Single-cell immune profiling of atherosclerosis: from omics to therapeutics

Depuydt, M.A.C.

Single-cell immune profiling of atherosclerosis

from omics to therapeutics

Marie Depuydt

Single-cell immune profiling of atherosclerosis

from omics to therapeutics

Marie Depuydt

Cover and layout design: © evelienjagtman.com
Printer: Optima, Rotterdam, The Netherlands

ISBN: 978-94-6361-967-7

Depuydt, Marie
Single-cell immune profiling of atherosclerosis – from omics to therapeutics

Proefschrift Leiden

Met literatuuropgave – met samenvatting in het Nederlands

Single-cell immune profiling of atherosclerosis

from omics to therapeutics

Proefschrift

ter verkrijging van
de graad van doctor aan de Universiteit Leiden,
op gezag van rector magnificus prof.dr.ir. H. Bijl,
volgens besluit van het college voor promoties
te verdedigen op donderdag 28 maart 2024
klokke 16.15 uur

door

Marie Antoinette Christiane Depuydt
geboren te Leiderdorp, Nederland
in 1994

Promotores	Prof. dr. J. Kuiper	
	dr. B. Slütter	
	dr. I. Bot	
Promotiecommissie	Prof. dr. H. Irth	
	Prof. dr. E.C.M. de Lange	
	Prof. dr. J.C. Sluimer	Maastricht University
	Prof. dr. H. Winkels	University of Cologne
	dr. H. Björkbacka	Lund University

The research described in this thesis was performed at the division of BioTherapeutics, Leiden Academic Centre for Drug Research (LACDR), Leiden University, the Netherlands. This thesis was financially supported by the Dutch Heart Foundation (CVON2017-20: GENIUS II). Financial support by the Dutch Heart Foundation for the publication of this thesis is gratefully acknowledged.

Table of Contents

Chapter 1

General Introduction

Cardiovascular disease

Cardiovascular diseases (CVDs) comprise all diseases affecting the heart or blood vessels and are responsible for the majority of mortality globally. On average, 17.9 million people die as a consequence of CVD each year worldwide.[1,2] Atherosclerotic cardiovascular disease (ASCVD) accounts for the majority (85%) of CVD-related deaths.[3] ASCVD refers to coronary heart disease, cerebrovascular diseases, peripheral artery disease and abdominal and descending thoracic aortic aneurysm.[4] All these conditions have atherosclerosis as common underlying cause. Atherosclerosis is characterized by chronic, lipid-driven vascular inflammation that induces atherosclerotic plaque formation in the intima of medium to large arteries.[5] The continuously advancing intimal plaques are eventually prone to rupture, resulting in thrombus formation and clinical manifestations due to ischemia of surrounding tissues, such as a myocardial infarction (MI) or stroke. ASCVD has multiple risk factors, including age, a sedentary lifestyle, an unhealthy diet, smoking, hypertension, dyslipidemia, obesity, diabetes mellitus and genetic predisposition, such as a mutation in the LDL receptor (LDLr) leading to familiar hypercholesterolemia.[6]

CVD has a major impact on the social-economic burden as it was estimated by the European Heart Network that CVD-related health care costs the European Union economy €210 billion on average. Currently, lifestyle interventions such as increased physical activity, a healthy diet, reduced smoking and alcohol consumption, are considered as the fundament of ASCVD treatment.[7] By alleviating multiple major risk factors at once, the risk of all-cause mortality can theoretically be reduced by 66%.[8] Furthermore, a reduced risk ratio was observed for both cardiovascular mortality and disease upon achieving improved cardiovascular health metrics (as defined by the American Heart Association).[9,10] Despite these efforts, additional pharmacological and surgical interventions are often still required.

For long, atherosclerosis has primarily been considered as lipid-driven disease. Reduction of circulating LDL cholesterol by means of statin treatment has led to great advances in cardiovascular disease treatment. Nevertheless, recurrent events have occurred in over 20% of patients that have suffered from acute coronary heart disease and received high dose statin treatment.[11,12] Currently, upon the occurrence of a cardiovascular event, therapies are mainly directed at revascularization. These include antithrombotic treatment and/or several surgical methods.[13] Percutaneous transluminal coronary angioplasty with or without stent placement is generally performed after MI incidence to reopen the coronary artery.[14] However, upon severe occlusion of multiple arteries or presence of diabetes and/or heart failure,

coronary artery bypass surgery is the preferred choice of surgical intervention.[15] For cerebrovascular ASCVD, carotid endarterectomy surgery is recommended for patients with ≥70–99% symptomatic stenosis in the carotid artery to reduce the risk of stroke.[16] Carotid endarterectomy surgery is solely performed if the overall benefit of surgery outweighs the potential peri-operative complications.[17]

Nowadays, it has become evident that apart from disturbed lipid metabolism, there is a prominent role for immune cells in the development of atherosclerosis. In the last decade, a handful of clinical trials have supported a pivotal role for the immune system in the treatment of atherosclerosis.[18] The CANTOS trial was the first to show that treatment with an anti-inflammatory monoclonal antibody against Interleukin (IL)-1β reduced the risk of cardiovascular events by 15%.[19] This study provided clear evidence that intersecting with the immune system ameliorates disease. Negative side-effects of general immune suppression were however also observed. Since the CANTOS trial, several other trials have been designed targeting the immune system in ASCVD. In the CIRT trial, patients with previous myocardial infarction and type 2 diabetes or metabolic syndrome were treated with methotrexate, but with no effect on cardiovascular outcomes. In the COLCOT, LoDoCo and LoDoCo2 trials patients with recent myocardial infarction were treated with colchicine and showed a significantly reduced risk of ischemic cardiovascular events.[20–22] The RESCUE trial has focused on the treatment of patients with elevated levels of high-sensitive C-Reactive Protein (hsCRP) and chronic kidney disease (CKD), which significantly increases cardiovascular disease risk. These patients were treated with Ziltivekimab, targeting IL-6, and showed a dose-dependent reduction in hsCRP levels at the end of the trial.[23] The RESCUE trial is at present being followed up by the ZEUS trial, in which a similar set up is executed, but additionally cardiovascular events will be monitored.[24] Finally, LILACS is a the second current ongoing clinical trial in which patients are treated with a low dose of IL-2 to induce an anti-inflammatory T cell response.[25] Altogether, these data further support the notion that the immune system is a promising target for future therapeutic strategies.

Atherosclerosis

Early lesion development

Arteries and veins consist of three layers: the intima, the smooth muscle cell-rich media and the adventitia. In the healthy vasculature, these layers are protected by a non-permeable endothelial cell layer. The endothelium acts as a selective barrier that allows the exchange of molecules between blood and tissues. It

consists of a continuous monolayer of endothelial cells linked by different types of adhesive structures or cellular junctions.[26] Furthermore, through the secretion of vasoconstrictor and vasorelaxant molecules endothelial cells modify smooth muscle cells thereby managing vascular tone.[27] Differences in blood flow result in a variety of hemodynamic forces that directly impact the endothelium. Whereas in unbranched areas of the artery a relatively uniform laminar blood flow occurs, a disturbed flow pattern is often observed in areas of bifurcation, branch points or major curvature.[28] Shear stress is necessary to maintain a proper vascular physiology. Through local mechanotransduction mechanisms, it is capable of modifying endothelial cell phenotype and barrier function.[29] However, at areas with disturbed flow patterns, oscillatory shear stress occurs, which causes endothelial damage and upregulation of adhesion molecules. In addition, endothelial dysfunction is in part mediated by pro-atherogenic factors like dyslipidemia and pro-inflammatory cytokines, altogether being the initiation trigger for atherosclerosis development. Endothelial cells are activated and upregulate the expression of leukocyte adhesion molecules, amongst which intercellular adhesion molecule-1 (ICAM-1), vascular cell adhesion molecule-1 (VCAM-1), E-selectin and P-selectin.[30,31]

Simultaneously, the endothelium becomes more permeable allowing the transmigration of lipoproteins. Circulating lipoproteins facilitate the transport of hydrophobic particles, *e.g.* cholesterol and triglycerides. Thereby they play an essential role in the distribution of respectively structural components for cell membranes and steroid hormones, and a key source for energy for the body.[32] There is a variety of lipoproteins that are characterized based on size, density and their associated apolipoproteins, including chylomicrons, very low density lipoprotein (VLDL), intermediate density lipoprotein (IDL), low density lipoprotein (LDL), high density lipoproteins (HDL) and lipoprotein (a) (Lp(a)).[33] Hyperlipidemia has been associated with atherosclerosis, in which elevated VLDL and primarily LDL have been described to promote atherosclerosis development. Apolipoprotein B100 (ApoB100), which is a part of LDL, binds to proteoglycans in the extracellular matrix of the damaged endothelial cell layer, thereby reducing retention of LDL.[34-36] These bound cholesterol-rich LDL particles are subsequently prone to chemical modification by *e.g.* oxidation into oxidized LDL (oxLDL).[37]

Concurrently, oxLDL stimulates the endothelial cells to secrete chemokines, such as C-C motif Chemokine Ligand 5 (CCL5) and CCL2, which leads to the recruitment of monocytes to atherosclerosis-prone sites. These monocytes crawl over the vessel wall and subsequently adhere to the endothelium by binding of integrins very late antigen-4 (VLA-4) and lymphocyte function-associated antigen 1 (LFA-1) to the upregulated

leukocyte adhesion molecules and infiltrate in the intima.[38,39] Secretion of macrophage colony stimulating factor (M-CSF) and granulocyte-macrophage colony stimulating factor (GM-CSF) by endothelial cells stimulates monocytes to differentiate into macrophages. Macrophages are phagocytes, meaning that they engulf debris, pathogens and dead cells.[40] Apart from monocyte-derived macrophages, there is also a population of resident macrophages that are of embryonic origin and reside in amongst others the arteries to act in the first line of defense.[41] In the intima, oxLDL is phagocytosed via scavenger receptors, such as CD36 and scavenger receptor class A, by resident macrophages at first and by monocyte-derived macrophages in later stages of disease development.[42–44] The continuous uptake of oxLDL by macrophages results in excessive lipid storage in the cells as seen by accumulating lipid droplets. These lipid-rich macrophages are called foam cells and are a hallmark for early atherosclerotic plaque development. Consequently, foam cells further contribute to atherosclerotic plaque progression by the secretion of multiple proinflammatory cytokines and chemokines thereby amplifying local inflammation.[45] The intimal thickening that is a result of intimal oxLDL, foam cell formation and initial immune infiltration is called a 'fatty streak'. If plasma cholesterol levels are sufficiently lowered, fatty streaks can almost completely regress.[46] However, fatty streak formation occurs in the subclinical phase of disease development and progress into more advanced lesions that induce clinical manifestations. In **Figure 1** the processes contributing to atherosclerosis development are summarized.

Advanced atherosclerosis

A sustained hyperlipidemic and pro-inflammatory environment increasingly exacerbates plaque development. After initial foam cell development, other immune cells, including T cells, also enter the fatty streak. By the secretion of proinflammatory cytokines, *e.g.* Interferon (IFN)-γ, T cells are capable of regulating both innate immune cells and smooth muscle cells.[47] Upon plaque progression, medial smooth muscle cells migrate into the intima and acquire different phenotypes. Whereas in the healthy medial layer smooth muscle cells have a quiescent contractile phenotype that is important to maintain vascular tone, they are capable of dedifferentiation into a synthetic state with advancing disease. Synthetic smooth muscle cells regain proliferative capacity and migrate into the intimal layer. This is a consequence of loss of expression of genes that encode for cytoskeletal proteins such as α-Smooth Muscle Actin (αSMA) and smooth muscle myosin heavy chains (MYH11). Instead, synthetic smooth muscle cells upregulate genes that express extracellular matrix-related proteins.[48–51] Consequently, these cells are a primary source of extracellular matrix in the atherosclerotic plaque.[52] Furthermore, synthetic smooth muscle cells are well known to accumulate underneath the breached endothelial layer thereby forming a so-called fibrous cap. This cap has a stabilizing function due to its collagen

and proteoglycan-rich matrix, which prevents the plaque from rupture and releasing its contents.[48,53] There is also accumulating evidence suggesting that smooth muscle cells can undergo a phenotypic switch towards a foam cell-like phenotype. Similar scavenger receptors as seen on foam cells, such as CD36 and SR-A1, are highly expressed on synthetic smooth muscle cells and concurrent phagocytic capacity of cholesterol-rich lipoproteins has been shown.[52,54,55] Krüppel-like factor 4 (KLF4) is an essential factor involved in the gain of macrophage-like properties by smooth muscle cells.[56] Interestingly, lineage tracing has shown that the majority of foam cells in the atherosclerotic plaques may have a smooth-muscle cell origin.[57]

The continuous lipid uptake by macrophages and smooth muscle cells becomes unsustainable as the plaque further expands. Although these cells express cholesterol efflux transporters such as ATP-binding cassette transporter A1 (ABCA1) and ABCG1, the excessive lipid uptake outweighs the efflux capacities at a certain stage. As a consequence, foam cells will go in apoptosis due to lipotoxicity. Efferocytosis is a highly regulated process that is initiated by phagocytes, such as macrophages, to take up apoptotic cells. Clearing of apoptotic cells is vital in maintaining tissue homeostasis in disease in order to avoid secondary necrosis and related induced inflammation.[58,59] With atherosclerosis progression, however, this process becomes impaired as the efferocytic capacity of phagocytes is reduced, leading to an increased number of apoptotic bodies and subsequent secondary necrosis.[60–62] This leads to formation of a necrotic core, which is characterized by the accumulation of apoptotic (immune) cells, cellular debris and lipid deposition.[63] Eventually, the growing necrotic core results in increased arterial stenosis and is associated with plaque instability.

Another key process in advanced atherosclerosis is the degradation of extracellular matrix and simultaneous fibrous cap thinning. The continuous cycle of lipoprotein infiltration, foam cell formation and necrotic core expansion occurs with a congruent chronic inflammatory response. Over time, the local inflammation in the plaque aggravates and significantly contributes to plaque destabilization. IFN-γ secreted by T cells for instance inhibits interstitial collagen production by smooth muscle cells[47,64] Furthermore, multiple immune cells that accumulate in the lesion are responsible for the secretion and activation of a variety of proteases that actively degrade the extracellular matrix. Matrix metalloproteases (MMPs) are commonly described to contribute to this process, of which primarily MMP-2 and MMP-9 that are secreted by activated macrophages and neutrophils.[65,66] Moreover, with atherosclerosis progression mast cells accumulate in the lesion as well.[67] Mast cells are well known to secrete proteases chymase and tryptase that independently degrade several collagen types, fibronectin and elastin. However, both chymase and tryptase amplify

the conversion pro-MMP-1 and pro-MMP-3 to their active forms, which subsequently activate *e.g.* MMP-2 and MMP-9, thereby further aggravating matrix degeneration in the atherosclerotic plaque and thus promote plaque instability.[68]

Altogether these processes will eventually destabilize the plaque to such an extent that the fibrous cap ruptures. Hereto, the necrotic content of the plaque which contains a large amount of thrombogenic factors, such as tissue factor, gets released in the vessel lumen and initiate thrombus formation and subsequent occlusion of the artery. Additionally, thrombus formation could also occur as a consequence of plaque erosion. Eroded plaques are often characterized by a less inflamed and more extracellular matrix-rich phenotype, which is more often found in patients treated with lipid-lowering drugs and is also more prevalent in women. Due to endothelial apoptosis, underlying collagen is exposed and initiates the accumulation of neutrophils and platelets and subsequent thrombus formation.[47,69,70] Both with plaque rupture and erosion, thrombus formation can lead to full occlusion of surrounding arteries, thereby inducing ischemia of the surrounding tissues and subsequent clinical events, such as stroke and myocardial infarction.

Experimental models of atherosclerosis

Due to the complex etiology of the atherosclerotic plaque, experimental studies are still largely dependent on *in vivo* atherosclerosis models. Despite recent advances in *in vitro* models of the healthy vasculature[71], to date these models are not applicable to model the advanced atherosclerotic plaque in culture. Atherosclerosis has been examined in a large variety of animal models, including rats, rabbits, pigs, and non-human primates. Nevertheless, mice remain the most common animal model for atherosclerosis.[72] Since the murine lipoprotein profile differs substantially from that in humans, atherosclerosis mouse models generally require a high fat and cholesterol diet, often referred to as western type diet, to accelerate disease development.[73] Nevertheless, wild type (C57BL/6) mice only developed small areas with fatty streaks after 14 weeks fed with a cholate containing high fat diet.[74] Instead, genetically modified murine models are used that specifically target the lipoprotein metabolism to increase circulating VLDL and LDL concentrations. The *apoE* and *Ldlr* deficient mouse models are most commonly used. ApoE is a constituent of VLDL and chylomicrons and is the main ligand for the clearance of these lipoproteins by the liver via several receptor systems, including the LDLr and the LDL receptor-related protein (LRP).[75] Deficiency of this gene already significantly elevates plasma cholesterol levels and this largely increases with a western type diet.[76] *ApoE*$^{-/-}$ mice naturally develop atherosclerotic plaques, which quickly become advanced upon diet feeding.[77] On the contrary, *Ldlr*$^{-/-}$ mice, which lack the LDLr required for clearance of VLDL and LDL particles by the liver, are characterized by modestly elevated levels of both VLDL and LDL in the blood. The advantage of this model is that the plasma cholesterol is largely

transported by LDL particles, which more closely resembles the human lipoprotein profile as compared to the *apoE*$^{-/-}$ mouse. Moreover, *LDLR* deficiency in humans is the underlying cause of familial hypercholesterolemia.[78,79] On a regular diet, these mice develop small atherosclerotic lesions in the first few months. Yet, with western type diet feeding they rapidly develop advanced atherosclerotic plaques. Of note, it has recently been shown that aged *Ldlr*$^{-/-}$ on a regular diet for two years, which reflects the average age of symptomatic cardiovascular patients, these mice develop advanced atherosclerosis as well.[80] Finally, atherosclerosis can also be induced in C57BL/6 mice via adeno-associated virus (AAV)-mediated overexpression of pro-protein convertase subtilisin/kexin type 9 (PCSK9)[81,82] PCSK9 is involved in hepatic LDLR recycling. It induces endocytosis and lysosomal degradation of the receptor, which results in reduced LDL uptake by the liver. Overexpression of this gene thus elevates circulating LDL and promotes atherosclerosis development. Nowadays, PCSK9 inhibitors have been introduced as treatment for both cardiovascular disease and familial hypercholesterolemia.[83]

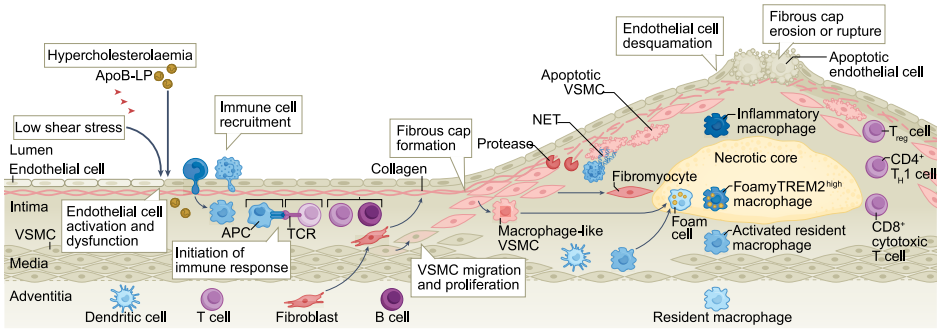

Figure 1. Development of atherosclerosis. Hypercholesterolemia and low shear stress damage the endothelial cell layer of the vessel wall resulting in endothelial dysfunction and activation. The endothelial cell layer becomes permeable and allows ApoB-containing lipoproteins (ApoB-LP) to enter the arterial wall. These ApoB-LPs get oxidized and further induce endothelial cell activation. Subsequently, monocytes are recruited, transmigrate and differentiate into macrophages. Both these macrophages and recruited vascular smooth muscle cells (VSMCs) in turn take up the oxLDL particles and differentiate into foam cells. This forms the fatty streak. As atherosclerosis progresses, the continuous uptake of lipoproteins by foam cells induces lipotoxicity and induces apoptosis. This is the foundation of the necrotic core that develops with aggravating disease. Furthermore, adaptive immune cells are also recruited to the atherosclerotic lesion. Antigen presentation by APCs induces T cell and B cell activation which will subsequently contribute to the pro-inflammatory environment in the lesion. Migration of VSMCs to the breached endothelial layer will induce fibrous cap formation. Over time, the plaque becomes unstable due to increased necrotic core formation alongside extracellular matrix degradation and apoptosis of VSMCs in the cap. As a consequence, the plaque will rupture and induce thrombosis leading to subsequent clinical manifestations. *Adapted and modified with permission from Engelen et al. (2022) Nat. Rev. Cardiol. 19(8):522-542.*[18]

The immune system in atherosclerosis

Although dyslipidemia has a pivotal role in atherosclerosis development, it has become evident that inflammation is a crucial process for disease progression. The immune system is responsible for protecting the body from infection and tissue injury.[84] Hereto, it employs two different arms: the innate and the adaptive immune system, otherwise referred to as respectively 'non-specific' and 'specific'.[85] The innate immune response is the first line of defense and becomes activated by the expression of pattern recognition receptors (PRRs).[86] These PRRs recognize pathogen-associated molecular patterns (PAMPs) and damage-associated molecular patterns (DAMPs). PAMPs are molecular structures not found in the host organism and therefore essential for innate immune cells to protect from pathogens. DAMPs on the other hand are endogenous molecular structures produced upon tissue damage and will be recognized as 'self' to activate natural immunity.[87] Multiple innate immune cells are capable of processing these PAMPs and/or DAMPs, which will induce a specific response based on the received signal. Subsequently, these cells are capable of presenting small peptide fragments of the pathogen on their surface to initiate the adaptive immune system. These fragments are called antigens or epitopes. Each adaptive immune cell has its own unique receptor that specifically binds the antigen presented by innate immune cells. Importantly, adaptive immune cells gain immunological memory after the first antigen encounter, which allows a rapid activation of these cells if they are rechallenged with the same antigen.[88] Therefore, the adaptive immune system is an important regulator for the resolution of inflammation. Both the innate and adaptive immune system are involved in atherosclerosis. The contribution of the different immune cells involved will be discussed below.

Innate immunity

The innate immune system plays a pivotal role in the initiation of atherosclerosis. The innate immune cells that are involved in disease development include monocytes, macrophages, dendritic cells, mast cells, neutrophils[89], natural killer cells[90] and innate lymphoid cells[91]. The cells that are relevant for this thesis are described more in detail below.

Monocytes and macrophages

Monocytes develop and mature from a hematopoietic stem cell origin in the bone marrow. There are two commonly described subsets: non-classical and classical monocytes.[92] Mon-classical monocytes are characterized as $Ly6C^{-}CCR2^{-}CX3CR1^{+}$ in mice and $CD14^{low}CD16^{+}$ in humans.[93] Their function is to patrol the vasculature to rapidly respond to, amongst others, endothelial damage. To do so, they recruit neutrophils that induce focal endothelial necrosis, and subsequently clear the

remaining cellular debris.[94,95] This subset of monocytes is often considered anti-inflammatory. Classical monocytes are defined as Ly6C^{hi}CCR2^{+}CX3CR1^{-} in mice and CD14^{+}CD16^{-} in humans and have a pro-inflammatory phenotype.[93] In contrast to non-classical monocytes, classical monocytes are specifically recruited to sites of inflammation or tissue remodeling. Here, they can extravasate from the blood and differentiate into monocyte-derived macrophages or dendritic cells.[92,96,97] As described above, monocytes are recruited upon endothelial damage and intimal (ox) LDL accumulation. Indeed, a positive correlation has been described between aortic monocytes and atherosclerotic lesion area.[98] Furthermore, in mice it was confirmed that classical monocytes develop into macrophages in the atherosclerotic aorta.[99] In line, the high expression of CCR2 rapidly redirects monocytes to the CCL2 secreting endothelial cells. Consequently, depletion of *Ccr2* in *ApoE*$^{-/-}$ mice significantly reduced atherosclerotic lesion size by three-fold. [100]

When entering the vascular intima, monocytes differentiate into macrophages upon stimulation with various cytokines and growth factors present in the plaque. Macrophages have a multitude of different phenotypes in health and disease. For years, a classical division was commonly used to distinguish two types of macrophages: M1 and M2 macrophages. The M1 phenotype is a pro-inflammatory subset that is polarized by either T helper 1 (Th1) secreted cytokines such as IFN-γ of TNFα or by recognition bacterial lipopolysaccharide (LPS) through the Toll-like receptor 4 (TLR4).[101] Their main function is phagocytosis of pathogens, after which M1 macrophages subsequently secrete a plethora of pro-inflammatory cytokines, including IL-1β, IL-6 and TNFα.[102] In atherosclerosis, oxLDL is also capable of inducing TLR4-associated macrophage activation, thereby promoting a pro-inflammatory environment in the plaque by the secretion of amongst others IL-6 and IL-1β secretion, of which the latter has been specifically targeted in the CANTOS trial.[19,103] M2 macrophages on the other hand have been generally considered anti-inflammatory and are polarized by secretion of *e.g.* IL-4 and IL-13 by Th2 cells. Generally, M2 macrophages are considered anti-inflammatory due to their increased secretion of IL-10 and TGFβ.[104,105] They play an important role in angiogenesis, wound healing and tissue remodeling and are potent scavenging cells.[104,106] Furthermore, they have pro-fibrotic capacities.[107] Based on these capacities, M2 macrophages have been described to resolve plaque inflammation.[108]

This distinction is largely based on *in vitro* assays assessing phenotypic changes of macrophages. However, at least in atherosclerosis, *in vivo* work has shown that the variety of macrophage phenotypes is way beyond just the pro- and anti-inflammatory subtypes. In the last decade, new techniques, such as cytometry by time-of-flight (CYTOF) and single-cell RNA sequencing, have shed new light on macrophage diversity

in the atherosclerotic plaque. Within the murine atherosclerotic aorta, five different subclasses of macrophages have been identified.[109,110] An inflammatory macrophage subset, which is characterized by expression of pro-inflammatory cytokines and genes that are involved in the inflammasome-induced conversion of pro-IL-1β into its active form. Furthermore, another pro-inflammatory subset of macrophage has been identified as type-I interferon inducible cells (IFNIC), which upregulate interferon-induced genes such as *Ifit3* and *Irf7*.[111] Both subsets are likely to be monocyte-derived. An anti-inflammatory foamy macrophage subset has mainly been characterized by the expression of *Trem2* (Triggering receptor expressed on myeloid cells 2).[112] These foamy macrophages were detected at different stages of atherosclerosis, yet not in healthy arteries. Expression of *Trem2* on BODIPY$^+$ lipid laden cells confirmed their foam cell-like phenotype, which additionally also expressed other genes associated with foam cell formation, including *Abca1*, *Abcg1* and *Cd36*. [41,113] Lastly, two resident macrophage subtypes have been characterized in murine atherosclerotic aortas. These macrophages reside both in healthy and diseased arteries. Lymphatic vessel endothelial hyaluronan receptor 1 (*Lyve1*)$^+$ resident macrophages are of embryonic origin and inhibit collagen synthesis by smooth muscle cells.[114,115] Recently, MAC^{AIR} (aortic-intima resident macrophage) macrophages were characterized. This subset of resident macrophages originates from blood monocytes shortly after birth and contribute to early lesion development by secretion of *Il1b*. They maintain by local proliferation in the aorta and are involved in the initial lipid uptake with atherosclerosis initiation. Yet, they encounter limited proliferation with plaque progression.[116] In human atherosclerosis macrophages have currently been generally divided in four subtypes, consisting of two types of pro-inflammatory macrophages, a TREM2$^+$ macrophage subset and resident-like macrophage population.[117–119] The pro-inflammatory macrophages are either characterized by expression of *IL1B* and associated genes that are involved in IL1β production or by expression of *TNF*. Of note, Fernandez *et al*. mainly detected *IL1B* expression in macrophages of asymptomatic patients.[119] The TREM2$^+$ macrophage subset is likely involved in lipid metabolism as supported by expression of *ABCA1*, *ABCG1*, *OLR1* and little proinflammatory genes. Furthermore, they express *CD9*, which has been associated to fibrosis in other diseases.[120] Finally, similar to murine atherosclerosis, a *LYVE1*$^+$ resident macrophage subset has been identified that may also affect antigen presentation and complement activation.[117]

Dendritic cells

Besides macrophages, dendritic cells (DCs) are classified as a distinct lineage of mononuclear phagocytes. The DC is the most potent antigen presenting cell (APC) and forms a bridge between the innate and adaptive immune system.[121] DCs regulate either antigen-specific T cell responses or tolerogenic responses to self-antigens. They reside

in both lymphoid and non-lymphoid tissues.[122] For long, a clear phenotypic distinction between macrophages and DCs has been a matter of debate as in inflammatory conditions they share expression of surface markers, such as CD11c.[123,124] Especially monocyte-derived cells have been shown to exhibit a very plastic phenotype as they acquire functional properties from both macrophages and dendritic cells (moDC) based on the microenvironment.[125–127] Nevertheless, the common DC progenitor (CDP) has been identified as unique precursor for both classical (cDC) and plasmacytoid DCs (pDC).[127,128] CDPs are localized in the bone marrow and either mature into pDCs within the bone marrow, or give rise to pre-DCs that enter the circulation, become immature DCs and mature into cDCs in lymphoid and non-lymphoid tissues. cDCs are divided in cDC1s and cDC2s, dependent on respectively BATF3 and IRF4 expression.[129,130]

Immature DCs patrol peripheral tissues to identify potential antigens. Upon internalization of antigens at inflammatory sites, DCs mature and migrate through the afferent lymphatic vessels to adjacent draining lymph nodes.[131] In this process, DCs downregulate their phagocytic capacity and gain antigen presenting properties by upregulation of CCR7 to enhance migration, and costimulatory molecules such as CD40, CD80 and CD86. Furthermore, they upregulate major histocompatibility complex (MHC) I or II, which are required for antigen presentation.[132,133] To induce an antigen-specific T cell response, the APC requires three signals: an interaction between the MHC and T cell receptor, a costimulatory or coinhibitory stimulation and finally cytokine secretion that altogether define whether the naive T cell gains an effector or an immunosuppressive function.[134,135] Of note, antigen presentation is not restricted to DCs, but could also be performed by other immune cells, such as macrophages, B cells and mast cells.[135,136]

DCs are present in the adventitia of healthy arteries. With atherosclerosis progression, they accumulate in advanced lesions, particularly in the rupture prone shoulder regions. [124,137,138] Furthermore, DCs are also found in adventitial tertiary lymphoid organs (ATLOs), which also significantly contribute to atherosclerosis progression.[139,140] Several studies have aimed to identify a causal contribution of DCs to atherosclerosis.[141] In early atherosclerosis, DCs have been shown to play an important role in cholesterol metabolism as upon dyphteria-toxin induced deletion of CD11c reduced plaque lipid content of *Ldlr*$^{-/-}$ mice.[142] In line, induction of a prolonged lifespan of DCs by overexpression of *Bcl2* resulted in an atheroprotective reduction of plasma cholesterol levels.[143] Interestingly, vaccination with *ex vivo* oxLDL-pulsed DCs significantly reduced atherosclerotic lesion size and increased plaque stability.[144] Additionally, adoptive transfer of ApoB100-loaded dendritic cells also significantly reduced atherosclerotic lesion size and reduced effector T cell activation, indicative of

a tolerogenic DC response.[145] These studies both underline the therapeutic potential of vaccination with tolerogenic DCs (tolDCs) for the treatment of atherosclerosis. Amongst others in rheumatoid arthritis, this strategy has been shown to effectively reduce disease burden and has resulted in the start of multiple clinical trials.[146,147] Nevertheless, a well-defined epitope to induce this tolerogenic response in atherosclerosis still remains to be identified.

Mast cells

Another prominent innate immune cell in atherosclerosis is the mast cell. This pro-inflammatory effector cell is widely distributed in several tissues and is predominantly found near surfaces exposed to the environment, such as the blood vessels, the skin, the airways and the gastrointestinal tract, allowing these cells to act as a first line of defense against pathogens.[148] Mast cells develop from hematopoietic stem cells, in particular a subset of granulocyte-monocyte progenitors, in the bone marrow.[149] These subsequently enter the circulation as mast cell progenitors.[150,151] Similar to macrophages, mast cells only mature within peripheral tissues. Mature mast cells are characterized by expression of c-Kit (CD117) and the Fcε receptor I (FcεRI).[152] Furthermore, they have a granule-rich cytoplasm that contains a plethora of inflammatory mediators. Upon activation, mast cells degranulate and release their mast-cell specific proteases tryptase and chymase, histamine and depending on the strength of the interaction they release amongst other cytokines, chemokines, leukotrienes and growth factors.[153,154] Mast cells are activated through a variety of mechanisms (**Figure 2**). Binding of an antigen-sensitized IgE to its high affinity receptor FcεRI results in a rapid degranulation and the concurrent release of proteases and lipid mediators, whereafter cytokines, chemokines and growth factors can be secreted as well.[154–157] This IgE-mediated activation is the most commonly known route of activation, however mast cells can also be activated via toll-like receptors, the FcγR, complement receptors and a number of neuropeptide receptors.[158] The secretion of mast cell mediators could have both pro- and anti-inflammatory functions on the surrounding cells. Additionally, mast cells have also been described as atypical antigen presenting cells by upregulation of MHC II molecules and could hereto induce T cell responses.[135,159,160]

Although mast cells are mostly known for their contribution to allergic reactions and airway diseases like asthma, they also play a significant role in atherosclerosis development. Mast cells are found in all stages of plaque development and their numbers have been shown to increase with disease progression.[161–163] Furthermore, a positive correlation has been observed between intraplaque mast cell numbers

and future cardiovascular events.[67] Multiple experimental atherosclerosis studies further outline the functional importance of mast cells in atherosclerosis. Systemic activation of mast cells exacerbates atherosclerosis development in *Apoe*$^{-/-}$ mice, which was resolved upon treatment with the mast cell stabilizer cromolyn.[164] Moreover, depletion of mast cells in *Ldlr*$^{-/-}$ mice significantly reduced atherosclerotic lesion size, which was restored after repopulation with bone-marrow derived mast cells.[165] The pro-atherogenic effects of mast cells are mainly attributed to the proteases they secrete upon activation. Chymase has been shown to induce apoptosis of both vascular smooth muscle cells and endothelial cells[166–169] and both chymase and tryptase activate matrix metalloproteases (MMPs) inducing matrix degradation and subsequent plaque remodeling.[170] Indeed, treatment with a chymase inhibitor not only reduced plaque size, but it also increased collagen content and reduced necrotic core size and the frequency and size of intraplaque hemorrhages, indicative of improved plaque stability.[171] Furthermore, in both *in vitro* and *in vivo* settings, mast cells can induce foam cell formation as heparin binds to LDL particles, resulting in complex formation and phagocytosis by plaque macrophages.[172–175] The secretion of pro-inflammatory cytokines also affects other surrounding immune cells thereby contributing to plaque progression.[176] Targeting mast cell activation or their migration to the atherosclerotic plaque are thus promising therapeutic approaches to improve disease outcome.

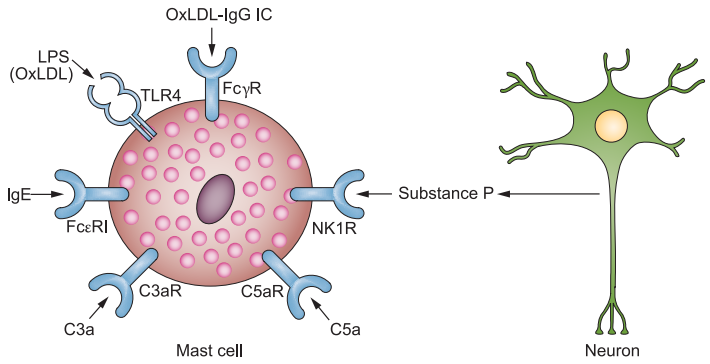

Figure 2. Different pathways of mast cell activation that occur during atherosclerosis development. Mast cell activation is considered pro-atherogenic. Multiple pathways have been described to induce mast cell activation with the progression of atherosclerosis. The most commonly known route of activation is upon binding and sensitization of IgE to the FcεRI, leading to subsequent degranulation of the mast cell. Furthermore, activation via the complement receptors C3aR and C5aR, TLR4, FcγR and NK1R result in degranulation and/or cytokine secretion by the mast cell. All pathways have been shown to independently contribute atherosclerosis. *Adapted with permission from Shi et al. (2015) Nat. Rev. Cardiol. 12(11):643-58.*[158]

Adaptive immunity

The adaptive immune response is initiated as secondary line of defense and it is mainly characterized by its immunological memory. The adaptive immune system consists of two different cell types: T and B cells. Both cell types play a prominent role in atherosclerosis.[177-181]

T cell development and activation

T cells originate from hematopoietic stem cells and migrate to the thymus to undergo maturation and selection before they enter the circulation. Within the thymus, $CD4^+CD8^+$ T cell precursors develop into two lineages depending on the T cell receptor chains they obtain: αβ or γδ T cells.[182,183] Each TCR has an antigen-binding site which is determined through V(D)J recombination. The α and γ chains are assembled from Variable (V) and Joining (J) segments, whereas the β and δ chain also have an additional diversity (D) segment.[184] Through somatic DNA recombination, a variable region is generated from these segments on the TCR that is unique for each individual T cell and specific for an antigen-MHC complex. Subsequently, the T cell precursors are selected based on their affinity for self-peptides and the strength of the TCR signal.[185] The majority of the T cell precursors are subject to death by neglect when they fail to sufficiently recognize a self-peptide-MHC complex or are unable to generate TCR signal that allows activation and differentiation of the T cell. T cell precursors that have too high affinity for self-peptides are negatively selected and go into apoptosis to avoid an autoimmune response. Finally, the positively selected T cell precursors have low self-reactivity and sufficient TCR signaling for maturation.[186,187] These cells will further differentiate into $CD4^+$ and $CD8^+$ T cells, dependent on their affinity for respectively MHCII or MHCI, and exit the thymus into the periphery. As a result, there is a large and diverse pool of different TCRs that are capable of responding to pathogen-derived antigens as well as preserving self-tolerance.

Naïve T cells get activated after encountering their cognate antigen presented by an APC. Upon antigen presentation, the naïve T cells will clonally expand and differentiate into a large pool of effector T cells with the same TCR. Activated T cells then migrate to the site of inflammation, such as the atherosclerotic plaque, and be primed again by local antigen presenting cells (**Figure 3**).[188] When the inflammation is resolved, the majority of the effector T cells go into apoptosis. However, a part of the effector T cells become circulating memory T cells that can elicit a quick response upon subsequent engagement with the same antigen.[189]

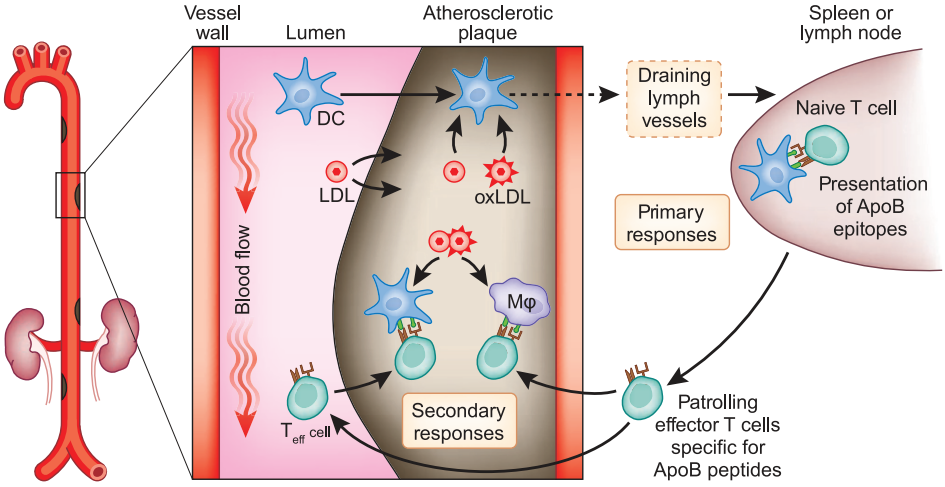

Figure 3. T cell activation in atherosclerosis. APCs, such as DCs patrol the circulation for antigens to present on their surface, for example peptides from ApoB100. APCs enter the plaque to take up antigens and subsequently migrate to draining lymphoid organs to present the antigen to naïve T cells. These will be activated and go back into the circulation as effector T cell. When they are recruited to the atherosclerotic plaque, they will undergo secondary activation by APCs residing in the lesion and exert their effector function. *Adapted with permission from Hansson et al. (2011) Nat. Immunol. 12, 204-212.*[188]

T cells play a prominent role in atherosclerosis development. A reduction in fatty streak formation was observed in *Ldlr*$^{-/-}$ mice lacking both B and T cells.[190] Similarly, a significant reduction in atherosclerotic plaque size was observed in immunodeficient *Apoe*$^{-/-}$ mice, yet upon reconstitution with CD4^{+} T cells atherosclerosis progression was accelerated.[191] Both CD4^{+} and CD8^{+} T cells have been detected in human atherosclerotic plaques[192] and contribute to multiple aspects of atherosclerosis progression.

CD4^{+} T cells

CD4^{+} T cells have a multifaceted role in atherosclerosis. Naïve CD4^{+} T cells develop into different T helper (Th) subsets dependent on the cytokines secreted with antigen presentation. Multiple CD4^{+} Th subsets have been described to affect disease progression. Th1, Th2, Th17 and regulatory T cells (T_{reg}) are most commonly studied in atherosclerotic plaques and will be discussed in more detail below. Apart from the beforementioned Th subsets, Th9[193,194], Th22[194,195], follicular T helper (Tfh) cells[196-198] and a subset of cytotoxic CD4^{+} T cells[199,200] have also been described in the context of atherosclerosis yet it remains elusive if they exert pro- or anti-atherogenic functions.

Th1 cells differentiate from naïve CD4+ T cells upon stimulation with IL-12. They are characterized by expression of the transcription factor T-bet and secretion of IFN-γ, IL-2 and TNFα.[178] Hereto, they contribute to the local pro-inflammatory environment in the atherosclerotic plaque. Indeed, T-bet deficient *Ldlr*$^{-/-}$ mice developed significantly smaller atherosclerotic lesions.[201] Furthermore, depletion of both IFN-γ and its receptor both resulted in a substantial reduction in plaque size[202,203], whereas treatment with IFN-γ concurrently aggravated disease.[204] Through secretion of IFN-γ, Th1 cells also promote plaque vulnerability as this cytokine inhibits smooth muscle cell proliferation, induces foam cell formation and promotes a pro-inflammatory phenotype for macrophages.[205-207] Altogether, these data provide clear evidence for the pro-atherogenic role of Th1 cells in atherosclerosis.

In contrast to Th1 cells, the function of Th2 cells in atherosclerosis is less evident. Th2 cells are defined by the expression of transcription factor GATA-3 and the secretion of IL-4, IL-5 and IL-13.[208] Th2 cells are well-known for their role in the protection of helminth infections and their contribution to asthma and allergic diseases.[209] In atherosclerosis however, conflicting results have been observed for these T cells. Since IL-4 was shown to inhibit Th1 responses, Th2 cells were initially thought to be atheroprotective.[210] However, whereas depletion of IL-4 ameliorated atherosclerosis in both *Ldlr*$^{-/-}$ and *Apoe*$^{-/-}$ mice[211,212], induction of an ApoB100-specific Th2 response did not alter disease progression.[213] On the contrary, IL-4 released from mononuclear leukocytes were associated with reduced risk of CVD and circulating Th2 cells were negatively associated with common carotid intima-media thickness.[214] Plasma IL-5 was shown to inversely correlate with carotid intima-media thickness in women.[215] Furthermore, immunization against modified LDL initiated a Th2-response, resulting in secretion of IL-5 which mitigated atherosclerosis development.[216] The cytokine IL-13 was reported to be anti-atherogenic as well.[217] Collectively, how Th2 exactly contribute to atherosclerosis progression remains ambiguous.

Differentiation of Th17 cells requires IL-23 and results in upregulation of the transcription factor RORγT and secretion of IL-17.[218] Like Th2 cells, there is still some discrepancy regarding the role of Th17 cells in atherosclerosis. Deficiency of IL-17 has been described to be either atheroprotective[219], pro-atherogenic[220] or not affecting atherosclerosis at all.[221] Yet, administration of IL-17 or anti-IL-17 antibodies demonstrated that this cytokine promotes atherosclerosis development.[222-224] Deficiency of the IL-23 receptor (IL-23R) reduced IL-17 production by CD4+ T cells but did not affect atherosclerosis in both a full-body knockout and upon adoptive transfer of IL-23R deficient CD4+ T cells into atheroprone immunodeficient mice.[225] In humans, a similar disparity is observed regarding how Th17 act on disease progression. Patients

with acute coronary syndrome exhibited higher numbers of peripheral Th17 cells as well as increased levels of IL-17 and IL-23 compared to controls.[226] Plasma IL-17 was also associated with patients with acute myocardial infarction and it was elevated in patients that had a complex lesion defined by angiographic analysis.[227] However, IL-17 has also been shown to promote collagen production by human vascular smooth muscle cells *in vitro* and *IL17A* and *RORC* (encoding for RORγT) expression were both positively associated with expression of *ACTA2* (α-SMA) and *COL1A1* (Procollagen 1α1) indicating that IL-17 promotes plaque stability.[228] This was further supported by another study that also found increased levels of IL-17 expression in plaques with a stable phenotype.[229] The complexity in which Th17 cells affect atherosclerosis could in part be explained by their plasticity.[230] Upon pro- stimulation with TGFβ3, Th17 cells could also upregulate IFN-γ[231], whereas stimulation with TGFβ1 and IL-6 could promote Th17 to secrete the anti-inflammatory cytokine IL-10.[232,233] Taken together, it appears that Th17 exert no clear pro- or anti-atherogenic role and that their function is largely dependent on the microenvironment they reside in.

T_{regs} are involved in preserving self-tolerance and resolving inflammation.[234] They are characterized by expression of forkhead box protein P3 (FOXP3), IL-2RA (CD25) and lack of CD127. Their differentiation is induced by TGF-β and IL-2 or by weak TCR interactions.[235,236] Upon activation they secrete the anti-inflammatory cytokine IL-10. Although the number of T_{regs} in atherosclerotic plaques are limited[237], several experimental atherosclerosis studies have determined an atheroprotective role for these cells. Depletion of T_{regs} significantly increased atherosclerotic lesion size[238,239], and adoptive transfer of T_{regs} correspondingly attenuated disease progression.[238,240] Furthermore, expansion of T_{regs} using an IL-2 complex ameliorated atherosclerosis and increased plaque stability.[241] A different approach for T_{reg} expansion even resulted in regression of existing atherosclerotic lesions.[242] In line, vaccination against FOXP3 reduced the percentage of T_{regs} and exacerbated atherosclerosis.[243] The suppressive function of T_{regs} in atherosclerosis is in part mediated by secretion IL-10 as lack of this gene promotes disease progression.[244-246] In brief, T_{regs} have an important atheroprotective function. Induction of T_{regs}, as examined in the LILACS trial, is therefore a promising strategy to treat CVD patients.

$CD8^+$ T cells

$CD8^+$ are commonly known to act in the defense against infectious pathogens, such as bacteria and viruses, and contribute to anti-tumor immunity.[247,248] The majority of $CD8^+$ T cells differentiate into a cytotoxic subset after encountering an antigen-MHC I complex. These cytotoxic $CD8^+$ T cells are subsequently capable of killing the infected cells that carry the presented antigen in three ways: (1) through secretion of IFN-γ and TNF-α, that

respectively promote the inflammatory response and induce apoptosis, (2) by interaction of Fas with the Fas receptor on the target cell to induce apoptosis and (3) by the secretion of granzymes and perforin which are responsible for lysis of the target cell.[249,250]

The role of $CD8^+$ T cells in atherosclerosis remains inconclusive. Interference with MHC-I-related antigen presentation significantly reduced $CD8^+$ T cell numbers, but did not affect atherosclerosis.[251] Furthermore, depletion of *Cd8a* in *Apoe*$^{-/-}$ mice did not alter atherosclerotic lesion size either.[252] Nevertheless, both pro-atherogenic and atheroprotective roles for $CD8^+$ T cells have been described in mice as well. High-fat diet rapidly induced $CD8^+$ T cell activation in *Apoe*$^{-/-}$ mice as measured by their increased IFN-γ production in draining lymph nodes of the aortic root.[253] Moreover, administration of monoclonal antibodies against CD8α and CD8β significantly reduced atherosclerotic plaque size and reduced necrotic core size in *Apoe*$^{-/-}$ mice.[254] In line, the same study showed that adoptive transfer of $CD8^+$ T cells aggravated atherosclerosis and induced plaque vulnerability. This was attributed to the secretion of perforin, granzyme B and TNFα, as reconstitution of $CD8^+$ T cells deficient for these proteins did not affect atherosclerosis in immunodeficient mice. In contrast, treatment with a CD8α-depleting antibody in *Ldlr*$^{-/-}$ mice with advanced atherosclerosis increased plaque vulnerability as seen by increased necrotic core area.[255] This protective role for $CD8^+$ T cells was further supported in another study in which immunization with the ApoB100-derived peptide p210 resulted in expansion of $CD8^+$ T cells and a subsequent reduction in atherosclerotic plaque size.[256]

It has been hypothesized that these opposing effects of $CD8^+$ T cell depletion in are due to the heterogeneity of $CD8^+$ T cells. A subset referred to as Tc17 cells, characterized by RORγT expression and IL-17 secretion, was shown to increase in atherosclerotic lesions compared to the spleen. Yet, transfer of Tc17 cells into *Cd8a*$^{-/-}$*Apoe*$^{-/-}$ mice did not directly affect plaque size.[257] On the other hand, regulatory $CD8^+$ T cells, defined by expression of CD25 and FOXP3, have been described to be atheroprotective.[258,259]

In humans, mainly a pro-atherogenic role for $CD8^+$ T cells has been described. Increased levels of circulating cytotoxic $CD8^+$ T cells were detected in patients with coronary artery disease.[260,261] Furthermore, $CD8^+$ T cells are found in large numbers in the human atherosclerotic plaque, particularly in the shoulder regions and fibrous caps.[192,261,262]

B cells

B cells play an important role in humoral and cellular immunity. They are well known for the production of antibodies, but also contribute to T cell activation through antigen presentation or the cytokines they secrete.[263] In atherosclerosis, B cells

were first described to have a protective function, as adoptive transfer of B cells into splenectomized mice and B cell deficiency resulted in respectively a reduction and an increase in plaque size[264,265] Since then, several subsets of B cells have been associated with atherosclerosis.[179,180] The B1 subset is characterized by the secretion of natural antibodies and protects from atherosclerosis.[266] B1 cells can be further subdivided in B1a and B1b cells. A prominent anti-atherogenic function is denoted for B1a cells, as they are the main producers of IgM antibodies.[267,268] Deletion of secreted IgM indeed significantly increased atherosclerotic lesion size, concurrent with an increase in IgE and a corresponding increase in mast cell activation.[269] IgM antibodies that resolve atherosclerosis by clearing oxLDL and necrotic debris are of specific interest.[270] The secretion of oxLDL-targeted IgM antibodies was found to be mediated through secretion of IL-5 by Th2 cells. In addition, an atheroprotective function for B1b cells was also described as they also produce IgM antibodies targeting oxidation specific epitopes on LDL.[271] B2 cells however are generally considered pro-atherogenic.[272] B2 cells can be divided in follicular (FO) and marginal zone (MZ) B cells. After encountering their cognate antigen, FO B cells migrate towards the T cell area in lymphoid organs and upon interaction with Th cells that recognize the same antigen, they can proliferate and undergo class switching.[273] FO B cells are subsequently capable of secreting amongst others IgG and IgE, which are both pro-atherogenic.[181,274] MZ B cells can secrete antibodies independent of T cell activation and can hereto rapidly produce IgM and IgG antibodies.[275] However, MZ B cells were also shown to be protective as they regulate Tfh cells which subsequently reduces FO B cell activation.[276] Finally, a subset of IL-10^{+} regulatory B cells has also been identified in atherosclerosis, yet their precise role in atherosclerosis is not fully elucidated yet.[277-279] Collectively, proper targeting of the humoral immune response in atherosclerosis could provide a beneficial therapeutic strategy against atherosclerosis.

Single-cell transcriptomics in atherosclerosis research

The introduction of single-cell transcriptomics has revolutionized biological research. Single-cell RNA sequencing was first applied in 2009, in which the mRNA transcriptome was uncovered from a manually isolated single cell.[280] Since then, the field of single-cell RNA sequencing has rapidly evolved, allowing for the analysis of single cell transcriptomes of thousands of cells per sample.[281] The great advantage of this technology lies in the fact that it provides an unbiased analysis of the different cells present in heterogenous tissue samples, whereas conventional methods like immunohistochemistry and flow cytometry rely on pre-defined markers. Furthermore, single cell transcriptomics are likely to identify small cellular populations that would

otherwise be diluted when using bulk RNA sequencing.[282] By now, the field of single-cell multi-omics has been complemented with several modalities to extend the single cell analysis.[283] This gives the possibility to include antibodies for proteomic characterization of for instance certain lineage markers necessary for proper cell annotation (CITE-seq). Furthermore, the epigenome can be assessed using single-cell ATAC sequencing and both TCR and BCR clones can be detected per single cell to assess clonal expansion for extensive immune profiling.

The application of single-cell transcriptomics has significantly advanced the field of atherosclerosis in the past decade. In 2018, single-cell RNA sequencing was first applied in both *Apoe*$^{-/-}$ and *Ldlr*$^{-/-}$ mice to map the cells present in atherosclerotic plaques.[112,284] This uncovered amongst others the presence of TREM2^{+} macrophages in atherosclerosis. Since then, a body of literature has been generated in which single-cell transcriptomics has been applied in both murine and human atherosclerosis. This has significantly enhanced our knowledge on the different cells present in (human) atherosclerosis. We will further elaborate on these findings in chapter 2 of this thesis.

Thesis outline

In this thesis, single-cell multi-omics were applied to generate a cellular atlas of the human atherosclerotic plaque. These data were subsequently further analyzed to identify and examine new potential targets to prevent atherosclerotic disease progression.

In **chapter 2** we provide an overview of how single-cell RNA sequencing has improved our knowledge in atherosclerosis and aneurysm formation. We describe the different cell populations identified in studies performed in diseased tissues of both murine and human origin. Finally, we elaborate on overlapping cellular subsets potentially contributing to both diseases. In **chapter 3** we unbiasedly mapped the cells present in human atherosclerotic plaques by using single-cell RNA and ATAC sequencing and discovered a large T cell population as well as cellular plasticity and intercellular communication pathways. Since we detected a large population of T cells in the advanced human plaque, we further investigated whether these T cells underwent clonal expansion indicative of an antigen-induced response. Hereto, in **chapter 4**, we applied single-cell TCR sequencing to assess T cell clonality in atherosclerosis. We identified a plaque-enriched clonally expanded CD4^{+} T cell subset, suggesting an autoimmune component in atherosclerosis. In **chapter 5** we developed a flow cytometry method to characterize mast cell phenotype in human atherosclerosis.

Here, we showed that the majority of mast cells express the activation marker CD63 in the human plaque. Moreover, a high percentage of these activated mast cells had IgE bound to their surface, indicating that the FcεRI-IgE pathway is of importance in mast cell activation in atherosclerosis. We elaborate on the mast cell in **chapter 6** in which we examined how aging affects mast cell phenotype, since this is a prominent risk factor for atherosclerosis. We describe that the aging microenvironment in the plaque increases mast cell activation in the atherosclerotic aorta and promotes the antigen-presenting capacities of these cells. Finally, we applied the human single-cell RNA sequencing data set to identify two genes that potentially affect atherosclerosis. In **chapter 7** we blocked BLT1 receptor to inhibit leukotriene B4-mediated mast cell migration to the plaque. This did neither affect atherosclerosis progression nor mast cell migration towards the plaque in *Ldlr*$^{-/-}$ mice. In **chapter 8** we used a small molecule to inhibit IL4I1, which was uniquely present on TREM2^{+} macrophages. Although this did induce a clear pro-inflammatory T cell response, atherosclerosis development was not altered. In **chapter 9** all data in this thesis will be summarized and discussed, including concluding remarks and future perspectives.

References

1. World Health Organization. Noncommunicable diseases. https://www.who.int/news-room/fact-sheets/detail/noncommunicable-diseases (2022).
2. Timmis, A. *et al.* European Society of Cardiology: cardiovascular disease statistics 2021. *Eur Heart J* **43**, 716–799 (2022).
3. World Health Organization. Cardiovascular diseases (CVDs). https://www.who.int/news-room/fact-sheets/detail/cardiovascular-diseases-(cvds) (2021).
4. Grundy, S. M. *et al.* 2018 AHA/ACC/AACVPR/AAPA/ABC/ACPM/ADA/AGS/APhA/ASPC/NLA/PCNA Guideline on the Management of Blood Cholesterol: Executive Summary. *J Am Coll Cardiol* **73**, (2019).
5. Bäck, M., Yurdagul, A., Tabas, I., Öörni, K. & Kovanen, P. T. Inflammation and its resolution in atherosclerosis: mediators and therapeutic opportunities. *Nature Reviews Cardiology 2019 16:7* **16**, 389–406 (2019).
6. Bays, H. E. *et al.* Ten things to know about ten cardiovascular disease risk factors. *Am J Prev Cardiol* **5**, 100149 (2021).
7. Libby, P. *et al.* Atherosclerosis. *Nature Reviews Disease Primers 2019 5:1* **5**, 1–18 (2019).
8. Loef, M. & Walach, H. The combined effects of healthy lifestyle behaviors on all cause mortality: A systematic review and meta-analysis. *Prev Med (Baltim)* **55**, 163–170 (2012).
9. Fang, N., Jiang, M. & Fan, Y. Ideal cardiovascular health metrics and risk of cardiovascular disease or mortality: A meta-analysis. *Int J Cardiol* **214**, 279–283 (2016).
10. Lloyd-Jones, D. M. *et al.* Defining and Setting National Goals for Cardiovascular Health Promotion and Disease Reduction. *Circulation* **121**, 586–613 (2010).
11. Cannon, C. P. *et al.* Intensive versus moderate lipid lowering with statins after acute coronary syndromes. *N Engl J Med* **350**, 1495–1504 (2004).
12. Libby, P., Ridker, P. M. & Hansson, G. K. Progress and challenges in translating the biology of atherosclerosis. *Nature* **473**, 317–325 (2011).
13. Collet, J.-P. *et al.* 2020 ESC Guidelines for the management of acute coronary syndromes in patients presenting without persistent ST-segment elevationThe Task Force for the management of acute coronary syndromes in patients presenting without persistent ST-segment elevation of the European Society of Cardiology (ESC). *Eur Heart J* **42**, 1289–1367 (2021).
14. Braunwald, E. The treatment of acute myocardial infarction: the Past, the Present, and the Future. *Eur Heart J Acute Cardiovasc Care* **1**, 9–12 (2012).
15. Michaels, A. D. & Chatterjee, K. Angioplasty Versus Bypass Surgery for Coronary Artery Disease. *Circulation* **106**, (2002).
16. Bonati, L. H. *et al.* European Stroke Organisation guideline on endarterectomy and stenting for carotid artery stenosis. *Eur Stroke J* **6**, I–XLVII (2021).
17. Calvillo-King, L., Xuan, L., Zhang, S., Tuhrim, S. & Halm, E. A. Predicting Risk of Perioperative Death and Stroke After Carotid Endarterectomy in Asymptomatic Patients: Derivation and Validation of a Clinical Risk Score. *Stroke; a journal of cerebral circulation* **41**, 2786 (2010).
18. Engelen, S. E., Robinson, A. J. B., Zurke, Y. X. & Monaco, C. Therapeutic strategies targeting inflammation and immunity in atherosclerosis: how to proceed? *Nat Rev Cardiol* **19**, 522–542 (2022).
19. Ridker, P. M. *et al.* Antiinflammatory Therapy with Canakinumab for Atherosclerotic Disease. *New England Journal of Medicine* **377**, 1119–1132 (2017).

20. Nidorf, S. M. *et al.* Colchicine in Patients with Chronic Coronary Disease. *New England Journal of Medicine* **383**, 1838–1847 (2020).
21. Tardif, J.-C. *et al.* Efficacy and Safety of Low-Dose Colchicine after Myocardial Infarction. *New England Journal of Medicine* **381**, 2497–2505 (2019).
22. Opstal, T. S. J. *et al.* Long-Term Efficacy of Colchicine in Patients With Chronic Coronary Disease: Insights From LoDoCo2. *Circulation* **145**, 626–628 (2022).
23. Ridker, P. M. *et al.* IL-6 inhibition with ziltivekimab in patients at high atherosclerotic risk (RESCUE): a double-blind, randomised, placebo-controlled, phase 2 trial. *The Lancet* **397**, 2060–2069 (2021).
24. Ridker, P. M. From RESCUE to ZEUS: will interleukin-6 inhibition with ziltivekimab prove effective for cardiovascular event reduction? *Cardiovasc Res* **117**, e138–e140 (2021).
25. Zhao, T. X. *et al.* Low-dose interleukin-2 in patients with stable ischaemic heart disease and acute coronary syndromes (LILACS): protocol and study rationale for a randomised, double-blind, placebo-controlled, phase I/II clinical trial. *BMJ Open* **8**, (2018).
26. Michiels, C. Endothelial cell functions. *J Cell Physiol* **196**, 430–443 (2003).
27. Peiró, C. *et al.* Influence of Endothelium on Cultured Vascular Smooth Muscle Cell Proliferation. *Hypertension* **25**, 748–751 (1995).
28. Gimbrone, M. A., Topper, J. N., Nagel, T., Anderson, K. R. & Garcia-Cardeña, G. Endothelial Dysfunction, Hemodynamic Forces, and Atherogenesisa. *Ann N Y Acad Sci* **902**, 230–240 (2000).
29. Cunningham, K. S. & Gotlieb, A. I. The role of shear stress in the pathogenesis of atherosclerosis. *Laboratory Investigation 2005 85:1* **85**, 9–23 (2004).
30. Cybulsky, M. I. & Gimbrone, M. A. Endothelial expression of a mononuclear leukocyte adhesion molecule during atherogenesis. *Science* **251**, 788–791 (1991).
31. Libby, P. The changing landscape of atherosclerosis. *Nature 2021 592:7855* **592**, 524–533 (2021).
32. Lu, Y. *et al.* The Functional Role of Lipoproteins in Atherosclerosis: Novel Directions for Diagnosis and Targeting Therapy. *Aging Dis* **13**, 491 (2022).
33. Bhargava, S., de la Puente-Secades, S., Schurgers, L. & Jankowski, J. Lipids and lipoproteins in cardiovascular diseases: a classification. *Trends in Endocrinology & Metabolism* **33**, 409–423 (2022).
34. Borén, J. *et al.* Identification of the principal proteoglycan-binding site in LDL. A single-point mutation in apo-B100 severely affects proteoglycan interaction without affecting LDL receptor binding. *Journal of Clinical Investigation* **101**, 2658 (1998).
35. Flood, C. *et al.* Molecular Mechanism for Changes in Proteoglycan Binding on Compositional Changes of the Core and the Surface of Low-Density Lipoprotein-Containing Human Apolipoprotein B100. *Arterioscler Thromb Vasc Biol* **24**, 564–570 (2004).
36. Tabas, I., Williams, K. J. & Borén, J. Subendothelial lipoprotein retention as the initiating process in atherosclerosis: update and therapeutic implications. *Circulation* **116**, 1832–1844 (2007).
37. Alique, M., Luna, C., Carracedo, J. & Ramírez, R. LDL biochemical modifications: a link between atherosclerosis and aging. *Food Nutr Res* **59**, (2015).
38. Moore, K. J. & Tabas, I. The Cellular Biology of Macrophages in Atherosclerosis. *Cell* **145**, 341 (2011).
39. Moore, K. J., Sheedy, F. J. & Fisher, E. A. Macrophages in atherosclerosis: a dynamic balance. *Nature Reviews Immunology 2013 13:10* **13**, 709–721 (2013).
40. Shapouri-Moghaddam, A. *et al.* Macrophage plasticity, polarization, and function in health and disease. *J Cell Physiol* **233**, 6425–6440 (2018).

41. Willemsen, L. & de Winther, M. P. J. Macrophage subsets in atherosclerosis as defined by single-cell technologies. *J Pathol* **250**, 705–714 (2020).
42. Goldstein, J. L., Ho, Y. K., Basu, S. K. & Brown, M. S. Binding site on macrophages that mediates uptake and degradation of acetylated low density lipoprotein, producing massive cholesterol deposition. *Proc Natl Acad Sci U S A* **76**, 333 (1979).
43. Kunjathoor, V. V. *et al.* Scavenger receptors class A-I/II and CD36 are the principal receptors responsible for the uptake of modified low density lipoprotein leading to lipid loading in macrophages. *J Biol Chem* **277**, 49982–49988 (2002).
44. Williams, J. W. *et al.* Limited proliferation capacity of aortic intima resident macrophages requires monocyte recruitment for atherosclerotic plaque progression. *Nat Immunol* **21**, 1194–1204 (2020).
45. Wilson, H. M. Macrophages heterogeneity in atherosclerosis – implications for therapy. *J Cell Mol Med* **14**, 2055–2065 (2010).
46. Björkegren, J. L. M. *et al.* Plasma Cholesterol-Induced Lesion Networks Activated before Regression of Early, Mature, and Advanced Atherosclerosis. *PLoS Genet* **10**, e1004201 (2014).
47. Libby, P. *et al.* Atherosclerosis. *Nature Reviews Disease Primers 2019 5:1* **5**, 1–18 (2019).
48. Allahverdian, S., Chaabane, C., Boukais, K., Francis, G. A. & Bochaton-Piallat, M. L. Smooth muscle cell fate and plasticity in atherosclerosis. *Cardiovasc Res* **114**, 540 (2018).
49. Owens, G. K., Kumar, M. S. & Wamhoff, B. R. Molecular regulation of vascular smooth muscle cell differentiation in development and disease. *Physiol Rev* **84**, 767–801 (2004).
50. Rensen, S. S. M., Doevendans, P. A. F. M. & van Eys, G. J. J. M. Regulation and characteristics of vascular smooth muscle cell phenotypic diversity. *Neth Heart J* **15**, 100–8 (2007).
51. Gomez, D. & Owens, G. K. Smooth muscle cell phenotypic switching in atherosclerosis. *Cardiovasc Res* **95**, 156–164 (2012).
52. Doran, A. C., Meller, N. & McNamara, C. A. Role of Smooth Muscle Cells in the Initiation and Early Progression of Atherosclerosis. *Arterioscler Thromb Vasc Biol* **28**, 812–819 (2008).
53. Bentzon, J. F., Otsuka, F., Virmani, R. & Falk, E. Mechanisms of Plaque Formation and Rupture. *Circ Res* **114**, 1852–1866 (2014).
54. Rong, J. X., Shapiro, M., Trogan, E. & Fisher, E. A. Transdifferentiation of mouse aortic smooth muscle cells to a macrophage-like state after cholesterol loading. *Proceedings of the National Academy of Sciences* **100**, 13531–13536 (2003).
55. Li, H., Freeman, M. W. & Libby, P. Regulation of smooth muscle cell scavenger receptor expression in vivo by atherogenic diets and in vitro by cytokines. *J Clin Invest* **95**, 122–133 (1995).
56. Shankman, L. S. *et al.* KLF4-dependent phenotypic modulation of smooth muscle cells has a key role in atherosclerotic plaque pathogenesis. *Nat Med* **21**, 628–637 (2015).
57. Wang, Y. *et al.* Smooth Muscle Cells Contribute the Majority of Foam Cells in ApoE (Apolipoprotein E)-Deficient Mouse Atherosclerosis. *Arterioscler Thromb Vasc Biol* **39**, 876–887 (2019).
58. Doran, A. C., Yurdagul, A. & Tabas, I. Efferocytosis in health and disease. *Nature Reviews Immunology 2019 20:4* **20**, 254–267 (2019).
59. Björkegren, J. L. M. & Lusis, A. J. Atherosclerosis: Recent developments. *Cell* **185**, 1630–1645 (2022).
60. Schrijvers, D. M., De Meyer, G. R. Y., Herman, A. G. & Martinet, W. Phagocytosis in atherosclerosis: Molecular mechanisms and implications for plaque progression and stability. *Cardiovasc Res* **73**, 470–480 (2007).
61. Tabas, I. Consequences and therapeutic implications of macrophage apoptosis in atherosclerosis: the importance of lesion stage and phagocytic efficiency. *Arterioscler Thromb Vasc Biol* **25**, 2255–2264 (2005).

62. Geng, Y. J. & Libby, P. Evidence for apoptosis in advanced human atheroma. Colocalization with interleukin-1 beta-converting enzyme. *Am J Pathol* **147**, 251 (1995).
63. Weber, C. & Noels, H. Atherosclerosis: current pathogenesis and therapeutic options. *Nature Medicine 2011 17:11* **17**, 1410–1422 (2011).
64. Hansson, G. K., Hellstrand, M., Rymo, L., Rubbia, L. & Gabbiani, G. Interferon gamma inhibits both proliferation and expression of differentiation-specific alpha-smooth muscle actin in arterial smooth muscle cells. *J Exp Med* **170**, 1595–1608 (1989).
65. Moore, K. J. & Tabas, I. Macrophages in the pathogenesis of atherosclerosis. *Cell* **145**, 341–355 (2011).
66. Soehnlein, O. Multiple Roles for Neutrophils in Atherosclerosis. *Circ Res* **110**, 875–888 (2012).
67. Willems, S. *et al*. Mast cells in human carotid atherosclerotic plaques are associated with intraplaque microvessel density and the occurrence of future cardiovascular events. *Eur Heart J* **34**, 3699–3706 (2013).
68. Johnson, J. L., Jackson, C. L., Angelini, G. D. & George, S. J. Activation of Matrix-Degrading Metalloproteinases by Mast Cell Proteases in Atherosclerotic Plaques. *Arterioscler Thromb Vasc Biol* **18**, 1707–1715 (1998).
69. Partida, R. A., Libby, P., Crea, F. & Jang, I. K. Plaque erosion: a new in vivo diagnosis and a potential major shift in the management of patients with acute coronary syndromes. *Eur Heart J* **39**, 2070–2076 (2018).
70. Libby, P. & Pasterkamp, G. Requiem for the 'vulnerable plaque'. *Eur Heart J* **36**, 2984–2987 (2015).
71. Moses, S. R., Adorno, J. J., Palmer, A. F. & Song, J. W. Vessel-on-a-chip models for studying microvascular physiology, transport, and function in vitro. *Am J Physiol Cell Physiol* **320**, C92–C105 (2021).
72. Daugherty, A. *et al*. Recommendation on Design, Execution, and Reporting of Animal Atherosclerosis Studies: A Scientific Statement From the American Heart Association. *Circ Res* **121**, e53–e79 (2017).
73. Getz, G. S. & Reardon, C. A. Diet and Murine Atherosclerosis. *Arterioscler Thromb Vasc Biol* **26**, 242–249 (2006).
74. Paigen, B., Morrow, A., Brandon, C., Mitchell, D. & Holmes, P. Variation in susceptibility to atherosclerosis among inbred strains of mice. *Atherosclerosis* **57**, 65–73 (1985).
75. Van Eck, M. *et al*. Essential role for the (hepatic) LDL receptor in macrophage apolipoprotein E-induced reduction in serum cholesterol levels and atherosclerosis. *Atherosclerosis* **154**, 103–112 (2001).
76. Meir, K. S. & Leitersdorf, E. Atherosclerosis in the Apolipoprotein E–Deficient Mouse. *Arterioscler Thromb Vasc Biol* **24**, 1006–1014 (2004).
77. Zhang, S. H., Reddick, R. L., Piedrahita, J. A. & Maeda, N. Spontaneous Hypercholesterolemia and Arterial Lesions in Mice Lacking Apolipoprotein E. *Science (1979)* **258**, 468–471 (1992).
78. Getz, G. S. & Reardon, C. A. Animal Models of Atherosclerosis. *Arterioscler Thromb Vasc Biol* **32**, 1104–1115 (2012).
79. Emini Veseli, B. *et al*. Animal models of atherosclerosis. *Eur J Pharmacol* **816**, 3–13 (2017).
80. Smit, V. *et al*. Single-cell profiling reveals age-associated immunity in atherosclerosis. *Cardiovasc Res* (2023) doi:10.1093/CVR/CVAD099.
81. Roche-Molina, M. *et al*. Induction of sustained hypercholesterolemia by single adeno-associated virus-mediated gene transfer of mutant hPCSK9. *Arterioscler Thromb Vasc Biol* **35**, 50–59 (2015).

82. Bjørklund, M. M. *et al.* Induction of atherosclerosis in mice and hamsters without germline genetic engineering. *Circ Res* **114**, 1684–1689 (2014).
83. Punch, E., Klein, J., Diaba-Nuhoho, P., Morawietz, H. & Garelnabi, M. Effects of PCSK9 Targeting: Alleviating Oxidation, Inflammation, and Atherosclerosis. *J Am Heart Assoc* **11**, 23328 (2022).
84. Medzhitov, R. Origin and physiological roles of inflammation. *Nature 2008 454:7203* **454**, 428–435 (2008).
85. Vivier, E. & Malissen, B. Innate and adaptive immunity: specificities and signaling hierarchies revisited. *Nature Immunology 2005 6:1* **6**, 17–21 (2004).
86. Li, D. & Wu, M. Pattern recognition receptors in health and diseases. *Signal Transduction and Targeted Therapy 2021 6:1* **6**, 1–24 (2021).
87. Bianchi, M. E. DAMPs, PAMPs and alarmins: all we need to know about danger. *J Leukoc Biol* **81**, 1–5 (2007).
88. Netea, M. G., Schlitzer, A., Placek, K., Joosten, L. A. B. & Schultze, J. L. Innate and Adaptive Immune Memory: an Evolutionary Continuum in the Host's Response to Pathogens. *Cell Host Microbe* **25**, 13–26 (2019).
89. Silvestre-Roig, C., Braster, Q., Ortega-Gomez, A. & Soehnlein, O. Neutrophils as regulators of cardiovascular inflammation. *Nature Reviews Cardiology 2020 17:6* **17**, 327–340 (2020).
90. Palano, M. T. *et al.* When a Friend Becomes Your Enemy: Natural Killer Cells in Atherosclerosis and Atherosclerosis-Associated Risk Factors. *Front Immunol* **12**, 5718 (2022).
91. Engelbertsen, D. & Lichtman, A. H. Innate lymphoid cells in atherosclerosis. *Eur J Pharmacol* **816**, 32–36 (2017).
92. Ginhoux, F. & Jung, S. Monocytes and macrophages: developmental pathways and tissue homeostasis. *Nature Reviews Immunology 2014 14:6* **14**, 392–404 (2014).
93. Ingersoll, M. A. *et al.* Comparison of gene expression profiles between human and mouse monocyte subsets. *Blood* **115**, (2010).
94. Auffray, C. *et al.* Monitoring of blood vessels and tissues by a population of monocytes with patrolling behavior. *Science* **317**, 666–670 (2007).
95. Carlin, L. M. *et al.* Nr4a1-dependent Ly6C(low) monocytes monitor endothelial cells and orchestrate their disposal. *Cell* **153**, 362–375 (2013).
96. Geissmann, F., Jung, S. & Littman, D. R. Blood monocytes consist of two principal subsets with distinct migratory properties. *Immunity* **19**, 71–82 (2003).
97. Buscher, K., Marcovecchio, P., Hedrick, C. C. & Ley, K. Patrolling Mechanics of Non-Classical Monocytes in Vascular Inflammation. *Front Cardiovasc Med* **4**, 80 (2017).
98. Swirski, F. K. *et al.* Monocyte accumulation in mouse atherogenesis is progressive and proportional to extent of disease. *Proc Natl Acad Sci U S A* **103**, 10340–10345 (2006).
99. Swirski, F. K. *et al.* Ly-6Chi monocytes dominate hypercholesterolemia-associated monocytosis and give rise to macrophages in atheromata. *J Clin Invest* **117**, 195–205 (2007).
100. C. Dawson, T., A. Kuziel, W., A. Osahar, T. & Maeda, N. Absence of CC chemokine receptor-2 reduces atherosclerosis in apolipoprotein E-deficient mice. *Atherosclerosis* **143**, 205–211 (1999).
101. Chen, Y. J. *et al.* Eps8 protein facilitates phagocytosis by increasing TLR4-MyD88 protein interaction in lipopolysaccharide-stimulated macrophages. *J Biol Chem* **287**, 18806–18819 (2012).
102. Shapouri-Moghaddam, A. *et al.* Macrophage plasticity, polarization, and function in health and disease. *J Cell Physiol* **233**, 6425–6440 (2018).
103. Geng, H. *et al.* The effects of ox-LDL in human atherosclerosis may be mediated in part via the toll-like receptor 4 pathway. *Mol Cell Biochem* **342**, 201–206 (2010).

104. Sica, A., Erreni, M., Allavena, P. & Porta, C. Macrophage polarization in pathology. *Cell Mol Life Sci* **72**, 4111–4126 (2015).
105. Wang, N., Liang, H. & Zen, K. Molecular mechanisms that influence the macrophage m1-m2 polarization balance. *Front Immunol* **5**, (2014).
106. Jetten, N. *et al.* Anti-inflammatory M2, but not pro-inflammatory M1 macrophages promote angiogenesis in vivo. *Angiogenesis* **17**, 109–118 (2014).
107. Braga, T. T., Agudelo, J. S. H. & Camara, N. O. S. Macrophages During the Fibrotic Process: M2 as Friend and Foe. *Front Immunol* **6**, (2015).
108. Moore, K. J., Sheedy, F. J. & Fisher, E. A. Macrophages in atherosclerosis: a dynamic balance. *Nature Reviews Immunology 2013 13:10* **13**, 709–721 (2013).
109. Roy, P., Orecchioni, M. & Ley, K. How the immune system shapes atherosclerosis: roles of innate and adaptive immunity. *Nature Reviews Immunology 2021 22:4* **22**, 251–265 (2021).
110. Zernecke, A. *et al.* Meta-Analysis of Leukocyte Diversity in Atherosclerotic Mouse Aortas. *Circ Res* **127**, 402–426 (2020).
111. King, K. R. *et al.* IRF3 and type I interferons fuel a fatal response to myocardial infarction. *Nat Med* **23**, 1481–1487 (2017).
112. Cochain, C. *et al.* Single-Cell RNA-Seq Reveals the Transcriptional Landscape and Heterogeneity of Aortic Macrophages in Murine Atherosclerosis. *Circ Res* **122**, 1661–1674 (2018).
113. Kim, K. *et al.* Transcriptome Analysis Reveals Nonfoamy Rather Than Foamy Plaque Macrophages Are Proinflammatory in Atherosclerotic Murine Models. *Circ Res* **123**, 1127–1142 (2018).
114. Ensan, S. *et al.* Self-renewing resident arterial macrophages arise from embryonic CX3CR1(+) precursors and circulating monocytes immediately after birth. *Nat Immunol* **17**, 159–168 (2016).
115. Lim, H. Y. *et al.* Hyaluronan Receptor LYVE-1-Expressing Macrophages Maintain Arterial Tone through Hyaluronan-Mediated Regulation of Smooth Muscle Cell Collagen. *Immunity* **49**, 326-341. e7 (2018).
116. Williams, J. W. *et al.* Limited proliferation capacity of aortic intima resident macrophages requires monocyte recruitment for atherosclerotic plaque progression. *Nature Immunology 2020 21:10* **21**, 1194–1204 (2020).
117. de Winther, M. P. J. *et al.* Translational opportunities of single-cell biology in atherosclerosis. *Eur Heart J* **44**, 1216–1230 (2023).
118. Depuydt, M. A. C. *et al.* Microanatomy of the Human Atherosclerotic Plaque by Single-Cell Transcriptomics. *Circ Res* **127**, 1437–1455 (2020).
119. Fernandez, D. M. *et al.* Single-cell immune landscape of human atherosclerotic plaques. *Natuere Medicine* **25**, 1576–1588 (2019).
120. Ramachandran, P. *et al. Resolving the fibrotic niche of human liver cirrhosis at single-cell level*. *Nature* vol. 575 (Springer US, 2019).
121. Subramanian, M. & Tabas, I. Dendritic cells in atherosclerosis. *Semin Immunopathol* **36**, 93–102 (2014).
122. Subramanian, M. & Tabas, I. Dendritic cells in atherosclerosis. *Semin Immunopathol* **36**, 93–102 (2014).
123. Satpathy, A. T. *et al.* Zbtb46 expression distinguishes classical dendritic cells and their committed progenitors from other immune lineages. *Journal of Experimental Medicine* **209**, 1135–1152 (2012).
124. Zernecke, A. Dendritic Cells in Atherosclerosis. *Arterioscler Thromb Vasc Biol* **35**, 763–770 (2015).
125. Tamoutounour, S. *et al.* Origins and Functional Specialization of Macrophages and of Conventional and Monocyte-Derived Dendritic Cells in Mouse Skin. *Immunity* **39**, 925–938 (2013).

126. Varol, C. *et al.* Intestinal Lamina Propria Dendritic Cell Subsets Have Different Origin and Functions. *Immunity* **31**, 502–512 (2009).
127. Guilliams, M. *et al.* Dendritic cells, monocytes and macrophages: a unified nomenclature based on ontogeny. *Nature Reviews Immunology 2014 14:8* **14**, 571–578 (2014).
128. Gil-Pulido, J. & Zernecke, A. Antigen-presenting dendritic cells in atherosclerosis. *Eur J Pharmacol* **816**, 25–31 (2017).
129. Hildner, K. *et al.* Batf3 deficiency reveals a critical role for CD8alpha+ dendritic cells in cytotoxic T cell immunity. *Science* **322**, 1097–1100 (2008).
130. Tamura, T. *et al.* IFN regulatory factor-4 and -8 govern dendritic cell subset development and their functional diversity. *J Immunol* **174**, 2573–2581 (2005).
131. Liu, J., Zhang, X., Cheng, Y. & Cao, X. Dendritic cell migration in inflammation and immunity. *Cellular & Molecular Immunology 2021 18:11* **18**, 2461–2471 (2021).
132. Guermonprez, P., Valladeau, J., Zitvogel, L., Théry, C. & Amigorena, S. Antigen Presentation and T Cell Stimulation by Dendritic Cells. *https://doi.org/10.1146/annurev.immunol.20.100301.064828* **20**, 621–667 (2003).
133. Bobryshev, Y. V. Dendritic cells in atherosclerosis: current status of the problem and clinical relevance. *Eur Heart J* **26**, 1700–1704 (2005).
134. Banchereau, J. & Steinman, R. M. Dendritic cells and the control of immunity. *Nature 1998 392:6673* **392**, 245–252 (1998).
135. Kambayashi, T. & Laufer, T. M. Atypical MHC class II-expressing antigen-presenting cells: can anything replace a dendritic cell? *Nature Reviews Immunology 2014 14:11* **14**, 719–730 (2014).
136. Ait-Oufella, H., Sage, A. P., Mallat, Z. & Tedgui, A. Adaptive (T and B Cells) Immunity and Control by Dendritic Cells in Atherosclerosis. *Circ Res* **114**, 1640–1660 (2014).
137. Yilmaz, A. *et al.* Emergence of dendritic cells in rupture-prone regions of vulnerable carotid plaques. *Atherosclerosis* **176**, 101–110 (2004).
138. Erbel, C. *et al.* Functional profile of activated dendritic cells in unstable atherosclerotic plaque. *Basic Res Cardiol* **102**, 123–132 (2007).
139. Mohanta, S. K. *et al.* Artery Tertiary Lymphoid Organs Contribute to Innate and Adaptive Immune Responses in Advanced Mouse Atherosclerosis. *Circ Res* **114**, 1772–1787 (2014).
140. Yin, C., Mohanta, S. K., Srikakulapu, P., Weber, C. & Habenicht, A. J. R. Artery tertiary lymphoid organs: Powerhouses of atherosclerosis immunity. *Front Immunol* **7**, 217268 (2016).
141. Zhao, Y., Zhang, J., Zhang, W. & Xu, Y. A myriad of roles of dendritic cells in atherosclerosis. *Clin Exp Immunol* **206**, 12–27 (2021).
142. Paulson, K. E. *et al.* Resident Intimal Dendritic Cells Accumulate Lipid and Contribute to the Initiation of Atherosclerosis. *Circ Res* **106**, 383–390 (2010).
143. Gautier, E. L. *et al.* Conventional Dendritic Cells at the Crossroads Between Immunity and Cholesterol Homeostasis in Atherosclerosis. *Circulation* **119**, 2367–2375 (2009).
144. Habets, K. L. L. *et al.* Vaccination using oxidized low-density lipoprotein-pulsed dendritic cells reduces atherosclerosis in LDL receptor-deficient mice. *Cardiovasc Res* **85**, 622–630 (2010).
145. Hermansson, A. *et al.* Immunotherapy With Tolerogenic Apolipoprotein B-100–Loaded Dendritic Cells Attenuates Atherosclerosis in Hypercholesterolemic Mice. *Circulation* **123**, 1083–1091 (2011).
146. Vigario, F. L., Kuiper, J. & Slütter, B. Tolerogenic vaccines for the treatment of cardiovascular diseases. *EBioMedicine* **57**, 102827 (2020).
147. Jansen, M. A. A. *et al.* Targeting of tolerogenic dendritic cells towards heat-shock proteins: a novel therapeutic strategy for autoimmune diseases? *Immunology* **153**, 51 (2018).

148. Galli, S. J., Gaudenzio, N. & Tsai, M. Mast Cells in Inflammation and Disease: Recent Progress and Ongoing Concerns. *https://doi.org/10.1146/annurev-immunol-071719-094903* **38**, 49–77 (2020).
149. St. John, A. L., Rathore, A. P. S. & Ginhoux, F. New perspectives on the origins and heterogeneity of mast cells. *Nature Reviews Immunology 2022 23:1* **23**, 55–68 (2022).
150. Dahlin, J. S. & Hallgren, J. Mast cell progenitors: Origin, development and migration to tissues. *Mol Immunol* **63**, 9–17 (2015).
151. Dahlin, J. S. *et al.* Lin− CD34hi CD117int/hi FcεRI+ cells in human blood constitute a rare population of mast cell progenitors. *Blood* **127**, 383–391 (2016).
152. El-Agamy, D. S. Targeting c-kit in the therapy of mast cell disorders: Current update. *Eur J Pharmacol* **690**, 1–3 (2012).
153. Krystel-Whittemore, M., Dileepan, K. N. & Wood, J. G. Mast cell: A multi-functional master cell. *Front Immunol* **6**, 165675 (2016).
154. Galli, S. J., Borregaard, N. & Wynn, T. A. Phenotypic and functional plasticity of cells of innate immunity: macrophages, mast cells and neutrophils. *Nature Immunology 2011 12:11* **12**, 1035–1044 (2011).
155. Nagata, Y. & Suzuki, R. FcεRI: A Master Regulator of Mast Cell Functions. *Cells* **11**, 622 (2022).
156. Sibilano, R., Frossi, B. & Pucillo, C. E. Mast cell activation: A complex interplay of positive and negative signaling pathways. *Eur J Immunol* **44**, 2558–2566 (2014).
157. Kalesnikoff, J. & Galli, S. J. New developments in mast cell biology. *Nature Immunology 2008 9:11* **9**, 1215–1223 (2008).
158. Shi, G. P., Bot, I. & Kovanen, P. T. Mast cells in human and experimental cardiometabolic diseases. *Nat Rev Cardiol* **12**, 643–658 (2015).
159. Dimitriadou, V. *et al.* Expression of functional major histocompatility complex class II molecules on HMC-1 human mast cells. *J Leukoc Biol* **64**, 791–799 (1998).
160. Poncet, P., Arock, M. & David, B. MHC class II-dependent activation of CD4+ T cell hybridomas by human mast cells through superantigen presentation. *J Leukoc Biol* **66**, 105–112 (1999).
161. Kaartinen, M., Penttilä, A. & Kovanen, P. T. Accumulation of activated mast cells in the shoulder region of human coronary atheroma, the predilection site of atheromatous rupture. *Circulation* **90**, 1669–1678 (1994).
162. Atkinson, J. B., Harlan, C. W., Harlan, G. C. & Virmani, R. The association of mast cells and atherosclerosis: a morphologic study of early atherosclerotic lesions in young people. *Hum Pathol* **25**, 154–159 (1994).
163. Kovanen, P. T., Kaartinen, M. & Paavonen, T. Infiltrates of activated mast cells at the site of coronary atheromatous erosion or rupture in myocardial infarction. *Circulation* **92**, 1084–1088 (1995).
164. Bot, I. *et al.* Perivascular mast cells promote atherogenesis and induce plaque destabilization in apolipoprotein E-deficient mice. *Circulation* **115**, 2516–2525 (2007).
165. Sun, J. *et al.* Mast cells promote atherosclerosis by releasing proinflammatory cytokines. *Nat Med* **13**, 719–724 (2007).
166. Leskinen, M. J., Lindstedt, K. A., Wang, Y. & Kovanen, P. T. Mast cell chymase induces smooth muscle cell apoptosis by a mechanism involving fibronectin degradation and disruption of focal adhesions. *Arterioscler Thromb Vasc Biol* **23**, 238–243 (2003).
167. Leskinen, M. J. *et al.* Mast cell chymase induces smooth muscle cell apoptosis by disrupting NF-kappaB-mediated survival signaling. *Exp Cell Res* **312**, 1289–1298 (2006).

168. Mäyränpää, M. I., Heikkilä, H. M., Lindstedt, K. A., Walls, A. F. & Kovanen, P. T. Desquamation of human coronary artery endothelium by human mast cell proteases: implications for plaque erosion. *Coron Artery Dis* **17**, 611–621 (2006).
169. Heikkilä, H. M. *et al.* Activated mast cells induce endothelial cell apoptosis by a combined action of chymase and tumor necrosis factor-alpha. *Arterioscler Thromb Vasc Biol* **28**, 309–314 (2008).
170. Johnson, J. L., Jackson, C. L., Angelini, G. D. & George, S. J. Activation of Matrix-Degrading Metalloproteinases by Mast Cell Proteases in Atherosclerotic Plaques. *Arterioscler Thromb Vasc Biol* **18**, 1707–1715 (1998).
171. Bot, I. *et al.* Mast cell chymase inhibition reduces atherosclerotic plaque progression and improves plaque stability in ApoE-/- mice. *Cardiovasc Res* **89**, 244–252 (2011).
172. Kokkonen, J. O. & Kovanen, P. T. Low-density-lipoprotein binding by mast-cell granules. Demonstration of binding of apolipoprotein B to heparin proteoglycan of exocytosed granules. *Biochem J* **241**, 583–589 (1987).
173. Kokkonen, J. O. & Kovanen, P. T. Stimulation of mast cells leads to cholesterol accumulation in macrophages in vitro by a mast cell granule-mediated uptake of low density lipoprotein. *Proc Natl Acad Sci U S A* **84**, 2287–2291 (1987).
174. Kokkonen, J. O. Stimulation of rat peritoneal mast cells enhances uptake of low density lipoproteins by rat peritoneal macrophages in vivo. *Atherosclerosis* **79**, 213–223 (1989).
175. Kaartinen, M., Penttilä, A. & Kovanen, P. T. Extracellular mast cell granules carry apolipoprotein B-100-containing lipoproteins into phagocytes in human arterial intima. Functional coupling of exocytosis and phagodytosis in neighboring cells. *Arterioscler Thromb Vasc Biol* **15**, 2047–2054 (1995).
176. Bot, I., Shi, G. P. & Kovanen, P. T. Mast cells as effectors in atherosclerosis. *Arterioscler Thromb Vasc Biol* **35**, 265 (2015).
177. Gisterå, A. & Hansson, G. K. The immunology of atherosclerosis. *Nature Reviews Nephrology 2017 13:6* **13**, 368–380 (2017).
178. Saigusa, R., Winkels, H. & Ley, K. T cell subsets and functions in atherosclerosis. *Nat Rev Cardiol* **17**, 387 (2020).
179. Douna, H. & Kuiper, J. Novel B-cell subsets in atherosclerosis. *Curr Opin Lipidol* **27**, 493–498 (2016).
180. Sage, A. P., Tsiantoulas, D., Binder, C. J. & Mallat, Z. The role of B cells in atherosclerosis. *Nature Reviews Cardiology 2018 16:3* **16**, 180–196 (2018).
181. Mallat, Z. & Binder, C. J. The why and how of adaptive immune responses in ischemic cardiovascular disease. *Nature Cardiovascular Research 2022 1:5* **1**, 431–444 (2022).
182. Anderson, G. & Jenkinson, E. J. Lymphostromal interactions in thymic development and function. *Nature Reviews Immunology 2001 1:1* **1**, 31–40 (2001).
183. Kumar, B. V, Connors, T. J. & Farber, D. L. Human T Cell Development, Localization, and Function throughout Life. (2018) doi:10.1016/j.immuni.2018.01.007.
184. Bassing, C. H., Swat, W. & Alt, F. W. The Mechanism and Regulation of Chromosomal V(D)J Recombination. *Cell* **109**, S45–S55 (2002).
185. Moran, A. E. & Hogquist, K. A. T-cell receptor affinity in thymic development. *Immunology* **135**, 261–267 (2012).
186. Hogquist, K. A. Signal strength in thymic selection and lineage commitment. *Curr Opin Immunol* **13**, 225–231 (2001).
187. Lutes, L. K. *et al.* T cell self-reactivity during thymic development dictates the timing of positive selection. *Elife* **10**, (2021).

188. Hansson, G. K. & Hermansson, A. The immune system in atherosclerosis. *Nat Immunol* **12**, 204–212 (2011).
189. Marshall, J. S., Warrington, R., Watson, W. & Kim, H. L. An introduction to immunology and immunopathology. *Allergy, Asthma and Clinical Immunology* **14**, 1–10 (2018).
190. Song, L., Leung, C. & Schindler, C. Lymphocytes are important in early atherosclerosis. *J Clin Invest* **108**, 251–259 (2001).
191. Zhou, X., Nicoletti, A., Elhage, R. & Hansson, G. K. Transfer of CD4(+) T cells aggravates atherosclerosis in immunodeficient apolipoprotein E knockout mice. *Circulation* **102**, 2919–2922 (2000).
192. van Dijk, R. A. *et al.* A change in inflammatory footprint precedes plaque instability: a systematic evaluation of cellular aspects of the adaptive immune response in human atherosclerosis. *J Am Heart Assoc* **4**, (2015).
193. Zhang, W. *et al.* IL-9 aggravates the development of atherosclerosis in ApoE-/- mice. *Cardiovasc Res* **106**, 453–464 (2015).
194. Lin, Y. Z. *et al.* Circulating Th22 and Th9 levels in patients with acute coronary syndrome. *Mediators Inflamm* **2013**, (2013).
195. Zhang, L. *et al.* Elevated frequencies of circulating Th22 cell in addition to Th17 cell and Th17/Th1 cell in patients with acute coronary syndrome. *PLoS One* **8**, (2013).
196. Nus, M. *et al.* Marginal zone B cells control the response of follicular helper T cells to a high-cholesterol diet. *Nat Med* **23**, 601–610 (2017).
197. Ryu, H. *et al.* Atherogenic dyslipidemia promotes autoimmune follicular helper T cell responses via IL-27. *Nat Immunol* **19**, 583–593 (2018).
198. Douna, H. *et al.* IFNγ-Stimulated B Cells Inhibit T Follicular Helper Cells and Protect Against Atherosclerosis. *Front Cardiovasc Med* **9**, 781436 (2022).
199. Liuzzo, G. *et al.* Unusual CD4+CD28null T Lymphocytes and Recurrence of Acute Coronary Events. *J Am Coll Cardiol* **50**, 1450–1458 (2007).
200. Tomas, L. *et al.* Low Levels of CD4+CD28null T Cells at Baseline Are Associated With First-Time Coronary Events in a Prospective Population-Based Case-Control Cohort. *Arterioscler Thromb Vasc Biol* **40**, 426–436 (2020).
201. Buono, C. *et al.* T-bet deficiency reduces atherosclerosis and alters plaque antigen-specific immune responses. *Proc Natl Acad Sci U S A* **102**, 1596–1601 (2005).
202. Buono, C. *et al.* Influence of interferon-gamma on the extent and phenotype of diet-induced atherosclerosis in the LDLR-deficient mouse. *Arterioscler Thromb Vasc Biol* **23**, 454–460 (2003).
203. Gupta, S. *et al.* IFN-gamma potentiates atherosclerosis in ApoE knock-out mice. *J Clin Invest* **99**, 2752–2761 (1997).
204. Whitman, S. C., Ravisankar, P., Elam, H. & Daugherty, A. Exogenous Interferon-γ Enhances Atherosclerosis in Apolipoprotein E−/− Mice. *Am J Pathol* **157**, 1819–1824 (2000).
205. Hansson, G. K., Hellstrand, M., Rymo, L., Rubbia, L. & Gabbiani, G. Interferon gamma inhibits both proliferation and expression of differentiation-specific alpha-smooth muscle actin in arterial smooth muscle cells. *J Exp Med* **170**, 1595–1608 (1989).
206. Yu, X. H., Zhang, J., Zheng, X. L., Yang, Y. H. & Tang, C. K. Interferon-γ in foam cell formation and progression of atherosclerosis. *Clin Chim Acta* **441**, 33–43 (2015).
207. Orecchioni, M., Ghosheh, Y., Pramod, A. B. & Ley, K. Macrophage Polarization: Different Gene Signatures in M1(LPS+) vs. Classically and M2(LPS-) vs. Alternatively Activated Macrophages. *Front Immunol* **10**, (2019).

208. Walker, J. A. & McKenzie, A. N. J. TH2 cell development and function. *Nature Reviews Immunology 2017 18:2* **18**, 121–133 (2017).
209. Sun, L., Su, Y., Jiao, A., Wang, X. & Zhang, B. T cells in health and disease. *Signal Transduction and Targeted Therapy 2023 8:1* **8**, 1–50 (2023).
210. Wurtz, O., Bajénoff, M. & Guerder, S. IL-4-mediated inhibition of IFN-gamma production by CD4+ T cells proceeds by several developmentally regulated mechanisms. *Int Immunol* **16**, 501–508 (2004).
211. King, V. L., Szilvassy, S. J. & Daugherty, A. Interleukin-4 deficiency decreases atherosclerotic lesion formation in a site-specific manner in female LDL receptor-/- mice. *Arterioscler Thromb Vasc Biol* **22**, 456–461 (2002).
212. Davenport, P. & Tipping, P. G. The Role of Interleukin-4 and Interleukin-12 in the Progression of Atherosclerosis in Apolipoprotein E-Deficient Mice. *Am J Pathol* **163**, 1117 (2003).
213. Engelbertsen, D. *et al*. Induction of T helper 2 responses against human apolipoprotein B100 does not affect atherosclerosis in ApoE-/- mice. *Cardiovasc Res* **103**, 304–312 (2014).
214. Engelbertsen, D. *et al*. T-helper 2 immunity is associated with reduced risk of myocardial infarction and stroke. *Arterioscler Thromb Vasc Biol* **33**, 637–644 (2013).
215. Silveira, A. *et al*. Plasma IL-5 concentration and subclinical carotid atherosclerosis. *Atherosclerosis* **239**, 125–130 (2015).
216. Binder, C. J. *et al*. IL-5 links adaptive and natural immunity specific for epitopes of oxidized LDL and protects from atherosclerosis. *J Clin Invest* **114**, 427–437 (2004).
217. Cardilo-Reis, L. *et al*. Interleukin-13 protects from atherosclerosis and modulates plaque composition by skewing the macrophage phenotype. *EMBO Mol Med* **4**, 1072–1086 (2012).
218. Peters, A., Lee, Y. & Kuchroo, V. K. The many faces of Th17 cells. *Curr Opin Immunol* **23**, 702–706 (2011).
219. Usui, F. *et al*. Interleukin-17 deficiency reduced vascular inflammation and development of atherosclerosis in Western diet-induced apoE-deficient mice. *Biochem Biophys Res Commun* **420**, 72–77 (2012).
220. Danzaki, K. *et al*. Interleukin-17A deficiency accelerates unstable atherosclerotic plaque formation in apolipoprotein E-deficient mice. *Arterioscler Thromb Vasc Biol* **32**, 273–280 (2012).
221. Madhur, M. S. *et al*. Role of interleukin 17 in inflammation, atherosclerosis, and vascular function in apolipoprotein e-deficient mice. *Arterioscler Thromb Vasc Biol* **31**, 1565–1572 (2011).
222. Gao, Q. *et al*. A critical function of Th17 proinflammatory cells in the development of atherosclerotic plaque in mice. *J Immunol* **185**, 5820–5827 (2010).
223. Erbel, C. *et al*. Inhibition of IL-17A attenuates atherosclerotic lesion development in apoE-deficient mice. *J Immunol* **183**, 8167–8175 (2009).
224. Smith, E. *et al*. Blockade of interleukin-17A results in reduced atherosclerosis in apolipoprotein E-deficient mice. *Circulation* **121**, 1746–1755 (2010).
225. Engelbertsen, D. *et al*. IL-23R deficiency does not impact atherosclerotic plaque development in mice. *J Am Heart Assoc* **7**, (2018).
226. Cheng, X. *et al*. The Th17/Treg imbalance in patients with acute coronary syndrome. *Clin Immunol* **127**, 89–97 (2008).
227. Hashmi, S. & Zeng, Q. T. Role of interleukin-17 and interleukin-17-induced cytokines interleukin-6 and interleukin-8 in unstable coronary artery disease. *Coron Artery Dis* **17**, 699–706 (2006).
228. Gisterå, A. *et al*. Transforming growth factor-β signaling in T cells promotes stabilization of atherosclerotic plaques through an interleukin-17-dependent pathway. *Sci Transl Med* **5**, (2013).

229. Taleb, S. *et al.* Loss of SOCS3 expression in T cells reveals a regulatory role for interleukin-17 in atherosclerosis. *Journal of Experimental Medicine* **206**, 2067–2077 (2009).
230. Taleb, S., Tedgui, A. & Mallat, Z. IL-17 and Th17 cells in atherosclerosis: subtle and contextual roles. *Arterioscler Thromb Vasc Biol* **35**, 258–264 (2015).
231. Hirota, K. *et al.* Fate mapping of IL-17-producing T cells in inflammatory responses. *Nat Immunol* **12**, 255–263 (2011).
232. McGeachy, M. J. *et al.* TGF-β and IL-6 drive the production of IL-17 and IL-10 by T cells and restrain TH-17 cell–mediated pathology. *Nature Immunology 2007 8:12* **8**, 1390–1397 (2007).
233. Lee, Y. *et al.* Induction and molecular signature of pathogenic Th17 cells. *Nat Immunol* **13**, 991–999 (2012).
234. Vignali, D. A. A., Collison, L. W. & Workman, C. J. How regulatory T cells work. *Nature Reviews Immunology 2008 8:7* **8**, 523–532 (2008).
235. Fu, S. *et al.* TGF-beta induces Foxp3 + T-regulatory cells from CD4 + CD25 - precursors. *Am J Transplant* **4**, 1614–1627 (2004).
236. De Rosa, V. *et al.* Glycolysis controls the induction of human regulatory T cells by modulating the expression of FOXP3 exon 2 splicing variants. *Nat Immunol* **16**, 1174 (2015).
237. de Boer, O. J., van der Meer, J. J., Teeling, P., van der Loos, C. M. & van der Wal, A. C. Low Numbers of FOXP3 Positive Regulatory T Cells Are Present in all Developmental Stages of Human Atherosclerotic Lesions. *PLoS One* **2**, e779 (2007).
238. Ait-Oufella, H. *et al.* Natural regulatory T cells control the development of atherosclerosis in mice. *Nat Med* **12**, 178–180 (2006).
239. Klingenberg, R. *et al.* Depletion of FOXP3+ regulatory T cells promotes hypercholesterolemia and atherosclerosis. *J Clin Invest* **123**, 1323–1334 (2013).
240. Mor, A. *et al.* Role of naturally occurring CD4+ CD25+ regulatory T cells in experimental atherosclerosis. *Arterioscler Thromb Vasc Biol* **27**, 893–900 (2007).
241. Foks, A. C. *et al.* Differential effects of regulatory T cells on the initiation and regression of atherosclerosis. *Atherosclerosis* **218**, 53–60 (2011).
242. Kita, T. *et al.* Regression of atherosclerosis with anti-CD3 antibody via augmenting a regulatory T-cell response in mice. *Cardiovasc Res* **102**, 107–117 (2014).
243. van Es, T. *et al.* Vaccination against Foxp3(+) regulatory T cells aggravates atherosclerosis. *Atherosclerosis* **209**, 74–80 (2010).
244. Mallat, Z. *et al.* Protective role of interleukin-10 in atherosclerosis. *Circ Res* **85**, (1999).
245. Pinderski Oslund, L. J. *et al.* Interleukin-10 blocks atherosclerotic events in vitro and in vivo. *Arterioscler Thromb Vasc Biol* **19**, 2847–2853 (1999).
246. Caligiuri, G. *et al.* Interleukin-10 Deficiency Increases Atherosclerosis, Thrombosis, and Low-density Lipoproteins in Apolipoprotein E Knockout Mice. *Molecular Medicine* **9**, 10 (2003).
247. Wong, P. & Pamer, E. G. CD8 T cell responses to infectious pathogens. *Annu Rev Immunol* **21**, 29–70 (2003).
248. Mittrücker, H. W., Visekruna, A. & Huber, M. Heterogeneity in the Differentiation and Function of CD8+ T Cells. *Arch Immunol Ther Exp (Warsz)* **62**, 449–458 (2014).
249. Andersen, M. H., Schrama, D., Thor Straten, P. & Becker, J. C. Cytotoxic T Cells. *Journal of Investigative Dermatology* **126**, 32–41 (2006).
250. Van Duijn, J., Kuiper, J. & Slutter, B. The many faces of CD8+ T cells in atherosclerosis. *Curr Opin Lipidol* **29**, 411–416 (2018).
251. Kolbus, D. *et al.* TAP1-Deficiency Does Not Alter Atherosclerosis Development in Apoe −/− Mice. *PLoS One* **7**, (2012).

252. Elhage, R. *et al.* Deleting TCRαβ+ or CD4+ T Lymphocytes Leads to Opposite Effects on Site-Specific Atherosclerosis in Female Apolipoprotein E-Deficient Mice. *Am J Pathol* **165**, 2013 (2004).
253. Kolbus, D. *et al.* CD8+ T cell activation predominate early immune responses to hypercholesterolemia in Apoe-/- mice. *BMC Immunol* **11**, 58 (2010).
254. Kyaw, T. *et al.* Cytotoxic and proinflammatory CD8+ T lymphocytes promote development of vulnerable atherosclerotic plaques in apoE-deficient mice. *Circulation* **127**, 1028–1039 (2013).
255. Van Duijn, J. *et al.* CD8+ T-cells contribute to lesion stabilization in advanced atherosclerosis by limiting macrophage content and CD4+ T-cell responses. *Cardiovasc Res* **115**, 729–738 (2019).
256. Chyu, K. Y. *et al.* CD8+ T cells mediate the athero-protective effect of immunization with an ApoB-100 peptide. *PLoS One* **7**, (2012).
257. Van Duijn, J. *et al.* Tc17 CD8+ T cells accumulate in murine atherosclerotic lesions, but do not contribute to early atherosclerosis development. *Cardiovasc Res* **117**, 2755 (2021).
258. Zhou, J. *et al.* CD8(+)CD25(+) T cells reduce atherosclerosis in apoE(-/-) mice. *Biochem Biophys Res Commun* **443**, 864–870 (2014).
259. Clement, M. *et al.* Control of the T follicular helper-germinal center B-cell axis by $CD8^+$ regulatory T cells limits atherosclerosis and tertiary lymphoid organ development. *Circulation* **131**, 560–570 (2015).
260. Bergström, I., Backteman, K., Lundberg, A., Ernerudh, J. & Jonasson, L. Persistent accumulation of interferon-γ-producing CD8+CD56+ T cells in blood from patients with coronary artery disease. *Atherosclerosis* **224**, 515–520 (2012).
261. Hwang, Y. *et al.* Expansion of CD8(+) T cells lacking the IL-6 receptor α chain in patients with coronary artery diseases (CAD). *Atherosclerosis* **249**, 44–51 (2016).
262. Gewaltig, J., Kummer, M., Koella, C., Cathomas, G. & Biedermann, B. C. Requirements for CD8 T-cell migration into the human arterial wall. *Hum Pathol* **39**, 1756–1762 (2008).
263. Lebien, T. W. & Tedder, T. F. B lymphocytes: how they develop and function. *Blood* **112**, 1570–1580 (2008).
264. Caligiuri, G., Nicoletti, A., Poirierand, B. & Hansson, G. K. Protective immunity against atherosclerosis carried by B cells of hypercholesterolemic mice. *J Clin Invest* **109**, 745–753 (2002).
265. Major, A. S., Fazio, S. & Linton, M. F. B-Lymphocyte Deficiency Increases Atherosclerosis in LDL Receptor–Null Mice. *Arterioscler Thromb Vasc Biol* **22**, 1892–1898 (2002).
266. Binder, C. J. & Silverman, G. J. Natural antibodies and the autoimmunity of atherosclerosis. *Springer Semin Immunopathol* **26**, 385–404 (2005).
267. Kyaw, T. *et al.* B1a B lymphocytes are atheroprotective by secreting natural IgM that increases IgM deposits and reduces necrotic cores in atherosclerotic lesions. *Circ Res* **109**, 830–840 (2011).
268. Hosseini, H. *et al.* Phosphatidylserine liposomes mimic apoptotic cells to attenuate atherosclerosis by expanding polyreactive IgM producing B1a lymphocytes. *Cardiovasc Res* **106**, 443–452 (2015).
269. Tsiantoulas, D. *et al.* Increased Plasma IgE Accelerate Atherosclerosis in Secreted IgM Deficiency. *Circ Res* **120**, 78–84 (2017).
270. Kyaw, T., Tipping, P., Bobik, A. & Toh, B. H. Protective role of natural IgM-producing B1a cells in atherosclerosis. *Trends Cardiovasc Med* **22**, 48–53 (2012).
271. Rosenfeld, S. M. *et al.* B-1b Cells Secrete Atheroprotective IgM and Attenuate Atherosclerosis. *Circ Res* **117**, e28 (2015).
272. Kyaw, T. *et al.* Conventional B2 B cell depletion ameliorates whereas its adoptive transfer aggravates atherosclerosis. *J Immunol* **185**, 4410–4419 (2010).

273. Crotty, S. T follicular helper cell differentiation, function, and roles in disease. *Immunity* **41**, 529–542 (2014).
274. Tay, C. *et al.* Follicular B Cells Promote Atherosclerosis via T Cell-Mediated Differentiation Into Plasma Cells and Secreting Pathogenic Immunoglobulin G. *Arterioscler Thromb Vasc Biol* **38**, e71–e84 (2018).
275. Cerutti, A., Cols, M. & Puga, I. Marginal zone B cells: virtues of innate-like antibody-producing lymphocytes. *Nature Reviews Immunology 2013 13:2* **13**, 118–132 (2013).
276. Douna, H. *et al.* B- and T-lymphocyte attenuator stimulation protects against atherosclerosis by regulating follicular B cells. *Cardiovasc Res* **116**, 295–305 (2020).
277. Sage, A. P. *et al.* Regulatory B cell-specific interleukin-10 is dispensable for atherosclerosis development in mice. *Arterioscler Thromb Vasc Biol* **35**, 1770–1773 (2015).
278. Strom, A. C. *et al.* B regulatory cells are increased in hypercholesterolaemic mice and protect from lesion development via IL-10. *Thromb Haemost* **114**, 835–847 (2015).
279. Douna, H. *et al.* Bidirectional effects of IL-10+ regulatory B cells in Ldlr-/- mice. *Atherosclerosis* **280**, 118–125 (2019).
280. Tang, F. *et al.* mRNA-Seq whole-transcriptome analysis of a single cell. *Nature Methods 2009 6:5* **6**, 377–382 (2009).
281. Svensson, V., Vento-Tormo, R. & Teichmann, S. A. Exponential scaling of single-cell RNA-seq in the past decade. *Nature Protocols 2018 13:4* **13**, 599–604 (2018).
282. Olsen, T. K. & Baryawno, N. Introduction to Single-Cell RNA Sequencing. *Curr Protoc Mol Biol* **122**, (2018).
283. Baysoy, A., Bai, Z., Satija, R. & Fan, R. The technological landscape and applications of single-cell multi-omics. *Nature Reviews Molecular Cell Biology 2023* 1–19 (2023) doi:10.1038/s41580-023-00615-w.
284. Winkels, H. *et al.* Atlas of the Immune Cell Repertoire in Mouse Atherosclerosis Defined by Single-Cell RNA-Sequencing and Mass Cytometry. *Circ Res* **122**, 1675–1688 (2018).

Chapter 2

The application of single-cell transcriptomics in healthy and diseased vasculature

Manuscript in preparation

Marie A.C. Depuydt[1]*, Carlijn M. Lems[1]*, Bram Slütter[1], Ilze Bot[1]

1. Division of BioTherapeutics, LACDR, Leiden University

*These authors contributed equally

Abstract

Despite therapeutic advances, cardiovascular complications such as atherosclerosis and aortic aneurysm (AA) continue to be the primary cause of death worldwide. This emphasizes the urgent need to elucidate the complex biological mechanisms that underpin vascular disease formation and progression. Recent advances in single-cell RNA sequencing have provided new insights into the heterogeneity of cell populations, cellular transitions into pathological phenotypes, and cell-cell communication within the diseased vascular wall.

In this review, we summarize these findings and discuss the future perspectives of single-cell transcriptomics applications in studies of atherosclerosis and AA. Single-cell RNA sequencing has revealed the cellular landscape of atherosclerotic plaques and AA tissues to be much more diverse than previously believed, in particular with regard to immune cells. It has also characterized the enormous potential of vascular cells, in particular smooth muscle cells, for phenotypic switching and how this contributes to disease. Additionally, single-cell RNA sequencing has contributed to elucidating the complex cellular interaction network that governs vascular disease, thereby discovering candidate signaling pathways and ligand-receptor pairs for drug discovery. Lastly, this technique has uncovered both striking similarities and distinct differences between atherosclerosis and AA.

Single-cell transcriptomics has been of immense value in deepening our understanding of atherosclerosis and AA pathogenesis, thereby paving the way for the development of novel therapies. The ever-increasing amount of available data offers a unique opportunity for integrated and cross-species analyses to unify cell population nomenclature. Directions for future research include combining single-cell RNA sequencing with various single-cell omics techniques and outcomes of genome-wide association studies.

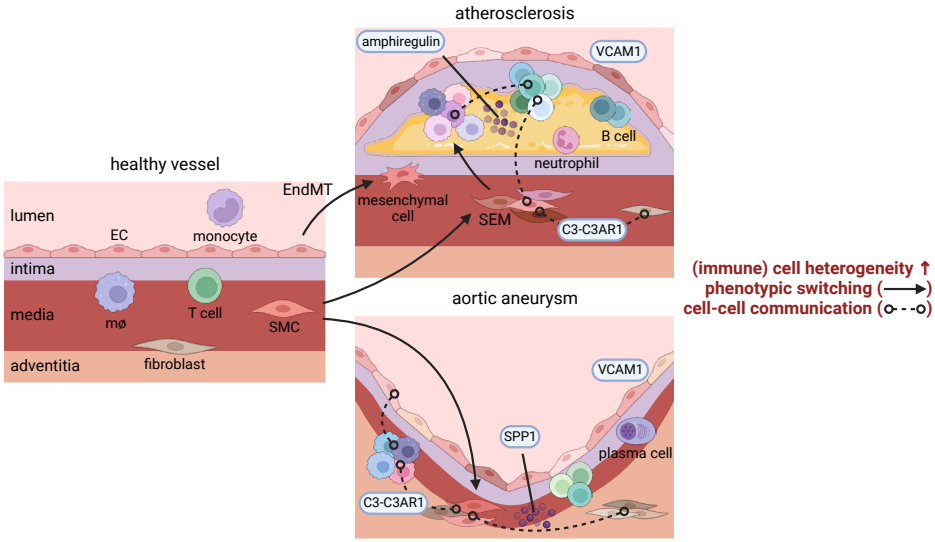

Graphical abstract. Summary of the cellular content, cellular plasticity and the main cellular crosstalk pathways in the healthy and diseased vasculature as described by single-cell transcriptomics. C3, complement component 3; C3AR1, complement C3a receptor 1; EC, endothelial cell; EndMT, endothelial-to-mesenchymal transition; mø, macrophage; SEM, stem cell, endothelial cell, monocyte; SPP1, secreted phosphoprotein 1; VCAM1, vascular cell adhesion molecule 1. The figure was created in BioRender.com.

Introduction

Cardiovascular disease is the leading cause of global mortality and its prevalence as well as its number of associated deaths are continuously increasing.[1] Common cardiovascular complications include atherosclerosis and aortic aneurysm (AA)[2]. Atherosclerosis (reviewed in [3]) is the primary underlying pathology of cardiovascular syndromes such as myocardial infarction or stroke worldwide and is characterized by chronic inflammation and the formation of atheromatous plaques in the vascular wall. Such plaques are typically covered with a thin fibrous cap and are rich in lipids and locally infiltrating inflammatory cells that promote the degradation of extracellular matrix (ECM) molecules such as collagen. Advanced atherosclerotic lesions can obstruct blood flow, either by gradually infringing on the arterial lumen or by provoking thrombus formation following plaque rupture or erosion, both leading to ischemia. This may trigger acute cardiovascular syndromes such as myocardial infarction or stroke. Established risk factors for atherosclerosis include hypercholesterolemia, diabetes, smoking, and hypertension. Genetic conditions such as familial hypercholesterolemia may also increase the risk of atherosclerosis.

After atherosclerosis, AA (reviewed in [4,5]), defined as a localized dilatation of the aorta, is the most common disease affecting the aorta. It results from structural changes in the aortic wall, including thinning of the outer layers due to the progressive loss of vascular smooth muscle cells (SMCs) and degradation of the ECM. This increases the susceptibility of the aorta to rupture, causing a potentially life-threatening hemorrhage. AAs can be subdivided into two groups based on anatomic location, namely thoracic aortic aneurysm (TAA) and abdominal aortic aneurysm (AAA). Important risk factors implicated causally in AAA formation are smoking, male sex, and the presence of atherosclerosis. Conversely, genetic predisposition plays a more prominent role in TAA, with conditions such as Marfan syndrome (MFS) comprising important risk factors.

For many years, researchers have sought to elucidate the various mechanisms that underpin vascular pathology development and progression. In the early years, knowledge was largely derived from pathology and histology research, which provided valuable information on healthy and diseased vascular tissue at the level of individual markers. This was then followed by the emergence of more modern techniques such as conventional bulk transcriptomics, which enabled the simultaneous characterization of entire gene expression profiles. Although this method has considerably increased our knowledge of differential gene expression in healthy versus diseased vascular systems, an important limitation is that it measures average gene expression across cells and hence does not allow for profiling populations on a single-cell level. A single-

cell resolution is required to adequately capture the large cellular heterogeneity in the arterial wall. Single-cell RNA sequencing (scRNA-seq) was first reported in 2009 and has quickly become a key technique in the domain of vascular pathology [6] Its main advantages lie in the identification of rare or *de novo* cell subpopulations[7], the ability to trace the lineage of cells[8], and the elucidation of cellular crosstalk.[9]

There is a rapidly growing body of literature on scRNA-seq efforts in atherosclerosis and AA. Additionally, exploration and re-analysis of the various publicly available datasets are facilitated by web portals such as PlaqView.[10,11] What remains unclear, however, is precisely what contribution scRNA-seq has made to enhancing our understanding of vascular diseases at a cellular level, and how this technique can be optimally employed in the future. This review aims to assess the value of scRNA-seq in vascular disease research by summarizing findings in healthy vasculature and the vascular pathologies atherosclerosis and aortic aneurysm, and by discussing future opportunities for its application in this field. This work offers a fresh perspective on the worth and untapped potential of a fairly new experimental approach in an increasingly important field of research and may guide future research efforts. First, we provide an overview of the current knowledge owing to scRNA-seq research in mice and humans on the cellular composition of normal and diseased vasculature, lineage-tracing experiments, and intercellular communication in the vascular wall. We then draw together these various findings to critically reflect on the added value of scRNA-seq in vascular disease research up until now. Finally, we propose several promising future research directions, such as spatial transcriptomics and single-cell multi-omics approaches.

Current knowledge of healthy and diseased vasculature: insights from scRNA-seq

Cellular composition of vasculature

Healthy vasculature comprises a wide variety of cell types, including endothelial cells (ECs), vascular SMCs, immune cells, and fibroblasts, all of which in turn consist of several subpopulations. ECs thinly line the interior surface of blood vessels, thereby functioning as a barrier between the circulation and tissues. Additionally, they control vascular relaxation and contraction by releasing vasoactive substances, and they regulate blood coagulation. Vascular SMCs are located in the media of the vascular wall. Here, they provide structural support and are primarily responsible for regulating arterial tone to control blood pressure and blood flow. Vascular SMCs exhibit two distinct phenotypes, namely a quiescent, contractile phenotype and a proliferative, undifferentiated, synthetic phenotype. Of note, based on a review of scRNA-seq data,

Yap *et al.* classified four different SMC phenotypes besides a contractile phenotype and a central dedifferentiated phenotype.[12] Hence, the authors argue that the classification of vascular SMCs should be expanded beyond the contractile and synthetic profiles. Some immune cell subsets, including T cells, B cells, and macrophages, 'patrol' the adventitia of healthy arteries[13], albeit in limited numbers compared to ECs and SMCs. In contrast, other immune cell subsets are sparsely found in normal arteries, such as neutrophils. Immune cells play a pivotal role in maintaining vascular health and are recruited from the vascular adventitia and lumen in response to inflammatory signals. Lastly, fibroblasts contribute to the structural framework of blood vessels through the production of ECM and the construction of fiber networks.

Single-cell transcriptomics has not only confirmed our previous knowledge of healthy vasculature but also underlies major recent advances in vascular biology (reviewed in [14]). Above all, it has enabled the identification and in-depth characterization of cellular subpopulations[15–19], including ECs[20–23], SMCs[24–26], and macrophages[27,28]. For instance, scRNA-seq of healthy murine aortas recently revealed 10 different cell clusters representing the four aforementioned primary vascular cell types.[20] Surprisingly, not SMCs but ECs showed the highest cellular heterogeneity. Kalluri *et al.* identified three functionally distinct EC subpopulations with concomitant gene expression profiles suggesting specialization in either angiogenesis, ECM production, and lipoprotein handling (ECs 1 and 2) or lymphatic function (EC 3).[20] Transcriptional markers that differentiate these three populations include, respectively, canonical EC markers (*Vcam1*), genes related to angiogenesis (*Flt1*) or lipid transport (*Cd36*, *Lpl*), and markers of lymphatic identity (*Lyve1*). With regard to vascular SMCs, Dobnikar *et al.* detected seven subpopulations in healthy mouse vessels, including a rare *Sca1*$^{+}$ population. [25] This *Sca1*$^{+}$ SMC subset showed a progressive downregulation of contractile genes (*Myh11*, *Actn4*) and upregulation of genes involved in ECM synthesis (*Mgp*, *Col8a1*, *Spp1*), migration (*Pak3*, *Igf1*, *Igfbp5*), and proliferation. Moreover, this study revealed that *Sca1* upregulation is a hallmark of SMC phenotypic switching. Furthermore, the emergence of single-cell transcriptomic atlases, such as the Tabula Sapiens[29], has uncovered tissue-specific features of cell types across human organs (reviewed in [30]), including in their blood vessels. This is of importance for understanding differences between vascular diseases affecting different tissues, e.g., the aorta and the heart.

Atherosclerosis

The cellular landscape of atherosclerotic plaques has been constructed the most extensively using single-cell transcriptomics. An overview of scRNA-seq experiments conducted in atherosclerosis research is presented in **Table 1**. In the next paragraphs, we will discuss the individual cell populations, including ECs, SMCs, and various immune cells.

Endothelial cells

Endothelial dysfunction is one of the main drivers of atherosclerosis initiation.[53] Wirka *et al.* identified two EC clusters, defined by genes such as *Pecam1*, *Egfl7*, and *Esam* (EC 1), and *Lrg1*, *Mmm1*, and *Ecscr* (EC 2), in mouse atherosclerotic aortas.[33] Together, these clusters mapped to a single EC cluster in diseased human coronary arteries. Conversely, several scRNA-seq studies report the presence of two major EC clusters in human carotid atherosclerotic plaques.[35,50,51] These populations were enriched in *COL4A1/2*[50,51], *SPARCL1*[50], and *PLVAP* (EC 1), and *MPZL2*, *SULF1*, and *VWF* (EC 2). Depuydt *et al.* additionally performed further subclustering to reveal four distinct EC subpopulations.[50] Three of these subpopulations represented activated endothelium characterized by angiogenic capacity (*PRCP*), cell adhesion, and the facilitation of leukocyte extravasation (*VCAM1*), thereby actively stimulating lesion inflammation. Furthermore, one EC subset displayed clear signs of endothelial-to-mesenchymal transition (EndMT) (*ACTA2*, *MYH11*)[50], a phenomenon that we discuss in more detail in the lineage tracing section below.[54] Another study showed that inflammatory ECs (*IL6*, *ACKR1*, *HLA-DQA1*) are located in the proximal adjacent region of diseased human carotid arteries[52], whereas ECs in the atherosclerotic core appear to be involved in intimal repair (*ITLN*, *DKK2*) and ECM modulation (*FN1*).

Smooth muscle cells

Similarly, single-cell transcriptomics has been applied to describe yet unknown layers of SMC phenotypic heterogeneity in atherosclerosis. The majority of findings concern the phenotypic switching or modulation of SMCs which is a hallmark of atherosclerosis.[55,56] We provide an in-depth discussion of SMC modulation-related findings generated through trajectory analysis the lineage tracing section below. An early scRNA-seq finding was that an equivalent of the abovementioned *Sca1*$^{+}$ SMC population found in healthy mouse vessels is present in murine atherosclerotic plaques [25]. This was confirmed by Wang *et al.*[39], who additionally showed that this highly de-differentiated *Sca1*$^{+}$ subset clonally expands during mouse atherogenesis. Aside from downregulating classic SMC markers, these SMCs were enriched in genes associated with inflammation, innate immunity, and the classical complement cascade, particularly *C3*. Although a gene signature resembling murine *Sca1*$^{+}$ SMCs was discovered in bulk RNA-seq data of human atherosclerosis[39], a homolog of *Sca1* is absent in humans.[57] In human carotid plaques, histone variant H2A.Z is pivotal for maintaining vascular SMC identity [48], as indicated by a downregulation of SMC marker genes (*CALD1*, *ACTA2*) and an upregulation of the proliferation-promoting gene *SMARCA4* in *H2AFZ*^{low} SMCs.

Table 1. Single-cell transcriptomics studies in atherosclerotic tissue.

Sex	Genotype	Tissue
Mouse		
Female	*ApoE*$^{-/-}$	Aorta CD45^{+}
Unknown	*Ldr*$^{-/-}$	Aorta CD45^{+}
Male	*LdlR*$^{-/-}$	Aorta CD45^{+}
Male	*ApoE*$^{-/-}$	Aortic foam cells
Male	C57BL/6	Aorta
Male	*ApoE*$^{-/-}$; *Myh11-CreERt2*; *Confetti*	Aorta
Male	*LdlR*$^{-/-}$	Aorta CD45^{+}
Female	*ApoE*$^{-/-}$	Aorta CD45^{+}
Male	C57BL/6J, *ApoE*$^{-/-}$	Aortic adventitia
Male	*ApoE*$^{-/-}$; *Tcf21*$^{+/+}$; *Tg*$^{Myh11\text{-}CreERT2}$; *ROSAtdT*$^{f/+}$, *ApoE*$^{-/-}$; *Tcf21*$^{\Delta SMC/\Delta SMC}$; *Tg*$^{Myh11\text{-}CreERT2}$; *ROSAtdT*$^{f/+}$	Aortic root/ascending aorta
Unknown	*Cx3cr1*$^{CreERT2\text{-}IRES\text{-}YFP/+}$; *Rosa26*$^{fl\text{-}tdTomato/+}$; *Ldr*$^{-/-}$ (AAV-mPCSK9)	Aortic arch
Male	*ROSA26*$^{ZsGreen1/+}$; *Ldr*$^{-/-}$; *Myh11-CreER*^{T2}, *ROSA26*$^{ZsGreen1/+}$; *ApoE*$^{-/-}$; *Myh11-CreER*^{T2}	Aorta
Unknown	C57BL/6	Aorta CD45^{+}
Unknown	*CX3CR1*$^{CreER/+}$; *Rosa26-LSL-Tomato*; *Ldr*$^{-/-}$	Aorta CD45^{+}
Male	*Myh11-Cre*^{ERT2}; *Rosa-eYFP*; *ApoE*$^{-/-}$	BCA
Male	*Myh11-Cre*^{ERT2}; *Rosa-eYFP*; *ApoE*$^{-/-}$, *Cdh5-Cre*^{ERT2}; *Rosa-eYFP*; *ApoE*$^{-/-}$, *Myh11-Cre*^{ERT2}; *Rosa-eYFP*; *ApoE*$^{-/-}$; *SMCKlf4*$^{WT/WT}$, *Myh11-Cre*^{ERT2}; *Rosa-eYFP*; *ApoE*$^{-/-}$; *SMCKlf4*$^{\Delta/\Delta}$	BCA
Male and female	*Myh11-Dre*^{ERT2}; *Lgals3-Cre*; *Rosa-tdTomato-eGFP*; *ApoE*$^{-/-}$	BCA

	Exposure	Cell type focus	References
	WD 12 weeks	Immune cells	Winkels *et al.*, 2018 [31]
	CHD 12 weeks		
	HCD 12 weeks		
	CHD 12 weeks		
	WD 12 weeks	Macrophages	Kim *et al.*, 2018 [32]
	WD 27 weeks		
	-	SMCs	Dobnikar *et al.*, 2018 [25]
	WD 14/18 weeks		
	HFD 11 weeks	Macrophages	Cochain *et al.*, 2018 [28]
	CHD 11 weeks		
	HFD 20 weeks		
	HFD 12 weeks		
	CHD	Immune cells, non-immune cells	Gu *et al.*, 2019 [15†,*]
	HFD 0/8/16 weeks	SMCs	Wirka *et al.*, 2019 [33]
	WD 20 weeks	Macrophages	Lin *et al.*, 2019 [34†]
	WD 18 weeks +		
	CHD 2 weeks + ApoB-ASO		
	WD 0/8/16/26 weeks	SMCs	Pan *et al.*, 2020 [35]
	-	Macrophages	Williams *et al.*, 2020 [36]
	HFD 3 weeks		
	-	SMCs	Alencar *et al.*, 2020 [37]
	WD 18 weeks		
	WD 18 weeks		

Table 1. Continued.

Sex	Genotype	Tissue
Male	*Ldlr*$^{-/-}$	Aorta CD45^{+}
Male	*Myh11-Cre*^{ERT2}; *Rosa26*$^{tdTomato/tdTomato}$; *ApoE*$^{-/-}$	Aortic arch
Male	*Tg*$^{Myh11\text{-}CreERT2}$; *ROSA*$^{tdT/tdT}$; *ApoE*$^{-/-}$, *Tg*$^{Myh11\text{-}CreERT2}$; *ROSA*$^{tdT/tdT}$; *ApoE*$^{-/-}$; *Ahr* $^{\Delta SMC/\Delta SMC}$	Aortic root
Female	*ApoE*$^{-/-}$	Aorta CD45^{+}
Male and female	C57BL6/J (AAV-mPCSK9)	Aortic arch CD45^{+}
Male	*Ntn1*$^{fl/fl}$*Cx3cr1*$^{CreERT2+}$, *Ntn1*$^{fl/fl}$*Cx3cr1*^{WT} (AAV-mPCSK9)	Aortic arch CD45^{+}
Male	*Ldlr*$^{-/-}$	Aortic arch CD45^{+}
Male	*ApoE*$^{-/-}$	Aorta CD45^{+}
Male	*ApoE*$^{-/-}$	Aorta CD45^{-}
Male	*Perk*$^{SMC+/+}$ (AAV-mPCSK9), *Perk*$^{SMC-/-}$ (AAV-mPCSK9)	Aortic root to distal aortic arch
Human		
Unknown		Carotid plaque
Male and female		Coronary artery
Male and female		Carotid plaque CD45^{+}, blood CD45^{+}
Male and female		Carotid plaque
Male and female		Carotid plaque
Male and female		Carotid plaque
Male and female		Carotid plaque
Unknown		Carotid plaque

AAV-mPCSK9, adeno-associated virus vector encoding mouse proprotein convertase subtilisin/kexin type 9; ApoB-ASO, antisense oligonucleotide to apolipoprotein B; BCA, brachiocephalic artery; CHD, chow diet; EC, endothelial cell; HCD, high-cholesterol diet; HFD, high-fat diet;

Exposure	Cell type focus	References
HFD 10-11 weeks CHD 10-11 weeks	Neutrophils	Vafadarnejad *et al.*, 2020 [38]
HFD 18 weeks	SMCs	Wang *et al.*, 2020 [39]
HFD 16 weeks	SMCs	Kim *et al.*, 2020 [40]
WD 12 weeks CHD 12 weeks	T cells	Wolf *et al.*, 2020 [41]
WD 20 weeks WD 20 weeks + CHD 3 weeks + ApoB-ASO + IgG or anti-CD25	T cells	Sharma *et al.*, 2020 [42]
WD 20 weeks WD 20 weeks + CHD 4 weeks	Monocytes/macrophages	Schlegel *et al.*, 2021 [43†]
WD 14 weeks + CHD 4 weeks + control anti-miR or anti-miR-33	Immune cells	Afonso *et al.*, 2021 [44]
NCD 16 weeks HCD 11 weeks	Macrophages	Burger *et al.*, 2022 [45]
NCD 16 weeks HCD 11 weeks	SMCs	Brandt *et al.*, 2022 [46]
HFD 12 weeks	SMCs	Chattopadhyay *et al.*, 2022 [47†]
	SMCs	Yao *et al.*, 2018 [48]
	SMCs	Wirka *et al.*, 2019 [33]
	Immune cells	Fernandez *et al.*, 2019 [49*]
	ECs, SMCs, immune cells	Depuydt *et al.*, 2020 [50*]
	SMCs	Pan *et al.*, 2020 [35]
	SMCs	Alencar *et al.*, 2020 [37]
	SMCs, ECs	Slenders *et al.*, 2021 [51]
	SMCs, ECs	Alsaigh *et al.*, 2022 [52]

miR, microRNA; NCD, normal cholesterol diet; SMC, smooth muscle cell; WD, western diet.

†This study additionally performed a trajectory analysis

*This study additionally performed a communication analysis

Overall, scRNA-seq efforts are in agreement that murine and/or human plaques comprise one or several vascular SMC subclusters with contractile characteristics (*Myh11*/*MYH11*, *Acta2*/*ACTA2*).[33,35,37,40,46,47,50,58,59] Each of these studies additionally reports one or multiple distinct SMC or SMC-derived subpopulations characterized by a loss of SMC markers, although the subpopulations in question markedly differ between studies. A recent meta-analysis of multiple scRNA-seq datasets of SMC lineage-traced atherosclerotic mouse models[33,35,37,40] provides more insight into the (dis)similarity of these SMC(-derived) subpopulations.[58] From this analysis, Conklin *et al.* conclude that a convergent finding is the presence of an SMC-derived intermediate cell state termed 'SEM' (stem cell, endothelial cell, monocyte).[58] Pan *et al.* previously reported a loss of contractile features and activation of ECM-related pathways (*Fn1*, *Col1a2*) in SEM cells and proposed that they represent an intermediate SMC phenotypic switching state.[35] Furthermore, Conklin *et al.* found strong evidence of SMC-derived macrophage-like cells, although there was a wide quantitative range between studies, likely due to technical differences.[58] Consistent with this, a recent study identified four phenotypically modulated SMC clusters in mouse atherosclerotic aortas, including a cluster of macrophagic calcific SMCs (*Gdf10*, *Hsd11b1*, *Pex5l*).[46] The other SMC subpopulations exhibited a mesenchymal chondrogenic (*Ifi27l2a*, *Gata4*, *Meox1*), an inflammatory and ECM regulation (*Pf4*, *Chad*, *Slc10a6*), or an inflammatory (*Ccl7*, *Ptx3*, *Ccl11*) phenotype.In the meta-analysis of Conklin *et al.*[58], a comparison with scRNA-seq data of human carotid lesions[35] showed many similarities, favoring the continued use of mouse models in atherosclerosis SMC research. In line with this, Depuydt *et al.* report a synthetic SMC cluster in human plaques that was derived from the plaque cap as suggested by the downregulation of typical SMC markers and the upregulation of ECM genes (*COL1A1*, *MGP*, *COL3A1*).[50] A small subset of this cluster was *KLF4*$^{+}$, which is indicative of differentiation into a more synthetic or macrophage-like phenotype. Additionally, Alencar *et al.* found that *KLF4*/*Klf4* regulates SMC transition to several phenotypes in advanced human carotid and murine plaques, including an *Lgals3*$^{+}$ osteogenic phenotype (*Runx2*, *Sox9*, *Cytl1*) that is likely detrimental for late-stage atherosclerotic lesion pathogenesis.[37] Similarly, Wirka *et al.* showed that *TCF21*/*Tcf21* regulates SMC phenotypic modulation in atherosclerotic lesions of human coronary and mouse arteries, specifically the transformation of SMCs into fibroblast-like cells termed 'fibromyocytes' (*Fn1*, *Lum*).[33] Another scRNA-seq study identified SMCs with enhanced calcification and ECM remodeling (*SPP1*, *IBSP*) in the atherosclerotic core versus SMCs with pro-inflammatory signaling (*C3*, *PLA2G2A*) in the proximal adjacent region of human carotid plaques.[52] Re-analysis of this dataset by Zhang *et al.* revealed SMC-derived *CD68*^{high}*ACTA2*^{low} macrophage-like cells enriched in phagocytic, inflammation, and cholesterol metabolism functions.[59]

Macrophages

An established hallmark of atherosclerosis development and progression is the accumulation of macrophages within the arterial intima, most of which are derived from monocytes that infiltrate the intima and subsequently differentiate into macrophages. The importance of monocyte recruitment for plaque progression was confirmed by Williams *et al.*, who combined scRNA-seq with fate mapping to reveal the limited proliferation capacity of specialized aortic intima resident macrophages (Mac^{AIR}) in murine aortic lesions.[36] Although this Mac^{AIR} population (*Itgax*, *Cx3cr1*, *Csf1R*) gave rise to the earliest foam cells in plaques, they were replaced entirely by recruited monocytes upon prolonged hypercholesterolemia. Still, the debate has long prevailed as to what macrophage populations are present in atherosclerotic lesions. The four most consistent macrophage phenotypes across scRNA-seq studies in mice include a resident-like macrophage (i), an inflammatory macrophage (ii), a triggering receptor expressed on myeloid cells-2 (Trem2) macrophage (iii), and an interferon (IFN)-inducible macrophage (IFNIC) (iv). The population representing resident-like macrophages (*Lyve1*) was consistently found in both healthy[28,31,60] and atherosclerotic[28,31,32,34,45,60] mouse aortas. One of these studies additionally revealed this subtype to highly express *Ccl24*, thereby promoting the trans-differentiation of SMCs to osteogenic-like cells in atherosclerosis.[45] All remaining populations were specific to atherosclerosis, including inflammatory macrophages (*Il1b*, *Cxcl2*)[28,60], otherwise referred to as non-foamy[32] or chemokine^{high} [34] macrophages. Trem2 macrophages, characterized by an upregulation of *Trem2*[28,32,34,60], were first described by Cochain *et al.*[28] and later shown to be identical to the lipid-laden foamy macrophages identified by Kim *et al.*[32] in diseased mouse aortas.[61,62] Furthermore, Kim *et al.* showed that Trem2 foamy macrophages are not pro-inflammatory, thereby resolving controversy in the field.[32] Of note, microRNA-33 (miR-33) silencing has been shown to reduce intraplaque inflammatory and Trem2 macrophage levels.[44] Silencing of miR-33[44] or netrin-1[43] additionally promotes atherosclerosis regression in part by altering macrophage transcriptomic profiles, either by upregulating genes associated with lipid metabolism (*Abcba*, *Ncoa1/2*) and chromatin remodeling/transcriptional regulation (*Brwd3*, *Ddx5*, *Hipk1*)[44] or by upregulating pathways involved in phagocytosis and migration (*Ccr7*).[43] The fourth macrophage population comprises IFNICs[32,34,60], which are enriched in IFN-inducible genes (*Ifit3*, *Irf7*, *Isg15*). While this subset was initially not found by Cochain *et al.*[28] and Winkels *et al.*[31], most likely due to the relatively small number of sequenced macrophages in these studies, a meta-analysis by Zernecke *et al.*[60] later revealed small numbers of IFNICs in these datasets. Moreover, this analysis verified all four previously established macrophage subsets in mice and expanded over the original studies by identifying a new subset resembling cavity macrophages (*Cd226*, *Itgax*).

The same group recently integrated scRNA-seq data of mouse and human atherosclerosis in an attempt further to refine the nomenclature of mononuclear phagocytes, including macrophages, and compare their transcriptomic signatures between mice and humans.[63] Integration of mouse data identified subpopulations with distinct gene expression profiles within the resident-like (*Cd209*^{high} and *Cd209*^{low}), inflammatory (*Ccr2*^{int}*MHCII*$^{+}$ and *Nlrp3*^{high}*Il1b*^{high}), and foamy (Mac^{AIR}, *Trem2*^{high}*Slamf9*, and *Trem2*^{high}*Gpnmb*) macrophage populations. In addition, cross-species comparison and data integration indicated conserved transcriptomic features of macrophages in mouse and human atherosclerosis. In particular, gene signatures of four major mouse macrophage subsets, i.e., resident-like, inflammatory, foamy/Trem2, and IFNIC macrophages, mapped to specific populations in human lesions. However, a subset of cavity macrophages (*Itgax*, *Cd226*) was detected only in mice, emphasizing that some, but not all, macrophage subclasses identified in mouse models are relevant to human atherosclerosis and should therefore be investigated further. Depuydt *et al*. found a different discrepancy between mice and humans, namely no significant overlap between human *IL1B*$^{+}$ pro-inflammatory macrophages and any macrophage populations present in mouse atherosclerotic plaques.[50] They did establish the presence of resident-like, inflammatory, and foamy TREM2 macrophage populations in human lesions, and additionally revealed resident-like macrophages to be pro-inflammatory with an upregulation of *TNF*. Moreover, the TREM2 foam cell-like population expressed smooth muscle actin (*ACTA2*), suggesting a transition from a macrophage to an SMC phenotype or vice versa, and displayed a fibrosis-promoting phenotype. While Fernandez *et al*. identified five distinct macrophage clusters in human carotid artery plaques, they functionally characterized only four.[49] Three subsets displayed activated (*HLA-DRA*, *CD74*) and pro-inflammatory (*CYBA*, *S100A9/8*, and *JUNB*, *NFKBIA*) states. The second of these macrophage populations (*CYBA*, *S100A9/8*) was enriched in TIMP metallopeptidase inhibitor 1 (*TIMP1*) and may therefore promote plaque stabilization by limiting ECM degradation. The final population showed a foam cell-like gene expression profile (*APOC1*, *APOE*) with, unsurprisingly, reduced pro-inflammatory signaling (*IL1*, *IFN*).

T cells

Even though atherosclerosis was traditionally perceived as a macrophage-dominated pathology, it has an immune component primarily involving T cells that was established in part due to scRNA-seq experiments. The accumulation of T cells in atherosclerotic lesions and the vascular adventitia was first observed through immunohistochemistry, according to which T cells comprised approximately 7.7-22% of all cells in human plaques depending on the region.[64,65] However, using scRNA-seq Fernandez *et al*. revealed that T cells in fact account for the majority of human

plaque immune cells.[49] Similarly, Depuydt *et al.* found that T cells comprised the majority (52%) of all cells analyzed from human lesions.[50] scRNA-seq studies in mice showed a somewhat smaller fraction of T cells, namely approximately 25% of all leukocytes in atherosclerotic aortas.[28,31] Of note, the apparent discrepancy between immunohistochemistry and scRNA-seq findings may partially be attributed to the enzymatic tissue digestion that precedes scRNA-seq. This may cause the loss of fragile cell types, such as macrophages, resulting in an overestimation of more durable cellular subsets, including T cells. Nonetheless, through histological analysis, Depuydt *et al.* confirmed that $CD3^+$ T cells indeed outnumbered $CD68^+$ macrophages in human plaques.[50]

Furthermore, scRNA-seq has uncovered considerable T-cell heterogeneity in atherosclerosis (reviewed in [66]). Overall, there are four consistent T-cell populations in murine atherosclerosis, namely $CD8^+$ cytotoxic T cells (i), naive T cells (ii), thymocyte-like T cells (iii), and multilineage-committed $CD4^+$ T cells expressing *Cxcr6* (iv). An integrative analysis of scRNA-seq data additionally identified a distinct cluster of regulatory T cells (T_{regs}) (*Tnfrsf4/18*, *Cd134*, *NT5e*).[60] $CD8^+$ cytotoxic T cells (*Cd8a/b*, *Ccl5*, *Gzmk*) were consistently present in healthy and diseased aortas but not in the adventitia.[15,28,31,60] Conversely, the other T-cell populations were atherosclerosis-specific and were also detected in the aortic adventitia. This includes a population of naive $Cd28^+Ccr7^+$ T cells, which additionally expressed *Lef1*, *Dapl*, and *Tcf7*.[15,28,31,60] The third cluster comprised T cells enriched in both CD4 and CD8 and was previously termed mixed.[28,31] It is important to note that due to the technical limitations of scRNA-seq, the presence of $CD8^+CD4^+$ T cells was not confirmed on a single-cell level. I.e., it was only proven that the cluster expressed both of these markers, not that the individual cells that comprise this cluster did so. Zernecke *et al.*[60] propose that this population represents immature T cells, and Winkels and Wolf[66] note that these cells indeed expressed the thymocyte genes *Tcf7*, *Rag1*, and *Ccr9*.[28,31] The final cluster of multilineage-committed $CD4^+$ T cells (*Cxcr6*, *Rora*, *Tmem176*)[15,28,31] was termed $Il17^+Cxcr6^+$ in the meta-analysis by Zernecke *et al.*[60] This population displayed a mixed T_{reg}-helper T (T_H)1-T_H17-T_H2 transcriptomic profile that differs markedly between studies, as discussed in more detail in the review by Winkels and Wolf.[66] They additionally propose that $Cxcr6^+$ T cells may be specific for apolipoprotein B (ApoB) based on overlapping gene signatures with ApoB-reactive T cells detected in mouse atherosclerosis.[41] These ApoB-reactive T cells displayed mixed T_{reg} and T_H1-T_H2-T_H17-follicular helper T (T_{FH}) transcriptional programs and support the notion that atherosclerosis has an autoimmune component. Integrative analysis of these datasets is, however, not available. Both Wolf *et al.*[41] and another study that identified a mixed T_{reg}-T_H phenotype in atherosclerotic mice[67] showed that these cells failed to protect

from atherosclerosis in adoptive transfers despite their T_{reg} origin. In line with this, Sharma *et al.*[42] found distinct gene signatures of T_{regs} in progressing versus regressing plaques in mice. In particular, T_{regs} in regressing plaques lacked *Nrp1*, a marker for thymus-derived or natural T_{regs}, suggesting they are induced in the periphery. Furthermore, scRNA-seq recently revealed that miR-33 silencing increases T_{reg} levels in murine plaques while reducing the accumulation of $CD8^+$ T cells and T_H1 cells.[44]

In contrast to the traditional T_H subsets in mice, two scRNA-seq studies of human atherosclerotic lesions report T-cell phenotypes primarily defined by their activation status.[49,50] Depuydt *et al.* identified a diverse landscape of activation-based $CD8^+$ and $CD4^+$ T-cell subclasses that varied from cytotoxic (*GZMA*, *GZMK*) to more quiescent (*LEF1*, *SELL*).[50] Similarly, Fernandez *et al.* found distinct T-cell subsets with gene signatures of T-cell activation (*NFATC2*, *FYN*), cytotoxicity (*GZMA*, *GZMK*), and exhaustion (*EOMES*, *PDCD1*) in plaques.[49] Conversely, blood T cells of the same patients displayed transcriptomic profiles associated with a resting phenotype (*KLF2*, *TXNIP*). Additionally, this study reports distinct differences in plaque T cells between asymptomatic and symptomatic patients, including an unexpected pro-inflammatory signature (*IFNG*) in the former. It remains unclear how T-cell populations in mice and humans overlap, highlighting the need for integrated cross-species analysis of scRNA-seq data.

B cells

With regard to B cells, scRNA-seq efforts have established that this cell type is less prevalent and displays less phenotypic heterogeneity than T cells in atherosclerotic plaques. Yet, it is important to consider that B cells predominantly populate artery tertiary lymphoid organs in the adventitia adjacent to advanced plaques.[31,68] Hence, scRNA-seq studies excluding the adventitial compartment are likely to find a smaller abundance of B cells in atherosclerotic vessels. This almost certainly applies to all studies with carotid endarterectomy patients given that this procedure involves the removal of the intima with the plaque from the artery without affecting the tunica media or adventitia. A meta-analysis by Zernecke *et al.*[60] of several scRNA-seq studies in mice[28,31,32,34] defined two B-cell clusters, namely a small cluster of B1-like cells and a larger cluster of B2-like cells that was also detected in healthy aortas.[28,31] Transcriptional markers that differentiated the B1- and B2-like subsets included, respectively, genes associated with B1 cells (*Tppp3*, *S100a6*, *Cd9*) and with germinal center and marginal zone B cells (*Fcer2a*, *Cd23*). In human lesions, Depuydt *et al.*[50] and Fernandez *et al.*[49] both detected one small, homogeneous B cell cluster. Fernandez *et al.* additionally showed that B cells, as expected, have a higher frequency in blood than in plaques.[49]

Neutrophils

Despite their small numbers, neutrophils play an important role in atherosclerosis and thrombosis.[69] In an integrated analysis of scRNA-seq data in mice, Zernecke *et al.*[60] found only a few neutrophils in multiple datasets of healthy[28,31] as well as diseased[28,31,32,34] aortas. Still, several of the individual studies failed to identify a neutrophil cluster[31,32], and to our knowledge, no scRNA-seq study to date has been able to detect a neutrophil population in human plaques.[49,50] Zernecke *et al.*[60] propose two intrinsic obstacles as potential explanations, namely the relatively low mRNA content of neutrophils and the degradation of RNA by the potent, readily releasable ribonucleases in which neutrophils are rich. The process of tissue digestion likely also poses a considerable problem. Despite these hindrances, Vafadarnejad *et al.* recently observed two distinct *Siglecf*^{high} and *Siglecf*^{low} neutrophil populations in mouse atherosclerosis that resembled those present in the murine heart after myocardial infarction.[38]

Aortic aneurysm

Single-cell transcriptomics has substantially contributed to mapping the cellular landscape of AAs. **Table 2** provides an overview of scRNA-seq studies performed in AA research. As with atherosclerosis, most experiments were conducted using mouse models due to difficulties in obtaining and processing human AA tissue. Of note, the field of experimental aneurysm research employs diverse modes of promoting AA in mice, including Angiotensin (Ang) II infusion[70], periaortic exposure to calcium chloride ($CaCl_2$)[71], elastase perfusion[72], and an MFS (Fbn1$^{C1041G/+}$) mouse model[73].

Table 2. Single-cell transcriptomics studies in aortic aneurysm tissue.

Sex	Genotype	Tissue
Mouse		
Unknown	*ApoE*$^{-/-}$	Abdominal aorta
Male and female	C57BL/6J, *Sting*$^{gt/gt}$	Ascending aorta
Male and female	*Fbn1*$^{C1041G/+}$	Aortic root/ascending aorta
Unknown	*TGFβR2*$^{iSMC\text{-}Apoe}$	Ascending aorta
Male	C57BL/6J	Infrarenal abdominal aorta
Male	*ApoE*$^{-/-}$	Suprarenal abdominal aorta
Male	C57BL/6J	Infrarenal abdominal aorta
Male	*Mef2c-Cre +/0*; *ROSA26R*$^{mT/mG}$	Ascending aorta
Male	C57BL/10	Ascending aorta/aortic arch
Male	*ApoE*$^{-/-}$	Suprarenal abdominal aorta
Male and female	*Fbn1*$^{C1041G/+}$; *Nkx2-5*$^{IRES\text{-}Cre}$; *Rosa*$^{tdTomato/tdTomato}$	Aortic root/ascending aorta
Human		
Male	MFS	Aortic root
Male and female		ATAA
Male and female		AAA
Male and female	MFS	Aortic root/ascending aortic aneurysm

AAA, abdominal aortic aneurysm; Ang II, angiotensin II; ATAA, ascending thoracic aortic aneurysm; BAPN, β-aminopropionitrile; $CaCl_2$, calcium chloride; CHD, chow diet; EC, endothelial cell; HCHFD, high-cholesterol high-fat diet; HFD, high-fat diet;

Endothelial cells

Even though endothelial dysfunction is an established contributor to AA formation and development, only a few scRNA-seq studies have comprehensively characterized EC populations in AA tissues. Li *et al*. identified two EC subclusters in healthy adult mice and an Ang II-induced mouse model of AAA, namely 'normal' ECs (*Pecam1*) and lymphatic ECs (*Pecam1*, *Lyve1*).[76] EC dysfunction in AAA was characterized by an upregulation of genes associated with EC proliferation as well as leukocyte migration and activation, the latter suggesting a role of ECs in inflammatory cell recruitment during AAA formation. These findings are partially supported by a recent study that found three EC clusters in Ang II-induced AAA and sham mouse models.[79] Two of these clusters had similar expression patterns and upregulated genes related to proliferation and regeneration (*Eng*, *Kdr*, *Chd5*). Conversely, the third EC cluster had a distinct gene signature and was enriched in inflammation and damage-

Exposure	Cell type focus	References
WD 2 weeks + Ang II 4 weeks	Macrophages	Hadi *et al.*, 2018 [70]
HFD 5 weeks + Ang II 1 week (during last week)	SMCs, macrophages	Luo *et al.*, 2020 [74]
4/24 weeks	SMCs	Pedroza *et al.*, 2020 [73†]
HCHFD 0/1/2/4 months	SMCs	Chen *et al.*, 2020 [75]
Elastase-induced AAA 7/14/28 days	SMCs, monocytes/macrophages	Zhao *et al.*, 2021 [72]
Ang II 4 weeks	Macrophages, fibrocytes	Li *et al.*, 2021 [76†]
$CaCl_2$-induced AAA	SMCs, fibroblasts, macrophages	Yang *et al.*, 2021 [71]
Ang II 3 days	Fibroblasts, SMCs	Sawada *et al.*, 2022 [77†,*]
BAPN 7/14/21 days	Macrophages	Liu *et al.*, 2022 [78*]
Ang II 4 weeks	Fibroblasts, SMCs, immune cells, ECs	Weng *et al.*, 2022 [79†,*]
16 weeks	SMCs	Pedroza *et al.*, 2022 [80]
	SMCs	Pedroza *et al.*, 2020 [73]
	Immune cells, non-immune cells	Li *et al.*, 2020 [81†,*]
	Monocytes/macrophages	Davis *et al.*, 2021 [82†]
	SMCs, fibroblasts, ECs	Dawson *et al.*, 2021 [83*]

MFS, Marfan syndrome; SMC, smooth muscle cell; WD, western diet.
†This study additionally performed a trajectory analysis
*This study additionally performed a communication analysis

related genes (*Vcam1*, *Vwf*, *Icam1*). During the process of AAA, the cell numbers of this pro-inflammatory phenotype increased, whereas those of the proliferative EC phenotypes decreased. The latter is not in line with the increased expression of EC proliferative genes observed by Li *et al.*[76] during AAA development. While Dawson *et al.*[83] also identified three EC clusters in ascending AA tissues from MFS patients and in non-aneurysmal control tissues, they appear to be somewhat dissimilar to those reported in mice. The largest EC cluster represented a baseline EC population and was enriched in *POSTN*, quiescence markers (*IL33*, *CDKN1A*), and genes associated with innate immune responses. This cluster also upregulated stress genes (*ATF4*, *JUN*, *FOS*), although the authors attributed this to artificial stress in response to tissue processing. The second-largest EC cluster represented a more activated EC phenotype termed 'healing ECs' and showed an upregulation of genes involved in angiogenesis (*FLT1*, *DLL4*, *NOTCH4*), collagen deposition, and remodeling. The smallest

cluster represented de-differentiated ECs and expressed genes associated with the coagulation pathway and gap junctions, as well as *COL1A2*, *CCND1*, and contractile genes. All EC clusters, in particular healing ECs, had an increased proportion in MFS compared to control tissues. By contrast, another study detected two EC subsets that were both decreased in ascending thoracic AA (ATAA) patients versus healthy controls.[81] Furthermore, one cluster (*SLC9A3R2*, *HLA-C*) exhibited higher cell-cell and cell-ECM junction scores than the other EC cluster (*CEMIP2*, *EMP1*), which is suggestive of lower cell motility and/or migration.

Smooth muscle cells

SMCs are widely considered the culprit cell type in the pathogenesis of AAs and have therefore been intensively studied in the context of this disease. scRNA-seq studies consistently report a loss of SMCs during AA formation in mice[71,72,75,76,78] and humans[81,84,85]. To our knowledge, the only exception is a recent study by Weng *et al.* that reports an SMC expansion in an Ang II-induced AAA mouse model.[79] Furthermore, several scRNA-seq experiments detected a distinct, frequently disease-enriched cluster of modulated SMCs.[73,78,80,81,83] Trajectory inference-based insights into SMC phenotypic switching in AAs will be further discussed below. In a study by Pedroza *et al.*, the principal distinction between MFS and control mouse aortic root/ascending aorta tissue was the presence of a disease-enriched subset of transcriptomically modulated SMCs with ECM organization- (*Fn1*, *Mgp*, *Eln*), proliferation-, and adhesion-related functions.[73] While modulated SMCs were not present in young Fbn1$^{C1041G/+}$ mice, the single SMC cluster observed in these mice upregulated genes associated with early SMC modulation, suggesting activation of this process. Despite finding similar patterns of SMC phenotypic switching in murine atherosclerosis, this study identified a transcriptomic profile specific to MFS (*Serpine1*, *Klf4*). scRNA-seq of an aortic root aneurysm sample from an MFS patient revealed modulated SMCs (*COL1A1*, *SERPINE1*, *TGFB1*) analogous to those found in adult MFS mice. The same group later identified a similar disease-enriched modulated SMC subtype (*Igfbp2*) in the same mouse model, together with quiescent SMCs (*Myh11*), *Tnnt2*$^{+}$ SMCs, and rare *Rgs5*$^{+}$ pericytes.[80] Consistent with their prior study[73], the SMC modulation signature was distinguished by highly expressed *Mmp2*, *Tgfb1*, and *Col1a1* and downregulated SMC contractile genes (*Cnn1*, *Myh11*, *Acta2*).[80] Pedroza *et al.* additionally investigated whether the embryologic origin of SMCs, either the second heart field (SHF) or the neural crest, influences their phenotypic switching.[80] Interestingly, although SMCs derived from both lineages underwent phenotypic modulation in the setting of MFS, they displayed different transcriptomic responses. In a β-aminopropionitrile (BAPN)-induced thoracic aortic aneurysm and dissection (TAAD) mouse model and control mice, Liu *et al.* found

13 SMC clusters that could be divided into *Rgs5^{low}* and *Rgs5^{high}* SMCs.[78] The latter represented phenotypically modulated SMCs and displayed an ECM remodeling (*Fn1*, *Mmp2*, *Col1a1*) and migratory transcriptomic profile similar to fibroblasts, with downregulation of SMC contractile markers (*Acta2*, *Mylk4*, *Myh11*). Notably, one *Rgs5^{high}* cluster was significantly expanded at the early stage of TAAD, while the other two were either expanded or contracted at the advanced stage.

Compared with Pedroza *et al.*[73], Li *et al.*[81] performed a more comprehensive scRNA-seq study on tissues from multiple ATAA patients and control subjects. They uncovered a cluster of fibromyocytes or modulated SMCs (*ACTA2*, *MYL9*, *COL1A2*) with a gene signature suggestive of high ECM production but not proliferation. Other SMC clusters included contractile SMCs (*ACTC1*, *ACTA2*, *MYL9*), stressed SMCs (*FOS*, *ATF3*, *JUN*), and two subsets of proliferating SMCs (*MGP*, *TPM4*, *MYH10*). Of note, the authors argue that the gene expression profile of the stressed SMC cluster may be induced by tissue dissociation and hence not truly represent its physiological molecular status. A study by Dawson *et al.*[83] conducted on multiple human MFS and control samples detected a similar cluster of fibromyocytes that expressed both contractile and ECM (*ELN*, *FLN1*, *VCAN*) genes and resembled the modulated SMCs described by Wirka *et al.*[33] in atherosclerosis. They additionally identified a de-differentiated, proliferative SMC phenotype (*CCND1*, *THY1*) increased in MFS tissues and speculated that this cluster may be similar to the modulated SMC cluster unique to MFS identified by Pedroza *et al.*[73]. Other SMC subtypes included mature contractile (*SMTN*, *CNN1*) and contractile SMCs (*MYH11*), stressed SMCs (*JUN*, *FOS*, *ATF3*) likely reflecting the technical artifacts of tissue processing, and intermediate SMCs with a similar gene signature as modulated SMCs but a higher expression of contractile genes. Furthermore, based on a consistent downregulation of the canonical transforming growth factor beta (TGFβ) pathway (*TGFBR2*) in SMCs, Dawson *et al.*[83] proposed that impaired TGFβ signaling contributes to disease pathology. This is consistent with the downregulation of major TGFβ receptors (*Lrp1*/*LRP1*, *Tgfbr2*/*TGFBR2*) in SMCs of Ang II-infused mice as well as human TAAs.[77]

Other studies found alternative evidence of SMC phenotypic transformation. For instance, Weng *et al.* observed a functional transformation of SMCs from a contractile to a secretory phenotype in an Ang II-induced AAA mouse model.[79] Both SMC clusters identified in this study expanded during AAA formation and upregulated secretory genes (*Spp1*, *Mgp*, *Eln*), while the expression of contractile genes (*Acta2*, *Cald1*, *Myh11*) was largely unaffected. Similarly, Li *et al.* report SMCs enriched in ECM-associated functions suggestive of a phenotypic transformation in response to Ang II infusion

in mice.[76] Another study found transcriptomic evidence of an SMC phenotypic switch from contractile to synthetic in the early phase of murine AAA.[71] The contractile SMC population (*Myh11*, *Acta2*, *Tagln*) was diminished in AAA, whereas the synthetic SMC cluster (*Acta2*, *Aqp1*), which highly expressed cell cycle-related genes, was increased. In contrast, Sawada *et al*. found that SMCs in Ang II-infused mice upregulated contractile genes (*Acta2*, *Cnn1*, *Tagln*) and ECM components (*Eln*, *Col1a1/2*, *Col4a1*), and downregulated proliferation genes (*Klf4*, *Egr1*).[77]

AA scRNA-seq experiments also revealed SMC gene signatures associated with stress response pathway activation and inflammation. Consistent with SMC depletion being a hallmark for AA, Li *et al*. found an upregulation of apoptotic signaling pathway regulation in SMCs of Ang II-induced AAA mice.[76] In another study, transcriptomic profiling highlighted the contribution of excessive activation of stress-responsive (*Egr1*) and Toll-like receptor (TLR) signaling (*Atf3*) pathways in SMCs at the onset of TAAD in mice.[78] Luo *et al*. induced sporadic AAD in mice with a combination of a high-fat diet and Ang II.[74] Aortic challenge induced *Sting* expression in two SMC clusters, accompanied by an upregulation of key genes associated with inflammation (*Il1b*, *Il6*, *Tnf*) and cell death via, e.g., apoptosis (*Casp3/7/9*, *Bak1*, *Bax*). Knockdown of *Sting* prevented this transcriptomic reprogramming, suggesting a crucial role for *Sting* in activating stress response and cell death pathways implicated in AA formation. Immunostaining of human sporadic ascending TAAD tissues suggested a similar activation of the stimulator of interferon genes (STING) pathway in SMCs. In healthy and elastase-induced aneurysmal infrarenal abdominal aortas (IAAs) of mice, Zhao *et al*. detected a small inflammatory-like SMC cluster (*Sparcl1*, *Thbs1*, *Notch3*) that proportionally increased during AAA progression, along with an upregulation of pro-inflammatory genes (*Cd68*, *Cxcl1/2*, *Il1r1*).[72] The other SMC subpopulations, namely quiescent-contractile SMCs (*Myh11*, *Acta2*, *Tagln*), proliferative-contractile SMCs (*Fos*, *Jun*, *Klf2/4*), and de-differentiated SMCs (*Mt1/2*, *Hk2*, *Gata6*), all decreased in AAA, accompanied with downregulation of contractile genes. Lastly, re-analysis of the human ATAA scRNA-seq dataset of Li *et al*.[81] revealed 16 distinct SMC clusters, which were further classified according to their canonical definitions into contractile, secreting (*COL1A1/2*), mesenchymal-like (*CD34*, *PDGFRA*), adipocyte-like (*FABP4*, *EBF2*), macrophage-like (*CD14*, *CD68*), and T-cell-like (*CD3D/G*) SMCs.[84] Only the contractile SMC phenotype was reduced in ATAA, whereas all other SMC phenotypes were significantly increased. All in all, scRNA-seq efforts in AA research have provided considerable evidence of SMC phenotypic switching commonly characterized by enhanced ECM regulation, as well as of increased stress-responsive and inflammatory signaling by SMCs.

Fibroblasts

Although a proportional decrease of fibroblasts is typically observed in AA using scRNA-seq[71,72,76,79,81,84,85], fibroblast heterogeneity plays a pivotal role in AA.[79] Nevertheless, there is no consensus on the number of fibroblast clusters in healthy aortic and AA tissue. As with SMCs, Pedroza *et al.* identified a different number of fibroblast clusters in young versus adult Fbn1$^{C1041G/+}$ mice, the difference being a distinct *Ly6a*$^{+}$ fibroblast cluster only detected in adult mice but not in young mice or an MFS patient.[73] Re-analysis of the adult mice scRNA-seq dataset by Zhou *et al.* revealed an additional, disease-specific *Spp1*$^{+}$ subpopulation of fibroblasts associated with enhanced ECM regulation.[86] However, other scRNA-seq studies report a decrease in ECM regulation in AAs along with an increase in proliferation. For instance, Ang II infusion induced a unique SHF-derived fibroblast subcluster in the ascending aorta of mice, characterized by downregulation of genes related to ECM components (*Col4a3*, *Eln*) and TGFβ signaling (*Tgfb2*, *Tgfbr2*) and upregulation of proliferative genes (*Cdk1*, *Mki67*, *Cks2*).[77] Another study observed a proportional decrease of quiescent fibroblasts that played a role in ECM turnover and collagen synthesis (*Dcn*, *Lum*, *Col1a1*) in an early-stage AAA mouse model compared with sham.[71] The second fibroblast cluster identified in this study had an inflammatory and proliferative gene signature (*Pclaf*, *Mki67*) and was slightly increased in AAA tissues. Aside from ECM modulation and proliferation, scRNA-seq studies have identified AA-associated fibroblast subtypes with various other functions. For example, Weng *et al.* identified 10 distinct fibroblast clusters in Ang II-induced AAA and sham mouse models, four of which increased in amount during the formation of AAA.[79] The expanded populations were defined as antigen-presenting (*Cd74*, *H2-Ab11*), activation (*Acta2*, *Pdgfrb*), tissue-repair (*Fn1*), and vascular (*Des*) fibroblasts. Enrichment analysis suggested that fibroblasts mainly participate in the AAA process through ECM metabolic homeostasis, but also via pathways such as oxidative phosphorylation and PI3K-Akt signaling. Similarly, Li *et al.* found a population of myofibroblasts (*Cd34*$^{-}$*Acta2*$^{+}$) involved in wound healing that increased significantly in AAA compared to healthy mouse tissues.[76] Other fibroblast clusters detected in this study included inactivated fibroblasts (*Cd34*$^{+}$*Acta2*$^{-}$) and an intermediate population, which were specifically enriched in the functions 'transmembrane receptor protein serine/threonine kinase signaling pathway' and 'connective tissue development', respectively.

Only two scRNA-seq studies provide an in-depth characterization of fibroblast populations in aneurysmal human aortic tissue.[81,83] Some, but not all, of their findings are comparable to those in mouse models, e.g., quiescent, proliferative, and healing gene signatures. Li *et al.* found two clusters of fibroblasts in both control and aneurysmal human ascending aortas.[81] One cluster upregulated *FBN1*

and proteoglycans (*LUM*, *DCN*), while the other highly expressed *ELN* and displayed higher cell-cell and cell-ECM junction scores. The former resembles the population of quiescent fibroblasts detected by Dawson *et al.* in both ascending AA tissues from MFS patients and control tissues.[83] This population showed an increased expression of genes related to fibroblast quiescence and ECM maintenance (*C1R/S*, *LUM*, *DCN*) and was additionally enriched in *ADAMTS* genes, which were previously linked to AA formation. As with ECs and SMCs, Dawson *et al.* also identified stressed fibroblasts (*CXCL2/3*, *IER3*, *ATF3*) that likely represented fibroblasts in a stressed state due to tissue processing rather than a truly distinct phenotype.[83] The final cluster was consistent with activated fibroblasts and displayed a proliferative and healing gene signature, with an increased expression of genes involved in, e.g., SMC contraction (*MYL9*, *TAGLN*, *ACTA2*) and angiogenesis (*NOTCH3*, *THBS2*, *COL18A1*). Only this population showed an increased fraction in MFS patients.

Macrophages

A principal feature of the pathogenesis of AA is the accumulation of immune cells, particularly macrophages, as confirmed by single-cell transcriptomics.[71,72,75,76,78,79,81,84,85,87] One common scRNA-seq finding with regard to macrophages is an AA-associated upregulation in pro-inflammatory signaling. Zhao *et al.*, for instance, found a cluster of inflammatory macrophages (*Ccl2*, *Il1b*, *Mmp9*) in IAAs of elastase-induced AAA mice and healthy controls.[72] Other subpopulations included two types of aortic-resident macrophages (*Cx3cr1*, *Flt3*), blood-derived monocytes (*Adgre1*, *Itgam*, *H2-Aa*), and blood-derived reparative macrophages (*Arg1*, *Egr2*, *Il1r2*). Elastase exposure induced significant expansion of all clusters except for *Cx3cr1*$^{+}$ resident macrophages. In a $CaCl_2$-induced mouse model of early-stage AAA and in control mice, Yang *et al.* identified a macrophage population with a similar inflammatory transcriptomic profile (*Il1b*, *H2-Ab1*).[71] Unlike in Zhao *et al.*[72], resident-like macrophages did not form a distinct cluster but were concentrated in an anti-inflammatory (*Pf4*, *Mrc1*) and a proliferating (*Stmn1*, *Mki67*) macrophage cluster.[71] Inflammatory macrophages were responsible for the observed accumulation of macrophages in an early stage of AAA development, while the importance of local macrophage proliferation in AA has yet to be proven. Through an integrated analysis of scRNA-seq data of both aforementioned studies[71,72], Cheng *et al.* uncovered four gene modules positively associated with AAA primarily functionally enriched in collagen-containing ECM, myeloid leukocyte migration, and the PI3K-Akt signaling pathway.[87] Additionally, *Clec4e*, *Il1b*, and *Thbs1* were identified as key monocyte/macrophage-related genes, and a high expression of *CLEC4E* and *IL1B* was discovered in the human AAA dataset of Davis *et al.*[82] Interestingly, in their original study, Davis *et al.* discovered that the activation of an inflammatory immune response (*REL*, *TNF*, *NFKB1*) can at least partly be attributed to a significant

enrichment of the histone demethylase *JMJD3* in macrophages and monocytes.[82] By integrating human TAA scRNA-seq data[81,88], Wang *et al.* revealed macrophages predominantly enriched in immune-related pathways such as antigen processing and presentation and T_H-cell differentiation.[85] Some of these pathways were also identified by bulk scRNA-seq, suggesting that macrophages are largely responsible for inducing inflammatory responses involved in TAA formation and progression.

Of note, although some studies determine the expression of traditional M1 and M2 macrophage markers[72,76,79,81], this panel is not sufficiently specific to fully capture the functional heterogeneity observed in macrophages in AA. This is illustrated by a recent study in Ang II-induced AAA and healthy mice, which found six monocyte/macrophage clusters, including three clusters of M2-type macrophages (*Arg1*, *Cd163*, *Stab1*) that decreased during AAA progression.[79] Reportedly, macrophages were simultaneously polarized in an inflammation-promoting direction, although there was no apparent increase in M1 marker genes (*Cd68*, *Tlr2*, *Ciita*), which were expressed irregularly in the clusters. Li *et al.* did detect three specific M1-like clusters (*TNF*, *IL1B*, *NFKB1*) with inflammatory (*CCL3L1*, *CCL4*, *TNF*), tissue remodeling (*EREG*, *TIMP1*, *VCAN*), and $CD8^+$ T cell-presenting (*HLA-F*) functions in human ATAA and control tissues.[81] They additionally found two M2-like clusters (*MRC1*, *STAB1*, *CD163*) with roles in glucose metabolism (*PDK4*), anti-inflammation, and phagocytosis, and clusters associated with the IFN response (*IFI44l*, *ISG15*, *IFIT1*), tissue remodeling (*IGFBP7*, *ADAMTS1*, *MMP2*), and proliferation (*H2AFZ*, *TUBB*, *CKS1B*). M1-like populations were proportionally increased in tissues of ATAA patients, whereas remodeling macrophages were decreased.

This decrease in tissue remodeling macrophages is not in line with several scRNA-seq studies that report AA-associated macrophages involved in maladaptive ECM degradation and tissue remodeling, e.g., through upregulation of matrix metalloproteinase (MMP) family proteins. Liu *et al.* identified three subpopulations of macrophages in TAAD and sham mouse models, i.e., $Lyve1^+$ resident-like, $Cd74^{high}$ antigen-presenting, and $Il1rn^+/Trem1^+$ pro-inflammatory macrophages, that were all significantly expanded at the advanced stage of TAAD.[78] Additionally, this study pinpoints the latter as the predominant source of most detrimental molecules that contribute to TAAD development, including MMPs and inflammatory cytokines. This finding was verified in human TAAD patients through bulk RNA-seq and is supported by another scRNA-seq study using a sporadic AAD mouse model.[74] Here, a $Sting^{high}$ macrophage cluster upregulated genes associated with both inflammation (*Il1b*, *Ccr2*, *Cxcr3*) and ECM degradation (*Mmp2/8/9*). This upregulation was prevented in $Sting^{gt/gt}$ mice. Conversely, another study found non-inflammatory

macrophages responsible for ECM degradation and remodeling.[76] In healthy mice and an Ang II-induced mouse model of AAA, Li *et al*. discovered three macrophage clusters, namely *Trem2*$^{+}$*Acp5*$^{+}$ osteoclast-like macrophages, *Mrc1*$^{+}$*Cd163*$^{+}$ M2-like macrophages, and *Il1b*$^{+}$*Ccr2*$^{+}$ M1-like macrophages.[76] Osteoclast-like macrophages were increased in AAA tissues, and both osteoclast-like and M2-like macrophages highly expressed MMPs and showed an upregulated expression of cathepsins in response to Ang II infusion.

T cells

Similar to macrophages, many scRNA-seq studies report a proportional increase in T cells in murine[72,76,78,87] and human[81,84,85] AA tissues. Conversely, Yang *et al*. found an unchanged percentage of T cells and other adaptive immune cells, including B cells, in early-stage murine AAA.[71] A possible explanation for this discrepancy is that the adaptive immune response has not yet been fully activated at this stage. However, another study identified fewer T and B cells in late-stage murine AAA compared to healthy mouse tissues.[79] Still, critical transcriptomic alterations occurred in T cells during AAA development, including significant upregulation of *Cd3* and *Cd8* while *Cd4* expression remained essentially unchanged. In addition, AAA-associated T cells were enriched in ribosomal protein synthesis and T-cell differentiation and activation mechanisms. Zhao *et al*. identified three T-cell subpopulations in elastase-induced AAA and control mice, one of which accounted for the majority of T cells (*Ly6c2*, *Cd8a*, *Cd8b1*) (T 1).[72] The other subpopulations were defined by *Gzma* (T 2), which is specific to cytotoxic T cells and NK cells, and *Cd4* and *Il2ra* (T 3), the latter of which is characteristic of T_{regs}. During the progression of AAA, the cytotoxic T and NK cell-like cluster was proportionally increased on day 7 and restored on day 14. In contrast, the other two clusters were decreased on day 7 and restored on day 14. A different study in mice showed T cells to be enriched in the function of NK-cell activation (*Klrb1c*, *Il2rb*) in response to Ang II infusion.[76] In human ATAA tissues, Li *et al*. found T cells to be the largest cell population and detected a total of 11 distinct clusters that were all expanded compared to control.[81] Three of these clusters comprised CD4^{+} T cells, namely active CD4^{+} T cells (*CREM*, *CXCR6*, *GZMB*), resting CD4^{+} T cells (*CCR7*, *IL7R*, *CCL20*), and T_{regs} (*IL2RA*, *CTLA4*, *TNFRSF18*). In addition, two clusters of CD8^{+} T cells were identified, i.e., active CD8^{+} T cells (*GZMK*, *CRTAM*, *CCL4*) and CD8^{+} terminally differentiated effector T cells (*GNLY*, *PRF1*, *CCL5*). Other clusters consisting of both CD4^{+} and CD8^{+} T cells included heat shock protein (HSP) T cells (*JUN*, *FOS*, *HSPA1A/B*), GTPase of the immune-associated nucleotide-binding protein (GIMAP) T cells (*GIMAP1/4/7*, *MALAT1*), stressed T cells (*JUN*, *FOS*, *DNAJA1*), proliferating T cells (*TUBA1B*, *HMGB1*, *CKS1B*), switched T cells (*TAGLN*, *MYH11*, *TPM1*), and IFN

response T cells (*ISG15*, *IFI44*, *LY6E*). The authors argue that the HSP and IFN response subtypes may have resulted from tissue processing and viral infection, respectively. Finally, Wang *et al.* demonstrated that T cells in human TAA are enriched in pathways such as 'ribosome', 'antigen processing and presentation', and, curiously, 'lipid and atherosclerosis'.[85]

B cells

An AA-associated expansion of B cells is also commonly found by scRNA-seq studies in mice[76,78] and patients[81,84,85]. By contrast, Zhao *et al.* observed a contraction of the B-cell population in IAAs of elastase-induced AAA versus healthy mice.[72] Interestingly, Li *et al.* showed that B cells in aortic tissues from an Ang II-induced AAA mouse model upregulated genes associated with an immunoglobulin-mediated immune response (*Cr2*, *Ighm*), which the authors relate to activation to plasma cells.[76] This is supported by another study using the same mouse model that reports an increase in plasma cells during AAA formation in spite of a decrease in B cells.[79] In the AAA process, B cells were predominantly enriched in B-cell receptor signaling, ribosomal protein synthesis, and NF-κB signaling pathways. In agreement with both aforementioned studies[76,79], Li *et al.* found a considerably expanded population of plasma cells (*MZB1*, *IGHA1*, *SSR4*) in human ATAA compared to control tissues.[81]

Lineage tracing

Single-cell transcriptomics has not only contributed to elucidating the cellular composition of tissues, but also to reconstructing lineage relationships between cells (reviewed in [8,89,90]). Traditional lineage tracing involves the genetic labeling of a cell and subsequent tracking of its progeny in, for instance, mouse model systems. This technique has been widely applied in vascular pathology research, especially in the fields of atherosclerosis[33,35–37,39–41,46,91–93] and AA[75,80]. For instance, Pan *et al.* used genetic lineage tracing to track SMC trans-differentiation in atherosclerotic mice and demonstrated that SMCs differentiate into multiple cell types or states, including macrophage-like cells (*Lgals3*, *Cd52*) and fibrochondrocytes (*Fn1*, *Col1a1/2*).[35] Furthermore, Chen *et al.* generated SMC lineage-tracing mice to establish that abrogation of TGFβ signaling in SMCs combined with hypercholesterolemia induces AAs by reprogramming SMCs into macrophage-like cells as well as into mesenchymal-like stem cells (MSCs) (*Ly6a*, *Cd34*, *Cd44*), from which chondrocytes (*Sox9*), osteoblasts (*Runx2*), and adipocytes (*Ppar γ*) arise.[75]

Alternatively, lineage or differentiation trajectories can be inferred based on scRNA-seq data using various bioinformatics tools (reviewed in [94]). Such tools detect the pattern of a dynamic process, e.g., cell differentiation, and subsequently arrange the transcriptomes of individual cells according to their differentiation status. The majority of computational methods rely on dimensionality reduction for ordering cells along a dimension otherwise known as 'pseudotime'.[8] One of the most commonly applied algorithms that performs such pseudotemporal ordering is Monocle.[95,96] RNA velocity is an alternative technique that infers cell state trajectories based on the splicing dynamics of transcripts.[97] While transcriptome-derived lineage predictions provide more detailed phenotypic information than genetic lineage tracing, they do not necessarily reflect true genetic relationships between cells. Concepts and limitations of cell trajectory inference from scRNA-seq data are reviewed in Tritschler *et al.*[98] In the remainder of this section, we will provide an in-depth discussion of the knowledge of healthy and diseased vasculature owing to scRNA-seq-based trajectory analysis.

Healthy vasculature

Some of the rapidly increasing number of scRNA-seq efforts have generated insights into the lineage of arterial cells in healthy vasculature.[15,17,19,21,23,24] For example, Lukowski *et al.* inferred pseudotime trajectories from mouse scRNA-seq data to define an endothelial hierarchy wherein endovascular progenitor cells (*Pdgfra*, *Il33*, *Sox9*) transition to mature, differentiated endothelial cells (*Sox18*, *Pecam1*, *Fabp4*) in aortic endothelium.[21] In human cardiac (aortic, pulmonary, and coronary) arteries, trajectory analysis arranged vascular SMCs of four clusters into one principal trajectory.[17] The proliferative (*Mt1a/m*, *Fabp4*) and aorta- and pulmonary artery-specific synthetic (*Cytl1*, *Lum*) SMC clusters were located on opposite ends of the differentiation trajectory, with contractile (*Cnn1*, *Rgs5*) and coronary artery-specific synthetic (*Fn1*, *Vcan*) SMCs located roughly in between. Pseudotime analysis has also been employed for obtaining independent evidence for the putative topography of vascular cell subpopulations. For instance, in developing a single-cell transcriptome atlas of murine ECs, Kalucka *et al.* captured the anatomical topography of various EC subtypes alongside the vascular tree.[23] Aside from revealing a differentiation trajectory from arteries to veins via capillaries, this analysis established several markers of, e.g., large arteries (*Fbln5*, *Cytl1*), capillaries (*Rgcc*), and large veins (*Lcn2*) in the brain. In healthy mouse aortas, Yu *et al.* observed that two spatially distributed SMC clusters, namely *Vim*$^{+}$ and *Malat1*$^{+}$ SMCs located in the abdominal and thoracic segments of the aorta, respectively, also developed into opposite differentiation directions.[19]

Atherosclerosis

Vascular cells in atherosclerotic plaques have a tremendous potential for undergoing phenotypic switching, otherwise referred to as phenotypic modulation or de-differentiation. Cell types with considerable differentiation potential include ECs and SMCs. EC plasticity plays a crucial role in atherosclerosis progression by giving rise to plaque-associated mesenchymal cells through EndMT.[54] EndMT can be induced by disturbed blood flow, a major contributor to atherosclerotic plaque formation as illustrated by the preferential development of lesions in vascular segments that are curved or branched. Andueza *et al.* investigated the effect of pro-atherogenic disturbed flow on the transcriptomic profile of ECs through scRNA-seq and single-cell assay for transposase accessible chromatin sequencing (scATAC-seq) of mouse arteries following partial carotid ligation.[99] Trajectory inference analysis revealed extensive endothelial reprogramming, with transitions to not only mesenchymal cells (EndMT) (*Tagln*, *Cnn1*) but also to hematopoietic stem cells (endothelial-to-hematopoietic transition, EndHT) (*Sox7*, *Sox17*), endothelial stem/progenitor cells (*Cd157*, *Sca1*), and an unforeseen immune cell-like phenotype (EndICLT) (*C1qa/b*, *C5ar1*). In a similar scRNA-seq study using a partial carotid ligation mouse model, Li *et al.* found a mechanosensitive *Dkk2*^{high} EC subpopulation that possibly transformed from *Klk8*^{high} ECs under disturbed flow.[100] This *Dkk2*^{high} subpopulation was enriched in biological processes related to flow disturbance, including epithelial-to-mesenchymal transition (EMT) and TGFβ signaling. Another important driver of atherosclerosis that has been shown to trigger endothelial changes is arterial stiffness. Zamani *et al.* performed scRNA-seq of human coronary artery ECs cultured *in vitro* on both physiological and pathological stiffness substrates.[101] RNA velocity analysis showed an EndMT trajectory as well as an unexpected reverse mesenchymal-to-endothelial transition (Mes-to-EndT) that was blocked by high stiffness. This is consistent with a model in which the pro-atherogenic stiffness-induced accumulation of mesenchymal cells is, at least partly, attributable to a reduced conversion back to an endothelial state. Of note, lineage tracing has not only generated insights into EC de-differentiation in atherosclerosis but also into EC differentiation. By integrating lineage-tracing mouse models with pseudotime analysis of scRNA-seq data, Deng *et al.* uncovered that vascular *c-Kit*$^{+}$ stem/progenitor cells in healthy and diseased mouse aortas display endothelial differentiation potential.[93] *c-Kit*$^{+}$ cells contributed not only to endothelial turnover in atheroprone regions during homeostasis but also to endothelial replacement in transplant atherosclerosis. Different from 'regular' atherosclerosis, recipient immune-mediated reactions to donor ECs and SMCs constitute an underlying mechanism in transplant atherosclerosis.[102]

A number of scRNA-seq studies have characterized the trajectories and fates of SMC phenotypic switching given its established role in atherosclerosis.[55,56] In hypercholesterolemic mice, Chattopadhyay *et al.* found that contractile SMCs initially undergo uniform phenotypic modulation, followed by a separation into two distinct modulated SMC clusters (*Lcn2*, *Serpina3n*, and *Lars2*, *C3*).[47] The former subpopulation further diverged into two major lineages, while the latter formed a single lineage that was absent upon *Perk* deletion in SMCs. A recent meta-analysis of murine atherosclerosis scRNA-seq datasets by Conklin *et al.* highlights the power of combining genetic lineage tracing with single-cell transcriptomics.[58] This study inferred re-differentiation trajectories of SMCs through pseudotime analysis and removed uncertainty about cells truly being SMC-derived by performing this analysis on data from SMC lineage-positive cells. They uncovered a multitude of state transition paths, many of which traversed the SEM population (*Vcam1*, *Fn1*). This is in agreement with the notion proposed by Pan *et al.* that SEM cells represent a de-differentiated stem cell-like state that gives rise to other SMC-derived cell types.[35] Interestingly, one trajectory traversed from contractile SMCs (*Myh11*, *Acta2*) to macrophage-like cells (*Lgals3*, *Cd68*) through a proliferative cell subpopulation (*Plk1*, *Birc5*, *Ccna2*). Recent findings by Schlegel *et al.* partially support the presence of SMC-derived macrophages in murine atherosclerotic plaques.[43] Monocytes and *Cx3cr1*$^{-}$ macrophages remained distinct in a pseudotime trajectory, suggesting these macrophages might be derived from a non-myeloid cell origin. However, as *Cx3cr1*$^{-}$ macrophages were enriched in some vascular SMC markers (*Fn1*, *Tagln2*) but not in others (*Myh11*, *Acta2*), their origins remain unclear. In their meta-analysis, Conklin *et al.* also found links connecting SMCs, SEM cells, and fibroblast-like cells.[58] This is consistent with a recent study in which pseudotemporal ordering of a published scRNA-seq dataset of diseased human coronary arteries[33] revealed distinct derivations of fibroblast-like cells from SMCs.[10] Key alterations in gene expression along the transition path included upregulation of inflammation (*C3/7*, *CXCL12*) and ECM (*FBLN1*) genes and downregulation of genes associated with healthy SMCs (*MYH11*, *IGFBP2*, *PPP1R14A*). Lastly, in the study by Li *et al.* on flow effect, disturbed flow induced *Spp1*^{high} SMCs as indicated by their location at the end of the pseudotime trajectory.[100] Interestingly, these SMCs were enriched in genes associated with vascular stiffening (*Thbs1*), osteoblast differentiation (*Mef2c*, *Tnc*), and fibrosis (*Ctgf*, *Col5a1/2*), suggesting a role in arterial stiffness.

Aortic aneurysm

The concept of cellular phenotypic plasticity over a continuous spectrum is not specific to atherosclerosis but is characteristic of AA as well. Cell types that possess the potency to differentiate in AA include not only SMCs but also macrophages and fibroblasts. Through pseudotime trajectory analysis of transcriptomes, Pedroza *et*

al. inferred that modulated SMCs gradually trans-differentiate from SMCs in MFS mice.[73] Additionally, this analysis revealed differentially expressed genes with multiple patterns of gene modulation along the spectrum of phenotypic switching. For instance, some genes were activated relatively early in pseudotime (*Serpine1*, *Klf4*), whereas others peaked at the end of the trajectory (*Tnfrsf11b*, *Vcam1*). In human ATAA, Li *et al.* described two re-differentiation trajectories from contractile SMCs toward (i) inflammatory non-immune cells expressing macrophage-specific genes (*C1QA/B*) and remodeling macrophages (*IGFBP7*, *ADAMTS1*), and (ii) inflammatory non-immune cells showing a T cell-like gene signature (*CXCR4*, *CCL4*) and switched T cells (*TAGLN*, *MYH11*, *TPM1*).[81] Integrated trajectory analysis of this and another scRNA-seq dataset[88] provided more insights into cellular transitions of macrophages and T cells during the formation of human TAA.[85] Interestingly, macrophages and T cells experienced respectively ten and seven different subtypes or states from the normal aorta to TAA along with trajectory progression. Davis *et al.* performed pseudotime analysis of human AAA tissues and inferred a differentiation trajectory from one monocyte cluster to macrophages via another monocyte cluster.[82] The increase in *JMJD3* expression along this trajectory was accompanied by a higher expression of *TNFAIP3*, *IL1B*, and *NFKBIA*. Based on trajectory analysis, Li *et al.* proposed the re-polarization of *Trem2*$^{+}$*Acp5*$^{+}$ osteoclast-like macrophages and M2-like macrophages toward M1-like macrophages in AAA pathogenesis in Ang II-infused mice.[76] During the M2-to-M1 transition, several genes associated with this polarization either increased (*Pgam1*, *Pkm*) or decreased (*Cd36*, *Klf4*) in expression. Furthermore, although a disease-enriched population of *Cd34*$^{+}$*Col1a2*$^{+}$ bone marrow-derived fibrocytes was initially classified as a macrophage subtype, further pseudotime analysis revealed no strong connection between this cluster and other macrophage clusters. Instead, fibrocytes resembled inactivated fibroblasts and tended to differentiate toward fibroblasts and subsequently myofibroblasts. Similarly, another study reconstituted the pseudotime of fibroblasts to predict their transformation over the course of disease in an Ang II-induced AAA mouse model.[79] One fibroblast cluster was identified as the starting point and ultimately differentiated into antigen-presenting (*Cd74*, *H2-Ab11*) and tissue-repair (*Fn1*) fibroblasts. Crucial reprogramming genes were predominantly enriched in immune system regulation (*Cfh*, *Cd55*). Lastly, Sawada *et al.* employed trajectory inference to demonstrate that the previously mentioned Ang II-induced SHF-derived fibroblasts in mice were derived from a fibroblast cluster also present in healthy mice.[77]

Cellular crosstalk

Single-cell transcriptomics also offers the opportunity to decipher cellular communication (reviewed in 9). In particular, cell-cell interactions can be inferred from the coordinated expression of ligands and their cognate receptors. Numerous intercellular signaling pathways are documented in available databases of ligand-receptor pairs.[103] Based on scRNA-seq data, a communication score can be estimated to quantify the potential ligand-receptor interaction between one set of ligand-expressing cells and another set of receptor-expressing cells[9] A communication score is typically computed for each ligand-receptor pair by applying a scoring function, such as expression threshold or product, on the expression of the corresponding genes. In addition, various bioinformatic tools that employ advanced statistical methods for imputing cellular crosstalk from scRNA-seq data have rapidly emerged (reviewed in 104). CellPhoneDB[105] and CellChat[106] are the most widely used computational tools in vascular physiology and pathology research.[10,16,18,19,50,78,79,84–86,107,108] Unlike most methods for cell communication inference, CellPhoneDB and CellChat consider multisubunit protein complexes by assessing whether all subunits of multimeric proteins are simultaneously expressed.[9] This better represents functional ligand-receptor interactions, thereby decreasing the risk of false-positive predictions. Other approaches consider information beyond ligand-receptor pairs, as exemplified by NicheNet[109], a tool that employs a network method to incorporate downstream targets and thereby uncover the activation of intracellular signaling. However, physical proximity is key for most communicative links between cells, and information on the spatial position of cells is lost with scRNA-seq. PIC-seq represents a novel approach for describing physical interactions that combines cell sorting with scRNA-seq to acquire and transcriptionally profile physically interacting cells (PICs).[110] However, to the best of our knowledge, this technique has not yet been applied to study vascular systems. In this section, we provide an overview of the discoveries of healthy and diseased vasculature enabled by cell-cell communication profiling based on scRNA-seq.

Healthy vasculature

A number of scRNA-seq experiments have contributed to elucidating the cell-cell interactions governing vascular homeostasis.[15–19] In a recent study of healthy mouse aortas, one EC subset (*Vcam1*, *Ace*) and one SMC subset (*Malat1*) were located in the center of the cell-to-cell interaction network, suggesting they play a vital role in aorta physiology.[19] Using the CCInx tool[111], Hu *et al.* revealed that cellular crosstalk between vascular SMCs and fibroblasts was predominant in human cardiac arteries and mainly relied on ECM molecules (*COL3A1*, *DCN*, *FN1*).[17] Cell-cell communication between ECs and macrophages through cell surface proteins (*CD74*, *B2M*) and cytokines (*CCL2*,

IL1B) also contributed to maintaining arterial structure and function. Moreover, interactions between ECs and immune cells (*ICAM1*/*VCAM1-ITGB2*) were speculated to increase in atherosclerosis. Another scRNA-seq study profiled cellular communication in both healthy and at-risk vasculature.[16] This study constructed intercellular networks of mouse aortas under normal conditions or with high glucose levels, dietary salt, or fat intake. This analysis revealed strong stromal cell-EC, stromal cell-SMC, and EC-SMC correlations. The last two were considerably diminished in the at-risk aorta, along with decreased interactions of these three cell types within their own subtypes.

Atherosclerosis

Cell-cell communication profiling of plaques has provided potential mechanisms of how cells collaboratively give rise to and advance atherosclerosis. For example, Gu *et al.* discovered enhanced cell intercommunication between a mesenchyme cluster (*Cd248*, *Procr*) and inflammatory cells (*Col1a1-Cd44*, *Ccl2-Ccr2*), especially inflammatory macrophages (*Ms4a6c*, *Gngt2*), in the adventitia of apolipoprotein E (ApoE)-deficient mice.[15] This implies a role for mesenchymal cells in initiating adventitial inflammation in early-stage atherosclerosis. In contrast, through ligand-receptor interaction analyses, Kan *et al.* showed extensive crosstalk between ECs, SMCs, and macrophages in the ascending aorta of mice fed a high-fat diet.[18] This was predominantly facilitated by chemokine signaling (*Cxcl12-Ackr3*, *Ccl6-Ccr2*), suggesting that cell-cell communication drives vascular inflammation in this setting. Ma *et al.*[10] inferred cell-to-cell communication from diseased human coronary artery scRNA-seq data[33] using both CellChat[106] and the network-based modeling method scTalk[112]. This analysis suggested that fibroblasts exert strong signals in laminin (*LAMB2-CD44*) and complement (*C3-C3AR1*) signaling pathways in the plaque microenvironment.[10] In particular, fibroblasts signal to SMCs, T cells, and pericytes through pro-inflammatory and repair molecules such as complement component 3 (C3), fibulin-1 (FBN1), and MMP2. Interestingly, a significant upregulation of these molecules was observed along the SMC-to-fibroblast trajectory as discussed previously. Another study applied CellPhoneDB[105] to the same dataset and found significant ligand-receptor relationships between T-cell-expressed *AREG*, which encodes the cytokine amphiregulin, and its receptors on both SMCs (*ICAM1*, *EGFR*) and macrophages (*ICAM1*).[108] These findings suggest that T cells interact with the aforementioned cell types by secreting amphiregulin, thereby promoting SMC proliferation and irreversible plaque formation. Instead of a bioinformatic tool, Fernandez *et al.*[49] employed an established scoring function that computes the average of the product of ligand and receptor expression of two cell types across all single-cell pairs.[113] This approach was used for predicting cellular interactions that promote the distinct functional and activation states of T cells and/or macrophages (e.g., pro-inflammatory) observed

in atherosclerotic lesions of asymptomatic and symptomatic patients.[49] Overall, T cell-T cell and T cell-macrophage intercellular communications carefully controlled the specialized functions of T cells. A key finding was the predicted interaction of the same ligand *(IL-15*) with distinct receptors on T cells in asymptomatic (*IL15RA*) versus symptomatic (*IL2RB*) plaques, either promoting cell proliferation, migration, and apoptosis inhibition or regulating T_H1 reprogramming and differentiation, respectively. Furthermore, the analysis revealed that while the functional states of macrophages are in part self-regulated, they also rely upon signals from T-cell ligands that bind to, e.g., TLRs. In contrast, Depuydt *et al*. report a limited number of potential ligand-receptor interactions between immune cells in human plaques.[50] This may be a consequence of the absence of T-cell receptor-related genes in the interaction database. Furthermore, in contrast to Fernandez *et al*.[49], this study also included non-immune cells in the analysis which potentially present more prominent cellular crosstalk pathways in the plaque. Indeed, cell intercommunication at the lesion site was most prevalent between myeloid cells, ECs, and SMCs. Interactions between myeloid cells and ECs were primarily associated with chemotaxis (*CCL2/CXCL8-ACKR151*) and extravasation of myeloid cells (*CD44-SELE*, *SELL-CD34*).

Aortic aneurysm

Lastly, intercellular communication inference has enhanced our understanding of the cell-cell interactions that underlie aortic dysfunction and AA development. Cell-cell communication profiling in a BAPN-induced TAAD mouse model uncovered a potential role of macrophages in stimulating tumor necrosis factor (TNF)-mediated SMC apoptosis (*Tnf-Tnfrsf1a*) and the activation of TGFβ signaling in SMCs (*Tgfb1-Tgfbr1*) in early-stage TAAD.[78] In addition, SMCs interact with fibroblasts, macrophages, and ECs via *Fgf1*-mediated paracrine signaling. Through expression thresholding, in which ligand-receptor pairs are considered 'active' if both genes are expressed above a certain threshold, Sawada *et al*. demonstrated enhanced cell-cell interactions among SMC and fibroblast clusters under Ang II infusion in mice.[77] The previously discussed unique subcluster of SHF-derived fibroblasts especially had more potential interactions with another fibroblast cluster from which they originate and with SMCs.

A number of scRNA-seq studies report a role for secreted phosphoprotein 1 (Spp1) in cellular signaling in AA. For instance, analysis of Spp1-mediated cell communication in data of $Fbn1^{C1041G/+}$ mice suggested that Spp1 regulates fibroblast and SMC crosstalk predominantly through the receptor *Itga8/Itgb1*.[73,86] In particular, Spp1 released by modulated SMCs as well as the disease-specific *Spp1*$^{+}$ fibroblast subset discussed previously governs the fibroblast and SMC functional changes that occur during TAA formation. In another study, ligand-receptor analyses revealed enhanced

collagen synthesis to be the most prominent feature of communication between fibroblasts and SMCs in Ang II-induced AAA mice, which was surprising considering that loss of collagen contributes to the development of AAA.[79] Interestingly, *Spp1-a9b1* comprised one of the ligand-receptor pairs either commonly significantly increased (*Spp1-a9b1*, *Fgfr1-Ncam1*) or decreased (*Nrp1-Vegfb*, *Pdgfr-Pdgfd*) in four expanded fibroblast clusters. Yang *et al.*[107] extensively inferred intercellular signaling from published scRNA-seq data of three experimental AAA models[70–72] as well as human AAA[82]. Important predictions include potential SPP1-mediated regulation of SMC phenotypic switching by inflammatory macrophages and altered thrombospondin (THBS) signaling in AAA.[107] This study also highlighted distinct differences between AAA mouse models, as exemplified by a contribution of vascular remodeling and fibrosis to early AAA progression in elastase- but not $CaCl_2$-induced AAA.

Other studies performed a more targeted analysis with a focus on specific interactions or ligand-receptor pairs. For instance, Dawson *et al.* performed junctional analyses of ligand-receptor pairs for *TGFB1-3* and bone morphogenic protein (BMP) ligands in human MFS and control tissues.[83] The highest TGFβ junctional scores were found between activated fibroblasts and all EC types, whereas BMP-mediated communication primarily occurred from de-differentiated ECs to all other non-immune cells. Another study estimated cell-cell and cell-ECM junction scores in ATAA patients and control subjects using the expression product method and found that modulated SMCs (fibromyocytes) exhibit higher junction scores, especially cell-ECM, than other SMC subsets.[81] The results of their analysis with regard to ECs and fibroblasts are discussed above. Cao *et al.* did comprehensively analyze the intercellular communication between immune cells and immune-related SMCs in this dataset, resulting in multiple important findings.[84] First, macrophages and macrophage-like SMCs showed the highest communication capabilities and acted as both signaling senders and receivers. Second, macrophage migration inhibitory factor (MIF) (*MIF-CD74*) and galectin (*LGALS9-CD44*) signaling stimulated SMC trans-differentiation into a macrophage-like phenotype, whereas C-X-C motif chemokine ligand (CXCL) (*CXCL12-CXCR4*) and galectin promoted SMC switching to a T-cell-like phenotype. Finally, the aforementioned signaling pathways together with complement (*C3-C3AR1*) and chemerin (*RARRES2-CMKLR1*) significantly contributed to AA progression by driving immune cell activation and migration. In agreement with the first finding, Wang *et al.* report that macrophages were the most notable signal senders and receivers in both TAA patients and controls, and together with ECs, fibroblasts, and SMCs comprised the most frequently interacting cells.[85] In TAA, their interactions with ECs and fibroblasts were significantly enhanced, whereas those with SMCs were reduced.

Conclusion and Future Perspectives

This review set out to shed light on the contribution that single-cell transcriptomics has made to expanding our knowledge of atherosclerosis and aortic aneurysm. Summarizing scRNA-seq findings has highlighted several remarkable similarities between these vascular pathologies. One striking parallel is an established immune component that is characterized in part by an accumulation of macrophages, some of which exhibit enhanced pro-inflammatory signaling (*Il1b*/*IL1B*, *TNF*). An increase in T cells is another shared feature, and comparable T-cell subsets include cytotoxic $CD8^+$ T cells (*Gzma*/*GZMA*, *Gzmk*/*GZMK*, *Ccl5*/*CCL5*) and T_{regs} (*tnfrsf18*/*TNFRSF18*). Additionally, EC dysfunction may further promote vascular inflammation in both atherosclerosis and AA by facilitating leukocyte recruitment (*Vcam1*/*VCAM1*). Another shared hallmark, as confirmed by trajectory inference, is the phenotypic modulation of SMCs. This phenomenon is often accompanied by an increase in ECM regulation (*Col1a1*/*COL1A1*, *Mgp*/*MGP*). With regard to cellular communication, shared frequently interacting cell types include fibroblasts, ECs, SMCs, and macrophages. Finally, complement signaling is an overlapping pathway that promotes immune cell activation and migration.

Nonetheless, our review also underscores differences between these vascular diseases. Notably, fibroblasts have been more prominently described in AA pathogenesis, whereas in atherosclerosis the immune component has a somewhat more pronounced role. There are also marked dissimilarities in immune cell subsets. For instance, foamy macrophages are a hallmark component of atherosclerotic lesions but were not particularly detected in AA tissues. Although, a $Trem2^+$ osteoclast-like macrophage has been described in AA as well. Instead, AA-associated macrophages contribute to ECM degradation and tissue remodeling by secreting MMPs. Similarly, some T-cell populations are seemingly unique to either atherosclerosis or AA, such as multilineage-committed $CD4^+$ T cells and switched T cells, respectively. Furthermore, within AA a clear plasma cell population has been described, whereas in single-cell studies of atherosclerosis the B cell lineage is not yet fully characterized. A notable discrepancy with regard to SMC modulation is that no equivalent of the SEM intermediate cell state in atherosclerosis has (yet) been identified in AA. Moreover, SMC-derived macrophages are more commonly found in atherosclerotic lesions, while SMCs in AA often activate stress response pathways, consistent with the greater loss of SMCs during AA formation. Other dissimilarities in cellular transitions are that EndMT is specific for atherosclerosis, whereas the re-differentiation of macrophages and fibroblasts occurs predominantly in AA. Major differences in cellular crosstalk include greater communication by T cells and macrophages in atherosclerosis and AA, respectively. Lastly, we did not identify any shared signaling pathways other than complement, with *C3-C3AR1* being the only common ligand-receptor pair.

The scRNA-seq findings presented here have a number of therapeutic implications. First, the disease-enriched cell populations identified through scRNA-seq provide potential therapeutic targets. miR-33 silencing has already been shown to drive plaque regression by reducing inflammatory and Trem2 macrophages.[44] Similarly, the success of the CANTOS (Canakinumab Anti-Inflammatory Thrombosis Outcome Study) trial, which targeted interleukin (IL)-1β[114], may be attributable to its impact on pro-inflammatory macrophages. Conversely, stimulating the aggregation of pro-resolving cell subtypes, such as M2 macrophages, may promote vascular disease regression. The next steps should focus on further elucidating and verifying the specific regulatory mechanisms and functions of these cell populations, in particular at different disease stages. Second, scRNA-seq has uncovered transcriptome factors involved in regulating SMC identity, such as *KLF4*.[37] Therapeutic strategies targeting such factors could manipulate SMC fates, halting disease progression or promoting its reversal. This applies not only to SMC phenotypic switching but also to other pathological transitions, such as EndMT. Of note, another potential approach for interfering with EndMT is to target two of its drivers as confirmed by scRNA-seq, i.e., arterial flow and stiffness. Further research should validate the factors that govern cellular plasticity and elucidate the mechanisms by which it contributes to disease development. Lastly, cellular communication profiling has revealed novel signaling pathways and ligand-receptor pairs that are active in vascular disease and hence consist of potential druggable targets. Examples include the cytokines amphiregulin and Spp1, which are specific for respectively atherosclerosis and AA, and the complement and CXCL signaling pathways, which seemingly contribute to both vascular pathologies. This knowledge provides a basis for therapeutic avenues that may disrupt this cellular crosstalk. However, further investigation is required to enhance our understanding of how this cell-cell communication drives vascular dysfunction and disease development. In particular, intervention studies should clarify whether the aforementioned shared signaling pathways play similar roles in atherosclerosis and AA. Additionally, drug-gene interaction analysis may facilitate the translation of scRNA-seq findings into new therapies by revealing candidate drug-gene interactions.[10]

It is essential for the findings that support novel therapeutic strategies to be corroborated by other studies. However, matching outcomes from different studies is currently being impeded by the considerable variation in transcriptome-based names of cell populations across studies.[58] This is illustrated by the variety of terms used for describing modulated SMCs. Hence, the field would benefit greatly from a unified nomenclature of cell populations. Future research should therefore focus on integrating the publicly available scRNA-seq data, especially for AA, since

meta-analyses in this field are currently lacking. This would not only help gain a comprehensive understanding of current studies but may also to some extent eliminate technical variance among studies, reveal novel cell subsets, and facilitate cross-species comparisons. Inter-species comparisons are of especially great importance considering that for many cell types it remains unclear how populations in mice and humans overlap. Lastly, a consensus in cell population nomenclature would simplify comparisons among vascular diseases.

Current limitations of scRNA-seq provide a multitude of opportunities for the future. One such limitation is the loss of spatial information, which has led to the emergence of spatial transcriptomics. This enables gene expression profiling across tissue space, allowing for pinpointing the location of specific cell populations in the vascular wall. It also helps decipher local networks of cell-cell communication by revealing ligand-receptor interactions between neighboring cells. Several techniques for spatial sequencing have been developed (reviewed in 115), including spatial barcoding and *in situ* hybridization. The application of these approaches in atherosclerosis and AA research would provide a more comprehensive functional landscape of these vascular pathologies. Still, no method is currently able to provide a full scope of the transcriptome at a single-cell resolution, highlighting the need for future advancements to make it an even more powerful tool.

Similarly, combining scRNA-seq with other single-cell omics approaches has the potential to greatly expand our knowledge of healthy and diseased vasculature. Such approaches may profile molecular features such as chromatin accessibility and histone modifications, providing insight into the epigenetic regulation of dynamic gene expression. Other single-cell omics assays measure the proteome or interactions between transcription factors and DNA. Two recent studies combined scRNA-seq with single-cell T-cell receptor sequencing (scTCR-seq) to map the T-cell repertoire in human coronary plaques[108] or human carotid lesions and matched peripheral blood mononuclear cell (PBMC) samples[116], finding evidence of clonal expansion. Future developments in integrative single-cell multi-omics technologies will allow us to measure multiple molecular profiles in the same cell, which will deepen our understanding of the complex biological processes that underlie atherosclerosis and AA development.

Another emerging trend that has the potential to provide profound information is the integration of scRNA-seq data with data from genome-wide association studies (GWASs). GWASs have uncovered numerous common genetic variants associated with vascular diseases, including coronary artery disease (CAD)[117]. However, translating

these genetic loci into biological mechanisms and candidate genes with clinical potential still poses a considerable challenge. To address this issue, three studies intersected GWAS summary statistics with scRNA-seq data of human plaques to map CAD susceptibility loci[50,118] or atherosclerotic and cardiovascular disease traits[51] to specific cell populations, thereby identifying potential atherosclerosis-associated gene-cell pairs. Thus, this approach represents a powerful tool for guiding future mechanistic research and discovering novel cell-specific drug targets for functional testing. Other (future) applications of scRNA-seq, such as understanding sex differences, the translation of observations from mice to men, and cardiovascular precision medicine, are discussed elsewhere.[119,120]

To conclude, single-cell transcriptomics has proven to be of tremendous value in the field of atherosclerosis and AA. On account of scRNA-seq, cell populations in the diseased vascular wall have been shown to be much more heterogeneous and dynamic than previously thought. Moreover, our understanding of cellular plasticity and cell-cell communication in disease pathogenesis has vastly improved. Still, the growing amount of scRNA-seq data amplifies the need for integrated analyses to unify cell population nomenclature and facilitate cross-species comparisons. Promising future opportunities lie in the combination of scRNA-seq with complementary technologies, such as spatial transcriptomics. We believe scRNA-seq will be instrumental in elucidating the molecular mechanisms underlying atherosclerosis and AA and in identifying candidate actionable pathways for drug discovery.

References

1. Roth, R., Kim, S., Kim, J. & Rhee, S. Single-cell and spatial transcriptomics approaches of cardiovascular development and disease. *BMB Rep* **53**, 393–399 (2020).
2. Tsao, C. W. *et al.* Heart Disease and Stroke Statistics-2022 Update: A Report From the American Heart Association. *Circulation* **145**, E153–E639 (2022).
3. Libby, P. *et al.* Atherosclerosis. *Nat Rev Dis Primers* **5**, 1–18 (2019).
4. Sakalihasan, N. *et al.* Abdominal aortic aneurysms. *Nat Rev Dis Primers* **4**, 1–22 (2018).
5. Senser, E. M., Misra, S. & Henkin, S. Thoracic Aortic Aneurysm: A Clinical Review. *Cardiol Clin* **39**, 505–515 (2021).
6. Tang, F. *et al.* mRNA-Seq whole-transcriptome analysis of a single cell. *Nat Methods* **6**, 377–382 (2009).
7. Nguyen, A., Khoo, W. H., Moran, I., Croucher, P. I. & Phan, T. G. Single cell RNA sequencing of rare immune cell populations. *Front Immunol* **9**, 1553 (2018).
8. Kester, L. & van Oudenaarden, A. Single-Cell Transcriptomics Meets Lineage Tracing. *Cell Stem Cell* **23**, 166–179 (2018).
9. Armingol, E., Officer, A., Harismendy, O. & Lewis, N. E. Deciphering cell–cell interactions and communication from gene expression. *Nat Rev Genet* **22**, 71–88 (2020).
10. Ma, W. F. *et al.* Enhanced single-cell RNA-seq workflow reveals coronary artery disease cellular cross-talk and candidate drug targets. *Atherosclerosis* **340**, 12–22 (2022).
11. Ma, W. F. *et al.* PlaqView 2.0: A comprehensive web portal for cardiovascular single-cell genomics. *Front Cardiovasc Med* **9**, (2022).
12. Yap, C., Mieremet, A., De Vries, C. J. M., Micha, D. & De Waard, V. Six Shades of Vascular Smooth Muscle Cells Illuminated by KLF4 (Krüppel-Like Factor 4). *Arterioscler Thromb Vasc Biol* **41**, 2693–2707 (2021).
13. Galkina, E. *et al.* Lymphocyte recruitment into the aortic wall before and during development of atherosclerosis is partially L-selectin dependent. *J Exp Med* **203**, 1273–1282 (2006).
14. Chavkin, N. W. & Hirschi, K. K. Single Cell Analysis in Vascular Biology. *Front Cardiovasc Med* **7**, 42 (2020).
15. Gu, W. *et al.* Adventitial Cell Atlas of wt (Wild Type) and ApoE (Apolipoprotein E)-Deficient Mice Defined by Single-Cell RNA Sequencing. *Arterioscler Thromb Vasc Biol* **39**, 1055–1071 (2019).
16. He, D. *et al.* Aortic heterogeneity across segments and under high fat/salt/glucose conditions at the single-cell level. *Natl Sci Rev* **7**, 881–896 (2020).
17. Hu, Z. *et al.* Single-Cell Transcriptomic Atlas of Different Human Cardiac Arteries Identifies Cell Types Associated With Vascular Physiology. *Arterioscler Thromb Vasc Biol* **41**, 1408–1427 (2021).
18. Kan, H. *et al.* Single-cell transcriptome analysis reveals cellular heterogeneity in the ascending aortas of normal and high-fat diet-fed mice. *Exp Mol Med* **53**, 1379–1389 (2021).
19. Yu, L. *et al.* An intersegmental single-cell profile reveals aortic heterogeneity and identifies a novel Malat1+ vascular smooth muscle subtype involved in abdominal aortic aneurysm formation. *Signal Transduct Target Ther* **7**, 1–14 (2022).
20. Kalluri, A. S. *et al.* Single-Cell Analysis of the Normal Mouse Aorta Reveals Functionally Distinct Endothelial Cell Populations. *Circulation* **140**, 147–163 (2019).
21. Lukowski, S. W. *et al.* Single-Cell Transcriptional Profiling of Aortic Endothelium Identifies a Hierarchy from Endovascular Progenitors to Differentiated Cells. *Cell Rep* **27**, 2748-2758.e3 (2019).

22. Jambusaria, A. *et al.* Endothelial heterogeneity across distinct vascular beds during homeostasis and inflammation. *Elife* **9**, (2020).
23. Kalucka, J. *et al.* Single-Cell Transcriptome Atlas of Murine Endothelial Cells. *Cell* **180**, 764-779. e20 (2020).
24. Gao, Y. K. *et al.* A regulator of G protein signaling 5 marked subpopulation of vascular smooth muscle cells is lost during vascular disease. *PLoS One* **17**, (2022).
25. Dobnikar, L. *et al.* Disease-relevant transcriptional signatures identified in individual smooth muscle cells from healthy mouse vessels. *Nat Commun* **9**, 1–17 (2018).
26. Tang, J. *et al.* Arterial Sca1+ Vascular Stem Cells Generate De Novo Smooth Muscle for Artery Repair and Regeneration. *Cell Stem Cell* **26**, 81-96.e4 (2020).
27. Weinberger, T. *et al.* Ontogeny of arterial macrophages defines their functions in homeostasis and inflammation. *Nat Commun* **11**, 1–16 (2020).
28. Cochain, C. *et al.* Single-Cell RNA-Seq Reveals the Transcriptional Landscape and Heterogeneity of Aortic Macrophages in Murine Atherosclerosis. *Circ Res* **122**, 1661–1674 (2018).
29. Jones, R. C. *et al.* The Tabula Sapiens: A multiple-organ, single-cell transcriptomic atlas of humans. *Science (1979)* **376**, (2022).
30. Elmentaite, R., Domínguez Conde, C., Yang, L. & Teichmann, S. A. Single-cell atlases: shared and tissue-specific cell types across human organs. *Nature Reviews Genetics 2022 23:7* **23**, 395–410 (2022).
31. Winkels, H. *et al.* Atlas of the Immune Cell Repertoire in Mouse Atherosclerosis Defined by Single-Cell RNA-Sequencing and Mass Cytometry. *Circ Res* **122**, 1675–1688 (2018).
32. Kim, K. *et al.* Transcriptome analysis reveals nonfoamy rather than foamy plaque macrophages are proinflammatory in atherosclerotic murine models. *Circ Res* **123**, 1127–1142 (2018).
33. Wirka, R. C. *et al.* Atheroprotective roles of smooth muscle cell phenotypic modulation and the TCF21 disease gene as revealed by single-cell analysis. *Nat Med* **25**, 1280–1289 (2019).
34. Lin, J. Da *et al.* Single-cell analysis of fate-mapped macrophages reveals heterogeneity, including stem-like properties, during atherosclerosis progression and regression. *JCI Insight* **4**, (2019).
35. Pan, H. *et al.* Single-Cell Genomics Reveals a Novel Cell State During Smooth Muscle Cell Phenotypic Switching and Potential Therapeutic Targets for Atherosclerosis in Mouse and Human. *Circulation* **142**, 2060–2075 (2020).
36. Williams, J. W. *et al.* Limited proliferation capacity of aortic intima resident macrophages requires monocyte recruitment for atherosclerotic plaque progression. *Nat Immunol* **21**, 1194–1204 (2020).
37. Alencar, G. F. *et al.* Stem Cell Pluripotency Genes Klf4 and Oct4 Regulate Complex SMC Phenotypic Changes Critical in Late-Stage Atherosclerotic Lesion Pathogenesis. *Circulation* **142**, 2045–2059 (2020).
38. Vafadarnejad, E. *et al.* Dynamics of Cardiac Neutrophil Diversity in Murine Myocardial Infarction. *Circ Res* **127**, E232–E249 (2020).
39. Wang, Y. *et al.* Clonally expanding smooth muscle cells promote atherosclerosis by escaping efferocytosis and activating the complement cascade. *Proceedings of the National Academy of Sciences* **117**, 15818–15826 (2020).
40. Kim, J. B. *et al.* Environment-sensing aryl hydrocarbon receptor inhibits the chondrogenic fate of modulated smooth muscle cells in atherosclerotic lesions. *Circulation* **142**, 575–590 (2020).
41. Wolf, D. *et al.* Pathogenic Autoimmunity in Atherosclerosis Evolves From Initially Protective Apolipoprotein B100-Reactive CD4+ T-Regulatory Cells. *Circulation* **142**, 1279–1293 (2020).
42. Sharma, M. *et al.* Regulatory T Cells License Macrophage Pro-Resolving Functions During Atherosclerosis Regression. *Circ Res* **127**, 335–353 (2020).

43. Schlegel, M. *et al.* Silencing Myeloid Netrin-1 Induces Inflammation Resolution and Plaque Regression. *Circ Res* **129**, 530–546 (2021).
44. Afonso, M. S. *et al.* miR-33 Silencing Reprograms the Immune Cell Landscape in Atherosclerotic Plaques. *Circ Res* **128**, 1122–1138 (2021).
45. Burger, F. *et al.* Single-Cell RNA-Seq Reveals a Crosstalk between Hyaluronan Receptor LYVE-1-Expressing Macrophages and Vascular Smooth Muscle Cells. *Cells* **11**, (2022).
46. Brandt, K. J. *et al.* Single-Cell Analysis Uncovers Osteoblast Factor Growth Differentiation Factor 10 as Mediator of Vascular Smooth Muscle Cell Phenotypic Modulation Associated with Plaque Rupture in Human Carotid Artery Disease. *Int J Mol Sci* **23**, (2022).
47. Chattopadhyay, A. *et al.* Preventing Cholesterol-Induced Perk (Protein Kinase RNA-Like Endoplasmic Reticulum Kinase) Signaling in Smooth Muscle Cells Blocks Atherosclerotic Plaque Formation. *Arterioscler Thromb Vasc Biol* **42**, 1005–1022 (2022).
48. Yao, F. *et al.* Histone Variant H2A.Z Is Required for the Maintenance of Smooth Muscle Cell Identity as Revealed by Single-Cell Transcriptomics. *Circulation* **138**, 2274–2288 (2018).
49. Fernandez, D. M. *et al.* Single-cell immune landscape of human atherosclerotic plaques. *Nat Med* **25**, 1576–1588 (2019).
50. Depuydt, M. A. C. *et al.* Microanatomy of the Human Atherosclerotic Plaque by Single-Cell Transcriptomics. *Circ Res* **127**, 1437–1455 (2020).
51. Slenders, L. *et al.* Intersecting single-cell transcriptomics and genome-wide association studies identifies crucial cell populations and candidate genes for atherosclerosis. *European Heart Journal Open* **2**, (2021).
52. Alsaigh, T., Evans, D., Frankel, D. & Torkamani, A. Decoding the transcriptome of calcified atherosclerotic plaque at single-cell resolution. *Commun Biol* **5**, 1–17 (2022).
53. Biswas, I., Khan, G. A., Biswas, I. & Khan, G. A. Endothelial Dysfunction in Cardiovascular Diseases. *Basic and Clinical Understanding of Microcirculation* (2019) doi:10.5772/INTECHOPEN.89365.
54. Souilhol, C., Harmsen, M. C., Evans, P. C. & Krenning, G. Endothelial-mesenchymal transition in atherosclerosis. *Cardiovasc Res* **114**, 565–577 (2018).
55. Bennett, M. R., Sinha, S. & Owens, G. K. Vascular Smooth Muscle Cells in Atherosclerosis. *Circ Res* **118**, 692–702 (2016).
56. Gomez, D. & Owens, G. K. Smooth muscle cell phenotypic switching in atherosclerosis. *Cardiovasc Res* **95**, 156–164 (2012).
57. Holmes, C. & Stanford, W. L. Concise review: stem cell antigen-1: expression, function, and enigma. *Stem Cells* **25**, 1339–1347 (2007).
58. Conklin, A. C. *et al.* Meta-Analysis of Smooth Muscle Lineage Transcriptomes in Atherosclerosis and Their Relationships to In Vitro Models. *Immunometabolism* **3**, (2021).
59. Zhang, Z., Huang, J., Wang, Y. & Shen, W. Transcriptome analysis revealed a two-step transformation of vascular smooth muscle cells to macrophage-like cells. *Atherosclerosis* **346**, 26–35 (2022).
60. Zernecke, A. *et al.* Meta-analysis of leukocyte diversity in atherosclerotic mouse aortas. *Circ Res* **127**, 402–426 (2020).
61. Cochain, C., Saliba, A. E. & Zernecke, A. Letter by Cochain et al regarding article, "Transcriptome analysis reveals nonfoamy rather than foamy plaque macrophages are proinflammatory in atherosclerotic murine models". *Circ Res* **123**, E49–E48 (2018).
62. Kim, K. & Choi, J. H. Response by Kim and Choi to Letter Regarding Article, 'Transcriptome Analysis Reveals Nonfoamy Rather Than Foamy Plaque Macrophages Are Proinflammatory in Atherosclerotic Murine Models'. *Circ Res* **123**, E50 (2018).

63. Zernecke, A. *et al.* Integrated single-cell analysis based classification of vascular mononuclear phagocytes in mouse and human atherosclerosis. *Cardiovasc Res* (2022) doi:10.1093/CVR/CVAC161.
64. Jonasson, L., Holm, J., Skalli, O., Bondjers, G. & Hansson, G. K. Regional Accumulations of T Cells, Macrophages, and Smooth Muscle Cells in the Human Atherosclerotic Plaque. *Arteriosclerosis* **6**, 131–138 (1986).
65. Hansson, G. K. & Jonasson, L. The discovery of cellular immunity in the atherosclerotic plaque. *Arterioscler Thromb Vasc Biol* **29**, 1714–1717 (2009).
66. Winkels, H. & Wolf, D. Heterogeneity of T Cells in Atherosclerosis Defined by Single-Cell RNA-Sequencing and Cytometry by Time of Flight. *Arterioscler Thromb Vasc Biol* **41**, 549–563 (2021).
67. Butcher, M. J. *et al.* Atherosclerosis-Driven Treg Plasticity Results in Formation of a Dysfunctional Subset of Plastic IFNγ+ Th1/Tregs. *Circ Res* **119**, 1190–1203 (2016).
68. Srikakulapu, P. *et al.* Artery Tertiary Lymphoid Organs Control Multilayered Territorialized Atherosclerosis B-Cell Responses in Aged ApoE-/- Mice. *Arterioscler Thromb Vasc Biol* **36**, 1174–1185 (2016).
69. Silvestre-Roig, C. *et al.* Externalized histone H4 orchestrates chronic inflammation by inducing lytic cell death. *Nature* **569**, 236–240 (2019).
70. Hadi, T. *et al.* Macrophage-derived netrin-1 promotes abdominal aortic aneurysm formation by activating MMP3 in vascular smooth muscle cells. *Nat Commun* **9**, 1–16 (2018).
71. Yang, H., Zhou, T., Stranz, A., Deroo, E. & Liu, B. Single-Cell RNA Sequencing Reveals Heterogeneity of Vascular Cells in Early Stage Murine Abdominal Aortic Aneurysm-Brief Report. *Arterioscler Thromb Vasc Biol* **41**, 1158–1166 (2021).
72. Zhao, G. *et al.* Single-cell RNA sequencing reveals the cellular heterogeneity of aneurysmal infrarenal abdominal aorta. *Cardiovasc Res* **117**, 1402–1416 (2021).
73. Pedroza, A. J. *et al.* Single Cell Transcriptomic Profiling of Vascular Smooth Muscle Cell Phenotype Modulation in Marfan Syndrome Aortic Aneurysm. *Arterioscler Thromb Vasc Biol* **40**, 2195 (2020).
74. Luo, W. *et al.* Critical Role of Cytosolic DNA and Its Sensing Adaptor STING in Aortic Degeneration, Dissection, and Rupture. *Circulation* **141**, 42–66 (2020).
75. Chen, P. Y. *et al.* Smooth Muscle Cell Reprogramming in Aortic Aneurysms. *Cell Stem Cell* **26**, 557 (2020).
76. Li, B. *et al.* Single-Cell Transcriptome Profiles Reveal Fibrocytes as Potential Targets of Cell Therapies for Abdominal Aortic Aneurysm. *Front Cardiovasc Med* **8**, 1635 (2021).
77. Sawada, H. *et al.* Second Heart Field-Derived Cells Contribute to Angiotensin II-Mediated Ascending Aortopathies. *Circulation* **145**, 987–1001 (2022).
78. Liu, X. *et al.* Single-cell RNA sequencing identifies an Il1rn+/Trem1+ macrophage subpopulation as a cellular target for mitigating the progression of thoracic aortic aneurysm and dissection. *Cell Discov* **8**, 1–21 (2022).
79. Weng, Y. *et al.* Single-Cell RNA Sequencing Technology Revealed the Pivotal Role of Fibroblast Heterogeneity in Angiotensin II-Induced Abdominal Aortic Aneurysms. *DNA Cell Biol* **41**, 498–520 (2022).
80. Pedroza, A. J. *et al.* Embryologic Origin Influences Smooth Muscle Cell Phenotypic Modulation Signatures in Murine Marfan Syndrome Aortic Aneurysm. *Arterioscler Thromb Vasc Biol* **42**, 1154–1168 (2022).

81. Li, Y. *et al.* Single-Cell Transcriptome Analysis Reveals Dynamic Cell Populations and Differential Gene Expression Patterns in Control and Aneurysmal Human Aortic Tissue. *Circulation* **142**, 1374–1388 (2020).
82. Davis, F. M. *et al.* Inhibition of macrophage histone demethylase JMJD3 protects against abdominal aortic aneurysms. *J Exp Med* **218**, (2021).
83. Dawson, A. *et al.* Single-Cell Analysis of Aneurysmal Aortic Tissue in Patients with Marfan Syndrome Reveals Dysfunctional TGF-beta Signaling. *Genes (Basel)* **13**, 95 (2021).
84. Cao, G. *et al.* Deciphering the Intercellular Communication Between Immune Cells and Altered Vascular Smooth Muscle Cell Phenotypes in Aortic Aneurysm From Single-Cell Transcriptome Data. *Front Cardiovasc Med* **9**, (2022).
85. Wang, Q. *et al.* Integrating Bulk Transcriptome and Single-Cell RNA Sequencing Data Reveals the Landscape of the Immune Microenvironment in Thoracic Aortic Aneurysms. *Front Cardiovasc Med* **9**, (2022).
86. Zhou, M. *et al.* Fibroblast-Secreted Phosphoprotein 1 Mediates Extracellular Matrix Deposition and Inhibits Smooth Muscle Cell Contractility in Marfan Syndrome Aortic Aneurysm. *J Cardiovasc Transl Res* (2022) doi:10.1007/S12265-022-10239-8.
87. Cheng, S. *et al.* Identification of key monocytes/macrophages related gene set of the early-stage abdominal aortic aneurysm by integrated bioinformatics analysis and experimental validation. *Front Cardiovasc Med* **9**, (2022).
88. Folkersen, L. *et al.* Unraveling divergent gene expression profiles in bicuspid and tricuspid aortic valve patients with thoracic aortic dilatation: the ASAP study. *Molecular medicine* **17**, 1365–1373 (2011).
89. Chen, C., Liao, Y. & Peng, G. Connecting past and present: single-cell lineage tracing. *Protein Cell* **13**, 790 (2022).
90. Wagner, D. E. & Klein, A. M. Lineage tracing meets single-cell omics: opportunities and challenges. *Nat Rev Genet* **21**, 410–427 (2020).
91. Shankman, L. S. *et al.* KLF4-dependent phenotypic modulation of smooth muscle cells has a key role in atherosclerotic plaque pathogenesis. *Nat Med* **21**, 628–637 (2015).
92. Gaddis, D. E. *et al.* Apolipoprotein AI prevents regulatory to follicular helper T cell switching during atherosclerosis. *Nat Commun* **9**, 1–15 (2018).
93. Deng, J. *et al.* Single-cell gene profiling and lineage tracing analyses revealed novel mechanisms of endothelial repair by progenitors. *Cellular and Molecular Life Sciences* **77**, 5299–5320 (2020).
94. Saelens, W., Cannoodt, R., Todorov, H. & Saeys, Y. A comparison of single-cell trajectory inference methods. *Nat Biotechnol* **37**, 547–554 (2019).
95. Trapnell, C. *et al.* The dynamics and regulators of cell fate decisions are revealed by pseudotemporal ordering of single cells. *Nat Biotechnol* **32**, 381–386 (2014).
96. Qiu, X. *et al.* Reversed graph embedding resolves complex single-cell trajectories. *Nat Methods* **14**, 979–982 (2017).
97. La Manno, G. *et al.* RNA velocity of single cells. *Nature* **560**, 494–498 (2018).
98. Tritschler, S. *et al.* Concepts and limitations for learning developmental trajectories from single cell genomics. *Development (Cambridge)* **146**, (2019).
99. Andueza, A. *et al.* Endothelial Reprogramming by Disturbed Flow Revealed by Single-Cell RNA and Chromatin Accessibility Study. *Cell Rep* **33**, (2020).
100. Li, F. *et al.* Single-cell RNA-seq reveals cellular heterogeneity of mouse carotid artery under disturbed flow. *Cell Death Discov* **7**, (2021).

101. Zamani, M. *et al.* Single-Cell Transcriptomic Census of Endothelial Changes Induced by Matrix Stiffness and the Association with Atherosclerosis. *Adv Funct Mater* 2203069 (2022) doi:10.1002/ADFM.202203069.
102. Von Rossum, A., Laher, I. & Choy, J. C. Immune-mediated vascular injury and dysfunction in transplant arteriosclerosis. *Front Immunol* **5**, (2015).
103. Ramilowski, J. A. *et al.* A draft network of ligand–receptor-mediated multicellular signalling in human. *Nat Commun* **6**, 1–12 (2015).
104. Almet, A. A., Cang, Z., Jin, S. & Nie, Q. The landscape of cell-cell communication through single-cell transcriptomics. *Curr Opin Syst Biol* **26**, 12–23 (2021).
105. Efremova, M., Vento-Tormo, M., Teichmann, S. A. & Vento-Tormo, R. CellPhoneDB: inferring cell–cell communication from combined expression of multi-subunit ligand–receptor complexes. *Nat Protoc* **15**, 1484–1506 (2020).
106. Jin, S. *et al.* Inference and analysis of cell-cell communication using CellChat. *Nat Commun* **12**, 1–20 (2021).
107. Yang, H., DeRoo, E., Zhou, T. & Liu, B. Deciphering Cell-Cell Communication in Abdominal Aortic Aneurysm From Single-Cell RNA Transcriptomic Data. *Front Cardiovasc Med* **9**, 831789 (2022).
108. Chowdhury, R. R. *et al.* Human Coronary Plaque T Cells Are Clonal and Cross-React to Virus and Self. *Circ Res* **130**, 1510–1530 (2022).
109. Browaeys, R., Saelens, W. & Saeys, Y. NicheNet: modeling intercellular communication by linking ligands to target genes. *Nat Methods* **17**, 159–162 (2019).
110. Giladi, A. *et al.* Dissecting cellular crosstalk by sequencing physically interacting cells. *Nat Biotechnol* **38**, 629–637 (2020).
111. Ximerakis, M. *et al.* Single-cell transcriptomic profiling of the aging mouse brain. *Nat Neurosci* **22**, 1696–1708 (2019).
112. Farbehi, N. *et al.* Single-cell expression profiling reveals dynamic flux of cardiac stromal, vascular and immune cells in health and injury. *Elife* **8**, (2019).
113. Kumar, M. P. *et al.* Analysis of Single-Cell RNA-Seq Identifies Cell-Cell Communication Associated with Tumor Characteristics. *Cell Rep* **25**, 1458-1468.e4 (2018).
114. Ridker, P. M. *et al.* Antiinflammatory Therapy with Canakinumab for Atherosclerotic Disease. *N Engl J Med* **377**, 1119–1131 (2017).
115. Longo, S. K., Guo, M. G., Ji, A. L. & Khavari, P. A. Integrating single-cell and spatial transcriptomics to elucidate intercellular tissue dynamics. *Nat Rev Genet* **22**, 627–644 (2021).
116. Depuydt, M. A. C. *et al.* Single-cell T cell receptor sequencing of paired human atherosclerotic plaques and blood reveals autoimmune-like features of expanded effector T cells. *Nature Cardiovascular Research 2023 2:2* **2**, 112–125 (2023).
117. Aragam, K. G. *et al.* Discovery and systematic characterization of risk variants and genes for coronary artery disease in over a million participants. *Nat Genet* **54**, 1803–1815 (2022).
118. Örd, T. *et al.* Single-Cell Epigenomics and Functional Fine-Mapping of Atherosclerosis GWAS Loci. *Circ Res* **129**, 240–258 (2021).
119. Slenders, L., Tessels, D. E., Laan, S. W. van der, Pasterkamp, G. & Mokry, M. The Applications of Single-Cell RNA Sequencing in Atherosclerotic Disease. *Front Cardiovasc Med* **9**, 826103 (2022).
120. Fernandez, D. M. & Giannarelli, C. Immune cell profiling in atherosclerosis: role in research and precision medicine. *Nat Rev Cardiol* **19**, 43–58 (2022).

Chapter 3

Microanatomy of the human atherosclerotic plaque by single-cell transcriptomics

Circulation Research 2020; 127:1437-1455

Marie A.C. Depuydt[1#], Koen H.M. Prange[2#], Lotte Slenders[3#], Tiit Örd[4], Danny Elbersen[5], Arjan Boltjes[3], Saskia C.A. de Jager[5], Folkert W. Asselbergs[3], Gert J. de Borst[6], Einari Aavik[4], Tapio Lönnberg[7], Esther Lutgens[2,8], Christopher K. Glass[9,10], Hester M. den Ruijter[11], Minna U. Kaikkonen[4], Ilze Bot[1], Bram Slütter[1], Sander W. van der Laan[3], Seppo Yla-Herttuala[4], Michal Mokry[3,11*], Johan Kuiper[1*], Menno P.J. de Winther[2,8*], Gerard Pasterkamp[3*]

1. Leiden Academic Centre for Drug Research, Division of Biotherapeutics, Leiden University, The Netherlands
2. Amsterdam University Medical Centers – location AMC, University of Amsterdam, Experimental Vascular Biology, Department of Medical Biochemistry, Amsterdam Cardiovascular Sciences, Amsterdam Infection and Immunity, The Netherlands
3. Laboratory of Clinical Chemistry and Haematology, University Medical Center, The Netherlands.
4. A.I.Virtanen Institute for Molecular Sciences, University of Eastern Finland, Finland
5. Laboratory for Experimental Cardiology, University Medical Center Utrecht, The Netherlands
6. Department of Vascular Surgery, University Medical Centre Utrecht, Heidelberglaan 100, Utrecht, The Netherlands
7. Turku Bioscience Centre, University of Turku and Åbo Akademi University, 20520 Turku, Finland
8. Institute for Cardiovascular Prevention (IPEK), Munich, Germany & German Center for Cardiovascular Research (DZHK), partner site Munich Heart Alliance, Munich, Germany
9. Cell and Molecular Medicine, University of California San Diego, San Diego, CA, USA
10. School of Medicine, University of California San Diego, San Diego, CA, USA
11. Department of Cardiology, University Medical Center Utrecht The Netherlands

#These authors contributed equally; *Shared last authors

Abstract

Rationale: Atherosclerotic lesions are known for their cellular heterogeneity, yet the molecular complexity within the cells of human plaques have not been fully assessed.

Objective: Using single-cell transcriptomics and chromatin accessibility we gained a better understanding of the pathophysiology underlying human atherosclerosis.

Methods and Results: We performed single-cell RNA and single-cell ATAC sequencing on human carotid atherosclerotic plaques to define the cells at play and determine their transcriptomic and epigenomic characteristics. We identified 14 distinct cell populations including endothelial cells, smooth muscle cells, mast cells, B cells, myeloid cells, and T cells and identified multiple cellular activation states and suggested cellular interconversions. Within the endothelial cell population we defined subsets with angiogenic capacity plus clear signs of endothelial to mesenchymal transition. $CD4^+$ and $CD8^+$ T cells showed activation-based subclasses, each with a gradual decline from a cytotoxic to a more quiescent phenotype. Myeloid cells included two populations of pro-inflammatory macrophages showing IL1B or TNF expression as well as a foam cell-like population expressing TREM2 and displaying a fibrosis-promoting phenotype. ATACseq data identified specific transcription factors associated with the myeloid subpopulation and T cell cytokine profiles underlying mutual activation between both cell types. Finally, cardiovascular disease susceptibility genes identified using public GWAS data were particularly enriched in lesional macrophages, endothelial and smooth muscle cells.

Conclusion: This study provides a transcriptome-based cellular landscape of human atherosclerotic plaques and highlights cellular plasticity and intercellular communication at the site of disease. This detailed definition of cell communities at play in atherosclerosis will facilitate cell-based mapping of novel interventional targets with direct functional relevance for the treatment of human disease.

Key words: atherosclerosis, single-cell RNA sequencing, single-cell ATAC sequencing, GWAS

Non-standard Abbreviations and Acronyms.

CVD	cardiovascular disease
GWAS	genome-wide association studies
CyTOF	cytometry by time of flight
scRNA-seq	single cell RNA sequencing
scATAC-seq	single cell ATAC sequencing
FACS	fluorescence-activated cell sorting
SMC	smooth muscle cell
EndoMT	endothelial to mesenchymal transition
MACE	major adverse cardiovascular events
TF	transcription factor
(ox)LDL	(oxidized) low-density lipoprotein
DC	dendritic cell
EC	endothelial cell
CAD	coronary artery disease
DEG	differentially expressed gene
LoF	loss-of-function

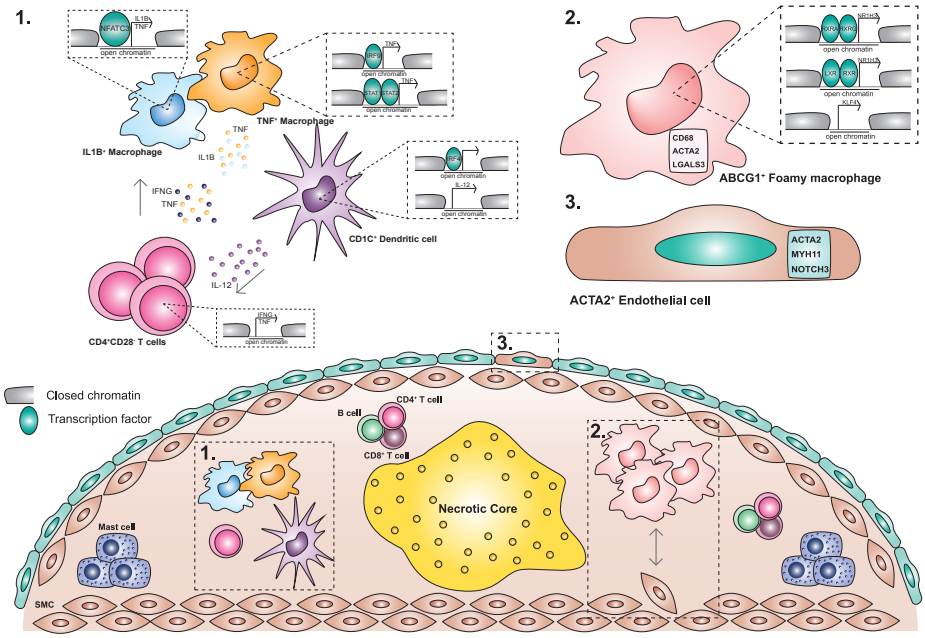

Graphical Abstract. Microanatomy of the human atherosclerotic plaque through scRNA-seq and scATAC-seq. Schematic overview of the retrieved cells in the human plaque, highlighting the local inflammation as found through the IL12-IFNγ axis between dendritic cells, $CD4^+CD28^-$ T cells and macrophages (1); the LXR_RXR induced foam cell phenotype (2) and the cellular plasticity in the plaque as seen by the $ACTA2^+$ macrophages and the $ACTA2^+$ endothelial cells that potentially undergo EndoMT .

Novelty and significance

What is known?

- Atherosclerotic lesions show a complex cellular composition that has mainly been studied using selected marker molecules
- The benefit of using single-cell RNA sequencing as unbiased method has been shown for immune cells in both murine and human atherosclerosis

What new information does this article contribute?

- Single-cell RNA sequencing of a broad cohort of human carotid plaques now provides a detailed cellular atlas of the various cell types and their phenotypes, including different clusters of endothelial and smooth muscle cells.
- Chromatin accessibility of macrophages and T cells is mapped at a single cell level and identifies relevant transcription factor binding sites.
- Mapping of cardiovascular susceptibility genes identified by GWAS to cellular subsets identifies potential cell specific targets.

It is important to determine the exact cell (sub)types and their interactions at play in atherosclerosis in order to devise novel therapeutic strategies. Here, we describe the total cellular composition of atherosclerotic plaques taken from carotid arteries of a broad cohort of patients. Our data suggests that the main immune cell subset consists of T cells, which can be subdivided by activation status. Macrophages are found in distinct populations with diverse activation patterns, inflammatory status, and foam cell characteristics. We shed light on plaque endothelial and smooth muscle cell gene expression and show cell clusters with gene expression patterns pointing towards characteristics of endothelial to mesenchymal transition. To further investigate the dynamic intra-plaque niche, we assessed ligand-receptor interactions driving our cell communities and investigated potential transcription factor activity underlying myeloid and T cell populations in the plaque by studying chromatin accessibility at the single cell level. Finally, we identified cell types enriched for cardiovascular susceptibility genes by integrating available GWAS data. Together, our data provide an in-depth map of the human atherosclerotic plaque and give valuable insights into cell types, pathways, and genes that are relevant for future research aiming at the development of novel therapeutic strategies.

Introduction

Atherosclerosis is characterized by chronic, lipid-driven vascular inflammation and is the main underlying cause of cardiovascular disease (CVD).[1] Many studies have defined cellular profiles of human atherosclerosis based on single or several marker proteins, but detailed description of the cells involved in the pathophysiology of atherogenesis is lacking. Moreover, genome-wide association studies (GWAS) have identified many loci associated with increased risk for CVD, but the translation of these findings into new therapies[2] has been hampered by the lack of information on specific cell communities in atherosclerotic plaques and the cell-specific expression patterns of druggable candidate genes at the site of disease. Recently, the immune cell composition of murine and human aortic atherosclerotic plaques has been described using cytometry by time of flight (CyTOF) and single cell RNA sequencing (scRNA-seq).[3-7] Yet, the full cellular composition of human carotid plaques, including non-immune cells, remains elusive. Therefore, we performed scRNA-seq and single-cell ATAC sequencing (scATAC-seq) on advanced human atherosclerotic plaques obtained during carotid endarterectomy and report a comprehensive overview of the various cell types in plaques and their activation status, which reveals an active, ongoing inflammation and multiple cellular interactions as well as cellular plasticity with respect to endothelial cells and macrophages. In addition, we identified cell type specific expression of GWAS risk loci for CVD.

Methods

Please see the Online Data Supplement for detailed methods.

Results

Single-cell RNA sequencing identifies 14 distinct cell populations in human atherosclerotic plaques

To examine the transcriptome of human atherosclerotic plaques, carotid endarterectomy tissue from 18 patients (77% male sex) was enzymatically digested, viable nucleated cells were isolated by fluorescence-activated cell sorting (FACS) (**Figure 1A**, **Online Figure 1A**, **Online Table 1**) and scRNA-seq libraries were prepared. After filtering cells based on the number of reported genes (see online methods), we applied unbiased clustering on 3282 cells, identifying 14 cell populations (**Figure 1B**, **C**, **Online Table 2**). Correlation of our scRNA-seq data with bulk RNA-seq

data (**Online Figure 1B**) and examining inter-patient variation of cluster distribution (**Online Figure 1C**) and size (**Online Figure 1D**) confirmed uniformity of the data except for patient 1. We assigned a cell type to each cluster based on differential expression of established lineage markers (**Figure 1B, D**). Cluster composition did not differ between sexes (**Online Figure 1E**) and cluster identities were confirmed by correlation with bulk RNA-seq datasets (**Figure 1E**).[8] We observed three non-immune cell clusters (clusters 8, 9 and 10; expressing *CD34* and *ACTA2*)[9,10] and eleven leukocyte clusters (**Figure 1B, D**). The latter included five lymphocyte clusters (clusters 0, 1, 3, 4, and 11; expressing *CD3E*, *CD4*, *CD8*, *CD79A*)[11,12], five myeloid clusters (clusters 5, 6, 7, 12 and 13; expressing *CD14*, *CD68*, *KIT*)[13–16], and one cluster containing a mixture of cells (cluster 2), which did not show a clear cell type-defining expression profile, but had similar gene expression levels as other clusters and seemed to mainly contain apoptotic myeloid and T cells (**Figure 1B, D, Online Figure 2A-D**). T cells appeared to be the most abundant population in our data set, encompassing 52.4% of all analyzed cells, whereas the myeloid populations represented 18.5% of all cells (**Online Figure 2E**). Histological analysis of matched samples confirmed that $CD3^+$ T cells indeed outnumbered the $CD68^+$ cells, which represent macrophages and to a limited extend smooth muscle cells[17], in the studied samples (number of $CD3^+$ T cells: 1880±449 vs. number of $CD68^+$ cells: 870±135) (**Online Figure 2F**).

ECs exhibited a gene expression profile indicative of activation and potential transdifferentiation

Endothelial cells were represented by cluster 9; expressing *COL4A1*, COL4A2, *SPARCL1*, and *PLVAP*, and cluster 10; expressing *MPZL2*, *SULF1*, *VWF*, and *EDN1* (**Figure 1B**, **C**, **Online Table** 2). Isolating and reclustering these clusters revealed four distinct subclasses (E.0-E.3, **Figure 2A**, **Online Table 2**). We could assign endothelial cell phenotypes to the subclasses by assessing marker genes (**Figure 2B**). E.0, E.1, and E.2 displayed classical endothelial markers *CD34* and *PECAM1*, and the vascular endothelial marker *TIE1*. E.0 showed distinct expression of *ACKR1*, which has been associated with venous endothelial cells and the vasa vasorum in mice[18,19] and *PRCP*[20], involved in angiogenesis and regeneration of damaged endothelium (**Figure 2B, C**). E.1 and E.2 separated on expression of extracellular matrix genes in E.1 and cell mobility markers *FGF18* and *HEG1* in E.2. Both populations expressed *VCAM1* (**Figure 2C**), which is expressed by activated endothelium and facilitates adhesion and transmigration of leukocytes such as monocytes and T cells.[21] Together, this suggests that E.0, E.1, and E.2 represent activated endothelium which actively aggravate inflammation in the advanced lesion by cell adhesion and neovascularization and mediating leukocyte extravasation.[22] Of note, subclass E.3 expressed typical smooth muscle cell markers such as *ACTA2*, *NOTCH3*, and *MYH11* next to the aforementioned endothelial markers

(**Figure 2C**). This, combined with its clustering among the endothelial cell clusters and enrichment of transitory and SMC related pathways (**Figure 2D**) indicated that this subset may be undergoing endothelial to mesenchymal transition (EndoMT) or vice-versa. To validate these findings we looked into the expression of ACTA2 and CD34 on sequential histological slides. **Figure 2E** shows cells lining the intraplaque vasculature that show overlapping expression.

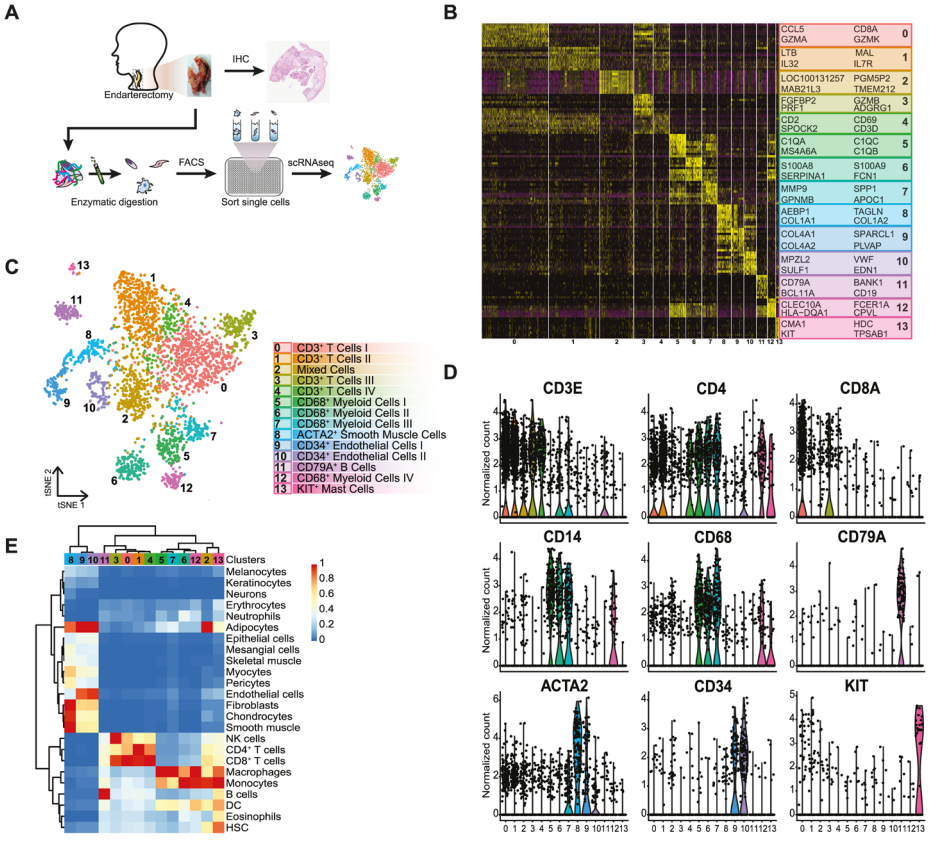

Figure 1. CCA clustering and tSNE visualization revealed 14 distinct populations. A) Experimental setup: plaque samples obtained from endarterectomy procedures were digested, single viable cells were FACS sorted in a PCR plate, and CEL-seq2 was performed. B) Heatmap of top marker genes per cluster. C) tSNE visualization of clustering revealed 14 cell populations. Population identities were determined based on marker gene expression. D) Violin plots of signature genes confirmed population identities, as well as E) by similarity to known cell type in reference RNA-seq data sets.

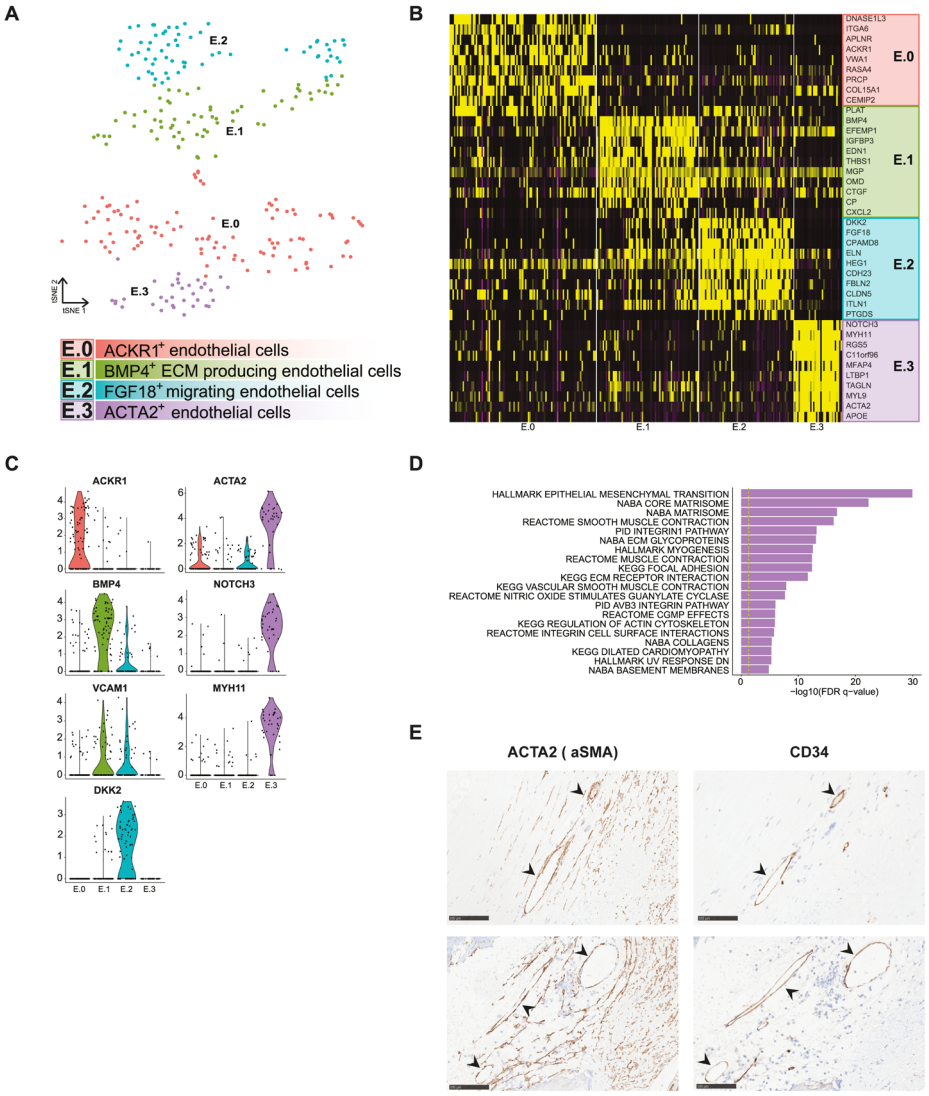

Figure 2. Subclustering of endothelial cells revealed 4 distinct populations. A) tSNE visualization of clustering revealed 4 distinct endothelial cell populations. B) Heatmap of top marker genes per cluster. C) Violin plots of endothelial cell-specific markers, genes involved in endothelial cell angiogenesis and activation and genes that are associated with EndoMT. D) Top pathways associated with cluster E.3. E) Examples of ACTA2 and CD34 expression in a monolayer of cells lining intraplaque vasculature on sequential histological slides of two different patients. Scale bars represent 100µm.

Synthetic phenotype dominates in plaque smooth muscle cells

Smooth muscle cells were represented by cluster 8; expressing *MYH11*, *PDGFRB*, *NOTCH3* and *MFAP4*[23-25] (**Figure 1B**, **C**, **Online Table 2**), which separated into two subclasses (**Online Figure 3A**): a cluster of SMCs with contractile characteristics (cluster S.1; expressing *MYH11*, *ACTA2* and *TAGLN*), and a cluster of synthetic-like SMCs (cluster S.0; expressing *COL1A1*, *MGP* and *COL3A1*)[26] (**Online Figure 3B**, **C**, **Online Table 2**). The low expression of typical SMC markers in cluster S.0 and upregulation of extracellular matrix genes suggested that a subset of these cells were derived from the established cap portion of the plaque. A limited number of cells within this cluster was *KLF4*$^{+}$ (**Online Figure 3D**), indicative of differentiation from vascular smooth muscle cells into either a synthetic or macrophage-like phenotype.

Intraplaque T cells are defined by activation status

Lymphocyte clusters consisted of one small, but homogenous cluster of B cells (cluster 11; expressing *CD79A*, *FCER2*, *CD22* and *CD79B*)[27-29] (**Figure 1B**, **C**, **Online Table 2**), and four T cell clusters. To define the T cells in more detail, we assessed the CD4^{+} T cells (expression *CD4* > *CD8*) and the CD8^{+} T cells (expression *CD8* > *CD4*) from *CD3* enriched clusters 0, 1, 3 and 4. Isolating and reclustering the CD4^{+} T cells revealed five subclasses (CD4.0-CD4.4, **Figure 3A**, **Online Table 2**) of which the primary difference was their activation state rather than the transcription factors and cytokines commonly used to define CD4^{+} T helper subsets (Figure 3B, C). CD4.0 and CD4.1 exerted a cytotoxic gene expression profile exemplified by expression of *GZMA*, *GZMK* and *PRF1*. Apart from these cytotoxic transcripts, cells in CD4.0 also showed very little *CD28* expression and some *GZMB* expression, suggesting that these cells are cytotoxic CD4^{+}CD28^{null} cells, that have previously been correlated with unstable angina and increased risk of Major Adverse Cardiovascular Events (MACE).[30,31] In addition, gene expression in this cluster confirmed an enrichment in pro-inflammatory pathways associated with adaptive immune responses (**Figure 3D**). Using flow cytometry, we confirmed the cytotoxic character of the CD4^{+}CD28^{null} cells, which showed that significantly more CD4^{+}CD28^{-} cells contained granzyme B as compared to the CD4^{+}CD28^{+} cells (**Figure 3E**, **Online Figure 4A**). CD4.2 and CD4.4 were characterized by expression of *IL7R, LEF1* and *SELL*, associated with a naïve and central-memory phenotype. The final CD4^{+} subclass (CD4.3) was identified as a regulatory T cell cluster based on the expression of the classical markers *FOXP3*, *IL2RA* (CD25) and *CTLA4*[32] (**Figure 3B**, **Online Table 2**). Interestingly, we also found some co-expression of FOXP3 with transcription factors RORA and GATA3 in this cluster (**Online Figure 4B**), which has respectively been associated with the enhanced immunosuppressive function of regulatory T cells[33] and with the prevention of polarization towards other T_H subsets[34]. Expression of the T helper (T_H) cell subset-

specific transcription factors *TBX21* (Tbet; Th1), *GATA3* (Th2) and *RORC* (RORγT; Th17) was not linked to a specific cluster (Online Figure 4C), which seems to be a common phenomenon when dealing with T cell scRNA-seq data.[35,36] By analyzing the CD4$^+$ T cells in a clustering-independent method by selecting all cells that have the expression of both CD3E and CD4 and subsequently analyzing the expression of single T_H specific transcription factors we find that a large population of T cells did not express a clear signal of the transcription factors (**Online Figure 4D**).

Analysis of CD8$^+$ T cells revealed three subclasses (**Online Figure 5A**, **B**), which were similarly to CD4$^+$ T cells defined by differences in activation state. CD8.0 was identified as an effector-memory subset, characterized by expression of *GZMK*, *GZMA*, and *CD69*, indicating recent T cell receptor activity (**Online Figure 5C**). A clear, terminally differentiated, cytotoxic CD8$^+$ T cell profile was observed in CD8.1, which showed expression of *GZMB*, *TBX21*, *NKG7*, *GNLY*, *ZNF683* and *CX3CR1* and in line, this subclass lacked *CD69* expression. Finally, CD8.2 displayed a quiescent, central-memory CD8$^+$ T cell phenotype with expression of *LEF1*, *SELL*, *IL7R* and *LTB*. In contrast to Fernandez *et al*.[7] and previous scRNA-seq data obtained from various cancers, we did not detect a clear exhausted phenotype in the CD8$^+$ T cells.[35-37] The CD8 clusters with reduced cytotoxic potential show expression of *CD69* suggesting recent TCR activation and it will be of future interest to examine how these CD8$^+$ populations were activated and how they affect the pathogenesis of atherosclerosis. This could indicate that not the cytotoxic, but the more quiescent CD8$^+$ T cell-subsets are responding to plaque-specific antigens and may be more relevant in the pathogenesis of atherosclerosis. Using experimental mouse models of atherosclerosis it has been shown that the majority of CD8$^+$ T cells in the plaque are antigen-specific[38], but so far little is known regarding the plaque-antigen(s) they respond to. Whereas CD4$^+$ T cells have been shown to respond to (ox)LDL and its related apoB100 peptide, plaque-antigen(s) for CD8$^+$ remain mostly indefinable.[39] Therefore, we are unable to define which antigens have activated the T cells in the atherosclerotic lesion.

Figure 3. Subclustering of CD4$^+$ T cells revealed 5 distinct populations. A) tSNE visualization of clustering revealed 5 distinct CD4$^+$ T cell populations. B) Dotplot of cluster-identifying genes and T cell transcription factors. C) Violin plots of CD4.0 characterizing cytotoxic genes. D) Flow cytometry analysis of Granzyme B production by CD4$^+$CD28$^-$ cells on defrosted plaque samples. E). Top pathways associated with cluster CD4.0. Data shown as mean±SD (n = 10; obtained from cohort 1 and 2). *p<0.05. ►

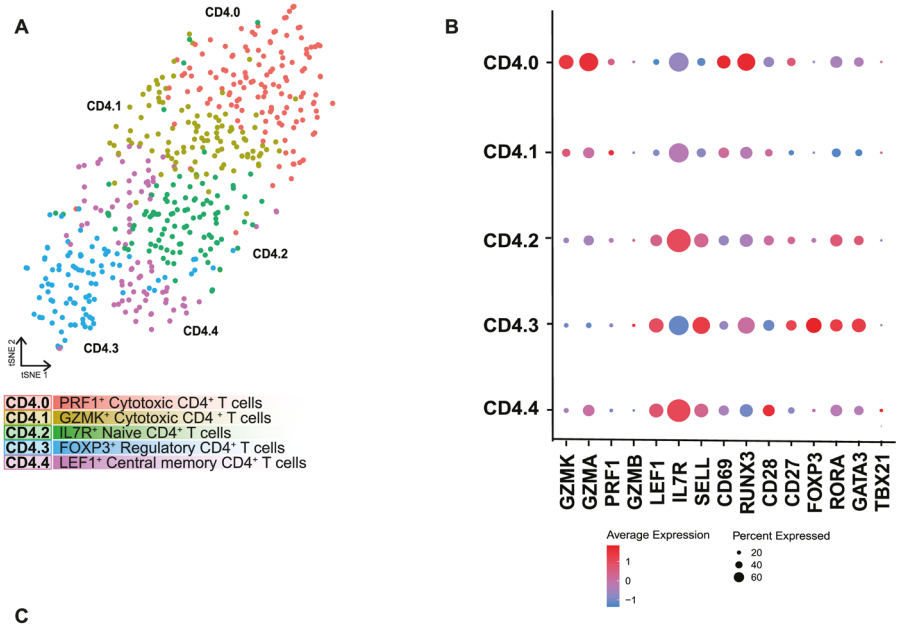
A
CD4.0
CD4.1
CD4.2
CD4.3
CD4.4
tSNE 2
tSNE 1
CD4.0 PRF1+ Cytotoxic CD4+ T cells
CD4.1 GZMK+ Cytotoxic CD4 + T cells
CD4.2 IL7R+ Naive CD4+ T cells
CD4.3 FOXP3+ Regulatory CD4+ T cells
CD4.4 LEF1+ Central memory CD4+ T cells
B
CD4.0
CD4.1
CD4.2
CD4.3
CD4.4
GZMK
GZMA
PRF1
GZMB
LEF1
IL7R
SELL
CD69
RUNX3
CD28
CD27
FOXP3
RORA
GATA3
TBX21
Average Expression
1
0
−1
Percent Expressed
20
40
60

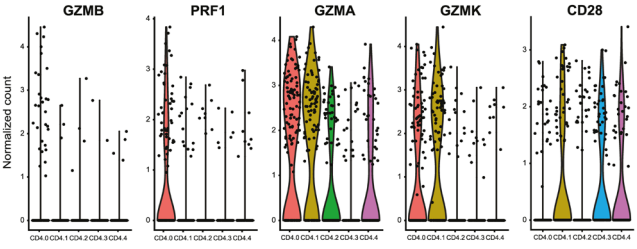
C
GZMB
PRF1
GZMA
GZMK
CD28
Normalized count
CD4.0 CD4.1 CD4.2 CD4.3 CD4.4

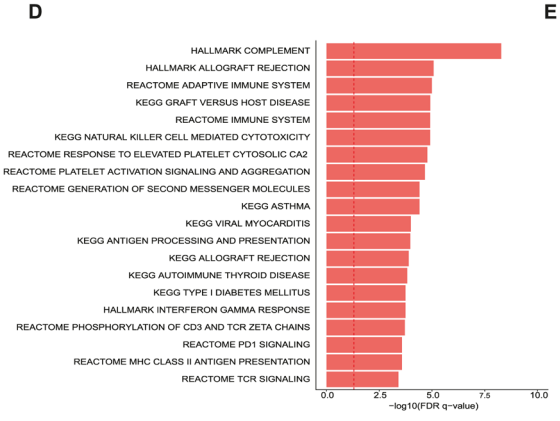
D
HALLMARK COMPLEMENT
HALLMARK ALLOGRAFT REJECTION
REACTOME ADAPTIVE IMMUNE SYSTEM
KEGG GRAFT VERSUS HOST DISEASE
REACTOME IMMUNE SYSTEM
KEGG NATURAL KILLER CELL MEDIATED CYTOTOXICITY
REACTOME RESPONSE TO ELEVATED PLATELET CYTOSOLIC CA2
REACTOME PLATELET ACTIVATION SIGNALING AND AGGREGATION
REACTOME GENERATION OF SECOND MESSENGER MOLECULES
KEGG ASTHMA
KEGG VIRAL MYOCARDITIS
KEGG ANTIGEN PROCESSING AND PRESENTATION
KEGG ALLOGRAFT REJECTION
KEGG AUTOIMMUNE THYROID DISEASE
KEGG TYPE I DIABETES MELLITUS
HALLMARK INTERFERON GAMMA RESPONSE
REACTOME PHOSPHORYLATION OF CD3 AND TCR ZETA CHAINS
REACTOME PD1 SIGNALING
REACTOME MHC CLASS II ANTIGEN PRESENTATION
REACTOME TCR SIGNALING
0.0
2.5
5.0
7.5
10.0
−log10(FDR q−value)

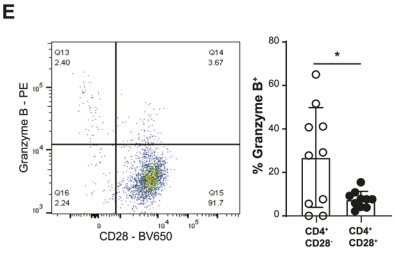
E
Granzyme B - PE
CD28 - BV650
Q13
2.40
Q14
3.67
Q16
2.24
Q15
91.7
% Granzyme B+
CD4+ CD28-
CD4+ CD28+
*

Both pro- and anti-inflammatory macrophage populations reside in the plaque

Atherosclerotic myeloid cells were represented by five clusters. A small, distinct mast cell population was defined by expression of *HDC*, *KIT*, *CMA1* and *TPSAB1*.[40] The remaining myeloid clusters, cluster 6, 7, 8, and 12, expressed *CD14* and *CD68* (**Figure 1B**, **C**) and isolating and reclustering of these cells revealed five distinct phenotypes (My.0-My.4, **Figure 4A**, **Online Figure 6A**, **Online Table 2**).

My.0, My.1 and My.2 most likely represented different macrophage activation states. Enrichment of pro-inflammatory marker genes (**Figure 4B**) and immune- and inflammatory pathways (**Figure 4C**) indicated that subclasses My.0 and My.1 consisted of pro-inflammatory macrophages. My.0 showed characteristics of recently recruited macrophages (''Leukocyte transendothelial migration'', Figure 4C and ''Leukocyte extravasation signaling'', **Figure 4D**) displaying inflammasome activation based on co-expression of *IL1B*, *CASP1* and *CASP4* (**Figure 4B**, **Online Figure 6B**). My.1 represented macrophages that differentially expressed *TNF* and toll-like receptors (**Figure 4B**). Interestingly, both My.0 and My.1 expressed *KLF4*, albeit at a low level, which is known to drive macrophages towards an anti-inflammatory phenotype by repressing the NF-κB gene program.[41] Our data may suggest that an inhibitory feedback loop in the pro-inflammatory macrophage populations is actively mediated by KLF4 expression.

In contrast to My.0 and My.1, My.2 showed absence of clear pro-inflammatory markers and showed signs of macrophages and foam cells. It expressed foam cell marker genes *ABCA1*[42], *ABCG1*, *MMP9*, and *OLR1*[43] (**Figure 4B**, **Online Figure 6A**), pro-fibrotic markers such as *TREM2* and *CD9*[44,45], and the enrichment of metabolic pathways hinted at a shift in metabolism (**Figure 4C** bottom). Interestingly, My.2 cells expressed smooth muscle actin (*ACTA2*), a hallmark of smooth muscle cells, in combination with macrophage markers such as *LGALS3* and *CD68* (**Online Figure 6C**, **D**). Expression of myeloid lineage transcription factors (TFs) PU.1 (SPI1) and C/EBPβ (CEBPB)[46] and absence of SMC lineage TFs myocardin (MYOCD) and MRTF-A (MRTFA)[47] in specifically the ACTA2^{+} cells of My.2 suggests that part of the My.2 myeloid cells gained characteristics of SMCs rather than that it originated from SMCs[17] (**Online Figure 6E**).

To further characterize the 3 subclasses, we next examined pathways differentially enriched per population (**Figure 4D**) as well as the upstream regulators that possibly govern these populations by Ingenuity Pathway Analysis (IPA; **Figure 4E**). My.0 and My.1 showed enrichment for classical inflammatory and immune pathways clearly suggesting cellular activation, recruitment and immune cell interactions driving their phenotype. In line, IPA predicted that My.0 and My.1 are mainly controlled by pro-inflammatory factors such as IL1A, IFNA, INFG and IL1B.

My.2 was enriched for metabolic pathways and LXR/RXR activation, consistent with a foamy phenotype. Hence, this cluster was uniquely driven by anti-inflammatory pathways such as STAT6 and had typical foam cell-related factors including APOE and the LXR family (Nr1h: NR1H2,3,4), which interestingly showed some overlap with My.1. The latter may indicate that unlike the more recently recruited My.0, My.1 cells are gaining foamy characteristics.

My.3 is characterized by dendritic cell (DC) markers such as *CD1C*, *CLEC10A*, and *FCER1A* **Online Figure 6A**) and this population most likely represents CD1c^{+} DCs.[13,48,49] In line with their DC phenotype, this cluster showed the highest expression of multiple class II HLA genes indicative of their enhanced activation status as a consequence of antigen-specific interaction with plaque T cells (**Online Figure 6F**). Cluster My.4 expressed *CD3E*, *GNLY*, *FOXP3*, and *CD2,* suggesting that My.4 potentially contains regulatory T cells. This mis-clustering might be a result of comparable CD4 expression levels in T cells and macrophages, since myeloid cells frequently expressed CD4 (**Online Figure 1E**).

Finally, we compared our macrophage subclasses with monocyte and macrophage populations from four recent papers on scRNA-seq analysis of atherosclerotic plaques in mice.[3–6] Eight mouse populations showed significant overlap with our human subclasses (**Figure 4F**). My.0 showed no statistically significant overlap, but most resembled inflammatory mouse macrophages (**Figure 4G**). My.1 resembled inflammatory, resident-like mouse macrophages, and My.2 overlapped with foamy, anti-inflammatory, Trem2^{+} macrophages. Together, this confirms the recently migrated and embedded inflammatory phenotypes we defined respectively for My.0 and My.1, and matches the foamy phenotype we saw in My.2. It also showcases a decent concordance between human patients and mouse models in relation to cell type diversity.

Intercellular communication drives inflammation within the plaque

We next examined potential ligand-receptor interactions between cell types to predict intercellular communication within the lesion based on CellPhone DB v2.0[50]. Lymphocytes and mast cells showed the lowest absolute numbers of potential interactions while myeloid, endothelial, and SMCs displayed higher numbers of interactions (**Figure 5A**). The low interaction between myeloid and T cells may be a consequence of the apparent lack of detection of TCR-related genes (*TRA, TRB, TRG)* in our scRNAseq dataset and the fact that CD4-class II and CD8-class I interactions are not included in this database.

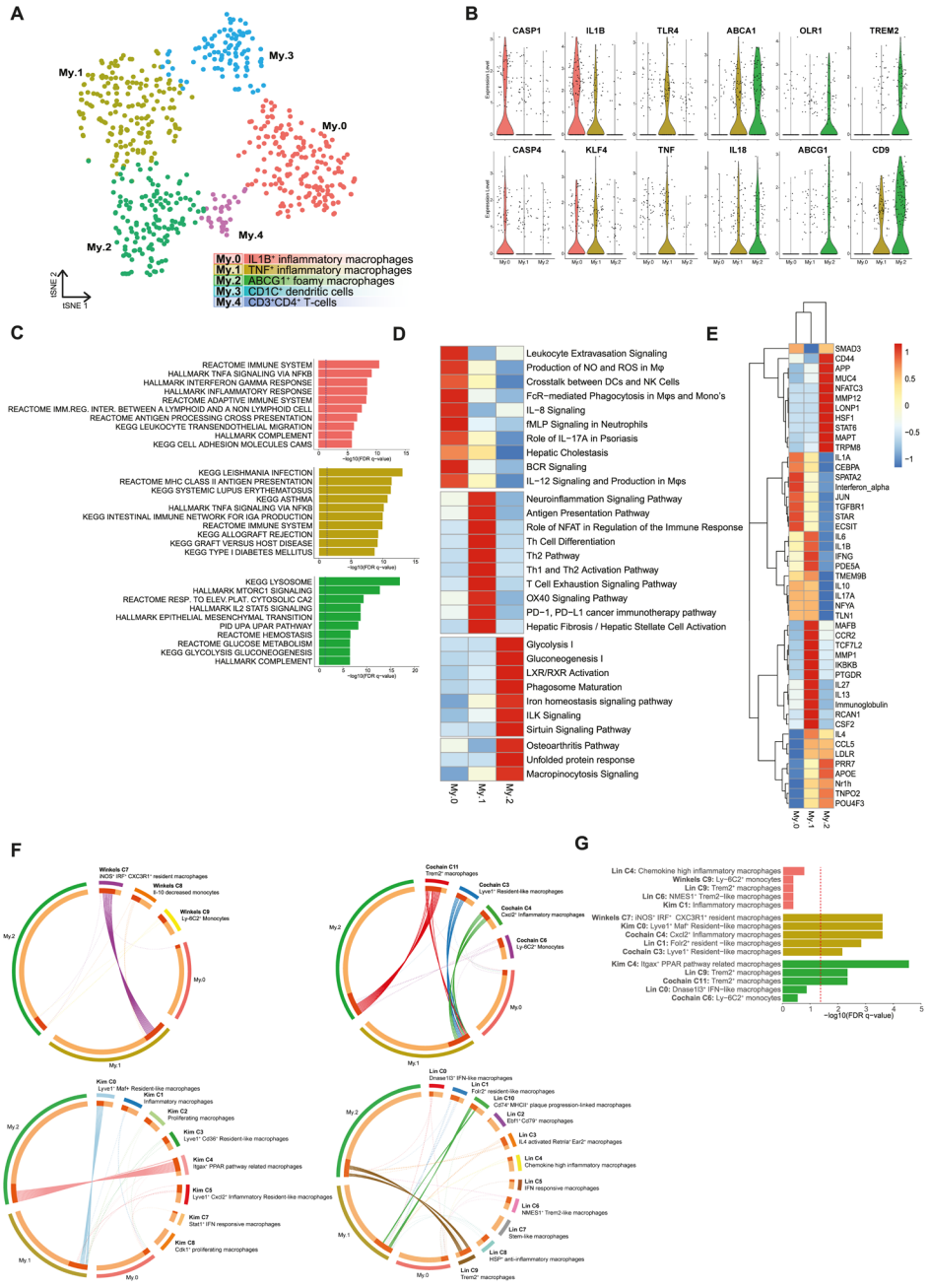
A
My.1
My.3
My.0
My.2
My.4
My.0 IL1B+ inflammatory macrophages
My.1 TNF+ inflammatory macrophages
My.2 ABCG1+ foamy macrophages
My.3 CD1C+ dendritic cells
My.4 CD3+CD4+ T-cells
tSNE 2
tSNE 1
B
CASP1
IL1B
TLR4
ABCA1
OLR1
TREM2
CASP4
KLF4
TNF
IL18
ABCG1
CD9
C
REACTOME IMMUNE SYSTEM
HALLMARK TNFA SIGNALING VIA NFKB
HALLMARK INTERFERON GAMMA RESPONSE
HALLMARK INFLAMMATORY RESPONSE
REACTOME ADAPTIVE IMMUNE SYSTEM
REACTOME IMM.REG. INTER. BETWEEN A LYMPHOID AND A NON LYMPHOID CELL
REACTOME ANTIGEN PROCESSING CROSS PRESENTATION
KEGG LEUKOCYTE TRANSENDOTHELIAL MIGRATION
HALLMARK COMPLEMENT
KEGG CELL ADHESION MOLECULES CAMS
KEGG LEISHMANIA INFECTION
REACTOME MHC CLASS II ANTIGEN PRESENTATION
KEGG SYSTEMIC LUPUS ERYTHEMATOSUS
KEGG ASTHMA
HALLMARK TNFA SIGNALING VIA NFKB
KEGG INTESTINAL IMMUNE NETWORK FOR IGA PRODUCTION
REACTOME IMMUNE SYSTEM
KEGG ALLOGRAFT REJECTION
KEGG GRAFT VERSUS HOST DISEASE
KEGG TYPE I DIABETES MELLITUS
KEGG LYSOSOME
HALLMARK MTORC1 SIGNALING
REACTOME RESP. TO ELEV.PLAT. CYTOSOLIC CA2
HALLMARK IL2 STAT5 SIGNALING
HALLMARK EPITHELIAL MESENCHYMAL TRANSITION
PID UPA UPAR PATHWAY
REACTOME HEMOSTASIS
REACTOME GLUCOSE METABOLISM
KEGG GLYCOLYSIS GLUCONEOGENESIS
HALLMARK COMPLEMENT
−log10(FDR q−value)
D
Leukocyte Extravasation Signaling
Production of NO and ROS in Mφ
Crosstalk between DCs and NK Cells
FcR−mediated Phagocytosis in Mφs and Mono's
IL−8 Signaling
fMLP Signaling in Neutrophils
Role of IL−17A in Psoriasis
Hepatic Cholestasis
BCR Signaling
IL−12 Signaling and Production in Mφs
Neuroinflammation Signaling Pathway
Antigen Presentation Pathway
Role of NFAT in Regulation of the Immune Response
Th Cell Differentiation
Th2 Pathway
Th1 and Th2 Activation Pathway
T Cell Exhaustion Signaling Pathway
OX40 Signaling Pathway
PD−1, PD−L1 cancer immunotherapy pathway
Hepatic Fibrosis / Hepatic Stellate Cell Activation
Glycolysis I
Gluconeogenesis I
LXR/RXR Activation
Phagosome Maturation
Iron homeostasis signaling pathway
ILK Signaling
Sirtuin Signaling Pathway
Osteoarthritis Pathway
Unfolded protein response
Macropinocytosis Signaling
My.0
My.1
My.2
E
SMAD3
CD44
APP
MUC4
NFATC3
MMP12
LONP1
HSF1
STAT6
MAPT
TRPM8
IL1A
CEBPA
SPATA2
Interferon_alpha
JUN
TGFBR1
STAR
ECSIT
IL6
IL1B
IFNG
PDE5A
TMEM9B
IL10
IL17A
NFYA
TLN1
MAFB
CCR2
TCF7L2
MMP1
IKBKB
PTGDR
IL27
IL13
Immunoglobulin
RCAN1
CSF2
IL4
CCL5
LDLR
PRR7
APOE
Nr1h
TNPO2
POU4F3
F
Winkels C7: iNOS+ IRF+ CXC3R1+ resident macrophages
Winkels C8: IL-10 decreased monocytes
Winkels C9: Ly-6C2+ Monocytes
Cochain C11: Trem2+ macrophages
Cochain C3: Lyve1+ Resident-like macrophages
Cochain C4: Cxcl2+ Inflammatory macrophages
Cochain C8: Ly-6C2+ Monocytes
Kim C0: Lyve1+ Maf+ Resident-like macrophages
Kim C1: Inflammatory macrophages
Kim C2: Proliferating macrophages
Kim C3: Lyve1+ Cd36+ Resident-like macrophages
Kim C4: Itgax+ PPAR pathway related macrophages
Kim C5: Lyve1+ Cxcl2+ Inflammatory Resident-like macrophages
Kim C7: Stat1+ IFN responsive macrophages
Kim C8: Cdk1+ proliferating macrophages
Lin C0: Dnase1l3+ IFN-like macrophages
Lin C1: Fcls2+ resident-like macrophages
Lin C10: Cd14+ MHCII+ plaque progression-linked macrophages
Lin C2: Ednrb+ Cd79+ macrophages
Lin C3: IL4 activated Retnla+ Ear2+ macrophages
Lin C4: Chemokine high inflammatory macrophages
Lin C5: IFN responsive macrophages
Lin C6: NME51+ Trem2-like macrophages
Lin C7: Stem-like macrophages
Lin C8: HSP+ anti-inflammatory macrophages
Lin C9: Trem2+ macrophages
My.0
My.1
My.2
G
Lin C4: Chemokine high inflammatory macrophages
Winkels C8: Ly−6C2+ monocytes
Lin C9: Trem2+ macrophages
Lin C6: NME51+ Trem2−like macrophages
Kim C1: Inflammatory macrophages
Winkels C7: iNOS+ IRF+ CXC3R1+ resident macrophages
Kim C0: Lyve1+ Maf+ Resident−like macrophages
Cochain C4: Cxcl2+ Inflammatory macrophages
Lin C1: Fcrl2+ resident −like macrophages
Cochain C3: Lyve1+ Resident−like macrophages
Kim C4: Itgax+ PPAR pathway related macrophages
Lin C9: Trem2+ macrophages
Cochain C11: Trem2+ macrophages
Lin C0: Dnase1l3+ IFN−like macrophages
Cochain C6: Ly−6C2+ monocytes
−log10(FDR q−value)

◂ **Figure 4. Subclustering of myeloid cells revealed 5 distinct populations.** A) tSNE visualization of clustering revealed 5 distinct myeloid populations. B) Violin plots of macrophage-specific activation genes and foam cell markers. C) Top pathways associated with the macrophage clusters. D) Unique pathways per macrophage cluster. E) IPA analysis of upstream regulators of the macrophage subsets. Both D and E depict data as Z-score. F) Circos plots displaying overlap of macrophage clusters with macrophage clusters of murine scRNA-seq papers. Dotted lines indicate no significant overlap, solid lines indicate significant overlap. G) Bar graph with top 5 overlapping clusters of human and murine macrophage clusters.

Subsequently, we specifically examined the top unique interactions within the myeloid populations, split by myeloid ligands (**Figure 5B**) and receptors (**Figure 5C**). We found multiple chemotactic interactions, including endothelial *ACKR1*[51] with myeloid derived *CCL2*, CXCL8, *CCL8* and *CXCL1*, of which the last two ligands were specifically expressed in My.1. We also observed an interaction between *CSF1R* on all myeloid subsets and *CSF1* on endothelial cells, smooth muscle cells, mast cells and myeloid cells. *CCR1* and *CCR5* interacted with CCL5 from both $CD4^+$ and $CD8^+$ T cells and *CXCR4* on B cells interacted with *CXCL12* on My.1 cells. In addition, we identified communication patterns that are potentially involved in extravasation of myeloid cells, including *CD44* (My) – *SELE* (EC), *SELL* (My) – *CD34* (EC), *SELPLG* (My) – *SELP* and *SELL* (both EC). Myeloid cells showed potential capability to attract other leukocytes, for example $CCR5^+$ T cells through expression of *CCL3* (My.1). Moreover, myeloid cells were also predicted to interact with T cells leading to mutual activation, through i.e. *SIRPA* (My) – *CD47* (T)[52], *ICAM1* (My) – *ITGAL* (CD8), inducing cytotoxicity, and multiple interactions involved in antigen presentation. Lastly, interaction of *PDGFB* on myeloid subsets with *PDGFBR* on endothelial cells suggest a possible myeloid-driven induction of angiogenesis, which has been associated with plaque destabilization.[53,54]

Chromatin accessibility of myeloid and T cell populations reveals transcription factors involved in gene regulation

Next, we aimed to further define the genomic landscape that accounts for the obtained cluster-specific patterns of gene expression and potentially uncover disease driving transcription factors. Using scATAC-seq we examined the open chromatin promoter and enhancer landscape of myeloid- and T cells in human plaques. We identified four myeloid and five T cell clusters by scATAC-seq. Population label transfer from scRNA-seq to scATAC-seq populations showed good agreement with the native scATAC-seq cluster borders and retrieved the majority of the scRNA-seq populations (**Figure 6A**, **B**). Open chromatin at macrophage (*CSF1R*, *IL1B*) and T cell specific genes (*NKG7*), as well as enrichment of motifs of cell-type TFs for macrophages and T cells (*SPI1*[55] and *ETS1*[56]), confirmed the delineation between cell types (**Figure 6C**, **D**). Transferred myeloid populations were reclustered analogous to the scRNA-seq clusters (**Figure 6E**).

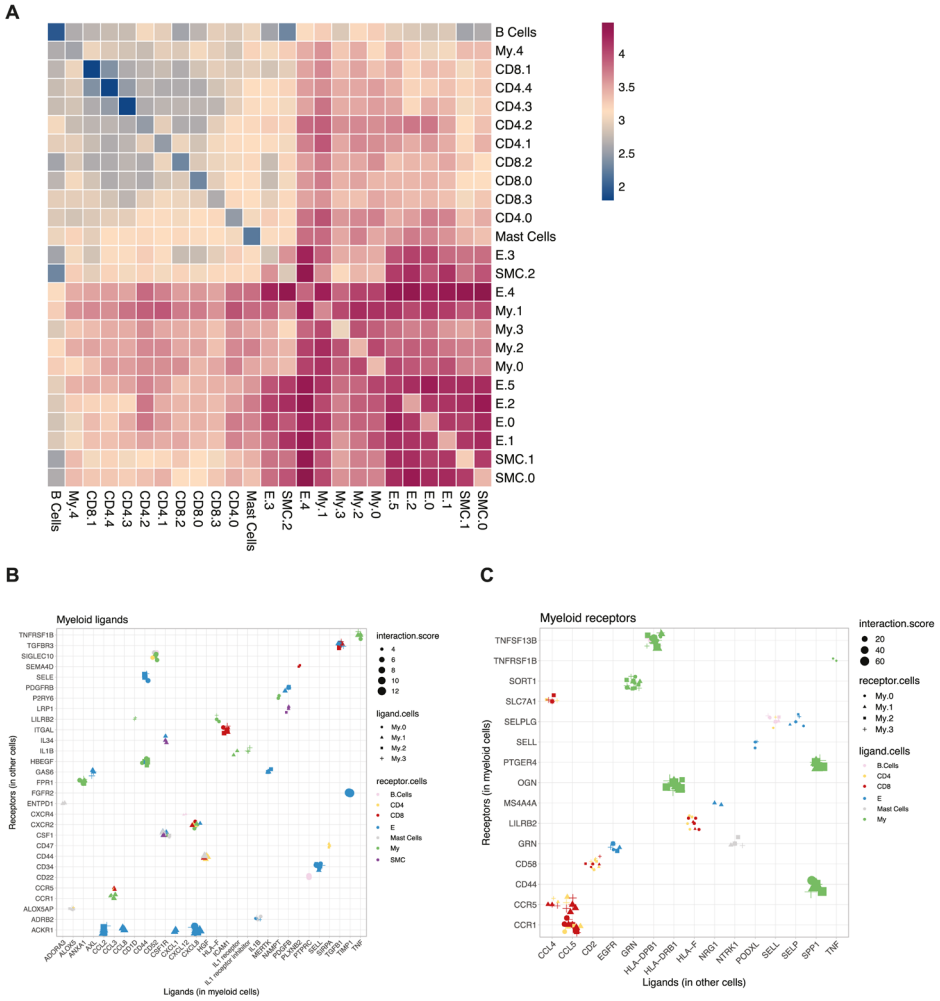

Figure 5. Ligand-receptor interaction analyses to asses intracellular communication in the plaque. A) Heatmap showing logarithmic interaction scores between all cell subsets. Top quartile of unique ligand-receptor interactions between all cells and myeloid cells for both B) ligands expressed by myeloid cells and C) receptors expressed by myeloid cells.

IRF4 has been shown to be a CD1c^{+} dendritic cell-specific transcriptional regulator[57] and its motif was indeed enriched in My.3 (**Figure 6F**). In line, we found specific open chromatin at the promoter region of *IL12A*, the subunit that is specific for the cytokine IL12, in all myeloid populations and an enhancer specifically in My.3 dendritic cells (**Online Figure 7E**). IL12 is required to induce a pro-inflammatory, T_H1-like cytotoxic phenotype of T cells and actively induces atherosclerosis.[58,59] Potentially, as a result of the My.3-specific IL12, we observed open chromatin at the *IFNG* and *TNF* loci in

CD4.0, confirming its activated, cytotoxic phenotype and suggesting that this cluster has T_H1-like properties. (**Online Figure 7G**, **H**). Additionally enriched accessible motifs within the T cells (**Online Figure 7A**, **B**) were observed for the *RUNX3* motif in CD4.0, normally a $CD8^+$ T cell linage specific TF that is also known to induce expression of cytotoxic genes in $CD4^+$ T cells[60–63], as well as the *STAT3* motif, which is downstream of IL6 and IL2 signaling. The BATF_JUN motif (**Online Figure 7C**) that is known to be critical for effector function in T cells, was also enriched in this cluster.[64] The effector function could be further confirmed by differential open chromatin of the *GZMB* and *GZMH* loci in both CD4.0 and all CD8 clusters (**Online Figure 7D**) and an open locus at *IL2* in CD4.0, CD4.1 and CD8.0.

In line with the scRNA-seq data My.1 showed enrichment of pro-inflammatory TF motifs (**Figure 6F**), which matches the pro-inflammatory gene expression seen in these cells. This cluster was especially enriched in interferon signaling induced TFs including IRF1, IRF9, STAT1 and STAT2. The STAT1-STAT2 complex is known to interact with IRF9 upon IFNγ stimulation and hence induces the upregulation of pro-inflammatory cytokines as TNF, indicating an IFNγ pathway driven activation, possibly secreted by the T cells.[65] Indeed, the IRF9 motif was accessible and the *IRF9* locus was open predominantly in My.1 cells (**Figure 6G**, **H**). Moreover, these IRF and STAT TFs are also key mediators of type I IFN responses which have previously been shown to associate with atherosclerotic disease as well.[66]

My.0 cells were specifically enriched for the NFATC3 motif (**Figure 6F**), a TF which has previously been linked to activated TLR-pathway signaling and has been shown to partially regulate subsequent TNFα and IL-1β secretion.[67,68] Finally, My.2 cells were enriched for anti-inflammatory, foam cell associated TFs in the scATAC-seq data similar as in the scRNA-seq data. We observed increased chromatin accessibility at loci harboring the KLF4 motif, which next to repressing pro-inflammatory programs was shown to implement an anti-inflammatory macrophage activation state and is also known to be involved in the transformation of vascular SMCs to macrophages[41,46,69] (**Figure 6F**). This is in contrast with the scRNA-seq data where KLF4 was expressed at a low level, indicating that while the KLF4 locus is poised, its associated gene program is not necessarily executed in all foamy macrophages. Furthermore, My.2 was enriched for the *de novo* motif MA1149.1, which was annotated to RAR_RXR, a motif with high similarity to the LXR_RXR motif (**Figure 6I**). Moreover, LXR_RXR motif accessibility is enriched in My.2 cells and the *NR1H3* (LXRα) locus is opened specifically in the My.2 population (**Figure 6J**). In line, the scRNA-seq data likewise shows *NR1H3* upregulation specifically in My.2 (**Figure 6K**).

We could not map the regulatory T cell cluster CD4.3 to an scATAC-seq cluster. The *FOXP3* locus hardly showed open chromatin in any population in the scATAC-seq data set and neither did the Treg-associated cytokine gene *IL10* (**Online Figure 7I**, **J**).

Cell type specific enrichment of genes in GWAS loci

Genome wide association studies (GWAS) have discovered 163 genetic susceptibility loci linked to coronary artery disease (CAD) through literature search and effects on expression[70]. However, the challenge remains in identifying the potential causal genes linked to these loci for functional testing as novel therapeutic targets. In part, this is due to the underlying genetic architecture where multiple causative variants in a gene might be involved and variants in linkage disequilibrium only show marginal significance in a GWAS. Another reason is that many of the risk variants are not causal and ambiguously linked to genes. A gene-centric analysis considers all variants in a gene and solves these issues, yet such analyses fail to identify the cells potentially involved. Here, we aimed to 1) identify genes associated to CAD, that are 2) also highly expressed in specific cell types, effectively identifying tangible candidates for functional follow-up. To this end, we mapped genes near GWAS loci associated to CAD, and assessed expression of these genes across our scRNA-seq cell populations to investigate their expression in disease relevant tissue. We prioritized 317 protein-coding genes based on the summary statistics of a recent CAD GWAS[71] (see **Online Methods**; **Online Table 3**). Next, we selected the genes that would best represent each individual cell population. To achieve this, we determined differentially expressed genes (DEGs) (**Online Figure 8**; Online Methods). 3876 genes were differentially expressed and DEGs were grouped into 15 gene expression patterns that best matched the scRNA-seq populations (**Figure 7A**). We overlapped the 317 CAD associated genes with the 3876 differentially expressed genes, resulting in a significant overlap (permutation over random data $p = 2{,}67e^{-5}$) of 74 genes. These genes are distributed over multiple individual CAD loci (**Online Table 3**), indicating that our methods are robust. We observed a significant accumulation of GWAS linked genes in patterns 3, 8 and 14 (permutation over random data p = 0.015, p = 0.006 and p = 0.015 respectively) (**Figure 7B**). Genes in pattern 3 are associated with higher expression in the endothelial cell clusters 9 and 10 (**Figure 7C**) and consisted of *SHE*, *KCNN3*, *VAMP5*, *SEMA3F*, *HDAC9*, *GIMAP1*, *NOS3*, and *DOCK6*. Pattern 8 is hallmarked by gene expression associated with all four macrophage populations (**Figure 7A**) and contained *AMPD2*, *CTSS*, *IL6R*, *CAPG*, *GPX1*, *GNAI2*, *TRIB1*, *SH2B3*, *FES*, *C19orf38* and *VASP* (**Figure 7B**, **D**). Genes in pattern 14 were predominantly associated with higher expression in both the smooth muscle cell population 8 and the *CD34*$^{+}$ endothelial cell population 10 (**Figure 7E**). This pattern contained *ITGB*, *ARHGEF26*, *CXCL12*, *PTPN11*, *COL4A1*, *COL4A2*, *KANK2* and *GGT5*. Our results suggest that macrophages, smooth muscle cells and endothelial cells are of particular interest as a starting point for functional testing.

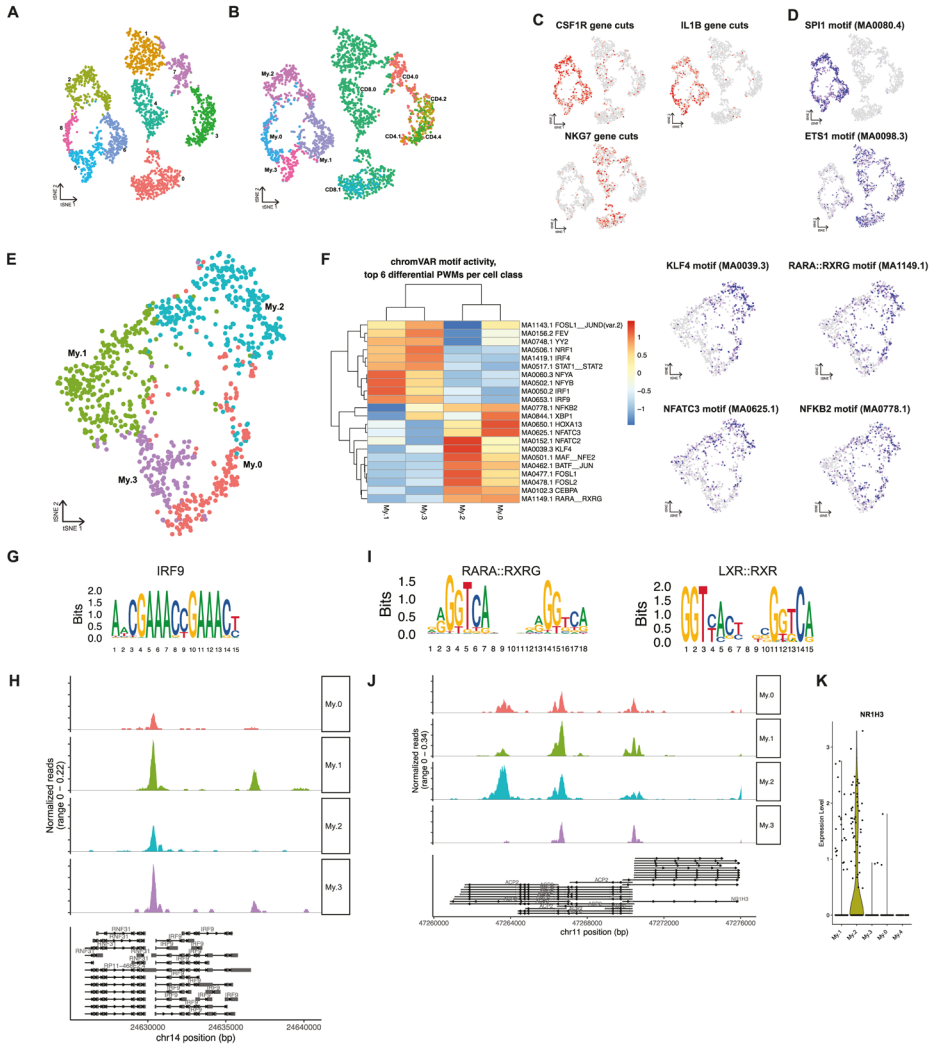

Figure 6. Chromatin accesibility of myeloid cells in human atherosclerotic plaques analyzed using scATAC-seq. A) tSNE visualization of myeloid and T cell clusters based on scATAC-seq. B) Projection of scRNA-seq myeloid and T cell labels over the scATAC-seq clusters. C) tSNE visualization of cell type-specific accessible gene loci. D) tSNE visualization of cell type-specific transcription factor motifs enriched in open chromatin regions. E) tSNE visualization of subclustered scATAC-seq myeloid clusters. F) Heatmap showing the top differential open chromatin TF motifs by chromVAR, with subcluster specific accessible TF motifs visualized as tSNE. G) IRF9 motif H) Pseudobulk genome browser visualization identifying the open chromatin regions of *IRF9* in different myeloidsubsets. I) RARA:RXRG and LXR:RXR motifs. J) Pseudobulk genome browser visualization identifying open chromatin regions of *NR1H3* (encoding LXRα) in different myeloid subsets. K) Violin plot of *NR1H3* gene expression from myeloid scRNA-seq data.

Furthermore, given that for many of the genes previously mapped to the 163 CAD loci the mechanisms and cellular expression are still unknown[70], we examine whether these genes show cell-type specific expression in carotid plaques. We found that 24 of the 75 genes previously classified as 'unknown' by Erdmann *et al*.[70] were differentially expressed between cell populations in carotid plaques, and included 3 genes that also showed association with CAD (*CHD13*, *SNRPD2* and *ARHGEF26*; **Online Table 3**) in our analysis.

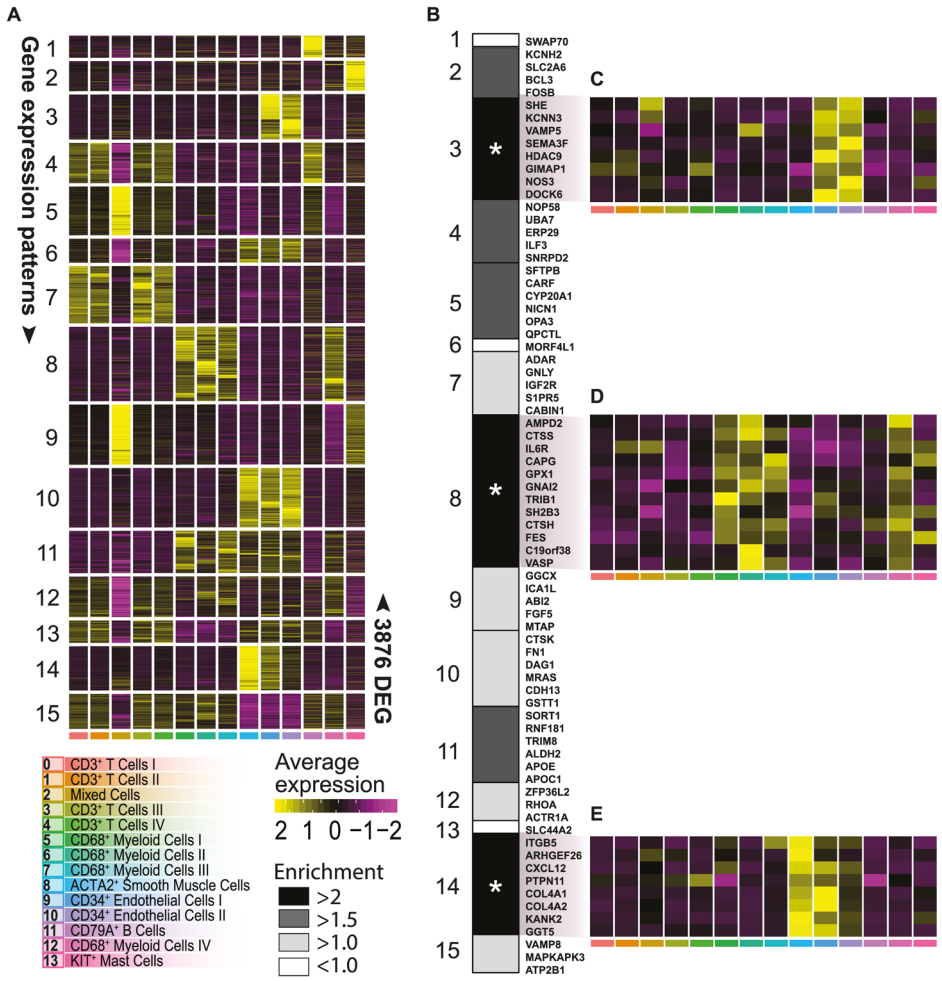

Figure 7. Projection of CAD GWAS associated genes. A) Heatmap of average expression of 3876 DEGs divided into 15 gene expression patters that best matched cluster or cell-type identity (for DEG selection, see **Online Figure 8**). B) Enrichment of 74 CAD GWAS associated genes across the 15 gene expression patterns. C, D, E) Heatmap of average relative expression of significantly enriched CAD genes from gene expression pattern #3, #8 and #14 respectively. Asterisk indicates significant enrichment. *p<0.05.

Discussion

In the past two years, single-cell technologies have advanced our knowledge in atherosclerosis tremendously. scRNA-seq has been applied to specifically describe the immune cell landscape of murine and human atherosclerotic lesions.[3–7] The recent study by Fernandez *et al*. gave a first overview of the human immune cell landscape during atherosclerosis by showing a data set based on extensive CyTOF analyses and by comparing RNA expression profiles of T cells and macrophages in plaque and blood of symptomatic and asymptomatic patients[7]. They provide insight into which immune cells reside in the plaque and described their different activation states. Yet, both the mouse and human studies lack coverage of non-immune cell types in the plaque and so far only a limited number of patients have been included in the scRNA-seq studies. Here, we applied scRNA-seq to all live cells in advanced human atherosclerotic plaques of 18 patients and revealed a highly diverse cellular landscape consisting of 14 main cell populations.

We detected a predominance of T cells in the leukocyte population of the human lesions. In contrast, murine scRNA-seq studies describe a more prominent presence of myeloid cells, which may be caused by the previously described declining myeloid content upon progression of human atherosclerotic plaques, whereas T cells reciprocally increase in human atherosclerosis.[72,73] Both $CD4^+$ and $CD8^+$ T cells subsets were characterized by their activation state, rather than classical T_H or T_C subclasses. We could confirm the presence of activated T cells that in the plaque could especially be characterized by the expression of multiple granzymes.[7] In addition, we show that these granzymes are not only expressed by $CD8^+$ T cells, but also by a substantial number of $CD4^+$ T cells in the plaque. The $CD4^+$ T cells showed a dominant cytotoxic T cell pool, characterized by expression of *PRF1* and multiple granzymes, with granzyme B production confirmed by flow cytometry. The lack of *CD28* expression in these cells indicates that this pool constitutes most likely a subset of cytotoxic $CD4^+CD28^{null}$ T cells, which has previously been associated with atherosclerosis as they have been detected in peripheral blood of CAD patients.[30,74] Although the presence of a similar TCR clone as observed in peripheral $CD4^+CD28^{null}$ cells was found in bulk coronary artery tissue[30,74], we can now confirm the presence of these cells on a single-cell level suggesting a functional role in patients with CVD. As cytokine expression could not be retrieved from the scRNA-seq data, but we were able to detect open chromatin at various cytokine gene loci within the T cell populations using scATAC-seq suggesting active cytokine genes. Amongst others, *IFNG* showed open chromatin in the cytotoxic and effector T cell subclasses. Apart from confirming the cytotoxic, T_H1-like phenotype within the plaque, this also suggests that the pro-inflammatory

macrophage subclasses we observe in our dataset may be primed for classical activation by secretion of IFNγ by the T cells.[75] These T_H1 cells acting on macrophages may in turn be driven by activated CD1c$^+$ dendritic cells that were characterized by an active *IL12* gene (i.e. open enhancer), which has previously been found on protein level in plaque lysates[76,77], and the enrichment of HLA-DR subtypes.[78,79]

Each of the macrophage clusters seemed to have been activated differently, one expressing *TNF* and *TLR4*, which can be activated by oxLDL and IFNγ[80], as well as IL1B, and the other more selectively expressing *IL1B*, which correlated with caspase expression suggesting inflammasome activation.[81] The recent CANTOS trial, which targeted IL-1β[82], might thus have been effective through impacting on the pro-inflammatory capacity of the My.0 and My.1 populations within the plaque. Chromatin accessibility confirmed the pro-inflammatory phenotype of these cells by showing open regions linked to inflammatory transcription factors. Particularly the TNF enriched macrophage cluster My.1 was enriched for motifs from IFN induced TFs (e.g. STATs, IRFs), which correlated with our upstream regulator analysis that suggested IFN as drivers of the macrophage phenotype and may be a result of the local IFNγ production by T cells. In line, the My.0 and My.1 populations correlated with inflammatory and resident-like macrophages as detected in murine lesions. [3–6]

The IL12–IFNγ-axis, as found in our scRNA-seq, data may form an important feature of T cell activation in the plaque, and subsequent activation of myeloid cells contributes to the inflammation profile within the plaque. This is in line with several experimental studies that show the pro-atherogenic role of both IL12 and IFNγ in cardiovascular disease.[59,83,84]

The more anti-inflammatory foam-cell-like cluster was characterized by expression of ABC cholesterol efflux transporters and lipid-related genes whose expression is most likely driven by intracellular lipid accumulation.[85] The lipid-phenotype was confirmed by the enriched LXR_RXR TF motifs in the scATAC-seq data. LXR is a well-known nuclear receptor, active in foam cells and inducing ABC transporters.[46,86] The notice that foam cell formation per se is not pro-inflammatory is a recent ongoing paradigm shift in the field. Several studies have previously shown clear pro-inflammatory characteristics of foam cell formation, either through engagement of TLRs by oxLDL[87–89], induction of oxidative responses[90] or through other pathways.[91–93] However, recent data studying foam cells in in vivo model systems[94] or isolating foam cells from murine plaques[5] clearly demonstrate that foam cells do not necessarily show pro-inflammatory characteristics and even may be considered anti-inflammatory.[94,95] In line, our data shows that cells exhibiting the foam-cell driven LXR activation program do not express

high levels of *IL1B* and *TNF*. This further confirms that lipid accumulation leads to *LXR* activation and induces an anti-inflammatory phenotype. We also observed *TREM2* and *CD9* expression within this cluster, resembling the TREM2$^+$ macrophages found in murine atherosclerosis.[4,6] In other tissues, these TREM2$^+$CD9$^+$ macrophages have been described as either Lipid Associated Macrophages (LAMs)[45] in obesity, or as Scar Associated Macrophages (SAMs)[44] in liver cirrhosis. Key phenotypes of these cells were shown to involve pro-fibrotic characteristics and this is also of high relevance for human atherosclerosis as it may indicate a plaque stabilizing macrophage population.

Our study provides further supports the notion that trans-differentiation of cells is likely to occur in human atherosclerosis. About a quarter of the My.2 macrophages expressed smooth muscle cell actin, which may indicate derivation from SMCs, or conversely macrophages showing a SMC cell-like fibrotic phenotype.[17,96] Presence of myeloid lineage specific TF expression in these cells (e.g. SPI and CEBPB) and absence of SMC TFs (e.g. MYOCD and MRTFA) suggests that the latter is more likely. This is in line with previous reports applying SMC lineage tracing that showed that unidentified SMC-derived cells in atherosclerotic lesions exhibit phenotypes of other cell lineages, including macrophages and mesenchymal stem cells.[17,97] Also endothelial cell cluster E.3 was characterized by expression of smooth muscle cell markers, such as *ACTA2*, *MYH11* and *NOTCH3*, suggesting that these cells could be in endothelial to mesenchymal transition. Mature endothelial cells can exhibit considerable heterogeneity and can transdifferentiate into mesenchymal-like cells, a biological process called EndoMT.[97] There is accumulating evidence that EndoMT plays a role in atherosclerotic lesion progression and which has been linked with inflammatory stress and endothelial dysfunction.[98,99] Our study shows that distinct EC clusters are present within atherosclerotic lesions and the gene signatures identify a cluster that shares both SMC and EC characteristics further providing human supportive evidence that EndoMT may occur in advanced human atherosclerotic plaques.

Apart from cellular plasticity within the endothelial and macrophage population, our study also provides new insights regarding intercellular communication within the plaque and its role in progression of atherosclerosis. We have shown that the within the plaque this was predicted to be most prevalent between myeloid, endothelial and smooth muscle cells. In addition to previous studies predicting interactions between macrophages and T cells in human lesions[7], we were also able to predict interactions between endothelial cells and SMCs, which were mainly involved with chemotaxis and extravasation of myeloid cells. We also show activation and recruitment of other immune cells, in particular T cells. Future development of therapeutics may benefit from detailing these interactions, providing specific pathways to target.

One of the significant post-GWAS challenges is the identification of candidate genes and pathways with clinical potential.[100] Here we mapped genes based on common variants (minor allele frequency > 1%) in susceptibility loci and used single-cell resolution expression in disease-relevant tissue to identify putative targets for future functional follow-up Our analysis showed enriched expression of CAD-associated genes in myeloid, endothelial, and smooth muscle cells. Furthermore, some of these genes are involved in cell-cell interactions, such as *SORT1* and *CXCL12*. Interestingly, the candidate genes did not show a significant overlap with T cells specific transcriptional signatures. Our approach is pragmatic in that we explicitly focus on 1) common variants in risk loci associated to CAD, and 2) map protein-coding genes that are associated to CAD to these risk loci, and 3) select CAD-associated genes that are also differentially expressed between cell populations. This identifies tangible potential targets as starting points for future functional testing in macrophages, endothelial and smooth muscle cells. However, we note that rare loss-of-function (LoF) variants and underrepresented genes may have significant effects in these and other cells. Future studies focusing on LoF variants and under-expressed genes could identify potentially other cell-specific targets.

There are several limitations that come with the use of human plaque endarterectomy samples. The vast majority of carotid endarterectomy samples also contain an inevitable small medial smooth muscle cell layer that potentially has contributed to the contractile smooth muscle cell cluster. There is a fine line between increasing digestion time to isolate more cells and generating a pure sample containing a high number of viable cells. We therefore not exclude that the ratio of cell types that we detected in the plaques based on gene expression profiles was affected by the digestion procedure.

In summary, we provide an in-depth characterization of the highly diverse cellular communities in advanced human atherosclerotic plaques. Based on RNA expression and chromatin accessibility profiles of individual cells, we uncover amongst others the presence of pro-inflammatory, cytotoxic T cell populations, multiple activation states of macrophages and their interactions, and functionally distinct endothelial cell populations that all can be considered modulators of human disease development. Furthermore, we show that by incorporating GWAS data, scRNA-seq data can be applied to map CVD susceptibility loci to specific cell populations and define potential patient-driven relevant targets for drug intervention of specific cell types. Our approach thus provides a powerful tool to aid research into the mechanisms underlying human disease and discover novel drug targets for intervention.

Funding

This work was supported by The Dutch Heart Foundation [CVON2017-20: Generating the best evidence-bases pharmaceutical targets and drugs for atherosclerosis (GENIUS II) to JK, MW, GP, SWvdL, MACD, IB, BS]; Spark-Holding BV [grant number 2015B002 to MW]; NWO-ZonMW [PTO program Inhibition of mast cell activation in atherosclerotic lesions using an anti-IgE antibody approach. [grant number 95105013, to MACD, IB, JK]; the European Union [ITN-grant EPIMAC to MW]; Fondation Leducq [Transatlantic Network Grants to MW, CKG, SY-H and GP]; EU 755320 Taxinomisis grant [GJdB, AB, GP]. We acknowledge the European Research Area Network on Cardiovascular diseases [ERA-CVD, grant number 01KL1802 to SWL, GP]; European Research Council (ERC) consolidator grant [grant number 866478 UCARE to HMdR]. MUK was supported by the ERC under the European Union's Horizon 2020 research and innovation programme [grant number 802825 to MUK], the Academy of Finland [Decisions 287478 and 319324], the Finnish Foundation for Cardiovascular Research and the Sigrid Jusélius Foundation. TÖ and MUK were supported by the Health from Science (TERVA) Programme of the Academy of Finland [Decision 314554]. TL was supported by the Academy of Finland [Decisions 311081 and 314557].

Acknowldegements

We would like to thank Judith Vivié and Dr. Mauro Muraro of Single Cell Discoveries for processing the plates for sequencing. We thank Dr. Anouk Wezel and Dr. Harm Smeets for sample collection at the Haaglanden Medisch Centrum. We acknowledge Biocenter Finland for infrastructure support. We are grateful to Kimmo Mäkinen for enabling sample acquisition at Kuopio University Hospital.

Author contributions

M.A.C.D., K.H.M.P. and L.S. drafted the manuscript and designed the figures. G.J.B. performed carotid endarterectomy procedures. M.A.C.D., D.E., I.B, B.S, S.C.A.J. and M.M. provided the pilot experiments. D.E. and M.A.C.D. executed the human plaque processing, FACS and flow cytometry. K.H.M.P. performed the clustering analyses. L.S. performed the GWAS analysis with help from M.M., S.W.L., A.B. and F.W.A. S.W.L. executed the FUMA data collection. M.A.C.D., K.H.M.P., L.S., A.B. I.B., B.S. and S.W.L. participated in conceptualization, data interpretation and provided critical feedback on the manuscript. S.C.A.J. and E.L. provided critical feedback on the manuscript. H.M.D.R. and C.K.G. provided funding and critical feedback on the manuscript. T.Ö., E.A. and T.L. processed the human plaque samples and carried out the experimental work for scATAC-seq, analyzed the data, and prepared the corresponding figures. M.U.K. and S.Y.-H. participated in the conceptualization,

funding and supervision of the scATAC-seq experiments and analysis. M.M., J.K., M.W. and G.P. participated in the conceptualization, funding and supervision of the scRNA-seq experiments and analysis and finalization of the manuscript. All authors provided feedback on the research, analyses and manuscript.

Disclosures

The authors have no conflicts of interest.

References

1. Benjamin, E. J. *et al.* Heart Disease and Stroke Statistics—2017 Update: A Report From the American Heart Association. *Circulation* **135**, e146–e603 (2017).
2. Turner, A. W., Wong, D., Dreisbach, C. N. & Miller, C. L. GWAS Reveal Targets in Vessel Wall Pathways to Treat Coronary Artery Disease. *Frontiers in Cardiovascular Medicine* **5**, 1–10 (2018).
3. Winkels, H. *et al.* Atlas of the Immune Cell Repertoire in Mouse Atherosclerosis Defined by Single-Cell RNA-Sequencing and Mass Cytometry. *Circ Res* **122**, 1675–1688 (2018).
4. Cochain, C. *et al.* Single-Cell RNA-Seq Reveals the Transcriptional Landscape and Heterogeneity of Aortic Macrophages in Murine Atherosclerosis. *Circ Res* **122**, 1661–1674 (2018).
5. Kim, K. *et al.* Transcriptome Analysis Reveals Nonfoamy Rather Than Foamy Plaque Macrophages Are Proinflammatory in Atherosclerotic Murine Models. *Circ Res* **123**, 1127–1142 (2018).
6. Lin, J.-D. *et al.* Single-cell analysis of fate-mapped macrophages reveals heterogeneity, including stem-like properties, during atherosclerosis progression and regression. *JCI Insight* **4**, (2019).
7. Fernandez, D. M. *et al.* Single-cell immune landscape of human atherosclerotic plaques. *Natuere Medicine* **25**, 1576–1588 (2019).
8. Aran, D. *et al.* Reference-based analysis of lung single-cell sequencing reveals a transitional profibrotic macrophage. *Nature Immunology* **20**, 163–172 (2019).
9. Müller, A. M. *et al.* Expression of the Endothelial Markers PECAM-1, vWf, and CD34 in Vivo and in Vitro. *Experimental and Molecular Pathology* **72**, 221–229 (2002).
10. Owens, G. K. Regulation of differentiation of vascular smooth muscle cells. *Physiological reviews* **75**, 487–517 (1995).
11. Germain, R. N. T-cell development and the CD4–CD8 lineage decision. *Nature Reviews Immunology* **2**, 309–322 (2002).
12. LeBien, T. W. & Tedder, T. F. B lymphocytes: how they develop and function. *Blood* **112**, 1570–80 (2008).
13. Ziegler-Heitbrock, L. *et al.* Nomenclature of monocytes and dendritic cells in blood. *Blood* **116**, e74-80 (2010).
14. Stöger, J. L. *et al.* Distribution of macrophage polarization markers in human atherosclerosis. *Atherosclerosis* **225**, 461–468 (2012).
15. Tabas, I. & Bornfeldt, K. E. Macrophage Phenotype and Function in Different Stages of Atherosclerosis. *Circulation research* **118**, 653–67 (2016).
16. Voehringer, D. Protective and pathological roles of mast cells and basophils. *Nature Reviews Immunology* **13**, 362–375 (2013).
17. Shankman, L. S. *et al.* KLF4-dependent phenotypic modulation of smooth muscle cells has a key role in atherosclerotic plaque pathogenesis. *Nat Med* **21**, 628–637 (2015).
18. Thiriot, A. *et al.* Differential DARC/ACKR1 expression distinguishes venular from non-venular endothelial cells in murine tissues. *BMC Biology* **15**, 1–19 (2017).
19. Kalucka, J. *et al.* Single-Cell Transcriptome Atlas of Murine Endothelial Cells. *Cell* **180**, 764-779. e20 (2020).
20. Adams, G. N. *et al.* Prolylcarboxypeptidase promotes angiogenesis and vascular repair. *Blood* **122**, 1522–1531 (2013).
21. Elices, M. J., Osborn, L., Luhowskyj, S., Hemler, M. E. & Lobb, R. R. VCAM-1 on activated endothelium interacts with the leukocyte integrin VLA-4 at a site distinct from the VLA-4.pdf. *Cell* **60**, 577–584 (1990).

22. Moreno, P. R., Purushothaman, K. R., Sirol, M., Levy, A. P. & Fuster, V. Neovascularization in human atherosclerosis. *Circulation* **113**, 2245–2252 (2006).
23. Zhu, L. *et al.* Mutations in myosin heavy chain 11 cause a syndrome associating thoracic aortic aneurysm / aortic dissection and patent ductus arteriosus. *Nature Genetics* **38**, 343–349 (2006).
24. Jin, S. *et al.* Notch Signaling Regulates Platelet-Derived Growth Factor Receptor-B Expression in Vascular Smooth Muscle Cells. *Circulation Research* **102**, 1483–1491 (2008).
25. Schlosser, A. *et al.* MFAP4 Promotes Vascular Smooth Muscle Migration ,. *Arterioscler Thromb Vasc Biol.* **36**, 122–133 (2016).
26. Rensen, S. S. M., Doevendans, P. A. F. M. & van Eys, G. J. J. M. Regulation and characteristics of vascular smooth muscle cell phenotypic diversity. *Neth Heart J* **15**, 100–8 (2007).
27. Luger, D. *et al.* Expression of the B-Cell Receptor Component CD79a on Immature Myeloid Cells Contributes to Their Tumor Promoting Effects. *PLoS ONE* **8**, e76115 (2013).
28. Tedder, T. F., Tuscano, J., Sato, S. & Kehrl, J. H. CD22 , A B LYMPHOCYTE – SPECIFIC ADHESION MOLECULE THAT REGULATES ANTIGEN RECEPTOR SIGNALING *. *Annu. Rev. Immunol* **15**, 481–504 (1997).
29. Liu, C., Richard, K., Melvin, W., Zhu, X. & Conrad, D. H. CD23 can negatively regulate B-cell receptor signaling. *Scientific reports* **6**, 1–8 (2016).
30. Liuzzo, G. *et al.* Monoclonal T-Cell Proliferation and Plaque Instability in Acute Coronary Syndromes. *Circulation* **102**, 2883–2888 (2000).
31. Liuzzo, G. *et al.* Unusual CD4+CD28null T Lymphocytes and Recurrence of Acute Coronary Events. *J Am Coll Cardiol* **50**, 1450–1458 (2007).
32. Mohr, A., Malhotra, R., Mayer, G., Gorochov, G. & Miyara, M. Human FOXP3+ T regulatory cell heterogeneity. *Clinical and Translational Immunology* **7**, 1–11 (2018).
33. Malhotra, N. *et al.* RORα-expressing T regulatory cells restrain allergic skin inflammation. *Science Immunology* **3**, 1–13 (2018).
34. Wohlfert, E. A. *et al.* GATA3 controls Foxp3 + regulatory T cell fate during inflammation in mice. *The journal of clinical investigation* **121**, 4503–4515 (2011).
35. Guo, X. *et al.* Global characterization of T cells in non-small-cell lung cancer by single-cell sequencing. *Nature medicine* **24**, 978–985 (2018).
36. Li, H. *et al.* Dysfunctional CD8 T Cells Form a Proliferative, Dynamically Regulated Compartment within Human Melanoma. *Cell* 1–15 (2018) doi:10.1016/j.cell.2018.11.043.
37. Wherry, E. J. & Kurachi, M. Molecular and cellular insights into T cell exhaustion. *Nature Reviews Immunology* **15**, 486–499 (2015).
38. van Duijn, J. *et al.* CD39 identifies a microenvironment-specific anti-inflammatory CD8 + T-cell population in atherosclerotic lesions. *Atherosclerosis* **285**, 71–78 (2019).
39. Chyu, K. Y. *et al.* CD8 + T cells mediate the athero-protective effect of immunization with an ApoB-100 peptide. *PLoS ONE* **7**, (2012).
40. Dwyer, D. F., Barrett, N. A., Austen, K. F., Immunological, T. & Consortium, G. P. Expression profiling of constitutive mast cells reveals a unique identity within the immune system. *Nature Immunology* **17**, 878–887 (2016).
41. Kapoor, N. *et al.* Transcription Factors STAT6 and KLF4 Implement Macrophage Polarization via the Dual Catalytic Powers of MCPIP. *The Journal of Immunology* **194**, 6011–6023 (2015).
42. Westerterp, M. *et al.* ATP-binding cassette transporters, atherosclerosis, and inflammation. *Circulation Research* **114**, 157–170 (2014).
43. Collot-Teixeira, S., Martin, J., McDermott-Roe, C., Poston, R. & McGregor, J. L. CD36 and macrophages in atherosclerosis. *Cardiovascular Research* **75**, 468–477 (2007).

44. Ramachandran, P. *et al. Resolving the fibrotic niche of human liver cirrhosis at single-cell level*. *Nature* vol. 575 (Springer US, 2019).
45. Jaitin, D. A. *et al.* Lipid-Associated Macrophages Control Metabolic Homeostasis in a Trem2-Dependent Manner. *Cell* **178**, 686-698.e14 (2019).
46. T, K., KHM, P., CK, G. & MPJ, de W. Transcriptional and epigenetic regulation of macrophages in atherosclerosis. *Nature Reviews Cardiology* (2019).
47. Wang, Z., Wang, D. Z., Pipes, G. C. T. & Olson, E. N. Myocardin is a master regulator of smooth muscle gene expression. *Proceedings of the National Academy of Sciences of the United States of America* **100**, 7129–7134 (2003).
48. Boltjes, A. & van Wijk, F. Human dendritic cell functional specialization in steady-state and inflammation. *Frontiers in Immunology* **5**, 1–13 (2014).
49. Villlani;, A.-C. *et al.* Single-cell RNA-Seq reveals new types of human blood dendritic cells, monocytes, and progenitors. *Science* **356**, (2017).
50. Efremova, M., Vento-Tormo, M., Teichmann, S. A. & Vento-Tormo, R. CellPhoneDB v2.0: Inferring cell-cell communication from combined expression of multi-subunit receptor-ligand complexes. *bioRxiv* 680926 (2019) doi:10.1101/680926.
51. Bonecchi, R. & Graham, G. J. Atypical Chemokine Receptors and Their Roles in the Resolution of the Inflammatory Response. *Frontiers in Immunology* **7**, (2016).
52. Engelbertsen, D. *et al.* Increased lymphocyte activation and atherosclerosis in CD47-deficient mice. *Scientific Reports* **9**, 1–12 (2019).
53. Sato, N. *et al.* Platelet-derived growth factor indirectly stimulates angiogenesis in vitro. *The American Journal of Pathology* **142**, 1119 (1993).
54. Corliss, B. A., Azimi, M. S., Munson, J., Peirce, S. M. & Murfee, W. L. Macrophages: An Inflammatory Link between Angiogenesis and Lymphangiogenesis. *Microcirculation (New York, N.Y. : 1994)* **23**, 95 (2016).
55. Lou, L., Zhang, P., Piao, R. & Wang, Y. Salmonella Pathogenicity Island 1 (SPI-1) and Its Complex Regulatory Network. *Frontiers in Cellular and Infection Microbiology* **9**, 270 (2019).
56. Cauchy, P. *et al.* Dynamic recruitment of Ets1 to both nucleosome-occupied and -depleted enhancer regions mediates a transcriptional program switch during early T-cell differentiation. *Nucleic Acids Research* **44**, 3567–3585 (2016).
57. Collin, M. & Bigley, V. Human dendritic cell subsets: an update. *Immunology* **154**, 3–20 (2018).
58. Akdis, M. *et al.* Interleukins (from IL-1 to IL-38), interferons, transforming growth factor β, and TNF-α: Receptors, functions, and roles in diseases. *Journal of Allergy and Clinical Immunology* **138**, 984–1010 (2016).
59. Hauer, A. D. *et al.* Blockade of interleukin-12 function by protein vaccination attenuates atherosclerosis. *Circulation* **112**, 1054–1062 (2005).
60. Tian, Y. *et al.* Unique phenotypes and clonal expansions of human CD4 effector memory T cells re-expressing CD45RA. *Nature Communications* **8**, (2017).
61. Mucida, D. *et al.* Transcriptional reprogramming of mature CD4 + helper T cells generates distinct MHC class II-restricted cytotoxic T lymphocytes. *Nature Immunology* **14**, 281–289 (2013).
62. Tian, Y., Sette, A. & Weiskopf, D. Cytotoxic CD4 T cells: Differentiation, function, and application to dengue virus infection. *Frontiers in Immunology* **7**, 531 (2016).
63. Reis, B. S., Rogoz, A., Costa-Pinto, F. A., Taniuchi, I. & Mucida, D. Mutual expression of the transcription factors Runx3 and ThPOK regulates intestinal CD4 + T cell immunity. *Nature Immunology* **14**, 271–280 (2013).

64. Kurachi, M. *et al.* The transcription factor BATF operates as an essential differentiation checkpoint in early effector CD8 + T cells. *Nature Immunology* **15**, 373–383 (2014).
65. Hoeksema, M. A., Stöger, J. L. & De Winther, M. P. J. Molecular pathways regulating macrophage polarization: Implications for atherosclerosis. *Current Atherosclerosis Reports* **14**, 254–263 (2012).
66. Goossens, P. *et al.* Myeloid type I interferon signaling promotes atherosclerosis by stimulating macrophage recruitment to lesions. *Cell Metabolism* **12**, 142–153 (2010).
67. Minematsu, H. *et al.* Nuclear presence of nuclear factor of activated T cells (NFAT) c3 and c4 is required for Toll-like receptor-activated innate inflammatory response of monocytes/macrophages. *Cellular Signalling* **23**, 1785–1793 (2011).
68. Fric, J. *et al.* NFAT control of innate immunity. *Blood* **120**, 1380–1389 (2012).
69. Kapoor, N. *et al.* Transcription factors STAT6 and KLF4 implement macrophage polarization via the dual catalytic powers of MCPIP. *Journal of Immunology* **194**, 6011–6023 (2015).
70. Erdmann, J., Kessler, T., Munoz Venegas, L. & Schunkert, H. A decade of genome-wide association studies for coronary artery disease: The challenges ahead. *Cardiovascular Research* **114**, 1241–1257 (2018).
71. Nelson, C. P. *et al.* Association analyses based on false discovery rate implicate new loci for coronary artery disease. *Nature Genetics* **49**, 1385–1391 (2017).
72. Van Dijk, R. A. *et al.* A Change in Inflammatory Footprint Precedes Plaque Instability: A Systematic Evaluation of Cellular Aspects of the Adaptive Immune Response in Human Atherosclerosis. doi:10.1161/JAHA.114.001403.
73. van Dijk, R. A., Virmani, R., von der Thüsen, J. H., Schaapherder, A. F. & Lindeman, J. H. N. The natural history of aortic atherosclerosis: a systematic histopathological evaluation of the peri-renal region. *Atherosclerosis* **210**, 100–6 (2010).
74. Téo, F. H. *et al.* Characterization of CD4+CD28null T cells in patients with coronary artery disease and individuals with risk factors for atherosclerosis. *Cell Immunol* **281**, 11–19 (2013).
75. Mosser, D. M. & Edwards, J. P. Exploring the full spectrum of macrophage activation. *Nature Reviews Immunology* **8**, 958–969 (2008).
76. Peeters, W. *et al.* Carotid atherosclerotic plaques stabilize after stroke insights into the natural process of atherosclerotic plaque stabilization. *Arteriosclerosis, Thrombosis, and Vascular Biology* **29**, 128–133 (2009).
77. Scholtes, V. P. W. *et al.* Type 2 diabetes is not associated with an altered plaque phenotype among patients undergoing carotid revascularization. A histological analysis of 1455 carotid plaques. *Atherosclerosis* **235**, 418–423 (2014).
78. Van Vré, E. A., Van Brussel, I., Bosmans, J. M., Vrints, C. J. & Bult, H. Dendritic cells in human atherosclerosis: from circulation to atherosclerotic plaques. *Mediators of inflammation* **2011**, 941396 (2011).
79. Villlani;, A.-C. *et al.* Single-cell RNA-Seq reveals new types of human blood dendritic cells, monocytes, and progenitors. *Science* **356**, (2017).
80. Howell, K. W. *et al.* Toll-like Receptor 4 Mediates Oxidized LDL-Induced Macrophage Differentiation to Foam Cells. *Journal of Surgical Research* **171**, e27–e31 (2011).
81. Karasawa, T. & Takahashi, M. Role of NLRP3 Inflammasomes in Atherosclerosis. *J Atheroscler Thromb* **24**, 443–451 (2017).
82. Ridker, P. M. *et al.* Antiinflammatory Therapy with Canakinumab for Atherosclerotic Disease. *New England Journal of Medicine* **377**, 1119–1132 (2017).

83. Buono, C. *et al.* Influence of interferon-γ on the extent and phenotype of diet-induced atherosclerosis in the LDLR-deficient mouse. *Arterioscler Thromb Vasc Biol* **23**, 454–460 (2003).
84. Gupta, S. *et al.* IFN-γ potentiates atherosclerosis in ApoE knock-out mice. *Journal of Clinical Investigation* **99**, 2752–2761 (1997).
85. Jessup, W., Gelissen, I. C., Gaus, K. & Kritharides, L. Roles of ATP binding cassette transporters A1 and G1, scavenger receptor BI and membrane lipid domains in cholesterol export from macrophages. *Current opinion in Lipidology* **17**, 247–257 (2006).
86. Tangirala, R. K. *et al.* Identification of macrophage liver X receptors as inhibitors of atherosclerosis. *Proc Natl Acad Sci U S A* **99**, 11896–11901 (2002).
87. Choi, S.-H. *et al.* Lipoprotein accumulation in macrophages via toll-like receptor-4-dependent fluid phase uptake. *Circulation research* **104**, 1355–63 (2009).
88. Xu, X. H. *et al.* Toll-like receptor-4 is expressed by macrophages in murine and human lipid-rich atherosclerotic plaques and upregulated by oxidized LDL. *Circulation* **104**, 3103–8 (2001).
89. Stewart, C. R. *et al.* CD36 ligands promote sterile inflammation through assembly of a Toll-like receptor 4 and 6 heterodimer. *Nature Immunology* **11**, 155–161 (2010).
90. Chou, M. Y. *et al.* Oxidation-specific epitopes are important targets of innate immunity. in *Journal of Internal Medicine* vol. 263 479–488 (John Wiley & Sons, Ltd, 2008).
91. Michelsen, K. S. *et al.* Lack of toll-like receptor 4 or myeloid differentiation factor 88 reduces atherosclerosis and alters plaque phenotype in mice deficient in apolipoprotein E. *Proceedings of the National Academy of Sciences of the United States of America* **101**, 10679–10684 (2004).
92. Monaco, C. *et al.* Toll-like receptor-2 mediates inflammation and matrix degradation in human atherosclerosis. *Circulation* **120**, 2462–9 (2009).
93. Duewell, P. *et al.* NLRP3 inflammasomes are required for atherogenesis and activated by cholesterol crystals. *Nature* **464**, 1357–1361 (2010).
94. Spann, N. J. *et al.* Regulated accumulation of desmosterol integrates macrophage lipid metabolism and inflammatory responses. *Cell* **151**, 138–152 (2012).
95. Baardman, J. *et al.* A Defective Pentose Phosphate Pathway Reduces Inflammatory Macrophage Responses during Hypercholesterolemia. *Cell Reports* **25**, 2044-2052.e5 (2018).
96. Neele, A. E. *et al.* Macrophage Kdm6b controls the pro-fibrotic transcriptome signature of foam cells. *Epigenomics* **9**, (2017).
97. Wesseling, M., Sakkers, T. R., de Jager, S. C. A., Pasterkamp, G. & Goumans, M. J. The morphological and molecular mechanisms of epithelial/endothelial-to-mesenchymal transition and its involvement in atherosclerosis. *Vascular Pharmacology* vol. 106 1–8 Preprint at https://doi.org/10.1016/j.vph.2018.02.006 (2018).
98. Cho, J. G., Lee, A., Chang, W., Lee, M.-S. & Kim, J. Endothelial to Mesenchymal Transition Represents a Key Link in the Interaction between Inflammation and Endothelial Dysfunction. *Frontiers in Immunology* **9**, 294 (2018).
99. Chen, P. Y. *et al.* Endothelial-to-mesenchymal transition drives atherosclerosis progression. *Journal of Clinical Investigation* **125**, 4514–4528 (2015).
100. Boyle, E. A., Li, Y. I. & Pritchard, J. K. An Expanded View of Complex Traits: From Polygenic to Omnigenic. *Cell* vol. 169 1177–1186 Preprint at https://doi.org/10.1016/j.cell.2017.05.038 (2017).
101. Verhoeven, B. A. N. *et al.* Athero-express: Differential atherosclerotic plaque expression of mRNA and protein in relation to cardiovascular events and patient characteristics. Rationale and design. *Eur J Epidemiol* **19**, 1127–1133 (2004).
102. Hellings, W. E. *et al.* Histological characterization of restenotic carotid plaques in relation to recurrence interval and clinical presentation: a cohort study. *Stroke* **39**, 1029–32 (2008).

103. Hashimshony, T. *et al*. CEL-Seq2: sensitive highly-multiplexed single-cell RNA-Seq. *Genome Biology* **17**, 77 (2016).
104. Li, H. & Durbin, R. Fast and accurate long-read alignment with Burrows-Wheeler transform. *Bioinformatics* **26**, 589–595 (2010).
105. Muraro, M. J. *et al*. A Single-Cell Transcriptome Atlas of the Human Pancreas. *Cell Systems* **3**, 385-394.e3 (2016).
106. R Core Team. R: A language and environment for statistical computing. https://www.r-project.org/ (2019).
107. Butler, A., Hoffman, P., Smibert, P., Papalexi, E. & Satija, R. Integrating single-cell transcriptomic data across different conditions , technologies , and species. *Nature Biotechnology* **36**, 411–420 (2018).
108. Martens, J. H. A. & Stunnenberg, H. G. BLUEPRINT: mapping human blood cell epigenomes. *Haematologica* **98**, 1487–1489 (2013).
109. Stuart, T. *et al*. Comprehensive Integration of Single-Cell Data. *Cell* **177**, 1888-1902.e21 (2019).
110. Schep, A. N., Wu, B., Buenrostro, J. D. & Greenleaf, W. J. ChromVAR: Inferring transcription-factor-associated accessibility from single-cell epigenomic data. *Nature Methods* **14**, 975–978 (2017).
111. Khan, A. *et al*. JASPAR 2018: Update of the open-access database of transcription factor binding profiles and its web framework. *Nucleic Acids Research* **46**, D260–D266 (2018).
112. Watanabe, K., Taskesen, E., van Bochoven, A. & Posthuma, D. Functional mapping and annotation of genetic associations with FUMA. *Nature communicationsommunications* **8**, 1–11 (2017).
113. Auton, A. *et al*. A global reference for human genetic variation. *Nature* vol. 526 68–74 Preprint at https://doi.org/10.1038/nature15393 (2015).
114. de Leeuw, C. A., Mooij, J. M., Heskes, T. & Posthuma, D. MAGMA: Generalized Gene-Set Analysis of GWAS Data. *PLoS Computational Biology* **11**, e1004219 (2015).

Online Data supplement

Expanded materials and methods

Patient population

Atherosclerotic plaques were obtained from 14 male and 4 female patients undergoing a carotid endarterectomy (CEA) procedure. All plaque specimens were included in the Athero-Express Biobank Study (AE, www.atheroexpress.nl), an ongoing biobank study at the University Medical Centre Utrecht (UMCU)[101] (Cohort 1). Only primary CEAs were included, restenotic plaques were excluded due to their difference in composition compared to primary atherosclerotic plaques[102]. The study was approved by the Medical Ethical Committee of the UMCU. For flow cytometry, seven plaques (5 male, 2 female) were used that were obtained from patients undergoing CEA procedure at Haaglanden Medical Center Westeinde (The Hague, The Netherlands) (Cohort 2). The study was approved by the Medical Ethical Committee of the HMC. For scATAC-Seq, atherosclerotic plaque samples were obtained from 3 patients undergoing CEA procedure at Kuopio University Hospital, Kuopio, Finland (Cohort 3). The studies were approved by Local Ethical Committee of Kuopio University Hospital. All studies were performed in accordance with the declaration of Helsinki and all patients gave written informed consent before start of the study.

Human plaque processing (Single Cell)

Human carotid plaques of Cohort 1 were collected during CEA; the culprit segment (5 mm) was used for histology and embedded in paraffin as described elsewhere[101]. Time between surgical removal and plaque processing did not exceed 10 minutes. The inclusion of a small medial layer in the dissected tissue could not be excluded during the surgical procedure. The plaques were characterized as fibrous (n = 6), fibro-atheromatous (n = 6) or atheromatous (n = 6). Characterization was in concordance with the Athero-Express Biobank Study protocols. The remainder of the plaque washed in RPMI and minced into small pieces with a razor blade. The tissue was then digested in RPMI 1640 containing 2.5 mg/mL Collagenase IV (ThermoFisher Scientific), 0.25 mg/mL DNAse I (Sigma), 2.5 mg/mL Human Albumin Fraction V (MP Biomedicals) and 1 mM Flavopiridol (Selleckchem) at 37°C for 30 minutes. Subsequently, the plaque cell suspension was filtered through a 70 µm cell strainer and washed with RPMI 1640. Cells were kept in RPMI 1640 with 1% Fetal Calf Serum until subsequent staining for fluorescence-activated cell sorting. Remaining, unstained cells were cryostored in liquid nitrogen.

Immunohistochemistry

Immunohistochemical staining of CD3, CD34, αSMA (ACTA2) and CD68 was performed fully automated (Benchmark, Ventana Medical Systems, Yuscon AZ). Stainings were performed on matched samples of patients from cohort 1 (n = 3). The CD3 antibody was purchased from DAKO and used at a dilution of 1:100. The CD68 antibody was purchased from Novocastra (cat. No. NCL-CD68-KP1) and used at a dilution of 1:3200. The CD34 antibody was purchased from Ventana Medical Systems (cat. No. 790-2927) and used at the dilution recommended by manufacturer. The αSMA antibody was purchased from Sigma (cat. No. A2547) and used at a dilution of 1:20000.

Human plaque processing (whole tissue)

Whole plaque tissue RNA-seq was obtained from two male Athero-Express biobank samples. RNA-seq library preparation was performed using the CEL-Seq2 Sample Preparation Protocol[103] and sequenced as 2 x 75bp paired-end on a Illumina NextSeq 500 (Utrecht Sequencing Facility). The reads were de-multiplexed and aligned to human cDNA reference using the BWA (v0.7.13)[104]. Downstream analysis was performed using custom R scripts.

Fluorescent activated cell sorting of viable cells

Single cell suspensions were stained with Calcein AM and Hoechst (ThermoFisher Scientific) in PBS supplemented with 5% Fetal Bovine Serum (FBS) and 0.2% ethylenediaminetetraacetic acid (EDTA) for 30 minutes at 37°C. After staining, cells were washed and filtered through a 70 μm FlowMi cell strainer (SP Scienceware). Viable cells, positive for both Calcein AM and Hoechst, were sorted using the Beckman Coulter MoFlo Astrios EQ.

Flow cytometry

Flow cytometry was performed on defrosted single cell suspensions of plaques from three patients of cohort 1 and on seven plaques single cell suspensions from cohort 2 (characterized as advanced plaques that showed luminal thrombosis, regions of intraplaque hemorrhage, large macrophage regions and a large necrotic core). All samples were digested according to the same protocol as described above for the scRNA-seq samples. The single plaque cells were stimulated with phorbol 12-myristate 13-acetate (PMA, 50 ng/mL, Sigma-Aldrich), ionomycin (500 ng/mL, Sigma-Aldrich) and Brefeldin A (ThermoFisher Scientific) for 3.5h in complete RPMI at 37°C and 5% CO_2. Subsequently, cells were stained with extracellular antibodies, fixated, permeabilized and stained with intracellular antibodies **(Online Table 4**). The fluorescently labeled plaque cells were measured using a Cytoflex S (Beckman

and Coulter) and analysed with FlowJo software. Statistical analysis was performed using Graphpad Prism 8 software. Data passed the Shapiro-Wilk normality test and an unpaired T-test was performed to determine significance.

Single cell RNA-sequencing

Using a Mosquito® HTS (TTP Labtech) 384 wells plates were filled with 50nL lysis buffer containing CELseq2-primers, spike-ins and dinucleotide triphosphates (dNTPs) and overlaid with mineral oil to prevent evaporation. Viable cells were sorted one cell per well into these 384 wells plates, fixed by lysis to preserve expression status, and immediately frozen at -80°C until further processing. First, cDNA was constructed using the SORT-seq protocol[105]. In short, cells were lysed for 5 min at 65°C and subsequently reverse transcription and second strand mixes were added using the Nanodrop II liquid handling platform (GC biotech). Next, cells were pooled in one library and the aqueous phase was separated from the oil phase, followed by in vitro transcription (IVT). A library was formed using the CEL-Seq2 protocol[103]. Primers consisted of a 24 bp polyT stretch, a 64bp random molecular barcode (UMI), a cell-specific 8bp barcode, the 5' Illumina TruSeq small RNA kit adaptor and a T7 promoter. For sequencing, TruSeq small RNA primers (Illumina) were added to the libraries and sequenced paired end at 75 bp read length using Illumina NextSeq 500.

scRNA-seq data processing and clustering

Single-cell sequencing data were processed as described previously[105]. Analyses were performed in an R 3.5 environment[106] using Seurat (version 2.3.4 and 3.0)[107]. Prior to processing, reads were filtered for mitochondrial and ribosomal genes, MALAT1, KCNQ1OT1, UGDH-AS1, and EEF1A. In order to omit doublets and low-quality cells, only cells expressing between 500 and 10.000 genes and genes expressed in at least 3 cells were used for further analysis. The following steps were performed using Seurat (version 2.3.4): data was log-normalized and scaled with the exclusion of unique molecular identifiers (UMIs). Top variable genes for all samples were used to combine samples into one object using Seurat function RunMultiCCA(), after which samples were aligned using AlignSubspace() with reduction.type=CCA and grouping.var="plate". Subsequently, canonical correlation analysis (CCA) reduction was performed with a resolution of 1.2 for 15 dimensions to identify clusters and to perform t-distributed stochastic neighbor embedding (tSNE). Cell types were assigned to cell clusters by evaluating gene expression of individual cell clusters using differential gene expression (Wilcoxon rank sum test) and analysis with SingleR[8] against BLUEPRINT[108] reference data. Sub-clustering of identified cell clusters was performed using CCA with a resolution of 0.9 or 1.5 for 15 dimensions (Seurat version 2.3.4). Downstream analysis of initial and sub-clusters was performed in a similar manner. Pathway analysis were

performed using the EGSEA (version 1.16.0) with Canonical pathway and hallmark gene set collections from broad institute GSEA (version 1.17.0) and FDR for multiple testing correction. tSNE plots, dot plots and violin plots were made with Seurat (version 2.3.4 and 3.0). Figure 1E and S2C were made using SingleR (version 1.2.4). Barplots were made using ggplot2. For full details, see ***Data access.***

Comparison whole- tissue and single-cell RNA-seq

Ilumina cell sequencing data was processed as described previously[105]. In summary, prior to processing reads were filtered for mitochondrial and ribosomal genes, MALAT1, KCNQ1OT1, UGDH-AS1 and EEF1A, and duplicate or unannotated entries. A "pseudobulk" patient was created by combining reads from all patients. Individual patients and the pseudobulk patient were compared to bulk RNA-seq as described above. Correlation coefficient was determined through Pearson correlation (CI 0.95). Scatterplot was made using ggplot2. All processing was performed using custom R scripts. For full details, see ***Data access***.

Integration of mouse datasets

Top 20 marker genes from all myeloid cell clusters in the 4 mouse datasets[3–6] were converted to human symbols using the ENSEMBL biomaRt R package (v2.42.0) in an R v3.5.3 environment. Subsequently, the overlap of genes in the mouse clusters with significant (p.adj < 0.1) marker genes from My.0, My.1, and My.2 was determined and significance calculated by hypergeometric test using standard R function phyper() with parameters q-1 and lower.tail = F. Finally, bar graphs were generated with ggplot2 and circos plots of overlaps were generated on http://metascape.org by uploading lists of marker genes per cluster, starting a custom analysis, and downloading the corresponding 'gene circos.svg' file from the 'ID conversion' tab. For full details, see ***Data access***.

Ligand-receptor interaction analysis

Ligand-receptor interactions were calculated using cellphonedb [v2.11 – database version 2.0.0][50] with default settings. Heatmap was made with cellphonedb. Top significant ($p < 0.05$) interactions were defined as > 3rd quartile and plotted using ggplot2. For full details, see ***Data access***.

Human plaque processing for scATAC-Seq

The tissue samples from cohort 3 (characterized as fibro-atheromatous) were minced with a scalpel and enzymatically dissociated using Miltenyi Biotec Multi-Tissue Dissociation Kit supplemented with 0.5% BSA and 20 mM HEPES buffer (pH 7.2-7.5) for 60 min at 37 °C with end-over-end rotation. The suspension was passed through a 30 µm strainer and viable cells were purified magnetically using the Dead Cell Removal

Kit (Miltenyi Biotec). For the isolation of nuclei from cells, the lysis buffer formulation recommended by 10x Genomics for scATAC-Seq nuclei preparation was used. The nuclei were purified by iodixanol (OptiPrep; Sigma) density gradient centrifugation at 3300g for 20 min at 4 °C. The nuclei were recovered at the interface of 29% and 35% iodixanol. The nuclei were resuspended in ice-cold 10x Genomics Nuclei Buffer and counted using fluorescence staining (DAPI). Approximately 5000-6000 nuclei per sample were processed on the 10x Genomics Chromium Controller instrument, followed by scATAC-Seq library preparation according to the manufacturer's protocol. The libraries were sequenced on an Illumina NextSeq sequencer using the standard protocol recommended by 10x Genomics for scATAC-Seq libraries.

scATAC-Seq data analysis

Sequencing data preprocessing, library quality control, cell calling and peak calling were done with the Cell Ranger ATAC pipeline (10x Genomics, version 1.1). Integration of scATAC-Seq samples, clustering of cells, and visualization of chromatin accessibility and pseudobulk coverage tracks was performed with Seurat (version 3.0)[109] and its extension Signac (version 0.15; https://github.com/timoast/signac). scATAC-Seq cells were matched to scRNA-Seq cell types using the scRNA-Seq as the reference data set in a cross-modal label transfer procedure, as described in Stuart *et al*.(2019).[109] Differential motif accessibility was calculated using chromVAR (version 1.5)[110] using the human motifs from the JASPAR CORE motif collection (2018 release)[111]. First, at the level of individual cells, the relative accessibility of each motif genome-wide ('motif activity') was computed as the deviation in motif occurrence in the accessible peaks compared to a set of background peaks matched for GC content, using the default parameters of the chromVAR method.[110] Subsequently, cell clusters were tested for differences (both positive and negative direction) in motif activity using a logistic regression test with the total peak count as a latent variable, as suggested for differential motif analysis by the authors of the Signac package109. $P < 0.05$ after correction for multiple testing using the Benjamini–Hochberg procedure was considered significant. Heatmaps were made using pheatmap (version 1.0.12), genome plots were made using Signac. For full details, see ***Data access***.

Differential gene expression analysis and mapping of GWAS loci

For the analysis and mapping of CAD associated gene to the single-cell RNAseq data, we applied three steps: 1) we prioritized genes based on the CAD GWAS summary statistics, 2) we determined the genes differentially expressed between cell type and therefore specific to these cell types, and 3) we overlapped the GWAS-derived genes and differentially expressed genes to identify genes associated to CAD and specific to a cell type.

Step 1: We used the summary statistics from the GWAS on CAD by Nelson *et al.* which included CARDIoGRAMplusC4D and UK Biobank data[71]. This data was annotated with a the Functional Mapping and Annotation of Genome-Wide Association Studies (FUMA v1.3.3b, https://fuma.ctglab.nl) platform.[112] FUMA can be used to annotate, prioritize, visualize and interpret GWAS results. In short, FUMA takes GWAS summary statistics as an input, it will map and match the results to a reference (in this case the 1000G EUR population, https://www.internationalgenome.org[113]), and provides extensive functional annotation for all SNPs (present in the summary statistics and the reference used) in genomic areas identified by lead SNPs. Various filters can be applied. Here, we applied genome-wide significance ($p = 5x10^{-8}$), a linkage disequilibrium $r^2 = 0.05$ for clumping of independent loci within 1000 kb of the lead variant (PLINK version 1.9), and included only variants with minor allele frequency (MAF) > 1%. Annotation and mapping of genes were based on 1) position (within 1000kb of the lead variant), 2) limited to blood and vascular bed derived data from the Genotype-Tissue Expression (GTEx version 7) Project only. This resulted in a list of 644 genes that mapped to CAD loci. To further prioritize these 644 genes, we calculated per-gene p-values based on the per-SNP p-values from the CAD GWAS summary statistics. To this end FUMA uses MAGMA (https://ctg.cncr.nl/software/magma, v1.06[114]). MAGMA first analyses the individual SNPs in a gene and combines the resulting SNP p-values into a gene test-statistic while taking into account the underlying LD structure. Using permutations based on a randomly generated test-statistic drawn from the standard normal distribution, a per-gene empirical (permuted) p-value is derived. This results in a per-gene p-value of association with CAD for all genes in a reference (here ENSEMBL v92 was used and we only included protein-coding genes). We further prioritized the 644 genes mapped to CAD loci by selecting genes with a MAGMA p-value < 0.05. This selection resulted in 317 CAD associated genes (mapped to CAD associated loci) which were used for the downstream single-cell analysis and mapping.

Step 2: For the single-cell analysis and mapping, we have focused only on genes that 1) are specific for the different cell types in plaque, and that 2) have a genetic association with CAD. The purpose of the analysis is to find those genes in each cell type to provide tangible starting points for functional testing. Genes that are highly specific (i.e., highly expressed) are more likely to have a specific function within the cells, making them interesting targets when these genes are also genetically correlated with the disease. To this end we performed a differential gene expression analysis, resulting in 3876 differentially expressed genes (DEG) listed in figure 7A, the second pillar of this analysis. For better interpretation and visualization, we sorted these genes into 15 gene expression patterns, which highlight the expression of genes in specific (related) cell types. Differential expression was tested between clusters by

Wilcoxon sum rank testing in both a "One cluster vs. One cluster" and "One cluster vs. Remaining clusters" fashion. Genes were deemed differentially expressed if they met 2 criteria: 1) >= 10% of cells within one cell cluster express the gene with log2 fold change of >= 0.6, and 2) the gene passes the Bonferroni adjusted significance threshold of p.adjusted < 0.05 for this test. The 3876 differentially expressed genes (DEG) were sorted into 15 gene expression patterns by K-means clustering based on average expression per cell type (**Online Table 3**).

Step 3: After this, the 317 CAD associated genes derived from the GWAS summary statistics and the 3876 DEGs derived from the scRNAseq data are overlapped. This resulted in 74 genes that are both highly expressed in scRNAseq data (a DEG), and are associated to CAD based on GWAS summary statistics. We calculated enrichment of the 74 DEGs in the 15 gene expression patterns using permutation analysis. We sampled 75000 random sets of 317 genes from 26180 genes that were possible to map. We then calculated positive enrichment for each gene expression pattern for the mapped GWAS genes compared to the random sets and determined the enrichment of DEGs. Downstream processing was performed using custom R scripts. Heatmap was made with Seurat (version 2.3.4) and bar graph with ggplot2. For full details, see ***Data access***.

Data access

In silico data analysis was performed using custom R scripts (R version 3.5.3) designed especially for this research and/or based on the recommended pipelines from the pre-existing packages listed in the individual segments above. R scripts are available on GitHub [https://github.com/AtheroExpress/MicroanatomyHumanPlaque_scRNAseq] Other data is available upon personal request to the corresponding authors (m.mokry@umcutrecht.nl; j.kuiper@lacdr.leidenuniv.nl; m.dewinther@amsterdamumc.nl; g.pasterkamp@umcutrecht.nl).

Supplemental Tables

For supplemental tables see https://doi.org/10.1161/CIRCRESAHA.120.316770

Supplemental Figures

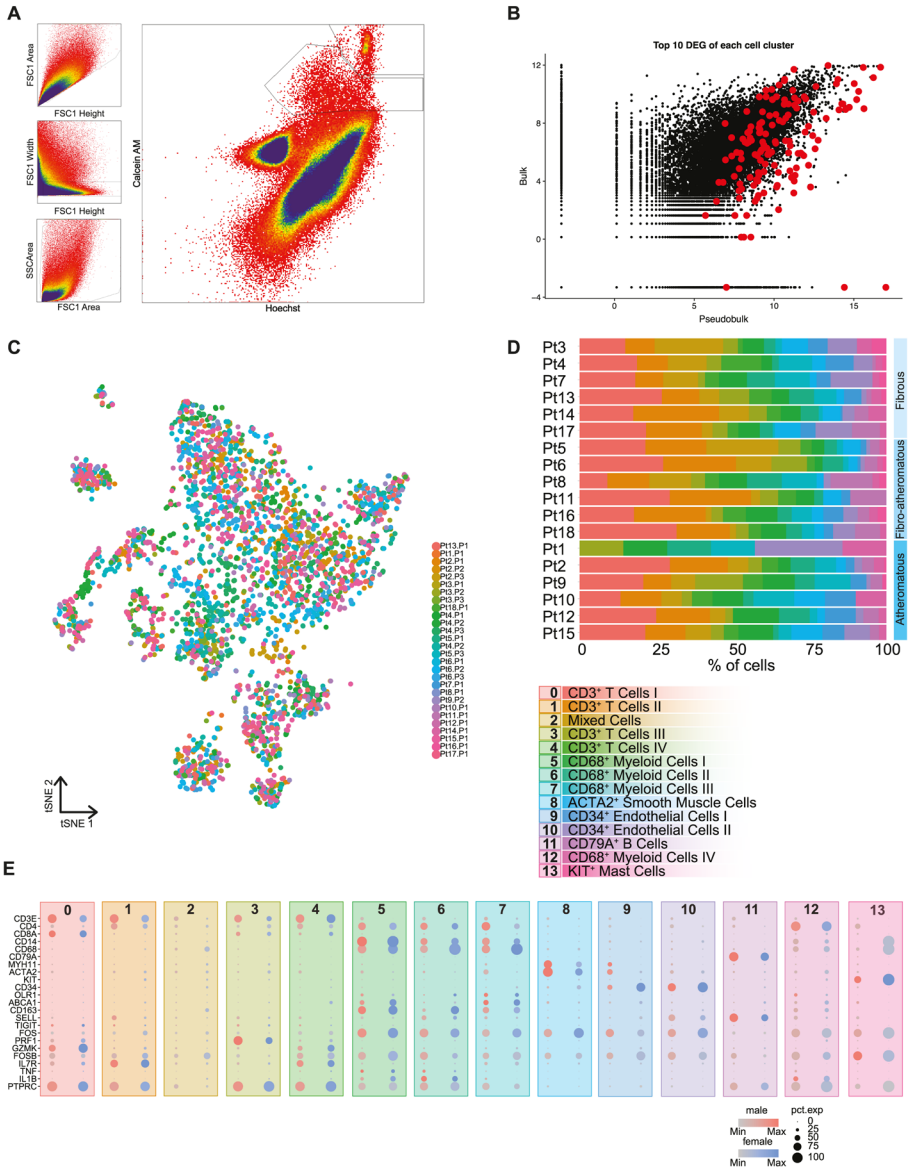

Online Figure 1. CCA clustering and tSNE visualization revealed 14 distinct populations. A) FACS plots showing gating directions for viable cells, positive for both Calcein AM and Hoechst B) Single cell CEL-seq2 libraries showed good correlation with plaque bulk RNA-seq libraries. Correlation 0.643 $p < 2.2e\text{-}10$. C) Clusters were not biased towards individual PCR plates or patients. D) Relative cluster sizes were comparable between patients. E) Dotplot of marker genes confirmed population identities and low inter-sex variance.

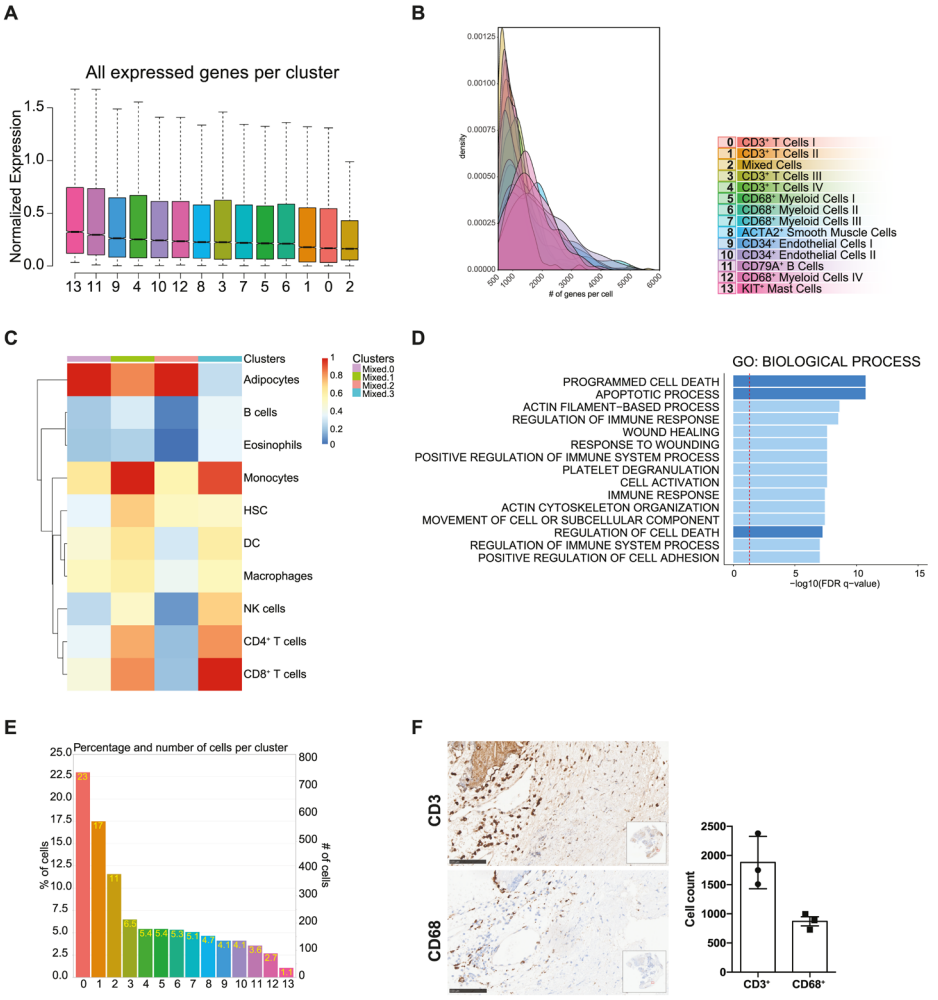

Online Figure 2. Refinement of population identities. A) Boxplots of normalized gene expression per cluster. B) Per cluster density plots of number of detected genes per cell. C) Heatmap of subclusters of unknown cluster 2's similarity to reference datasets of known cell types. D) Top pathways associated with cluster 2. E) Distribution of number of cells per cluster. F) Immunostaining of 3 representative endarterectomy samples. Top left: CD3$^+$ T cells. Bottom Left: CD68$^+$ macrophages. Right: Barplots of positive cell counts, data shown as mean±SD (n = 3). Scale bars represent 100µm.

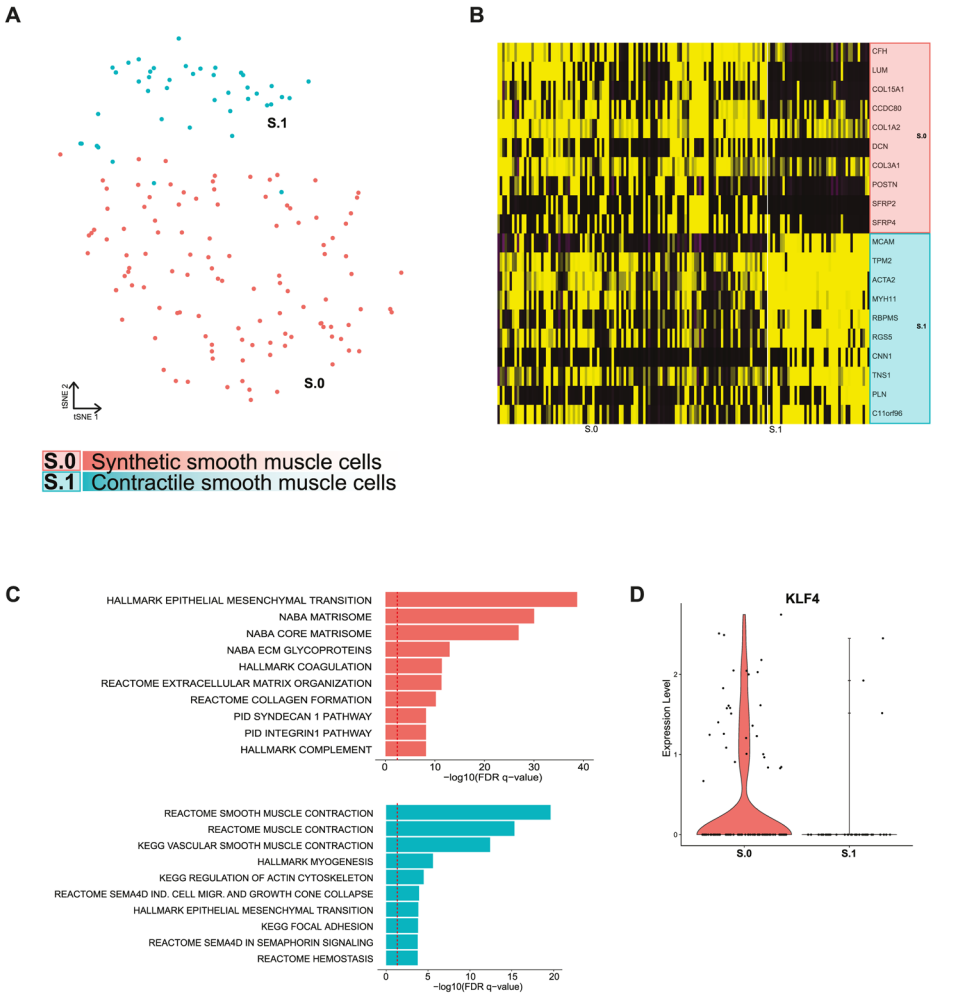

Online Figure 3. Subclustering of smooth muscle cells revealed 2 distinct populations. A) tSNE visualization of clustering revealed 2 distinct smooth muscle cell populations. B) Heatmap of top marker genes per cluster. C) Top pathways associated with each population.

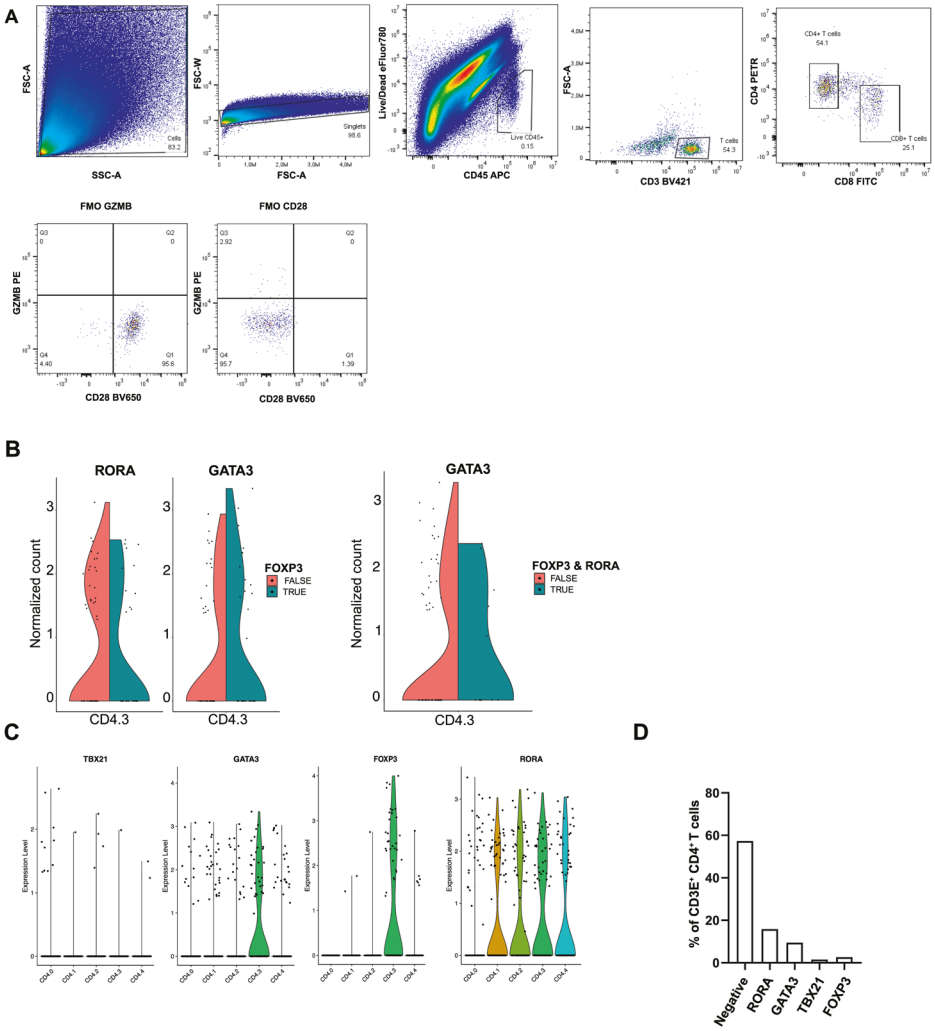

Online Figure 4. Representation of potential T_H-subsets in the human plaque. A) Gating strategy for GZMB staining within $CD4^+CD28^{null}$ T cells. B) Split-violins showing a correlation between expression of FOXP3 and respectively RORA and GATA3; and cells that express all three transcription factors. C) Violin plots showing expression of helper T cell subset-related transcription factors within the $CD4^+$cluters. D) Independent analysis of all $CD3E^+CD4^+$ T cells. Negative $CD4^+$ T cells are negative for all transcription factors. Other bars represent the percentage of $CD4^+$ T cells that specifically express the noted transcription factor. RORC was not detected in our dataset.

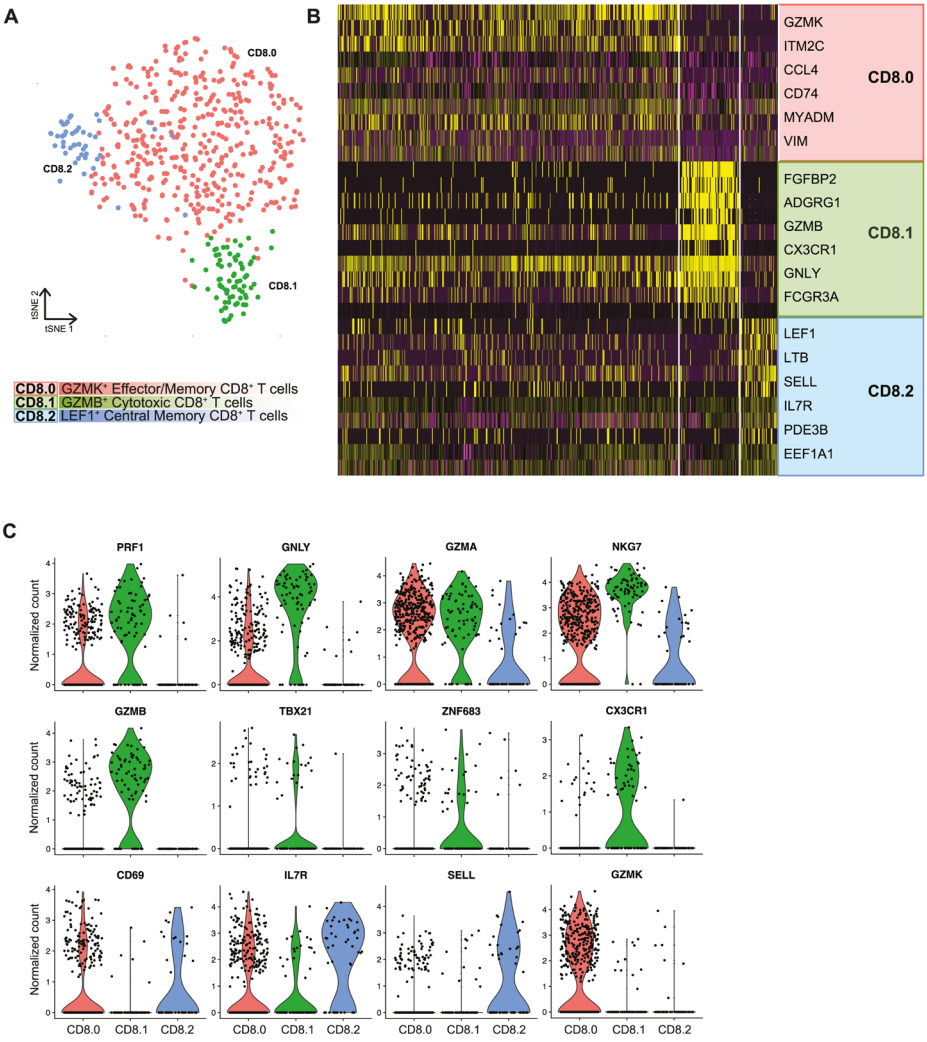

Online Figure 5. Subclustering of CD8⁺ T cells revealed 3 distinct populations. A) tSNE visualization of clustering revealed 4 distinct CD8⁺ T cell populations. B) Heatmap of top marker genes per cluster. C) Violin plots of marker genes associated with CD8⁺ T cell cytotoxicity and quiescence.

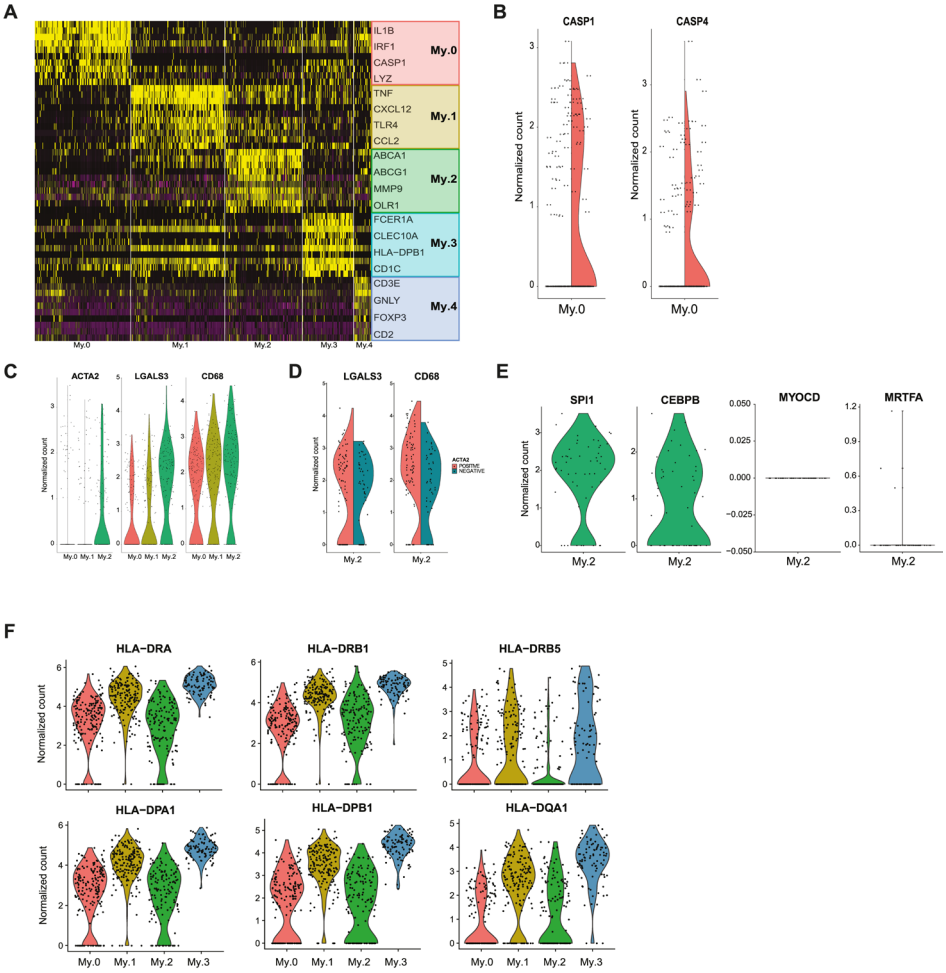

Online Figure 6. Myeloid population marker genes and SMC related gene expression. A) Heatmap of top marker genes per cluster. B) Split violin plot showing *CASP1* and *CASP4* expression in *IL1B*$^{-}$ (left side of violins) and *IL1B*$^{+}$ cells (right side of violins). C) Violin plot showing genes associated with the transition of smooth muscle cell to macrophage. D) Correlation of ACTA2 expression with CD68 and LGALS3 levels in cluster My.2. E) Violin plots of *ACTA2*$^{+}$ cells in cluster My.2 showing expression of myeloid lineage transcription factors *SPI1* and *CEBPB* and smooth muscle cell lineage transcription factors *MYOCD* and *MRTFA*. F) Violin plots of class II HLA subtypes expressed by cluster My.0 – My.4.

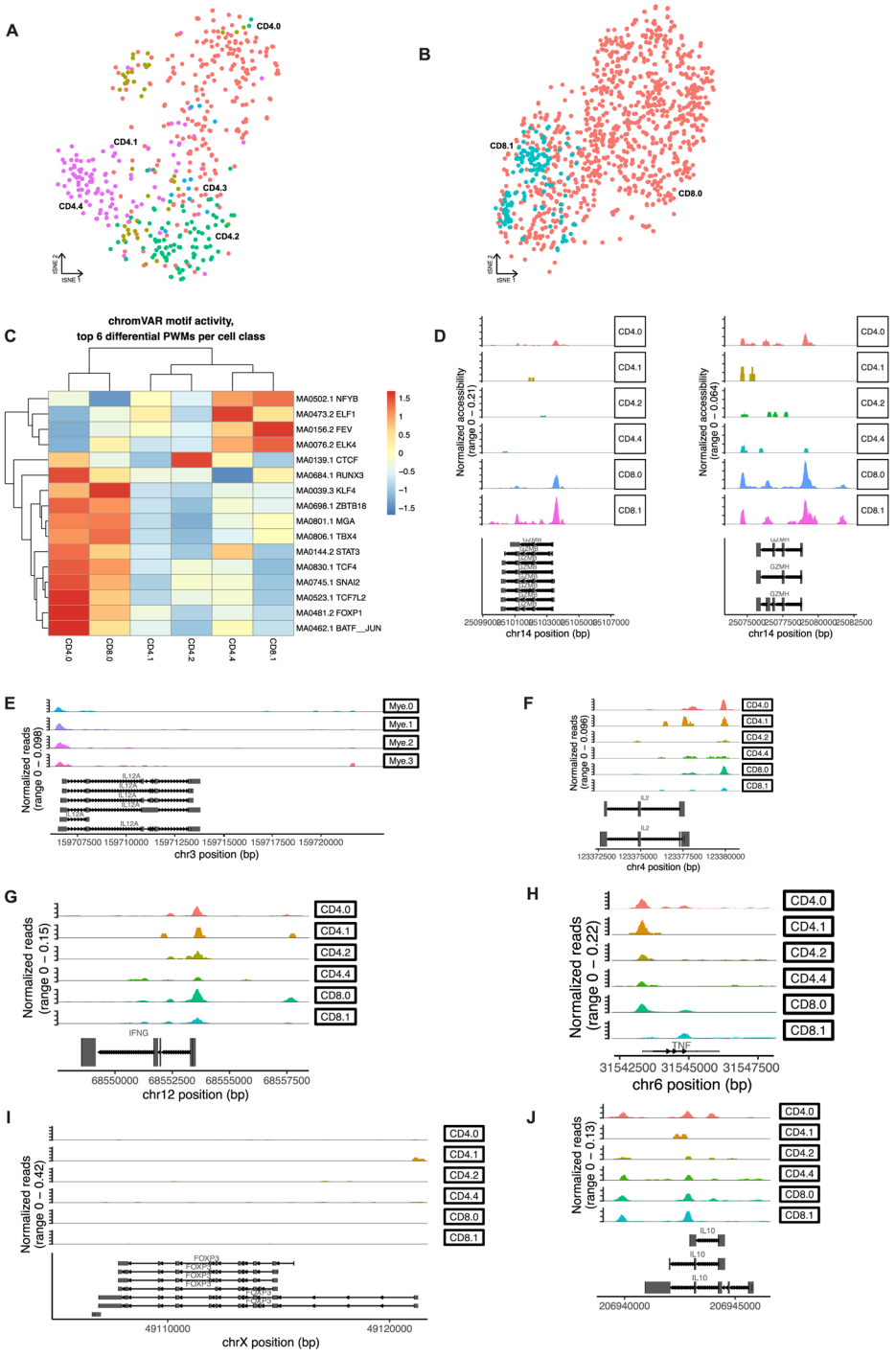
A
CD4.0
CD4.1
CD4.3
CD4.4
CD4.2
tSNE 2
tSNE 1
B
CD8.1
CD8.0
C
chromVAR motif activity,
top 6 differential PWMs per cell class
MA0502.1 NFYB
MA0473.2 ELF1
MA0156.2 FEV
MA0076.2 ELK4
MA0139.1 CTCF
MA0684.1 RUNX3
MA0039.3 KLF4
MA0698.1 ZBTB18
MA0801.1 MGA
MA0806.1 TBX4
MA0144.2 STAT3
MA0830.1 TCF4
MA0745.1 SNAI2
MA0523.1 TCF7L2
MA0481.2 FOXP1
MA0462.1 BATF::JUN
CD4.0
CD8.0
CD4.1
CD4.2
CD4.4
CD8.1
D
Normalized accessibility
(range 0 – 0.21)
Normalized accessibility
(range 0 – 0.064)
CD4.0
CD4.1
CD4.2
CD4.4
CD8.0
CD8.1
chr14 position (bp)
E
Normalized reads
(range 0 – 0.096)
Mye.0
Mye.1
Mye.2
Mye.3
IL12A
chr3 position (bp)
F
Normalized reads
(range 0 – 0.096)
IL2
chr4 position (bp)
G
Normalized reads
(range 0 – 0.15)
IFNG
chr12 position (bp)
H
Normalized reads
(range 0 – 0.22)
TNF
chr6 position (bp)
I
Normalized reads
(range 0 – 0.42)
FOXP3
chrX position (bp)
J
Normalized reads
(range 0 – 0.13)
IL10

◂ Online Figure 7. Chromatin accessibility of T cells in human atherosclerotic plaques analyzed using scATAC-seq. A) tSNE visualization of $CD4^+$ T cell subclusters. B) tSNE visualization of $CD8^+$ T cell subclusters. C) Heatmap showing the top differential TF motifs based on chromVAR. Pseudobulk genome browser visualization identifying the open chromatin regions of E) *IL12*, F) *IL2*, G) *IFNG*, H) *TNF*, I) *FOXP3* and J) *IL10*.

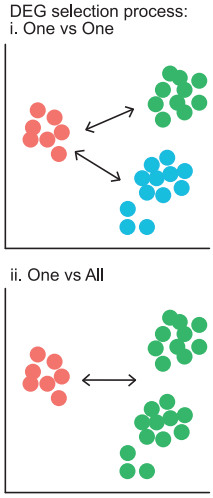

Online Figure 8. Projection of CAD GWAS associated genes: DEG selection process. Schematic overview of differentially expressed gene (DEG) selection. Top: DEG were called comparing all clusters against one another. Bottom: DEG were called comparing one cluster against all others aggregated.

Chapter 4

Single-cell T-cell Receptor sequencing of paired human atherosclerotic plaques and blood reveals autoimmune-like features of expanded effector T-cells

Nature Cardiovascular Research 2023; 2:112-125

Marie A.C. Depuydt[1]*, Frank H. Schaftenaar[1]*, Koen H.M. Prange[2], Arjan Boltjes[3], Esmeralda Hemme[1], Lucie Delfos[1], Jill de Mol[1], Maaike J.M. de Jong[1], Mireia N.A. Bernabé Kleijn[1], Judith A.H.M. Peeters[4], Lauren Goncalves[4], Anouk Wezel[4], Harm J. Smeets[4], Gert J. de Borst[5], Amanda C. Foks[1], Gerard Pasterkamp[3], Menno P.J. de Winther[2], Johan Kuiper[1], Ilze Bot[1#], Bram Slütter[1#]

1. Leiden Academic Centre for Drug Research, Division of Biotherapeutics, Leiden University, Einsteinweg 55, 2333 CC Leiden, The Netherlands
2. Amsterdam University Medical Centers - location University of Amsterdam, Experimental Vascular Biology, Department of Medical Biochemistry, Amsterdam Cardiovascular Sciences, Amsterdam Infection and Immunity, Meibergdreef 9, Amsterdam, The Netherlands
3. Central Diagnostic Laboratory, University Medical Center, Utrecht University, Heidelberglaan 100, Utrecht, The Netherlands
4. Department of Surgery, Haaglanden Medisch Centrum Westeinde, 2512 VA The Hague, The Netherlands
5. Department of Vascular Surgery, University Medical Centre Utrecht, Heidelberglaan 100, Utrecht, The Netherlands

*These authors contributed equally; #Shared last authors

Abstract

Atherosclerosis is a lipid-driven chronic inflammatory disease, however, whether it can be classified as an autoimmune disease remains unclear. Here we apply single-cell TCR sequencing (scTCRseq) on human carotid artery plaques and matched PBMC samples to assess the extent of TCR clonality and antigen specific activation within the various T-cell subsets. We observed the highest degree of plaque-specific clonal expansion in effector $CD4^+$ T-cells and these clonally expanded T-cells expressed genes such as *CD69*, *FOS* and *FOSB* indicative of recent TCR engagement suggesting antigen-specific stimulation. CellChat analysis suggested multiple potential interactions of these effector $CD4^+$ T-cells with foam cells. Finally, we integrated a published scTCRseq dataset of the autoimmune disease psoriatic arthritis and report various commonalities between the two diseases. In conclusion, our data suggest that atherosclerosis has an autoimmune component driven by autoreactive $CD4^+$ T-cells.

Main

Atherosclerosis is the major underlying pathology of acute cardiovascular events, such as myocardial infarction and stroke. It is characterized by accumulation of lipids and subsequent inflammation of the medium and large arteries. As low-density lipoprotein (LDL) particles are important instigators of atherosclerosis, cardiovascular disease (CVD) has primarily been treated as a lipid-driven disorder with a treatment focus on lowering LDL cholesterol levels. Nonetheless, inflammation plays a critical role in perpetuating the growth and instability of atherosclerotic lesions, highlighted by the success of recent clinical trials with anti-inflammatory agents.[1,2] Elucidating the dominant inflammatory pathways that drive atherosclerosis may therefore allow identification of new druggable targets independent of cholesterol lowering.

Single-cell RNA sequencing (scRNAseq) and mass cytometry have allowed detailed mapping of the leukocyte contents of atherosclerotic plaques.[3,4] These studies show that T-cells are the largest leukocyte population and show that the number of effector T-cells within the lesion associates with plaque instability. In combination with previous murine work, this suggests inflammatory processes inside the plaque are driven by T-cells and atherosclerosis could be considered an autoimmune like disease. In support of that, autoreactive (LDL-specific) $CD4^+$ T-cells have previously been reported in the human atherosclerotic lesions and have been identified in elevated levels in the circulation CVD patients.[5–7] Moreover, vaccination approaches aimed at the reduction of self-reactive T-cells or induction of regulatory T-cells (T_{regs}) have shown promise in murine models of atherosclerosis.[8,9] However, when self-reactive $CD4^+$ T-cells are indeed the culprit T-cells that propagate disease, clonal expansion and accumulation of these cells in the lesions is to be expected. Interestingly, recent work examining the T-cell Receptor (TCR) distribution in human coronary plaques showed primarily clonal expansion of $CD8^+$ T-cells inside the plaque and identified some of these TCRs to be specific for common viral antigens such as Influenza, Cytomegalovirus (CMV) and SARS-CoV2.[10] However, this work did not include patient-matched PBMC controls, rendering it impossible to assess whether the virus-specific $CD8^+$ T-cells were specifically enriched in the plaque and/or had recently undergone antigen-specific interactions.

Here we present an approach to identify the T-cell subsets that are specifically enriched in atherosclerotic lesions and whether these subsets underwent antigen-specific interaction in the plaque. We combine scRNAseq and single-cell TCR seq (scTCRseq) of human carotid plaques and matched PBMC samples. With this approach, we observe the highest degree of plaque-specific clonal expansion in both effector

CD4+ T-cells and to a smaller extent in the T_{reg} population. By integrating the data from our patients with atherosclerosis with scTCRseq data from psoriatic arthritis patients, we show that atherosclerosis has major similarities with another prominent autoimmune disease. Thus, our data suggest that atherosclerosis is characterized by an autoimmune component driven by autoreactive CD4+ T-cells.

Results

Signature of antigen-specific T-cell in atherosclerosis

Recent scRNAseq studies in human atherosclerosis have shown a prominent accumulation of T-cells in the plaque.[3,4] Yet, it remains unclear whether these T-cells are bystanders or whether they actively contribute to lesion progression through antigen-specific activation. To examine potential recent antigen encounter and activation, CD69 expression was measured on the surface of both PBMC and plaque T-cells using flow cytometry (Cohort 1; **Fig. 1a, Supplementary Table 1**). A significant increase in CD69+ CD4+ (PBMC: 0.82% ± 0.71, plaque: 51.45% ± 16.39; *P*-value <0.0001) and CD8+ T-cells (PBMC: 4.95% ± 6.49, Plaque: 55.20% ± 19.40; *P*-value <0.0001) was observed in the plaque compared to PBMCs (**Fig. 1b, Extended Data Fig. 1a, b**). Since CD69 is known to rapidly upregulate after TCR/HLA engagement on T-cells[11], these data suggest that T-cells actively engage in TCR-specific interactions within the atherosclerotic plaque.

Yet, CD69 expression may also indicate the presence of resident memory T-cells or may be upregulated by exposure to type I Interferon (IFN).[12,13] To determine whether the elevated CD69 expression was due to antigen-specific interactions in the plaque, we aimed to assess whether these T cells were clonally expanded as well. We combined scRNAseq with scTCRseq on paired PBMCs and carotid artery plaques from 3 male patients (Cohort 2; **Supplementary Table 1**). The plaques were enzymatically digested and live CD45+ cells were isolated by fluorescent-activated cell sorting (FACS) (**Extended Data Fig. 2a**). Both PBMC and plaque cells were stained for CD3, CD4, CD8 and CD14 on a protein level with feature barcoding to properly distinguish between myeloid and T-cell subsets on both RNA and protein level. All cells were subsequently processed with droplet-based single-cell 5' RNA sequencing (10X Genomics) and sequenced (**Fig. 2a**). Unsupervised clustering revealed clusters comprised of T-cells, NK cells, myeloid cells and B cells, originating from both PBMC and plaque cells and with limited interpatient variability (**Extended Data Fig. 2b-e**). We did not further characterize all non T-cells as we specifically focused on characterizing T-cells to assess their clonal expansion in atherosclerosis. Therefore, all T-cells were selected based on both RNA and protein expression and subsequently unsupervised clustering was

performed independent of the variable TCR genes to prevent clustering based on clonality (see **Online methods**). Subclustering of both PBMC and plaque T-cells revealed 13 distinct T-cell subsets (**Fig. 2b, c, Extended Data Fig 2f**). Within the T-cells we observed one memory (C0) and three naive (C1, C2 and C10) T-cell clusters based on different expression levels of *TCF7*, *LEF1*, *SELL* and *CCR7* (**Fig. 2b, d, Supplementary Table 2)**. Furthermore, three effector T-cell clusters were detected (C3, C4, C5) expressing a multitude of different cytotoxic genes, amongst others *GZMB*, *GZMK*, *GZMA* (**Fig. 2b, d, Supplementary Table 2**). A T_{reg} cluster was defined based on expression of *FOXP3*, *IL2RA* and *TIGIT* (C6; **Fig 2b, d, Supplementary Table 2**).[14] In addition, an exhausted T-cell cluster characterized by expression of *HAVCR2*, *PDCD1* and *TOX*[15,16] (C7; **Fig. 2b, d, Supplementary Table 2**), and two γδ-T-cell clusters expressing *TRGC1*, *TRGC2*, *TRDC* (C8, C9; **Fig. 2b, d, Supplementary Table 2**) were detected. Lastly, we observed two small clusters consisting of mast cells (C11; **Fig. 2b, Supplementary Table 2**) and mucosal-invariant T-cells (MAIT; C12; **Fig. 2b, d, Supplementary Table 2**).

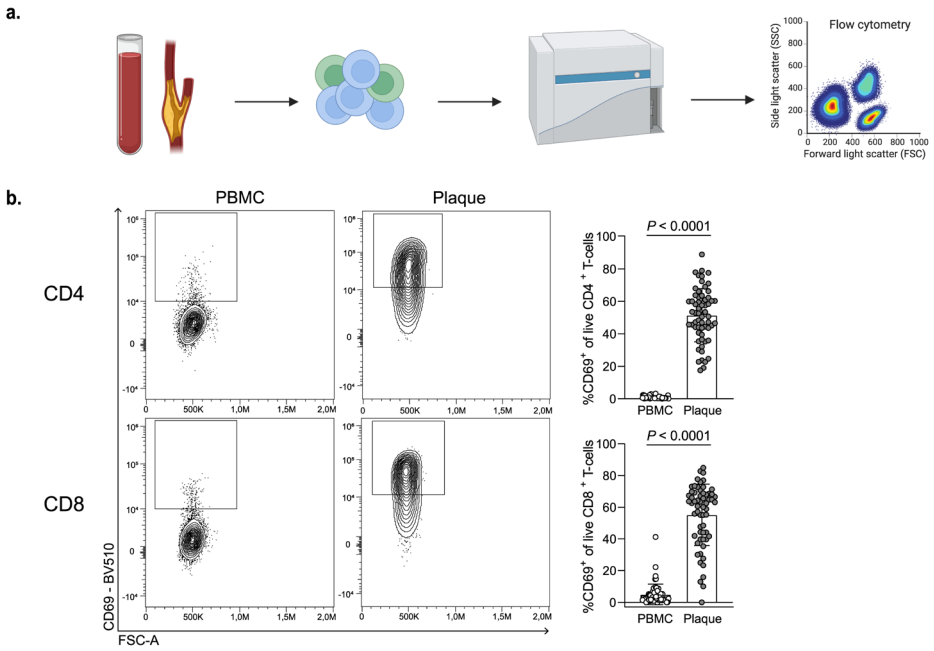

Fig. 1. Significant increase in CD69⁺ T-cells in the atherosclerotic plaque suggests an antigen-specific T-cell response. a. Experimental set up: single cells from PBMC and plaque samples were stained with fluorescently labeled antibodies and measured with flow cytometry. **b.** Flow cytometry analysis of CD69 expression on PBMC and plaque live CD4⁺ and CD8⁺ T-cells. *P*-values are depicted in the figure panels. Data are presented as mean values ± SD. PBMC n = 58; plaque n = 61. Statistical analyses were performed using an unpaired Mann-Whitney T-test.

Next, we compared expression of *CD69*, as well as *FOS* and *FOSB*, genes which are also upregulated downstream of TCR signaling[17], between plaque and blood. In line with the increased CD69$^+$ protein expression measured with flow cytometry, all three genes showed an increased mRNA expression in plaque T-cells compared to their PBMC counterparts (**Fig. 2e**). Subsequently, we applied VDJ sequencing to map paired α- and β-chains of the TCR and to define the clonal composition of the paired PBMC and plaque T-cells. Clonal expansion levels were calculated to indicate the clonotype abundance as percentage of the total measured TCRs per patient per tissue (**Fig. 2f**, see **Online Methods**). 'Single' represents a single clonotype occurrence. Expanded T-cells were divided in multiple categories characterized by increasing frequencies of clonotype occurrences, labeled as respectively 'Small', 'Medium', 'Large' and 'Hyperexpanded'.

Fig. 2. Single-cell TCR sequencing reveals clonal expansion and antigen-specific activation of T-cells in the plaque. a. Schematic overview of the study design. Human plaques were enzymatically digested and live CD45$^+$ cells were sorted using fluorescent-activated cell sorting (FACS). Matched blood samples were processed to isolate PBMCs. Both plaque and PBMC cells were then further processed using 10X Genomics and sequenced. **b.** UMAP depicting 13 distinct T-cell clusters resulting from unsupervised clustering (n = 24443). **c.** UMAP showing contribution of PBMC or plaque to the T-cell clusters. **d.** Heatmap with average expression of T-cell function-associated genes. **e.** Violin plot with expression of *CD69*, *FOS* and *FOSB* in PBMC and plaque T-cells. **f.** UMAP visualization of clonotype expansion levels among T-cells between PBMC and plaque. **g.** Barplot with quantification of clonal expansion levels between plaque and PBMC T-cells. **h.** Barplot with quantification of tissue enrichment scores of clonotypes. **i.** Circle plots depicting tissue-enrichment scores of all T-cells per tissue and per patient. **j.** Barplot with quantification of clonal expansion levels between PBMC and plaque T-cells of bulk TCR-sequencing data (Cohort 3, n = 10). **k.** Barplot with quantification of Tissue enrichment scores of bulk TCR-sequencing data (Cohort 3). Clonotype expansion levels: Single (1 occurrence), Medium (>0.1 & ≤1%), Large (>1 & ≤10%), Hyperexpanded (>10%), percentage of all T-cells. Tissue enrichment scores: Plaque-enriched (Frequency expanded clone higher in Plaque vs. PBMC), Single (1 occurrence), Unenriched (Frequency expanded clone similar in PBMC vs. Plaque), PBMC-enriched (Frequency expanded clone higher in PBMC vs Plaque). ►

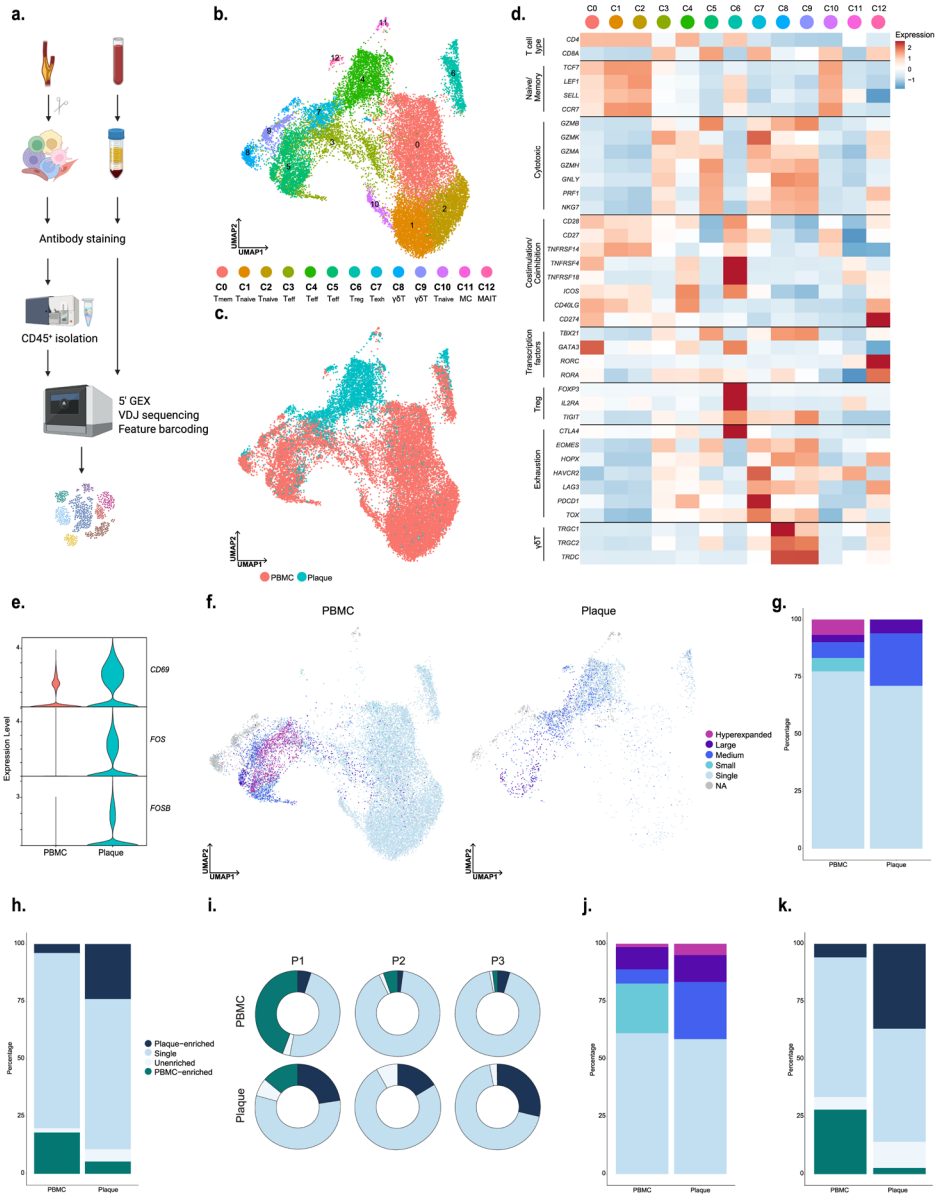
a.
Antibody staining
CD45+ isolation
5' GEX
VDJ sequencing
Feature barcoding
b.
C0 C1 C2 C3 C4 C5 C6 C7 C8 C9 C10 C11 C12
Tmem Tnaive Tnaive Teff Teff Teff Treg Texh γδT γδT Tnaive MC MAIT
c.
PBMC Plaque
d.
C0 C1 C2 C3 C4 C5 C6 C7 C8 C9 C10 C11 C12
Expression
T cell type
Naive/ Memory
Cytotoxic
Costimulation/ Coinhibition
Transcription factors
Treg
Exhaustion
γδT
CD4
CD8A
TCF7
LEF1
SELL
CCR7
GZMB
GZMK
GZMA
GZMH
GNLY
PRF1
NKG7
CD28
CD27
TNFRSF14
TNFRSF4
TNFRSF18
ICOS
CD40LG
CD274
TBX21
GATA3
RORC
RORA
FOXP3
IL2RA
TIGIT
CTLA4
EOMES
HOPX
HAVCR2
LAG3
PDCD1
TOX
TRGC1
TRGC2
TRDC
e.
Expression Level
CD69
FOS
FOSB
PBMC Plaque
f.
PBMC
Plaque
Hyperexpanded
Large
Medium
Small
Single
NA
g.
Percentage
PBMC Plaque
h.
Percentage
Plaque−enriched
Single
Unenriched
PBMC−enriched
PBMC Plaque
i.
P1 P2 P3
PBMC
Plaque
j.
Percentage
PBMC Plaque
k.
Percentage
PBMC Plaque

Taken together, a small increase in the percentage of total expanded T-cells is observed in the plaque compared to PBMCs (PBMC 23% vs. Plaque 29%; **Fig. 2f, g, Extended Data Fig. 3a, b, c, Supplementary Table 3**). One clonotype, originating from patient 1, was defined as hyperexpanded in the PBMC and large in the plaque. The TCRα-sequence of this clonotype matched with a TCRα-sequence previously associated with CMV in the VDJdb database (https://vdjdb.cdr3.net/).[18] The CD8⁺ T-cell specific clonotype, however, was only expressed on T-cells that had little expression of *CD69*, *FOS* and *FOSB*, suggesting that this was not an active viral infection (**Extended Data Fig. 4a-c**). In addition, the tissue enrichment of clonotypes was assessed to investigate whether certain clonotypes specifically accumulated within either of the tissues, or whether the clonotype abundance was unaffected by the location. T-cells with clonotypes more present in the PBMC were identified as PBMC-enriched and vice versa for plaque-enriched T-cells. Indeed, within the plaque an increased percentage of plaque-enriched T-cells was observed in all patients, suggesting a potential plaque-restricted antigen-induced clonal expansion (**Fig. 2h, i, Extended Data Fig. 3d, e, Supplementary Table 3**). To confirm these findings, bulk TCRβ sequencing was performed on matched blood and plaque T-cells from 10 patients (Cohort 3; **Supplementary Table 1**). Both clonal expansion levels as well as tissue-enrichment were comparable between TCRβ bulk sequencing and the scTCRseq data (**Fig. 2j, k, Extended data Fig. 5a**).

Increased percentage of expanded CD8⁺ T-cells in PBMCs

In order to properly isolate CD4⁺ and CD8⁺ T-cells for further analysis, a selection was made of CD4⁺ and CD8⁺ single positive T-cells based on expression of these proteins as measured by feature barcoding (**Extended Data Fig. 6a**). Subclustering of CD8⁺ T-cells resulted in 11 distinct subsets. The majority of the CD8⁺ T-cells had an activated phenotype as indicated by expression of multiple genes with a cytotoxic signature. One naive (C6) and one memory (C2) cluster were mainly detected in the PBMC (*TCF7*, *LEF1*, *SELL*, *CCR7*; **Fig. 3a, Extended Data Fig. 6b, c, Supplementary Table 2**). Four effector clusters were characterized of which C0 and C10 mostly reside in PBMC and C3 and C5 predominantly in plaque. C0, C3 and C10 expressed a multitude of different cytotoxic genes, including *GZMK* and *GZMA*, at different levels. C5 was characterized by expression of *CD69*, *FOS*, *FOSB* (**Fig. 3a, Extended Data Fig. 6b, c, Supplementary Table 2**). Furthermore, three terminally differentiated effector memory T-cell (T_{EMRA}) clusters were defined by expression of e.g. *GZMB*, *PRF1*, *NKG7* and lack of *CD27* and *CD28* (C1, C4, C7; **Fig. 3a, Extended Data Fig. 6b, c, Supplementary Table 2**). T_{EMRA} clusters were primarily associated with a gradual increase in expression of amongst others *KLRD1, KLRG1* and *FCGR3A*, indicating various stages of terminal

differentiation (**Extended Data Fig. 6d**). Using Seurat multimodal reference mapping, which maps your data set to a large PBMC data set with feature barcoding data, expression of CD45RA and CD45RO could be predicted. Indeed, T_{EMRA} subsets were predicted to express CD45RA, whereas the effector T-cells were predicted to be CD45RO$^+$ (**Extended Data Fig. 6e**). Finally, a cluster of γδ-T-cells (C8) and a cluster of MAIT (C9) were detected within the CD8$^+$ T-cell subsets (**Fig. 3a, Extended Data Fig. 6a, b, Supplementary Table 2**). Subsequently, clonal expansion levels were examined and quantified within the CD8$^+$ T-cells in PBMC and plaque. A large percentage of clonally expanded CD8$^+$ T-cells was detected in the plaque, however a higher percentage of expanded CD8$^+$ T-cells was detected in the PBMC (**Fig. 3b, c, Extended Data Fig. 6f, Supplementary Table 3**). Nevertheless, within the plaque, the majority of the expanded CD8$^+$ T-cells remained plaque-enriched (**Fig. 3d, Extended Data Fig. 6g, Supplementary Table 3**). Expanded CD8$^+$ T-cells showed upregulation of multiple genes involved in CD8 cytotoxicity, eg. *GZMH*, *KLRD1*, *PRF1*, *GZMB* (**Fig. 3e**). Interestingly, when comparing PBMC-enriched versus plaque-enriched CD8$^+$ T-cells, PBMC-enriched cells expressed cytotoxic genes such as *GNLY*, *PRF1* and members of the killer cell lectin-like subfamily (*KLRG1*, *KLRD1*), whereas plaque-enriched CD8$^+$ T-cells seemed to have experienced recent antigen-induced TCR activation (**Fig. 3f**). To further illustrate the plaque-expanded CD8$^+$ T-cell clusters, we selected C1, C3, C5 and C9 which had relatively the most plaque-enriched expansion (**Fig. 3g**). C1, C3 and C5 all expressed a multitude of cytotoxic genes. C1 highly expressed *NKG7*, *GNLY* and *GZMB*, of which the latter was increased in plaque, whereas C3 and C5 had increased expression of *GZMA* and *GZMK* in the plaque. C5 plaque T-cells had the highest expression of *CD69*, *FOS* and *FOSB*. Finally, MAIT-cells (C9) showed high expression of genes unique for this cell type (*TRAV1-2*, *ZBTB16*, *IL23R*)[19] and of TCR activation genes. To identify potential dynamics of different CD8$^+$ populations, we applied lineage tracing analyses using Monocle3 and RNA velocity. RNA velocity shows that within the CD8$^+$ clusters, cells tend to be less prone to switch into another subset. A small trajectory appeared between the memory CD8$^+$ T-cells (C2) and the antigen-experienced effector T-cells (C5), yet this was not clearly retrieved with pseudotime analysis (**Fig. 3i, j**).

Increased percentage of expanded CD4$^+$ T-cells in plaque

Unsupervised clustering revealed 11 subsets of CD4$^+$ T-cells (**Fig. 4a**). As previously described, CD4$^+$ T-cell clusters are mainly defined by a shift in activation status.[3,4] Two naive T-cell clusters (C1, C2) and a memory T-cell cluster (C0) were mainly detected within the PBMC (**Fig. 4a, Extended Data Fig. 7a, b, Supplementary Table 2**). Furthermore, a T-helper (T_h) 17-like cluster (C4) expressing *RORC*, *RORA* and *CCR6* as

well as a T_{reg} cluster (C5; **Fig 4a, Extended Data Fig. 7b, Supplementary Table 2**) were identified. Whereas T_{regs} were found in both PBMC and plaque, T_{h17}-like cells were mainly detected in PBMCs (**Extended Data Fig. 7c**). A T-cell cluster with genes involved in cell migration (T_{migr}, C6) mainly resided in PBMCs (**Supplementary Table 2**). Two different effector subsets were characterized, of which one more plaque-specific with high expression of *CD69*, *FOS*, *JUN* and *GZMA* (C3) and one found in both tissues specifically enriched for *GZMK* (C8; **Fig. 4a, Extended Data Fig. 7a, b, Supplementary Table 2**). Moreover, a cytotoxic $CD4^+$ T-cell cluster, that resembled the previously described $CD4^+CD28^{null}$ cells[3,20,21], was defined by expression of *GZMB*, *PRF1* and lack of *CD28* and was found in both PBMC and plaque (**Fig. 4a, Extended Data Fig. 6a, b, Supplementary Table 2**). Finally, a cluster of T-cells was observed in the PBMCs that expressed genes involved in IFN I signaling and a small mast cell cluster in the plaque (**Fig. 4a**, **Supplementary Table 2**). Subsequently, $CD4^+$ T-cell clonality was assessed. Clonal expansion levels were projected on the $CD4^+$ T-cell UMAP and quantified. In line with a recent study by Chowdhury *et al*.[10], the percentage of clonal expanded $CD8^+$ T-cells in the plaque is larger than those in $CD4^+$ T-cells. However, in contrast to $CD8^+$ T-cells, a marked increase in the percentage of expanded $CD4^+$ T-cells in the plaque was revealed compared to the PBMCs (**Fig. 4b, c, Extended Data Fig. 7e, Supplementary Table 3**). Furthermore, the expanded clonotypes in the plaque $CD4^+$ T-cells were mostly plaque-enriched (**Fig. 4d, Extended Data Fig. 7f, Supplementary Table 3**). When comparing expanded $CD4^+$ T-cells to their single counterparts with a unique clonotype, upregulation of genes involved in T-cell activation and cytotoxicity, such as *GNLY*, *GZMH*, *PRF1*, *CX3CR1*, were particularly observed in the expanded T-cells, whereas single T-cells expressed genes upregulated in naive and memory T-cells (*CCR7*, *LTB*, *LEF1*, *SELL*, *CD27*)(**Fig. 4e**). Interestingly, when comparing clonally expanded PBMC-enriched versus the plaque-enriched expanded $CD4^+$ T-cells, plaque-enriched $CD4^+$ T-cells showed enhanced expression of genes upregulated shortly after antigen-specific TCR interaction (*JUN*, *CD69*, *FOS*, *FOSB*) (**Fig. 4f**), suggesting there are $CD4^+$ T-cells that undergo antigen-specific interactions in the plaque. Next, we quantified the absolute number of plaque-enriched clones per $CD4^+$ T-cell cluster (**Fig. 4g**), which revealed cluster C3 as the major contributor in absolute number of plaque-specific clonally expanded T-cells. Furthermore, C7 and C8 consisted of a relatively large number of plaque-enriched clones compared to the other $CD4^+$ T-cell clusters. The C7 cluster, characterized by an increase in cytotoxic genes, including *GZMB*, *NKG7* and *PRF1*, has little to no expression of *CD69*, *FOS*, *FOSB*, indicating that although these cells have significant expanded clonotypes, they do not express genes involved in antigen-induced activation (**Fig. 4h**). The effector populations C3 and C8 displayed increased expression of TCR proximal genes *CD69*, *FOS* and *FOSB*. Interestingly, whereas we did not observe increased accumulation of clonally

expanded T_{regs} (C5) in plaque, we did observe upregulation of *FOS*, *FOSB* and *JUN* in plaque-derived T_{regs} compared to PBMC-derived T_{regs}, suggesting T_{regs} are encountering antigen in the plaque. Expression of various functional T_{reg} markers (*FOXP3*, *IL2RA*, *TIGIT*, *CTLA4*, *TNFRSF4* (OX40) and *TNFRSF18* (GITR)) in the plaque compared to the PBMC, indicated increased activity of T_{regs} (**Fig. 4h, 4i**).

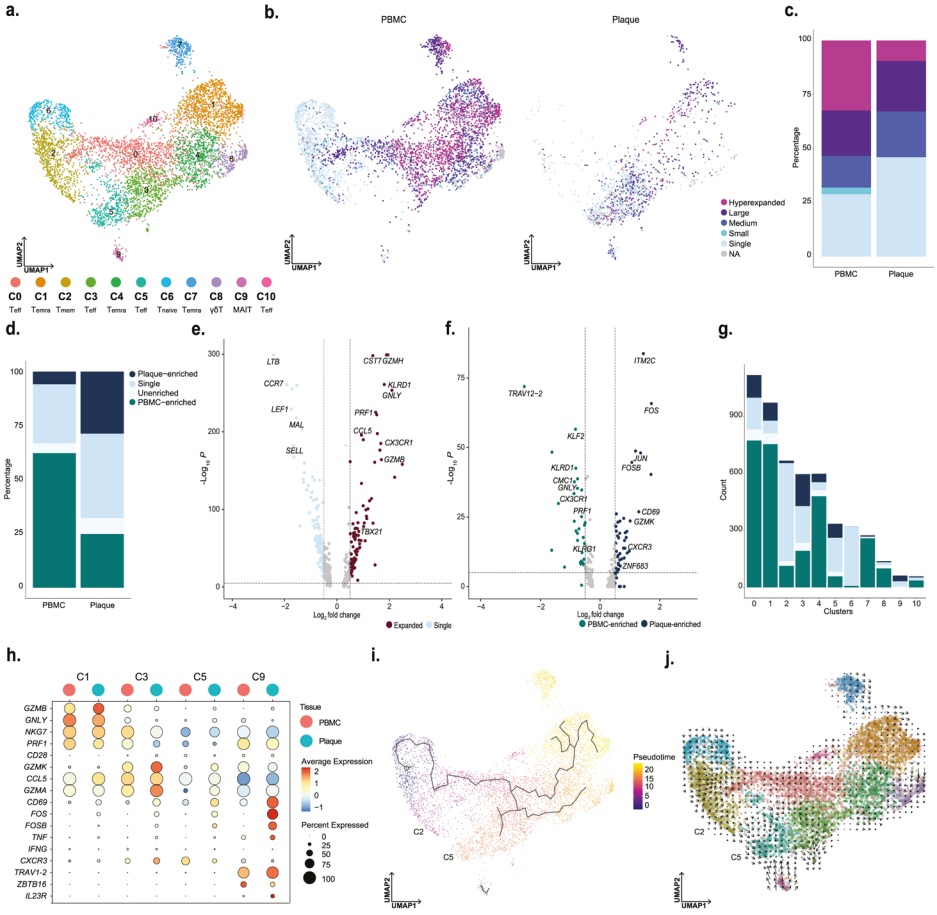

◂ **Fig. 3. Limited clonal expansion in plaque CD8⁺ T-cells compared to PBMC. a.** UMAP visualization of unsupervised clustering revealed 11 distinct CD8⁺ T-cell populations (n = 5730). **b.** UMAP visualization of different levels of clonotype expansion among CD8⁺ T-cells between PBMC and plaque. **c.** Quantification of clonal expansion levels between PBMC and plaque CD8⁺ T-cells. **d.** Quantification of tissue enrichment scores of clonotypes in CD8⁺ T-cells of PBMC and plaque. **e.** Volcano plot with differentially expressed genes between CD8⁺ T-cells with Single clonotypes and all expanded clonotypes (Small-Large). Genes were considered significant with a *P*-value < $10e^{-6}$ and a fold change of 0.5. For all Volcano plots, Bonferroni corrected *P*-values were calculated based on the total number of genes in the dataset. **f.** Volcano plot with differentially expressed genes of PBMC-enriched versus plaque-enriched CD8⁺ T-cells. Genes were considered significant with a *P*-value < $10e^{-6}$ and a fold change of 0.5. **g.** Barplot with quantification of tissue-enrichment score of individual CD8⁺ T-cell clusters. **h.** Dotplot of average expression of upregulated genes in cluster 1, 3, 5 and 9. **i.** UMAP visualization of pseudotime analysis of CD8⁺ T-cells. C2 indicates cluster 2; C5 indicates cluster 5. **j.** UMAP visualization of RNA velocity analysis of CD8⁺ T-cells. Clonotype expansion levels: Single (1 occurrence), Medium (>0.1 & ≤1%), Large (>1 & ≤10%), Hyperexpanded (>10%), percentage of all CD8⁺ T-cells. Tissue enrichment scores: Plaque-enriched (Frequency expanded clone higher in Plaque vs. PBMC), Single (1 occurrence), Unenriched (Frequency expanded clone similar in PBMC vs. Plaque), PBMC-enriched (Frequency expanded clone higher in PBMC vs Plaque).

Fig. 4. Increased percentage of expanded and plaque-enriched CD4⁺ T-cells in the atherosclerotic plaque. a . UMAP visualization of unsupervised clustering revealed 11 distinct CD4⁺ T-cell populations (n = 17073). **b.** UMAP visualization of different levels of clonotype expansion among CD4⁺ T-cells between PBMC and plaque. **c.** Barplot with quantification of clonal expansion levels between PBMC and plaque CD4⁺ T-cells. **d.** Barplot with quantification of tissue enrichment scores of clonotypes in CD4⁺ T-cells of PBMC and plaque. **d.** Volcano plot with differentially expressed genes between CD4⁺ T-cells with Single clonotypes and all expanded clonotypes (Small-Large). Genes were considered significant with a *P*-value < $10e^{-6}$ and a fold change of 0.5. For all Volcano plots, Bonferroni corrected *P*-values were calculated based on the total number of genes in the dataset. **f.** Volcano plot with differentially expressed genes of PBMC-enriched versus plaque-enriched CD4⁺ T-cells. Genes were considered significant with a *P*-value < $10e^{-6}$ and a fold change of 0.5. **g.** Barplot with quantification of tissue-enrichment score of individual CD4⁺ T-cell clusters. **h.** Dotplot of average expression of upregulated genes in cluster 3, 5, 7 and 8. **i.** Volcano plot with differentially expressed genes between regulatory T-cells in PBMC and plaque. Genes were considered significant with a *P*-value < $10e^{-6}$ and a fold change of 0.5. **j.** UMAP visualization of pseudotime analysis of CD4⁺ T-cells. Two branches of the analysis have been indicated with 1 and 2.**k.** UMAP visualization of RNA velocity analysis of CD4⁺ T-cells with close-up of branch 1 and 2. **l**. UMAP visualization of four overlapping clonotypes between cluster 6 and cluster 3. Open circles indicate PBMC CD4⁺ T-cells, closed circles indicate plaque CD4⁺ T-cells. Clonotype expansion levels: Single (1 occurrence), Medium (>0.1 & ≤1%), Large (>1 & ≤10%), percentage of all CD4⁺ T-cells. Tissue enrichment scores: Plaque-enriched (Frequency expanded clone higher in Plaque vs. PBMC), Single (1 occurrence), Unenriched (Frequency expanded clone similar in PBMC vs. Plaque), PBMC-enriched (Frequency expanded clone higher in PBMC vs Plaque). ▸

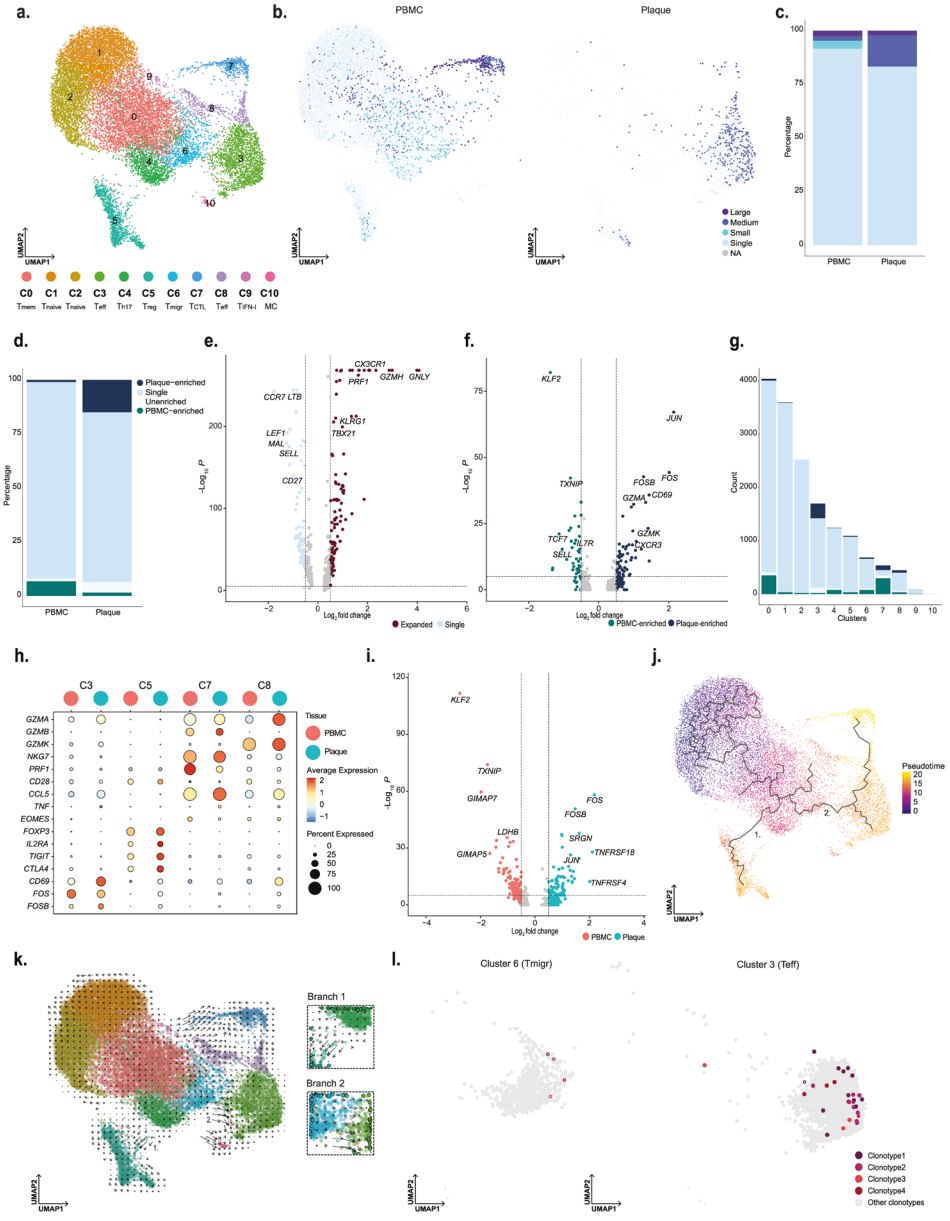
a.
b.
PBMC
Plaque
c.
C0 C1 C2 C3 C4 C5 C6 C7 C8 C9 C10
Tmem Tnaive Tnaive Teff Th17 Treg Tmigr TCTL Teff TIFN-I MC
Large
Medium
Small
Single
NA
Percentage
d.
Plaque−enriched
Single
Unenriched
PBMC−enriched
e.
f.
g.
Expanded
Single
PBMC-enriched
Plaque-enriched
Clusters
h.
C3 C5 C7 C8
GZMA GZMB GZMK NKG7 PRF1 CD28 CCL5 TNF EOMES FOXP3 IL2RA TIGIT CTLA4 CD69 FOS FOSB
Tissue
PBMC
Plaque
Average Expression
Percent Expressed
i.
j.
Pseudotime
k.
Branch 1
Branch 2
l.
Cluster 6 (Tmigr)
Cluster 3 (Teff)
Clonotype1
Clonotype2
Clonotype3
Clonotype4
Other clonotypes

To identify the origin of the antigen-specific effector CD4$^+$ T-cell subsets in the plaque, we applied lineage tracing analyses to define the dynamics of the different CD4$^+$ T-cell populations. Pseudotime analysis using Monocle3 showed a trajectory ranging from naive T-cells towards either the T_{regs} (Branch 1) or towards the effector T-cell population (Branch 2; **Fig. 4j**). The first pseudotime branch directing towards T_{regs} is projected through the T_{h17}-like CD4$^+$ T-cell cluster, potentially suggesting a plasticity between both subtypes. Yet, if the complementary RNA velocity analysis is assessed (time-resolved analysis based on spliced and unspliced mRNA[22]), the T_{reg} cluster does not seem to be derived from the T_{h17}-like cells (Branch 1; **Fig. 4k**). Moreover, T_{regs} in tissue also cluster further away from the circulating T_{h17}-like cells compared to the PBMC T_{regs}, indicating that the plaque environment is less likely to induce a phenotype switch from T_{regs} to T_{h17}. In addition, no overlapping clonotypes were found between both clusters and *FOXP3* and *RORC* did not co-express (**Extended Data Fig. 7b, c**), suggesting that in our data set we were not able to detect the previously described T_{reg}/T_{h17} plasticity.[23] Looking at the other branch in both pseudotime analysis and RNA velocity (Branch 2), a clear path ranging from the T_{migr} cluster (C6) towards the CD69$^+$ T_{eff} cluster (C3) is observed. Their migratory phenotype, highlighted by expression of *CCR4* and *CCR10* previously described to be expressed on infiltrating T-cells in the inflamed skin[24], suggests that this T_{migr} subset could be the precursor population for the antigen-specific CD4$^+$ T-cells in the plaque (**Extended Data Fig. 7d**). Indeed, when comparing overlap in TCR sequence between the different CD4$^+$ subpopulations, 37 clonotypes overlapped between both cluster C6 and C3. Within the top 5 most expanded clonotypes, 4 plaque-enriched clonotypes were detected and exhibited marked expansion in C3 compared to C6, further confirming our hypothesis that the clonally expanded T_{eff} cells could originate from the circulating migratory T-cell subset (**Fig. 4l, Extended Data Fig. 7c**).

TREM2$^+$ macrophages can activate antigen-induced CD4$^+$ T-cells

Our data suggests atherosclerotic plaques harbor one major CD4$^+$ T-cell subset that regularly undergoes antigen-specific interactions. To understand whether and how these clonally expanded T-cells interacted with myeloid subsets in the plaque, we selected five plaque myeloid cell populations from the overall data set: myeloid-derived dendritic cells (DC-M), plasmacytoid DCs (DC-P), proliferating macrophages (M-Prol), inflammatory macrophages (M-Inf) and foamy TREM2^{hi} macrophages (M-TREM2) (**Extended data Fig. 8a**).[3] Using CellChat we examined potential signaling pathways between these myeloid subsets and the CD4$^+$ and CD8$^+$ T-cells in the plaque.[25] CellChat can predict incoming (receptor), and outgoing (ligand) activity of cell-signaling pathways based on scRNA-seq data, accounting for the multimeric structure of ligand-receptor complexes, and the effect of co-factors on the ligand-receptor

interactions. Predicted outgoing and incoming pathway signaling were displayed per cluster. Overlap between outgoing and incoming signals of a certain pathway within or between clusters, indicate a possible interaction through this pathway. The different CD4$^+$ T-cell clusters showed different levels of relative signaling strength in the outgoing signaling patterns (top barplot heatmap, relative to outgoing signals of all pathways in the heatmap), whereas CD8$^+$ T-cells showed little difference between the clusters (**Fig. 5a, Extended data Fig. 8b**). In general, the most upregulated signaling pathway was MHCII as outgoing signal on all myeloid subsets and incoming signals in multiple CD4$^+$ T-cell subsets, including cluster 3 (C3). The plaque-enriched CD69$^+$ C3 displayed elevated outgoing signaling patterns. Interestingly, one of the pathways that was enriched in this cluster, is the CD40 pathway, involved in antigen-specific T-cell activation.[26] Next, we assessed whether the CD40 pathway was also enriched as incoming signaling pattern (**Fig. 5b**). Specific enrichment was observed in the M-TREM2 (foam cell) subset. Apart from the CD40 pathway, multiple other enriched pathways involved in immune synapse formation and co-stimulation could be defined between C3 and M-TREM2, including the CD99, CD6, CD40, Macrophage Inhibitory Factor (MIF) and Annexin A1 pathways (**Fig. 5b**).[27-30] Together, this suggests that M-TREM2 could be involved in activation of the clonally expanded CD4$^+$ T-cells in atherosclerotic lesions.

Common autoimmune phenotype in expanded plaque T-cells

Based on the accumulation of plaque-enriched CD4$^+$ and CD8$^+$ T-cell clonotypes, we hypothesized that human atherosclerosis could be characterized as an autoimmune driven T-cell response. To further confirm this hypothesis, we integrated a scTCRseq data set of the autoimmune disease psoriatic arthritis (PSA), containing data from PBMC and synovial fluid (SF).[31] As in this study CD45RA$^-$ T-cells were isolated, we excluded the naive T-cell clusters from our data set. Moreover, this study did not include feature barcoding. CD4$^+$ and CD8$^+$ T-cells were therefore selected based on the labels predicted by multimodal reference mapping (**Extended Data Fig. 9a-f**). Subsequently, CD4$^+$ and CD8$^+$ T-cells of both diseases were integrated (**Extended Data Fig. 9g, h**) and projected on the atherosclerosis CD4$^+$ and CD8$^+$ UMAP as reference. Remarkably, a clear overlap between PBMCs from atherosclerosis and PSA was observed in both CD4$^+$ and CD8$^+$ T-cells. In addition, this overlap was also seen between plaque and SF for both T-cell subsets (**Fig. 6a, b**). Next, clonal expansion levels were recalculated for both atherosclerosis and PSA (percentage of all CD4$^+$ or CD8$^+$ detected TCRs). Indeed, clonally expanded T-cells were found in similar CD4$^+$ and CD8$^+$ T-cell clusters in both diseases (**Fig. 6c, e**). Moreover, quantification of this clonal expansion revealed a similar distribution. An increased percentage of expanded CD8$^+$ T-cells versus expanded CD4$^+$ T-cells was detected in SF. However,

as seen in atherosclerosis, the percentage of expanded CD4⁺ T-cells was increased in SF compared to PBMC, whereas expanded CD8⁺ T-cells did not differ between both tissues (**Fig. 6d, f**). Tissue-enrichment scores were also determined and again displayed similarities between atherosclerosis and PSA. Tissue-enriched T-cells were located in overlapping clusters in both diseases. Quantification resulted in an increase in tissue-enriched T-cells in both CD4⁺ and CD8⁺ in plaque and SF compared to their matched PBMCs, although this enrichment was more prominent in SF versus plaque T-cells (**Fig. 6g-j**). Finally, we defined the genes supporting the overlap between the atherosclerosis and PSA subsets in C3 and C5 of both CD4⁺ and CD8⁺ T-cells. CD4⁺ T-cells from C3 were characterized by high expression of *CCL5*, *GZMK* and *GZMA* in both plaque and SF (**Fig. 6k, Extended Data Fig. 10a**). Atherosclerosis-specific C3 CD4⁺ T-cells had slightly increased *GZMA* expression compared to PSA PBMC and SF. In both diseases, *FOS* and *JUN* were upregulated in tissue compared to PBMC, whereas *FOSB* was specifically upregulated in plaque T-cells. Furthermore, regulatory CD4⁺ T-cells in both affected tissues appeared more active by upregulation of activation markers, including *IL2RA*, *TNFRSF4*, *TNFRSF18*, *TNFSF1B* and *CTLA4*, compared to the PBMC counterpart (**Fig. 6l, Extended Data Fig. 10b**). Nevertheless the Treg subset showed some disparity between SF and plaque derived cells as plaque T_{regs} also increasingly expressed *ICOS* and *ENTPD1*, compared to PSA SF derived T_{regs}. Interestingly, atherosclerosis T_{regs} in both PBMC and plaque had increased expression of *TGFB1* compared to the PSA T_{regs}. In both PSA and atherosclerosis CD8⁺ C3 T-cells, expression profiles displayed a comparable phenotype with high expression of T-cell effector genes, eg. *CCL5*, *GZMH*, *GZMA*, *GZMK* and *NKG7* (**Fig. 6m, Extended Data Fig. 10c**). Lastly, CD8⁺ T-cells from C5 showed upregulation of genes involved in antigen-induced TCR activation in both affected tissues (*FOS*, *JUN*) (**Fig. 6n, Extended Data Fig. 10d**). *FOSB* was upregulated in plaque only, similar to CD4⁺ C3 and *JUNB* expression was increased in PSA compared to atherosclerosis. Furthermore, increased expression of *ZNF683* was observed in both diseased tissues. *GZMH* was particularly upregulated in plaque CD8⁺ T-cells. To summarize, these data support the hypothesis that atherosclerosis has a significant autoimmune component as it has phenotypically similar clonally expanded T-cells compared to the autoimmune disease PSA.

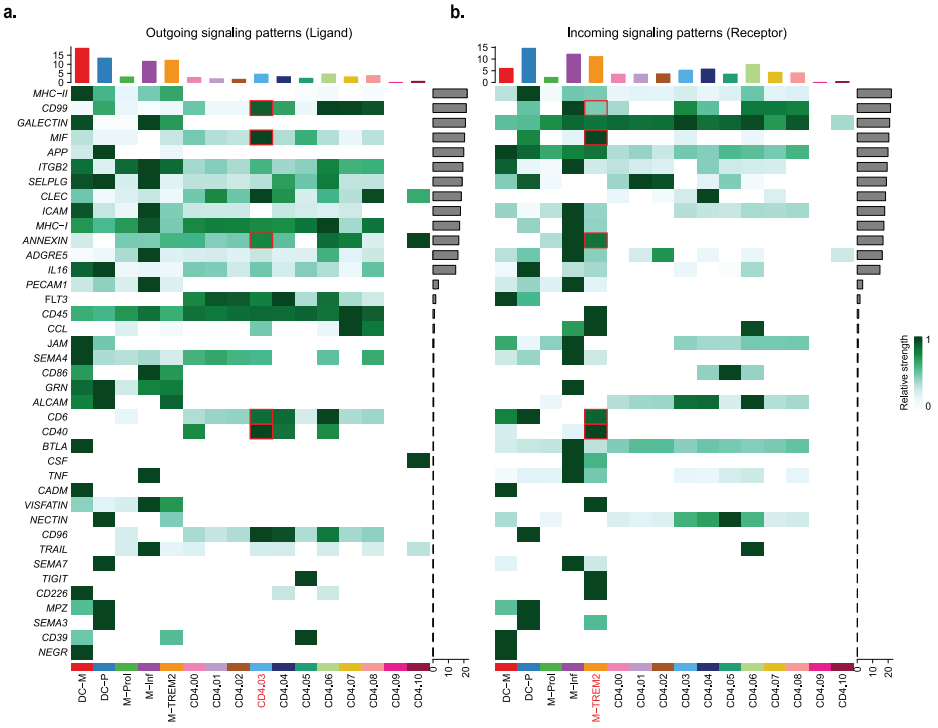

Fig. 5. Enriched interaction pathways between CD4⁺ T_{eff} cells and TREM^{hi} macrophages. a. Heatmaps displaying outgoing (Ligand) and **b.** incoming signaling (Receptor) patterns of pathways describing potential ligand-receptor interactions. Scale above heatmap indicates the relative signaling strength of a cell cluster based on all signaling pathways displayed in the heatmap. Grey bars right of the heatmap show the total signaling strength of a pathway in all cell clusters. The relative signaling strength indicated by ranging color from white (low) to green (high). DC-M indicates myeloid-derived dendritic cell (DC); DC-P indicates plasmacytoid DC; M-PROL indicates proliferating macrophages; M-Inf indicates inflammatory macrophage; M-TREM2 indicates TREM2^{hi} macrophages. All cells included in these graphs originate from the plaque.

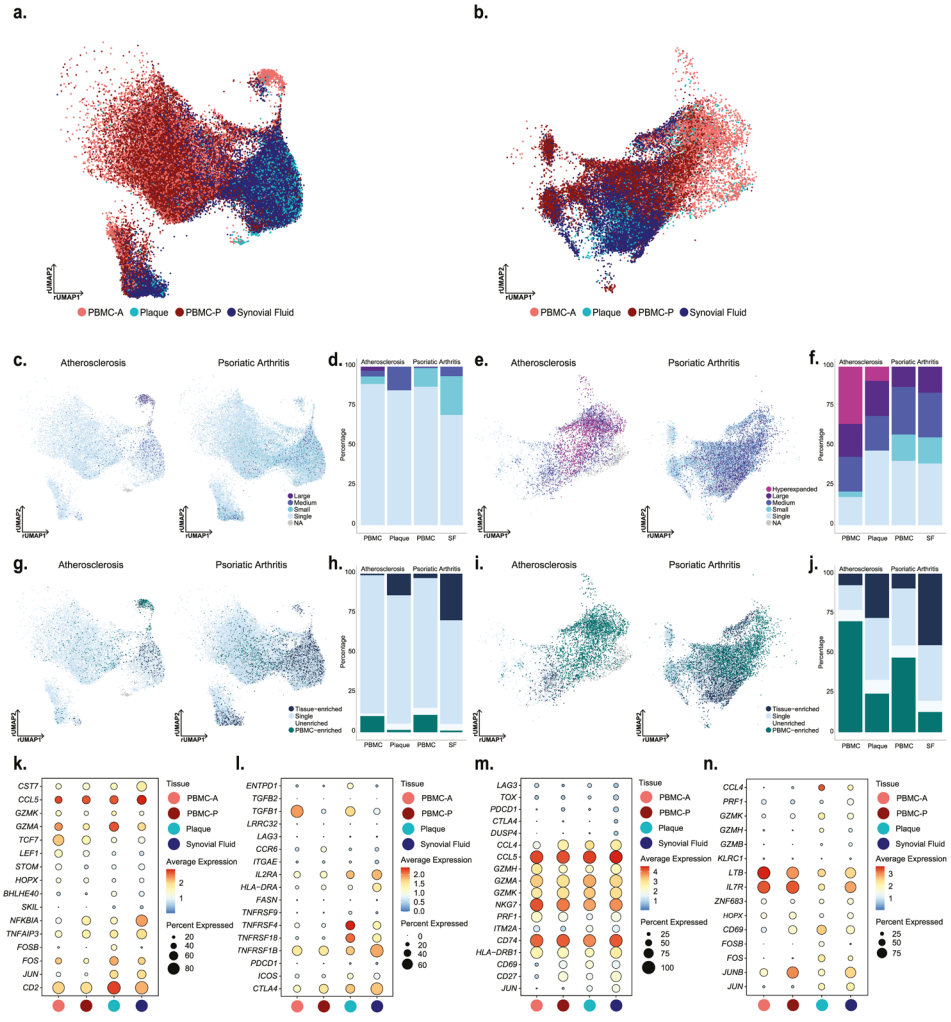
a.
b.
PBMC-A
Plaque
PBMC-P
Synovial Fluid
c.
Atherosclerosis
Psoriatic Arthritis
d.
e.
f.
g.
h.
i.
j.
k.
l.
m.
n.
Tissue
Average Expression
Percent Expressed

◂ Fig. 6. Tissue-enriched clonal expanded CD4⁺ and CD8⁺ T-cells of atherosclerosis and psoriatic arthritis have phenotypic commonalities. a. Atherosclerosis and psoriatic arthritis CD4⁺ T-cells of PBMC, plaque and synovial fluid projected on an atherosclerosis CD4⁺ T-cells reference UMAP (rUMAP). **b.** Atherosclerosis and psoriatic arthritis CD8⁺ T-cells of PBMC, plaque and synovial fluid projected on an atherosclerosis CD8⁺ T-cells reference UMAP (rUMAP). **c.** rUMAP projecting clonal expansion levels of CD4⁺ T-cells in atherosclerosis and psoriatic arthritis. **d.** Quantification of clonal expansion levels of CD4⁺ T-cells in atherosclerosis, split over PBMC and tissue. **e.** rUMAP projecting clonal expansion levels of CD8⁺ T-cells in atherosclerosis and psoriatic arthritis. **f.** Barplot displaying quantification of clonal expansion levels of CD8⁺ T-cells in atherosclerosis, split over PBMC and tissue. **g.** rUMAP projecting tissue enrichment scores of clonotypes in CD4⁺ T-cells of atherosclerosis and psoriatic arthritis. **h.** Barplot with quantification of tissue enrichment scores of CD4⁺ T-cells in atherosclerosis and psoriatic arthritis, split by PBMC, and tissue. **i.** rUMAP projecting tissue enrichment scores of clonotypes in CD8⁺ T-cells of atherosclerosis and psoriatic arthritis.. **j.** Quantification of tissue enrichment scores of CD8⁺ T-cells in atherosclerosis and psoriatic arthritis, split by PBMC, and tissue. **k-n.** Dotplots with average expression of genes characterizing the genes underlying the overlap between atherosclerosis and psoriatic arthritis in CD4⁺ T_{regs} (C5, **k**) and T_{effs} (C3, **l**) and in CD8⁺ T_{effs} (C3, **m**; C5**; n**). Clonotype expansion levels: Single (1 occurrence), Medium (>0.1 & ≤1%), Large (>1 & ≤10%), Hyperexpanded (>10%), percentage of respectively CD4⁺ and CD8⁺ T-cells. Tissue enrichment scores: Tissue-enriched (Frequency expanded clone higher in Tissue vs. PBMC), Single (1 occurrence), Unenriched (Frequency expanded clone similar in PBMC vs. Tissue), PBMC-enriched (Frequency expanded clone higher in PBMC vs Tissue).

Discussion

Atherosclerosis has a long history of being treated as metabolic and/or lifestyle disease, with its inflammatory component being overlooked as a potential target of intervention. Ground-breaking work earlier this century has shown that inflammation is an integral part of the disease pathophysiology and significant health benefits can be obtained by intervening in inflammatory cascades. Our work here takes these observations a step further and suggests that atherosclerosis is an autoimmune-like disease, with autoreactive T-cells driving the inflammation process inside the plaque (**Fig. 7**). Classic autoimmune diseases that involve inflammation of distinct tissue, such as Type I diabetes, multiple sclerosis, and rheumatoid and psoriatic arthritis are usually associated with specific HLA Class II alleles, suggesting a pathogenic CD4⁺ T-cell response is a major cause of disease. Moreover, accumulation of antigen-specific T-cells at the site of inflammation is a hallmark of autoimmune disease. The absence of clear associations of HLA alleles and atherosclerosis argue against the autoimmune theory in CVD[32], yet the multifactorial nature of the disease and the large population that it affects, make such associations difficult to establish. Accumulation of T-cells in atherosclerotic plaques however is well established. Moreover, earlier studies investigating TCR diversity using TCRβ sequencing in the plaque indicated an increased clonality in the lesions compared

to blood samples from CVD patients.[33] By taking advantage of scTCRseq here, we can combine data on distribution of TCRs with their activation state and functionality. Using this approach we show that a select number of effector CD4⁺ T-cells and CD8⁺ T-cells accumulate in the lesions and likely undergo antigen-specific activation similar to autoimmune diseases such as psoriatic arthritis. Recent work by Chowdhury *et al*. using a similar approach reached the same conclusion[10], however by using matched PBMC controls we were able to determine that a large fraction of clonally expanded CD8⁺ T-cells did not specifically accumulate in the plaque and were equally represented or even overrepresented in the circulation. One CD8⁺ T-cell clone in particular, whose Vα TCR sequence was identified as specific for CMV, was hyperexpanded and accounted for a significant percentage of clonally expanded T-cells in the plaque, while also contributing to the clonally expanded CD8⁺ T-cell pool in the PBMC of this patient. Moreover, this clone did not show a signature of recent antigen encounter. Apart from classical CD4⁺ and CD8⁺ T-cells, we also identified a proinflammatory MAIT population. MAITs have been described in multiple autoimmune and inflammatory diseases, including psoriatic arthritis, with contradicting or unknown contributions to disease development. How MAITs contribute to atherosclerosis development and whether they are activated through their non-polymorphic MHC class I-like protein MR1 or through TCR independent activation induced by i.e. IL-12 and IL-18[34–36], needs further elucidation.

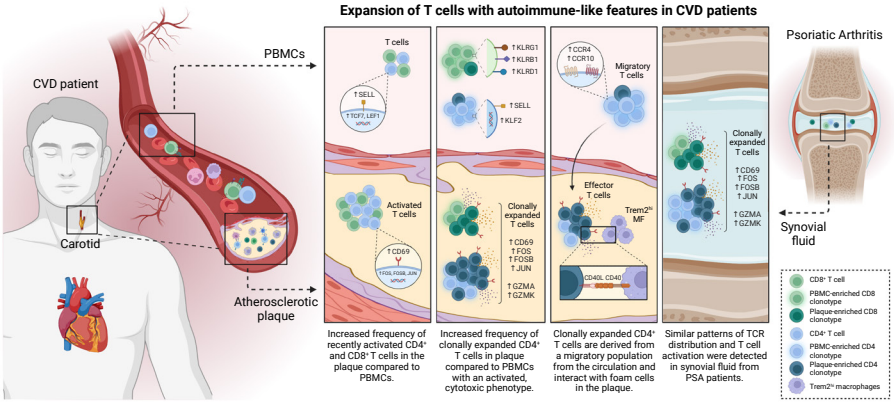

Fig. 7. Schematic presentation of the main conclusions.

By instead focusing on the clonally enriched T-cells specific for the plaque, we observed that one subset of effector CD4⁺ T-cells was significantly enriched in clonally expanded TCRs and expressed genes indicative of recent antigen engagement. Although we found two such populations in the CD8⁺ T-cells, their clonal enrichment was less pronounced. Interestingly, we also observed an antigen activation signature in the

plaque residing T_{regs} suggesting these T-cells undergo antigen-specific interactions in the plaque. However these T_{regs} did not show significant clonal expansion, suggesting these cells do not expand in the plaque. Instead, RNA velocity analysis suggests T_{regs} are not derived from any other T-cell population we detected in PBMC or plaque. Also, we observed minimal overlapping TCR sequences between T_{reg} and other T-cells in the plaque, in contrast to the effector $CD4^+$ T-cell population, which showed significant TCR overlap with a migratory $CD4^+$ T-cell subset in the circulation. Previous work suggests that T_{regs} can lose their suppressive capacity and gain expression of proinflammatory markers.[37] A shift of autoreactive (ApoB100-specific) T_{regs} towards a T_{h17} phenotype has been associated with severity of CVD. Although the authors show in mice that this shift happens independent of the TCR clonotypes, our data argues against such a shift and suggests T_{regs} and effector $CD4^+$ T-cells do not derive from the same ancestor, but rather develop independent of one another. Alternatively, the number of TCRs detected here may not have been sufficient to find overlapping sequences between T_{regs} and effector $CD4^+$ T-cells. Also, it is unknown whether ApoB100-specific T-cells undergo antigen-specific interaction in the plaque and because the antigen-specificity of T-cells investigated in this study are unknown, it is possible we did not examine ApoB100-specific $CD4^+$ and $CD8^+$ T-cells here.

We attempted to cluster the TCRs in silico using GLIPH2 and GIANA algorithms[38,39], which are based on CDR3β similarity, as this is proposed to be an attractive way to cluster TCRs for a specific antigen together. However, a convincing clustering of plaque-enriched clonotypes was not observed in our dataset. The current clustering algorithms may have some limitations, which in our data was illustrated by co-clustering of $CD4^+$ T cell and $CD8^+$ T cell derived clonotypes, which was only resolved if the CDR3α sequence was included. Moreover, we observed diffuse clustering of clonotypes previously reported as ApoB100-specific[40] suggesting that the current algorithms are not specific enough to resolve TCR clustering in atherosclerosis. Therefore, we believe that a more stringent approach that includes both CDR3α and CDR3β needs to be developed.

As we observe antigen-specific activation in both the effector as well as T_{reg} subsets, it is currently unclear what the overall effect of TCR engagement in the lesion is. Previous work in mice has shown mixed results with $MHCII^{-/-}$ $apoE^{-/-}$ mice suggesting this interaction is protective, whereas various papers suggest a pathogenic role for $CD4^+$ T-cells in atherosclerosis.[41,42] Interestingly, our work identifies several pathways involved in costimulation and immunological synapse formation that potentially drive pathogenic interactions of effector $CD4^+$ T-cells with the M-TREM2 (foam cell) population. When limited to effector $CD4^+$ T-cell populations these may be specific and druggable targets.

For instance, the expression of *CD40LG* on the clonally enriched effector population, suggests active signaling to foam cells through CD40. This costimulatory pathway and that of other TNF superfamily member has been extensively studied in mouse models of atherosclerosis and is subject of a clinical study.[43,44] The observation of antigen-specific T_{reg} interaction also provides a rationale for potential therapeutic possibilities, such as expanding these cells by means of vaccination or development of tolerogenic CAR T-cells. Identification of the antigen(s) driving T_{reg} interaction in the plaque will be crucial for this development. Potential antigens such ApoB100, Heat Shock Proteins, and fibronectin have been suggested as potential self-antigens and have shown therapeutic potential as antigens in mouse models[45–47] and may serve as potential starting point for vaccine development. Thus, here we highlight an autoimmune component to the pathophysiology of atherosclerosis, and confirm a rationale for immunotherapeutic interventions in cardiovascular disease.

Methods

Patient cohorts

For flow cytometry (Cohort 1) and bulk TCRβ sequencing (Cohort 3), whole blood and atherosclerotic plaques were obtained from respectively 61 and 10 patients that underwent carotid endarterectomy surgery (CEA) at the Haaglanden Medical Center Westeinde (HMC; The Hague, The Netherlands). The study was approved by the Medical Ethics Committee of the HMC (Study approval number Cohort 1: 17-046, protocol number NL57482.098.17 and Cohort 3: Z19.075, protocol number NL71516.058.19). For single-cell TCR sequencing, whole blood and atherosclerotic plaques were obtained from 3 male patients that underwent CEA (Cohort 2). Patients were included in the AtheroExpress biobank (AE, www.atheroexpress.nl), an ongoing biobank study at the University Medical Centre Utrecht (UMCU).[48] The study was approved by the Medical Ethics Committee of the UMCU (Study approval number: TME/C-01.18, protocol number 03/114). All blood samples were collected by venipuncture prior to surgery. Atherosclerosis specimens were obtained from primary CEAs, restenotic plaques were excluded due to their different plaque composition as compared to primary atherosclerotic plaques.[49] Informed consent was obtained from all patients involved in this study.

Whole blood processing

Peripheral venous blood was collected in K2-EDTA blood tubes (BD Vacutainer). For single-cell TCR sequencing, blood was processed within 10 minutes after withdrawal (Cohort 2). For both Cohort 1 and 2, blood was diluted 1:2 in Phosphate Buffered Saline (PBS) containing 2% Fetal Calf Serum (FCS). A density gradient was created using SepMate™

PBMC isolation tubes (STEMCELL Technologies) containing Ficoll-Paque Premium™ (GE Healthcare). Cells were centrifuged at 1200xg for 10 minutes at room temperature. The intermediate layer containing peripheral blood mononuclear cells (PBMC) was isolated and washed twice with PBS + 2% FCS (250xg, 10 minutes, room temperature). Cells were taken up in PBS + 1% Bovine Serum Albumin (BSA) until further processing. For Cohort 3, whole blood samples were lysed twice with ACK lysis buffer in PBS(1:10) for 10 minutes at RT and washed with PBS (300xg, 5 minutes). Cells were taken up in RPMI + 1% FCS and cryostored in Cryostor cell cryopreservation medium (Sigma-Aldrich) until further use.

Human atherosclerotic plaque cell isolation

Human carotid plaques were collected during CEA; the culprit segment (5 mm) was used for histology and embedded in paraffin as described elsewhere.[48] In brief, culprit segments were fixed in 4% formaldehyde and decalcified in 10% EDTA pH 7.5. Afterwards, culprit segments were embedded in paraffin. Time between surgical removal and plaque processing did not exceed 10 minutes. The inclusion of a small medial layer in the dissected tissue could not be excluded during the surgical procedure. The remainder of the plaque washed in RPMI and minced into small pieces with a razor blade. The tissue was then digested in RPMI 1640 containing 2.5 mg/mL Collagenase IV (ThermoFisher Scientific), 0.25 mg/mL DNAse I (Sigma), 2.5 mg/mL Human Albumin Fraction V (MP Biomedicals) at 37°C for 30 minutes. In Cohort 2, 1 µM Flavopiridol (Selleckchem) was added to the digestion mixture. Subsequently, the plaque cell suspension was filtered through a 70 µm cell strainer and washed with RPMI 1640. Cells were kept in RPMI 1640 with 1% Fetal Calf Serum until subsequent staining for flow cytometry (Cohort 1), Feature Barcoding and fluorescence-activated cell sorting (Cohort 2) or cryostored in Cryostor cell cryopreservation medium (Sigma-Aldrich) until further use.

Flow cytometry

Single cell suspensions from blood and plaque from Cohort 1 were stained with a mixture of extracellular antibodies for 30 minutes at 37°C (**Supplementary Table 4**). All measurements were performed on a Cytoflex S (Beckman and Coulter, USA) and analysed with FlowJo v10.7 (Treestar, San Carlos, CA, USA). A Shapiro log normality test was performed and a two-tailed Mann Whitney test was performed using GraphPad analysis software to determine significance.

Antibody staining for Feature Barcoding and fluorescent activated cell sorting

PBMC

PBMCs of Cohort 2 were stained with TotalSeq-C antibodies against CD3, CD4, CD8 and CD14 (**Supplemental Table 4**). Antibody pools containing 0.25 µg per antibody were prepared in labeling buffer (PBS + 1% BSA), spun down at 14.000xg for 10

minutes at room temperature and supernatant was collected for further staining. First, cells were stained with Human Trustain FcX (Biolegend) for 10 minutes at 4°C. Next, the antibody pool supernatant was added and incubated for 30 minutes at 4°C. Cells were washed thrice with labeling buffer at 400xg for 5 minutes at 4°C. Next, cells were taken up in PBS + 0.4% BSA and further processed with 10X genomics.

Plaque
Single cell suspensions of plaques of Cohort 2 were stained with TotalSeq-C antibodies against CD3, CD4, CD8 and CD14 (**Supplemental Table 4**). Antibody pools containing 0.25 µg/antibody and plaque (1 µg/antibody) single cell suspensions were prepared in labeling buffer (PBS + 1% BSA), spun down at 14.000xg for 10 minutes at room temperature and supernatant was collected for further staining. First, cells were stained with Human Trustain FcX (Biolegend) for 10 minutes at 4°C. Next, the antibody pool supernatant was added together with Calcein AM (1:1000; ThermoFisher), Hoechst (1:000; ThermoFisher) and CD45-PECy7 (1:200, Clone HI30, BD Biosciences) and incubated for 30 minutes at 4°C. Cells were washed thrice with labeling buffer at 400xg for 5 minutes at 4°C. Next, cells were taken up in PBS + 2% FBS. Live $CD45^+$ plaque cells were sorted using the BD FACS Aria II (BD Biosciences) in PBS + 0.04% BSA and further processed with 10X genomics.

Single-cell TCR sequencing by 10X Genomics
Single-cell TCR sequencing was performed on PBMCs and live $CD45^+$ plaque cell suspensions from Cohort 2 using the 10X Genomics 5' Single Cell Immune Profiling technology (10X Genomics, USA). Sequencing libraries were prepared using the 5' V1.1 chemistry following standard 10X Genomics protocol (10X Genomics, USA). Sequencing was performed using the Illumina Novaseq 6000 (Novogene).

Bulk TCRβ sequencing
Genomic DNA was extracted from plaque single cell suspensions and matched PBMC samples (Cohort 3) using a DNA extraction kit in accordance to the manufacturer's instructions (Qiagen, Hilden Germany). Sequencing of the VDJ locus was performed using the Adaptive Biotechnologies (Seattle WA) TCRβ sequencing platform.

Single-cell TCR sequencing data processing , clustering, and clonotype quantification
Single-cell TCR sequencing data analyses were executed in R-4.0.1 and R-4.1.3 environments, primarily using Seurat (version 4.0.0 – 4.1.1).[50,51] scTCR-seq data were processed as previously described.[51,52] In short, reads were filtered for mitochondrial, ribosomal genes, and long noncoding RNA genes. To remove apoptotic cells, low quality cells, and doublets, only cells with a gene expression below 2% for KCNQ1OT1, below 2% for UGDH-AS1 , below 2 % for GHET1, and expressing between 200 and 5000 genes

were used for further analysis. QC-filtered PBMC and plaque Seurat-objects were first merged per patient, after which the patient-merged Seurat-objects were normalized using the SCT method, integrated using rpca reduction with, and clustered according to the Seurat "scRNA-seq integration"-vignette. VDJ-sequencing data were imported into Seurat using the combineExpression function of scRepertoire (version 1.4.0).[53] The complete integrated dataset was mapped to the pbmc_multimodal.h5seurat dataset (https://atlas.fredhutch.org/data/nygc/multimodal/pbmc_multimodal.h5seurat) to transfer cell type labels to the integrated Seurat-object.

For subclustering, T-cells were selected from the complete integrated dataset, taking the clusters with protein expression of CD3, CD4 and CD8, and without CD14 expression (ADT assay). Before reclustering the T-cells, variable TCR genes were removed from the variable genes list, before PCA and clustering to avoid clustering based on TCR, interfering with clustering on T-cell phenotype. Yet, TCR genes were not removed from the data set. Separate $CD4^+$ T-cell and $CD8^+$ T-cell objects were then created by subsetting the T-cell object based on respectively protein expression of CD4>0.75 and CD8>1.0 in the ADT assay. Custom clonotype counting functions were used to quantify the clonotype content of the individual samples based on the amino acid sequences of the TCRs. Clonotype frequencies relating to the total TCR repertoire per patient, per tissue are depicted in the atherosclerosis figures. Volcano plots were created using EnhancedVolcano (version 1.8.0).[54] For all Volcano plots, the FindMarkers function of Seurat was used to define differential genes between both groups by using a non-parametric Wilcoxon Rank sum test to determine significance. To assess the differentiation trajectories of the $CD4^+$ T-cells and $CD8^+$ T-cells Monocle (version 3) and velocyto.R (version 0.6) were utilized.[22,55] To assess possible interactions of antigen presenting cells and T-cells in the plaque CellChat (version 1.4.0) was utilized.[25]

Definition of clonotype expansion levels and tissue-enrichment scores

The TCR amino acid sequences were used to define the clonotypes. The clonotype abundance of a clonotype was calculated as the percentage of cells expressing a certain clonotype within a tissue of a patient, divided by the total number of cells in which a TCR was detected in the same tissue of the same patient. Based on the number and percentage of cells expressing the same Clonotype, Clonotypes were classified as either, Hyperexpanded, Large, Medium, Small, or Single in the tissues of the patients (**Supplementary Table 5**). Furthermore the tissue enrichment of clonotypes was determined according to the parameters listed in **Supplementary Table 6**.

Integration with psoriatic arthritis scTCRseq data

T-cells from our scTCRseq atherosclerosis dataset were compared with TCRseq data from donor-matched PBMC and Synovial Tissue from Psoriatic arthritis (PSA) patients (ArrayExpress: E-MTAB-9492, European Genome-phenome Archive: EGAS00001002104).[31] The same QC, and processing steps were performed for the PSA dataset as described above for our atherosclerosis data set. Subsequently, the integrated PSA dataset was mapped to the UMAP reduction of our complete T-cell object, using our atherosclerosis dataset as reference. Because $CD4^+$ T-cells and $CD8^+$ T-cells could not be separated cleanly based on the clustering and the PSA dataset does not contain protein expression data, the atherosclerosis dataset and the PSA dataset were divided based on the predicted cell type (CD4 T-cell or CD8 T-cell), derived from the pbmc_multimodal.h5seurat dataset. Subsequently, the atherosclerosis and PSA $CD4^+$ T-cell and $CD8^+$ T-cell datasets were split by patient and reintegrated as previously described for the atherosclerosis object, to form a $CD4^+$ T-cell object and a $CD8^+$ T-cell object containing atherosclerosis and PSA derived T-cells. Then, the integrated datasets were mapped to our original $CD4^+$ T-cell and $CD8^+$ T-cell UMAP reductions. Since the PSA dataset is devoid of naïve T-cells due to the T-cell isolation procedure utilized by Penkava *et al.* , naïve T-cell clusters were removed from the $CD4^+$ T-cell dataset (cluster1 and 2) and $CD8^+$ T-cell dataset (cluster 6) before quantification of the clonotype abundance.[31]

Data availability

The raw single-cell TCR sequencing data from the Athero-Express cohort are not publicly available due to research participant privacy/consent. These data and the bulk TCRβ sequencing data can be accessed via DataverseNL at this address: https://doi.org/10.34894/DDYKLL. There are restrictions on use by commercial parties, and on sharing openly based on (inter)national laws and regulations and the written informed consent. Therefore, these data (and additional clinical data) are only available upon discussion and signing a Data Sharing Agreement (see Terms of Access in DataverseNL) and within a specially designed UMC Utrecht provided environment.

Open source single-cell TCR sequencing data from donor-matched PBMC and Synovial Tissue from Psoriatic arthritis (PSA) patients that we used in this study are publicly available (ArrayExpress: E-MTAB-9492, European Genome-phenome Archive: EGAS00001002104).[31]

Code availability

In silico data analysis was performed using custom made R scripts designed specifically for this study and/or based on the recommended pipelines from pre-existed packages listed above. R scripts are available via Zenodo (https://doi.org/10.5281/zenodo.7415207).

Supplemental Tables

For supplemental tables see https://doi.org/10.1038/s44161-022-00208-4

Ackowledgements

This work was supported by The Netherlands Heart Foundation [CVON2017-20: GENIUS II supporting JK, MW, GP, MACD, IB, BS], Dekker Fellowship [2018T051 to ACF]; Spark-Holding BV [grant number 2015B002 to MW]; NWO-ZonMW [PTO program grant number 95105013, supporting MACD, IB, JK]; the European Union [ITN-grant EPIMAC to MW]; Fondation Leducq [Transatlantic Network Grants to MW and GP]; EU 755320 Taxinomisis grant [supporting GJdB, AB, GP] and European Research Area Network on Cardiovascular diseases [ERA-CVD, 2018T092 supporting MJMJ, BS and 2019T107 supporting JM, ACF]; NWO Veni [VI.Veni.212.196 to KHMP]; NWO-ZonMW [Open competition 09120011910025 to MW]. Established investigator of the Netherlands Heart Foundation [2019T067, supporting EH, LD, IB].

We would like to thank Single Cell Discoveries (Utrecht) for processing 10X genomics samples. Study set up figures and the graphical abstract were created in BioRender.

Author contributions

M.A.C.D., F.H.S., I.B, J.K, A.C.F and B.S. drafted the manuscript and designed the figures. J.A.H.M.P, L.G., A.W., H.J.S and G.J.B. performed carotid endarterectomy procedures and collected patient material. M.A.C.D., A.B., E.H., L.D., J.M., M.N.A.B.K and M.J.M.J executed the human plaque processing, FACS and flow cytometry. M.A.C.D., K.H.M.P., F.S, J.K., I.B., B.S. participated in conceptualization, data interpretation and provided critical feedback on the manuscript. J.K., M.W., G.P., I.B and B.S participated in the conceptualization, funding and supervision of the scRNAseq experiments and analysis and finalization of the manuscript. All authors provided feedback on the research, analyses and manuscript.

Competing interests

The authors declare no competing interests.

References

1. Ridker, P. M. *et al.* Antiinflammatory Therapy with Canakinumab for Atherosclerotic Disease. *N. Engl. J. Med.* **377**, 1119–1132 (2017).
2. Nidorf, S. M. *et al.* Colchicine in Patients with Chronic Coronary Disease. *N. Engl. J. Med.* **383**, 1838–1847 (2020).
3. Depuydt, M. A. C. *et al.* Microanatomy of the Human Atherosclerotic Plaque by Single-Cell Transcriptomics. *Circ. Res.* **127**, 1437–1455 (2020).
4. Fernandez, D. M. *et al.* Single-cell immune landscape of human atherosclerotic plaques. *Natuere Med.* **25**, 1576–1588 (2019).
5. Stemme, S. *et al.* T lymphocytes from human atherosclerotic plaques recognize oxidized low density lipoprotein. *Med. Sci.* **92**, 3893–3897 (1995).
6. Wolf, D. *et al.* Pathogenic Autoimmunity in Atherosclerosis Evolves From Initially Protective Apolipoprotein B 100-Reactive CD4 + T-Regulatory Cells. *Circulation* **142**, 1279–1293 (2020).
7. Roy, P. *et al.* Immunodominant MHC-II (Major Histocompatibility Complex II) Restricted Epitopes in Human Apolipoprotein B. *Circ. Res.* **131**, 258–276 (2022).
8. Benne, N. *et al.* Anionic 1,2-distearoyl-sn-glycero-3-phosphoglycerol (DSPG) liposomes induce antigen-specific regulatory T cells and prevent atherosclerosis in mice. *J. Control. Release* **291**, 135–146 (2018).
9. Gisterå, A. *et al.* Vaccination against T-cell epitopes of native ApoB100 reduces vascular inflammation and disease in a humanized mouse model of atherosclerosis. *J. Intern. Med.* **281**, 383–397 (2017).
10. Chowdhury, R. R. *et al.* Human Coronary Plaque T Cells Are Clonal and Cross-React to Virus and Self. *Circ. Res.* **130**, 1510–1530 (2022).
11. Cibrián, D. & Sánchez-Madrid, F. CD69: from activation marker to metabolic gatekeeper. *Eur. J. Immunol.* **47**, 946–953 (2017).
12. Schenkel, J. M. *et al.* T cell memory. Resident memory CD8 T cells trigger protective innate and adaptive immune responses. *Science* **346**, 98–101 (2014).
13. Kranzer, K. *et al.* CpG-oligodeoxynucleotides enhance T-cell receptor-triggered interferon-gamma production and up-regulation of CD69 via induction of antigen-presenting cell-derived interferon type I and interleukin-12. *Immunology* **99**, 170–178 (2000).
14. Mohr, A., Malhotra, R., Mayer, G., Gorochov, G. & Miyara, M. Human FOXP3+ T regulatory cell heterogeneity. *Clin. Transl. Immunol.* **7**, 1–11 (2018).
15. Wherry, E. J. & Kurachi, M. Molecular and cellular insights into T cell exhaustion. *Nat. Rev. Immunol.* **15**, 486–499 (2015).
16. Khan, O. *et al.* TOX transcriptionally and epigenetically programs CD8 + T cell exhaustion. *Nature* **571**, 211–218 (2019).
17. Padhan, K. & Varma, R. Immunological synapse: A multi-protein signalling cellular apparatus for controlling gene expression. *Immunology* **129**, 322–328 (2010).
18. Bagaev, D. V. *et al.* VDJdb in 2019: database extension, new analysis infrastructure and a T-cell receptor motif compendium. *Nucleic Acids Res.* **48**, D1057–D1062 (2020).
19. Vorkas, C. K. *et al.* Single-Cell Transcriptional Profiling Reveals Signatures of Helper, Effector, and Regulatory MAIT Cells during Homeostasis and Activation. *J. Immunol.* **208**, 1042–1056 (2022).
20. Liuzzo, G. *et al.* Monoclonal T-Cell Proliferation and Plaque Instability in Acute Coronary Syndromes. *Circulation* **102**, 2883–2888 (2000).

21. Liuzzo, G. *et al.* Unusual CD4+CD28null T Lymphocytes and Recurrence of Acute Coronary Events. *J. Am. Coll. Cardiol.* **50**, 1450–1458 (2007).
22. La Manno, G. *et al.* RNA velocity of single cells. *Nature* **560**, 494 (2018).
23. Ali, A. J., Makings, J. & Ley, K. Regulatory T Cell Stability and Plasticity in Atherosclerosis. *Cells* **9**, (2020).
24. Wang, X. *et al.* Visualizing CD4 T-cell migration into inflamed skin and its inhibition by CCR4/CCR10 blockades using in vivo imaging model. *Br. J. Dermatol.* **162**, 487–496 (2010).
25. Jin, S. *et al.* Inference and analysis of cell-cell communication using CellChat. *Nat. Commun.* **12**, (2021).
26. Foks, A. C. & Kuiper, J. Immune checkpoint proteins: exploring their therapeutic potential to regulate atherosclerosis. *Br. J. Pharmacol.* **174**, 3940–3955 (2017).
27. Kwon, I. O. *et al.* CD99 activates T cells via a costimulatory function that promotes raft association of TCR complex and tyrosine phosphorylation of TCR ζ. *Exp. Mol. Med.* **39**, 176–184 (2007).
28. Bixel, G. *et al.* Mouse CD99 participates in T-cell recruitment into inflamed skin. *Blood* **104**, 3205–3213 (2004).
29. Calandra, T. & Roger, T. Macrophage migration inhibitory factor: a regulator of innate immunity. *Nat. Rev. Immunol.* **3**, 791–800 (2003).
30. D'Acquisto, F. *et al.* Annexin-1 modulates T-cell activation and differentiation. *Blood* **109**, 1095–1102 (2007).
31. Penkava, F. *et al.* Single-cell sequencing reveals clonal expansions of pro-inflammatory synovial CD8 T cells expressing tissue-homing receptors in psoriatic arthritis. *Nat. Commun.* **11**, (2020).
32. Björkbacka, H. *et al.* Weak associations between human leucocyte antigen genotype and acute myocardial infarction. *J. Intern. Med.* **268**, 50–58 (2010).
33. Lin, Z. *et al.* Deep sequencing of the T cell receptor β repertoire reveals signature patterns and clonal drift in atherosclerotic plaques and patients. *Oncotarget* **8**, 99312–99322 (2017).
34. Treiner, E. *et al.* Selection of evolutionarily conserved mucosal-associated invariant T cells by MR1. *Nature* **422**, 164–169 (2003).
35. Godfrey, D. I., Koay, H. F., McCluskey, J. & Gherardin, N. A. The biology and functional importance of MAIT cells. *Nat. Immunol.* **20**, 1110–1128 (2019).
36. Van Wilgenburg, B. *et al.* MAIT cells are activated during human viral infections. *Nat. Commun.* **7**, (2016).
37. Kleinewietfeld, M. & Hafler, D. A. The plasticity of human Treg and Th17 cells and its role in autoimmunity. *Semin. Immunol.* **25**, 305–312 (2013).
38. Huang, H., Wang, C., Rubelt, F., Scriba, T. J. & Davis, M. M. Analyzing the Mycobacterium tuberculosis immune response by T-cell receptor clustering with GLIPH2 and genome-wide antigen screening. *Nat. Biotechnol. 2020 3810* **38**, 1194–1202 (2020).
39. Zhang, H., Zhan, X. & Li, B. GIANA allows computationally-efficient TCR clustering and multi-disease repertoire classification by isometric transformation. *Nat. Commun. 2021 121* **12**, 1–11 (2021).
40. Saigusa, R. *et al.* Single cell transcriptomics and TCR reconstruction reveal CD4 T cell response to MHC-II-restricted APOB epitope in human cardiovascular disease. *Nat. Cardiovasc. Res. 2022 15* **1**, 462–475 (2022).
41. Wigren, M. *et al.* Lack of Ability to Present Antigens on Major Histocompatibility Complex Class II Molecules Aggravates Atherosclerosis in ApoE -/- Mice. *Circulation* **139**, 2554–2566 (2019).
42. Tabas, I. & Lichtman, A. H. Monocyte-Macrophages and T Cells in Atherosclerosis. *Immunity* **47**, 621–634 (2017).

43. Smeets, E., Meiler, S. & Lutgens, E. Lymphocytic tumor necrosis factor receptor superfamily co-stimulatory molecules in the pathogenesis of atherosclerosis. *Curr. Opin. Lipidol.* **24**, 518–524 (2013).
44. Seijkens, T. T. P. *et al.* Targeting CD40-Induced TRAF6 Signaling in Macrophages Reduces Atherosclerosis. *J. Am. Coll. Cardiol.* **71**, 527–542 (2018).
45. Chyu, K. Y. *et al.* Immunization using ApoB-100 peptide-linked nanoparticles reduces atherosclerosis. *JCI insight* **7**, (2022).
46. Van Puijvelde, G. H. M. *et al.* Induction of oral tolerance to HSP60 or an HSP60-peptide activates T cell regulation and reduces atherosclerosis. *Arterioscler. Thromb. Vasc. Biol.* **27**, 2677–2683 (2007).
47. Dunér, P. *et al.* Immunization of apoE-/- mice with aldehyde-modified fibronectin inhibits the development of atherosclerosis. *Cardiovasc. Res.* **91**, 528–536 (2011).
48. Verhoeven, B. A. N. *et al.* Athero-express: Differential atherosclerotic plaque expression of mRNA and protein in relation to cardiovascular events and patient characteristics. Rationale and design. *Eur. J. Epidemiol.* **19**, 1127–1133 (2004).
49. Hellings, W. E. *et al.* Histological characterization of restenotic carotid plaques in relation to recurrence interval and clinical presentation: a cohort study. *Stroke* **39**, 1029–32 (2008).
50. R Core Team. R: A language and environment for statistical computing. https://www.r-project.org/ (2019).
51. Butler, A., Hoffman, P., Smibert, P., Papalexi, E. & Satija, R. Integrating single-cell transcriptomic data across different conditions , technologies , and species. *Nat. Biotechnol.* **36**, 411–420 (2018).
52. Stuart, T. *et al.* Comprehensive Integration of Single-Cell Data. *Cell* **177**, 1888-1902.e21 (2019).
53. Borcherding, N., Bormann, N. L. & Kraus, G. scRepertoire: An R-based toolkit for single-cell immune receptor analysis. *F1000Research* **9**, (2020).
54. Blighe, K., Rana, S. & Lewis, M. EnhancedVolcano: Publication-ready volcano plots with enhanced colouring and labeling. (2018).
55. Cao, J. *et al.* The single-cell transcriptional landscape of mammalian organogenesis. *Nature* **566**, 496–502 (2019).

Extended Data

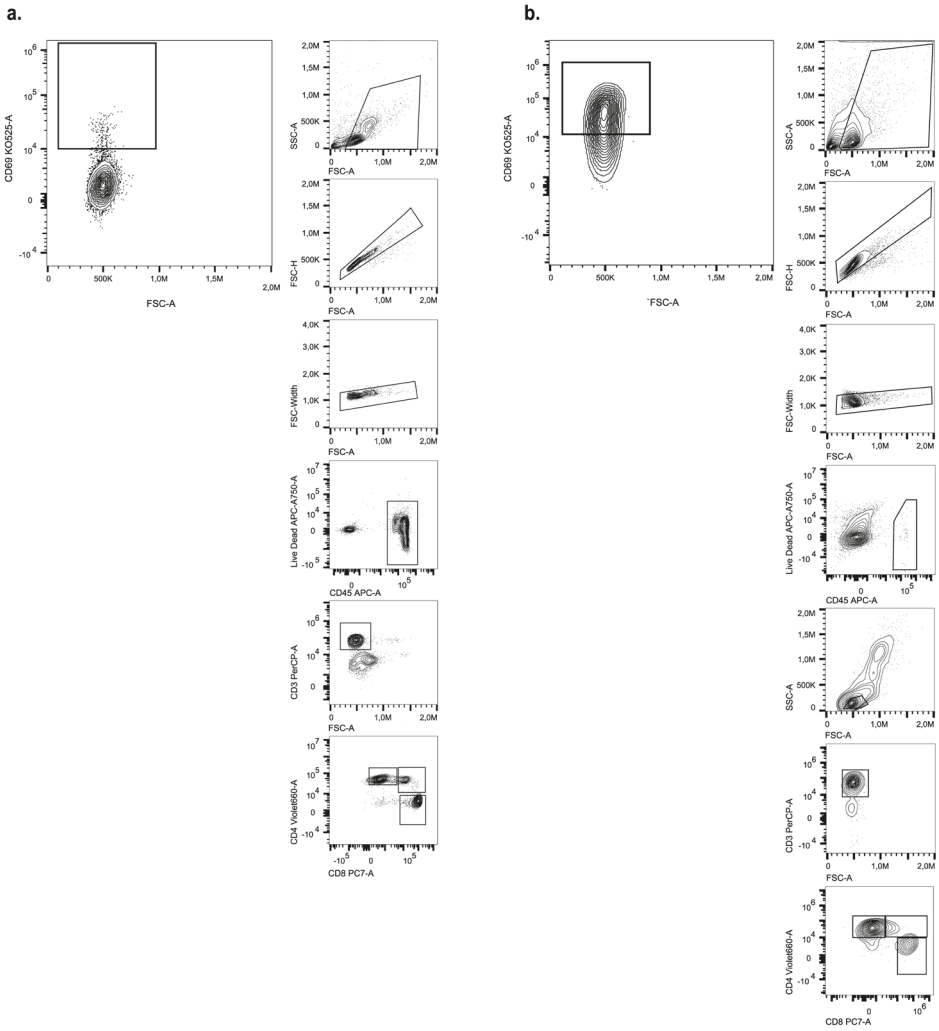

Extended Data Fig. 1. Gating strategy of flow cytometry of CD69⁺ T-cells. a. Example of gating and gating ancestry of CD69⁺ T-cells in PBMC. **b.** Example of gating and gating ancestry of CD69⁺ in the plaque.

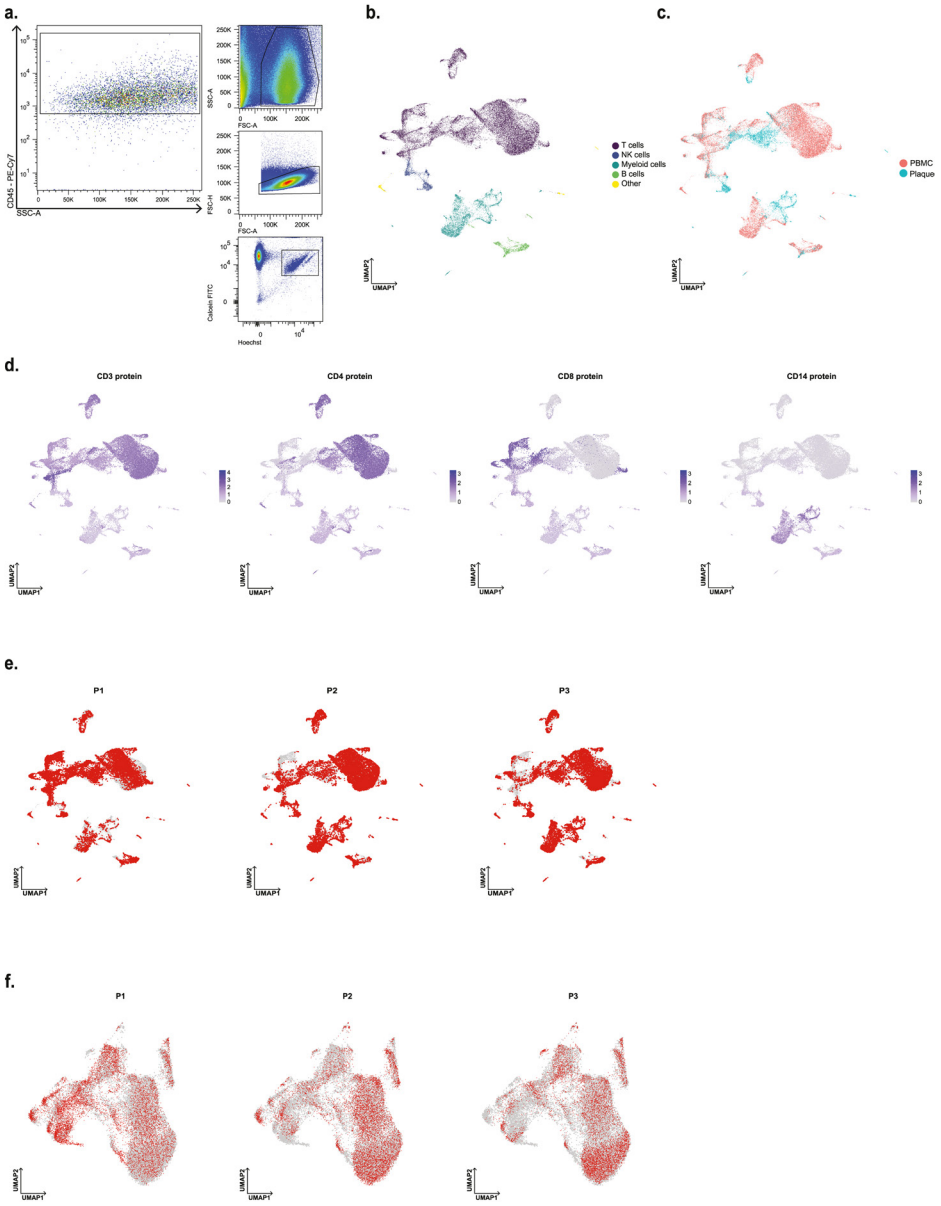

Extended Data Fig. 2. Single-cell RNA sequencing of PBMC and live CD45⁺ plaque cells. a. Gating strategy used for fluorescent-activated cell sorting (FACS) to isolate plaque live CD45⁺ cells for 10X Genomics and sequencing. **b.** UMAP projection of all PBMC and plaque cells, depicting multiple leukocyte types (n = 33249). **c.** UMAP visualization of tissue distribution of PBMC and plaque cells. **d.** UMAP projection of protein expression of CD3, CD4, CD8 and CD14 on all PBMC and plaque cells. **e.** Patient contribution to UMAP of all PBMC and plaque cells. Red dots indicate cells that are retrieved from the abovementioned patient. **f.** Patient contribution to UMAP of PBMC and plaque T-cells. Red dots indicate cells that are retrieved from the abovementioned patient.

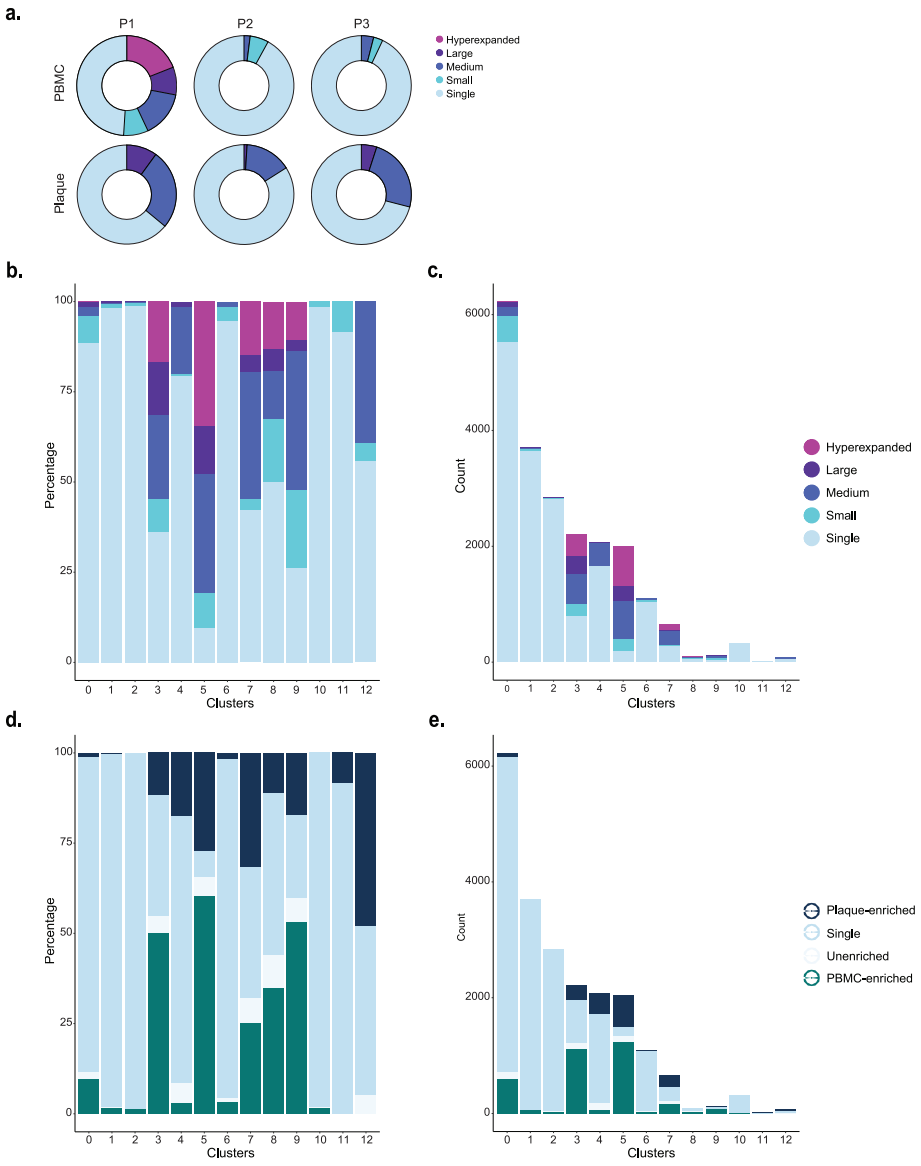

Extended Data Fig. 3. Distribution of clonal expansion levels and tissue-enrichment scores in T-cell clusters. a. Circle plots depicting clonal expansion levels of all T-cells per tissue and per patient. **b**. Barplot with relative quantification of clonal expansion levels per cluster. **c**. Barplot with absolute quantification of clonal expansion levels per cluster. **d.** Relative quantification of tissue enrichment scores per cluster. **e.** Barplot with absolute quantification of tissue enrichment scores per cluster. Clonotype expansion levels: Single (1 occurrence), Medium (>0.1 & ≤1%), Large (>1 & ≤10%), Hyperexpanded (>10%), percentage of all T-cells. Tissue enrichment scores: Plaque-enriched (Frequency expanded clone higher in Plaque vs. PBMC), Single (1 occurrence), Unenriched (Frequency expanded clone similar in PBMC vs. Plaque), PBMC-enriched (Frequency expanded clone higher in PBMC vs Plaque).

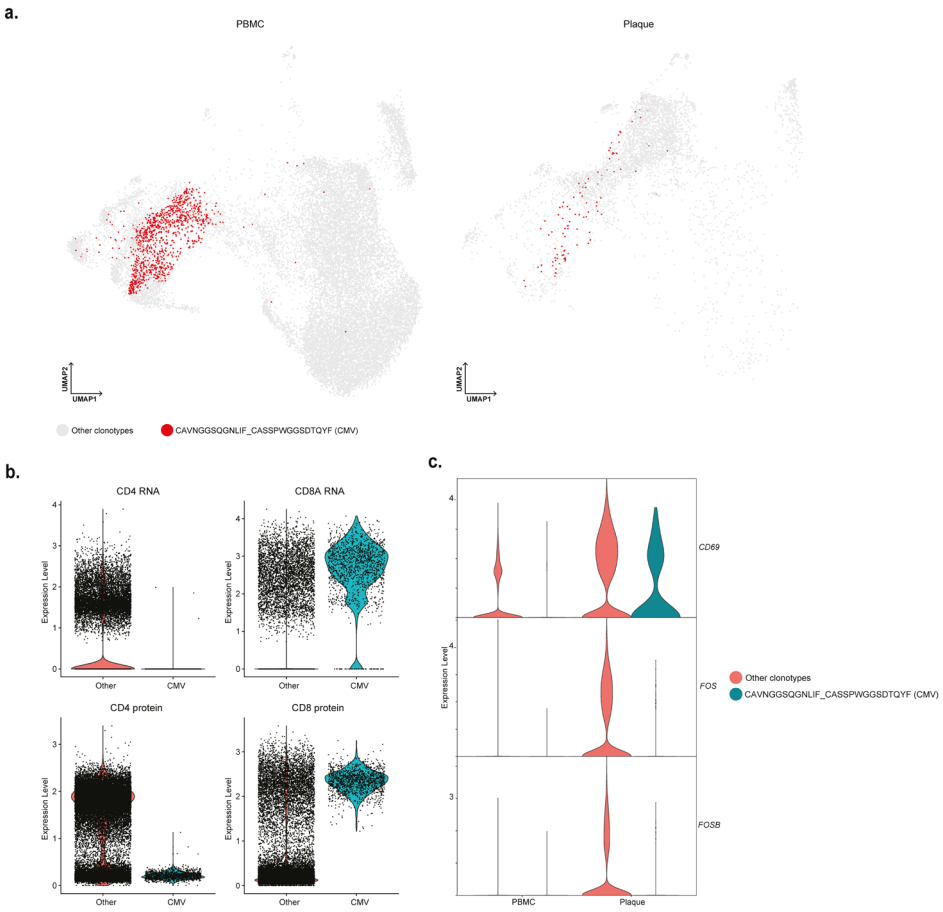

Extended Data Fig. 4. Hyperexpanded CMV clonotype does not show signs of recent T-cell activation. a. UMAP projection of clonotype CAVNGGSQGNLIF_CASSPWGGSDTQYF (CMV) on PBMC and plaque T-cells. Red dots indicate T-cells with clonotype CAVNGGSQGNLIF_CASSPWGGSDTQYF, grey dots indicate T-cells with other clonotypes. **b.** Violin plots projecting gene expression of *CD4*, *CD8A* and protein expression of CD4 and CD8 split by T-cells with and without clonotype CAVNGGSQGNLIF_CASSPWGGSDTQYF. **c**. Violin plots projecting expression of *CD69*, *FOS* and *FOSB* split by tissue and presence of clonotype CAVNGGSQGNLIF_CASSPWGGSDTQYF.

a.

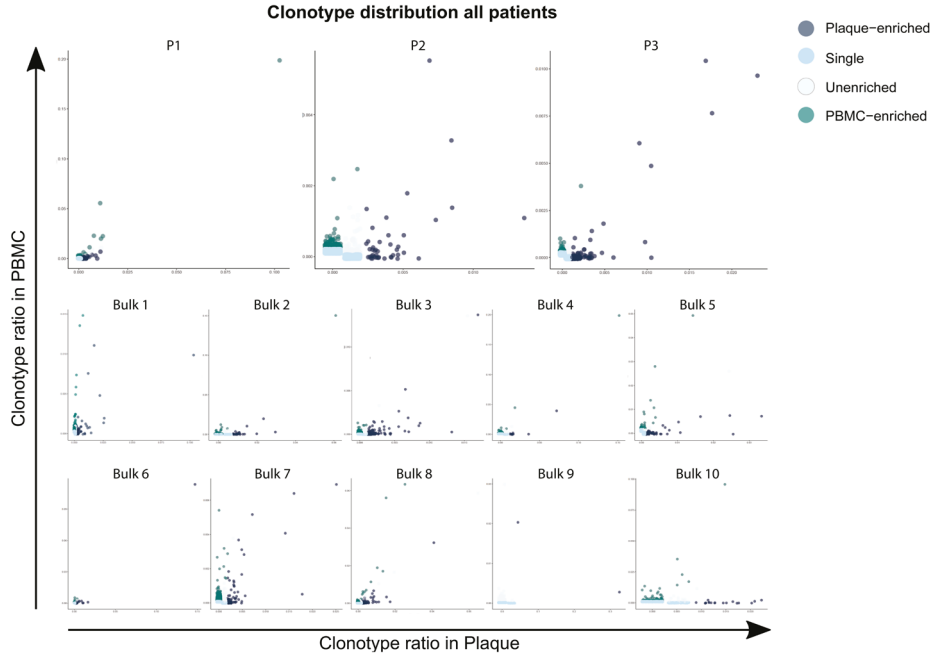

Extended Data Fig. 5. Distribution of expanded TCRs in scTCR-seq and TCR*β* bulk data sets. **a.** Scatterplot projecting frequencies of clonotypes and their tissue enrichment scores in PBMC and plaque per patient of the single-cell TCR sequencing dataset (Cohort 2) and the TCRβ bulk sequencing data set (Cohort 3). Tissue enrichment scores: Plaque-enriched (Frequency expanded clone higher in Plaque vs. PBMC), Single (1 occurrence), Unenriched (Frequency expanded clone similar in PBMC vs. Plaque), PBMC-enriched (Frequency expanded clone higher in PBMC vs Plaque).

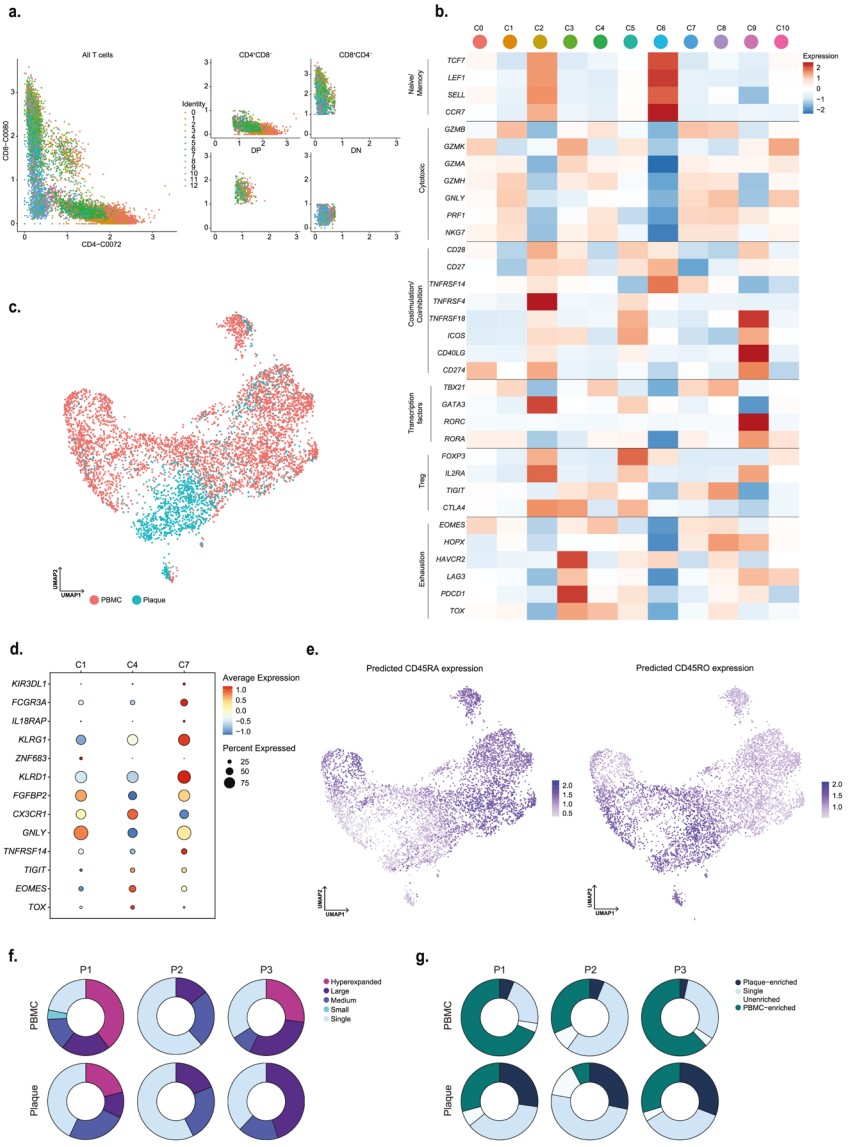

Extended Data Fig. 6. CD8⁺ T-cell marker genes and tissue distribution. a. CD4 and CD8 protein expression on all T-cells colored by cluster ID. Visualization of selection of $CD4^+CD8^-$, $CD4^-CD8^+$, double positive (DP) and double negative (DN) cells. $CD4^+CD8^-$ cells were used for subclustering of $CD4^+$ T-cells. $CD4^-CD8^+$ cells were used for subclustering of $CD8^+$ T-cells. **b.** UMAP projection of tissue distribution of PBMC and plaque $CD8^+$ T-cells. **c.** Heatmap with expression of T-cell function-associated genes in $CD8^+$ T-cell clusters. d. Dot plot visualization of a selection of differentially regulated genes, excluding TCR complex genes, between clusters 1, 4 and 7. **e.** Predicted expression of CD45RA and CD45RO based on mapping the data with Seurat multimodal reference mapping. **f.** Circle plots depicting clonal expansion levels of $CD8^+$ T-cells per tissue and per patient. **g**. Circle plots depicting tissue-enrichment scores of $CD8^+$ T-cells per tissue and per patient.

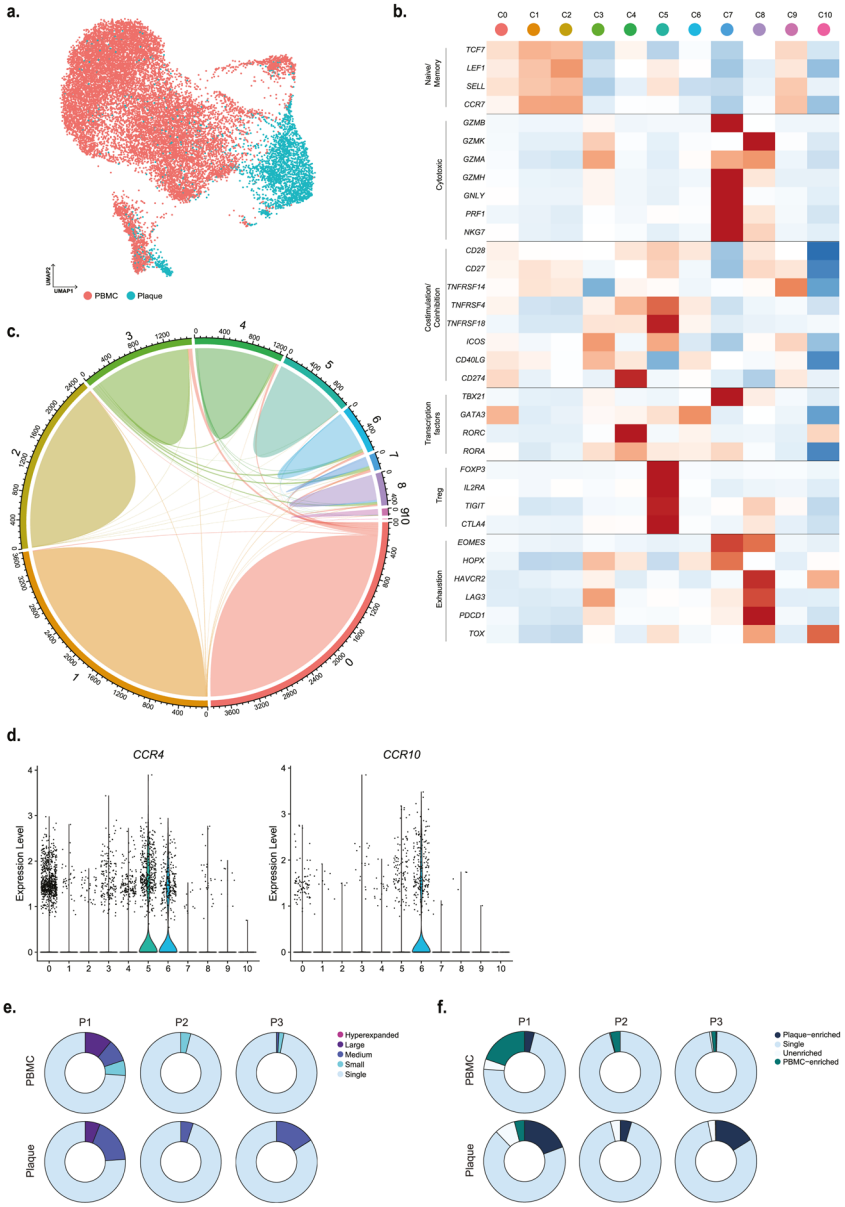

Extended Data Fig. 7. CD4⁺ T-cell marker genes and tissue distribution. a. UMAP visualization of tissue distribution of PBMC and plaque CD4⁺ T-cells. **b.** Heatmap with expression of T-cell function-associated genes in CD4⁺ T-cell clusters. **c.** Circle plot visualizing the overlap of clonotypes between all CD4⁺ clusters. Each color represents a different cluster. Axis indicates the number of TCRs. Line thickness indicates the number of overlapping clonotypes. **d.** Violin plots depicting expression of *CCR4* and *CCR10* in CD4⁺ T-cell clusters. **e.** Circle plots depicting clonal expansion levels of CD4⁺ T-cells per tissue and per patient. **f**. Circle plots depicting tissue-enrichment scores of CD4⁺ T-cells per tissue and per patient.

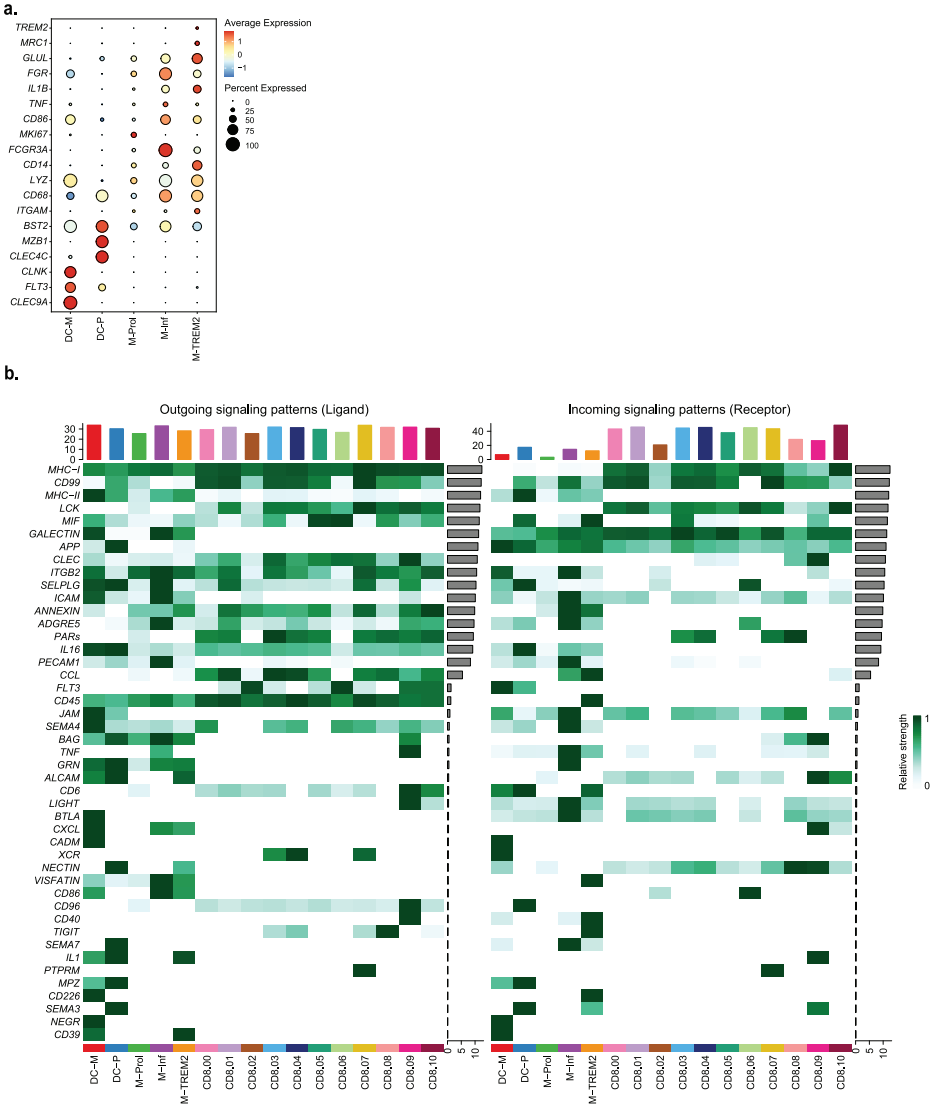

Extended Data Fig. 8. CellChat interaction pathways between CD8⁺ T-cells and myeloid cells. a. Dotplot displaying average expression of genes describing the different dendritic cell and macrophage clusters. DC-M indicates myeloid-derived dendritic cell (DC); DC-P indicates plasmacytoid DC; M-PROL indicates proliferating macrophages; M-Inf indicates inflammatory macrophage; M-TREM2 indicates TREM2^{hi} macrophages. **b.** Heatmaps displaying outgoing (Ligand) and incoming (Receptor) signaling patterns of pathways describing potential ligand-receptor interactions. Scale above heatmap indicates the relative signaling strength of a cell cluster based on all signaling pathways displayed in the heatmap. Grey bars right of the heatmap show the total signaling strength of a pathway in all cell clusters. The relative signaling strength indicated by ranging color from white (low) to green (high). All cells included in these graphs originate from the plaque.

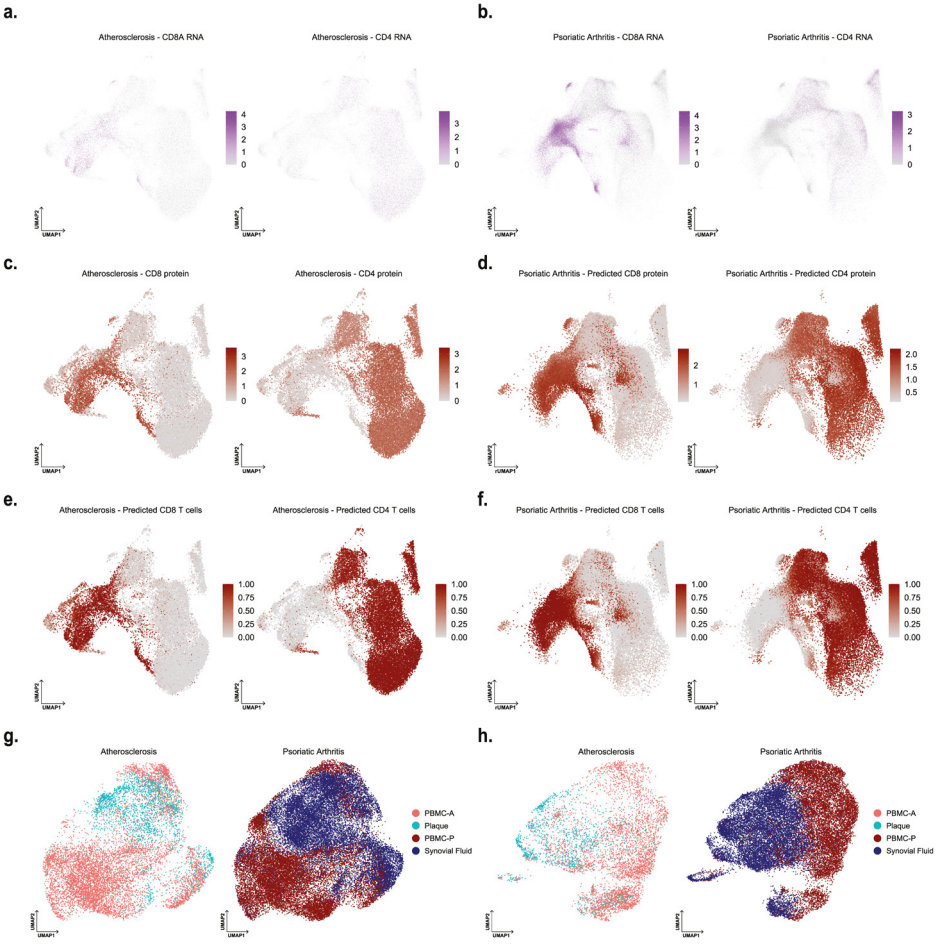

Extended Data Fig. 9. Projection of CD4⁺ and CD8⁺ T-cells of integrated atherosclerosis and psoriatic arthritis single-cell TCR sequencing data on the reference UMAP projection of CD4⁺ and CD8⁺ atherosclerosis data. a UMAP visualization of RNA expression of CD8A and CD4 on atherosclerosis T-cells. **b.** rUMAP visualization of RNA expression of CD8A and CD4 on psoriatic arthritis T-cells. **c.** UMAP visualization of protein expression of CD8 and CD4 on atherosclerosis T-cells. **d.** rUMAP visualization of predicted protein expression of CD8 and CD4 on psoriatic arthritis T-cells. **e.** UMAP visualization of selected CD8⁺ and CD4⁺ atherosclerosis T-cells. **f.** UMAP visualization of selected CD8⁺ and CD4⁺ psoriatic arthritis T-cells. **g.** UMAP of integrated CD4⁺ T-cells split by diseased and grouped by tissue type. **h.** UMAP of integrated CD8⁺ T-cells split by diseased and grouped by tissue type.

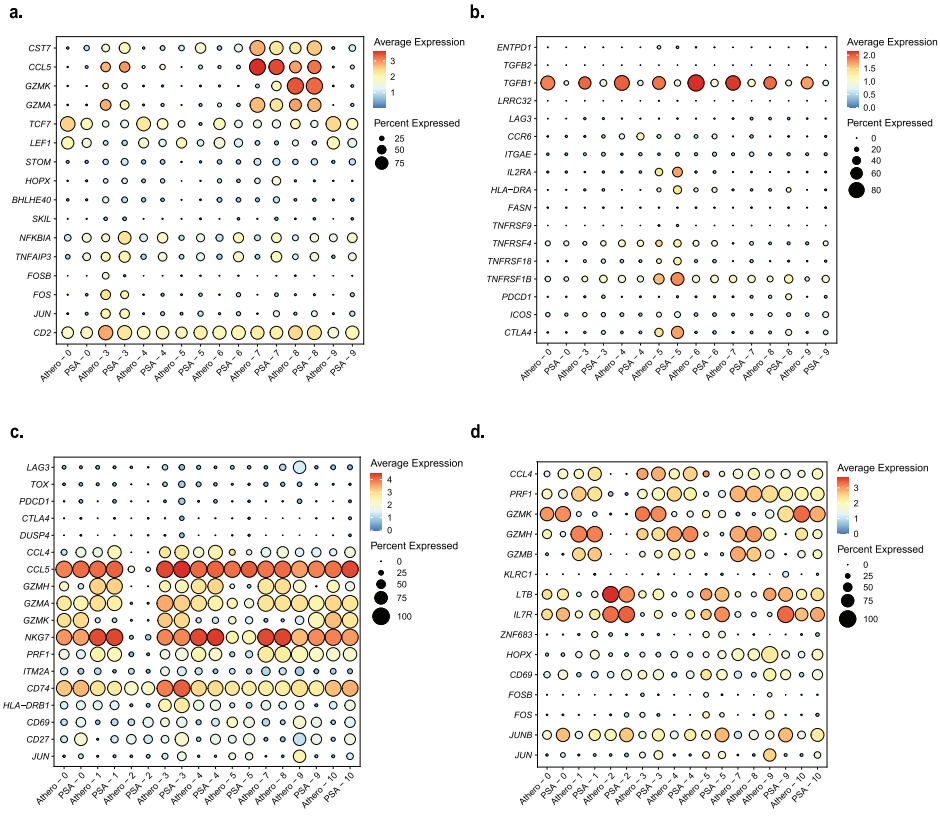

Extended Data Fig. 10. Extended dot plots with characterizing genes for atherosclerosis and psoriatic arthritis overlapping clonal expanded T-cells. Dotplots with genes used to characterize overlapping clusters of atherosclerosis and psoriatic arthritis per disease and per cluster of respectively CD4⁺ cluster 3 genes(**a**), CD4⁺ cluster 5 genes (**b**) CD8⁺ cluster 3 genes(**c**) and CD8⁺ cluster 5 genes (**d**).

Chapter 5

Flow Cytometry-Based Characterization of Mast Cells in Human Atherosclerosis

Cells 2019; 8(4): 334

Eva Kritikou[1], Marie A.C. Depuydt[1], Margreet R. de Vries[2,3], Kevin E. Mulder[1], Arthur M. Govaert[2,3], Marrit D. Smit[2,3], Janine van Duijn[1], Amanda C. Foks[1], Anouk Wezel[4], Harm J. Smeets[4], Bram Slütter[1], Paul H.A. Quax[2,3], Johan Kuiper[1] and Ilze Bot[1]

1 Division of BioTherapeutics, Leiden Academic Centre for Drug Research, Leiden University, 2333 CC, Leiden, The Netherlands
2 Department of Surgery, Leiden University Medical Center, 2333 ZC, Leiden, The Netherlands
3 Einthoven Laboratory for Experimental Vascular Medicine, Leiden University Medical Center, 2333 ZC, Leiden, The Netherlands
4 Department of Surgery, HMC Westeinde, 2512 VA, The Hague, The Netherlands

Abstract

The presence of mast cells in human atherosclerotic plaques has been associated with adverse cardiovascular events. Mast cell activation, through the classical antigen sensitized-IgE binding to their characteristic Fcε-receptor, causes the release of their cytoplasmic granules. These granules are filled with neutral proteases such as tryptase, but also with histamine and pro-inflammatory mediators. Mast cells accumulate in high numbers within human atherosclerotic tissue, particularly in the shoulder region of the plaque. These findings are largely based on immunohistochemistry, which does not allow for the extensive characterization of these mast cells and of the local mast cell activation mechanisms. In this study, we thus aimed to develop a new flow-cytometry based methodology in order to analyze mast cells in human atherosclerosis. We enzymatically digested 22 human plaque samples, collected after femoral and carotid endarterectomy surgery, after which we prepared a single cell suspension for flow cytometry. We were able to identify a specific mast cell population expressing both CD117 and the FcεR and observed that most of the intraplaque mast cells were activated based on their CD63 protein expression. Furthermore, most of the activated mast cells had IgE fragments bound on their surface, while another fraction showed IgE-independent activation. In conclusion, we are able to distinguish a clear mast cell population in human atherosclerotic plaques, and this study establishes a strong relationship between the presence of IgE and the activation of mast cells in advanced atherosclerosis. Our data pave the way for potential therapeutic intervention through targeting IgE-mediated actions in human atherosclerosis.

Keywords: atherosclerosis; flow cytometry; mast cell; plaque stability; tryptase.

Introduction

Up to the present day, atherosclerosis, the main underlying pathology of acute cardiovascular syndromes like stroke or myocardial infarction, is the major cause of human mortality.[1] As in most pathological conditions, the response of the immune system is crucial in the advancement of atherosclerosis, with mast cells being key mediators in this process.[2] Mast cells are innate immune cells, unique for their notorious granular load release upon activation with antigen-sensitized IgE fragments, in allergic reactions.[3] Aside from allergic inflammation, mast cells have long been established to play an important pro-inflammatory role in the development of atherosclerosis in experimental studies, as well as in human subjects.[4] Mast cells reside at low numbers in normal arterial tissue, however, their numbers increase in the arteries where a lipid-rich atherosclerotic plaque is formed.[5] In fact, as human atherosclerosis progresses, mast cells become increasingly activated and excrete their granules in the surrounding tissue.[6] The degranulated material consists mainly of proinflammatory cytokines, histamine, and neutral proteases, such as chymase and tryptase.[7] Mast cell activation is reported to augment plaque progression[8], enhance plaque destabilization[9], and increase the levels of intraplaque hemorrhage incidence[10]. Previous attempts to characterize mast cells and their protease content in human atheromata, by the means of immunohistochemistry, have revealed that mast cells comprise a heterogeneous population; the majority of cells contain only tryptase, while a smaller proportion contains chymase and tryptase.[11] Both of these proteases have been investigated in experimental studies of atherosclerosis. In these studies, tryptase has been implicated in atherosclerotic plaque destabilization[12], while the inhibition of chymase limited atherosclerotic plaque development and progression[13].

In human plaques, mast cells have furthermore been found to correlate with typical atherogenic immune populations, such as dendritic cells and T cells.[14] Importantly, in a human study of 270 patients, intraplaque mast cells emerged as the primary immune cell type to be positively associated with future cardiovascular events[15] and may thus actively contribute to atherosclerotic plaque destabilization. Until this day however, the means by which mast cells get activated inside atherosclerotic plaques have not been elucidated in full detail. However, it is suggested that the classical IgE-sensitized pathway[16,17] is involved to a certain extent. Moreover, there is increasing in vivo evidence that additional atherosclerosis-specific mechanisms can trigger mast cell activation, independently of IgE-binding[18,19], such as activation through Toll-like receptors (TLRs)[20], complement receptors[21], or neuropeptide[22] receptors. Thus far however, the proportional effect of these distinct pathways involved in atherosclerosis has not been clarified.

The presence of mast cells has thus far only been established by means of immunohistochemical staining. While this provides important information regarding the location of mast cells in the lesion, this method is limited by the number of markers that can be used to identify a cell type and its activation status. To be able to characterize the mast cell population in human atherosclerotic lesions in more detail using multiple markers simultaneously, we aimed to develop a novel flow cytometry-based technique to identify the mast cell population in human atherosclerosis, and to determine its activation status.

Methods

Sample Collection and Processing

The atherosclerotic plaque material of 22 anonymous human subjects was collected peri-operatively from carotid (n = 10) and femoral (n = 12) artery endarterectomy (from July to December 2016 at the Haaglanden Medical Center Westeinde, The Hague, The Netherlands). The handling of all of the human samples complied with the "Code for Proper Secondary Use of Human Tissue", METC number 16-071. The plaque samples were placed in RPMI (Lonza, Breda, The Netherlands) directly after removal from the patient. The culprit part of the plaques was collected as described previously[23], and stored in Shandon Zinc Formal-Fixx (Thermo Scientific, Waltham, MA, USA) for histology purposes. The remainder (~90%) of the plaques were processed into single cell suspensions by a 2-h digestion step in 37 °C, with an enzyme mix consisting of collagenase IV (Thermo Scientific, Waltham, MA, USA) and DNase (Sigma, Zwijndrecht, The Netherlands), as previously described.[24] Subsequently, the samples were filtered through a 70 µm cell strainer to obtain single cells, which were kept in RPMI/1% Fetal Calf Serum (FCS) until further analysis.

Histology

The culprit part of atherosclerotic samples was placed in Kristensen's buffer for three to seven days for decalcification, after which the plaques were embedded in paraffin. Next, the plaques were sectioned in 5-µm thick sections using a microtome RM2235 (LEICA Biosystems, Amsterdam, The Netherlands). A Movat's pentachrome staining was routinely performed, and subsequently, the plaques were analyzed for histological parameters, as described in Table 1 (three sections/plaque), based on the semiquantitative scoring systems of the AtheroExpress biobank[23] and the Oxford Plaque Study[25]. In short, the plaques were assessed for the presence of unstable plaque features such as the presence of a necrotic core, inflammatory cells, and intraplaque hemorrhage, as well as stable plaque features such as smooth muscle

cell (SMC)-rich extracellular matrix (ECM). To identify the mast cells in the lesion, atherosclerotic plaque sections were immunohistochemically stained for tryptase using an alkaline phosphatase-conjugated antibody directed against tryptase (1:250, clone G3, Sigma, Zwijndrecht, The Netherlands), after which nitro-blue tetrazolium and 5-bromo-4-chloro-3′-indolyphosphate were used as a substrate. Nuclear Fast Red was used as a counterstaining for the nuclei. For the morphologic analysis, slides were analyzed using a Leica DM-RE microscope (Leica Ltd., Cambridge, UK).

Flow Cytometry

The single plaque cells were stained with extracellular antibodies containing a fluorescent label, or were fixated and permeabilized (BD Biosciences, San Jose, CA, USA) for intracellular staining (Table 2). The fluorescently labeled samples were measured on a FACS Canto II (BD Biosciences, San Jose (CA), USA) or Cytoflex (Beckman Coulter, Miami, FL, USA), and were analyzed using FlowJo software (v10).

Statistics

All of the data are depicted using GraphPad Prism 7.00. The values were tested for normalcy. Upon non-Gaussian distribution, an unpaired Mann–Whitney U-test was performed. In the case of more than two groups, a one way-ANOVA analysis was used. Differences lower than $p < 0.05$ were considered statistically significant.

Table 1. Semiquantitative grading scale for the histology score of human endarterectomy specimen.

Grade	0	1
Necrotic Core	No sign of necrotic core	<20% of the arterial area
Calcification	No sign of calcification	<10% of the arterial area
Foam Cells	No sign of foam cells	Small * A few small sized clusters (~5) of foam cells
Cholesterol Crystal	No sign of cholesterol crystal	<10% of the necrotic core
Neovascularization	No sign of neovascularization	<25 neovessels in the whole tissue
Inflammatory Cells	No sign of inflammatory cells	Small A few (1 or 2) small sized (~50 cells) clusters of inflammatory cells or a few cells occasionally spread throughout the arterial area
Shoulder	Not detectable*	No sign of shoulder regions
Intraplaque hemorrhage (IPH)	No sign of IPH	<10% IPH of the arterial area
SMC-rich ECM area of total ECM area	No SMC visible	<20% of the ECM area
Luminal thrombosis	No	Yes (rupture)

SMC—smooth muscle cell; ECM—extracellular matrix.

2	3	4
20%–40% of the arterial area	40%–70% of the arterial area	>70%
10%–40% of the arterial area	>40% of the arterial area	
Intermediate	Large	
* Multiple small (~5) or medium sized (~10) clusters of foam cells	* At least 1 large sized cluster (~15) of foam cells or foam cells scattered around ~70% of the arterial area	
10%–40% of the necrotic core	>40% of the necrotic core	
25–50 neovessels in whole tissue	>50 neovessels in the whole tissue	
Intermediate Multiple (~5) small sized (~50 cells) clusters of inflammatory cells	Large At least 1 large sized (~100 cells) cluster of inflammatory cells or cells scattered around ~70% of the arterial area	
One sided shoulder region	Two-sided shoulder region	
10%–40% IPH of the arterial area	>40% IPH of the arterial area	
20%–40% of the ECM area	>40% of the ECM area	

Table 2. List of extracellular and *intracellular* antibodies used.

Antibody	Fluorochrome	Clone	Concentration	Company
Fixable Viability Dye	eFluor 780	-	0.1µg/sample	eBioscience
CD45	PB	2D1	0.25µg/sample	eBioscience
FcεRIα	APC/PE Cy7	AER-37	0.12 µg/sample	eBioscience
CD117	PercP Cy5.5	104D2	0.1µg/sample	eBioscience
CD63	PE	H5C6	0.1µg/sample	eBioscience
IgE	PE Cy7/FITC	Ige21	0.25µg/sample	eBioscience
Tryptase/TPSAB1	*PE*	-	0.1µg/sample	LSBio

Results

We analyzed the culprit part of the carotid and femoral plaques for its histology characteristics, based on the Movat's pentachrome staining (**Figure 1A**). The characteristics of the individual plaques and the assessment of the plaque stability parameters are shown in **Figure 1B**. Overall, the presence of a necrotic core, inflammatory cells, and intraplaque hemorrhage establish that the majority of the plaques can be classified as advanced, as expected.

Next, we prepared single cell suspensions of the remainder of the individual plaques, and stained the cells for the surface markers to be analyzed using flow cytometry. In **Figure 2A**, we demonstrate the gating strategy that we followed in order to detect the human intraplaque immune cells. Specifically, we pre-selected all of the cells from the debris present in the human plaques based on their size (forward scatter, FSC) and granularity (side scatter, SSC). Of these, single cells were further separated according to their width (FSC-W) and area (FSC-A). In addition, the viability was detected according to the negative signal for a fluorescent viability dye (FVD−). Viable white blood cells were identified according to the expression of the pan-leukocyte marker CD45. As the femoral plaques were generally bigger in size upon surgical removal compared with the carotid plaques, we were able to isolate more $CD45^+$ immune cells from the femoral arteries (carotid: $12 \times 10^5 \pm 4.7 \times 10^5$ leukocytes vs. femoral: $76 \times 10^5 \pm 27 \times 10^5$ leukocytes; **Figure 2B**).

Within these cells, we detected the population of intraplaque mast cells based on the high expression of their characteristic markers FcεRIα, the receptor for IgE[26], and of CD117–the receptor for stem cell factor, a growth factor required for the end-stage maturation of mast cells[27] (**Figure 2C**). Accordingly, we observed that the percentage of mast cells out of all of the viable leukocytes present inside the atherosclerotic plaques is 1.19% ± 0.31% for the

carotid arteries (n = 9), and 1.32% ± 0.21% for the femoral arteries (n = 13) (**Figure 2D**). Of note, a number of leukocytes may have been retained in the excluded debris material. Nonetheless, we enumerated the viable cells after manual quantification using Trypan Blue in relation to the percentage of viable $CD45^+$ cells observed according to our gating strategy. We detected that the carotid plaques consisted of a mean 12 ± 5 × 10^3 mast cells, while the femoral plaques contained 94 ± 37 × 10^3 mast cells. Thus, because of the higher total number of leukocytes, we identified higher absolute mast cell numbers in the femoral plaques compared with the carotid plaques (**Figure 2E**).

A

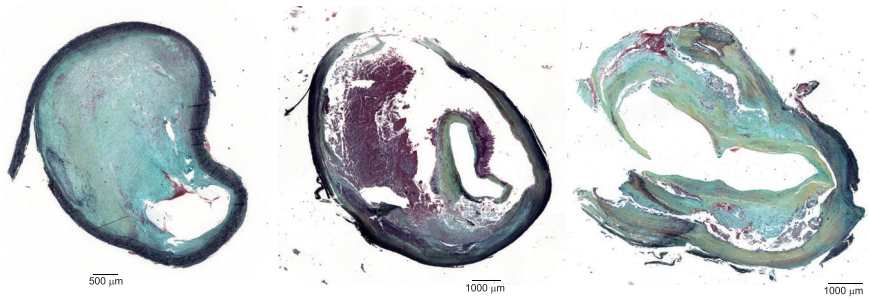

B

Sample number	Necrotic core	Calcification	Foam cells	Cholesterol chrystals	Neovascularization	Inflammatory cells	Shoulder	Intraplaque Hem.	SMC-rich ECM	Luminal thrombosis
5	3.00	1.00	0.33	0.33	1.00	1.00	1.00	0.33	1.00	yes
7	3.67	2.00	1.00	0.67	1.00	1.00	0.00	1.00	2.00	rupture
8	3.00	1.00	0.00	0.00	0.67	1.00	1.00	1.00	3.00	rupture
9	2.33	1.00	0.00	0.00	0.56	0.33	0.33	1.00	3.00	rupture
10	3.67	2.00	0.00	0.00	0.33	0.00	0.00	2.00	1.33	rupture
11	3.00	1.33	2.67	1.33	0.67	2.33	1.00	1.00	2.00	rupture
12	3.00	1.78	1.89	0.78	0.22	1.78	0.67	1.33	1.67	rupture
13	3.67	2.00	0.33	0.00	0.33	0.33	0.00	2.00	2.00	rupture
14	1.67	1.67	2.33	1.00	1.00	2.00	0.00	1.33	1.00	rupture
15	3.00	1.67	1.33	2.67	1.00	1.00	0.33	1.33	2.00	no
16	4.00	3.00	0.00	0.00	0.00	0.00	0.00	3.00	0.00	rupture
18	2.00	1.00	0.33	0.00	0.33	1.67	0.00	2.00	1.67	rupture
19	1.00	1.00	1.00	1.00	0.67	1.00	0.00	1.00	1.00	no
21	1.00	0.33	1.00	0.00	0.67	1.00	0.00	1.00	2.67	no
23	1.33	0.33	0.67	0.00	0.00	1.00	0.00	0.67	1.67	no
24	2.33	1.67	2.00	0.33	1.33	1.33	0.00	1.33	1.33	no
27	4.00	3.00	0.00	0.00	0.00	0.00	0.00	2.33	0.00	no
28	1.00	0.00	0.00	0.00	0.00	1.00	0.00	1.00	2.00	no
29	2.67	1.67	0.33	0.00	0.67	0.67	0.00	1.67	2.00	no
33	2.33	1.00	1.67	1.00	2.00	0.67	2.00	2.00	1.00	no
35	1.33	0.00	0.00	0.00	0.33	1.00	0.00	0.00	3.00	no
36	2.33	1.00	1.33	2.00	1.67	0.33	0.00	1.00	1.00	no

Figure 1. Human plaque characteristics. (**A**) Examples of Movat's pentachrome stained human endarterectomy plaques. (**B**) Assessment of the plaque stability parameters of the individual plaques used for mast cell flow cytometry. SMC– smooth muscle cell; ECM–extracellular matrix.

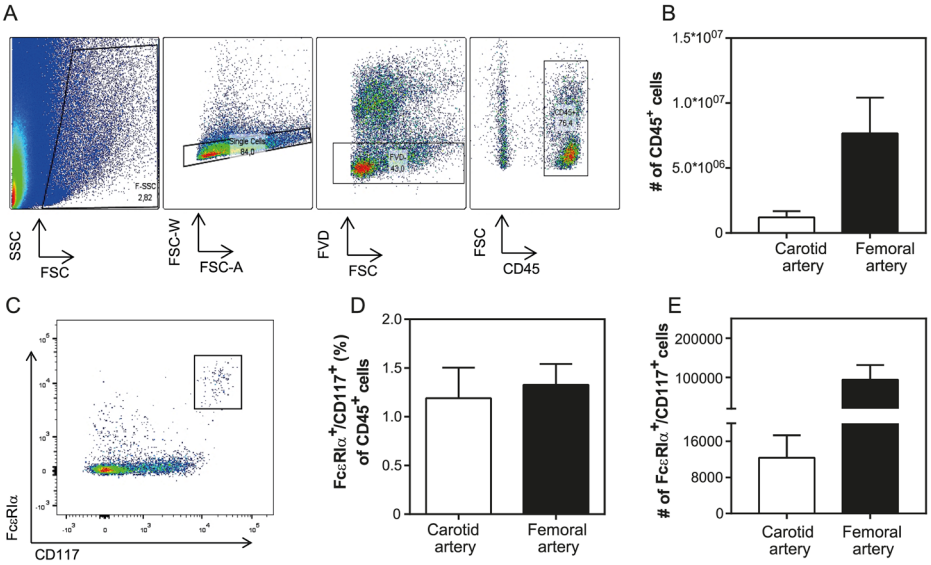

Figure 2. Mast cell content in human plaques. (A) Human plaque cell gating strategy using flow cytometry. Human intraplaque cells were selected based on their size and area. The viable cells were further separated according to the negative incorporation of fluorescent viability dye (FVD−). Immune cells were detected using the pan-leukocyte marker CD45⁺. (B) Both the femoral and carotid artery plaques contain CD45⁺ immune cells. (C) The human mast cell population was further classified using antibodies against the characteristic markers FcεRIα⁺ and CD117⁺. (D) Mast cell percentage inside human plaques isolated upon endarterectomy surgeries in carotid and femoral arteries. (E) Absolute mast cell numbers of human carotid and femoral artery samples. The data are depicted as mean ± standard error of the mean (SEM); (n = 10–12/grp).

We proceeded to further characterize the human intraplaque cells with respect to their activation status. We therefore screened our cells for the expression of CD63, a lysosomal protein that fuses with the membrane upon the release of cellular content, and marks mast cell activation.[28] We detected 7.0 ± 3.5 × 10^3 CD63⁺ mast cells in carotid plaques, which indicates that about 56% of these cells are in an activated state, while the femoral plaques showed 57 ± 23 × 10^3 activated mast cells, at a total percentage of 61% (**Figure 3A,B**). As the mast cell activation in, for example allergic reactions, predominantly occurs via IgE bound to its receptor (FcεR), we also stained the cells for the levels of IgE bound on their surface, and observed that inside the carotid arteries 7.8 ± 3.4 × 10^3 intraplaque mast cells, or approximately 63% of the total mast cell population, contained IgE, whereas in the femoral plaques 77 ± 36 × 10^3 mast cells, or 74% of all of the mast cells had IgE on their surface (**Figure 3C**). Because IgE binding generally implies mast cell degranulation, we analyzed, within each arterial plaque sample, the population of mast cells that showed both bound IgE

and CD63 expression (IgE^+CD63^+), as opposed to only IgE-binding (IgE^+CD63^-) and only a CD63 expression (IgE^-CD63^+) (**Figure 3D**). We observed that 23.8% ± 3.7% of all human plaque mast cells have IgE bound on their surface without expressing CD63, whereas the majority of mast cells, with 40.0% ± 3.9%, appeared to have IgE bound on their surface, and had also undergone degranulation. Interestingly, a proportion of mast cells, namely 19.6% ± 2.9%, appeared to be activated without showing any IgE-fragments bound on their surface, suggesting that this mast cell fraction had been activated via alternative mast cell activation pathways. The IgE-activated population was however significantly higher than the cells subjected to non-IgE mediated activation (p = 0.0005), and also higher than the mast cell population that showed a binding of IgE without being activated (p = 0.0067). When analyzing the carotid and femoral arteries separately, similar expression patterns were observed (**Figure 3E**), suggesting that intraplaque mast cell activation mechanisms do not differ much between plaque locations.

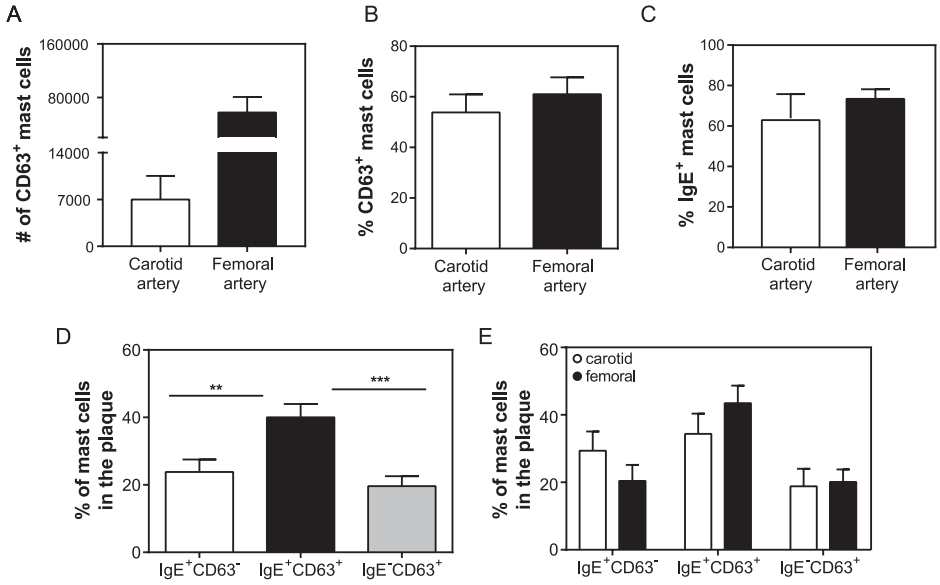

Figure 3. Activation of human intraplaque mast cells. (A) Number of activated mast cells, as defined by marker CD63, inside the carotid and femoral artery human plaques. (B) Percentage of activated mast cells in human atherosclerotic plaques. (C) Percentage of IgE+ mast cells in human atherosclerotic plaques. (D) Percentage of IgE^+CD63^-, IgE^+CD63^+, and of IgE^-CD63^+ mast cells of both carotid and femoral human atherosclerotic plaques combined. (E) Percentage of IgE^+CD63^-, IgE^+CD63^+, and of IgE^-CD63^+ mast cells displayed separately for carotid and femoral arteries, showing a similar pattern per plaque location. Data are depicted as mean ± SEM; A, B, C, and E: n = 10–12/grp; D: n = 22.

As tryptase is the preferred marker to determine the presence of mast cells in tissue by means of immunohistochemistry (**Figure 4A**), we also quantified the CD117^{+}FcεRI^{+} mast cell populations that contained tryptase in a smaller sample of the same patients using flow cytometry (n = 7). We determined that 6.8 ± 1.4 × 10^{3} of the carotid intraplaque mast cells, and 71 ± 27 × 10^{3} of the femoral intraplaque mast cells were stained positive for tryptase (**Figure 4B**). In **Figure 4C**, a flow cytometry plot of an atherosclerotic plaque with a low number of tryptase+ mast cells (left panel) and one with a very high number of tryptase^{+} mast cells (right panel) are shown. As not all intraplaque mast cells seem to stain positive for tryptase, these data indicate that one may underestimate the number of mast cells using immunohistochemistry. In addition, the amount of tryptase^{+} mast cells in the plaque can apparently differ between patients, which may be caused by recent degranulation of the intraplaque mast cells. However, this remains to be further investigated in larger patient populations.

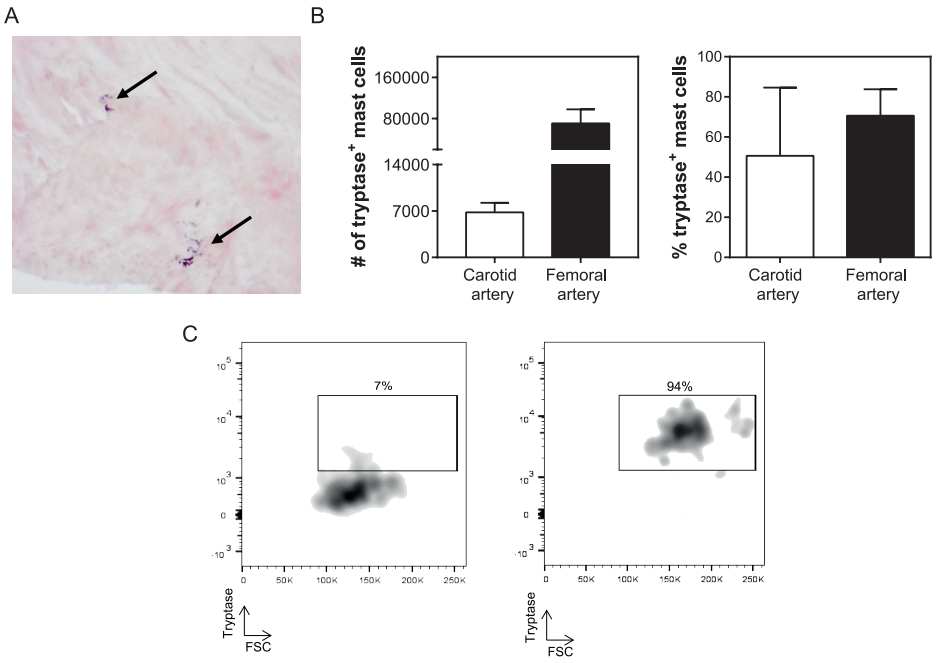

Figure 4. Tryptase content of mast cells in human atherosclerotic plaques. (A) Immunohistochemical tryptase staining of a human atherosclerotic plaque. Arrows indicate activated mast cells. (B) Number (left panel) and percentage (right panel) of mast cells containing tryptase in human carotid and femoral arteries based on flow cytometry. (C) Flow cytometry plot examples of tryptase^{+} mast cells, that is, left panel: low tryptase expression (7% of the mast cell population) vs. right panel: high tryptase expression (94% of the mast cell population). Values are depicted as mean ± SEM.

Discussion

In this study, we provide a novel flow cytometry-based approach to identify and characterize the mast cells in human atherosclerotic plaques. We classified ~1% of the total CD45$^+$ leukocyte population obtained from the plaque tissue as mast cells, based on the CD117 and FcεRI expression. Previous data have established that these mast cells, although present in relatively low numbers in the plaque, can have a severe impact on plaque stability and on the risk of future cardiovascular events.[15]. The majority of the mast cells present in arteries with advanced atherosclerosis are activated through IgE-binding, while a smaller fraction can undergo non-IgE-dependent activation. While IgE levels in the circulation[17] have been linked to increased incidence of acute cardiovascular events, and IgE fragments have been reported inside human atheromatic tissue[16], up until now, it was not clear to what extent this pathway affects mast cell activation in the area. Our data confirm that most mast cells present in the atherosclerotic plaques are activated[5,10], as it has been shown previously, specifically, for the shoulder region. We show here that the main activating mechanism is through classical antigen-sensitized IgE binding on their surface Fcε-receptors. In addition, we show that a small proportion of cells bind IgE without undergoing activation. The circulating IgE can thus bind on the surface of the intraplaque mast cells and sensitize them prior to antigen binding. The exact antigenic fragment that may cause intraplaque mast cell activation has not yet been identified, but the binding of lipid-specific antigenic fragments may be a possible mechanism.[20] Furthermore, the detection of IgE fragments inside the plaque tissue confirms that these fragments can surpass the endothelial wall and accumulate in the plaque area, which may explain why circulating IgE levels correlate with end-stage cardiovascular events like atherothrombosis[29] and myocardial infarction[30]. Therefore, it is reasonable to acknowledge IgE as an important risk factor in cardiovascular episodes, even though it still remains to be elucidated whether it is a causative element.[31] In addition, our data raise an interesting question regarding patients who suffer from other syndromes with increased circulating IgE levels. The development of atherosclerosis is a chronic process, which spans from the formation of a fatty streak, during an individual's teenage years, and may result in an unfortunate acute event of an end-stage plaque rupture and vessel occlusion.[32] In the course of those years, a fraction of humans may be diagnosed with allergic inflammatory conditions, associating with high levels of circulating IgE.[33] This may mean that IgE has an increased chance to migrate through the endothelium and bind the intraplaque mast cells, raising the likelihood for a future cardiovascular event. In fact, there is compiling evidence that allergic asthma and atherosclerosis are linked[34], and mast cells are seemingly paramount in this[33]. In addition, patients with a genetic condition called

hyper-IgE syndrome have recently been demonstrated to show signs of subclinical coronary atherosclerosis[35], and patients with systemic mastocytosis were recently described with a higher prevalence of cardiovascular disease events as compared to controls[36]. Interestingly, our group has demonstrated that the mast cell stabilizer cromolyn acts in a protective manner in atherosclerosis experimental studies.[37] Therefore, a mast cell stabilization approach may be an interesting preventive strategy in individuals who show high circulating IgE levels, but who have not yet been diagnosed with cardiovascular disease. In addition, we identified a group of mast cells that are activated without IgE binding, which suggests that this activation pathway is not the only way by which mast cells are activated in human atherosclerosis. We have previously established, in experimental atherosclerosis models, that mast cells in the vessel wall can be activated via neuropeptides such as Substance P[22] or Neuropeptide Y[38], or via complement components such as C5a[21]. These factors have also been shown to be present in human lesions.[21,22] It however remains to be established which of its receptors may induce mast cell activation in human atherosclerosis. The technical approach described in this study may be able to provide answers to these questions, by, for example, analyzing the expression of specific activating receptors on the intraplaque mast cells. It is still unclear what this implies in terms of mediator release. It would be interesting to further characterize the intracellular content of these cells to examine whether different activation pathways lead to the release of different proteases and cytokines, and how this may possibly affect the surrounding environment. Using this technique on a larger patient cohort may also reveal whether mast cell activation is affected by gender. A larger patient population will also allow for determining whether mast cell numbers or activation status relate to specific atherosclerotic plaque characteristics.

Our data provide an additional important point of attention when using tryptase-based immunohistochemistry to identify mast cells in tissue. Our flow cytometry data provide evidence that not all mast cells stain positive for tryptase, which can be explained by the fact that the recently degranulated mast cells may have released their tryptase content. One should therefore keep in mind that when using tryptase-immunohistochemistry only, the number of (activated) mast cells in the tissue may be an underestimation, and one may opt for a second quantification method, for example, a flow cytometry-based method using multiple markers.

In conclusion, in this study, we made use of flow cytometry to characterize mast cells in the advanced atherosclerotic plaques of human subjects. We confirm that the major pathway for the activation of mast cells inside the plaque tissue is IgE-mediated, and that the intraplaque mast cells are highly activated. This is particularly important,

as it suggests that already available modes of therapy like mast cell stabilization agents[39] or anti-IgE treatment[40] may prove beneficial in patients suffering from atherosclerosis. We expect that larger scale patient studies and the analysis of more characterization markers, for instance through mass cytometry, will reveal new pathways via which mast cells may act in atherosclerosis, opening new ways to intervene in cardiovascular disease.

Author Contributions

Conceptualization, E.K., A.W., J.K., and I.B.; methodology, E.K, B.S., A.W., and I.B.; validation, M.R.d.V. and I.B.; formal analysis, E.K.; investigation, E.K., M.A.C.D., M.R.d.V., K.E.M., A.M.G., M.D.S., B.S., J.v.D., A.C.F.; data curation, E.K., A.W., and I.B.; writing (original draft preparation), E.K. and I.B.; writing (review and editing), all of the authors; supervision, H.J.S., J.K., and P.H.A.Q.; project administration, A.W. and I.B.; funding acquisition, J.K. and I.B.

Funding

This project is funded by grant 95105013 (program translational research from ZonMW and the Dutch Heart Foundation).

Conflicts of Interest

The authors declare no conflict of interest.

References

1. Benjamin, E.J.; Blaha, M.J.; Chiuve, S.E.; Cushman, M.; Das, S.R.; Deo, R.; de Ferranti, S.D.; Floyd, J.; Fornage, M.; Gillespie, C.; et al. Heart Disease and Stroke Statistics–2017 Update: A Report From the American Heart Association. *Circulation* **2017**, *135*, e146–e603.
2. Bot, I.; Shi, G.-P.; Kovanen, P.T. Mast cells as effectors in atherosclerosis. *Arterioscler. Thromb. Vasc. Biol.* **2015**, *35*, 265–271.
3. Amin, K. The role of mast cells in allergic inflammation. *Respir. Med.* **2012**, *106*, 9–14.
4. Shi, G.-P.; Bot, I.; Kovanen, P.T. Mast cells in human and experimental cardiometabolic diseases. *Nat. Rev. Cardiol.* **2015**, *2*, 643–658.
5. Kaartinen, M.; Penttila, A.; Kovanen, P.T. Accumulation of activated mast cells in the shoulder region of human coronary atheroma, the predilection site of atheromatous rupture. *Circulation* **1994**, *90*, 1669–1678.
6. Kovanen, P.T.; Kaartinen, M.; Paavonen, T. Infiltrates of activated mast cells at the site of coronary atheromatous erosion or rupture in myocardial infarction. *Circulation* **1995**, *92*, 1084–1088.
7. Bot, I.; Biessen, E.A.L. Mast cells in atherosclerosis. *Thromb. Haemost.* **2011**, *106*, 820–826.
8. Ramalho, L.S.; Oliveira, L.F.; Cavellani, C.L.; Ferraz, M.L.; de Oliveira, F.A.; Miranda Corrêa, R.R.; de Paula Antunes Teixeira, V.; De Lima Pereira, S.A. Role of mast cell chymase and tryptase in the progression of atherosclerosis: Study in 44 autopsied cases. *Ann. Diagn. Pathol.* **2013**, *17*, 28–31.
9. Mayranpaa, M.I.; Heikkila, H.M.; Lindstedt, K.A.; Walls, A.F.; Kovanen, P.T. Desquamation of human coronary artery endothelium by human mast cell proteases: Implications for plaque erosion. *Coron. Artery Dis.* **2006**, *17*, 611–621.
10. Kaartinen, M.; Penttila, A.; Kovanen, P.T. Mast cells accompany microvessels in human coronary atheromas: Implications for intimal neovascularization and hemorrhage. *Atherosclerosis* **1996**, *123*, 123–131.
11. Kaartinen, M.; Penttila, A.; Kovanen, P.T. Mast cells of two types differing in neutral protease composition in the human aortic intima. Demonstration of tryptase- and tryptase/chymase-containing mast cells in normal intimas, fatty streaks, and the shoulder region of atheromas. *Arterioscler. Thromb. Vasc. Biol.* **1994**, *14*, 966–972.
12. Zhi, X.; Xu, C.; Zhang, H.; Tian, D.; Li, X.; Ning, Y.; Yin, L. Tryptase promotes atherosclerotic plaque haemorrhage in ApoE$^{-/-}$ mice. *PLoS One* **2013**, *8*, e60960.
13. Bot, I.; Bot, M.; van Heiningen, S.H.; van Santbrink, P.J.; Lankhuizen, I.M.; Hartman, P.; Gruener, S.; Hilpert, H.; van Berkel, T.J.; Fingerle, J.; et al. Mast cell chymase inhibition reduces atherosclerotic plaque progression and improves plaque stability in ApoE$^{-/-}$ mice. *Cardiovasc Res.* **2011**, *89*, 244–252.
14. Rohm, I.; Sattler, S.; Atiskova, Y.; Kretzschmar, D.; Pistulli, R.; Franz, M.; Jung, C.; Mall, G.; Kronert, T.; Schulze, P.C.; et al. Increased Number of Mast Cells in Atherosclerotic Lesions Correlates with the Presence of Myeloid but not Plasmacytoid Dendritic Cells as well as Pro-inflammatory T Cells. *Clin. Lab.* **2016**, *62*, 2293–2303.
15. Willems, S.; Vink, A.; Bot, I.; Quax, P.H.; de Borst, G.J.; de Vries, J.P.; van de Weg, S.M.; Moll, F.L.; Kuiper, J.; Kovanen, P.T.; et al. Mast cells in human carotid atherosclerotic plaques are associated with intraplaque microvessel density and the occurrence of future cardiovascular events. *Eur. Heart J.* **2013**, *34*, 3699–3706.

16. Wang, J.; Cheng, X.; Xiang, M.X.; Alanne-Kinnunen, M.; Wang, J.A.; Chen, H.; He, A.; Sun, X.; Lin, Y.; Tang, T.T.; et al. IgE stimulates human and mouse arterial cell apoptosis and cytokine expression and promotes atherogenesis in Apoe$^{-/-}$ mice. *J. Clin. Invest.* **2011**, *121*, 3564–3577.
17. Guo, X.; Yuan, S.; Liu, Y.; Zeng, Y.; Xie, H.; Liu, Z.; Zhang, S.; Fang, Q.; Wang, J.; Shen, Z. Serum IgE levels are associated with coronary artery disease severity. *Atherosclerosis* **2016**, *251*, 355–360.
18. Kelley, J.; Hemontolor, G.; Younis, W.; Li, C.; Krishnaswamy, G.; Chi, D.S. Mast cell activation by lipoproteins. *Methods Mol. Biol.* **2006**, *315*, 341–348.
19. Yu, Y.; Blokhuis, B.R.; Garssen, J.; Redegeld, F.A. Non-IgE mediated mast cell activation. *Eur. J. Pharmacol.* **2016**, *778*, 33–43.
20. Meng, Z.; Yan, C.; Deng, Q.; Dong, X.; Duan, Z.M.; Gao, D.F.; Niu, X.L. Oxidized low-density lipoprotein induces inflammatory responses in cultured human mast cells via Toll-like receptor 4. *Cell. Physiol. Biochem.* **2013**, *31*, 842–853.
21. de Vries, M.R.; Wezel, A.; Schepers, A.; van Santbrink, P.J.; Woodruff, T.M.; Niessen, H.W.; Hamming, J.F.; Kuiper, J.; Bot, I.; Quax, P.H. Complement factor C5a as mast cell activator mediates vascular remodelling in vein graft disease. *Cardiovasc. Res.* **2013**, *97*, 311–320.
22. Bot, I.; de Jager, S.C.; Bot, M.; van Heiningen, S.H.; de Groot, P.; Veldhuizen, R.W.; van Berkel, T.J.; von der Thüsen, J.H.; Biessen, E.A. The neuropeptide substance P mediates adventitial mast cell activation and induces intraplaque hemorrhage in advanced atherosclerosis. *Circ. Res.* **2010**, *106*, 89–92.
23. Verhoeven, B.A.; de Vries, J.P.; Pasterkamp, G.; Ackerstaff, R.G.; Schoneveld, A.H.; Velema, E.; de Kleijn, D.P.; Moll, F.L. Carotid atherosclerotic plaque characteristics are associated with microembolization during carotid endarterectomy and procedural outcome. *Stroke* **2005**, *36*, 1735–1740.
24. Van Brussel, I.; Ammi, R.; Rombouts, M.; Cools, N.; Vercauteren, S.R.; De Roover, D.; Hendriks, J.M.H.; Lauwers, P.; Van Schil, P.E.; Schrijvers, D.M. Fluorescent activated cell sorting: An effective approach to study dendritic cell subsets in human atherosclerotic plaques. *J. Immunol. Methods* **2015**, *417*, 76–85.
25. Lovett, J.K.; Gallagher, P.J.; Hands, L.J.; Walton, J.; Rothwell, P.M. Histological correlates of carotid plaque surface morphology on lumen contrast imaging. *Circulation* **2004**, *110*, 2190–2197.
26. Burd, P.R.; Rogers, H.W.; Gordon, J.R.; Martin, C.A.; Jayaraman, S.; Wilson, S.D.; Dvorak, A.M.; Galli, S.J.; Dorf, M.E. Interleukin 3-dependent and -independent mast cells stimulated with IgE and antigen express multiple cytokines. *J. Exp. Med.* **1989**, *170*, 245–257.
27. Tsai, M.; Takeishi, T.; Thompson, H.; Langley, K.E.; Zsebo, K.M.; Metcalfe, D.D.; Geissler, E.N.; Galli, S.J. Induction of mast cell proliferation, maturation, and heparin synthesis by the rat c-kit ligand, stem cell factor. *Proc. Natl. Acad. Sci. U. S. A.* **1991**, *88*, 6382–6386.
28. Kraft, S.; Jouvin, M.H.; Kulkarni, N.; Kissing, S.; Morgan, E.S.; Dvorak, A.M.; Schröder, B.; Saftig, P.; Kinet, J.P. The tetraspanin CD63 is required for efficient IgE-mediated mast cell degranulation and anaphylaxis. *J. Immunol.* **2013**, *191*, 2871–2878.
29. Sinkiewicz, W.; Błazejewski, J.; Bujak, R.; Zekanowska, E.; Sobański, P.; Kubica, J.; Dudziak, J.; Karasek, D.; Małyszka, P.; Balak, W.; et al. Immunoglobulin E as a marker of the atherothrombotic process in patients with acute myocardial infarction. *Cardiol. J.* **2007**, *14*, 266–273.
30. Langer, R.D.; Criqui, M.H.; Feigelson, H.S.; McCann, T.J.; Hamburger, R.N. IgE predicts future nonfatal myocardial infarction in men. *J. Clin. Epidemiol.* **1996**, *49*, 203–209.
31. Lippi, G.; Cervellin, G.; Sanchis-Gomar, F. Immunoglobulin E (IgE) and ischemic heart disease. Which came first, the chicken or the egg? *Ann. Med.* **2014**, *46*, 456–463.

32. Insull, W.J. The pathology of atherosclerosis: Plaque development and plaque responses to medical treatment. *Am. J. Med.* **2009**, *122*, S3–S14.
33. Laske, N.; Bunikowski, R.; Niggemann, B. Extraordinarily high serum IgE levels and consequences for atopic phenotypes. *Ann. Allergy. Asthma Immunol.* **2003**, *91*, 202–204.
34. Wang, L.; Gao, S.; Xu, W.; Zhao, S.; Zhou, J.; Wang, N.; Yuan, Z. Allergic asthma accelerates atherosclerosis dependent on Th2 and Th17 in apolipoprotein E deficient mice. *J. Mol. Cell. Cardiol.* **2014**, *72*, 20–27.
35. Abd-Elmoniem, K.Z.; Ramos, N.; Yazdani, S.K.; Ghanem, A.M.; Holland, S.M.; Freeman, A.F.; Gharib, A.M. Coronary atherosclerosis and dilation in hyper IgE syndrome patients: Depiction by magnetic resonance vessel wall imaging and pathological correlation. *Atherosclerosis* **2017**, *258*, 20–25.
36. Indhirajanti, S.; van Daele, P.L.A.; Bos, S.; Mulder, M.T.; Bot, I.; Roeters van Lennep, J.E. Systemic mastocytosis associates with cardiovascular events despite lower plasma lipid levels. *Atherosclerosis* **2018**, *268*, 152–156.
37. Bot, I.; de Jager, S.C.; Zernecke, A.; Lindstedt, K.A.; van Berkel, T.J.; Weber, C.; Biessen, E.A. Perivascular mast cells promote atherogenesis and induce plaque destabilization in apolipoprotein E-deficient mice. *Circulatio*n **2007**, *115*, 2516–2525.
38. Lagraauw, H.M.; Westra, M.M.; Bot, M.; Wezel, A.; van Santbrink, P.J.; Pasterkamp, G.; Biessen, E.A.; Kuiper, J.; Bot, I. Vascular neuropeptide Y contributes to atherosclerotic plaque progression and perivascular mast cell activation. *Atherosclerosis* **2014**, *235*, 196–203.
39. Finn, D.F.; Walsh, J.J. Twenty-first century mast cell stabilizers. *Br. J. Pharmacol.* **2013**, *170*, 23–37.
40. Logsdon, S.L.; Oettgen, H.C. Anti-IgE therapy: Clinical utility and mechanistic insights. *Curr. Top. Microbiol. Immunol.* **2015**, *388*, 39–61.

Chapter 6

Aging promotes mast cell activation and antigen presenting capacity in atherosclerosis

Manuscript in preparation

Marie A.C. Depuydt*[1], Virginia Smit*[1], Frank H. Schaftenaar[1], Esmeralda Hemme[1], Lucie Delfos[1], Femke Vlaswinkel[1], Conor Simpson[1], Petri T. Kovanen[2], Bram Slütter[1], Johan Kuiper, Ilze Bot#, Amanda C. Foks#

1 Division of BioTherapeutics, Leiden Academic Centre for Drug Research, Leiden University, 2333 CC, Leiden, The Netherlands
2 Wihuri Research Institute, Helsinki, Finland.

*These authors contributed equally; #Shared last authors.

Abstract

Aging is an independent and dominant risk factor for atherosclerosis and is associated with a low-grade chronic inflammation termed inflammaging. This age-induced pro-inflammatory environment may have great impact on plaque-residing immune cells, including mast cells. Mast cells have been found to accumulate in the human atherosclerotic plaque upon disease progression and have been associated with plaque instability. However, it is currently unknown whether aging drives the pro-atherogenic effects of mast cells in atherosclerosis.

To assess the effects of aging on mast cell phenotype, we examined mast cell populations in young and old male *Ldlr*$^{-/-}$ mice fed either a chow or Western-type diet. We found that in atherosclerotic tissue both mast cell number and activation status increased upon aging. Furthermore, we identified that aged bone-marrow derived mast cells displayed increased basal CD63 expression compared to young cells, indicative of intrinsic low-grade activation. Moreover, we demonstrated that aging increases the amount of MHCII^{+} mast cells in atherosclerosis, allowing them to act as antigen-presenting cells, which correspondingly led to increased CD4^{+} T cell proliferation *in vitro*. Finally, single-cell RNA sequencing of human atherosclerotic plaques confirmed mast cell-specific expression of MHC-II orthologs.

To conclude, we established that aging induces phenotypic changes of mast cells in atherosclerosis, regarding both activation status and antigen presenting capacity, which can contribute to disease progression.

Introduction

Acute cardiovascular syndromes are the principal cause of death in the Western society. The main pathology underlying the majority of cardiovascular diseases is atherosclerosis, which is caused by the accumulation of lipids and inflammatory cells in the vessel wall. Upon progression and destabilization of an atherosclerotic plaque, the risk of plaque rupture increases. Rupture or erosion of an atherosclerotic plaque can subsequently lead to vessel-occluding thrombosis, potentially resulting in acute cardiovascular syndromes such as myocardial infarction or stroke.[1]

The mast cell, a potent immune effector cell primarily involved in host defense responses[2,3], has been implicated in atherosclerotic plaque destabilization. Previously, we and others established that mast cells contribute to plaque development in experimental models of atherosclerosis[4,5]. Excessive mast cell activation resulted in an increased incidence of intraplaque hemorrhage, a hallmark of plaque instability in murine atherosclerosis[4]. Also in human atherosclerotic plaques, mast cell numbers increased upon plaque progression and were significantly elevated in plaques that contained an intraplaque hemorrhage[6]. Strikingly, mast cell numbers in advanced carotid artery plaques, obtained with carotid endarterectomy, were elevated in patients that suffered a clinical event during follow-up[6]. Together, these data suggest that mast cells actively contribute to atherosclerotic plaque progression and destabilization. Age is an important risk factor for atherosclerosis.[7] However, aging also leads to structural changes in immune responses with skewing towards myeloid at the cost of lymphoid lineages[8] and to an enduring state of low-grade inflammation (inflammaging), in which mast cells may participate as well. Few studies have investigated the effects of aging on mast cells.[9–11] In gut and brain for example, increasing numbers of mast cells were reported upon aging, which were implicated in prolonged inflammatory responses in a mouse model of stroke.[10] Also in human skin, mast cells accumulate upon aging, with altered functionality.[11] In these aged skin samples, a reduced gene expression of for example Substance P was observed compared to young, which has previously been described as potent mast cell activator via different receptors. This illustrates the importance of taking age into account upon therapeutic intervention. It is however unknown how aging impacts mast cells in atherosclerosis. Combined with the fact that mast cell numbers increase with disease progression, detailed mechanistic insights in age-associated changes in mast cell behavior is highly relevant in advanced atherosclerosis. In this study, we therefore aimed to assess the effects of aging on mast cell phenotype and activation status in atherosclerosis.

Methods

Animals

All animal experiments were performed in compliance with the guidelines of the Dutch government and the Directive 2010/63/EU of the European Parliament. The experiments were approved by the Ethics Committee for Animal Experiments and the Animal Welfare Body of Leiden University (Project 106002017887).

Aging cohort

Male young (10-12 weeks) and old (75-83 weeks) in-house bred *Ldlr*$^{-/-}$ mice on a C57BL/6 background (n = 8-9/group) were provided with food and water *ad libitum*. Young mice were either fed a regular chow diet or a Western-type diet (0.25% cholesterol, 15% cocoa butter, Special Diet Services, Essex, UK) for 5 weeks. Old mice were fed a regular chow diet. Mice were randomized based on weight and serum cholesterol levels. At week 5, mice were sacrificed upon subcutaneous injection of anaesthetics (ketamine (100 mg/kg), atropine (0.6 mg/kg) and xylazine (10 mg/kg)), followed by orbital bleeding, after which peritoneal lavage was performed with PBS. Next, mice were perfused with phosphate-buffered saline (PBS) through the left cardiac ventricle. Subsequently, organs were collected for analysis.

Adoptive transfer cohort

Male 15-22 week old *apoE*$^{-/-}$*Kit*$^{W\text{-}sh/W\text{-}sh}$ (n = 9-12/group) were provided with food and water *ad libitum*. Mice were randomized based on age, weight and serum cholesterol levels. At the start of the experiment, mice were injected intravenously with 10*10^{6} bone marrow-derived mast cells originating from either young or old *Ldlr*$^{-/-}$ mice and simultaneously put on a Western-type diet. After 14 weeks, mice were sacrificed as described above.

DSCG cohort

Male old (68-73 weeks) *Ldlr*$^{-/-}$ mice on a C57BL/6 background (n=13-14/group) were provided with food and water *ad libitum*. Mice were randomized based on age, weight and serum cholesterol levels and were fed a chow diet throughout the experiment. Mice were treated with disodium cromoglycate (DSCG; 50 mg/kg i.p.) or PBS control three times a week. After 6 weeks of treatment, mice were sacrificed as described above.

OT-II mice

OT-II mice were purchased from the Jackson Laboratory and further bred in house. Male 18 week old OT-II mice were sacrificed by cervical dislocation. Next, spleens were obtained for isolation of CD4^{+} T cells.

Histology

Hearts were dissected, embedded and frozen in Tissue-Tek OCT compound (Sakura). 10 µm cryosections of the aortic root were prepared for histological analysis. Mean plaque size and the percentage plaque area of total vessel area (vessel occlusion) were assessed by Oil-Red-O (ORO) staining. From the first appearance of the three aortic valves, 5 consecutive slides with 80 µm distance between the sections were analysed for total lesion size within the three valves, after which the average lesion size was calculated. Naphthol AS-D chloroacetate staining (Sigma-Aldrich) was performed to manually quantify resting and activated mast cells in the atherosclerotic aortic root. A mast cell was considered resting when all granula were maintained inside the cell, while mast cells were assessed as activated when granula were deposited in the tissue surrounding the mast cell. Collagen content of the plaque was measured using either a Sirius Red staining in the adoptive transfer study or a Masson's trichrome staining in the DSCG study. Similarly, the average necrotic core size was quantified by measuring the acellular debris-rich areas of the plaque of three sections per mouse. For all stainings, three sections per mouse were analysed and averaged unless stated otherwise. Sections were obtained using either a Leica DMRE microscope (Leica Systems) or digitalised using a Panoramic 250 Flash III slide scanner (3DHISTECH, Hungary). Blinded analysis was performed using ImageJ software.

Cell isolation

Blood samples were lysed with ACK lysis buffer (0.15 M NH_4Cl, 1 mM $KHCO_3$, 0.1 mM Na_2EDTA, pH 7.3) to obtain a single white blood cell suspension. Spleens were passed through a 70 µm cell strainer (Greiner, Bio-one, Kremsmunster, Austria) and splenocytes were subsequently lysed with ACK lysis buffer. Aortic arches were cut into small pieces and enzymatically digested in a digestion mix containing collagenase I (450 U/mL), collagenase XI (250 U/mL), DNAse (120 U/mL), and hyaluronidase (120 U/mL; all Sigma-Aldrich) for 30 minutes at 37°C while shaking. After incubation, all samples were passed through a 70 µm cell strainer (Geiner, Bio-one, Kremsmunster, Austria). Single cell suspensions were then used for flow cytometry analysis.

Flow cytometry

Single cell suspensions from the aortic arch, peritoneum, blood and spleen were extracellularly stained with a mixture of selected fluorescent labelled antibodies for 30 minutes at 4°C. For intracellular stainings, cells were fixed and permeabilized with the Foxp3 Transcription Factor Staining buffer set (ThermoFisher) according to the manufacturer's protocol and stained with intracellular antibodies for 30

minutes at 4°C.The antibodies used for flow cytometry are listed in **Table S1**. All measurements were performed on a Cytoflex S (Beckman and Coulter, USA) and analysed with FlowJo v10.7 (Treestar, San Carlos, CA, USA).

Serum IgE measurement

Serum was collected through centrifugation at 8000 rpm for 10 minutes at 4°C and stored at -80°C until further use. IgE was measured using an IgE ELISA kit (Biolegend) according to manufacturer's instructions.

Bone-marrow derived mast cell culture

To obtain bone marrow-derived mast cells (BMMCs), bone marrow cells from young and old *Ldlr*$^{-/-}$ mice were cultured in RPMI 1640 containing 25 mM HEPES (Lonza) and supplemented with 10% fetal calf serum, 1% L-glutamine (Lonza), 100 U/mL mix of penicillin/streptomycin (PAA), 1% sodium pyruvate (Sigma-Aldrich), 1% non-essential amino acids (MEM NEAA; Gibco) and 5 ng/mL IL-3 (Immunotools). Cells were incubated at 37°C and 5% CO_2 and were kept at a density of 0.25*10^6 cells per mL by weekly subculturing. BMMCs were cultured for 4 weeks in total to obtain mature mast cells.

In vitro mast cell stimulation

The mast cell activation assay was performed using 1*10^6 young or old BMMCs. All mast cells were first sensitized with anti-DNP IgE (1µg/mL, Sigma-Aldrich) for 2.5 hours at 37°C and 5% CO_2. Subsequently, DNP-HSA (20 ng/mL, Sigma-Aldrich) or medium control was added for 30 min at 37°C and 5% CO_2 to obtain respectively stimulated and unstimulated mast cells. Mast cell activation was measured as percentage CD63$^+$ of live CD117$^+$FcεRI$^+$ mast cells. Cytokines in the supernatant were measured using a Legendplex assay (Biolegend), which was performed according to the manufacturers protocol.

Mast cell – OT-II CD4$^+$ T cell co-culture

Young and old BMMCs were cultured as described above. To induce MHC-II expression, mast cells were stimulated with IFN-γ (50 ng/mL) and IL-4 (20 ng/mL) for 48 hours. After 24 hours the medium was supplemented with new cytokines. MHC-II expression was measured as percentage MHC-II$^+$ of live CD117$^+$FcεRI$^+$ cells. CD4$^+$ T cells from OT-II mice were obtained using magnetic bead isolation by negative selection (Miltenyi Biotec) and stained with CFSE for 10 minutes at 37°C and 5% CO_2. Subsequently, the CD4$^+$ T cells were stimulated with anti-CD3 (1 µg/mL) and anti-CD28 (0.5 µg/mL) for 24 hours. Next, cells were washed and the OT-II CD4$^+$ T cells were seeded with the MHC-II$^+$ mast cells in a 1:1 ratio. Finally, 1 µg/mL

ovalbumin (OVA) was added to the co-cultured cells for 48 hours. All cells in this experiment were cultured in RPMI supplemented with 10% Fetal Bovine Serum, 1% Penicillin and Streptomycin, 1% L-glutamine and 0.05mM 2-mercaptoethanol. Subsequently, $CD4^+$ T cell proliferation was assessed by flow cytometry as the $\%CFSE^-$ of live $CD4^+$ T cells.

Single-cell RNA sequencing of human atherosclerotic plaques

Human carotid artery plaques were collected from 46 patients (26 male, 20 female) that underwent carotid endarterectomy surgery as part of AtheroExpress, an ongoing biobank study at the University Medical Centre Utrecht (Study approval number TME/C-01.18, protocol number 03/114).[12] Single cells were obtained and processed for single-cell RNA sequencing as previously described.[13] All studies were performed in accordance with the Declaration of Helsinki. Informed consent was obtained from all subjects involved in the study.

Statistical analysis

All data are represented as mean ± SEM and analysed in GraphPad Prism 9. Shapiro-Wilkson normality test was used to test data for normal distribution. In the aging cohort, statistical analysis was performed using one-way ANOVA or, if not normal distributed data, a Kruskal-Wallis test. For both the adoptive transfer study and the DSCG study, an unpaired two-tailed Student *t*-test or, in case of not normally distributed data, Mann-Whitney test was used. $P < 0.05$ was considered to be significant.

Results

Increased number of activated mast cells in the aged atherosclerotic aorta

Multiple age-related changes in mast cells have been described so far. Mast cells have been reported to accumulate in the skin, gut and brain with aging, however changes in mast cell activation differ per tissue.[10,11,14,15] Here, we first examined whether increased age affects mast cell numbers and activation status in the atherosclerotic environment. To this extent, we assessed mast cell phenotype in young male *Ldlr*$^{-/-}$ mice on either a chow (non-atherosclerotic, CD) or Western type diet (5 weeks, atherosclerotic, WD) and aged male *Ldlr*$^{-/-}$ mice on a CD that gradually developed atherosclerosis over time (**Fig. 1a**).[16]

Using flow cytometry, we observed a strong 6-fold increase in the total number of $CD117^+$ $Fc\varepsilon RI^+$ mast cells in the aortic arch of aged *Ldlr*$^{-/-}$ mice compared to young CD- and WD-fed *Ldlr*$^{-/-}$ mice (YC: 4.5±0.7, YW: 45.3±15.2, OC: 279.4±9 cells per aorta, YC vs.

OC $p<0.01$, YW vs. OC $p<0.01$; **Fig. 1b, c, Supplemental Fig. 1**). Additionally, a significant increase in mast cells as percentage of live CD45$^+$ immune cells was detected both in the aged atherosclerotic aorta and in the aged peritoneum (**Fig. 1d, e**).

To examine whether age also affects mast cell activation status, we measured CD63$^+$ expression, which is a marker that is upregulated upon mast cell degranulation.[17] In the aortic arch, a significant increase in the absolute number of CD63$^+$ mast cells was detected in the aged group compared to both young groups (YC: 1.8±0.6, YW: 41.3±13.6, OC: 259.7±85.4 per aorta, YC vs. OC $p<0.01$, YW vs. OC $p<0.01$; **Fig. 1f**). Correspondingly, an increased percentage of CD63$^+$ mast cells of live CD45$^+$ was observed in both young and old atherosclerotic aortas compared to young non-atherosclerotic aorta's (**Fig. 1g**). Of note, the difference in mast cell activation between young WD-fed and old *Ldlr*$^{-/-}$ mice is mainly attributed to the amount of mast cells and not the level of CD63 expression (**Supplemental Fig. 2a**). Similar to the aortic arch the percentage of CD63$^+$ peritoneal mast cells was significantly increased in aged mice as compared to young, indicating that overall the proportion of activated mast cells in a model of aged atherosclerosis is augmented (**Fig. 1h**). Subsequently, we histologically assessed mast cell quantity and activation status in the aortic root. While we did not observe a difference in the number of adventitial mast cells between the groups (**Fig. 1i, j**), the percentage of activated (degranulated) mast cells was increased in the adventitia of aged *Ldlr*$^{-/-}$ mice compared to both young counterparts (YC: 49±3, YW: 45±3, OC: 63±2, YC vs. OC $p<0.001$, YW vs. OC $p<0.01$; **Fig. 1i, k**).

As the Immunoglobulin E (IgE)-FcεRI pathway is the most commonly known mast cell activation pathway[18], we measured circulating total IgE levels. We observed significantly elevated IgE levels in serum of aged compared to young *Ldlr*$^{-/-}$ mice (YC: 44.1±9.9 ng/mL, YW: 44.2±19.0 pg/mL, 163.4±32.0 pg/mL, YC vs. OC $p<0.05$, YW vs. OC $p<0.01$; **Fig. 1l**), supporting the possibility of enhanced IgE-mediated mast cell activation in the aorta.

We next examined whether aging also induced mast cell-intrinsic changes. No differences in maximal activation were observed between *in vitro* stimulated young and old BMMCs, however increased basal CD63 expression was observed on old BMMCs compared to young (Young: 0.14±0.006% vs. Old: 4.4±0.2%, $p<0.05$; **Fig. 1m, n**). Moreover, a significant increase of CC chemokine ligand 2 (CCL2) was observed in the supernatant of old stimulated BMMCs (Young: 198.5±5.4 pg/mL vs. Old: 238.0±11.8 pg/mL, $p<0.05$; **Fig. 1o**). No differences were observed for CCL3, CCL4, Interleukin (IL)-4, IL-6 and TNF-α (**Supplemental Fig 2b-f**). For unstimulated samples, all chemokines and cytokines measured had values below the detection limit.

Increased MHCII$^+$ expression on mast cells of old miceinduces vigorous CD4$^+$ T cell proliferation

Although mast cells are most commonly known for their pro-inflammatory secretome, there is accumulating evidence that they also act as atypical antigen presenting cells.[19] Therefore, we subsequently examined whether age affects Major Histocompatibility Complex (MHC)-II expression on mast cells. A respectively 63- and 4-fold increase in the number of MHC-II$^+$ mast cells was observed in aged compared to young CD-fed and WD-fed *Ldlr*$^{-/-}$ mice (YC: 2.5±0.5, YW: 40.8±14.7, OC: 157.7±40.5 per aorta, YC vs. OC $p<0.001$, YW vs. OC $p<0.01$; **Fig. 2a**). Similarly, the proportion of MHCII$^+$ mast cells accumulated was also significantly enlarged in the aged atherosclerotic aorta (YC: 0.1±0.03% vs OC: 3.0±0.6, $p<0.001$; **Fig. 2a**). This particular difference was also detected in peritoneal mast cells (**Fig. 2b**). Subsequently, we assessed whether aged mast cells have increased potential to induce CD4$^+$ T cell proliferation. We first stimulated BMMCs derived from both young and aged bone marrow with IFN-γ and IL-4 for two days to enhance MHCII expression as previously described.[20,21] A significant increase in MHC-II expression was detected on aged BMMCs versus young upon stimulation (**Fig. 2c**). Subsequently, co-culture of aged BMMCs with CD4$^+$ T cells resulted in significantly increased CD4$^+$ T cell proliferation (Young: 35.2±1.2% vs. Old: 45.8±1.2%, $p<0.001$ **Fig. 2d**). Finally, we examined expression of human MHC-II orthologs on mast cells detected in a single-cell RNA sequencing data set of 43 atherosclerotic plaques obtained by carotid endarterectomy surgery from aged patients. Expression of *HLA-DPA1*, *HLA-DRA* and *HLA-DRB1* was observed on the majority of the detected mast cells, suggesting that mast cells can act as antigen presenting cells in the human atherosclerotic plaque as well (**Fig. 2e**).

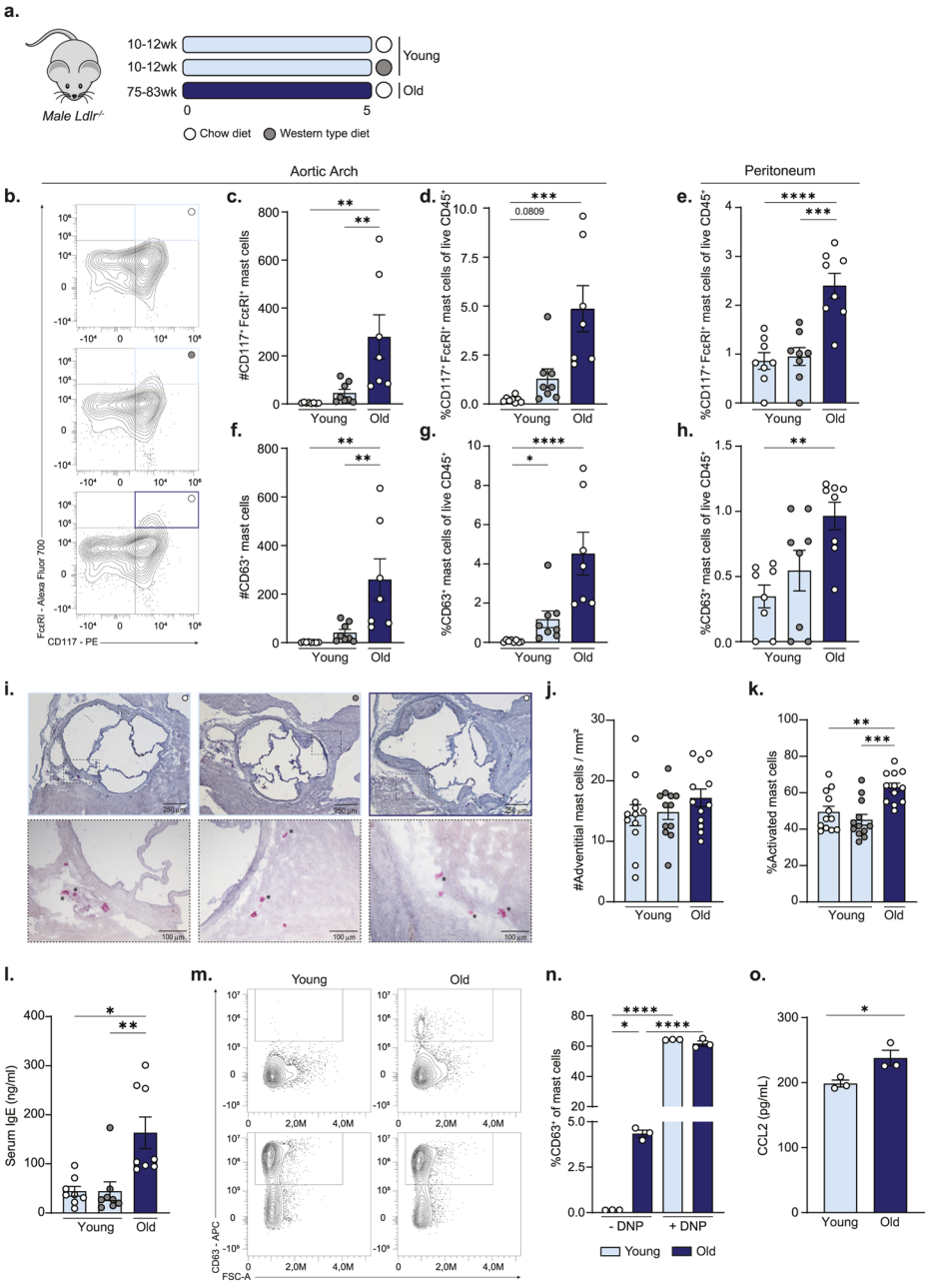
a.
Male Ldlr-/-
10-12wk
10-12wk
75-83wk
Young
Old
0
5
Chow diet
Western type diet
Aortic Arch
Peritoneum
b.
FcεRI - Alexa Fluor 700
CD117 - PE
c.
#CD117+ FcεRI+ mast cells
d.
%CD117+ FcεRI+ mast cells of live CD45+
0.0809
e.
%CD117+ FcεRI+ mast cells of live CD45+
f.
#CD63+ mast cells
g.
%CD63+ mast cells of live CD45+
h.
%CD63+ mast cells of live CD45+
Young
Old
i.
j.
#Adventitial mast cells / mm²
k.
%Activated mast cells
l.
Serum IgE (ng/ml)
m.
Young
Old
CD63 - APC
FSC-A
n.
%CD63+ of mast cells
- DNP
+ DNP
o.
CCL2 (pg/mL)

◂ **Figure 1. Age-induced accumulation of activated mast cells in the atherosclerotic aorta. a.** Experimental set-up: young 10-12 weeks old (light blue bars) and old 75-83 weeks old (dark blue bars) male *Ldlr*$^{-/-}$ mice were fed a chow diet (white dots) or western type diet (grey dots) for 5 weeks. **b.** Flow cytometry was used to detect the **c.** absolute number and **d.** percentage of mast cells of live CD45^{+} cells in the aortic arch and **e.** the peritoneal cavity. Mast cell activation was investigated by flow cytometric analysis of CD63. **f.** the absolute number of CD63^{+} mast cells in the aortic arch and the percentage of CD63^{+} mast cells within live CD45^{+} leukocytes was quantified in **g.** the aortic arch and **h.** the peritoneal cavity. **i.** Mast cells were stained with a napthol AS-D choloroacetate staining. **j.** The total number of mast cells per mm^{2} and **k.** the percentage of activated mast cells in the aortic root were quantified. **e.** Representative images of flow cytometry analysis of CD117^{+}FcεRI^{+} mast cells in the aortic arch. **l.** Total IgE concentrations were measured in the serum. **m.** Bone-marrow derived mast cells from young and old *Ldlr*$^{-/-}$ mice were stimulated *in vitro* stimulation with anti-IgE DNP and analyzed with flow cytometry. **n.** Activation was quantified by means of CD63 expression on live CD117^{+}FcεRI^{+} mast cells. **o.** CCL2 secretion by stimulated mast cells was detected with legendplex analysis. All representative pictures are taken at optical magnification 5x (top) and 20x (bottom); the bar indicates 250 μm (top) and 100 μm (bottom); asterix indicates activated mast cell. n = 7-8 per group for flow cytometry analysis, n=12 per group for histological analysis and n=3 per group for *in vitro* assays. Data represent mean ± SEM.

The age-associated mast cell phenotype is lost in a young atherosclerotic micro-environment

Next, we aimed to examine if the age-related intrinsic changes of mast cells impact atherosclerosis progression or whether the aged micro-environment drives this proatherogenic phenotype. Therefore, we adoptively transferred BMMCs derived from young versus aged *Ldlr*$^{-/-}$ mice into young mast cell deficient *apoE*$^{-/-}$*Kit*$^{W\text{-}sh/W\text{-}sh}$ mice (**Fig. 3a**). Both young (MC_Y) and aged (MC_O) mast cells were detected in similar levels in the peritoneal cavity of the acceptor mice (**Fig. 3b**), demonstrating equal repopulation efficiency. No differences were observed in the percentage of CD63^{+} and of MHC-II^{+} peritoneal mast cells between the groups (**Fig. 3c, d**), already indicating that the age-associated mast cell phenotype as described above is lost in a young micro-environment. As aged activated mast cells *in vitro* secreted more CCL2, a chemokine involved in monocyte recruitment towards the atherosclerotic plaque[22], the percentage of CD11b^{+}F4/80^{+} macrophages was measured in the peritoneal cavity, which were similar between both groups (**Fig. 3e**). Also, the percentage of CD4^{+} T cells did not differ in both the peritoneum and the aortic arch, neither did the percentage of Ki67 expression on these CD4^{+} T cells, indicating that T cell proliferation was not affected (**Fig. 3f-i**). Finally, no differences in atherosclerotic plaque size (**Fig. 3j, k**), percentage vessel occlusion (**Fig. 3j, l**), collagen content (**Fig. 3m, n**) and necrotic core size (**Fig. 3m, o**) were observed. Together, these data indicate that the intrinsic phenotypic changes observed *in vitro*, do not maintain in a long-term *in vivo* setting and that the continued exposure to the aging microenvironment controls mast cell phenotype in atherosclerosis.

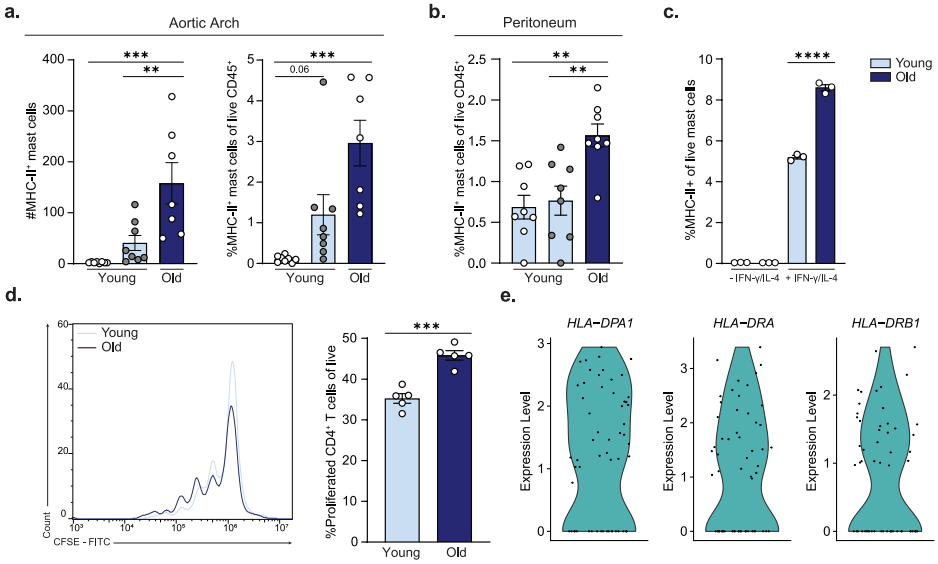

Figure 2. MHCII⁺ expression on aged mast cells induces increased CD4⁺ T cell proliferation. Flow cytometry was used to detect the **a.** absolute number and percentage of MHC-II mast cells of live CD45⁺ cells in the aortic arch and **b.** the peritoneal cavity. **c.** *In vitro* stimulation of young and old bone-marrow derived mast cells with IFN-γ and IL-4 induced MHC-II expression as measured and quantified by flow cytometry. **d.** To assess antigen presenting capacities of young and old bone-marrow derived mast cells, a co-culture was performed of IFN-γ and IL-4 stimulated mast cells with αCD3/αCD28-stimulated OT-II T cells with ovalbumin for 3 days. CD4⁺ T cell proliferation was measured by CFSE staining using flow cytometry. Proliferation was quantified as the percentage of CFSE⁻ CD4⁺ T cells of live cells. **e.** Single-cell RNA sequencing data of human carotid atherosclerotic plaques of 43 patients revealed expression of human MHC-II orthologs *HLA-DPA1*, *HLA-DRA* and *HLA-DRB1* in the mast cell cluster. n = 7-8 per group for flow cytometry analysis and n = 3-5 per group for *in vitro* assays. Data represent mean ± SEM.

Mast cell stabilization reduces the percentage of systemic effector T cells in aged mice

Based on these and our previous findings[21], we hypothesized that mast cells contribute to the local inflammatory environment in the plaque. To specifically address whether the aged mast cell impacts inflammation in the atherosclerotic plaque, we treated aged *Ldlr*$^{-/-}$ mice with a common mast cell stabilizer DSCG (**Fig. 4a**). DSCG treatment did not affect the percentage of mast cells in the aorta or the peritoneal cavity (**Fig. 4b, c; Supplemental Fig. 3b,c**), but did result in a 46% reduction in CD63 expression on peritoneal mast cells (Control: 32.4±4.6% vs. DSCG: 17.5±4.2%, $p<0.05$; **Fig. 4d**). Although the percentage CD63⁺ of mast cells was not affected in the atherosclerotic aorta (**Supplemental Fig. 3a**), a trend towards a decrease in the gMFI of CD63 within aortic mast cells was observed, suggesting that DSCG did affect the activation state of mast cells at the site of disease (**Fig. 4e**).

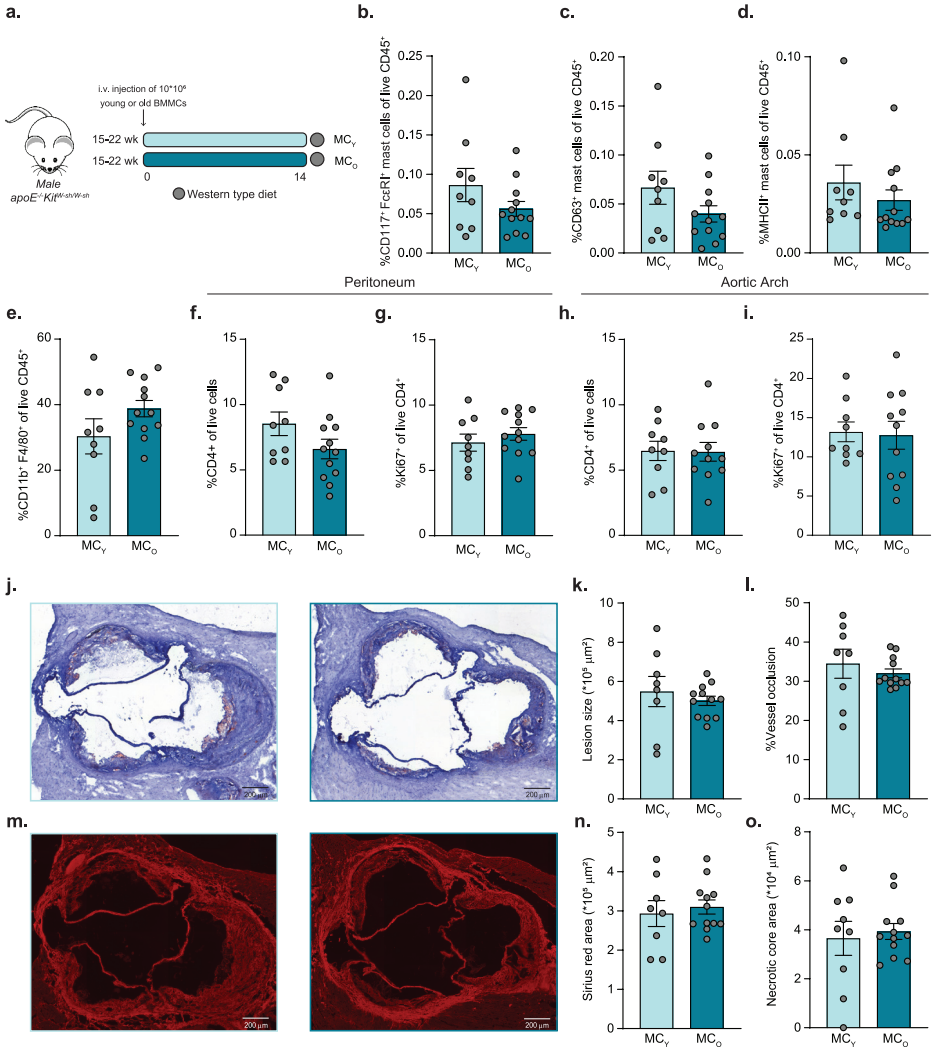
a.
b.
c.
d.
i.v. injection of 10*10⁶ young or old BMMCs
15-22 wk
15-22 wk
MCY
MCO
0
14
Western type diet
Male
apoE-/- KitW-sh/W-sh
%CD117+ FcεRI+ mast cells of live CD45+
%CD63+ mast cells of live CD45+
%MHCII+ mast cells of live CD45+
Peritoneum
Aortic Arch
e.
f.
g.
h.
i.
%CD11b+ F4/80+ of live CD45+
%CD4+ of live cells
%Ki67+ of live CD4+
%CD4+ of live cells
%Ki67+ of live CD4+
j.
k.
l.
m.
n.
o.
Lesion size (*10³ µm²)
%Vessel occlusion
Sirius red area (*10³ µm²)
Necrotic core area (*10⁴ µm²)
200 µm

◂ **Figure 3. Adoptive transfer of young and old mast cells does not alter atherosclerosis progression. a.** Experimental set up: $10*10^6$ young (MC_Y) and old (MC_O) bone marrow-derived mast cells were injected into young mast cell deficient *apoE*$^{-/-}$*Kit*$^{W\text{-}sh/W\text{-}sh}$ mice and simultaneously a western type diet (grey dots) was started for 14 weeks until sacrifice. **b.** Using flow cytometry, reconstitution of mast cells was assessed by measuring CD117$^+$FcεRI$^+$ mast cells of live cells in the peritoneum. **c.** Activation by means of the percentage of CD63$^+$ mast cells of live CD45$^+$ and **d.** antigen presenting capacities by means of the percentage of MHC-II$^+$ mast cells of live CD45$^+$ was quantified in the peritoneum by flow cytometry. **e.** The percentage of CD11b$^+$F4/80$^+$ peritoneal macrophages of live CD45$^+$ was quantified. Subsequently, the percentage of total CD4$^+$ and proliferating Ki67$^+$CD4$^+$ was measured by flow cytometry in respectively the peritoneum (**f., g.**) and the aortic arch (**h., i.**). **j.** Atherosclerotic plaques in the aortic root were stained by Oil Red O staining to measure **k.** lesion size in μm^2 and **l.** the percentage of vessel occlusion. **m.** Atherosclerotic plaque stability was examined by Sirius Red staining of the aortic root to identify the **n.** Sirius red stained collagen area in μm^2 and **o.** the necrotic core area in μm^2. All representative pictures are taken at optical magnification 5x; the bar indicates 200 μm. n = 9-12 per group. Data represent mean ± SEM.

Subsequently, we investigated whether this mast cell stabilization affected the systemic and local CD4$^+$ T cell content. No difference was detected in the total percentage of CD4$^+$ T cells in (**Supplemental Fig. 3b-d**), the percentage of proliferating CD4$^+$ T cells and the percentage of central memory CD4$^+$ T cells (CD44$^+$CD62L$^+$, **Fig. 5a, b**) in the organs analysed. However, a reduction was observed in circulating and splenic effector CD4$^+$ T cells with DSCG treatment (CD44$^+$CD62L$^+$, Blood: Control: 51.1±2.9% vs. DSCG: 39.5±2.5%, $p<0.05$; Spleen: Control: 58.0±3.0 vs. DSCG: 46.9±2.6%, $p<0.05$; **Fig. 5c**). Moreover, a trend towards a decrease was observed for regulatory T cells in both the spleen and the aortic arch (**Fig. 5d**). In the spleen, Th1 cells were also significantly lower in the DSCG treated group versus control (Control: 23.0±1.0 vs. DSCG: 17.7±1.4, $p<0.05$; **Fig. 5e**). No difference was observed in the percentage of MHCII$^+$ mast cells in respectively the peritoneum and the aortic arch with DSCG treatment (**Fig. 5f, g**). This suggests that the differences in CD4$^+$ T cell phenotype are not due to changes in direct antigen-presentation, but could be mediated by the pro-inflammatory mediators secreted by mast cells. While a 6-weeks DSCG treatment in aged *Ldlr*$^{-/-}$ mice was effective in reducing atherogenic CD4$^+$ T cell content, this did not translate into effects on the aged atherosclerotic plaque size (**Fig. 5h, i**), or morphology as measured by collagen and necrotic core content in this time-frame (**Fig. 5h-k**).

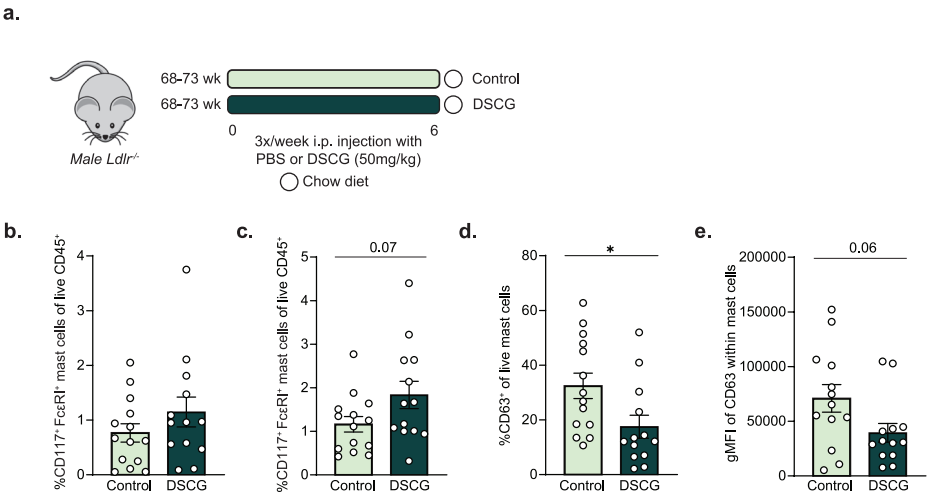

Figure 4. Treatment with DSCG reduces mast cell activation in aged mice. a. Experimental set-up: aged 68-73 weeks old mice were treated with DSCG (50mg/kg) of PBS control three times a week for six weeks. Mice were fed a chow diet (white dots) until sacrifice. Flow cytometry analysis was performed to examine the percentage of mast cells of live CD45$^+$ in **b.** the peritoneum and **c.** the aortic arch. Subsequently DSCG efficacy was examined by measuring **d.** the percentage of CD63$^+$ mast cells of live CD45$^+$ in the peritoneum and **e.** the geometric mean fluorescent intensity of CD63 on mast cells in the aortic arch. n = 13-14 per group. Data represent mean ± SEM.

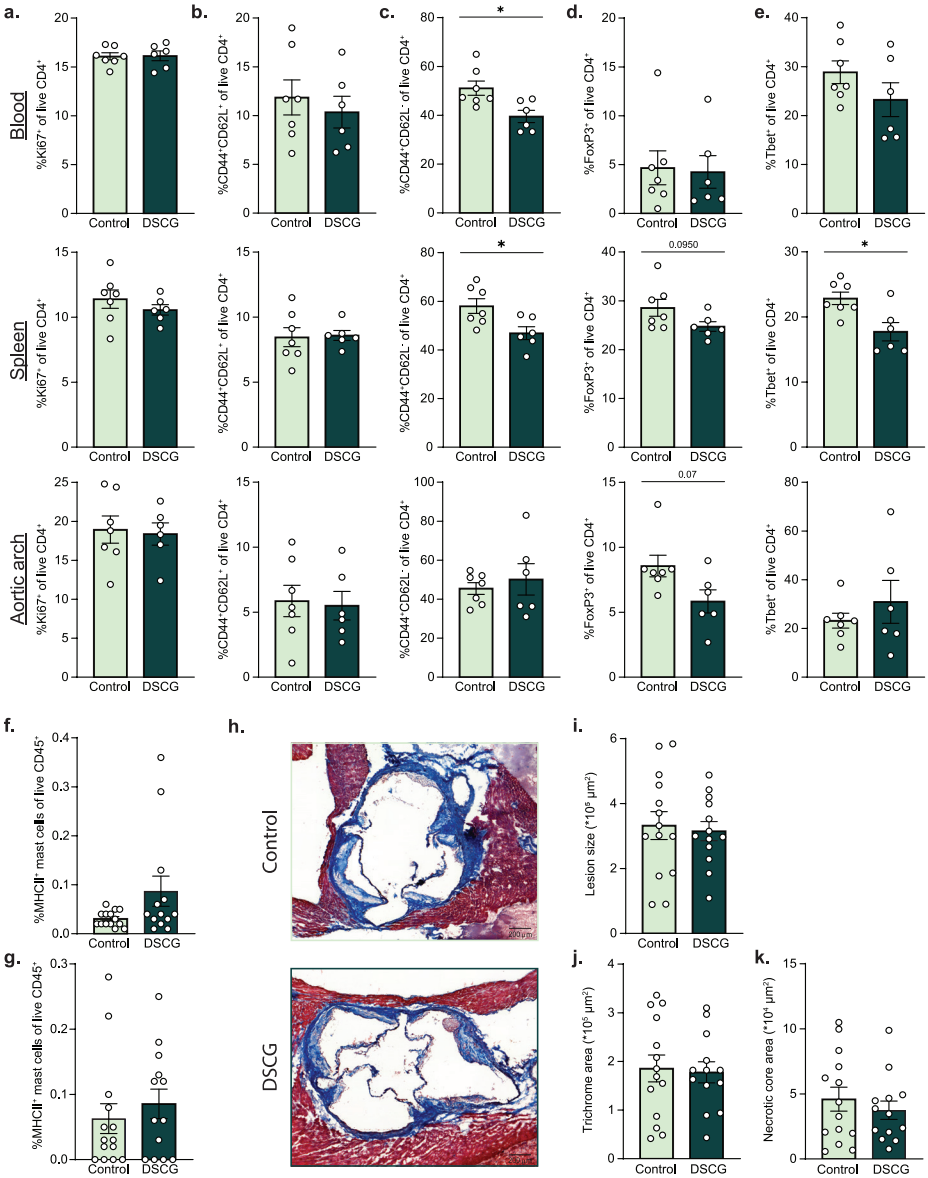
a.
b.
c.
d.
e.
Blood
Spleen
Aortic arch
%Ki67+ of live CD4+
%CD44+CD62L- of live CD4+
%FoxP3+ of live CD4+
%Tbet+ of live CD4+
Control
DSCG
*
0.0950
0.07
f.
g.
h.
i.
j.
k.
%MHCII+ mast cells of live CD45+
Control
DSCG
Lesion size (*10⁶ µm²)
Trichrome area (*10⁵ µm²)
Necrotic core area (*10⁴ µm²)

◂ **Figure 5. Treatment with DSCG reduces effector CD4⁺ T cells but not atherosclerotic plaque size.** Flow cytometry analysis was performed on the blood, spleen and aortic arch to identify respectively the percentage of **a.** Ki67⁺, **b.** CD44⁺CD62L⁺, **c.** CD44⁺CD62L⁻, **d.** Foxp3⁺ and **e.** Tbet⁺ of live CD4⁺ (all vertical). The percentage of MHC-II⁺ mast cells of live CD45⁺ was identified in **f.** the peritoneum and **g.** the aortic arch. **h.** Atherosclerotic plaques in the aortic root were stained by Masson's Trichrome to measure **i.** lesion size in μm^2 and to examine plaque stability by measuring the **j.** trichrome stained collagen area in μm^2 and **k.** the necrotic core area in μm^2. All representative pictures are taken at optical magnification 5x; the bar indicates 200 μm. n = 6-7 per group for flow cytometry analysis and n = 13-14 per group for histological analysis. Data represent mean ± SEM.

Discussion

Aging is a prominent risk factor for the development of atherosclerosis amongst others due to the inflammaging-related proinflammatory environment it induces. Previously, age-associated changes in intraplaque immune cells have been described[16], yet whether age also affects mast cells remained elusive. In this study, we therefore aimed to examine age-induced phenotypic changes of mast cells in atherosclerosis. Here we show that the aged microenvironment promotes local accumulation of mast cells and its activation which subsequently affects local and systemic CD4⁺ T cell proliferation and phenotype.

Interestingly, mast cell accumulation has previously been reported to associate with aging and age-related disease. Increased mast cell numbers were detected in the aged skin[11,14], gut and brain[10], as well as the brain of Parkinson's disease patients.[23,24] Additionally, gut mast cell numbers further expanded after middle cerebral artery occlusion, which mimics stroke. In line, we describe an increase in the proportion of mast cells in the peritoneum and atherosclerotic aortic arch upon aging.

Besides increased numbers of mast cells in aged atherosclerosis, our data also show that they exert a predominantly activated phenotype both in the peritoneum and the atherosclerotic aortic arch. The effects of age on mast cell activation and degranulation are to date still rather contradictory and differ per tissue. Whereas mast cells surrounding the mesenteric lymphatic vessels showed a 400% increase in activation in resting mesenterium of aged mice, less degranulation was observed in the papillary dermis of old individuals.[11,15] Nevertheless, in cardiovascular disease serum tryptase levels have been found twice as high in patients with acute myocardial infarction versus unsubstantial coronary heart disease patients.[25] Furthermore, a significant correlation has been found between serum tryptase level and age in these patients. Congruently, when comparing patients with ST Segment Elevation Myocardial

Infarction (STEMI) with healthy controls a similar increase in serum tryptase was detected as well as a positive correlation with age.[26] Moreover, in human carotid atherosclerotic plaques, the vast majority of detected mast cells were positive for CD63.[27] These data further support the hypothesis that mast cells have an increased activated phenotype in aged cardiovascular disease patients. A possible explanation for the activated mast cell phenotype in atherosclerosis could be an increase in activation via the IgE-FcεR-pathway. Serum IgE levels are generally described to be associated to cardiovascular disease and[28] we previously found the majority of the activated human intraplaque mast cells to have IgE bound to the surface. In addition, elevated levels of IgE sensitive to α-Gal were positively correlated with increased atheroma burden and an unstable plaque phenotype.[27,29] In this study, we observed an elevated serum IgE concentration in aged *Ldlr*$^{-/-}$ mice as well, together suggesting a prominent role for the IgE-FcεRI mediated pathway of activation.

Although we detected intrinsic changes in mast cell activation using BMMCs from aged mice, this did not sustain upon adoptive transfer in young mast cell deficient *apoE*$^{-/-}$*Kit*$^{W\text{-}sh/W\text{-}sh}$ mice. Mast cell phenotype can be altered by the local cytokine content.[30–34] Hereto, the inflammaging could indeed induce phenotypic changes, not only by the pro-inflammatory cytokines, but also due to interactions with neighboring aged immune cells. Indeed, our data emphasize the importance of the aging microenvironment on mast cell phenotype in atherosclerosis.

Recently, a prominent role for CD4$^+$ T cells in atherosclerosis has been proposed by reporting a plaque-specific clonal expansion suggesting that atherosclerosis has autoimmune-like components.[35] These CD4$^+$ T cells can be activated via interaction with classical antigen-presenting cells, including dendritic cells and macrophages. However, mast cells act as atypical antigen-presenting cells as well.[19] Gaudenzio *et al*. showed that in the skin of psoriasis patients, mast cells were observed in close contact with CD4$^+$ T cells.[36] Furthermore, in a murine model of multiple sclerosis, a reduction of CD44 expression as well as reduced T cell infiltration in the central nervous system was observed upon mast cell depletion.[37] In the context of atherosclerosis, previous work of our lab not only showed that hyperlipidemic serum upregulated MHC-II expression on mast cells, but that these mast cells were also capable of antigen presentation *in vivo* and that mast cell deficiency significantly reduced CD4$^+$ T cell proliferation in the atherosclerotic aorta.[21] Since we established an increased number of MHC-II$^+$ mast cells in the aged atherosclerotic aorta, we sought to examine whether this could affect the intraplaque CD4$^+$ T cells as well. Indeed, we observed increased CD4$^+$ T cell proliferation, indicating that the aged MHC-II$^+$ mast cells were capable of direct antigen presentation. Moreover, this *in vitro* assay also presented

evidence that mast cells are able to internalize ovalbumin and present it to $CD4^+$ T cells. This aligns with previous work reporting that mast cells are capable of IFN-γ independent uptake of soluble and particulate antigens.[38] Additionally, they state that mast cell degranulation increases surface delivery of antigen to the MHC-II molecule, further enhancing $CD4^+$ T cell proliferation. *In vivo*, however, upregulation of MHC-II is probably dependent on the aged microenvironment in which the mast cell resides, since with adoptive transfer this phenotype and effect on $CD4^+$ T cell proliferation was lost. Nevertheless, this implies that the expression of human orthologs of MHC-II on human intraplaque mast cells could thus contribute to $CD4^+$ T cell proliferation in the human atherosclerotic lesion of aged CVD patients.

Although direct antigen presentation by mast cells likely occurs in the plaque, we hypothesized that the pro-inflammatory cytokines secreted by activated mast cells could even have more impact on $CD4^+$ T cell proliferation during disease development. Indeed, mast cells have been described to affect T cell migration and polarization by their cytokine secretion upon activation.[39] By using the mast cell stabilizer DSCG as tool to inhibit degranulation, we could subsequently investigate the contribution of the mast cell secretome on $CD4^+$ T cell proliferation and phenotype in aged atherosclerotic mice. Although we did not find differences in $CD4^+$ T cell proliferation, we do report reduced systemic and intraplaque effector $CD4^+$ T cells as a consequence of reduced mast cell activation. Furthermore, particularly $FoxP3^+$ and $Tbet^+$ $CD4^+$ T cells were reduced by mast cell stabilization. Correspondingly, mast cells have been described to play a crucial role in the migration of tolerogenic dendritic cells as well as priming dendritic cells to promote subsequent Th1 and Th17 responses.[39–41] This suggest that the pro-inflammatory cytokines secreted by mast cells indeed affects $CD4^+$ T cell phenotype in atherosclerosis, yet further functional studies will be necessary to confirm this hypothesis.

To conclude, we report an age-induced accumulation of activated mast cells in the atherosclerotic plaque. Moreover, we demonstrate that mast cells contribute to intraplaque $CD4^+$ T cell proliferation and differentiation and emphasize how these changes are dependent on the aged microenvironment. It is thus of great importance to consider age in future research targeting mast cells, and other immune cells, in the development of new treatments for atherosclerosis.

Funding

This work was supported by the Dutch Heart Foundation (grant number 2018T051 to ACF), and the European Research Area Network on Cardiovascular Diseases (ERA-CVD) B-eatATHERO consortium (to ACF). IB is an Established Investigator of the Dutch Heart Foundation (2019T067). M.A.C.D., B.S., J.K., I.B. are supported by the

Dutch Heart Foundation (Generating the best evidence-based pharmaceutical targets and drugs for atherosclerosis (GENIUS II); grant number CVON2017-20). M.A.C.D., I.B., J.K. are supported by the NWO-ZonMW (PTO program grant number 95105013).

Disclosures

The authors have no conflicts of interest to disclose.

References

1. Libby, P. *et al.* Atherosclerosis. *Nature Reviews Disease Primers 2019 5:1* **5**, 1–18 (2019).
2. Krishnaswamy, G., Ajitawi, O. & Chi, D. S. The human mast cell: an overview. *Methods Mol Biol* **315**, 13–34 (2006).
3. Valent, P. *et al.* Mast cells as a unique hematopoietic lineage and cell system: From Paul Ehrlich's visions to precision medicine concepts. *Theranostics* **10**, 10743–10768 (2020).
4. Bot, I. *et al.* Perivascular mast cells promote atherogenesis and induce plaque destabilization in apolipoprotein E-deficient mice. *Circulation* **115**, 2516–2525 (2007).
5. Sun, J. *et al.* Mast cells promote atherosclerosis by releasing proinflammatory cytokines. *Nat Med* **13**, 719–724 (2007).
6. Willems, S. *et al.* Mast cells in human carotid atherosclerotic plaques are associated with intraplaque microvessel density and the occurrence of future cardiovascular events. *Eur Heart J* **34**, 3699–3706 (2013).
7. Niccoli, T. & Partridge, L. Ageing as a risk factor for disease. *Curr Biol* **22**, (2012).
8. Ho, Y. H. *et al.* Remodeling of Bone Marrow Hematopoietic Stem Cell Niches Promotes Myeloid Cell Expansion during Premature or Physiological Aging. *Cell Stem Cell* **25**, 407-418.e6 (2019).
9. Kutukova, N. A., Nazarov, P. G., Kudryavtseva, G. V. & Shishkin, V. I. Mast cells and aging. *Advances in Gerontology* **7**, 68–75 (2017).
10. Blasco, M. P. *et al.* Age-dependent involvement of gut mast cells and histamine in post-stroke inflammation. *J Neuroinflammation* **17**, (2020).
11. Pilkington, S. M., Barron, M. J., Watson, R. E. B., Griffiths, C. E. M. & Bulfone-Paus, S. Aged human skin accumulates mast cells with altered functionality that localize to macrophages and vasoactive intestinal peptide-positive nerve fibres. *Br J Dermatol* **180**, 849–858 (2019).
12. Verhoeven, B. A. N. *et al.* Athero-express: Differential atherosclerotic plaque expression of mRNA and protein in relation to cardiovascular events and patient characteristics. Rationale and design. *Eur J Epidemiol* **19**, 1127–1133 (2004).
13. Depuydt, M. A. C. *et al.* Microanatomy of the Human Atherosclerotic Plaque by Single-Cell Transcriptomics. *Circ Res* **127**, 1437–1455 (2020).
14. Gunin, A. G., Kornilova, N. K., Vasilieva, O. V. & Petrov, V. V. Age-related changes in proliferation, the numbers of mast cells, eosinophils, and cd45-positive cells in human dermis. *J Gerontol A Biol Sci Med Sci* **66**, 385–392 (2011).
15. Chatterjee, V. & Gashev, A. A. Aging-associated shifts in functional status of mast cells located by adult and aged mesenteric lymphatic vessels. *Am J Physiol Heart Circ Physiol* **303**, (2012).
16. Smit, V. *et al.* Single-cell profiling reveals age-associated immunity in atherosclerosis. *Cardiovasc Res* (2023) doi:10.1093/CVR/CVAD099.
17. Orinska, Z., Hagemann, P. M., Halova, I. & Draber, P. Tetraspanins in the regulation of mast cell function. *Med Microbiol Immunol* **209**, 531–543 (2020).
18. Bot, I., Shi, G. P. & Kovanen, P. T. Mast cells as effectors in atherosclerosis. *Arterioscler Thromb Vasc Biol* **35**, 265 (2015).
19. Kambayashi, T. & Laufer, T. M. Atypical MHC class II-expressing antigen-presenting cells: can anything replace a dendritic cell? *Nature Reviews Immunology 2014 14:11* **14**, 719–730 (2014).
20. Gaudenzio, N. *et al.* Cell-cell cooperation at the T helper cell/mast cell immunological synapse. *Blood* **114**, 4979–4988 (2009).

21. Kritikou, E. *et al.* Hypercholesterolemia Induces a Mast Cell-CD4+ T Cell Interaction in Atherosclerosis. *J Immunol* **202**, 1531–1539 (2019).
22. Kim, K. W., Ivanov, S. & Williams, J. W. Monocyte Recruitment, Specification, and Function in Atherosclerosis. *Cells* **10**, (2021).
23. Kempuraj, D. *et al.* Mast Cell Proteases Activate Astrocytes and Glia-Neurons and Release Interleukin-33 by Activating p38 and ERK1/2 MAPKs and NF-κB. *Mol Neurobiol* **56**, 1681–1693 (2019).
24. Zhang, X. *et al.* Immune Profiling of Parkinson's Disease Revealed Its Association With a Subset of Infiltrating Cells and Signature Genes. *Front Aging Neurosci* **13**, (2021).
25. Xiang, M. *et al.* Usefulness of serum tryptase level as an independent biomarker for coronary plaque instability in a Chinese population. *Atherosclerosis* **215**, 494–499 (2011).
26. Lewicki, L. *et al.* Elevated Serum Tryptase and Endothelin in Patients with ST Segment Elevation Myocardial Infarction: Preliminary Report. *Mediators Inflamm* **2015**, (2015).
27. Kritikou, E. *et al.* Flow Cytometry-Based Characterization of Mast Cells in Human Atherosclerosis. *Cells* **8**, (2019).
28. Kounis, N. G. & Hahalis, G. Serum IgE levels in coronary artery disease. *Atherosclerosis* **251**, 498–500 (2016).
29. Wilson, J. M. *et al.* IgE to the Mammalian Oligosaccharide Galactose-α-1,3-Galactose Is Associated With Increased Atheroma Volume and Plaques With Unstable Characteristics-Brief Report. *Arterioscler Thromb Vasc Biol* **38**, 1665–1669 (2018).
30. da Silva, E. Z. M., Jamur, M. C. & Oliver, C. Mast cell function: a new vision of an old cell. *J Histochem Cytochem* **62**, 698–738 (2014).
31. Galli, S. J. *et al.* Mast cells as 'tunable' effector and immunoregulatory cells: recent advances. *Annu Rev Immunol* **23**, 749–786 (2005).
32. Reber, L. L., Sibilano, R., Mukai, K. & Galli, S. J. Potential effector and immunoregulatory functions of mast cells in mucosal immunity. *Mucosal Immunol* **8**, 444–463 (2015).
33. Franceschi, C., Garagnani, P., Parini, P., Giuliani, C. & Santoro, A. Inflammaging: a new immune-metabolic viewpoint for age-related diseases. *Nat Rev Endocrinol* **14**, 576–590 (2018).
34. Tan, Q., Liang, N., Zhang, X. & Li, J. Dynamic Aging: Channeled Through Microenvironment. *Front Physiol* **12**, (2021).
35. Depuydt, M. A. C. *et al.* Single-cell T cell receptor sequencing of paired human atherosclerotic plaques and blood reveals autoimmune-like features of expanded effector T cells. *Nature Cardiovascular Research 2023 2:2* **2**, 112–125 (2023).
36. Gaudenzio, N., Laurent, C., Valitutti, S. & Espinosa, E. Human mast cells drive memory CD4+ T cells toward an inflammatory IL-22+ phenotype. *J Allergy Clin Immunol* **131**, (2013).
37. Gregory, G. D., Robbie-Ryan, M., Secor, V. H., Sabatino, J. J. & Brown, M. A. Mast cells are required for optimal autoreactive T cell responses in a murine model of multiple sclerosis. *Eur J Immunol* **35**, 3478–3486 (2005).
38. Lotfi-Emran, S. *et al.* Human mast cells present antigen to autologous CD4+ T cells. *J Allergy Clin Immunol* **141**, 311-321.e10 (2018).
39. Bulfone-Paus, S. & Bahri, R. Mast Cells as Regulators of T Cell Responses. *Front Immunol* **6**, (2015).
40. de Vries, V. C. *et al.* Mast cells condition dendritic cells to mediate allograft tolerance. *Immunity* **35**, 550–561 (2011).
41. Morita, H., Saito, H., Matsumoto, K. & Nakae, S. Regulatory roles of mast cells in immune responses. *Semin Immunopathol* **38**, 623–629 (2016).

Supplemental Figures

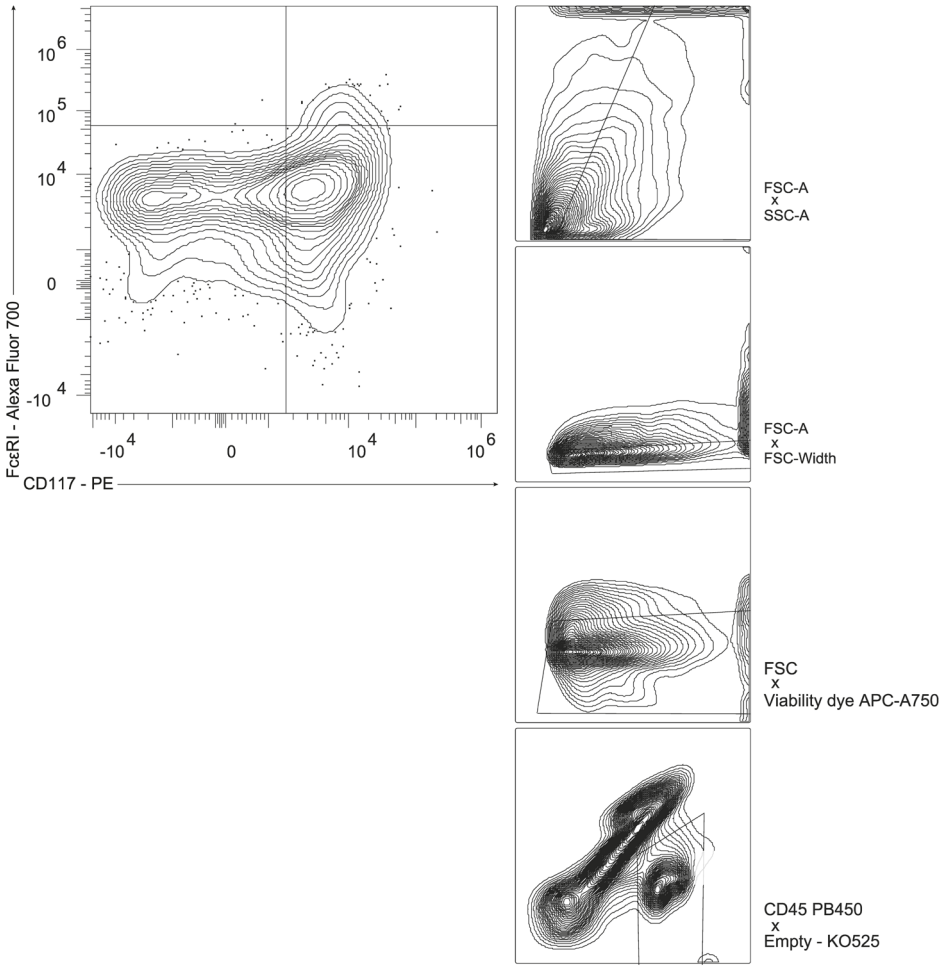

Supplemental figure 1. Gating strategy of mast cells in the aortic arch. First cells were selected (FSC-A x SSC-A), singlets were gated (FSC-A x FSC-W). Subsequently live cells were gated as Viability Dye negative population of singlets. CD45^{+} cells were isolated by gating against an empty channel. Finally CD117^{+}FcεRI^{+} cells were gated as mast cells for the analysis.

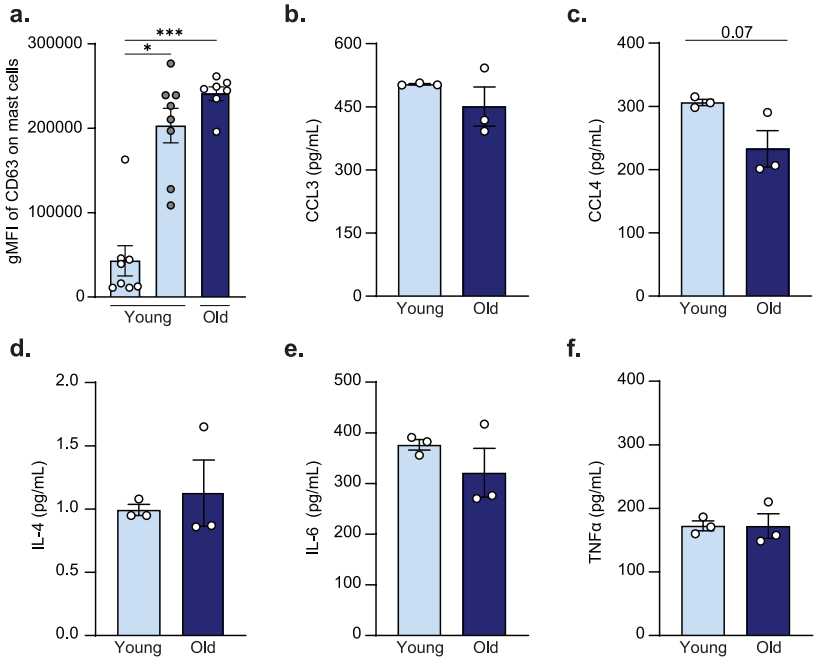

Supplemental figure 2. Increase in gMFI of CD63⁺ on mast cells with both WD and age in the atherosclerotic aorta. a. Flow cytometric analysis of the gMFI of CD63⁺ mast cells of live CD45⁺ in the aortic arch. Legendplex analysis of the supernatant of *in vitro* IgE-DNP stimulated young and old bone marrow-derived mast cells measuring the concentration of **b.** CCL3, **c.** CCL4, **d.** IL-4**, e.** IL-6 and **f.** TNFα in pg/mL. n = 7-8 for flow cytometry data. n = 3 for *in vitro* analysis. Data represent mean ± SEM.

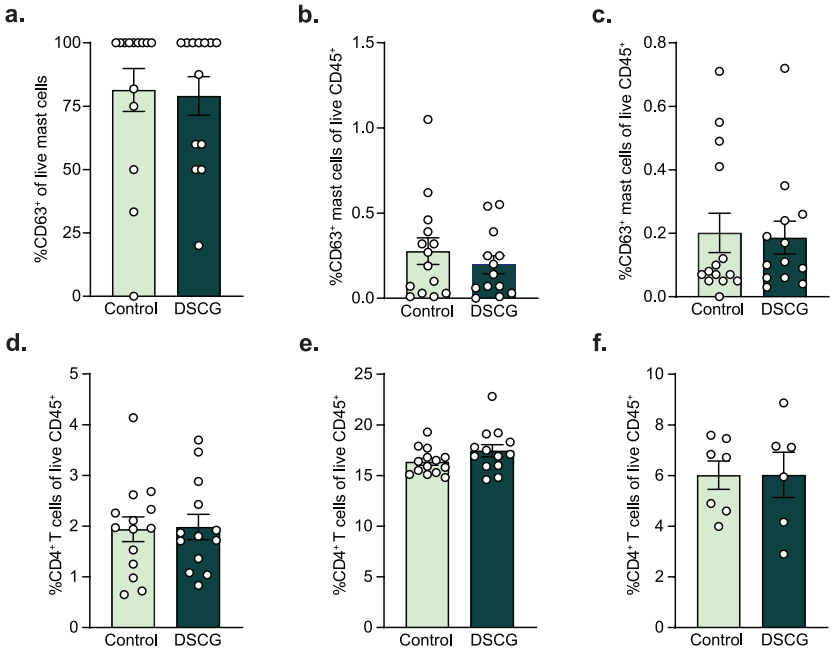

Supplemental figure 3. No difference in the percentage of CD63⁺ mast cells of live CD45⁺ in the peritoneum and aortic arch. a. Flow cytometry analysis of the percentage of CD63⁺ of live mast cells in the aortic arch. No difference was observed in the percentage of CD63⁺ mast cells of live CD45⁺ in both **b.** the peritoneum and **c.** the aortic arch with flow cytometry. Furthermore, the percentage of total CD4⁺ T cells of live CD45⁺ was measured in respectively **d.** the blood, **e.** the spleen and **f.** the aortic arch. n = 13-14 per group for flow cytometry analysis. n = 6-7 per group for CD4⁺ T cell analysis in the aortic arch. Data represent mean ± SEM.

Chapter 7

Blockade of the BLT1-LTB4 axis does not affect mast cell migration towards advanced atherosclerotic lesions in LDLr-/- mice.

Scientific Reports 2022; 12, 18362

Marie A.C. Depuydt[1], Femke D. Vlaswinkel[1], Esmeralda Hemme[1], Lucie Delfos[1], Mireia N.A. Bernabé Kleijn[1], Peter J. van Santbrink[1], Amanda C. Foks[1], Bram Slütter[1], Johan Kuiper[1] and Ilze Bot[1]

1 Division of BioTherapeutics, Leiden Academic Centre for Drug Research, Leiden University, 2333 CC, Leiden, The Netherlands

Abstract

Mast cells have been associated with the progression and destabilization of advanced atherosclerotic plaques. Reducing intraplaque mast cell accumulation upon atherosclerosis progression could be a potent therapeutic strategy to limit plaque destabilization. Leukotriene B_4 (LTB_4) has been reported to induce mast cell chemotaxis *in vitro*. Here, we examined whether antagonism of the LTB_4-receptor BLT1 could inhibit mast cell accumulation in advanced atherosclerosis.

Expression of genes involved in LTB_4 biosynthesis was determined by single-cell RNA sequencing of human atherosclerotic plaques. Subsequently, Western-type diet fed $LDLr^{-/-}$ mice with pre-existing atherosclerosis were treated with the BLT1-antagonist CP105,696 or vehicle control three times per week by oral gavage. In spleen, a significant reduction in $CD11b^{+}$ myeloid cells was observed, including $Ly6C^{lo}$ and $Ly6C^{hi}$ monocytes as well as dendritic cells. However, atherosclerotic plaque size, collagen and macrophage content in the aortic root remained unaltered upon treatment. Finally, BLT1 antagonism did not affect mast cell numbers in the aortic root.

Here, we show that human intraplaque leukocytes may be a source of locally produced LTB_4. However, BLT1 antagonism during atherosclerosis progression does not affect either local mast cell accumulation or plaque size, suggesting that other mechanisms participate in mast cell accumulation during atherosclerosis progression.

Keywords: Atherosclerosis; Immunology; Mast cell; Leukotriene B_4; Plaque instability

Introduction

The mast cell, a cell type of our innate immune system that acts in the first line of defence against pathogens, has been shown to promote the development and progression of atherosclerosis. Upon activation, mast cells secrete the proteases chymase and tryptase and pro-inflammatory cytokines such as IFN-γ, which have been shown to promote atherogenesis and to lead to destabilization of the plaque.[1,2] Systemic activation of mast cells in dinitrophenyl hapten (DNP)-challenged apolipoprotein E (apoE)$^{-/-}$ mice for example resulted in an increased plaque size and incidence of intraplaque haemorrhage[1], whereas mast cell deficiency was shown to reduce atherosclerotic plaque development.[2,3] In humans, mast cells have been shown to accumulate in advanced and ruptured coronary plaques.[4] More recently, the association of mast cells with disease progression in cardiovascular disease patients was established, as significantly increased serum tryptase levels were observed in patients with acute coronary syndromes[5] and intraplaque mast cell numbers were seen to increase upon atherosclerotic plaque destabilization.[6] In addition, in that study an independent association of intraplaque mast cell numbers in carotid plaques with the incidence of clinical cardiovascular events was revealed.[6] In patients with systemic mastocytosis, a disease characterized by the accumulation of mast cells in different organs, the prevalence of cardiovascular events was increased, despite a reduction in circulating low density lipoprotein levels.[7] Together, the contribution of mast cells and their activation to atherosclerosis has been well established as has also been reviewed[8,9], however it remains elusive what factors contribute to mast cell migration towards these plaques.

Apart from various chemokines and cytokines that have been implicated in mast cell migration, lipid mediators have been described to provoke a chemotactic response in mast cells.[10,11] Leukotriene B_4 (LTB_4) is a pro-inflammatory lipid mediator well known for its chemotactic effect on myeloid and lymphoid cells.[12] Intracellular biosynthesis of LTB_4 occurs in a two-step enzymatic reaction in which arachidonic acid is metabolized by 5-lipoxygenase (5-LOX), 5-lipoxygenase activating protein (FLAP) and LTA_4 hydrolase (LTA_4H).[13] Monocytes, macrophages and mast cells are able to release LTB_4 in response to stimulation with factors such as Complement component 5a (C5a), Interleukin-1 (IL-1), Leukemia Inhibitory Factor (LIF) and Tumor Necrosis Factor α (TNFα).[14] Synthesis and subsequent release of LTB_4 by these leukocytes will elicit a directed migration of vascular smooth muscle cells, neutrophils, eosinophils, basophils, monocytes, macrophages, dendritic cells and T cells but also of mast cell progenitors through binding with its receptor BLT1[14-20]. Previous *in vitro* studies showed an autocrine manner of mast cell migration towards LTB_4, which mainly recruits mast cell progenitors from the bone marrow as BLT1 expression is significantly reduced upon mast cell maturation.[19]

LTB_4 and its associated mediators have been suggested to participate in atherogenesis. Heterozygous deficiency of 5-LOX for example resulted in a 95%-decrease in lesion size in Low Density Lipoprotein receptor $(LDLr)^{-/-}$ mice.[21] Moreover, BLT1 deficiency in $apoE^{-/-}$ mice resulted in decreased plaque development.[15,22] Aiello *et al.* showed that antagonism of BLT1 through CP105,696 caused a decrease in the infiltration of monocytes into the lesions as well as reduced monocyte activation.[23] In these studies however, the authors primarily assessed initial lesion development and the number of mast cells in these lesions was not assessed.

As mast cell numbers particularly accumulate in advanced atheromatous human plaques, it may be of therapeutic interest to identify whether the LTB_4-BLT1 axis is involved in mast cell recruitment to advanced atherosclerosis. In our study, we thus first aimed to determine whether cells in the advanced plaque are able to produce LTB_4 and next investigated whether LTB_4 participates in the chemotaxis of mast cells towards pre-established atherosclerotic plaques and would thereby contribute to further progression of the disease. Here, we administered the BLT1-antagonist CP105,696 to $LDLr^{-/-}$ mice with pre-existing atherosclerosis and analysed its effect on plaque progression. In this study, treatment with CP105,696 resulted in reduced splenic myeloid cell content, but did not affect plaque morphology and mast cell accumulation in advanced atherosclerosis.

Results

Single cell RNA sequencing reveals expression of ALOX5 on human plaque mast cells

Blockade of mast cell recruitment to atherosclerotic lesions may be a promising intervention target to reduce plaque destabilization. Mast cells have previously been described to be involved in their own recruitment,[11,24] in which LTB_4 can act as an autocrine chemoattractant in multiple diseases.[19,20,25,26] Moreover, transcriptome analysis of *ex vivo* skin mast cells using deep-CAGE sequencing revealed expression of *ALOX5* (5-LOX), *ALOX5AP* (FLAP) and *LTA4H* (LTA_4H), the rate-limiting enzymes needed for biosynthesis of LTB_4.[27] Yet, it remains unknown whether plaque cells, among which mast cells, can produce LTB_4 in atherosclerotic lesions. In a previous study, we performed single-cell RNA sequencing on human atherosclerotic plaques obtained from carotid endarterectomy surgery from 18 patients.[28] Fourteen different cell clusters were found, of which one distinctly represented mast cells (cluster 13, **Figure 1A**). Within this data set, we analysed the expression of the aforementioned genes involved in LTB_4 biosynthesis. Indeed, we observed expression of *ALOX5*, *ALOX5AP* and *LTA4H* in several myeloid cell populations, including mast

cells, from human atherosclerotic plaques. Whereas *ALOX5AP* and *LTA4H* was ubiquitously expressed by all leukocytes, mast cells showed the highest expression of *ALOX5* (**Figure 1B**). To assess whether these genes are also expressed in murine atherosclerotic plaques, we examined a publicly available murine single-cell RNA sequencing data set by Cochain *et al*.[29] In this study, single-cell RNA sequencing was performed on CD45$^+$ cells isolated from aortas from LDLr$^{-/-}$ mice fed a chow diet, 11 weeks high fat diet and 20 weeks high fat diet, representing respectively the healthy aorta, early atherosclerotic and advanced atherosclerotic aortas. Integrating data from all three mouse models revealed 17 different clusters (**Figure S1A-B**). *Alox5*, *Alox5ap* and *Lta4h* were mainly found in the *Cd14*$^+$ *Cd68*$^+$ *Itgam*$^+$ myeloid cell clusters (**Figure S1C**). Therefore, we isolated all myeloid cells (clusters 0, 2, 3, 4, 6, 8, 13, 15 and 16) and examined whether expression of these three genes differed per plaque stage. *Alox5* was mainly expressed in myeloid cells of healthy aorta's compared to atherosclerotic aorta's (**Figure S1D**). Expression of *Alox5ap* and *Lta4h* showed no differences between plaque stages. Finally, we confirmed the expression of *Alox5*, *Alox5ap* and *Lta4h* in murine bone-marrow derived mast cells (BMMCs) (**Figure 1C**). Together, these data imply that LTB_4 can be produced locally in the plaque and that intraplaque mast cells may be its main source in the human plaque. We next aimed to determine whether blockade of the LTB_4 receptor affects mast cell migration towards the advanced atherosclerotic lesion.

CP105,696 treatment significantly lowers percentage of myeloid cells in the spleen

Next, we studied the effects of BLT1-antagonist CP105,696 treatment in our LDLr$^{-/-}$ mouse model with pre-existing atherosclerosis. CP105,696 treatment did not affect total body weight throughout the experiment (t=9 weeks, Control: 24.0±0.7 g vs. CP105,696: 23.9±0.5 g; **Figure 2A**). Serum total cholesterol levels were decreased in both groups during treatment (w5 vs. w9, Control: 1809.7±98.6 mg/dL vs. 1354.8±44.1 mg/dL, p = 0.0002 and CP105,696: 1866.2±92.2 mg/dL vs. 1351.9±42.7 mg/dL, p = 0.00002), but no differences were found between control and CP105,696 (**Figure 2B**). The decline in cholesterol level can be ascribed to the Tween 80 in the solvent as polysorbates were previously reported to induce cholesterol lowering.[30] No differences in serum triglyceride levels were detected (**Figure 2C**).

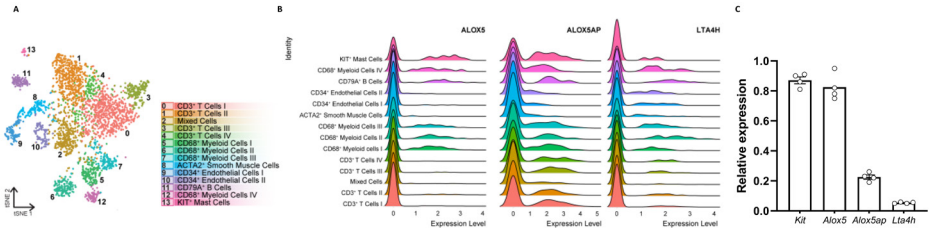

Figure 1. Expression of *ALOX5*, *ALOX5AP* and *LTA4H* in both human atherosclerotic plaque cells and murine bone-marrow derived mast cells. A) Single-cell RNA sequencing of human atherosclerotic plaque cells revealed 14 distinct cell clusters, including one mast cell cluster (cluster 13).[28] In these clusters, we measured the expression of B) *ALOX5, ALOX5AP* and *LTA4H*. C) Expression of *Kit*, *Alox5*, *Alox5ap* and *Lta4h* in murine bone-marrow derived mast cells. Human data n = 18; murine data: n = 4. Data represent mean ± SEM.

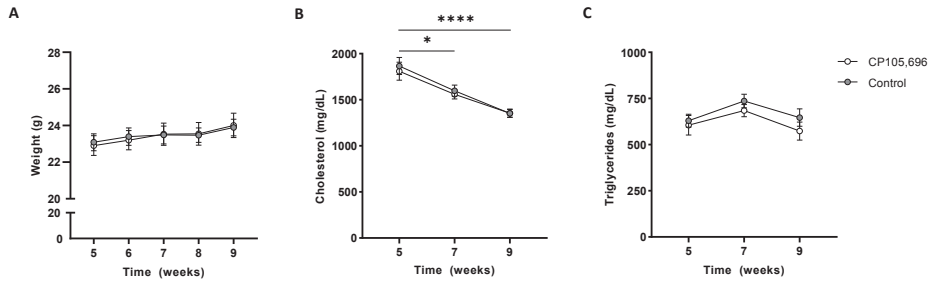

Figure 2. Body weight and plasma lipid levels upon CP105,696 treatment in *LDLr*$^{-/-}$ mice. A) Body weight of mice was measured weekly during treatment and was not affected by CP105,696 treatment. B) Plasma cholesterol and C) triglyceride concentrations were obtained at t=5, t=7 and t=9. *n* = 15 per group. Data represent mean ± SEM. **P*<0.05; *****P*<0.0001.

The BLT1-LTB$_4$ axis has previously been described to affect migration of multiple myeloid cells, including monocytes and dendritic cells.[31] To confirm that CP105,696 inhibited the BLT1 receptor *in vivo*, we used flow cytometry to measure myeloid subsets in blood and spleen. In the circulation, no differences were found in the total percentage of myeloid cells (CD11b$^+$; **Figure 3A**). The percentage of the different monocyte subtypes (CD11b$^+$Ly6C^{hi}, CD11b$^+$Ly6C^{mid} and CD11b$^+$Ly6C^{lo}) and of CD11b$^+$CD11c$^+$ cells, which predominantly characterize dendritic cells, also remained unaltered upon treatment (**Figure 3B-E**). In the spleen we observed a clear effect of treatment with the BLT1-antagonist. The percentage of total myeloid cells was significantly reduced upon treatment with CP105,696 (Control: 11.3±0.48% vs CP105,696: 9.4±0.56%; p = 0.016; **Figure 3F**). Both the percentage of inflammatory monocytes (Ly6C^{hi}; Control: 0.96±0.067% vs. CP105,696: 0.69±0.069%; p = 0.011; **Figure 3G, K**)

and that of the patrolling monocytes (Ly6C^{lo}; Control: 0.80±0.032 vs. CP105,696: 0.71±0.36; p = 0.07; **Figure 3I, K**) showed respectively a significant decrease and a trend towards a decrease after BLT1 inhibition, whereas Ly6C^{int} monocyte levels did not differ between groups (**Figure 3H, K**). Furthermore, we observed a reduced accumulation of CD11b^{+}CD11c^{+} dendritic cells in the spleen of treated mice (Control: 4.8±0.16 vs. CP105,696: 4.2±0.17; p = 0.016; **Figure 3J**).

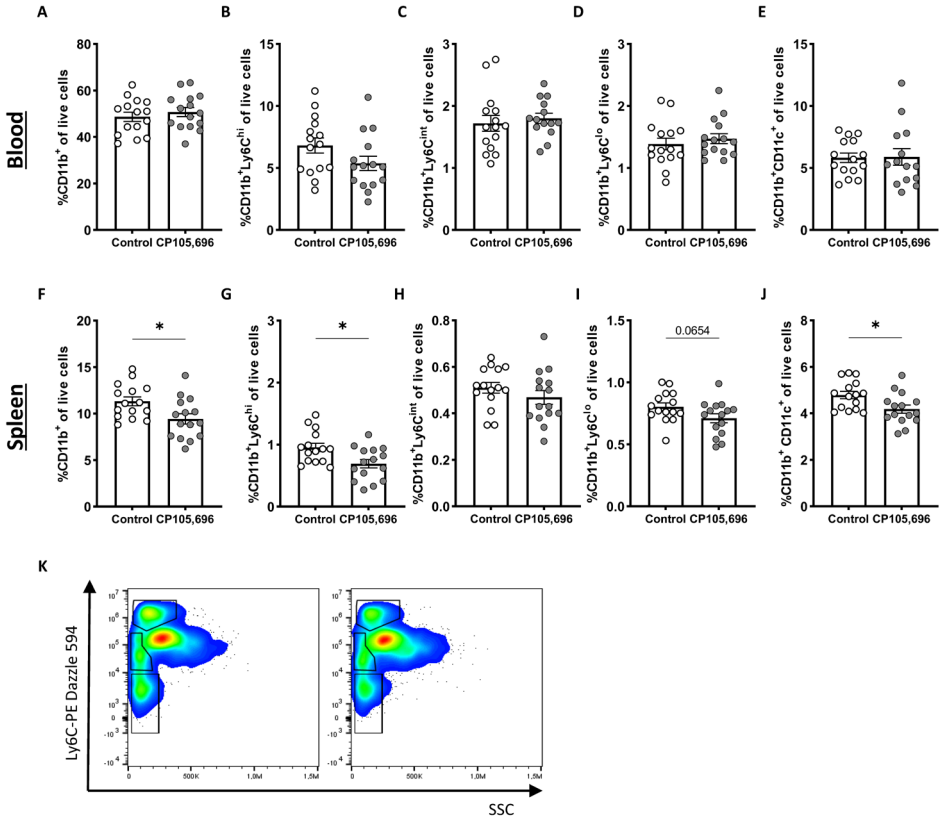

Figure 3. Myeloid cells significantly decreased with BLT1-antagonism in the spleen. Upon sacrifice, blood and spleen were collected and processed to obtain a single cell suspension for flow cytometry analysis. In the blood, the percentage of A) CD11b^{+} myeloid cells, B) Ly6C^{hi} monocytes, C) Ly6C^{int} monocytes, D) Ly6C^{lo} monocytes and E) CD11b^{+}CD11c^{+} dendritic cells was not different between the CP105,696 treated and the control group. In the spleen, a significant reduction in the percentage of F) CD11b^{+} myeloid cell content was found with CP105,696 treatment. Specifically, BLT1-antagonism resulted in a decrease in G) the percentage of CD11b^{+}Ly6C^{hi} monocytes, no difference in H) the percentage of CD11b^{+}Ly6C^{int} monocytes and I) a trend towards a decrease in the percentage of CD11b^{+}Ly6C^{lo} monocytes. J) Furthermore, we observed a significant decrease in the percentage of CD11b^{+} CD11c^{+} dendritic cells. K) Representative Flow Cytometry plot of monocytes in the spleen, left: control, right: CP105,696. *n* = 14-15 per group. Data represent mean ± SEM. *P<0.05.

Treatment with CP105,696 did not affect plaque progression in advanced atherosclerosis

Next, we assessed whether BLT1-antagonism affected the size and morphology of advanced lesions. CP105,696 treatment did not affect aortic root plaque area (Control: $3.7\pm0.3*10^5$ μm^2 vs. CP105,696: $3.9\pm0.2*10^5$ $\mu m2$; p = 0.60) and the percentage of Oil Red O staining in the plaque (Control: 34.5±3.3% vs. CP105,696: 32.3±5.1%; p = 0.18; **Figure 4A**). The degree of stenosis (Control: 36±2% vs. CP105,696: 39±1%; p = 0.233) as well as the total lesion area and plaque volume (Control: $1212\pm86*10^5$ μm^3 vs. CP105,696: $1264\pm64*10^5$ tm^3; p = 0.633) were unaltered by BLT1 antagonism (**Figure S3A-C).** We also examined collagen content and necrotic core size by Sirius Red staining. Both parameters did not change upon treatment with CP105,696 (**Figure 4B**). Furthermore, no differences in macrophage content were observed between the groups (**Figure 4C**). In addition, flow cytometry analysis of the atherosclerotic aortic arch did not reveal any differences in the percentage of live $CD45^+$ leukocytes of the single cell population and the percentage of total lymphocytes in the $CD45^+$ cell population (data not shown) between the groups. Also, the percentage of $CD11b^+$ myeloid cells and that of $CD11b^+CD11c^+$ dendritic cells in the $CD45^+$ cell population (**Figure S4A-C**) were not affected by CP105,696 treatment. Thus, BLT1-antagonism did not affect plaque morphology or myeloid cell content in a model of pre-existing atherosclerosis.

No difference in mast cell accumulation in the aortic root upon BLT1-antagonism

Subsequently, we aimed to investigate whether LTB_4 is a chemoattractant for the recruitment of mast cells towards the atherosclerotic plaque. We first assessed the percentage of mast cell progenitors (MCps) in blood and thereby examined whether BLT1-antagonism affected their migration. No differences were observed in $CD34^+Lin^-CD127^-CD16/32^+CD117^+FC\varepsilon RI^+$ MCps in blood between groups (Control: 0.010±0.002% vs. CP105,696: 0.012±0.002%; p = 0.34; **Figure 5A**). We also determined mast cell numbers in the aortic root of treated and non-treated mice. In line with the data on mast cell progenitors, no differences were found in total mast cell numbers (Control: 16.0±1.5 mast cells/mm^2 vs. CP105,696: 16.5±1.3 mast cells/mm^2; p = 0.80; **Figure 5B, D**) and in the percentage of activated mast cells (Control: 46±2% vs. CP105,696: 51±2%; p = 0.12; **Figure 5C**) in the aortic root.

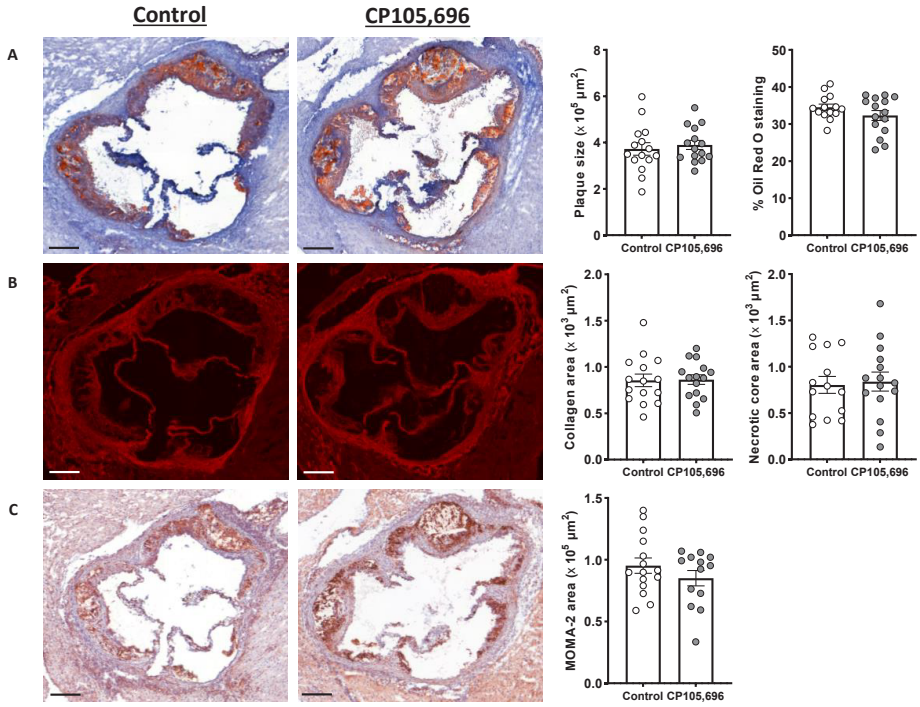

Figure 4. Inhibition of the BLT1-LTB4 axis did not alter plaque morphology in advanced atherosclerosis. A) Atherosclerotic plaque size and percentage Oil Red O staining in the plaque did not differ upon treatment with CP105,696 as assessed by Oil-Red O staining of the aortic root. B) Sirius red staining of the aortic root did not reveal differences in plaque collagen and necrotic core area in CP105,696 treated mice versus controls. C) BLT1 antagonism did not affect the MOMA-2 macrophage area in the aortic root. All representative pictures are taken at optical magnification 5x; the bar indicates 200µm. n = 13-15 per group. Data represent mean ± SEM.

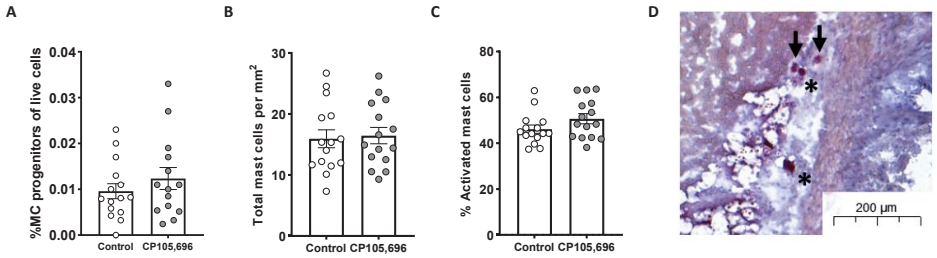

Figure 5. Mast cell accumulation in advanced atherosclerotic plaques. A) BLT1 antagonism did not affect the percentage of $CD34^+Lin^-CD127^-CD16/32^+CD117^+FC\varepsilon RI^+$ mast cell progenitors in blood. B) The total number of mast cells per mm^2 perivascular tissue of the aortic root tissue and C) the percentage of activated mast cells did not differ between the CP105,696 treated and control group. D) Representative image of mast cell staining in the aortic root section. Asterix indicates resting mast cells, arrows indicate activated mast cells. n = 14-15 per group. Data represent mean ± SEM.

Discussion

Mast cells actively contribute to progression and destabilization of advanced atherosclerotic lesions. Prevention of mast cell recruitment to atherosclerotic lesion could thus be a promising therapeutic strategy to limit plaque destabilization. In this study, we aimed to investigate whether inhibition of the BLT1-LTB_4 axis via BLT1 antagonism limits mast cell accumulation in advanced atherosclerosis and via this way prevent plaque instability. Although we observed expression of genes involved in LTB_4 biosynthesis in the human atherosclerotic plaque, including prominent expression in mast cells, inhibition of BLT1 *in vivo* did not affect plaque morphology and the number of mast cells in the advanced atherosclerotic plaque.

The LTB_4 biosynthesis pathway has previously been examined in atherosclerosis. ALOX5 (5-LO), ALOX5AP (FLAP) and LTA_4H have been found to be expressed in human atherosclerotic plaques, and were generally seen to colocalize with macrophages.[32–34] As we show here, these genes are also detected in the murine single-cell RNA sequencing data[29], while protein expression of ALOX5 and LTA_4H has been established in murine plaques and adventitial macrophages as well.[34] These proteins have also been targeted in experimental atherosclerosis studies. Similar to CP105,696, promising effects on atherosclerosis development have been shown with FLAP inhibitors like MK-886 and BAYx1005[35,36] Studies examining 5-LO in atherosclerosis have been less evident. 5-LO deficiency alone was not sufficient to limit atherosclerosis development, only in combination with 12-15-LO deficiency an effect was observed.[37] Furthermore, in humans, 5-LO inhibition using VIA-2291 gave

rather conflicting results. Gaztanaga *et al*. reported that treatment with VIA-2291 was not associated with significant reductions in vascular inflammation in patients after an acute coronary syndrome, while Matsumoto *et al*. showed that VIA-2291 resulted in slower plaque progression as measured by CT-angiography.[38,39]

It must be noted that all experimental studies in mice focussed on the effects of treatment during lesion initiation. As our single-cell RNA sequencing data of advanced human plaques revealed that mast cells have high expression of the LTB_4 biosynthesis-related genes, we aimed to examine the effect of LTB_4 inhibition in advanced atherosclerosis.

In our study, we observed a significant reduction in splenic myeloid cells, of which the most pronounced effects were found on both the inflammatory and patrolling monocyte subsets as well as on dendritic cells. This may be a result of direct inhibition of BLT1 on these cell subsets, but may also be indirectly related as LTB_4 has previously been shown to upregulate Monocyte Chemoattractant Protein (MCP-) 1.[40] Huang *et al*. showed that in human monocytes, LTB_4 interacts with BLT1 to upregulate mRNA expression and active synthesis of MCP-1 by monocytes to induce a feed-forward amplification loop for their chemotaxis.[41] Furthermore, it was shown that LTB_4 induced increased avidity and/or affinity of β1-integrin and β2-integrin to their endothelial ligands, further stimulating firm arrest of monocytes under physiologic flow.[42] Moreover, in both studies pharmacological inhibition of the LTB_4-BLT1 axis abrogated these effects. In line with these reported findings, CP105,696 reduced splenic myeloid cell and dendritic cell levels, of which the most pronounced effects were found on inflammatory and patrolling monocytes, which both have been found to migrate towards MCP-1.[43,44]

In atherosclerosis, BLT1 has already been a target in multiple studies. In line with the chemotactic effects on monocytes, Heller *et al*. showed that BLT1 deficiency resulted in a significant reduction in lesion size as well as macrophage content in apoE deficient mice.[15] Furthermore, in both apoE and LDLr deficient mice, a 35-day treatment with BLT1-antagonist CP105,696 led to a significant reduction in plaque size and $CD11b^+$ cells in the circulation.[23] In these studies however, intervention in the LTB1-BLT_4 axis occurred immediately upon lesion initiation. As mast cells are known to accumulate in later stages of disease,[6,9] we aimed to assess the effect of BLT1 blockade on pre-existing plaques. However, we did not observe any differences in plaque morphology as neither plaque and necrotic core size, nor plaque collagen and macrophage content were affected by BLT1 antagonism. Furthermore, flow cytometry analysis of the atherosclerotic aortic arch did not reveal any effects on total leukocyte and myeloid

cell content upon CP105,696 treatment. Apparently, blockade of BLT1 is not sufficient to affect plaque size and composition at this stage of the disease. Indeed, Aiello *et al*. described that more distinct effects of CP105,696 were observed in apoE$^{-/-}$ mice of 15 weeks old, with smaller and thus less complex lesions as compared to 24 weeks old mice with more advanced atherosclerosis.[23] In addition, in a BLT1$^{-/-}$apoE$^{-/-}$ mouse model on a western type diet, differences in lesion size were only detected after 4 weeks of diet, whereas after 8 weeks and 19 weeks of diet, lesion size was similar in both BLT1$^{-/-}$apoE$^{-/-}$ and apoE$^{-/-}$ mice.[22] This may be explained by the fact that monocyte influx into the plaque is a less dominant mechanism in advanced atherosclerosis as compared to early atherogenesis. In addition, macrophage egress has been shown to decrease with atherosclerosis progression.[45,46] Combined, this results in differences in myeloid cell dynamics between early and advanced atherosclerosis and effects observed upon BLT1 antagonism may thus be disease stage specific. Alternatively, in later stages of disease, other factors in the plaque microenvironment may contribute to the recruitment of different cell types to the plaque, which means that the decrease in myeloid content in the spleen due to BLT1 antagonism may not directly translate into effects in the plaque.

LTB_4 has previously been described to induce directed migration of mast cells and their progenitors.[20] *In vitro*, LTB_4 eluted from the supernatant of activated BMMCs elicited chemotaxis of immature mast cells. In mice, increased recruitment of CMFDA-labelled mast cell progenitors was detected upon injection of LTB_4 into the dorsal skin. LTB_4 was shown to be a potent chemoattractant for immature c-kit$^+$ human umbilical cord blood-derived mast cells (CBMCs), whereas mature c-kit$^+$ mast cells remained unresponsive.[19] Nevertheless, in our study we did not observe any differences in the percentage of circulating mast cell progenitors after 4 weeks of treatment with CP105,696. Moreover, the total number of mast cells and the percentage of activated mast cells in the aortic root also remained unaffected, suggesting that LTB_4 does not act as a chemoattractant for mast cells in advanced atherosclerosis via the LTB_4 receptor BLT1. Assessment of mast cell accumulation in other sites of advanced atherosclerosis may be warranted to confirm our findings. *In vitro* cultured murine and human mast cells have however also shown expression of the LTB_4 low affinity receptor BLT2. Lundeen *et al*. showed that inhibition with a selective BLT2 antagonist dose-dependently reduced migration of mast cells towards LTB_4 *in vitro*, suggesting that this interaction of BLT2 and LTB_4 could be involved in mast cell chemotaxis.[20] As CP105,696 is a selective BLT1-antagonist, we cannot exclude BLT2-induced mast cell recruitment towards the plaque in our experiment. Future studies may aim to investigate whether BLT2 is involved in mast cell chemotaxis to the advanced plaque independent of BLT1.

Although we did not see any differences in mast cell recruitment towards the atherosclerotic plaque in CP105,696 treated mice compared to our controls, single-cell RNA sequencing of human carotid atherosclerotic lesions suggests that mast cells may contribute to the local LTB_4 concentrations in the plaque as intraplaque mast cells highly expressed genes involved in LTB_4 biosynthesis. Interestingly, *ALOX5*, encoding for 5-LOX, was most prominently expressed in intraplaque mast cells as compared to other plaque cell types. In line, Spanbroek *et al*. showed that 5-LOX colocalized with tryptase$^+$ mast cells in carotid arteries and that the number of 5-LOX expressing cells increased in later stages of disease.[47] Furthermore, 5-LOX expression was mainly found in the shoulder regions of atherosclerotic lesions,[48] where mast cells have also been shown to reside and accumulate.[49] Together, this suggest that although mast cells may not induce an autocrine loop for their recruitment towards murine atherosclerotic lesions, that they may induce migration of other leukocytes towards the lesion via LTB_4. We cannot exclude species-induced differences here, however based on current literature, we do not expect any differences as both mouse and human mast cells in culture were seen to migrate towards LTB_4.[19,20]

To conclude, here we show that BLT1-antagonism does not affect plaque size and morphology during advanced stages of atherosclerosis, which suggests that LTB_4 is not involved in the progression of advanced atherosclerotic lesions. Moreover, we show that LTB_4 does not seem to be involved in mast cell migration towards atherosclerotic plaques, but that mast cells are able contribute to local LTB_4 production in the lesion. To identify novel therapeutic intervention strategies, further research should be aimed at the elucidation of mechanisms that induce directed migration of mast cells towards the advanced atherosclerotic plaque.

Methods

Single-cell RNA sequencing

Human carotid artery plaques were collected from 18 patients (14 male, 4 female) that underwent carotid endarterectomy surgery as part of AtheroExpress, an ongoing biobank study at the University Medical Centre Utrecht (Study approval number TME/C-01.18, protocol number 03/114).[50] Single cells were obtained and processed for single-cell RNA sequencing as previously described.[28] All studies were performed in accordance with the Declaration of Helsinki. Informed consent was obtained from all subjects involved in the study. Murine single-cell RNA sequencing data sets were obtained from Cochain *et al*.[29] and processed as previously described.[51,52] Briefly, data

sets were processed using the SCTransform normalization method[53], integrated using rpca reduction and subsequently clustered, all according to the Seurat "scRNA-seq integration" vignette.[54] All data analyses were executed in R-4.0.2.

Animals

All animal experiments were performed in compliance with the guidelines of the Dutch government and the Directive 2010/63/EU of the European Parliament. The experiment was approved by the Ethics Committee for Animal Experiments and the Animal Welfare Body of Leiden University (Project 106002017887, Study number 887,1-103).

Female 7-10 week old LDLr$^{-/-}$ mice (C57BL/6 background) (n=15/group) that were bred in-house were provided with food and water *ad libitum*. From the start of the experiment, the mice were fed a cholesterol-rich western-type diet (0.25% cholesterol, 15% cocoa butter, Special Diet Services, Essex, UK), which continued for 9 weeks in total. At week 5, the mice were randomized in groups based on age, weight and serum cholesterol levels. Previous work from our group showed that mast cell accumulation in the aortic root starts at approximately 6 weeks after the start of western-type diet feeding.[55] Therefore, from week 5 onwards, mice received either 20 mg/kg of BLT1-antagonist CP105,696 (Sigma-Aldrich) or vehicle control (0.6% Tween 80, 0.25% methylcellulose in phosphate-buffered saline (PBS)) three times per week via oral gavage for 4 weeks (n=15 per group). A detailed schedule of the experimental setup is provided in **Figure S2**. Blood was drawn by tail vein bleeding at week 5 and week 7. At week 9, the mice were sacrificed upon subcutaneous administration of anaesthetics (ketamine (40 mg/mL), atropine (0.1 mg/mL) and xylazine (8 mg/mL)). Blood was collected via orbital bleeding, after which the mice were perfused with PBS through the left cardiac ventricle. Next, organs were collected for analysis.

Cholesterol and Triglyceride Assay

Serum was collected through centrifugation at 8000 rpm for 10 minutes at 4°C and stored at -80°C until further use. Total cholesterol levels were determined through an enzymatic colorimetric assay (Roche/Hitachi, Mannheim, Germany). Triglyceride levels in serum were measured by an enzymatic colorimetric assay (Roche Diagnostics). For both assays, Precipath standardized serum (Roche Diagnostics) was used as an internal standard.

Cell Isolation

Blood samples were lysed with ACK lysis buffer (0.15 M NH_4Cl, 1 mM $KHCO_3$, 0.1 mM Na_2EDTA, pH 7.3) to obtain a single white blood cell suspension. Spleens were passed through a 70 µm cell strainer (Greiner, Bio-one, Kremsmunster,

Austria) and splenocytes were subsequently lysed with ACK lysis buffer. Aortic arches were cut into small pieces and enzymatically digested in a digestion mix containing collagenase I (450 U/mL), collagenase XI (250 U/mL), DNAse (120 U/mL), and hyaluronidase (120 U/mL; all Sigma–Aldrich) for 30 minutes at 37°C while shaking. After incubation, all samples were passed through a 70 µm cell strainer (Geiner, Bio-one, Kremsmunster, Austria). Single cell suspensions were then used for flow cytometry analysis.

Flow Cytometry

Single cell suspensions from blood and spleen were extracellularly stained with a mixture of selected fluorescent labelled antibodies for 30 minutes at 4°C. The antibodies used for flow cytometry are listed in **Table S1**. All measurements were performed on a Cytoflex S (Beckman and Coulter, USA) and analysed with FlowJo v10.7 (Treestar, San Carlos, CA, USA).

Histology

After euthanasia, the hearts were dissected, embedded and frozen in Tissue-Tek OCT compound (Sakura). 10 µm cryosections of the aortic root were prepared for histological analysis. Mean plaque size and the percentage plaque area of total vessel area (vessel occlusion) were assessed by Oil-Red-O (ORO) staining. From the first appearance of the three aortic valves, 5 consecutive slides with 80 µm distance between the sections were analysed for total lesion size within the three valves, after which the average lesion size was calculated. Average lesion size was also calculated in relation to distance from the start of the three-valve area. Subsequently, plaque volume was calculated as area under the curve. Collagen content of the plaque was measured using a Sirius Red staining after which fluorescent staining of three section per mouse was analysed and averaged. Similarly, the average necrotic core size was measured using the Sirius Red staining by measuring the acellular debris-rich areas of the plaque of three sections per mouse. Macrophage content was determined by using MOMA-2 antibody (1:1000; rat IgG2b; Bio-Rad). Naphthol AS-D chloroacetate staining (Sigma-Aldrich) was performed to manually quantify resting and activated mast cells in the plaques. Mast cells were identified and counted in the perivascular tissue of the aortic root at the site of atherosclerosis. A mast cell was considered resting when all granula were maintained inside the cell, while mast cells were assessed as activated when granula were deposited in the tissue surrounding the mast cell. Sections were digitalised using a Panoramic 250 Flash III slide scanner (3DHISTECH, Hungary). Analysis was performed using ImageJ software.

Cell Culture

Bone marrow-derived mast cells (BMMCs) from 7-10 weeks LDLr$^{-/-}$ mice were cultured in RPMI 1640 containing 25 mM HEPES (Lonza) and supplemented with 10% fetal calf serum, 1% L-glutamine (Lonza), 100 U/mL mix of penicillin/streptomycin (PAA), 1% sodium pyruvate (Sigma-Aldrich), 1% non-essential amino acids (MEM NEAA; Gibco) and 5 ng/mL IL-3 (Immunotools). Cells were incubated at 37°C and 5% CO_2 and were kept at a density of 0.25*10^6 cells per mL by weekly subculturing. BMMCs were cultured for 4 weeks in total to obtain mature mast cells.

RNA isolation and gene expression analysis

RNA isolation from 1*10^6 mast cells was performed using the guanine isothiocyanate method.[56] Using RevertAid M-MuLV reverse transcriptase cDNA was isolated according to the manufacturer's instructions. Quantitative gene expression analysis was performed with the SYBR Green Master Mix technology on a QuantStudio 6 Flex (Applied Biosystems by Life Technologies). A list of qPCR primers can be found in **Table S2**.

Statistical analysis

The data are presented as mean ± SEM and analysed in GraphPad Prism 9. Shapiro-Wilkson normality test was used to test data for normal distribution. Outliers were identified by a Grubbs' test. Data was analysed using an unpaired two-tailed Student *t*-test or Mann-Whitney test. $P < 0.05$ was considered to be significant.

Acknowledgments

The authors would like to thank Robin A.F. Verwilligen and Virginia Smit for technical assistance.

Author Contributions

Conceptualization, M.A.C.D. and I.B.; data acquisition, M.A.C.D., F.D.V., E.H., L.D., M.N.A.B., P.S., A.C.F. and I.B.; data analysis and interpretation, M.A.C.D., F.D.V. and I.B.; writing—original draft preparation, M.A.C.D., F.D.V. and I.B.; writing—review and editing, all authors; funding acquisition, A.C.F., J.K. and I.B. All authors have read and agreed to the published version of the manuscript.

Competing interests

The authors declare no competing interests.

Data availability

The data presented in this study are available on request from the corresponding author. The human scRNAseq data presented in this study are retrieved from Depuydt *et al*. Circ Res. 2020.[28] R scripts are available on GitHub (https://github.com/AtheroExpress/MicroanatomyHumanPlaque_scRNAseq). Other data is available upon request from the corresponding authors of this paper.

Funding

This research was funded by The Dutch Heart Foundation, grant number CVON2017-20: Generating the best evidence-based pharmaceutical targets and drugs for atherosclerosis (GENIUS II). M.A.C.D., I.B., J.K. are supported by the NWO-ZonMW (PTO program grant number 95105013). A.C.F. is supported by the Dutch Heart Foundation (2018T051). I.B. is an Established Investigator of the Dutch Heart Foundation (2019T067).

Ethics declarations

All experiments have been performed in accordance with the ARRIVE guidelines.

Human samples: The study was conducted according to the guidelines of the Declaration of Helsinki, and approved by the Medical Ethical Committee of the University Medical Centre Utrecht (UMCU). All samples were included in the Athero-Express Study (www.atheroexpress.nl), an ongoing biobank study at the UMCU. Informed consent was obtained from all subjects involved in the study.

Animal studies: All animal experiments were performed in compliance with the guidelines of the Dutch government and the Directive 2010/63/EU of the European Parliament. The experiment was approved by the Ethics Committee for Animal Experiments and the Animal Welfare Body of Leiden University (project 106002017887, study number 887,1-103).

References

1. Bot, I. *et al.* Perivascular mast cells promote atherogenesis and induce plaque destabilization in apolipoprotein E-deficient mice. *Circulation* **115**, 2516–2525 (2007).
2. Sun, J. *et al.* Mast cells promote atherosclerosis by releasing proinflammatory cytokines. *Nat. Med.* **13**, 719–724 (2007).
3. Heikkilä, H. M. *et al.* Mast cells promote atherosclerosis by inducing both an atherogenic lipid profile and vascular inflammation. *J. Cell. Biochem.* **109**, 615–623 (2010).
4. Laine, P. *et al.* Association between myocardial infarction and the mast cells in the adventitia of the infarct-related coronary artery. *Circulation* **99**, 361–369 (1999).
5. Morici, N. *et al.* Mast cells and acute coronary syndromes: relationship between serum tryptase, clinical outcome and severity of coronary artery disease. *Open Hear.* **3**, (2016).
6. Willems, S. *et al.* Mast cells in human carotid atherosclerotic plaques are associated with intraplaque microvessel density and the occurrence of future cardiovascular events. *Eur. Heart J.* **34**, 3699–3706 (2013).
7. Indhirajanti, S. *et al.* Systemic mastocytosis associates with cardiovascular events despite lower plasma lipid levels. *Atherosclerosis* **268**, 152–156 (2018).
8. Hermans, M., Van Lennep, J. R., Van Daele, P. & Bot, I. Mast Cells in Cardiovascular Disease: From Bench to Bedside. *Int. J. Mol. Sci.* **20**, (2019).
9. Kovanen, P. T. & Bot, I. Mast cells in atherosclerotic cardiovascular disease - Activators and actions. *Eur. J. Pharmacol.* **816**, 37–46 (2017).
10. Collington, S. J., Williams, T. J. & Weller, C. L. Mechanisms underlying the localisation of mast cells in tissues. *Trends Immunol.* **32**, 478–485 (2011).
11. Halova, I., Draberova, L. & Draber, P. Mast cell chemotaxis - chemoattractants and signaling pathways. *Front. Immunol.* **3**, (2012).
12. Funk, C. D. Prostaglandins and leukotrienes: advances in eicosanoid biology. *Science* **294**, 1871–1875 (2001).
13. Wan, M., Tang, X., Stsiapanava, A. & Haeggström, J. Z. Biosynthesis of leukotriene B 4. *Semin. Immunol.* **33**, 3–15 (2017).
14. Subramanian, B. C., Majumdar, R. & Parent, C. A. The role of the LTB 4-BLT1 axis in chemotactic gradient sensing and directed leukocyte migration. *Semin. Immunol.* **33**, 16–29 (2017).
15. Heller, E. A. *et al.* Inhibition of atherogenesis in BLT1-deficient mice reveals a role for LTB4 and BLT1 in smooth muscle cell recruitment. *Circulation* **112**, 578–586 (2005).
16. Yokomizo, T. Two distinct leukotriene B4 receptors, BLT1 and BLT2. *J. Biochem.* **157**, 65–71 (2015).
17. Tager, A. M. *et al.* Leukotriene B4 receptor BLT1 mediates early effector T cell recruitment. *Nat. Immunol.* **4**, 982–990 (2003).
18. Koga, T. *et al.* Expression of leukotriene B 4 receptor 1 defines functionally distinct DCs that control allergic skin inflammation. *Cell. Mol. Immunol.* **18**, 1437–1449 (2021).
19. Weller, C. L. *et al.* Leukotriene B4, an activation product of mast cells, is a chemoattractant for their progenitors. *J. Exp. Med.* **201**, 1961–1971 (2005).
20. Lundeen, K. A., Sun, B., Karlsson, L. & Fourie, A. M. Leukotriene B4 receptors BLT1 and BLT2: expression and function in human and murine mast cells. *J. Immunol.* **177**, 3439–3447 (2006).
21. Mehrabian, M. *et al.* Identification of 5-lipoxygenase as a major gene contributing to atherosclerosis susceptibility in mice. *Circ. Res.* **91**, 120–126 (2002).

22. Subbarao, K. *et al.* Role of leukotriene B4 receptors in the development of atherosclerosis: potential mechanisms. *Arterioscler. Thromb. Vasc. Biol.* **24**, 369–375 (2004).
23. Aiello, R. J. *et al.* Leukotriene B4 receptor antagonism reduces monocytic foam cells in mice. *Arterioscler. Thromb. Vasc. Biol.* **22**, 443–449 (2002).
24. Jamur, M. C. & Oliver, C. Origin, maturation and recruitment of mast cell precursors. *Front. Biosci. (Schol. Ed).* **3**, 1390 (2011).
25. Miyahara, N. *et al.* Leukotriene B4 release from mast cells in IgE-mediated airway hyperresponsiveness and inflammation. *Am. J. Respir. Cell Mol. Biol.* **40**, 672–682 (2009).
26. Ohnishi, H., Miyahara, N. & Gelfand, E. W. The role of leukotriene B(4) in allergic diseases. *Allergol. Int.* **57**, 291–298 (2008).
27. Motakis, E. *et al.* Redefinition of the human mast cell transcriptome by deep-CAGE sequencing. *Blood* **123**, e58-67 (2014).
28. Depuydt, M. A. C. *et al.* Microanatomy of the Human Atherosclerotic Plaque by Single-Cell Transcriptomics. *Circ. Res.* **127**, 1437–1455 (2020).
29. Cochain, C. *et al.* Single-Cell RNA-Seq Reveals the Transcriptional Landscape and Heterogeneity of Aortic Macrophages in Murine Atherosclerosis. *Circ. Res.* **122**, 1661–1674 (2018).
30. Li, X. *et al.* Polysorbates as novel lipid-modulating candidates for reducing serum total cholesterol and low-density lipoprotein levels in hyperlipidemic C57BL/6J mice and rats. *Eur. J. Pharmacol.* **660**, 468–475 (2011).
31. Shin, E. H., Lee, H. Y. & Bae, Y. S. Leukotriene B4 stimulates human monocyte-derived dendritic cell chemotaxis. *Biochem. Biophys. Res. Commun.* **348**, 606–611 (2006).
32. Cipollone, F. *et al.* Association Between 5-Lipoxygenase Expression and Plaque Instability in Humans. *Arterioscler. Thromb. Vasc. Biol.* **25**, 1665–1670 (2005).
33. Zhou, Y. J. *et al.* Expanding expression of the 5-lipoxygenase/leukotriene B4 pathway in atherosclerotic lesions of diabetic patients promotes plaque instability. *Biochem. Biophys. Res. Commun.* **363**, 30–36 (2007).
34. Qiu, H. *et al.* Expression of 5-lipoxygenase and leukotriene A4 hydrolase in human atherosclerotic lesions correlates with symptoms of plaque instability. *Proc. Natl. Acad. Sci. U. S. A.* **103**, 8161–8166 (2006).
35. Jawien, J. *et al.* Inhibition of five lipoxygenase activating protein (FLAP) by MK-886 decreases atherosclerosis in apoE/LDLR-double knockout mice. *Eur. J. Clin. Invest.* **36**, 141–146 (2006).
36. Jawien, J., Gajda, M., Olszanecki, R. & Korbut, R. BAY x 1005 attenuates atherosclerosis in apoE/LDLR - double knockout mice. *J. Physiol. Pharmacol.* **58**, 583–588 (2007).
37. Poeckel, D., Berry, K. A. Z., Murphy, R. C. & Funk, C. D. Dual 12/15- and 5-lipoxygenase deficiency in macrophages alters arachidonic acid metabolism and attenuates peritonitis and atherosclerosis in ApoE knock-out mice. *J. Biol. Chem.* **284**, 21077–21089 (2009).
38. Gaztanaga, J. *et al.* A phase 2 randomized, double-blind, placebo-controlled study of the effect of VIA-2291, a 5-lipoxygenase inhibitor, on vascular inflammation in patients after an acute coronary syndrome. *Atherosclerosis* **240**, 53–60 (2015).
39. Matsumoto, S. *et al.* Effect of treatment with 5-lipoxygenase inhibitor VIA-2291 (atreleuton) on coronary plaque progression: a serial CT angiography study. *Clin. Cardiol.* **40**, 210–215 (2017).
40. Matsukawa, A. *et al.* Endogenous monocyte chemoattractant protein-1 (MCP-1) protects mice in a model of acute septic peritonitis: cross-talk between MCP-1 and leukotriene B4. *J. Immunol.* **163**, 6148–54 (1999).
41. Huang, L. *et al.* Leukotriene B4 strongly increases monocyte chemoattractant protein-1 in human monocytes. *Arterioscler. Thromb. Vasc. Biol.* **24**, 1783–1788 (2004).

42. Friedrich, E. B. *et al.* Mechanisms of leukotriene B4--triggered monocyte adhesion. *Arterioscler. Thromb. Vasc. Biol.* **23**, 1761–1767 (2003).
43. Xu, L. L., Warren, M. K., Rose, W. L., Gong, W. & Wang, J. M. Human recombinant monocyte chemotactic protein and other C-C chemokines bind and induce directional migration of dendritic cells in vitro. *J. Leukoc. Biol.* **60**, 365–371 (1996).
44. Gschwandtner, M., Derler, R. & Midwood, K. S. More Than Just Attractive: How CCL2 Influences Myeloid Cell Behavior Beyond Chemotaxis. *Front. Immunol.* **10**, (2019).
45. Gerrity, R. G. & Naito, H. K. Lipid clearance from fatty streak lesions by foam cell migration. *Artery* **8**, 215–219 (1980).
46. Moore, K., Sheedy, F. & Fisher, E. Macrophages in atherosclerosis: a dynamic balance. *Nat. Rev. Immunol.* **13**, 709–721 (2013).
47. Spanbroek, R. *et al.* Expanding expression of the 5-lipoxygenase pathway within the arterial wall during human atherogenesis. *Proc. Natl. Acad. Sci. U. S. A.* **100**, 1238–1243 (2003).
48. Sánchez-Galán, E. *et al.* Leukotriene B4 enhances the activity of nuclear factor-kappaB pathway through BLT1 and BLT2 receptors in atherosclerosis. *Cardiovasc. Res.* **81**, 216–225 (2009).
49. Kaartinen, M., Penttilä, A. & Kovanen, P. T. Accumulation of activated mast cells in the shoulder region of human coronary atheroma, the predilection site of atheromatous rupture. *Circulation* **90**, 1669–1678 (1994).
50. Hellings, W. E. *et al.* Histological characterization of restenotic carotid plaques in relation to recurrence interval and clinical presentation: a cohort study. *Stroke* **39**, 1029–32 (2008).
51. Butler, A., Hoffman, P., Smibert, P., Papalexi, E. & Satija, R. Integrating single-cell transcriptomic data across different conditions , technologies , and species. *Nat. Biotechnol.* **36**, 411–420 (2018).
52. Stuart, T. *et al.* Comprehensive Integration of Single-Cell Data. *Cell* **177**, 1888-1902.e21 (2019).
53. Hafemeister, C. & Satija, R. Normalization and variance stabilization of single-cell RNA-seq data using regularized negative binomial regression. *Genome Biol.* **20**, 1–15 (2019).
54. Stuart, T., Hoffman, P. & Satija, R. Seurat Signac Package. (2020).
55. Bot, I. *et al.* Mast cell chymase inhibition reduces atherosclerotic plaque progression and improves plaque stability in ApoE-/- mice. *Cardiovasc. Res.* **89**, 244–252 (2011).
56. Chomczynski, P. & Sacchi, N. Single-step method of RNA isolation by acid guanidinium thiocyanate-phenol-chloroform extraction. *Anal. Biochem.* **162**, 156–159 (1987).

Supplemental Data

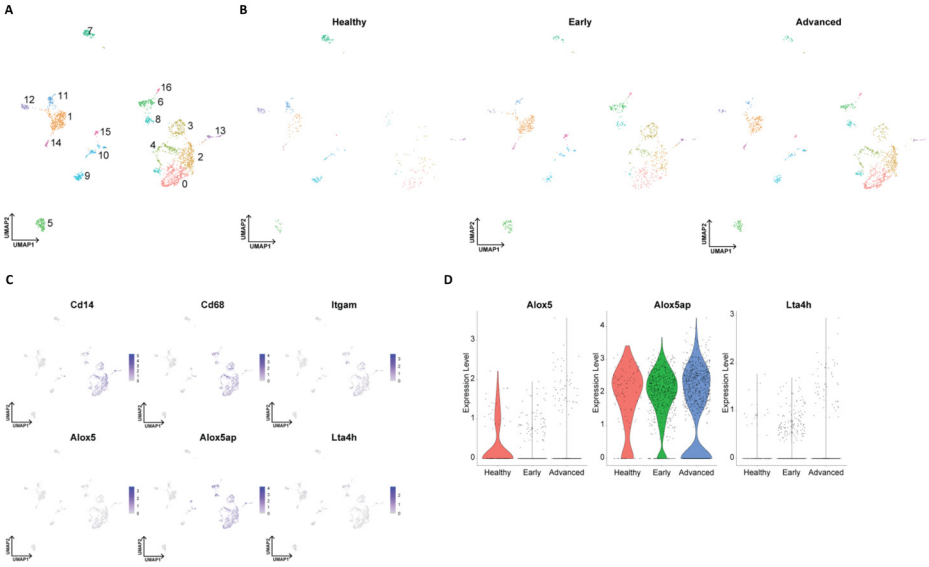

Figure S1. Single-cell RNA sequencing reveals expression of Alox5, Alox5ap, and Lta4h in healthy (chow diet), early atherosclerotic (11wk HFD) and advanced atherosclerotic aortas (20wk HFD) of LDLr$^{-/-}$ mice.[29] (A) Integrated analysis of CD45+ cells of aorta's from LDLr$^{-/-}$ in different plaque stages reveals UMAP with 17 clusters. (B) UMAP depicting distribution of CD45^{+} cells of healthy, early atherosclerotic and advanced atherosclerotic aortas. (C) *Alox5*, *Alox5ap* and *Lta4h* are mainly expressed in myeloid cell clusters (*Cd14*$^{+}$, *Cd68*$^{+}$, *Itgam*$^{+}$). (D) Expression of *Alox5*, *Alox5ap* and *Lta4h* in all myeloid cell clusters divided by plaque stage.

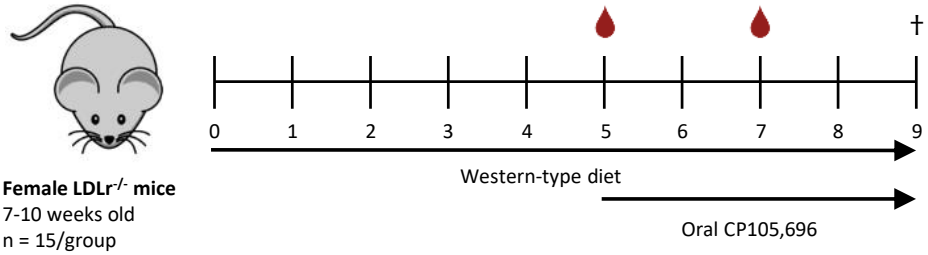

Figure S2. Schematic overview of the experimental set-up. Female *LDLr*$^{-/-}$ were put on a western type diet for 9 weeks and were treated with 20mg/kg CP105,696 or vehicle control three times a week by oral gavage from week 5 up to week 9. Blood was drawn via tail vein bleeding at week 5 and week 7. At week 9, all mice were sacrificed, after which organs were collected and processed for analysis.

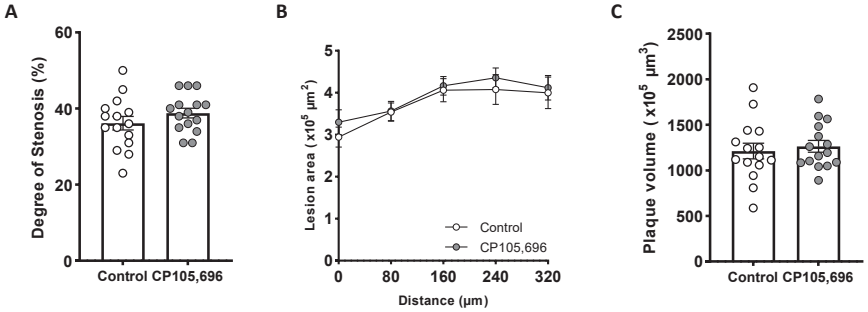

Figure S3. The degree of stenosis and plaque volume did not differ upon treatment with CP105,696. Oil red O staining did not reveal differences in (A) the degree of stenosis (percentage plaque area of total vessel area), (B) the lesion area and (C) plaque volume between the CP105,696 versus vehicle control mice. Data represents mean ± SEM.

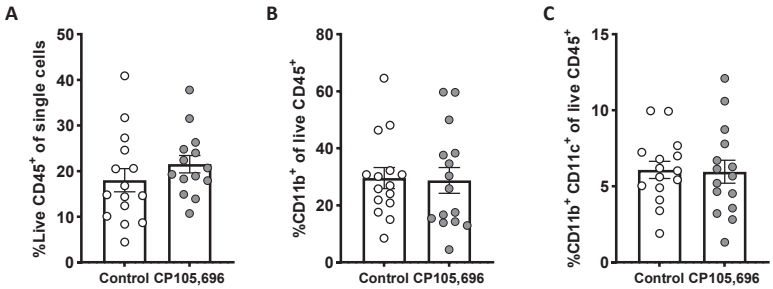

Figure S4. BLT1-antagonism did not affect the percentage of myeloid cells in the aortic arch. A) Flow cytometry analysis of the aortic arch revealed no differences in the percentage of aortic leukocytes (live CD45$^+$) within the single cell population upon treatment with CP105,696. Furthermore, the percentages of B) CD11b$^+$ myeloid cells and C) CD11b$^+$CD11c$^+$ dendritic cells within the CD45$^+$ cell population did not differ between groups. n = 14-15 per group. Data represent mean ± SEM.

Table S1. Extracellular antibodies used for flow cytometry analysis.

Antibody	Fluorochrome	Company
CD16/32	Brilliant violet 421	Biolegend
CD127	Brilliant violet 605	Biolegend
CD11c	FITC	Biolegend
CD45R	FITC (Lineage)	Biolegend
CD11b	FITC (Lineage)	eBioscience
Gr-1	FITC (Lineage)	eBioscience
CD3	FITC (Lineage)	eBioscience
Ter119	FITC (Lineage)	Biolegend
CD19	FITC (Lineage)	eBioscience
CD4	FITC (Lineage)	eBioscience
Sca-1	PE	BD Biosciences
CD11b	PE	Biolegend
Ly6C	PE-CF594	BD Biosciences
CD34	PE-Cy7	Biolegend
cKit/CD117	APC	eBioscience
Fcer1	AF700	Biolegend
Fixable Viability dye	eFluor780	ThermoFisher Scientific
Fc Block	n/a	Biolegend

Table S2. Primers used for quantitative reverse transcription PCR (RT-qPCR). For all analyses, *36b4* and *Rpl27* were included as housekeeping genes.

Gene	Forward primer	Reverse Primer
36b4	ctgagtacaccttcccacttactga	cgactcttcctttgcttcagcttt
Rpl27	cgccaagcgatccaagatcaagtcc	agctgggtccctgaacacatccttg
Kit	tggtcaaaggaaatgcacgactgcc	catccctgggtaggggctgcttc
Alox5	gcagatcgtggatactctaccagacc	aaatgctcctctgggtacatgcctag
Alox5ap	aagcaagcatggatcaagaggctgtg	aagcttctcccattatgcgccttgc
Lta4h	acggctctgcattcaatcgaaatgg	ggacagcttgatcatgggatttgtcg

Cat. No.	Clone	Dilution
101331	93	1:400
135025	A7R34	1:400
117306	N418	1:800
103206	RA3-6B2	1:400
11-0112-85	M1/70	1:400
11-5931-82	RB6-8C5	1:400
11-0031-85	145-2C11	1:400
116206	TER-119	1:400
11-0191-85	MB19-1	1:400
11-0041-85	GK1.5	1:400
553336	E13-161.7	1:400
101208	M1/70	1:1000
562728	AL-21	1:800
119325	MEC14.7	1:400
17-1171-82	3B8	1:400
134324	MAR-1	1:400
65-0865-14	n/a	1:2000
101320	n/a	1:250

Size	Accession number
885-1033	NM_007475.5
400-529	NM_011289.3
2542-2690	NM_001122733.1
1912-2031	NM_009662.2
102-234	NM_009663.2
1734-1873	NM_008517.2

Chapter 8

Inhibition of Interleukin-4 Induced Gene 1 (IL4I1) stimulates a pro-inflammatory immune environment without affecting early atherosclerotic lesion development in LDL receptor knockout mice.

Manuscript in preparation

M.A.C. Depuydt[1*], R.A.F. Verwilligen[1*], S. Taei[1], M.N.A. Bernabé Kleijn[1], V. Smit[1], B. Slütter[1], I. Bot[1], A. C. Foks[1], M. Hoekstra[1,2,3], M. Van Eck[1,2,3], J. Kuiper[1]

1 Division of BioTherapeutics, Leiden Academic Centre for Drug Research, Leiden University, 2333 CC, Leiden, The Netherlands
2 Systems Pharmacology and Pharmacy, Leiden Academic Centre for Drug Research, Leiden University, Leiden, The Netherlands
3 Pharmacy Leiden, Leiden, The Netherlands

*These authors contributed equally

Abstract

Interleukin-4 Induced Gene 1 (IL4I1) is produced by antigen presenting cells upon T cell activation. It functions as a suppressor of cytotoxic T cell activation and inhibition of IL4I1 has been proposed as a promising therapeutic strategy for cancer. However, immune therapy in cancer has been associated with cardiovascular health problems. In this study, the role of IL4I1 in atherosclerosis was investigated.

Single-cell RNA sequencing data from human atherosclerotic plaques revealed IL4I1 expression on foamy TREM2^{hi} macrophages. Female low-density lipoprotein receptor deficient (LDLr$^{-/-}$) mice were fed a Western-type diet for 6 weeks to induce atherosclerosis development and treated either with the IL4I1 inhibitor CB-668 (25 mg/kg) or vehicle control twice a day by oral gavage. Treatment with CB-668 had no effect on the main immune cell populations in the circulation. However, CB-668 administration did lead to a shift from naïve to effector and/or central memory CD4^{+} and CD8^{+} T cells and an increase in cytotoxic CD8^{+} T cells in the spleen and the atherosclerotic aorta. Histological analysis of the three-valve area in the heart showed that CB-688 did not affect atherosclerotic lesion size nor composition compared to the controls.

Our data show that inhibition of IL4I1 using the small molecule inhibitor CB-668 could result in a more pro-inflammatory immune environment but does not affect early atherosclerotic lesion development. This is the first indication that application of CB-668 in anti-cancer therapy likely does not lead to an increased risk of atherosclerosis.

Keywords: inflammation, the immune system, atherosclerosis, macrophage, IL4I1

Introduction

Interleukin 4 induced gene 1 (IL4I1) is a secreted amino-acid catabolizing enzyme which converts its substrate L-phenyl alanine into phenyl pyruvate, ammonia, and hydrogen peroxide.[1] IL4I1 was initially discovered in a rare type of B-cell lymphoma[2-4], and is currently known to be overexpressed in different types of cancer, including breast cancer, renal cancer, and melanoma. In experimental studies in murine models, overexpression of IL4I1 is associated with a poor diagnosis due to negative regulation of the antitumor effects of $CD8^+$ T cells and thereby stimulating tumor immune evasion.[5,6] Recently, a selective small molecule inhibitor of IL4I1, named CB-668, has been described as a potent novel anti-cancer therapy.[7] Blockade of IL4I1 using CB-668 in murine tumor models resulted in increased expression of pro-inflammatory immune genes in the tumor and led to reduced tumor growth, particularly in combination with anti-programmed cell death 1 (PD1) ligand therapy. This implies a key role for IL4I1 in suppression of the immune response in cancer. Indeed, recent studies have shown that IL4I1 limited T cell proliferation and differentiation as well as B cell proliferation.[1,8]

In immune cells, IL4I1 is primarily produced by antigen presenting cells such as macrophages and dendritic cells and secreted in the immune synapse at the interface between the antigen presenting cell and the T cell. It is crucial for cell-cell communication and functions as a negative regulator of T cell activation. Aubatin *et al.* have demonstrated that IL4I1 modulates T cell activation by interfering with signaling pathways downstream of the T cell receptor independently of its enzymatic activity.[9] Besides antigen presenting cells, certain T cell subtypes are also able to produce IL4I1, including T helper 17 cells (T_{h17}) and regulatory T cells (T_{regs}).[10,11] Production of IL4I1 by T_{h17} cells is induced in an autocrine manner and blocks T_{h17} cell cycle progression through the inhibitory effects of Tob1, a member of the TOB/BTG 1 family of anti-proliferative proteins and thus functions as a cell cycle inhibitor.[12] In addition, Cousin *et al.* demonstrated that IL4I1 promotes the differentiation of naïve T cells into regulatory $FOXP3^+$ T cells *in vitro*. Notably, increased numbers of $FOXP3^+$ T cells have been associated with augmented tumorigenesis, an effect related to their T cell suppression activity.[13,14]

In summary, IL4I1 is an important immunoregulator and has shown to be a promising therapeutic target in cancer to limit immune evasion in the tumor microenvironment. However, important to note is that blockade of immune checkpoints inhibits the natural "brake" on the immune response. Although this is beneficial in cancer therapy in which an augmented immune response is essential for effective removal of the aberrant cancer cells, it does increase the risk for an autoimmune response. Recent studies

showed substantial accumulation of T cells in human atherosclerotic plaques[15,16], making it likely that checkpoint inhibitors will affect T cell immune responses in atherosclerosis. In line, checkpoint inhibitors that are successful in cancer therapy, such as anti-PD-L1 and anti-T lymphocyte-associated protein 4 (CTLA4) have been associated with an increased risk for atherosclerosis.[17-20] Yet, it remains unknown whether blockade of the immunoregulator IL4I1 stimulates atherosclerosis risk.

In the current study we determined if IL4I1 is expressed in atherosclerotic plaques and established the effects of IL4I1 inhibition on atherosclerosis development in hypercholesterolemic low-density lipoprotein receptor (LDLr) knockout mice *in vivo*.

Material and methods

Single-cell RNA sequencing of human atherosclerotic plaques

Human carotid atherosclerotic plaques were obtained from 18 patients (14 male, 4 female) during carotid endarterectomy surgery and included in the AtheroExpress biobank.[18] Briefly, single cells were isolated, live cells were sorted into 384-wells plates and processed for single-cell RNA sequencing, as previously described.[15] All studies were performed in accordance with the Declaration of Helsinki. Informed consent was obtained from all patients involved in the study.

Mice

Female 8-10 weeks old Low-Density Lipoprotein receptor knockout (LDLr-/-) mice were bred in-house and provided with food and water *ad libitum*. Mice were housed in a standard laboratory setting and fed a Western-type diet (0.25% cholesterol, 15% cocoa butter, Special Diet Services, Essex, UK) for six weeks to induce atherosclerosis development. The mice were treated with either the IL4I1 inhibitor CB-668 (25 mg/kg, Calithera Biosciences) or a vehicle control (Ctrl) (n = 14-15 per group) twice daily through oral gavage. Blood was drawn from by tail vein bleeding in week 2 and 4. At week 6, mice were sacrificed after subcutaneous injection of anaesthetics (ketamine (40 mg/mL), atropine (0.1 mg/mL), and xylazine (8 mg/mL)). Blood was collected by orbital bleeding in regular tubes (Eppendorf), for serum analysis) or in K2-EDTA blood tubes (Sarstedt AG & Co. KG) for flow cytometry) and mice were perfused with PBS through the left cardiac ventricle. Subsequently, organs were collected for analysis. All animal experiments were approved by the Ethics Committee for Animal Experiments and the Animal Welfare Body of Leiden University, and performed in compliance with the European Parliament's Directive 2010/63/EU on the protection of animals used for research purposes.

Serum cholesterol levels

Serum was collected by centrifugation of whole blood at 8000 rpm for 10 minutes at 4°C and stored at -80°C until further use. Serum concentrations of total cholesterol were determined using enzymatic colorimetric assays.[21] Precipath (Roche Diagnostics) was used as internal standard.

Cell isolation

To obtain a white blood cell suspension, whole blood was lysed with ACK lysis buffer (0.15 M NH_4Cl, 1 mM $KHCO_3$, 0.1 mM Na_2EDTA, pH 7.3). Spleens were passed through a 70 µm cell strainer and subsequently lysed with ACK lysis buffer to obtain a splenocyte suspension. Heart lymph nodes were passed through a 70 µm cell strainer to obtain a single cell suspension. Aortic arches were cut into small pieces and digested using an enzyme mix containing collagenase I (450 U/mL), collagenase XI (250 U/mL), DNAse (120 U/mL), and hyaluronidase (120 U/mL; all Sigma-Aldrich) for 30 minutes at 37°C while shaking. Next, digested samples were passed through a 70 µm cell strainer. All single cell suspensions were subsequently used for flow cytometry.

Flow cytometry

Single cell suspensions were stained with a mixture of fluorescent antibodies directed extracellular markers for 30 minutes at 4°C. Intracellular staining was performed using the FoxP3 Transcription Factor Staining Buffer Set (ThermoFisher) following the manufacturer's instructions. Briefly, cells were fixed for 45 minutes at 4oC and washed twice at 1500 rpm for 5 minutes. Fixed cells were stained with a mixture of intracellular antibodies for 30 minutes at 4°C, washed, and subsequently measured with flow cytometry. The antibodies used for flow cytometry are listed in **Table 2**. All measurements have been performed on a Cytoflex S (Beckman Coulter) and analysed with FlowJo V10.7 (Treestar).

Histological analysis

Hearts were isolated, dissected, embedded, and frozen in Tissue-Tek OCT compound (Sakura). Prior to histological analyses, cryosections of 10 µm were made of the aortic root. Neutral lipids were stained with Oil-Red-O (Sigma Aldrich) to assess mean plaque size and vessel occlusion. Aortic root sections were stained with Masson's Trichrome to measure collagen content and necrotic core size. The monocyte/macrophage area was stained using a MOMA-2 primary antibody (1:1000; rat IgG2b; Bio-Rad) and visualized using a secondary biotinylated rabbit α-rat IgG antibody (1:100, Vector) and the Vectastain ABC HRP kit and Vector ImmPACT NovaRed (Vector). Sections were digitalized with a Panoramic 250 Flash III slide scanner (3DHistech) and quantified using ImageJ software.

Table 2. List of extracellular and intracellular antibodies used.

Marker	Fluorochrome	Clone	Supplier
CD3e	BV650	145-2C11	BD biosciences
CD4	PercP	RM4-5	BD biosciences
CD8	BV510	53-6.7	Biolegend
CD11b	BV605	M1/70	Biolegend
CD11c	APC	N418	eBioscience
CD25	PE-texas red	PC61.5	Biolegend
CD44	APC	IM7	eBioscience
CD45	AF700	30-F11	Biolegend
CD45	PE	30-F11	Biolegend
CD62L	BV605	MEL14	Biolegend
F4/80	FITC	BM8	Biolegend
Foxp3	eFluor 450	FJK-16s	eBioscience
Ly6C	BV510	HK1.4	Biolegend
Ly6G	PerCP-Cy5.5	1A8	Biolegend
MHCII	BV650	M5/114.15.2	Biolegend
ROR γT	PE	AFJKS-9	eBioscience
T-bet	PE-Cy7	eBio4B10	eBioscience

Statistical analysis

Data are depicted as mean ± SEM and analysed using GraphPad Prism 9 software. Normal distribution was tested using a Shapiro Wilk test. Outliers were identified by a Grubb's outlier test. A two-tailed Student's t-test was performed with normal distributed data, otherwise, the Mann–Whitney test was used. Probability values of $p<0.05$ were considered statistically significant.

Results

IL4I1 expression on human plaque TREM2⁺ macrophages detected by single-cell RNA sequencing

IL4I1 is known to be expressed by antigen presenting cells in multiple diseases. Apart from cancer, IL4I1⁺ macrophages accumulate in both inflammatory and infectious diseases, such as rheumatoid arthritis and COVID19.[22,23] Furthermore, in sarcoidosis and tuberculosis IL4I1 is highly expressed by macrophages and dendritic cells in Th1 granulomas.[24] However, whether IL4I1 is also expressed in antigen presenting cells in human atherosclerotic plaques remains unknown. Recently, we applied single-

cell RNA sequencing (scRNAseq) on human carotid atherosclerotic plaques of 18 patients.[15] Fourteen distinct cell clusters (0-13) were identified amongst which four myeloid cell clusters consisting of both macrophages and dendritic cells (cluster 5, 6, 7, 12) (**Fig. 1A**). Indeed, *IL4I1* expression was detected in this data set, primarily in the *TREM2* (Triggering receptor expressed on myeloid cells 2) expressing macrophages (**Fig. 1B**).[15,16,25] To confirm IL4I1 expression in murine plaque antigen presenting cells, we used PlaqView (www.plaqview.com) to look up *Il4i1* in an integrated data set of 12 data sets of murine atherosclerotic aorta's and, as described earlier by Zernecke *et al*., this gene was mainly expressed by cells of the mature dendritic cell cluster.[26,27] Together, these data show that IL4I1 is expressed in the atherosclerotic plaque and this expression is restricted to antigen presenting cells. We next aimed to determine whether inhibition of IL4I1 affected T cell polarization in the atherosclerotic plaque.

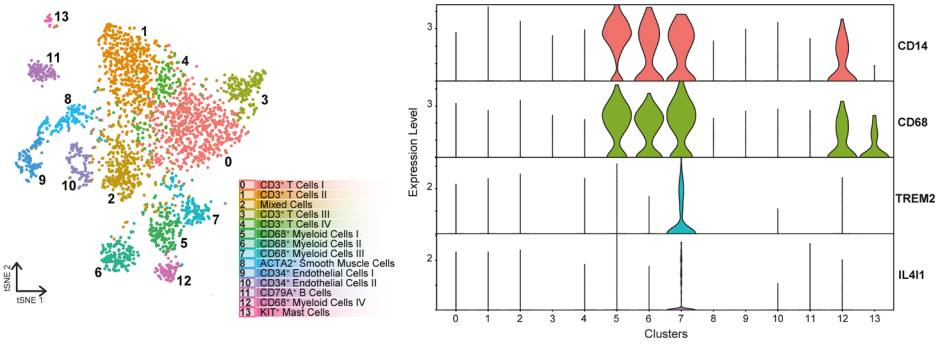

Figure 1. Single cell RNA sequencing reveals expression of IL4I1 on TREM2⁺ macrophages in human atherosclerotic lesions. (A) Single-cell RNA sequencing of human carotid atherosclerotic plaques reveals tSNE with 14 distinct clusters. **(B)** Violin plots of expression of CD14, CD68, TREM2 and IL4I1.

Inhibition of IL4I1 does not affect immune cell populations in the circulation and spleen

Because scRNAseq has shown that IL4I1 is expressed locally in the atherosclerotic lesion by myeloid cells, we have examined whether inhibition of IL4I1 could affect immune activation and atherosclerotic plaque development. Female LDLr$^{-/-}$ mice (8-10 weeks old) were fed a Western-type diet for 6 weeks to induce atherosclerosis. During these 6 weeks, mice were treated with CB-668, a small molecule inhibitor of IL4I1, or with vehicle control via oral gavage twice a day (25mg/kg)(**Fig. 2A**). Inhibition of IL4I1 using CB-668 did not affect the body weight throughout the experiment (t=6 weeks, Ctrl: 21.1±0.4 g vs. CB-668: 20.6±0.4 g; **Fig. 2B**). As expected, Western-type diet feeding led to an increase of serum total cholesterol levels in both groups

(**Fig. 2C**). IL4I1 inhibition did not significantly affect the serum cholesterol levels during the 6 weeks of treatment (t=6 weeks, Ctrl 1733.8±91.3 mg/dL vs. CB-668 1907.2±84 mg/dL; **Fig. 2C**). To study the systemic immune effects of IL4I1 inhibition using CB-668, general immune cell populations were assessed in the blood and spleen. In the circulation, no differences were found in either lymphocytes or myeloid cell subsets upon CD-668 treatment (**Fig. 2D**). In spleen, however, CB-668 did induce a significant decrease in $CD4^+$ (Ctrl: 15.70±0.84%, CB-668: 14.50±0.61%, $p<0.05$) and $CD8^+$ (Ctrl: 11.70±0.49%, CB-668: 10.80±0.44%, $p<0.05$) T cells. Furthermore, inflammatory monocytes were slightly increased ($CD11b^+Ly6C^{hi}$; Ctrl: 0.58±0.055%, CB-668: 0.81±0.091%, $p<0.05$). No differences were observed in splenic B cells, $CD11b^+$ cells, $Ly6G^+$ Neutrophils, or $CD11b^+$ $CD11c^+$ dendritic cells.

Treatment with CB-668 leads to a shift from naïve to effector or central memory $CD4^+$ and $CD8^+$ T cells

Because IL4I1 has been described as an immune regulator that may be involved in T cell proliferation and function[28], we have examined whether inhibition of IL4I1 could affect the T cell activation state in different immune organs such as the spleen, heart lymph nodes (HLN), and in the atherosclerotic aortic arch (AA). The percentages of naïve $CD4^+$ and $CD8^+$ T cells (T_{naive})($CD44^-CD62L^+$) were decreased in the spleen as well as in the HLN (spleen: $CD4^+$ T_{naive} -14.0%, $CD8^+$ T_{naive} -14,0%, HLN: $CD4^+$ T_{naive} -17.0%, $CD8^+$ T_{naive} -7.0%; $p<0.05$)(**Fig. 3A-B**). Moreover, this decrease was accompanied by an increase of effector T cells (T_{eff}) ($CD44^+CD62L^-$) and/or central memory T cells (T_{cm}) ($CD44^+CD62L^+$). Splenic $CD8^+$ T_{eff} cells were increased upon IL4I1 inhibition ($CD8^+$ T_{eff} +66.0%, $p<0.05$)(**Fig. 3A**), whereas there was no difference of $CD8^+$ T_{eff} cells in the HLN (**Fig. 3B**). Central memory $CD8^+$ T cells in the spleen as well as central memory $CD4^+$ and $CD8^+$ cells in the HLN were increased upon treatment with CB-668 (spleen: $CD8^+$ T_{cm} +15.0%, HLN: $CD4^+$ T_{cm} +39.0%, $CD8^+$ T_{cm} +11%, $p<0.05$)(**Fig. 3A-B**). In the atherosclerotic aorta, no differences were found in the activation state of $CD4^+$ T cells. However, we did observe a trend towards lower naïve $CD8^+$ T cells and an increase in effector $CD8^+$ T cells was observed ($CD8^+$ T_{eff} +45.8%, $p<0.01$)(**Fig. 3C**).

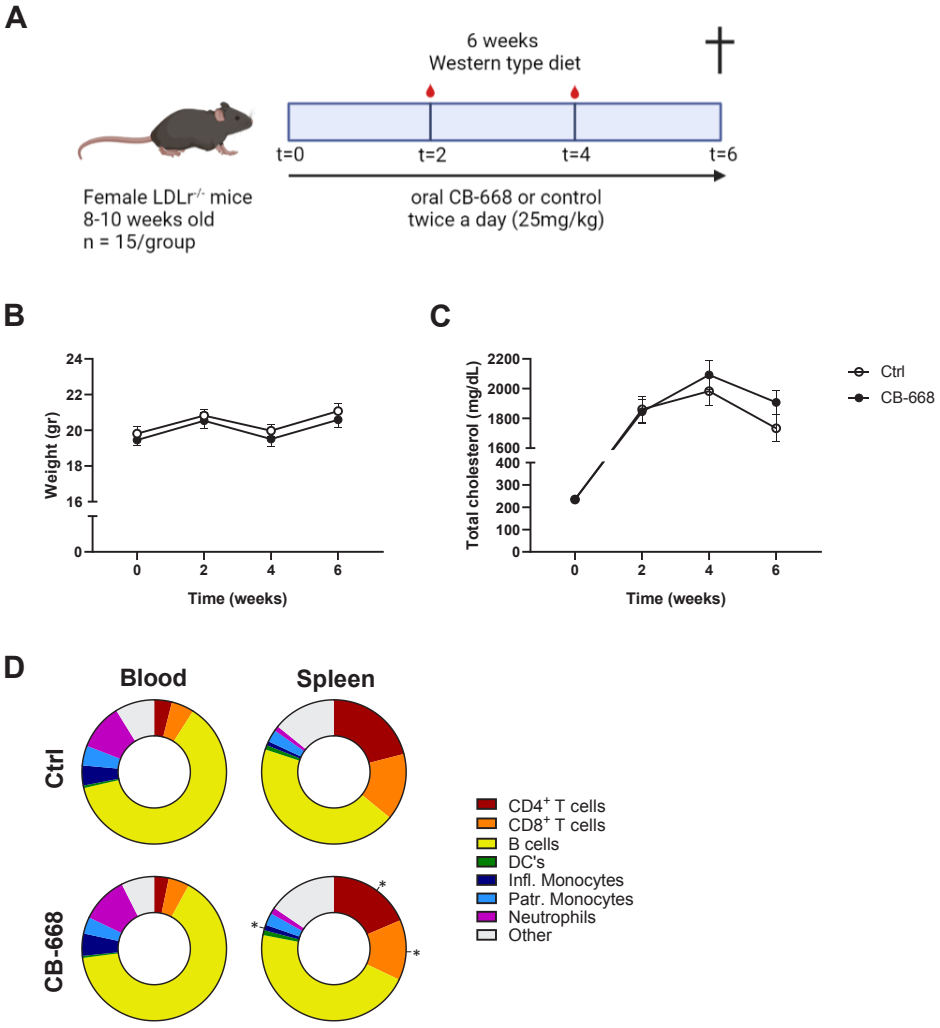

Figure 2. IL4I1 inhibition does not affect the bodyweight, serum cholesterol levels and general immune cells in blood and spleen. (A) Schematic overview of the experimental set-up. Female LDLr$^{-/-}$ were put on a western type diet for 6 weeks and were treated with 0.25 mg/kg CB-668 or vehicle control twice a day by oral. Blood was drawn via tail vein bleeding at week 2 and week 4. At week 6, all mice were sacrificed, after which organs were collected and processed for analysis. **(B)** Body weight of mice was measured every two weeks during treatment and was not affected by CB-668. **(C)** Plasma cholesterol levels were obtained at t=0, t=2, t=4 and t=6. **(D)** The frequency of CD4^{+} T cells, CD8^{+} T cells, CD19^{+} B cells, CD11b^{+} myeloid cells, CD11b^{+}CD11c^{+} Dendritic cells (DCs), CD11b^{+}Ly6c^{Hi} inflammatory monocytes (Inf. monocytes), CD11b^{+}Ly6c^{lo} patrolling monocytes (Patr. monocytes) and CD11b^{+}Ly6G^{Hi} Neutrophils was assessed and displayed as parts-of-whole of the live cell population. Statistical significance was determined using an unpaired Students t-test ($p<0.05$*). Data represent mean ± SEM (n = 14-15 per group).

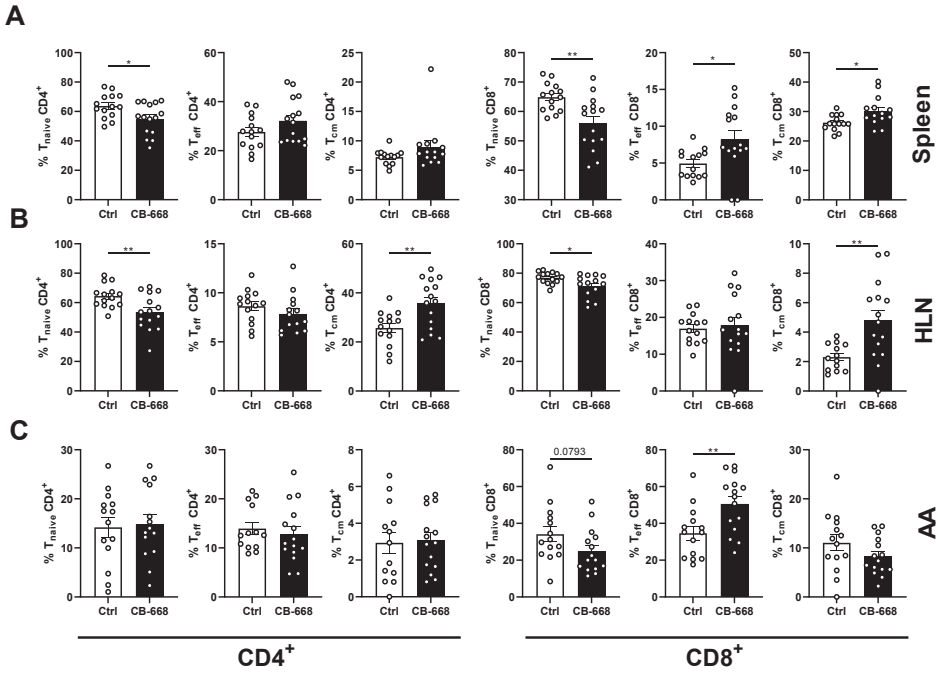

Figure 3. IL4I1 inhibition leads to a shift from naïve to effector or central memory CD4⁺ and CD8⁺ T cells (A) Naïve T cell (T_{naive}; $CD44^{-}CD62L^{+}$), effector T cells (T_{eff}; $CD44^{+}CD62L^{-}$) and central memory T cell (T_{cm}; $CD44^{+}CD62L^{+}$)(of live CD4 or CD8 cells) populations in the spleen, **(B)** HLN and **(C)** aortic arch (AA). Statistical significance was determined using an unpaired Students t-test ($p<0.05$*, $p<0.01$**). Data represent mean ± SEM (n = 14-15 per group).

Subsequently, we assessed whether CB-668 treatment also affected specific T helper (T_h) cell subsets. Whereas CB-668 treatment did not alter the percentages of T_h17 ($ROR\gamma T^{+}$ $CD4^{+}$) and regulatory T cells (T_{reg}; $Foxp3^{+}CD4^{+}$), it did lead to an increase of T_h1 cells ($Tbet^{+}CD4$ +98.0%) in the HLN and an increase in splenic cytotoxic $CD8^{+}$ T cells ($Tbet^{+}CD8^{+}$; T_c1 +33.0%)(**Fig. 4A-B**). A trend towards increased cytotoxic $CD8^{+}$ T cells was observed in the aortic arch as well (+37%; p=0.07) (**Fig. 4C**). Together, this suggests that IL4I1 inhibition induced a shift towards a central or effector T cell phenotype, mainly by an increase of T_c1 cells in the spleen and trend towards increase in the aortic arch and an increase in T_h1 cells in the HLN.

Inhibition of IL4I1 does not affect lesion development

Innate as well as the adaptive inflammatory immune responses are known to drive the development and progression of atherosclerosis. Because IL4I1 inhibition has been reported to affect these immune responses, we have examined whether IL4I1 inhibition could affect initial atherosclerosis development. Oil-red-O staining of aortic

root sections did not reveal any differences in both plaque size (Ctrl 169788±22661 μm^2 vs CB-668 184507±24990 μm^2) and vessel occlusion (Ctrl 16.9±2.0% vs CB-668 19.2±2.5%)(**Fig. 5A**). Further analysis of the plaque composition revealed that CB-668 treatment also did not affect the monocyte/macrophage positive area (Ctrl 26975±4382 μm^2 vs CB-668 24055±4289 μm^2) or macrophage content (Ctrl 56.4±3.2% vs CB-668 55.1±3.0%)(**Fig. 5B**). In addition, inhibition of IL4I1 did not have an effect on the collagen area (Ctrl 7596±1665 μm^2 vs CB-668 7695±1662 μm^2) or relative collagen content (Ctrl 21.8±2.2% vs CB-668 22.0±1.9%)(**Fig. 5C**). These data indicate that CB-668 treatment did not affect plaque development and composition and therefore does not lead to an increased risk of atherosclerosis in LDLr-/- mice.

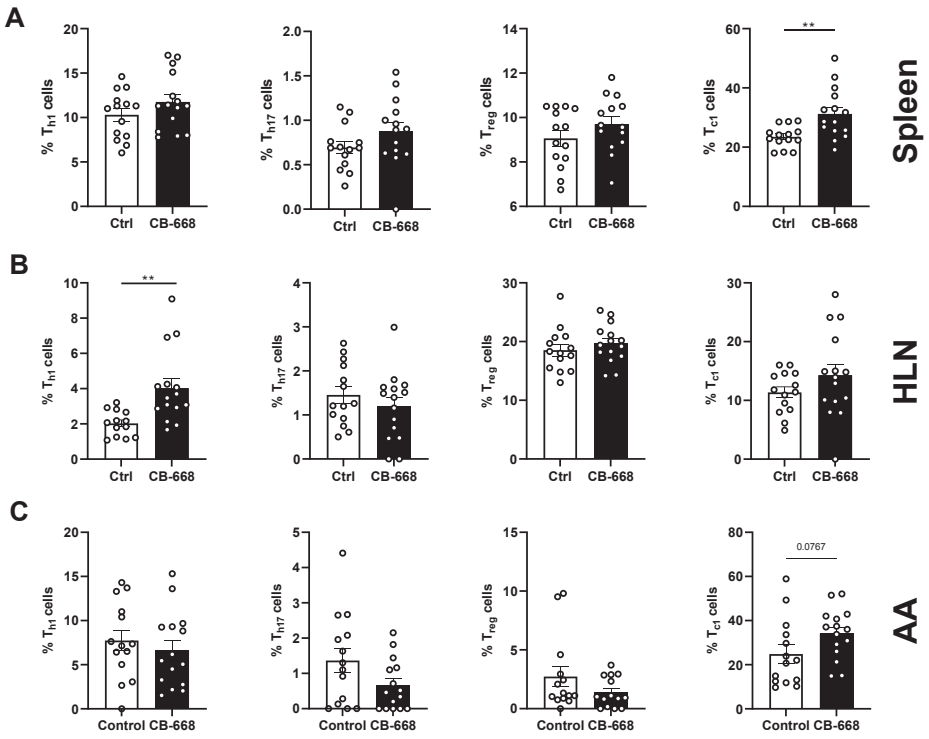

Figure 4. Blockage of IL4i1 does not have major effects on the CD4$^+$ and CD8$^+$ T cell subsets. **(A)** The percentages of T_h1 (CD4$^+$Tbet$^+$), T_h17 (CD4$^+$RORγT$^+$), regulatory T cells (T_{regs}; CD4$^+$FoxP3$^+$) and cytotoxic T cells (T_c1; CD8$^+$Tbet$^+$)(of live CD4 or CD8 cells) were determined in **(A)** the spleen, **(B)** HLN and **(C)** aortic arch (AA). Statistical significance was determined using an unpaired Students t-test ($p<0.05$*, $p<0.01$**). Data represent mean ± SEM (n = 14-15 per group).

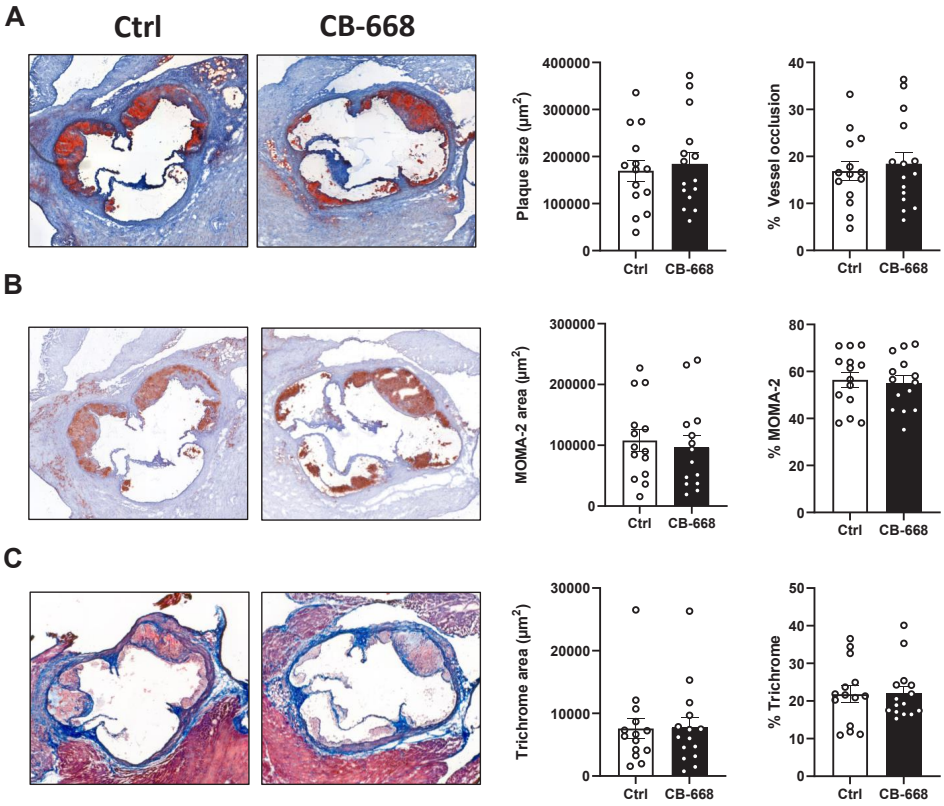

Figure 5. Inhibition of IL4I1 does not affect initial lesion development Representative pictures of aortic root atherosclerotic lesions stained with **(A)** Oil-red-O to visualize neutral lipids and quantification of the lesion size and vessel occlusion. **(B)** MOMA-2 antibodies for quantification of the absolute and relative macrophage content, and **(C)** Masson trichrome for quantification of the absolute and relative collagen content. Significance was determined using a Student's T-test. Individual data points and mean ± SEM (n = 14-15 per group).

Discussion

IL4I1 has been shown to be a promising immunological target for cancer treatment, as blockade induces cytotoxic $CD8^+$ T cell responses.[7] Cancer and atherosclerosis share multiple immunological pathways contributing to both diseases in different manners. Specific T cell responses are for example beneficial in cancer, but not in atherosclerosis. Moreover, scRNAseq data from human and murine atherosclerosis has shown that IL4I1 is highly expressed in myeloid cell subsets.[29] Intervening in the IL4I1 pathway could thus also affect this disease.

Our data demonstrate that IL4I1 inhibition by CB-668 treatment did not induce major effects on general immune cells on a systemic level. However, IL4I1 inhibition did lead to a shift from naïve to effector or central memory T cells, mainly by an increase in cytotoxic $CD8^+$ T cells in the spleen and a trend towards increased cytotoxic $CD8^+$ T cells the aortic arch. These results are in line with the effects observed in cancer, in which IL4I1 inhibition induced an accumulation of IFNγ-producing T_{c1} $CD8^+$ T cells in the tumor, which normally are activated through this pathway and impede tumor escape.[5,7] This suggests that IL4I1 secretion might be used as an immune evasion strategy by the tumor. Whereas cytotoxic $CD8^+$ T cells are beneficial in cancer, the role of these T cells in atherosclerosis is ambiguous. Both the phenotype induced by local stimuli present in the atherosclerotic lesion as well as the stage of atherosclerosis determines whether $CD8^+$ T cells exert pro-atherogenic or athero-protective functions.[30] Although the shift of naïve to effector or central memory T cells was abundant in the $CD8^+$ T cells, we did also observe this shift in $CD4^+$ T cells in the HLN. Olsen *et al*. has shown that decreased naïve and increased memory $CD4^+$ T cells are linked to subclinical atherosclerosis.[31] Although we observed increased effector and central memory $CD4^+$ T cells, we could not confirm the previously described *in vitro* effects of IL4I1 on T_{h17} and T_{regs} in our *in vivo* atherosclerosis model.[12,13] Nevertheless, we did see an increase in T_{h1} $CD4^+$ T cells in the HLN which, which corresponds with a previous *in vitro* study highlighting IL4I1 as inhibitor of T_{h1} proliferation upon interaction with IL4I1 secreting antigen presenting cells.[24]

IL4I1 inhibition results in a more systemic pro-inflammatory environment and a slight increase in T cell activation that might contribute to atherosclerosis development and progression. However, we did not find any differences in atherosclerotic plaque development or composition. The findings in our murine model suggest that treatment with the IL4I1 inhibitor to repress cancer might not induce the risk of atherosclerosis initiation. It, however, remains to be established if CD-668 treatment affects the progression or stability of advanced lesions, as human atherosclerosis is often asymptomatic and diagnosed at an advanced stage.[32] T cells predominantly play a role in the chronic inflammatory response leading to the formation of advanced atherosclerotic lesions.[33] Furthermore, in human atherosclerotic lesions, T cells make up the biggest and most diverse leukocyte population.[34] T cells constitute more than half of all leukocytes in human plaques, whereas in initial murine plaques T cells are less common and account for only between 6% to 25% of total leukocytes.[34–37] In advanced murine atherosclerotic lesions, the percentage T cells of total leukocytes is reported to increase.[34]

While murine models do not perfectly mimic human disease pathophysiology, they remain useful in the portrayal of immune cell-mediated immune responses in atherosclerosis.[39] In addition, comparison of coronary artery disease associated pathways from human genome wide associated studies with mouse studies has shown that the pathways involved in the immune system are highly overlapping.[40]

It is therefore likely that the increased pro-inflammatory $CD4^+$ and $CD8^+$ T cell subsets upon treatment with CB-668 in our study, could potentially affect advanced stages of atherosclerosis to a bigger extent. Furthermore, it would be of interest to examine if treatment with CB-668 in cancer patients with cardiovascular disease could lead to changes in the atherosclerotic plaque microenvironment to confirm in human subjects that this anticancer therapy is not correlated with an increased risk of cardiovascular disease development.[41]

In conclusion, our study demonstrated that inhibition of IL4I1 results in a more pro-inflammatory immune environment but does not affect initial atherosclerotic lesion development in $LDLr^{-/-}$ mice. Therefore, this study highlights that the use of CB-668 as an anti-cancer treatment does not lead to increased risk of atherosclerosis initiation. Still, further research will have to confirm whether inhibition of IL4I1 using CB-668 does not add to the risk of atherosclerosis progression and plaque destabilization, for example by including carotid intima-media thickness tests and the occurrence of major adverse cardiovascular events in clinical trial design.

References

1. Boulland, M.-L. *et al.* Human IL4I1 is a secreted L-phenylalanine oxidase expressed by mature dendritic cells that inhibits T-lymphocyte proliferation. *Blood* **110**, 220–227 (2007).
2. Copie-Bergman, C. *et al.* Interleukin 4–induced gene 1 is activated in primary mediastinal large B-cell lymphoma. *Blood* **101**, 2756–2761 (2003).
3. Carbonnelle-Puscian, A. *et al.* The novel immunosuppressive enzyme IL4I1 is expressed by neoplastic cells of several B-cell lymphomas and by tumor-associated macrophages. *Leukemia* **23**, 952–960 (2009).
4. Molinier-Frenkel, V., Prévost-Blondel, A. & Castellano, F. The IL4I1 Enzyme: A New Player in the Immunosuppressive Tumor Microenvironment. *Cells* **8**, 757 (2019).
5. Lasoudris, F. *et al.* IL4I1: an inhibitor of the CD8$^+$ antitumor T-cell response in vivo. *Eur. J. Immunol.* **41**, 1629–1638 (2011).
6. Bod, L. *et al.* IL4-induced gene 1 promotes tumor growth by shaping the immune microenvironment in melanoma. *Oncoimmunology* **6**, e1278331 (2017).
7. MacKinnon, A. *et al.* 705 Anti-tumor activity of CB-668, a potent, selective and orally bioavailable small-molecule inhibitor of the immuno-suppressive enzyme Interleukin 4 (IL-4)-Induced Gene 1 (IL4I1). in *Regular and young investigator award abstracts* A423.2-A424 (BMJ Publishing Group Ltd, 2020). doi:10.1136/jitc-2020-SITC2020.0705.
8. Bod, L. *et al.* IL-4-Induced Gene 1: A Negative Immune Checkpoint Controlling B Cell Differentiation and Activation. *J. Immunol. Baltim. Md 1950* **200**, 1027–1038 (2018).
9. Aubatin, A. *et al.* IL4-induced gene 1 is secreted at the immune synapse and modulates TCR activation independently of its enzymatic activity. *Eur. J. Immunol.* **48**, 106–119 (2018).
10. Santarlasci, V. *et al.* Rarity of human T helper 17 cells is due to retinoic acid orphan receptor-dependent mechanisms that limit their expansion. *Immunity* **36**, 201–214 (2012).
11. Scarlata, C.-M., Celse, C., Pignon, P., Ayyoub, M. & Valmori, D. Differential expression of the immunosuppressive enzyme IL4I1 in human induced Aiolos+, but not natural Helios+, FOXP3+ Treg cells. *Eur. J. Immunol.* **45**, 474–479 (2015).
12. Santarlasci, V. *et al.* IL-4-induced gene 1 maintains high Tob1 expression that contributes to TCR unresponsiveness in human T helper 17 cells. *Eur. J. Immunol.* **44**, 654–661 (2014).
13. Cousin, C. *et al.* The immunosuppressive enzyme IL4I1 promotes FoxP3(+) regulatory T lymphocyte differentiation. *Eur. J. Immunol.* **45**, 1772–1782 (2015).
14. Takeuchi, Y. & Nishikawa, H. Roles of regulatory T cells in cancer immunity. *Int. Immunol.* **28**, 401–409 (2016).
15. Depuydt Marie AC *et al.* Microanatomy of the Human Atherosclerotic Plaque by Single-Cell Transcriptomics. *Circ. Res.* **0**,.
16. Kim, K. *et al.* Transcriptome Analysis Reveals Nonfoamy Rather Than Foamy Plaque Macrophages Are Proinflammatory in Atherosclerotic Murine Models. *Circ. Res.* **123**, 1127–1142 (2018).
17. Liang, Y., Li, L., Chen, Y., Xiao, J. & Wei, D. PD-1/PD-L1 immune checkpoints: Tumor vs atherosclerotic progression. *Clin. Chim. Acta* **519**, 70–75 (2021).
18. Poels, K. *et al.* Antibody-Mediated Inhibition of CTLA4 Aggravates Atherosclerotic Plaque Inflammation and Progression in Hyperlipidemic Mice. *Cells* **9**, 1987 (2020).
19. Mocan-Hognogi, D. L. *et al.* Immune Checkpoint Inhibitors and the Heart. *Front. Cardiovasc. Med.* **8**, (2021).

20. Foks, A. C. & Kuiper, J. Immune checkpoint proteins: exploring their therapeutic potential to regulate atherosclerosis. *Br. J. Pharmacol.* **174**, 3940–3955 (2017).
21. Out, R. *et al.* Macrophage ABCG1 Deletion Disrupts Lipid Homeostasis in Alveolar Macrophages and Moderately Influences Atherosclerotic Lesion Development in LDL Receptor-Deficient Mice. *Arterioscler. Thromb. Vasc. Biol.* **26**, 2295–2300 (2006).
22. K, M. *et al.* Cross-tissue single-cell landscape of human monocytes and macrophages in health and disease. *Immunity* **54**, (2021).
23. Kuo, D. *et al.* HBEGF+ macrophages in rheumatoid arthritis induce fibroblast invasiveness. *Sci. Transl. Med.* **11**, eaau8587 (2019).
24. Marquet, J. *et al.* Dichotomy between factors inducing the immunosuppressive enzyme IL-4-induced gene 1 (IL4I1) in B lymphocytes and mononuclear phagocytes. *Eur. J. Immunol.* **40**, 2557–2568 (2010).
25. Willemsen, L. & de Winther, M. P. Macrophage subsets in atherosclerosis as defined by single-cell technologies. *J. Pathol.* **250**, 705–714 (2020).
26. Zernecke, A. *et al.* Integrated scRNA-seq analysis identifies conserved transcriptomic features of mononuclear phagocytes in mouse and human atherosclerosis. 2020.12.09.417535 Preprint at https://doi.org/10.1101/2020.12.09.417535 (2020).
27. Ma, W. F. *et al.* Enhanced single-cell RNA-seq workflow reveals coronary artery disease cellular cross-talk and candidate drug targets. *Atherosclerosis* **340**, 12–22 (2022).
28. Romagnani, S. IL4I1: Key immunoregulator at a crossroads of divergent T-cell functions. *Eur. J. Immunol.* **46**, 2302–2305 (2016).
29. Zernecke, A. *et al.* Meta-Analysis of Leukocyte Diversity in Atherosclerotic Mouse Aortas. *Circ. Res.* **127**, 402–426 (2020).
30. Schäfer, S. & Zernecke, A. CD8+ T Cells in Atherosclerosis. *Cells* **10**, E37 (2020).
31. Olson, N. C. *et al.* Decreased Naive and Increased Memory CD4+ T Cells Are Associated with Subclinical Atherosclerosis: The Multi-Ethnic Study of Atherosclerosis. *PLoS ONE* **8**, e71498 (2013).
32. Gatto, L. & Prati, F. Subclinical atherosclerosis: how and when to treat it? *Eur. Heart J. Suppl.* **22**, E87–E90 (2020).
33. Packard, R. R. S., Lichtman, A. H. & Libby, P. Innate and adaptive immunity in atherosclerosis. *Semin. Immunopathol.* **31**, 5–22 (2009).
34. Winkels, H. & Wolf, D. Heterogeneity of T Cells in Atherosclerosis Defined by Single-Cell RNA-Sequencing and Cytometry by Time of Flight. *Arterioscler. Thromb. Vasc. Biol.* **41**, 549–563 (2021).
35. Cochain, C. *et al.* Single-Cell RNA-Seq Reveals the Transcriptional Landscape and Heterogeneity of Aortic Macrophages in Murine AtherosclerosisNovelty and Significance. *Circ. Res.* **122**, 1661–1674 (2018).
36. Winkels, H. *et al.* Atlas of the Immune Cell Repertoire in Mouse Atherosclerosis Defined by Single-Cell RNA-Sequencing and Mass Cytometry. *Circ. Res.* **122**, 1675–1688 (2018).
37. Cole, J. E. *et al.* Immune cell census in murine atherosclerosis: cytometry by time of flight illuminates vascular myeloid cell diversity. *Cardiovasc. Res.* **114**, 1360–1371 (2018).
38. Paul, V. S. V., Paul, C. M. P. & Kuruvilla, S. Quantification of Various Inflammatory Cells in Advanced Atherosclerotic Plaques. *J. Clin. Diagn. Res. JCDR* **10**, EC35–EC38 (2016).
39. Bartlett, B., Ludewick, H. P., Misra, A., Lee, S. & Dwivedi, G. Macrophages and T cells in atherosclerosis: a translational perspective. *Am. J. Physiol. Heart Circ. Physiol.* **317**, H375–H386 (2019).

40. von Scheidt, M. *et al*. Applications and Limitations of Mouse Models for Understanding Human Atherosclerosis. *Cell Metab.* **25**, 248-261 (2017).
41. Mladosievicova, B. *et al*. Atherosclerosis in cancer patients. *Bratisl. Lek. Listy* **120**, 636-640 (2019).

Chapter 9

General discussion

Summary

Cardiovascular disease (CVD) remains the principal cause of mortality by comprising 32% of all deaths worldwide.[1,2] The majority of these cardiovascular deaths are attributed to myocardial infarction and stroke, with atherosclerosis as underlying cause of disease.[3] Atherosclerosis is characterized by excessive lipid accumulation in the arterial wall and a subsequent ongoing local inflammation. This chronic inflammatory disease induces continuous intimal growth of medium to large arteries resulting in the formation of atherosclerotic plaques.[4] With disease progression, these plaques further develop, become unstable and eventually rupture, leading to thrombus formation, ischaemia and subsequent clinical events. Revascularisation by means of anti-thrombotic treatment and/or surgical procedures is the primary therapeutic strategy upon a cardiovascular event. However, these surgical interventions, which include percutaneous transluminal coronary angioplasty, bypass surgery and carotid endarterectomy surgery, are highly invasive and may require repetition due to restenosis of the arteries.[5–8] Patients with either a history of CVD, or with familiar hypercholesterolemia and thus a high risk for disease development, are mainly treated with lipid-lowering therapeutics, such as statins and PCSK9 inhibitors. Although statins effectively lower circulating LDL cholesterol levels, recurrent events occur in over 20% of the symptomatic patients on high-dose statin treatment.[9,10] Considering that a large body of (experimental) studies have proven that the immune system plays a pivotal role in atherosclerosis development and progression, recent advances have been made to therapeutically target the ongoing chronic inflammation in CVD patients. Multiple clinical trials have provided proof-of-principle that targeting inflammation could alleviate CVD burden. The CANTOS trial was the first to prove this as treatment with a monoclonal antibody against IL-1β reduced the risk on recurrent cardiovascular events.[11] This was followed up by several other trials that applied immunosuppressive or anti-inflammatory agents, such as anti-TNF, methotrexate and colchicine, of which only the latter effectively reduced risk of ischemic cardiovascular events.[12–15] However, adverse effects caused by general immune suppression have also been described in these trials. As immunotherapy could also affect the host-defence response, the next challenge lies in the identification of more specific therapeutic targets that particularly target plaque-residing immune cells.

In the past decade, the rapid development of single-cell transcriptomics has revolutionized the bio-medical research field. Single-cell RNA sequencing (scRNA-seq) provides the full transcriptome on a per cell basis, thereby allowing a completely unbiased analysis of cellular phenotypes in heterogenous samples.[16] Single-cell RNA sequencing was first applied in 2009 by Tang *et al.*, who measured the whole-

transcriptome of a single cell.[17] By now, the technology has developed to such an extent that by using plate-based and microfluidic-based methods over thousands of single cells can be measured simultaneously.[18,19] The advantage of this technique is that it generates data at a much higher resolution, which results in a more detailed description of the cells and the possibility to detect rare cell populations that might become undetectable when applying more conventional techniques such as qPCR, microarray and bulk RNA sequencing.[20] Other approaches that measure on a single cell-level, such as immunohistochemistry, flow cytometry and cytometry by time-of-flight (CYTOF), are restricted by the use of a limited number of pre-defined targets that can be included for analysis.[20-22] Still, it remains of vital importance to keep using these techniques complementary to scRNA-seq analyses, especially as gene expression does not always correlate with protein levels. The field of single-cell transcriptomics has improved in such an extent, that currently the field moves towards single-cell multi-omics. This provides the opportunity to additionally identify the single-cell epigenome by measuring open chromatin regions (scATAC-seq), to assess clonality of respectively T and B cells by single-cell TCR and BCR sequencing and the opportunity to add an, in theory, indefinite number of monoclonal antibodies to simultaneously profile cell phenotype on protein level.[23] Altogether, single-cell multi-omics has proven to be a valuable tool in the understanding of disease development and in the identification of potential druggable targets.

This thesis

In this thesis, we applied single-cell multi-omics to generate a detailed cellular atlas of human atherosclerosis. We aimed to better characterize the cells that accumulate in advanced disease and subsequently employed this data set to define cells and genes that could be of therapeutic interest.

In the field of cardiovascular research, scRNA-seq has rapidly accelerated our understanding of vascular pathologies, including atherosclerosis and aortic aneurysm (AA). AA is the second aortic disease leading to cardiovascular death.[24,25] Due to progressive loss of vascular smooth muscle cells and extracellular matrix degradation the vascular wall becomes prone to rupture which results in severe clinical complications. In **chapter 2** we have provided an overview of the studies that have applied scRNA-seq to examine the cellular content of both diseases and reflect on potential similarities and differences between both diseases. Whereas AA is generally considered to be prominently affected by dysfunctional non-immune cells, including vascular smooth muscle cells, endothelial cells and fibroblasts,

scRNA-seq studies have strikingly described an established immune component to this disease as well. Both macrophages and T cells have been described in AA pathology, of which amongst others pro-inflammatory *IL1B*$^{+}$ macrophages and regulatory T cells were described with a similar phenotype in atherosclerosis. In AA, there has been more attention for a detailed description of fibroblasts compared to atherosclerosis, indicating the importance of these cells for this pathology. However, more recently, scRNA-seq has been applied to highlight the importance of fibroblasts in atherosclerosis as well.[26] Both in atherosclerosis and in AA, phenotypic modulation of smooth muscle cells is prominently described, often characterized by expression of genes involved in extracellular matrix regulation. In atherosclerosis, smooth muscle cell to macrophage transition is commonly described, whereas in AA the increased stress response leading to the loss of these cells in this disease is more pronounced. Endothelial dysfunction as consequence of inflammation was observed in both pathologies, however endothelial to mesenchymal transition was only observed in atherosclerosis studies. In both pathologies, the majority of the cellular communication pathways were between non-immune cells and macrophages, in which chemotaxis-related pathways were most commonly found. Yet, the only overlapping ligand-receptor pair between both diseases was the *C3-C3AR1* complement pathway. Although one could suggest that by targeting these pathways two birds are hit with one stone, this should be carefully interpreted as these cell subsets and pathways could have different functional properties in both diseases. Overall, this review highlights the extensive increased knowledge in vascular pathology that is obtained by scRNA-seq. The cellular content of both diseases has been shown to be much more diverse and dynamic than previously thought. ScRNA-seq will therefore be instrumental in further defining disease mechanisms and candidate targets for drug development.

Cellular atlas of the human atherosclerotic plaque by single cell transcriptomics

Atherosclerotic plaques are characterized by their heterogeneity in cellular content. To generate an unbiased immune cell atlas of murine atherosclerosis, in 2018, scRNA-seq was for the first time applied in atherosclerosis.[27,28] This showed the enormous potential of this technique as it led to the identification of amongst others TREM2^{+} macrophages, which by now have been proven to play a prominent role in atherosclerosis.[29,30] Subsequently, the immune cell content of human atherosclerotic plaques was first investigated by Fernandez *et al*. using a combination of CYTOF and scRNA-seq.[31] Yet, a full description of the cellular landscape of human atherosclerosis, including non-immune cells, was still lacking. Therefore, in **chapter 3**, we performed scRNA-seq and scATAC-seq on advanced human carotid plaques of a cohort of 18

patients and provide an overview of the various cell (sub)types present. We revealed 14 main cell populations and described their activation status, cellular plasticity and we examined potential pathways of intercellular communication. Finally, we integrated our data with existing cardiovascular GWAS data to map susceptibility genes to our identified cell populations.

Interestingly, we detected that the intraplaque leukocyte population predominantly consisted of T cells, encompassing over 50% of the analysed cells. Although the proportions of the cells present in the plaque could be affected by tissue dissociation[32], we could confirm by histological analysis that T cells indeed outnumbered myeloid cells in the human carotid atherosclerotic plaques. We showed that both $CD4^+$ and $CD8^+$ T cell subsets were mainly distinguished based on their activation status, rather than the conventional transcription factors that are classically used. Specifically of interest was the population of cytotoxic $CD4^+$ T cells that lacked *CD28* expression but did express *PRF1* and multiple granzymes, including Granzyme B. These cells had been previously found in the circulation of coronary artery disease patients [33,34], and now we could confirm their presence in the plaque on a cellular level as well. Whereas we were unable to detect cytokine expression, we did detect open chromatin regions of *IFNG* in this population.

Within the myeloid compartment, we observed one *CD1C* expressing dendritic cell cluster and three macrophage subsets, of which two proinflammatory and one anti-inflammatory foam cell-like cluster. The *IL1B*$^+$ macrophages express genes that are associated with inflammasome and caspase activity.[35,36] Likely, this subset could have been a target in the CANTOS trial, as well as in the LoDoCo trials, since colchicine has been shown to reduce NLRP3 activation.[11,13,15,37,38] The second pro-inflammatory subset was characterized by expression of *TNF* and *TLR4*, but also showed an enrichment for motifs from IFN-induced transcription factors. We hypothesized that the IFN-γ secreted by the $CD4^+CD28^{null}$ T cells could, in part, induce this pro-inflammatory macrophage phenotype. In line, scATAC-seq also revealed gene activation of *IL12* in the dendritic cell cluster, further confirming that the previously described IFN-γ-IL-12 loop could contribute to the local pro-inflammatory environment in the human plaque.[39–41] The last macrophage subset was characterized as a foam cell-like subset due to expression of *TREM2* and other lipid accumulation-associated genes, such as *ABCA1* and *ABCG1* and enrichment for lipid-associated LXR_RXR transcription factor motifs.[42,43] Whereas for long foam cells were considered pro-inflammatory, both *in vivo* and single-cell studies have shown that these cells are of anti-inflammatory nature instead.[29,44]

Due to the high resolution obtained with single-cell technologies, subtle phenotypic differences, such as cellular plasticity, can be detected. In this chapter, we also provided evidence for trans-differentiation of cells in the human plaque. Within the *TREM2* macrophage cluster, we detected expression of smooth-muscle cell associated genes. Lineage tracing studies in mice have reported that smooth muscle cells are also capable of lipid uptake and of differentiation into a macrophage-like cell.[45-47] Within the endothelial cells, we observed a similar phenomenon. Apart from angiogenesis-related gene signatures, we found a subset of *ACTA2*$^{+}$ endothelial cells, indicative of endothelial cells that underwent endothelial-to-mesenchymal transition, which occurs in inflammatory conditions.[48,49]

Apart from an extensive characterization of the cellular content of the plaque, we envisioned this data set as tool to simultaneously aid research into novel drug targets. Hereto, we predicted intercellular communication routes within the plaque. We mainly identified interactions involved in chemotaxis and extravasation of myeloid cells between endothelial cells and smooth muscle cells. Moreover, we predicted pathways that could be involved in t cell recruitment and activation. Finally, we used this data set to map candidate genes that have common variants in coronary artery disease (CAD) GWAS susceptibility loci on a single cell level. Even though GWAS has provided many genes of interest that could be causally related to cardiovascular disease, it remains challenging to identify which candidate genes have clinical potential and how to target them. By mapping them on a single cell level, direct functional tests can be performed to assess patient-driven druggable targets. We observed significant enrichment of these CAD GWAS hits in the macrophages, endothelial cells and smooth muscle cells. Future pre-clinical studies using both *in vitro* and *in vivo* models will be required to examine the function of the mapped CAD target genes in these cells to address how they contribute to disease progression.

Altogether, we have defined the microanatomy of the human atherosclerotic plaque by single cell technologies and provided two examples of how this data can be employed in the future. Throughout the rest of the chapters of this thesis, we have used this data set as basis for the definition of cells of interest and specific target finding and have validated these subsequently.

An autoimmune-like component in atherosclerosis

The role of T cells in atherosclerosis has been studied extensively. Within experimental studies, both atherogenic and atheroprotective mechanisms have been described for the different subsets.[50-53] As described in **chapter 3** and by Fernandez *et al.*[31], a large number of T cells can be found in human atherosclerotic plaques. Yet, what drives these T cells to migrate to the plaque and if they undergo antigen-specific activation remained elusive.

For this reason, in **chapter 4**, we performed single-cell TCR sequencing (scTCR-seq) on matched PBMC and human advanced carotid plaques investigate the extent of TCR clonality in the plaque and to assess the activation status of these antigen-specific T cells. In line with previous work, we observed that $CD8^+$ T cells were considerably more expanded in the plaque compared to $CD4^+$ T cells.[54] However, by using matched PBMC samples we showed that the proportion of clonally expanded $CD8^+$ T cells was equally represented or even overrepresented in the circulation, whereas we did observe an increased fraction of clonally expanded $CD4^+$ T cells in the plaque compared to PBMC. We identified one specific plaque-enriched clonally expanded $CD4^+$ T cell subset, that had a gene signature indicative of recent antigen-induced activation. Apart from this effector subset, we also detected a clear regulatory T cell (T_{reg}) subset with an antigen activation signature. Nevertheless, we only detected a small proportion of clonally expanded T_{regs}, which were furthermore detected in similar proportions in both environments. Interestingly, by applying lineage tracing we detected a clear path from the *CCR4*$^+$*CCR10*$^+$ migratory subset in the PBMC towards the plaque-enriched effector $CD4^+$ T cells. This suggests that these migratory cells could be a circulating precursor, which was further supported by the multiple overlapping TCR clones between both cell types of which a considerable amount was enriched in the plaque. Subsequently, we were interested to see whether we could identify interactions between these effector $CD4^+$ T cells and local antigen presenting cells in the plaque. There is contrasting evidence regarding how antigen-presentation in the lesion contributes to disease progression. The current hypothesis is that the location of the antigen-presentation is essential for the outcome of the T cell activation, in which the plaque environment should induce an atheroprotective T cell response.[55,56] Yet, we showed that pathogenic interactions may also occur in the lesion, as we predicted a co-stimulatory interaction through the CD40-CD40L pathway between lesional *TREM2*$^+$ myeloid cells and the plaque-enriched effector $CD4^+$ T cells. By showing an accumulation of antigen-specific T cells in the plaque, we hypothesized that there may be an autoimmune component to atherosclerosis. We therefore compared the transcriptome of the $CD4^+$ T cells to that in the synovial fluid of patients with the autoimmune disease psoriatic arthritis and found substantial similarities which supported this theory. In line with our results, scTCR-seq of atherosclerotic plaques, artery tertiary lymphoid organs (ATLOs) and draining lymph nodes of aged *apoE*$^{-/-}$ displayed similar clonal expansion of $CD4^+$ T cells in the plaque and ATLOs of these mice and revealed a predominantly pro-inflammatory phenotype of dendritic cells in ATLOs as well.[57] Altogether, these data support the notion that the pathophysiology of atherosclerosis has an autoimmune component, highlighting its potential for the development of novel therapeutic targets.

Mast cell activation and migration in advanced atherosclerosis

Whereas the largest population of immune cells was ascribed to T cells in **chapter 3**, the smallest population was a distinct cluster of mast cells. Albeit in low numbers, mast cells have been proven to significantly contribute to atherosclerosis progression. In experimental models for atherosclerosis, mast cells promote plaque vulnerability amongst others due to the proteases they secrete.[58–61] Moreover, the number of intraplaque mast cells was positively associated with future cardiovascular events independent of the main CVD risk factors.[62] Here, we aimed to further characterize human intraplaque mast cells, examine whether we could detect age-related changes and investigated whether we could inhibit mast cell migration towards the plaque.

In **chapter 5**, we set up a flow-cytometry based approach to better characterize mast cell numbers and phenotype in a cohort of plaques obtained from both carotid and femoral endarterectomy surgery. First, we established that approximately 1% of all $CD45^+$ leukocytes consists of mast cells, as identified by high expression of classical mast cell markers CD117 and FcεRI. Subsequently, we investigated mast cell activation status. Whereas mast cell activation in human atherosclerosis was generally assessed with immunohistochemical tryptase staining to visualize degranulation, we applied flow cytometry to address mast cell activation status. Notably, the majority of the intraplaque mast cells were found to be activated as measured by CD63 expression, a tetraspanin upregulated upon mast cell degranulation.[63] The most prominent route of mast cell activation is the FcεRI-IgE pathway.[64–67] Circulating IgE has been positively correlated to acute cardiovascular events[68,69], however whether IgE was also bound to the activated mast cells was yet to be determined. Therefore, we subsequently measured IgE on the intraplaque mast cells. Indeed, the majority of the activated mast cells had IgE bound to their surface. As in experimental models of atherosclerosis mast cell stabilization has been proven to moderate atherosclerosis development[58], a potential therapeutic strategy could be to limit circulating IgE thereby aiming for reduced intraplaque mast cell activation. In addition, we also observed a population of IgE^-CD63^+ mast cells, which have likely been activated through other pathways. It remains to be determined which pathways underlie this activation. Finally, we showed by flow cytometry that not all mast cells are positive for tryptase, indicating that immunohistochemical staining may not include all mast cells present in atherosclerosis. Therefore, we believe that this flow cytometry approach is a valid method to examine mast cells in human atherosclerosis. Future studies in larger cohorts could shed light on how certain activation patterns of mast cells may be correlated to clinical outcomes, thereby paving the way for new therapeutic approaches to target mast cells in atherosclerosis.

Aging is an independent risk factor for atherosclerosis. This is in part mediated by the low-grade chronic inflammation, termed inflammaging, that occurs with age. The pro-inflammatory conditions significantly affect the plaque-residing immune cells. Recent work has described multiple age-associated changes in intraplaque immune cells and confirmed these findings in human CVD patients.[70] Mast cells function has also been shown to alter with age[71–74], however it remained unknown whether they also undergo age-associated changes in atherosclerosis. Therefore, in **chapter 6**, we examined the effect of aging on mast cell phenotype and activation status. We examined mast cell populations in young and old *Ldlr*$^{-/-}$ mice and show an increased accumulation of mast cells in the aged atherosclerotic aorta and peritoneum. There is some disparity between tissues as to whether aging induces or inhibits mast cell activation.[72,74] Here, we observed that with age, mast cells exert a predominantly activated phenotype. Moreover, we observed increased serum IgE levels in aged *Ldlr*$^{-/-}$ mice, suggesting that the IgE-FcεRI pathway is involved in this increased activation. Congruently, we observed a similar mast cell phenotype in **chapter 5** in human plaques, which are generally obtained from elderly patients. Interestingly, we detected intrinsic mast cell activation in aged bone-marrow derived mast cells, which was accompanied by increased CCL2 secretion upon stimulation. The low-grade activation phenotype was not sustained upon adoptive transfer of these aged cells into young mast-cell deficient *apoE*$^{-/-}$*Kit*$^{W\text{-}sh/W\text{-}sh}$ mice and no differences were observed in myeloid cell recruitment as well. This can in part be explained by the fact that mast cell phenotype is largely dependent on the inflammatory environment in which the mast cell resides.[75–79] These results therefore highlight an instrumental role of the microenvironment for mast cell phenotype in atherosclerosis.

Although mast cell activation and degranulation are the most prominent line of investigation, mast cells have also been described to act as atypical antigen-presenting cell.[80] Indeed, mast cells have been found in close proximity to CD4$^+$ T cells in the skin of psoriasis patients and mast cell depletion resulted in reduced CD4$^+$ T cell infiltration and activation in a murine model of multiple sclerosis.[81,82] Furthermore, previous work from our lab has shown that hypercholesterolemia significantly upregulates MHC-II expression on mast cells.[83] Moreover, these mast cells were proven to be capable of functional antigen-presentation to CD4$^+$ T cells *in vivo* and mast cell depletion reduced CD4$^+$ T cell numbers in the atherosclerotic aorta. Considering the in **chapter 3** and **4** described importance of CD4$^+$ T cells in human atherosclerosis, we were particularly interested to examine whether aging also affects these antigen-presenting capacities of mast cells. Increased numbers of MHC-II$^+$ mast cells were retrieved in the aged atherosclerotic aorta compared to young. Notably, we reported increased CD4$^+$ T cell proliferation upon incubation with aged MHC-II$^+$ mast cells versus their young

counterparts, indicating that aged mast cells are capable of antigen internalization and direct presentation to $CD4^+$ T cells. However, similar to the activation profile of the mast cells, MHC-II upregulation is likely also influenced by the microenvironment as this was also lost upon reintroduction in a young microenvironment. Apart from direct antigen presentation, mast cells have also been shown to affect $CD4^+$ T cell polarization by the cytokines secreted upon activation.[84] So, we hypothesized that, although local antigen-presentation by mast cells could take place in the plaque, the aged mast cell secretome is likely to play a more important role in $CD4^+$ T cell differentiation. Indeed, we observed that treatment of aged *Ldlr*$^{-/-}$ mice with the mast cell stabilizer DSCG significantly reduced systemic and intraplaque effector $CD4^+$ T cells, in particular $FoxP3^+$ and $T\text{-}bet^+$ $CD4^+$ T cells. Conclusively, we show that aging and the inflammaging microenvironment significantly contributes to mast cell phenotype and function in atherosclerosis. This affects both their activation and degranulation as well as the subsequent changes on $CD4^+$ T cell phenotype in the plaque. It is therefore essential to consider age as important factor when further investigating mast cells for novel therapeutic interventions for atherosclerosis.

Because of the increased accumulation and activation of mast cells in advanced atherosclerosis [85], a promising therapeutic strategy could be to inhibit mast cell recruitment towards the atherosclerotic lesion to prevent plaque destabilization. One way of targeting this migration is through lipid mediators.[86,87] Leukotriene B4 (LTB_4) is a pro-inflammatory lipid mediator which has the leukotriene B4 receptor (BLT1) as its most potent receptor.[88] LTB_4 is synthesized as a result of the enzymatic reaction of arachidonic acid by 5-lipoxygenase (5-LOX), 5-lipoxygenase activating protein (FLAP) and LTA4 hydrolase (LTA4H).[89] The BLT1-LTB_4 axis has been shown to play a role in the recruitment of multiple immune cells, including myeloid cells and mast cell progenitors.[90–92] This chemotactic pathway has already been extensively researched in the context of atherosclerosis. Both genetic deletion and pharmacological inhibition of BLT1 or 5-LOX have been shown to reduce initial atherosclerosis development, in part due to reduced macrophage content in the plaque.[93–96] Yet, whether this lipid mediator also contributes to immune cell, and in particular mast cell, recruitment in pre-existing atherosclerosis remained elusive. Therefore, in **chapter 7** we examined whether BLT1-inhibition could reduce mast cell migration in advanced atherosclerosis. We first examined expression of the previously mentioned genes involved in the biosynthesis of LTB_4 were expressed in our single-cell human plaque atlas (**chapter 3**). Indeed, we detected expression of all genes in the myeloid compartment, but particularly high expression in the mast cells. Subsequently, we treated *Ldlr*$^{-/-}$ with established atherosclerosis with the BL1-antagonist CP105,696. We observed significantly reduced splenic myeloid cells, which is could be a direct effect of BLT1

inhibition, but is also congruent with the notion that upon LTB_4 binding, monocytes can actively synthesize monocyte-chemoattractant protein 1 (MCP-1) to enhance their recruitment.[97,98] We did not observe any changes in plaque size and morphology upon treatment with CP105,696. Likely, this treatment is less sufficient in more advanced atherosclerosis, which is in line with a previous study from Aiello *et al.*, who described the most pronounced effect of BLT1 antagonism in early lesions.[94] Finally, we did not observe any changes in the numbers of circulating mast cell progenitors nor the number of mast cells in the atherosclerotic aortic root. This suggests that in advanced atherosclerosis the BLT1-LTB_4 axis is not involved in mast cell recruitment to the site of disease. Of note, the low affinity BLT2 receptor could also induce mast cell migration.[92] As CP105,696 is BLT1-specific, we cannot exclude potential BLT2-induced mast cell migration in this study and this will need further investigation. Although BLT1-antagonism is apparently not the right approach to intervene with mast cell migration in advanced atherosclerosis, we did establish local LTB_4 production by mast cells in the human atherosclerotic plaque, which consequently could contribute to the intraplaque (immune) cell content. Overall, we are convinced that targeting mast cell migration, albeit through a different pathway, remains a promising strategy to intervene with atherosclerosis progression.

Single cell atlas as tool for the identification of druggable targets

Many potential targets have already been investigated for atherosclerosis, yet unfortunately the translation to the clinic is often unsuccessful. As previously mentioned, we generated the cellular atlas in **chapter 3** to improve the understanding of the pathophysiology of atherosclerosis and to aid in the definition of druggable targets. In **chapter 8** we employed this tool and found specific expression of *IL4I1* within the *TREM2*$^+$ macrophages. Interleukin-4-induced gene-1 (IL4I1) is an enzyme which is primarily produced by antigen-presenting cells and it induces the conversion of its substrate L-phenyl alanine into phenyl pyruvate, ammonia and hydrogen peroxide.[99,100] IL4I1 specifically accumulates in the immune synapse and subsequently interferes with T cell proliferation and promotes differentiation towards T_{regs}.[101] IL4I1 was originally discovered in different types of cancer and inhibition of this enzyme has been shown to significantly reduce tumor growth by increasing the cytotoxic $CD8^+$ T cell response.[102] Recently, a specific small-molecule IL4I1-inhibitor, CB-668, was reported to reduce tumor growth by interference with the $CD8^+$ T cell response.[103] Although cancer and atherosclerosis share mutual inflammatory pathways, the favorable response is often contradictory. Especially with immune checkpoint therapies, increased risk for cardiovascular disease has been reported repeatedly.[104,105] We therefore examined whether IL4I1-inhibition with CB-668 affected atherosclerosis progression in *Ldlr*$^{-/-}$ mice. In line

with the previously highlighted results, we observed a shift from naive towards effector and central memory T cells in the spleen. Furthermore, we observed an increase in splenic cytotoxic $CD8^+$ T cells and a trend towards an increase in the atherosclerotic aorta. Within the draining lymph node, we also observed an increase in pro-inflammatory T_{h1} $CD4^+$ T cells, altogether emphasizing the pro-inflammatory response induced upon CB-668 treatment. Nevertheless, we did not observe any changes in atherosclerotic lesion size and composition. Here, we examined IL4I1 inhibition in initial atherosclerosis, whereas more pronounced effects could occur in more advanced stages of the disease. So, even though our data demonstrated that IL4I1 antagonism does not affect initial atherosclerosis development, future studies will have to pinpoint if the induced pro-inflammatory microenvironment will further promote disease progression in advanced stages.

Future perspectives

Recent advances in the field have proven the enormous potential for targeting the immune system to treat atherosclerosis. Multiple trials targeting the immune system in atherosclerotic cardiovascular disease patients have proven beneficial cardiovascular outcomes. However, not all immunotherapies were successful in ameliorating disease burden. The heterogenous and plastic immune cells in the atherosclerotic plaque harbor both atherogenic and atheroprotective populations, each affecting disease progression differently. It is therefore essential to provide a more tailored approach to identify specific processes that can be targeted to restore the immunological balance within the lesion. The rapidly evolving single-cell technologies will become of vital importance when advancing towards precision medicine for atherosclerosis.

In the past decade, the datasets generated by single-cell multi-omics have provided an important tool for future therapeutic targeting of atherosclerosis. These studies have highlighted the delicate changes in cellular phenotype and provided crucial new insights in the disease. Apart from a detailed description of the transcriptome of the cells present in the plaque, advanced computational analyses of this data have also elucidated trajectories of cellular differentiation. For instance, in this thesis we describe a circulating precursor for the intraplaque antigen-specific effector $CD4^+$ T cell subset and recent work has extensively described macrophage plasticity in atherosclerosis which revealed that the anti-inflammatory *TREM2*$^+$ macrophages could also further differentiate into a pro-inflammatory lipid-associate macrophage phenotype.[106] It will be also of interest to correlate specific cell populations or gene signatures to clinical parameters to identify causal relationships. Importantly,

recent work has applied single-cell data as tool for drug repurposing to identify new therapeutic strategies for atherosclerosis.[107] By using a systems-immunology based approach, inflammatory signatures were screened for existing drugs that may target prominent pathways. This targeted approach allows for more rapid pre-clinical testing and accelerates the transition to the clinic.

Another common practice in single-cell analysis, is the prediction of intercellular communication to highlight important pathways for intervention.[31,108] Although this provides a proper idea on what cells could potentially interact, it also touches upon one of the limitations of single-cell technologies. As a single-cell suspension is needed, tissue dissociation is required. This could not only slightly affect the ratio of cell types present in the plaque, but you also lose the spatial architecture of the tissue.[32] Spatial transcriptomics have been introduced to overcome this issue.[109] In the context of this thesis it will be very valuable to apply this technique to examine interactions between antigen-presenting cells, including mast cells, and T cells to further define whether indeed the CD40-CD40L pathway is as important for antigen-specific activation of plaque $CD4^+$ T cells or if there are other more pronounced pathways involved in this process.

Now that we have established the accumulation of plaque-enriched antigen-specific T cells in the plaque, this immediately raises the question which antigen(s) initiate this T cell response. Several candidate antigens have been examined in atherosclerosis, including heat shock proteins, plasma protein β2-glycoprotein Ib and fibronectin.[110] Yet, T cell responses against peptides originating from Apolipoprotein B100 (ApoB100) have been investigated most prominently. Since vaccination with LDL and ox-LDL were shown to be atheroprotective[111–113], several methods have been applied to further define the exact antigens involved. This includes epitope-binding assays as well as prediction models that calculate MHC-II binding affinity.[114,115] Altogether these discovered auto-antigens have been proven to have therapeutic potential in experimental models of atherosclerosis.[116–118] However, with the advance of single-cell TCR sequencing and the identification of clonally expanded T cells in the tissue itself, there is a need to bridge the gap from TCR to peptide. Bioinformatic tools such as GLIPH2 and GIANA have been applied in atherosclerosis previously,[54,119,120] Although theses computational approaches have high potential, in our data this did not give the desired accuracy yet. An upcoming different approach to examine auto-antigen is by the use of immunopeptidomics. This technique allows the measurement of peptides presented on MHC molecules at the site of disease.[121] It will be of great importance to apply this technique to human atherosclerosis and to define its immunopeptidome, which may be a great tool for future vaccine development.

Finally, we provide evidence that targeting mast cells in atherosclerosis could be an effective therapeutic strategy. Either through inhibiting their highly activated state or by targeting mast cell recruitment to the plaque, atherosclerotic burden can be ameliorated. As our data demonstrate that IgE could significantly contribute to intraplaque mast cell activation, it will be of interest to treat patients with IgE-blocking antibodies, such as Omalizumab[122], to see how this affects atherosclerosis progression. Even though we were not yet able to define the prominent pathways involved in mast cell migration to the atherosclerotic plaque, we believe it is crucial to further examine this in the future.

Apart from drug target finding and validation, single-cell technologies could also be applied for diagnostic approaches. Currently, early detection of atherosclerotic cardiovascular disease is a prominent focus point in the research field. Therefore, it is essential to define new biomarkers for this disease. As mentioned before, if clinical parameters could be associated to certain pathological cell subsets, this could improve risk prediction. Additionally, by examining whether the cell subsets detected in the plaque also occur in the circulation or if we can find pre-cursors of pathogenic subsets, these could potentially be used as biomarker. Based on the work in this thesis, it could be of interest to further define if the $CCR4^{+}CCR10^{+}$ precursor $CD4^{+}$ T cells could be associated to future cardiovascular outcomes. Furthermore, investigating if circulating $CD4^{+}CD28^{null}$ cells could also be correlated to their intraplaque counterparts could be very relevant. In addition, measuring mast cell progenitors in the circulation could potentially also be a tool to predict plaque stability. Lastly, there lies great potential in the use of single-cell technologies for patient stratification and to predict drug response by the presence or absence of therapeutically relevant markers. In cancer, this has already been applied to define patients that are more likely to be a good responder to chemo- or immunotherapy.[20,123] In atherosclerosis, differences between immune cells of symptomatic and asymptomatic patients have been described previously on a single cell level[31], but gene signatures predicting response to cardiovascular therapeutics are yet to be determined. To aid in the challenges described above, it is of importance to assess whether there is similarity in cellular content between all vascular beds, or even to pinpoint significant differences. Currently, scRNA-seq is applied in human plaques originating from either carotid or coronary arteries. In a recent study, an integrated analysis has been performed on mononuclear phagocytes from two studies that used respectively carotid and coronary plaques.[31,124,125] This showed that, apart from some interpatient variability in the proportions, all myeloid subclusters were conserved in both tissues. To define proper biomarkers for all atherosclerosis patients, it will be valuable to further increase this meta-analysis by increasing the number of patients and studies and to elaborate on all cells detected within both vascular beds.

In conclusion, the work in this thesis shows that single-cell transcriptomics is a valuable tool to examine the pathophysiology of atherosclerosis in detail and to identify novel targets for intervention. It will be intriguing to see how the untapped potential of single-cell technologies will aid in tackling the challenges that lie ahead towards a tailored therapy for atherosclerosis.

References

1. World Health Organization. Cardiovascular diseases (CVDs). https://www.who.int/news-room/fact-sheets/detail/cardiovascular-diseases-(cvds) (2021).
2. World Health Organization. Noncommunicable diseases. https://www.who.int/news-room/fact-sheets/detail/noncommunicable-diseases (2022).
3. Timmis, A. *et al.* European Society of Cardiology: cardiovascular disease statistics 2021. *Eur Heart J* **43**, 716–799 (2022).
4. Bäck, M., Yurdagul, A., Tabas, I., Öörni, K. & Kovanen, P. T. Inflammation and its resolution in atherosclerosis: mediators and therapeutic opportunities. *Nature Reviews Cardiology 2019 16:7* **16**, 389–406 (2019).
5. Braunwald, E. The treatment of acute myocardial infarction: the Past, the Present, and the Future. *Eur Heart J Acute Cardiovasc Care* **1**, 9–12 (2012).
6. Michaels, A. D. & Chatterjee, K. Angioplasty Versus Bypass Surgery for Coronary Artery Disease. *Circulation* **106**, (2002).
7. Bonati, L. H. *et al.* European Stroke Organisation guideline on endarterectomy and stenting for carotid artery stenosis. *Eur Stroke J* **6**, I–XLVII (2021).
8. Calvillo-King, L., Xuan, L., Zhang, S., Tuhrim, S. & Halm, E. A. Predicting Risk of Perioperative Death and Stroke After Carotid Endarterectomy in Asymptomatic Patients: Derivation and Validation of a Clinical Risk Score. *Stroke; a journal of cerebral circulation* **41**, 2786 (2010).
9. Cannon, C. P. *et al.* Intensive versus moderate lipid lowering with statins after acute coronary syndromes. *N Engl J Med* **350**, 1495–1504 (2004).
10. Libby, P., Ridker, P. M. & Hansson, G. K. Progress and challenges in translating the biology of atherosclerosis. *Nature* **473**, 317–325 (2011).
11. Ridker, P. M. *et al.* Antiinflammatory Therapy with Canakinumab for Atherosclerotic Disease. *New England Journal of Medicine* **377**, 1119–1132 (2017).
12. Chung, E. S., Packer, M., Lo, K. H., Fasanmade, A. A. & Willerson, J. T. Randomized, Double-Blind, Placebo-Controlled, Pilot Trial of Infliximab, a Chimeric Monoclonal Antibody to Tumor Necrosis Factor-α, in Patients With Moderate-to-Severe Heart Failure. *Circulation* **107**, 3133–3140 (2003).
13. Nidorf, S. M. *et al.* Colchicine in Patients with Chronic Coronary Disease. *New England Journal of Medicine* **383**, 1838–1847 (2020).
14. Tardif, J.-C. *et al.* Efficacy and Safety of Low-Dose Colchicine after Myocardial Infarction. *New England Journal of Medicine* **381**, 2497–2505 (2019).
15. Opstal, T. S. J. *et al.* Long-Term Efficacy of Colchicine in Patients With Chronic Coronary Disease: Insights From LoDoCo2. *Circulation* **145**, 626–628 (2022).
16. Kashima, Y. *et al.* Single-cell sequencing techniques from individual to multiomics analyses. *Experimental & Molecular Medicine 2020 52:9* **52**, 1419–1427 (2020).
17. Tang, F. *et al.* mRNA-Seq whole-transcriptome analysis of a single cell. *Nature Methods 2009 6:5* **6**, 377–382 (2009).
18. Svensson, V., Vento-Tormo, R. & Teichmann, S. A. Exponential scaling of single-cell RNA-seq in the past decade. *Nature Protocols 2018 13:4* **13**, 599–604 (2018).
19. Aldridge, S. & Teichmann, S. A. Single cell transcriptomics comes of age. *Nature Communications 2020 11:1* **11**, 1–4 (2020).
20. Van de Sande, B. *et al.* Applications of single-cell RNA sequencing in drug discovery and development. *Nature Reviews Drug Discovery 2023 22:6* **22**, 496–520 (2023).

21. Cheung, R. K. & Utz, P. J. CyTOF—the next generation of cell detection. *Nature Reviews Rheumatology 2011 7:9* **7**, 502–503 (2011).
22. Nassar, A. F., Ogura, H. & Wisnewski, A. V. Impact of recent innovations in the use of mass cytometry in support of drug development. *Drug Discov Today* **20**, 1169–1175 (2015).
23. Baysoy, A., Bai, Z., Satija, R. & Fan, R. The technological landscape and applications of single-cell multi-omics. *Nature Reviews Molecular Cell Biology 2023 24:10* **24**, 695–713 (2023).
24. Sakalihasan, N. *et al.* Abdominal aortic aneurysms. *Nat Rev Dis Primers* **4**, 1–22 (2018).
25. Senser, E. M., Misra, S. & Henkin, S. Thoracic Aortic Aneurysm: A Clinical Review. *Cardiol Clin* **39**, 505–515 (2021).
26. van Kuijk, K. *et al.* Human and murine fibroblast single-cell transcriptomics reveals fibroblast clusters are differentially affected by ageing and serum cholesterol. *Cardiovasc Res* **119**, 1509–1523 (2023).
27. Winkels, H. *et al.* Atlas of the Immune Cell Repertoire in Mouse Atherosclerosis Defined by Single-Cell RNA-Sequencing and Mass Cytometry. *Circ Res* **122**, 1675–1688 (2018).
28. Cochain, C. *et al.* Single-Cell RNA-Seq Reveals the Transcriptional Landscape and Heterogeneity of Aortic Macrophages in Murine Atherosclerosis. *Circ Res* **122**, 1661–1674 (2018).
29. Kim, K. *et al.* Transcriptome Analysis Reveals Nonfoamy Rather Than Foamy Plaque Macrophages Are Proinflammatory in Atherosclerotic Murine Models. *Circ Res* **123**, 1127–1142 (2018).
30. Willemsen, L. & de Winther, M. P. J. Macrophage subsets in atherosclerosis as defined by single-cell technologies. *J Pathol* **250**, 705–714 (2020).
31. Fernandez, D. M. *et al.* Single-cell immune landscape of human atherosclerotic plaques. *Natuere Medicine* **25**, 1576–1588 (2019).
32. Fernandez, D. M. & Giannarelli, C. Immune cell profiling in atherosclerosis: role in research and precision medicine. *Nature Reviews Cardiology 2021 19:1* **19**, 43–58 (2021).
33. Liuzzo, G. *et al.* Unusual CD4+CD28null T Lymphocytes and Recurrence of Acute Coronary Events. *J Am Coll Cardiol* **50**, 1450–1458 (2007).
34. Téo, F. H. *et al.* Characterization of CD4+CD28null T cells in patients with coronary artery disease and individuals with risk factors for atherosclerosis. *Cell Immunol* **281**, 11–19 (2013).
35. Duewell, P. *et al.* NLRP3 inflammasomes are required for atherogenesis and activated by cholesterol crystals. *Nature* **464**, 1357–1361 (2010).
36. Karasawa, T. & Takahashi, M. Role of NLRP3 Inflammasomes in Atherosclerosis. *J Atheroscler Thromb* **24**, 443–451 (2017).
37. Libby, P. Interleukin-1 Beta as a Target for Atherosclerosis Therapy: Biological Basis of CANTOS and Beyond. *J Am Coll Cardiol* **70**, 2278–2289 (2017).
38. Amaral, N. B. *et al.* Colchicine reduces the activation of NLRP3 inflammasome in COVID-19 patients. *Inflammation Research* **72**, 895–899 (2023).
39. Hauer, A. D. *et al.* Blockade of interleukin-12 function by protein vaccination attenuates atherosclerosis. *Circulation* **112**, 1054–1062 (2005).
40. Buono, C. *et al.* Influence of interferon-γ on the extent and phenotype of diet-induced atherosclerosis in the LDLR-deficient mouse. *Arterioscler Thromb Vasc Biol* **23**, 454–460 (2003).
41. Gupta, S. *et al.* IFN-gamma potentiates atherosclerosis in ApoE knock-out mice. *J Clin Invest* **99**, 2752–2761 (1997).
42. Huang, Z. H., Fitzgerald, M. L. & Mazzone, T. Distinct cellular loci for the ABCA1-dependent and ABCA1-independent lipid efflux mediated by endogenous apolipoprotein E expression. *Arterioscler Thromb Vasc Biol* **26**, 157–162 (2006).

43. Tangirala, R. K. *et al.* Identification of macrophage liver X receptors as inhibitors of atherosclerosis. *Proc Natl Acad Sci U S A* **99**, 11896–11901 (2002).
44. Spann, N. J. *et al.* Regulated accumulation of desmosterol integrates macrophage lipid metabolism and inflammatory responses. *Cell* **151**, 138–152 (2012).
45. Owens, G. K., Kumar, M. S. & Wamhoff, B. R. Molecular regulation of vascular smooth muscle cell differentiation in development and disease. *Physiol Rev* **84**, 767–801 (2004).
46. Gomez, D. & Owens, G. K. Smooth muscle cell phenotypic switching in atherosclerosis. *Cardiovasc Res* **95**, 156–164 (2012).
47. Shankman, L. S. *et al.* KLF4-dependent phenotypic modulation of smooth muscle cells has a key role in atherosclerotic plaque pathogenesis. *Nat Med* **21**, 628–637 (2015).
48. Chen, P. Y. *et al.* Endothelial-to-mesenchymal transition drives atherosclerosis progression. *Journal of Clinical Investigation* **125**, 4514–4528 (2015).
49. Cho, J. G., Lee, A., Chang, W., Lee, M.-S. & Kim, J. Endothelial to Mesenchymal Transition Represents a Key Link in the Interaction between Inflammation and Endothelial Dysfunction. *Front Immunol* **9**, 294 (2018).
50. Tse, K., Tse, H., Sidney, J., Sette, A. & Ley, K. T cells in atherosclerosis. *Int Immunol* **25**, 615–622 (2013).
51. Foks, A. C., Lichtman, A. H. & Kuiper, J. Treating atherosclerosis with regulatory T cells. *Arterioscler Thromb Vasc Biol* **35**, 280–7 (2015).
52. van Duijn, J., Kuiper, J. & Slütter, B. The many faces of CD8+ T cells in atherosclerosis. *Curr Opin Lipidol* 1 (2018) doi:10.1097/MOL.0000000000000541.
53. Mallat, Z. & Binder, C. J. The why and how of adaptive immune responses in ischemic cardiovascular disease. *Nature Cardiovascular Research 2022 1:5* **1**, 431–444 (2022).
54. Chowdhury, R. R. *et al.* Human Coronary Plaque T Cells Are Clonal and Cross-React to Virus and Self. *Circ Res* **130**, 1510–1530 (2022).
55. Wigren, M. *et al.* Lack of Ability to Present Antigens on Major Histocompatibility Complex Class II Molecules Aggravates Atherosclerosis in ApoE -/- Mice. *Circulation* **139**, 2554–2566 (2019).
56. Slütter, B. & Kuiper, J. Immune Responses in Context: An Anti-Inflammatory Role for Major Histocompatibility Complex Class II Presentation in the Atherosclerotic Lesion? *Circulation* **139**, 2567–2569 (2019).
57. Wang, Z. *et al.* Pairing of single-cell RNA analysis and T cell antigen receptor profiling indicates breakdown of T cell tolerance checkpoints in atherosclerosis. *Nature Cardiovascular Research 2023 2:3* **2**, 290–306 (2023).
58. Bot, I. *et al.* Perivascular mast cells promote atherogenesis and induce plaque destabilization in apolipoprotein E-deficient mice. *Circulation* **115**, 2516–2525 (2007).
59. Bot, I. *et al.* Mast cell chymase inhibition reduces atherosclerotic plaque progression and improves plaque stability in ApoE-/- mice. *Cardiovasc Res* **89**, 244–252 (2011).
60. Bot, I., Shi, G. P. & Kovanen, P. T. Mast cells as effectors in atherosclerosis. *Arterioscler Thromb Vasc Biol* **35**, 265 (2015).
61. Shi, G. P., Bot, I. & Kovanen, P. T. Mast cells in human and experimental cardiometabolic diseases. *Nat Rev Cardiol* **12**, 643–658 (2015).
62. Willems, S. *et al.* Mast cells in human carotid atherosclerotic plaques are associated with intraplaque microvessel density and the occurrence of future cardiovascular events. *Eur Heart J* **34**, 3699–3706 (2013).
63. Orinska, Z., Hagemann, P. M., Halova, I. & Draber, P. Tetraspanins in the regulation of mast cell function. *Med Microbiol Immunol* **209**, 531–543 (2020).

64. Galli, S. J., Borregaard, N. & Wynn, T. A. Phenotypic and functional plasticity of cells of innate immunity: macrophages, mast cells and neutrophils. *Nature Immunology 2011 12:11* **12**, 1035–1044 (2011).
65. Nagata, Y. & Suzuki, R. FcεRI: A Master Regulator of Mast Cell Functions. *Cells* **11**, 622 (2022).
66. Sibilano, R., Frossi, B. & Pucillo, C. E. Mast cell activation: A complex interplay of positive and negative signaling pathways. *Eur J Immunol* **44**, 2558–2566 (2014).
67. Kalesnikoff, J. & Galli, S. J. New developments in mast cell biology. *Nature Immunology 2008 9:11* **9**, 1215–1223 (2008).
68. Sinkiewicz, W. *et al.* Immunoglobulin E as a marker of the atherothrombotic process in patients with acute myocardial infarction. *Cardiol J* **14**, 266–73 (2007).
69. Langer, R. D., Criqui, M. H., Feigelson, H. S., McCann, T. J. & Hamburger, R. N. IgE predicts future nonfatal myocardial infarction in men. *J Clin Epidemiol* **49**, 203–209 (1996).
70. Smit, V. *et al.* Single-cell profiling reveals age-associated immunity in atherosclerosis. *Cardiovasc Res* (2023) doi:10.1093/CVR/CVAD099.
71. Blasco, M. P. *et al.* Age-dependent involvement of gut mast cells and histamine in post-stroke inflammation. *J Neuroinflammation* **17**, (2020).
72. Pilkington, S. M., Barron, M. J., Watson, R. E. B., Griffiths, C. E. M. & Bulfone-Paus, S. Aged human skin accumulates mast cells with altered functionality that localize to macrophages and vasoactive intestinal peptide-positive nerve fibres. *Br J Dermatol* **180**, 849–858 (2019).
73. Gunin, A. G., Kornilova, N. K., Vasilieva, O. V. & Petrov, V. V. Age-related changes in proliferation, the numbers of mast cells, eosinophils, and cd45-positive cells in human dermis. *J Gerontol A Biol Sci Med Sci* **66**, 385–392 (2011).
74. Chatterjee, V. & Gashev, A. A. Aging-associated shifts in functional status of mast cells located by adult and aged mesenteric lymphatic vessels. *Am J Physiol Heart Circ Physiol* **303**, (2012).
75. da Silva, E. Z. M., Jamur, M. C. & Oliver, C. Mast cell function: a new vision of an old cell. *J Histochem Cytochem* **62**, 698–738 (2014).
76. Galli, S. J. *et al.* Mast cells as 'tunable' effector and immunoregulatory cells: recent advances. *Annu Rev Immunol* **23**, 749–786 (2005).
77. Reber, L. L., Sibilano, R., Mukai, K. & Galli, S. J. Potential effector and immunoregulatory functions of mast cells in mucosal immunity. *Mucosal Immunol* **8**, 444–463 (2015).
78. Franceschi, C., Garagnani, P., Parini, P., Giuliani, C. & Santoro, A. Inflammaging: a new immune-metabolic viewpoint for age-related diseases. *Nat Rev Endocrinol* **14**, 576–590 (2018).
79. Tan, Q., Liang, N., Zhang, X. & Li, J. Dynamic Aging: Channeled Through Microenvironment. *Front Physiol* **12**, (2021).
80. Kambayashi, T. & Laufer, T. M. Atypical MHC class II-expressing antigen-presenting cells: can anything replace a dendritic cell? *Nature Reviews Immunology 2014 14:11* **14**, 719–730 (2014).
81. Gaudenzio, N., Laurent, C., Valitutti, S. & Espinosa, E. Human mast cells drive memory CD4+ T cells toward an inflammatory IL-22+ phenotype. *J Allergy Clin Immunol* **131**, (2013).
82. Gregory, G. D., Robbie-Ryan, M., Secor, V. H., Sabatino, J. J. & Brown, M. A. Mast cells are required for optimal autoreactive T cell responses in a murine model of multiple sclerosis. *Eur J Immunol* **35**, 3478–3486 (2005).
83. Kritikou, E. *et al.* Hypercholesterolemia Induces a Mast Cell-CD4+ T Cell Interaction in Atherosclerosis. *J Immunol* **202**, 1531–1539 (2019).
84. Bulfone-Paus, S. & Bahri, R. Mast Cells as Regulators of T Cell Responses. *Front Immunol* **6**, (2015).
85. Kovanen, P. T. & Bot, I. Mast cells in atherosclerotic cardiovascular disease - Activators and actions. *Eur J Pharmacol* **816**, 37–46 (2017).

86. Collington, S. J., Williams, T. J. & Weller, C. L. Mechanisms underlying the localisation of mast cells in tissues. *Trends Immunol* **32**, 478–485 (2011).
87. Halova, I., Draberova, L. & Draber, P. Mast cell chemotaxis - chemoattractants and signaling pathways. *Front Immunol* **3**, (2012).
88. Funk, C. D. Prostaglandins and leukotrienes: advances in eicosanoid biology. *Science* **294**, 1871–1875 (2001).
89. Wan, M., Tang, X., Stsiapanava, A. & Haeggström, J. Z. Biosynthesis of leukotriene B 4. *Semin Immunol* **33**, 3–15 (2017).
90. Subramanian, B. C., Majumdar, R. & Parent, C. A. The role of the LTB 4-BLT1 axis in chemotactic gradient sensing and directed leukocyte migration. *Semin Immunol* **33**, 16–29 (2017).
91. Weller, C. L. *et al.* Leukotriene B4, an activation product of mast cells, is a chemoattractant for their progenitors. *J Exp Med* **201**, 1961–1971 (2005).
92. Lundeen, K. A., Sun, B., Karlsson, L. & Fourie, A. M. Leukotriene B4 receptors BLT1 and BLT2: expression and function in human and murine mast cells. *J Immunol* **177**, 3439–3447 (2006).
93. Heller, E. A. *et al.* Inhibition of atherogenesis in BLT1-deficient mice reveals a role for LTB4 and BLT1 in smooth muscle cell recruitment. *Circulation* **112**, 578–586 (2005).
94. Aiello, R. J. *et al.* Leukotriene B4 receptor antagonism reduces monocytic foam cells in mice. *Arterioscler Thromb Vasc Biol* **22**, 443–449 (2002).
95. Subbarao, K. *et al.* Role of leukotriene B4 receptors in the development of atherosclerosis: potential mechanisms. *Arterioscler Thromb Vasc Biol* **24**, 369–375 (2004).
96. Mehrabian, M. *et al.* Identification of 5-lipoxygenase as a major gene contributing to atherosclerosis susceptibility in mice. *Circ Res* **91**, 120–126 (2002).
97. Matsukawa, A. *et al.* Endogenous monocyte chemoattractant protein-1 (MCP-1) protects mice in a model of acute septic peritonitis: cross-talk between MCP-1 and leukotriene B4. *Journal of immunology* **163**, 6148–54 (1999).
98. Huang, L. *et al.* Leukotriene B4 strongly increases monocyte chemoattractant protein-1 in human monocytes. *Arterioscler Thromb Vasc Biol* **24**, 1783–1788 (2004).
99. Boulland, M. L. *et al.* Human IL4I1 is a secreted L-phenylalanine oxidase expressed by mature dendritic cells that inhibits T-lymphocyte proliferation. *Blood* **110**, 220–227 (2007).
100. Mulder, K. *et al.* Cross-tissue single-cell landscape of human monocytes and macrophages in health and disease. *Immunity* **54**, 1883-1900.e5 (2021).
101. Aubatin, A. *et al.* IL4-induced gene 1 is secreted at the immune synapse and modulates TCR activation independently of its enzymatic activity. *Eur J Immunol* **48**, 106–119 (2018).
102. Lasoudris, F. *et al.* IL4I1: an inhibitor of the CD8⁺ antitumor T-cell response in vivo. *Eur J Immunol* **41**, 1629–1638 (2011).
103. MacKinnon, A. *et al.* 705 Anti-tumor activity of CB-668, a potent, selective and orally bioavailable small-molecule inhibitor of the immuno-suppressive enzyme Interleukin 4 (IL-4)-Induced Gene 1 (IL4I1). *J Immunother Cancer* **8**, A423.2-A424 (2020).
104. Mocan-Hognogi, D. L. *et al.* Immune Checkpoint Inhibitors and the Heart. *Front Cardiovasc Med* **8**, 726426 (2021).
105. Poels, K. *et al.* Antibody-Mediated Inhibition of CTLA4 Aggravates Atherosclerotic Plaque Inflammation and Progression in Hyperlipidemic Mice. *Cells* **9**, (2020).
106. Dib, L. *et al.* Lipid-associated macrophages transition to an inflammatory state in human atherosclerosis, increasing the risk of cerebrovascular complications. *Nature Cardiovascular Research 2023 2:7* **2**, 656–672 (2023).

107. Amadori, L. *et al.* Systems immunology-based drug repurposing framework to target inflammation in atherosclerosis. *Nature Cardiovascular Research 2023 2:6* **2**, 550–571 (2023).
108. Depuydt, M. A. C. *et al.* Microanatomy of the Human Atherosclerotic Plaque by Single-Cell Transcriptomics. *Circ Res* **127**, 1437–1455 (2020).
109. Williams, C. G., Lee, H. J., Asatsuma, T., Vento-Tormo, R. & Haque, A. An introduction to spatial transcriptomics for biomedical research. *Genome Med* **14**, 1–18 (2022).
110. Nilsson, J. & Hansson, G. K. Vaccination Strategies and Immune Modulation of Atherosclerosis. *Circ Res* **126**, 1281–1296 (2020).
111. Zhou, X., Caligiuri, G., Hamsten, A., Lefvert, A. K. & Hansson, G. K. LDL Immunization Induces T-Cell–Dependent Antibody Formation and Protection Against Atherosclerosis. *Arterioscler Thromb Vasc Biol* **21**, 108–114 (2001).
112. Palinski, W., Miller, E. & Witztum, J. L. Immunization of low density lipoprotein (LDL) receptor-deficient rabbits with homologous malondialdehyde-modified LDL reduces atherogenesis. *Proceedings of the National Academy of Sciences* **92**, 821–825 (1995).
113. Freigang, S., Hörkkö, S., Miller, E., Witztum, J. L. & Palinski, W. Immunization of LDL Receptor–Deficient Mice With Homologous Malondialdehyde-Modified and Native LDL Reduces Progression of Atherosclerosis by Mechanisms Other Than Induction of High Titers of Antibodies to Oxidative Neoepitopes. *Arterioscler Thromb Vasc Biol* **18**, 1972–1982 (1998).
114. Fredrikson, G. N. *et al.* Identification of Immune Responses Against Aldehyde-Modified Peptide Sequences in ApoB Associated With Cardiovascular Disease. *Arterioscler Thromb Vasc Biol* **23**, 872–878 (2003).
115. Tse, K. *et al.* Atheroprotective vaccination with MHC-II restricted peptides from ApoB-100. *Front Immunol* **4**, 74978 (2013).
116. Seijkens, T. T. P. *et al.* Targeting CD40-Induced TRAF6 Signaling in Macrophages Reduces Atherosclerosis. *J Am Coll Cardiol* **71**, 527–542 (2018).
117. Chyu, K. Y. *et al.* Immunization using ApoB-100 peptide-linked nanoparticles reduces atherosclerosis. *JCI Insight* **7**, (2022).
118. Van Puijvelde, G. H. M. *et al.* Induction of oral tolerance to HSP60 or an HSP60-peptide activates T cell regulation and reduces atherosclerosis. *Arterioscler Thromb Vasc Biol* **27**, 2677–2683 (2007).
119. Huang, H., Wang, C., Rubelt, F., Scriba, T. J. & Davis, M. M. Analyzing the Mycobacterium tuberculosis immune response by T-cell receptor clustering with GLIPH2 and genome-wide antigen screening. *Nature Biotechnology 2020 38:10* **38**, 1194–1202 (2020).
120. Zhang, H., Zhan, X. & Li, B. GIANA allows computationally-efficient TCR clustering and multi-disease repertoire classification by isometric transformation. *Nature Communications 2021 12:1* **12**, 1–11 (2021).
121. Shapiro, I. E. & Bassani-Sternberg, M. The impact of immunopeptidomics: From basic research to clinical implementation. *Semin Immunol* **66**, 101727 (2023).
122. Kawakami, T. & Blank, U. From IgE to Omalizumab. *J Immunol* **197**, 4187–4192 (2016).
123. Aissa, A. F. *et al.* Single-cell transcriptional changes associated with drug tolerance and response to combination therapies in cancer. *Nat Commun* **12**, (2021).
124. Zernecke, A. *et al.* Integrated single-cell analysis-based classification of vascular mononuclear phagocytes in mouse and human atherosclerosis. *Cardiovasc Res* **119**, 1676–1689 (2023).
125. Wirka, R. C. *et al.* Atheroprotective roles of smooth muscle cell phenotypic modulation and the TCF21 disease gene as revealed by single-cell analysis. *Nat Med* **25**, 1280–1289 (2019).

Appendix

Nederlandse samenvatting

Introductie

Hart- en vaatziekten, ofwel cardiovasculaire aandoeningen, omvatten alle ziekten die het hart en/of de bloedvaten aantasten. Jaarlijks sterven wereldwijd gemiddeld 17,9 miljoen mensen als gevolg van hart- en vaatziekten. Cardiovasculaire aandoeningen zijn daarmee tezamen de meest voorkomende doodsoorzaak ter wereld[1,2] en hebben daarom een grote maatschappelijke impact. Uit cijfers van de Nederlandse Hartstichting blijkt dat in Nederland 1,7 miljoen mensen te maken hebben met een vorm van cardiovasculair lijden. Het feit dat er dagelijks 103 sterfgevallen zijn als gevolg van deze ziekten, illustreert de noodzaak voor een betere behandeling voor deze patiënten. 85% van de hart- en vaatziekten wordt gecategoriseerd als *atherosclerotische cardiovasculaire ziekten*.[3] Hieronder vallen onder andere een hartinfarct, een herseninfarct en een aneurysma.[4] Al deze aandoeningen hebben één gemeenschappelijke onderliggende oorzaak: slagaderverkalking of *atherosclerose*.

Atherosclerose

Atherosclerose wordt gekenmerkt door een verdikking van de binnenwand van de middelgrote tot grote slagaders.[5] Deze verdikking wordt een *plaque* of een *laesie* genoemd. Het ontstaan van deze plaque is het gevolg van een excessieve ophoping van vetten in de vaatwand met een daaropvolgende chronische ontstekingsreactie. Er zijn meerdere risicofactoren die de ontwikkeling van slagaderverkalking versnellen, waaronder veroudering, een sedentaire levensstijl, een ongezond dieet, roken, hoge bloeddruk, verhoogd cholesterol, obesitas, diabetes type II en genetische aanleg.[6]

Slagaderverkalking begint met schade aan het bloedvat. Onder andere een verhoogde bloeddruk en een toename van het *lage-dichtheids lipoproteine (LDL-) cholesterol* in het bloed zorgen ervoor dat de cellen die de vaten bekleden, de *endotheelcellen*, beschadigd raken. De endotheelcellen voorkomen normaliter dat ongewenste substanties vanuit het bloed in het omliggend weefsel terecht komen. Echter, met de initiatie van atherosclerose, wordt deze endotheellaag doorlaatbaar, waardoor er LDL-cholesterol in de vaatwand terecht kan komen. Deze endotheelcellen worden vervolgens geactiveerd en brengen verschillende signaalmoleculen tot expressie. Deze signaalmoleculen zorgen ervoor dat ontstekingscellen, of *immuuncellen*, naar de beschadigde vaatwand migreren. In de vaatwand wordt het LDL-cholesterol deeltje gemodificeerd en vormt *oxLDL*. Dit oxLDL wordt gezien als een lichaamsvreemde stof, die door de immuuncellen opgeruimd moet worden. Hiermee start de chronische ontstekingsreactie. *Monocyten* uit het bloed worden door de geactiveerde

endotheelcellen aangetrokken, waarna deze de vaatwand ingaan. Door verschillende lokale factoren zullen de monocyten in de vaatwand verder ontwikkelen tot *macrofagen*. De macrofaag is een cel die is gespecialiseerd in het opruimen van resten van dode cellen of lichaamsvreemde stoffen. Dit proces wordt ook wel *fagocytose* genoemd. In de vaatwand neemt de macrofaag de oxLDL-deeltjes op. De continue opname van deze cholesteroldeeltjes leidt tot het vormen van vetdruppeltjes in de macrofaag. Onder de microscoop krijgen deze vetrijke macrofagen een schuimig uiterlijk en daarom worden deze cellen ook wel *schuimcellen* of *foam cells* genoemd. De initiele verdikking van de vaatwand door de endotheelschade, de accumulatie van oxLDL en de infiltratie van de eerste ontstekingscellen wordt een *fatty streak* genoemd. Als de cholesterolconcentraties in het bloed voldoende verlaagd worden, kan deze fatty streak weer bijna volledig verdwijnen. Echter, de vorming van een fatty streak ontstaat vaak zonder enige klinische symptomen en wordt dus vaak niet op tijd opgemerkt. Daardoor zal de slagaderverkalking verder ontwikkelen in meer geavanceerde plaques die leiden tot klinische verschijnselen.

Als het cholesterolgehalte in het bloed voor langere tijd te hoog blijft, wordt de hoeveelheid oxLDL in de vaatwand zo hoog dat de schuimcellen het niet goed meer op kunnen ruimen. De schuimcellen zijn niet meer in staat de grote hoeveelheid oxLDL te verwerken en zullen overgaan op geprogrammeerde celdood, *apoptose*. Tegelijkertijd zullen er ook andere ontstekingscellen worden aangetrokken door de signaalstoffen die worden uitgescheiden door zowel de geactiveerde endotheelcellen als de levende en apoptotische schuimcellen. Deze ontstekingscellen, bestaande uit *neutrofielen*, *dendritische cellen*, *mestcellen*, *B-* en *T-cellen*, zullen ook ophopen in de vaatwand waardoor de verdikking van het vat nog meer toeneemt. Als gevolg van de ontstekingsreactie die plaatsvindt, raken ook de *gladde spiercellen* van het bloedvat geactiveerd. Normaliter zijn de gladde spiercellen betrokken bij het samentrekken van het bloedvat wat nodig is om een goede bloedstroom te creëren. Door de verergerde ontstekingsreactie in het vat zullen deze cellen migreren naar de plaque en zich ophopen onder de endotheellaag. Hiermee vormen ze een beschermende laag, de *fibrous cap*, over de laesie en produceren ze stabiliserende factoren zoals collageen om te voorkomen dat de plaque gaat scheuren. Recent onderzoek heeft ook uitgewezen dat gladde spiercellen zich zo kunnen differentiëren dat ze ook oxLDL-deeltjes kunnen opnemen en zo ook een schuimceluiterlijk krijgen. [7–10] Hieruit blijkt dat deze cellen dus ook al betrokken kunnen zijn bij de formatie van de fatty streak. Zolang de plaque een intacte fibrous cap heeft, wordt hij stabiel geacht. Echter, deze stabiele plaque leidt wel tot een vernauwing van het bloedvat, ook wel *stenose* genoemd. Deze stenose zorgt voor een verminderde bloedtoevoer naar het omliggend weefsel. Dit kan de eerste klinische symptomen veroorzaken, waaronder kortademigheid en pijn op de borst (*angina pectoris*).

Acute complicaties ontstaan echter op het moment dat de plaque instabiel wordt. De toenemende inflammatoire omgeving zorgt ervoor dat niet alleen de schuimcellen, maar ook andere immuuncellen in de plaque, een gecontroleerde vorm van celdood zullen ondergaan. Deze dode cellen worden dan ook niet goed meer opgeruimd. Hierdoor vormt zich in de plaque een zogeheten *necrotische kern*, die bestaat uit een ophoping van afgestorven ontstekingscellen, vetten en andere afvalstoffen. Daarnaast scheiden de immuuncellen in de plaque verschillende pro-inflammatoire stoffen uit, die het weefsel wat de plaque stabiliseert, afbreken. Dit leidt tot het verdunnen van de fibrous cap. Dit zorgt er gezamenlijk voor dat de fibrous cap kan scheuren en dat de inhoud van de plaque, waaronder de necrotische kern, in contact komt met het bloed. Hierbij vormt zich een bloedstolsel of een *thrombus*. Deze thrombusvorming leidt dan tot een volledige afsluiting van de slagader (*occlusie*), waardoor er geen zuurstof meer vervoerd wordt naar de omliggende weefsels. Afhankelijk van de locatie leidt dit tot klinische complicaties zoals een hart- en herseninfarct.

De huidige primaire behandelmethode bij acute cardiovasculaire complicaties is revascularisatie. Dit omvat antitrombotische medicatie en/of verschillende chirurgische ingrepen om de doorbloeding van het vat te herstellen. Bij een hartinfarct vindt de occlusie plaats in de kransslagader van het hart, waardoor de hartspier niet van voldoende zuurstof kan worden voorzien. Over het algemeen is *dotteren* de eerste keus voor het chirurgisch herstellen van de aangedane vaten. Hierbij wordt een slangetje via een (slag)ader in de lies of in de arm naar de vernauwing gebracht. Op de plek van de occlusie wordt dan een klein ballonnetje opgeblazen die de ruimte waardoor het bloed kan stromen vergroot. Vaak wordt er dan ook nog een *stent* geplaatst, wat voorkomt dat het bloedvat weer afsluit na het dotteren. Soms is de occlusie zo ernstig dat het nodig is om een omleiding te maken rondom de vernauwede vaten, wat een *bypassoperatie* wordt genoemd. Bij een herseninfarct kan er ook voor gekozen worden om de volledige plaque uit de halsslagader te verwijderen. Deze operatie wordt een *carotide endarterectomie* genoemd. Ondanks dat deze chirurgische ingrepen op kortere termijn een oplossing bieden, zijn de operaties zeker niet risicovrij. Er kunnen peri-operatieve complicaties ontstaan die de kwaliteit van leven beïnvloeden. Verder bestaat er ook een kans dat er opnieuw een vernauwing in het geopereerde bloedvat ontstaat, ook wel *restenose* genoemd. Het tijdig herkennen en behandelen van slagaderverkalking is dus essentieel om chirurgische ingrepen in de toekomst te voorkomen.

Preventieve behandeling van slagaderverkalking start met het aanpassen van de levensstijl, zoals meer beweging, een gezond dieet en minder roken en alcoholconsumptie. De meest voorkomende farmacologische interventie is het

gebruik van *statines*. Gedurende lange tijd is slagaderverkalking gezien als een cholesterol-gedreven ziekte. Door middel van statines wordt het circulerend LDL-cholesterol verlaagd, wat geleid heeft tot een grote vooruitgang in de behandeling van hart- en vaatziekten. Desondanks zijn er terugkerende cardiovasculaire complicaties opgetreden bij meer dan 20% van de patiënten die na een acute klinische complicaties met een hoge dosis statines behandeld werd. Inmiddels is er ook een nieuwe strategie gevonden om de LDL concentratie in het bloed te verminderen. Het eiwit PCSK9 is verantwoordelijk voor het afbreken van de LDL receptor, waardoor de opname en klaring van LDL geremd wordt. Door het remmen van PCSK9 zijn er aanzienlijke verbeteringen in de cholesterolhuishouding verkregen in patiënten met hart- en vaatziekten.

In de afgelopen decennia heeft een groot aantal (experimentele) onderzoeken aangetoond dat het immuunsysteem een cruciale rol speelt bij de ontwikkeling en progressie van atherosclerose. Dit heeft ertoe geleid dat er recentelijk meerdere klinische studies zijn gestart waarbij therapeutisch wordt ingegrepen op de voortdurende chronische ontsteking bij patiënten met slagaderverkalking. De CANTOS studie was de eerste klinische studie waarbij werd behandeld met een antilichaam tegen de ontstekingsfactor *Interleukine 1β*.[11] Dit is een toonaangevende studie gebleken, aangezien deze studie het eerste bewijs leverde dat aangrijpen op het immuunsysteem het risico op cardiovasculaire verschijnselen kon verlagen. Dit werd gevolgd door verschillende andere studies die ontstekingsremmende middelen toepasten, zoals anti-TNF, methotrexaat en colchicine, waarvan alleen de laatste effectief het risico op cardiovasculaire verschijnselen verminderde.[12–15] Echter, er werden ook negatieve bijwerkingen van algemene immuunsuppressie waargenomen in deze studies. Aangezien immuuntherapie ook de algemene immuunrespons tegen bijvoorbeeld virussen en bacteriën kan beïnvloeden, ligt de volgende uitdaging in de identificatie van meer specifieke therapeutische aangrijpingspunten om enkel de ontstekingsreactie in de plaque te remmen.

Het immuunsysteem

Het immuunsysteem is verantwoordelijk voor de bescherming van het lichaam tegen infecties en weefselschade. Bij de ontwikkeling van immuuncellen, of witte bloedcellen, worden ze getraind in het onderscheiden van lichaamseigen en lichaamsvreemde cellen en moleculen. Het immuunsysteem wordt onderverdeeld in twee takken: het aangeboren en het adaptieve immuunsysteem, ook wel respectievelijk 'niet-specifiek' en 'specifiek' genoemd.

Het aangeboren immuunsysteem reageert als eerste en wordt of geactiveerd door fragmenten van lichaamsvreemde ziekteverwekkers, zoals bacteriën en virussen, of door signalen die worden verstrekt als gevolg van weefselschade (lichaamseigen). Afhankelijk van het ontvangen signaal reageren de aangeboren immuuncellen op de juiste manier. Immuuncellen die hierin een rol spelen zijn onder andere monocyten, macrofagen, dendritische cellen, neutrofielen en mestcellen. Een belangrijke functie van het aangeboren immuunsysteem is het activeren van het adaptieve immuunsysteem. Macrofagen en dendritische cellen controleren het lichaam op lichaamsvreemde stoffen. Zodra deze cellen die tegenkomen, worden deze stoffen verwerkt en zullen de macrofagen en dendritische cellen een klein fragment, een *antigeen*, hiervan op het celmembraan presenteren aan de specifieke afweer. Deze cellen worden dan ook *antigeen-presenterende cellen* genoemd.

De cellen die betrokken zijn bij de specifieke afweer zijn B- en T-cellen. T-cellen worden ontwikkeld in de thymus. Er zijn twee types T-cel die hier gevormd worden: de $CD4^+$ en de $CD8^+$ T-cel. $CD4^+$ T-cellen zijn met name betrokken bij het reguleren van de ontstekingsreactie door ook omliggende cellen te activeren of remmen. $CD8^+$ T-cellen staan vooral bekend om hun cytotoxische functie waarbij ze direct cellen die zijn geïnfecteerd met lichaamsvreemde ziekteverwekkers kunnen doden. In de thymus krijgt elke T-cel een unieke receptor (*T-cel receptor – TCR*) die aan één uniek antigeen kan binden. T-cellen worden geactiveerd als dat antigeen gepresenteerd wordt door een antigeen-presenterende cel. Voor deze activatie zijn drie signalen nodig: de eerste is de interactie tussen de TCR en het *MHC-molecuul* waarop het antigeen zit wat gepresenteerd wordt; het tweede en derde signaal zijn een *co-signalerend signaal* en een ontstekingseiwit, een *cytokine*, wat geproduceerd wordt door de antigeen-presenterende cel. Met de laatste twee signalen wordt bepaald wat voor functie de T-cel krijgt na activatie. De functie van T-cellen is grofweg te onderscheiden in twee componenten: een pro-inflammatoire effector functie en een ontstekingsremmende regulatoire functie. Zodra de T-cel geactiveerd wordt zal deze zich gaan vermenigvuldigen en zo vormt zich een populatie van T-cellen met eenzelfde TCR. Dit proces wordt *klonale expansie* genoemd. Deze klonaal geëxpandeerde T-cellen zullen vervolgens migreren naar de plek waar het antigeen vandaan komt om het daar uit het lichaam te verwijderen. B-cellen hebben ook een unieke receptor (*B-cel receptor – BCR*). In tegenstelling tot T-cellen produceren B-cellen antistoffen na herkenning van het BCR-specifieke antigeen. Deze antistoffen circuleren in het bloed en zijn in staat om direct het antigeen te neutraliseren. Zowel B- als T-cellen vormen na de activatie een populatie *geheugencellen*. Dit zorgt ervoor dat deze B- en T-cellen bij een volgende infectie zich sneller kunnen vermenigvuldigen om hun anti-inflammatoire eigenschappen te kunnen uitvoeren. Het verkrijgen van dit

immunologisch geheugen is ook de basis van vaccinaties. Bij een vaccinatie wordt een onschadelijk stukje van de ziekteverwekker geïntroduceerd. Dit wordt gedaan om een eerste activatie van de specifieke afweercellen te initiëren en met name om geheugencellen te ontwikkelen die bij een infectie met de ziekteverwekker sneller kunnen reageren.

Single-cell RNA sequencing als tool voor target identificatie voor atherosclerose

Zoals hierboven beschreven heeft het ingrijpen op het immuunsysteem als behandeling voor slagaderverkalking veel potentie, maar is het essentieel om een atherosclerose-specifiek aangrijpingspunt hiervoor te identificeren. In het afgelopen decennium heeft er een hele snelle ontwikkeling plaatsgevonden van een techniek die daarbij van cruciale waarde kan zijn: *single-cell RNA sequencing (scRNA-seq)*.[16] Met scRNA-seq kan men het volledige genexpressie profiel meten per individuele cel. Het voordeel hiervan is dat het data genereert met een hele hoge resolutie, waardoor een gedetailleerde beschrijving gemaakt kan worden van de cellen die in het weefsel zitten. Bij de meer conventionele analysemethodes is het nodig om op voorhand bepaalde cellulaire markers uit te kiezen om op basis daarvan cellen te onderscheiden. Het aantal markers wat meegenomen kan worden is echter beperkt. Het voordeel van scRNA-seq ten opzichte van deze technieken is dan ook dat door het meten van alle genen het mogelijk is om zeldzame celpopulaties te onderscheiden, die met de gekozen markers bij de andere technieken mogelijk niet aan het licht waren gekomen. Het single-cell veld is inmiddels al zodanig doorontwikkeld dat er naast genexpressie per cel, er ook additionele parameters per cel gemeten kunnen worden. Denk hierbij aan het meten van bijvoorbeeld de TCR of BCR (*single-cell TCR of BCR sequencing*), maar ook kan er inmiddels per cel bekeken worden hoe de genen op DNA niveau gereguleerd kunnen worden (*single-cell ATAC sequencing*). De verzamelnaam van deze geavanceerde technieken is *single-cell multi-omics*.

Dit proefschrift

In dit proefschrift hebben we single-cell multi-omics toegepast om een gedetailleerde cellulaire atlas van humane atherosclerose te genereren, met als doel de cellen die zich ophopen in de vergevorderde plaque beter te karakteriseren. Deze informatie kan vervolgens gebruikt worden om cellen en genen te definiëren die van therapeutisch belang kunnen zijn.

De opkomst van scRNA-seq heeft het cardiovasculair onderzoek in een stroomversnelling gebracht door de nieuwe inzichten in vasculaire ziekten, waaronder atherosclerose en aneurysma. Incidentie van aneurysma is de tweede aortaziekte die leidt tot cardiovasculaire sterfte. Door progressief verlies van gladde spiercellen en afbraak van bloedvat-verstevigend weefsel (*extracellulaire matrix*) wordt de vaatwand vatbaar voor scheuren, wat resulteert in ernstige klinische complicaties. In **hoofdstuk 2** hebben we een overzicht gemaakt van de studies die scRNA-seq hebben toegepast om de verschillende celtypes in beide ziekten te onderzoeken en om mogelijke overeenkomsten en verschillen tussen beide ziekten in kaart te brengen. Terwijl aneurysma over het algemeen wordt gekoppeld aan disfunctionele cellen die niet tot het immuunsysteem behoren, waaronder vasculaire gladde spiercellen, endotheelcellen en fibroblasten, is er in meerdere scRNA-seq-studies opvallend genoeg ook een immuuncomponent van deze ziekte beschreven. Zowel macrofagen als T-cellen zijn gevonden in aneurysmaweefsels, waarvan onder andere de pro-inflammatoire IL-1β^{+} macrofagen en de regulatoire T-cellen een overeenkomstig fenotype hebben met die in atherosclerose. Bij aneurysma is er meer onderzoek gedaan naar het karakteriseren van fibroblasten dan bij atherosclerose, wat wijst op het belang van deze cellen voor deze pathologie. Recentelijk is er een scRNA-seq studie geweest die ook het belang van fibroblasten bij atherosclerose heeft benadrukt.[17] Als gevolg van het ziekteproces, is recent aan het licht gekomen dat bepaalde cellen een ander fenotype kunnen krijgen. Ze 'switchen' naar een fenotype wat vergelijkbaar kan zijn met dat van een volledig ander celtype, een proces wat *phenotype switching* wordt genoemd. Zowel bij atherosclerose als bij aneurysma kan zo een fenotypische modulatie van gladde spiercellen voorkomen, vaak gekenmerkt door expressie van genen die betrokken zijn bij extracellulaire matrixregulatie. Bij atherosclerose wordt de transitie van gladde spiercellen naar macrofagen vaak beschreven, terwijl bij aneurysma het verlies van deze cellen als gevolg van de verhoogde stressrespons een belangrijkere rol speelt. Endotheeldisfunctie als gevolg van ontsteking werd waargenomen in beide ziektebeelden, maar de transitie van endotheel cellen naar gladde spiercellen werd alleen waargenomen in atherosclerose. Met scRNA-seq kun je ook een voorspelling doen welke cellen mogelijk met elkaar communiceren. In beide ziektebeelden waren de meeste intercellulaire communicatieroutes tussen cellen die niet tot het immuunsysteem behoren en macrofagen, wat met name processen omvatte die de migratie van macrofagen naar het zieke weefsel induceren. Niettemin was de enige gemeenschappelijke communicatieroute in beide ziekten een route die een rol speelt in het complement system, wat een belangrijke anti-microbiële rol heeft maar ook betrokken is bij de activatie van immuuncellen. Hoewel men zou kunnen suggereren dat door op deze route te aan te grijpen er twee vliegen in één klap kunnen worden geslagen, moet dit voorzichtig worden geïnterpreteerd omdat deze celsubets en pathways verschillende functionele eigenschappen zouden kunnen hebben in beide

ziekten. Samengevat geeft deze review een overzicht van de uitgebreide toegenomen kennis in vasculaire pathologie die wordt verkregen door scRNA-seq. De cellen die betrokken zijn bij beide ziekten blijken veel meer divers en plastisch te zijn dan eerder werd gedacht. ScRNA-seq zal daarom van groot belang zijn bij het verder definiëren van ziektemechanismen en kandidaat-aangrijpingspunten voor medicijnontwikkeling.

Cellulaire atlas van de humane atherosclerotische plaque door middel van single-cell technologieën

Atherosclerotische plaques bestaan uit een zeer heterogene celpopulatie. In 2018 is scRNA-seq voor het eerst toegepast om een atlas van de immuuncellen te creëren in een experimenteel muismodel voor atherosclerose.[18,19] Dit toonde het enorme potentieel van deze techniek, omdat het leidde tot de identificatie van onder andere TREM2$^+$ macrofagen, waarvan inmiddels is aangetoond dat ze een prominente rol spelen in atherosclerose.[20,21] Niet veel later is ditzelfde experiment ook uitgevoerd voor humane atherosclerotische plaques.[22] Toch was de beschrijving van de verschillende cellen in humane plaques nog onvolledig aangezien de cellen die niet tot het immuunsysteem behoren ontbraken. Daarom hebben we in **hoofdstuk 3** scRNA-seq en scATAC-seq uitgevoerd op plaques van patiënten die een endarterectomie van de halsslagader ondergaan hebben. We hebben hiervoor een cohort gebruikt van 18 patiënten en een overzicht gegeven van de verschillende aanwezige cel(sub) types in de laesie. In deze studie hebben we 14 belangrijke celtypes, met daarbij de activatiestatus, mogelijke phenotype switching en potentiële intercellulaire communicatieroutes beschreven. Tot slot hebben we onze data gebruikt om de genen die in genoombrede associatiestudies (GWAS) in verband zijn gebracht met slagaderverkalking te herleiden naar een specifiek celtype.

Verrassend genoeg bleek dat de immuuncelpopulatie in de humane plaque met name uit T-cellen bestond, die meer dan 50% van de geanalyseerde cellen uitmaakten. Ondanks dat bij het prepareren van het weefsel voor scRNA-seq er verschillen kunnen ontstaan in de verhoudingen van bepaalde celpopulaties, konden we door middel van histologie aantonen dat er inderdaad meer T-cellen dan macrofagen in de humane plaque aanwezig waren. Uit onze studie bleek dat de T-cellen met name te onderscheiden waren op basis van de mate van activatie in tegenstelling tot de andere cellulaire markers die veelvuldig gebruikt worden met de meer conventionele technieken. Een populatie CD4$^+$ T-cellen werd gekarakteriseerd door het gebrek aan expressie van CD28, een cosignalerend molecuul, en was van interesse omdat deze eerder zijn gevonden in de circulatie van patiënten met atherosclerose in de kransslagader. Met onze studie konden we bevestigen dat deze cellen niet alleen in het bloed, maar ook in de plaque aanwezig zijn.

Verder observeerden we een type dendritische cellen en drie soorten macrofagen, waarvan er twee een pro-inflammatoir fenotype en één een anti-inflammatoir schuimcelachtig fenotype hadden. Een van de pro-inflammatoire macrofagen werd gekarakteriseerd door expressie van IL1β, waarop is aangegrepen in een recente succesvolle klinische studie (CANTOS trial). Aan de hand van de scRNA-seq en scATAC-seq data konden we bekijken welke genen tot expressie kwamen en ook hoe die genexpressie mogelijk gereguleerd werd op DNA-niveau. Hiermee hebben we de hypothese gesteld dat er in de plaque een activatiecyclus plaatsvindt waarbij de dendritische cellen mogelijk de hierboven genoemde T-celpopulatie kan (her) activeren, wat leidt tot de activatie van de pro-inflammatoire macrofagen. Hiermee kan deze cyclus dus bijdragen aan de lokale pro-inflammatoire omgeving in de humane plaque. De laatste macrofaag subset werd gekarakteriseerd als een schuimcel-achtige subset door expressie van *TREM2* en andere vetophoping-geassocieerde genen. Terwijl schuimcellen lang beschouwd werden als pro-inflammatoir, hebben zowel in vivo als single-cell studies aangetoond dat deze cellen juist anti-inflammatoir van aard zijn.

Door de hoge resolutie die met single-cell technologieën wordt verkregen, kunnen subtiele fenotypische verschillen, zoals cellulaire plasticiteit, worden gedetecteerd. In dit hoofdstuk leverden we ook bewijs voor transdifferentiatie van cellen in de humane plaque. Binnen het *TREM2*$^{+}$ macrofaagcluster ontdekten we expressie van gladde spiercel geassocieerde genen wat suggereert dat er phenotype switching heeft plaatsgevonden. Eerder is aangetoond dat gladde spiercellen ook in staat zijn om lipiden op te nemen en te differentiëren naar een macrofaagachtige cel.[10,23,24] Binnen de endotheelcellen hebben we een vergelijkbaar fenomeen waargenomen. We vonden een subset van *ACTA2*$^{+}$ endotheelcellen, wat impliceert dat deze cellen een transitie naar een gladde spiercelfenotype hebben ondergaan, een fenomeen wat optreedt in inflammatoire omstandigheden.

Naast een uitgebreide karakterisatie van de celpopulaties in de plaque, is in deze studie ook beschreven hoe deze dataset als hulpmiddel kan worden toegepast bij het onderzoek naar nieuwe aangrijpingspunten voor medicijnen. Hiervoor hebben we intercellulaire communicatieroutes voorspeld in de plaque. We identificeerden voornamelijk interacties tussen macrofagen en zowel endotheel- als gladde spiercellen die betrokken zijn bij het mobiliseren van immuuncellen. Bovendien voorspelden we routes die betrokken zouden kunnen zijn bij het rekruteren en activeren van T-cellen. Tot slot hebben we deze dataset gebruikt om genen die in grote GWAS studies zijn geassocieerd met kransslagaderverkalking op celniveau in kaart te brengen. Deze GWAS studies hebben, mede door de grote hoeveelheid patiënten die geïncludeerd

worden, meerdere interessante genen geïdentificeerd die geassocieerd worden met een verhoogd risico op slagaderverkalking. Desondanks blijft het een uitdaging om te bepalen welke genen therapeutische potentie hebben en hoe men hier goed op kan aangrijpen. Door de genen op celniveau te kunnen bekijken, kunnen directe functionele experimenten worden uitgevoerd om patiënt-gedreven kandidaatgenen voor nieuwe medicatie te kunnen onderzoeken. In deze studie zagen we dat de GWAS-genen met name tot expressie kwamen in macrofagen, endotheelcellen en gladde spiercellen. Toekomstige preklinische studies met zowel celkweek als experimentele diermodellen zullen nodig zijn om de functie van de in kaart gebrachte kandidaatgenen in deze cellen te onderzoeken om te bestuderen hoe ze bijdragen aan de progressie van de ziekte.

Samengevat hebben we een cel atlas van de humane atherosclerotische plaque ontwikkeld met behulp van single-cell technologieën. We hebben twee voorbeelden gegeven van hoe deze gegevens in de toekomst gebruikt kunnen worden voor medicijnonderzoek. In de overige hoofdstukken van dit proefschrift hebben we deze dataset gebruikt als basis voor het vaststellen van mogelijke interessante celtypes en aangrijpingspunten, en deze vervolgens gevalideerd in verschillende experimentele modellen.

Een auto-immuuncomponent in atherosclerose

De rol van T-cellen in atherosclerose is reeds uitgebreid bestudeerd. In experimentele studies zijn verschillende subtypes T-cellen beschreven die atherosclerose kunnen verergeren of een beschermende functie hebben. Zoals beschreven in **hoofdstuk 3** en een bestaande literatuur, bevatten humane atherosclerotische plaques een groot aantal T-cellen. Echter, wat deze T-cellen ertoe aanzet om naar de plaque te migreren en of ze antigeen-specifieke activatie ondergaan, was nog onduidelijk.

Hiertoe hebben we in **hoofdstuk 4** scTCR-seq toegepast op om te bepalen of de T-cellen in de plaque klonale expansie hadden ondergaan en om de activatiestatus van deze antigeen-specifieke T-cellen in kaart te brengen. Hiervoor hebben we van dezelfde endarterectomiepatiënten zowel de cellen in het bloed als in de plaque onderzocht. Aangezien antigeen-specifieke T-cellen naar de plek van het antigeen migreren, was de hypothese dat als de T-cellen zijn geactiveerd door een plaque-specifiek antigeen, er meer klonaal geëxpandeerde T-cellen in de laesie zouden zitten ten opzichte van het bloed. Eerdere studies hadden al aangetoond dat er in de plaque meer klonaal geëxpandeerde $CD8^+$ T cellen te vinden zijn ten opzichte van $CD4^+$ T-cellen.[25] Echter, met onze studie konden we aantonen dat alleen bij de $CD4^+$ T-cellen er een verrijking te zien was in de plaque in vergelijking met het bloed. Één specifieke plaque-verrijkte klonaal geëxpandeerde $CD4^+$ T-celsubset werd gekarakteriseerd door een set genen die hoger

tot expressie komen na antigeen-presentatie door een antigeen-presenterende cel. Doordat met scRNA-seq minimale verschillen in genexpressie gedetecteerd kan worden, is het mogelijk om met een algoritme te bepalen hoe de cellen zich ontwikkelen over tijd. Hiermee identificeerden we in het bloed een mogelijke voorlopercel van de hierboven benoemde antigeen-specifieke effector T-cellen. Deze T-cel wordt gekenmerkt door expressie van *CCR4* en *CCR10*, welke beiden betrokken zijn van de rekrutering van T-cellen naar inflammatoire locaties. Deze migratoire T-celsubset in het bloed had bovendien meerdere overeenkomstige TCRs met de geëxpandeerde T-cellen in de plaque, wat suggereert dat ze op hetzelfde antigeen hebben gereageerd.

Vervolgens hebben we onderzocht of we in de plaque lokale interacties konden voorspellen tussen deze effector T-cellen en antigeen-presenterende cellen. Er is tegenstrijdig bewijs over hoe antigeen-presentatie in de laesie bijdraagt aan ziekteprogressie. De huidige consensus is dat de locatie van de antigeen-presentatie essentieel is voor het resultaat van de T-celactivatie, waarbij de plaqueomgeving een beschermende T-celrespons zou moeten induceren.[26,27] Toch hebben we laten zien dat pathogene interacties ook in de laesie kunnen optreden, aangezien we een co-signalerende interactie tussen TREM2$^+$ macrofagen en de plaque-verrijkte effector CD4$^+$ T-cellen konden voorspellen. Aangezien de plaque voornamelijk uit lichaamseigen stoffen bestaat, lijkt de grote hoeveelheid geëxpandeerde T-cellen mogelijk op een lichaamseigen antigeen te reageren, wat een auto-immuunziekte definieert. Dit suggereert dat atherosclerose mogelijk een auto-immuuncomponent heeft. Echter, omdat we niet precies weten op welk antigeen de T-cellen reageren en of dit inderdaad lichaamseigen is, hebben we een andere strategie toegepast om deze hypothese verder te onderzoeken. We vergeleken daarom het genexpressieprofiel van de CD4$^+$ T-cellen met die in de synoviale vloeistof van patiënten met de auto-immuunziekte psoriatische artritis en vonden aanzienlijke overeenkomsten. Ook de verdeling van de geëxpandeerde CD4$^+$ T-cellen tussen bloed en het ziekteweefsel was vergelijkbaar. Kortom, deze data ondersteunen de theorie dat de pathofysiologie van atherosclerose een auto-immuuncomponent heeft. Om dit volledig te bevestigen is er verder onderzoek nodig naar wat het antigeen is waar de T-cellen op reageren. Desalniettemin benadrukt dit wel dat het aangrijpen op de antigeen-specifieke T-celactivatie veel therapeutische potentie heeft.

Mestcelactivatie en -migratie in vergevorderde atherosclerose

Terwijl de grootste populatie immuuncellen in **hoofdstuk 3** T-cellen bleek te zijn, bestond de kleinste populatie uit mestcellen. Hoewel ze in lage aantallen aanwezig zijn in de plaque, is bewezen dat mestcellen aanzienlijk bijdragen aan de progressie van atherosclerose. In experimentele modellen voor atherosclerose bevorderen

mestcellen de instabiliteit van plaques, onder andere doordat deze cellen eiwitten, *proteases*, produceren die de extracellulaire matrix van de plaque afbreken.[28–31] De meest voorkomende proteases zijn *chymase* en *tryptase*. Bovendien heeft een andere studie aangetoond dat het aantal intraplaque mestcellen positief geassocieerd kan worden met toekomstige cardiovasculaire gebeurtenissen, waarbij gecorrigeerd is voor de belangrijkste risicofactoren voor hart- en vaatziekten.[32] In de volgende hoofdstukken was het doel om de humane intraplaque mestcellen verder te karakteriseren, te onderzoeken of ze leeftijds-gerelateerde veranderingen ondergaan en te onderzoeken of we de migratie van mestcellen naar de plaque konden remmen.

In **hoofdstuk 5** hebben we flow cytometrie toegepast om het aantal mestcellen en hun fenotype beter te karakteriseren in een cohort van plaques verkregen uit zowel carotis als femorale endarterectomiechirurgie. Eerst stelden we vast dat ongeveer 1% van alle immuuncellen uit mestcellen bestaat. Om mestcellen te identificeren hebben we twee klassieke mestcelmarkers gemeten, namelijk CD117 en FcεRI. Vervolgens onderzochten we de activatiestatus van mestcellen. Waar voorheen mestcelactivatie in humane atherosclerose voornamelijk werd onderzocht door een histologische kleuring van tryptase, hebben wij hier flow cytometrie toegepast om dit beter in kaart te brengen. Een mestcel zit vol met kleine bolletjes, *granules*, waarin de proteases zijn opgeslagen. Zodra een mestcel geactiveerd raakt, zal deze *degranuleren*, wat inhoudt dat het zijn granules met proteases zal uitscheiden. Om mestcelactivatie beter te meten, hebben we gekozen voor de marker CD63, die op het cel oppervlak komt tijdens de degranulatie. De belangrijkste route van mestcelactivatie is als *immunoglobulin (Ig) E* bindt aan FcεRI. Zodra IgE aan deze receptor gebonden is, is enkel nog een antigeen nodig om de mestcel te activeren en te laten degranuleren. Circulerend IgE is positief gecorreleerd aan acute cardiovasculaire complicaties[33,34], maar of IgE ook gebonden is aan de geactiveerde mestcellen moest nog worden bepaald. Daarom hebben we vervolgens IgE gemeten op de intraplaque mestcellen. De meerderheid van de geactiveerde mestcellen had inderdaad IgE aan hun oppervlak gebonden. Aangezien in experimentele modellen van atherosclerose is aangetoond dat stabilisatie van mestcellen de progressie van de plaque kan remmen[28], zou het beperken van circulerend IgE, gericht op een verminderde intraplaque mestcelactivatie, een potentiële therapeutische strategie kunnen zijn. Daarnaast hebben we ook een populatie $IgE^{-}CD63^{+}$ mestcellen waargenomen, die waarschijnlijk via andere routes geactiveerd zijn. Het moet nog worden vastgesteld welke eiwitten betrokken zijn bij deze activatie. Tot slot toonden we met flow cytometrie aan dat niet alle mestcellen positief zijn voor tryptase, wat aangeeft dat histologische kleuring mogelijk niet alle mestcellen aankleurt die aanwezig zijn in atherosclerose. Daarom zijn wij van mening dat deze flow cytometrie benadering een valide methode is om mestcellen in humane

atherosclerose te onderzoeken. Toekomstige studies in grotere cohorten kunnen meer inzicht geven in hoe bepaalde activatiepatronen van mestcellen gecorreleerd kunnen worden aan klinische complicaties, waardoor de weg wordt vrijgemaakt voor nieuwe therapeutische benaderingen om mestcellen in atherosclerose aan te pakken.

Veroudering is een onafhankelijke risicofactor voor atherosclerose. Dit wordt gedeeltelijk veroorzaakt door een chronische laaggradige ontsteking, ook wel *inflammaging* genoemd, die zich ontwikkeld over tijd. Het inflammaging proces heeft aanzienlijk invloed op de immuuncellen in de plaque. Een recente studie heeft meerdere verouderings-gerelateerde veranderingen aangetoond in de intraplaque immuuncellen en heeft deze bevindingen ook bevestigd in een cohort van slagaderverkalking patiënten.[35] Er zijn meerdere studies die hebben aangetoond dat mestcellen ook leeftijds-gerelateerde veranderingen ondergaan[36-39], maar of dit ook in atherosclerose het geval is, was nog onbekend. Daarom hebben we in **hoofdstuk 6** het effect van veroudering op het fenotype en de activatiestatus van mestcellen in atherosclerose onderzocht. We hebben hiervoor de mestcelpopulatie geanalyseerd in een jong en een verouderd experimenteel muismodel voor atherosclerose. We observeerden dat in de verouderde groep de mestcellen meer geactiveerd waren. Bovendien zagen we in de oude muizen dat er meer IgE in het serum circuleerde. Dit suggereert dat de IgE-FcεRI route betrokken kan zijn bij de verhoogde activatie. In **hoofdstuk 5** zagen we een vergelijkbaar mestcelfenotype in humane plaques, die over het algemeen afkomstig zijn van oudere patiënten. We hebben ook jonge en oude mestcellen vergeleken door deze vanuit het beenmerg te laten ontwikkelen in de celkweek. Hier ontdekten we dat de oude mestcellen intrinsieke activatie vertoonde doordat ze CD63 tot expressie brachten zonder een stimulus. Om te onderzoeken of dit ten grondslag ligt aan de verhoogde activatie in het verouderd muismodel voor atherosclerose, hebben we deze vanuit het beenmerg ontwikkelde mestcellen getransplanteerd in een mestceldeficiënt muismodel en hier ook atherosclerose laten ontwikkelen. We zagen hier niet meer een verschil in activatie tussen de groep die jonge en oude mestcellen getransplanteerd hebben gekregen. Dit kan gedeeltelijk verklaard worden door het feit dat het fenotype van mestcellen grotendeels afhankelijk is van de inflammatoire omgeving waarin de mestcel zich bevindt. Deze resultaten benadrukken dus een belangrijke rol voor het verouderde inflammaging milieu voor het fenotype van de mestcellen in de atherosclerotische plaque.

Hoewel mestcelactivatie en degranulatie het meest onderzocht worden, zijn mestcellen ook beschreven als atypische antigeen-presenterende cellen. Mestcellen zijn inderdaad gevonden in de nabijheid van $CD4^+$ T-cellen in de huid van psoriasispatiënten en mestceldepletie resulteerde in verminderde $CD4^+$ T-celinfiltratie en -activatie in een

muis model voor multiple sclerose. Verder heeft eerder werk uit ons laboratorium aangetoond dat verhoogd cholesterol in het bloed de expressie van MHC-II, waarop het antigeen gepresenteerd wordt, op mestcellen significant is verhoogd. Bovendien is aangetoond dat deze mestcellen in staat zijn tot functionele antigeen-presentatie aan $CD4^+$ T-cellen in een muismodel en dat de depletie van mestcellen het aantal $CD4^+$ T-cellen in de atherosclerotische aorta vermindert. Gezien het in **hoofdstuk 3** en **4** beschreven belang van $CD4^+$ T cellen in humane atherosclerose, waren we vooral geïnteresseerd om te onderzoeken of veroudering ook invloed heeft op de antigeen-presenterende capaciteiten van mestcellen. De hoeveelheid $MHC\text{-}II^+$ mestcellen in de atherosclerotische aorta van verouderde muizen was hoger dan die in de jonge groep. Om te onderzoeken of dit ook functioneel van waarde is, hebben we het antigeen presentatie-proces in de celkweek nagebootst. We hebben wederom vanuit het beenmerg van jonge en oude muizen mestcellen laten groeien en die samen met $CD4^+$ T-cellen in kweek gezet. Bij incubatie met de oude mestcellen vonden we meer proliferatie van $CD4^+$ T-cellen, wat suggereert dat de mestcellen in staat zijn tot het presenteren van antigenen en dit direct kunnen presenteren aan $CD4^+$ T-cellen. Echter, ook de verhoogde expressie van MHC-II bleek een gevolg te zijn van de verouderde omgeving waarin de mestcellen zich bevinden, aangezien het verschil bij herintroductie in een jong milieu wederom verdween. Naast proteases, kunnen mestcellen ook cytokines produceren na activatie. Eerdere studies hebben aangetoond dat deze cytokines de functie van de T-cellen kunnen beïnvloeden door bij te dragen aan de inflammatoire omgeving.[40] Onze hypothese was daarom dat, ondanks dat er lokale antigen presentatie door mestcellen in de plaque kan plaatsvinden, de pro-inflammatoire cytokines die ze uitscheiden hoogstwaarschijnlijk een belangrijke rol spelen in T-cel activatie. We zagen inderdaad dat op het moment dat we verouderde muizen behandelden met DSCG, een stof die mestcel activatie remt, er minder effector $CD4^+$ T-cellen terug te vinden waren in het bloed en in de plaque. Samengevat hebben we met deze studie aangetoond dat veroudering en de bijbehorende inflammatoire omgeving significant bijdragen aan het fenotype en de functie van mestcellen in atherosclerose. Dit beïnvloedt zowel hun activatie en degranulatie als de daaropvolgende veranderingen in het $CD4^+$ T-celfenotype in de plaque. Het is daarom essentieel om leeftijd als belangrijke factor te beschouwen bij verder onderzoek naar mestcellen voor nieuwe therapeutische interventies voor atherosclerose.

Vanwege de verhoogde accumulatie en activatie van mestcellen in gevorderde atherosclerose zou het remmen van de rekrutering van mestcellen een veelbelovende therapeutische strategie kunnen zijn om destabilisatie van de plaque te voorkomen. Eén manier om deze migratie aan te pakken is door aan te grijpen op *lipide mediatoren*.

Leukotrieen B4 (*LTB_4*) is een ontstekingsbevorderende lipide mediator de hoogste affiniteit heeft voor de leukotrieen B4-receptor (BLT1). Er is aangetoond dat de BLT1-LTB4-as een rol speelt bij de rekrutering van meerdere immuuncellen, waaronder macrofagen en mestcelvoorlopers. Deze rekruteringsroute is al uitgebreid onderzocht in de context van atherosclerose. Zowel genetische deletie als farmacologische inhibitie van BLT1 of het enzym verantwoordelijk voor de biosynthese van LTB_4 hebben geleidt tot een vermindering van atherosclerose in een vroeg stadium, deels door een verlaagd aantal macrofagen in de plaque.[41–44] Echter, slagaderverkalking wordt vaak pas herkend als het al in een vergevorderd stadium zit. Of deze lipide mediatoren ook bijdragen aan de rekrutering van immuuncellen, en in het bijzonder mestcellen, in reeds bestaande plaques was nog onbekend. Daarom hebben we in **hoofdstuk 7** onderzocht of inhibitie van BLT1 de migratie van mestcellen naar gevorderde atherosclerose kan verminderen. We gebruikten eerst onze single-cell atlas van humane atherosclerose (**hoofdstuk 3**) om te analyseren of er in de plaque genen tot expressie worden gebracht die betrokken zijn bij de biosynthese van LTB4. We vonden dat macrofagen al deze genen tot expressie brachten, maar de hoogste expressie werd gevonden in de mestcellen. In deze studie hebben we muizen met vergevorderde atherosclerose behandeld met de BLT1-remmer CP105.696. We zagen significant minder macrofagen in de milt. Dit zou een direct effect kunnen zijn van BLT1-remming, maar monocyten produceren na binding van LTB_4 het eiwit *monocyte-chemoattractant protein 1* (*MCP-1*) wat rekrutering van nieuwe monocyten induceert. We zagen geen veranderingen in plaquegrootte en stabiliteit na behandeling met CP105.696. Waarschijnlijk is deze behandeling minder effectief in meer gevorderde atherosclerose, wat correspondeert met een eerdere studie die het grootste effect van BLT1-antagonisme in vroege laesies heeft beschreven.[42] Tenslotte zagen we geen veranderingen in het aantal circulerende mestcelvoorlopers of het aantal mestcellen in de plaque. Dit suggereert dat in gevorderde atherosclerose de BLT1-LTB4 as geen invloed heeft op de migratie van mestcellen naar de laesie. Hierbij moet wel vermeld worden dat de BLT2-receptor met lage affiniteit voor LTB_4 ook mestcelmigratie zou kunnen induceren. Aangezien CP105.696 BLT1-specifiek is, kunnen we in deze studie mogelijke BLT2-geïnduceerde mestcelmigratie niet uitsluiten en zal dit verder moeten worden onderzocht. Hoewel BLT1-antagonisme blijkbaar niet de juiste aanpak is om in te grijpen tegen mestcelmigratie in gevorderde atherosclerose, hebben we wel lokale LTB_4-productie door mestcellen in de humane atherosclerotische plaque gedetecteerd, die wel zou kunnen bijdragen aan de rekrutering van andere immuun cellen naar de plaque. Desalniettemin zijn we ervan overtuigd dat het aanpakken van mestcelmigratie, zij het via een andere route, een veelbelovende strategie blijft om in te grijpen op de progressie van atherosclerose.

Single-cell atlas als middel voor de identificatie van nieuwe aangrijpingspunten voor geneesmiddelen

Er zijn al veel potentiële targets voor atherosclerose onderzocht, maar helaas is de vertaling naar de kliniek vaak niet succesvol. Zoals eerder vermeld, hebben we de cellulaire atlas in **hoofdstuk 3** gegenereerd om het begrip van de pathofysiologie van atherosclerose te verbeteren en om te helpen bij het definiëren van nieuwe aangrijpingspunten voor medicijnen. In **hoofdstuk 8** gebruikten we dit hulpmiddel en vonden we specifieke expressie van *Interleukin-4-induced gene-1* (*IL4I1*) binnen de TREM2$^+$ macrofagen. IL4I1 is een enzym dat voornamelijk wordt geproduceerd door antigeen-presenterende cellen en het induceert de omzetting van zijn substraat L-fenylalanine in fenylpyruvaat, ammoniak en waterstofperoxide. IL4I1 is met name actief op het moment dat de antigeen-presenterende cel en de T-cel interactie hebben via het MHC-molecuul en de TCR. Hier interfereert het vervolgens met de T-cel proliferatie en bevordert het de ontwikkeling naar regulatoire CD4$^+$ T-cellen. IL4I1 werd oorspronkelijk ontdekt in verschillende soorten kanker en er is aangetoond dat remming van dit enzym de tumorgroei aanzienlijk vermindert door de cytotoxische CD8$^+$ T-celrespons te verhogen.[45] Onlangs werd gerapporteerd dat een specifieke IL4I1-remmer, CB-668, de tumorgroei vermindert door de CD8$^+$ T-celrespons te verstoren.[46] Hoewel kanker en atherosclerose gemeenschappelijke ontstekingsroutes hebben, is het doel bij kanker vaak om de ontstekingsreactie te activeren om de kankercellen te elimineren waarbij bij atherosclerose de ontstekingsreactie juist liever geremd wordt. Bij immuuntherapie tegen kanker wordt er dan ook herhaaldelijk een melding gemaakt van een verhoogd risico op hart- en vaatziekten, mogelijk door de geactiveerde ontstekingsreactie.[47,48] Daarom onderzochten we of IL4I1-inhibitie met CB-668 de progressie van atherosclerose in een muismodel zou beïnvloeden. In lijn met de eerder genoemde resultaten zagen we een vermindering van het aantal naïeve T-cellen en een toename van de effector en geheugencellen in de milt. Ook zagen we een toename van cytotoxische CD8$^+$ T-cellen in de milt en de atherosclerotische aorta. In de naastgelegen lymfeklier zagen we ook een toename van pro-inflammatoire effector CD4$^+$ T-cellen, wat op basis van eerdere studies waarschijnlijk een gevolg is van de CB-668 behandeling. Desondanks namen we geen veranderingen waar in de grootte en samenstelling van de plaques. In deze studie hebben welL4I1-remming in initiële atherosclerose onderzocht, terwijl meer uitgesproken effecten zouden kunnen optreden in meer gevorderde stadia van de ziekte. Ondanks dat onze studie aangetoond heeft dat IL4I1-inhibitie de ontwikkeling van atherosclerose initieel niet beïnvloedt, zullen toekomstige studies moeten uitwijzen of de door CB-668 geïnduceerde toegenomen ontsteking de progressie van de ziekte in een gevorderd stadia zal versnellen.

Toekomstperspectieven

In de afgelopen jaren is het onderzoeksveld zodanig ontwikkeld dat er een toegenomen aandacht is voor het aangrijpen op het immuunsysteem als behandeling voor atherosclerose. Meerdere klinische studies die de ontstekingsreactie getracht hebben te verminderen in patiënten met slagaderverkalking hebben een verlaging van het aantal acute cardiovasculaire complicaties beschreven. Echter, niet alle benaderingen bleken succesvol te zijn en de kwaliteit van leven te verbeteren. Doordat in atherosclerose er een delicate balans is tussen cellen die de ziekte verergeren of juist beschermen, is het essentieel om een op maat gemaakte therapeutische strategie te ontwerpen en om op specifieke processen aan te kunnen grijpen. De snelle ontwikkeling van single-cell technologieën zullen van vitaal belang zijn om dit te kunnen te bewerkstelligen.

In het afgelopen decennium is gebleken dat de datasets die zijn gegenereerd door single-cell multi-omics een belangrijk hulpmiddel zijn voor het identificeren van therapeutische aangrijppunten voor atherosclerose. Door de delicate veranderingen in het cel fenotype aan het licht te brengen, hebben deze studies tot belangrijke nieuwe inzichten in de ziekte geleid. Naast een gedetailleerde beschrijving van het genexpressieprofiel van de cellen in de plaque, kan er aan de hand van geavanceerde computationele analyses ook gekeken worden hoe de cellen zich ontwikkelen. Hiermee kunnen bijvoorbeeld voorlopercellen geïdentificeerd worden of processen beschreven worden die mogelijk kunnen voorkomen dat een pathogeen celtype zich in de plaque verder ontwikkelt. In dit proefschrift beschrijven we bijvoorbeeld de voorlopercellen in het bloed die zich in de plaque tot de antigeen-specifieke effector $CD4^+$ T-cellen ontwikkelen. Verder onderzoek naar het voorkomen van de rekrutering van deze voorlopercellen kan mogelijk een strategie zijn voor de behandeling van atherosclerose. Verder is het ook interessant om te kijken of bepaalde genen of celpopulaties te correleren zijn aan klinische parameters om mogelijk causale verbanden te identificeren. Een andere veelbelovende toepassing van deze single-cell datasets is onderzoeken of er al bestaande geneesmiddelen zijn die aangrijpen op genen die in atherosclerose een mogelijke pathogene rol spelen. Deze gerichte aanpak zorgt ervoor dat er sneller preklinische testen gedaan kunnen worden en versnelt de overgang naar de kliniek.

Een andere methode die in dit proefschrift ook veelvuldig aan bod is gekomen is het onderzoeken van mogelijke intercellulaire communicatie routes om op aan te grijpen. Hoewel dit een goed idee geeft van welke cellen mogelijk met elkaar zouden kunnen interacteren, heeft het een grote limitatie. Vanwege de methode die nodig is

om het weefsel goed te prepareren voor single-cell sequencing, is het onmogelijk te achterhalen of de cellen waarvan we voorspellen dat ze met elkaar communiceren ook daadwerkelijk in elkaars omgeving liggen. Om dit probleem te verhelpen is recentelijk *spatial transcriptomics* ontwikkeld, waarbij men het weefsel intact kan laten en alsnog een gedetailleerd genexpressie profiel van de cellen kunt genereren. In de context van dit proefschrift zal deze techniek een waardevolle bijdrage kunnen leveren om meer inzicht te krijgen in de interacties tussen de antigeen-presenterende cellen en de antigeen-specifieke T-cellen.

Nu we de accumulatie van plaque-verrijkte antigeen-specifieke T-cellen in de plaque is vastgesteld, is natuurlijk de meest prangende vraag op welke antigenen deze T-cellen mogelijk reageren. Er is al veel onderzoek gedaan naar dit mogelijke antigeen en er zijn meerdere kandidaat antigenen beschreven die nog verder onderzocht moeten worden.[49] Een voorbeeld hiervan is een stukje van het eiwit *Apolipoproteïne B100* (*ApoB100*), wat een onderdeel is van het LDL-cholesteroldeeltje. In experimentele muismodellen is aangetoond dat vaccinatie met LDL en oxLDL een beschermend effect heeft op de ontwikkeling van atherosclerose.[50–52] Echter, om het humane antigeen te bepalen zijn geavanceerdere methodes nodig. Tegenwoordig zijn er veel ontwikkelingen op computationeel gebied waarbij getracht wordt om vanuit de TCR sequentie een voorspelling te doen op welk antigeen de T-cellen reageren. Ondanks dat deze benadering veel potentie heeft, gaven ze bij onze data niet de gewenste nauwkeurigheid. Een andere benadering om het antigeen te onderzoeken is *immunopeptidomics*. Bij deze techniek is het mogelijk om de antigenen die op de MHC-moleculen van de antigeen-presenterende cellen in de plaque zitten, los te koppelen en te meten. Deze techniek is veelbelovend om nieuwe kandidaat antigenen te identificeren om zo mogelijk een stap in de richting van een vaccinatie voor atherosclerose te maken.

Tot slot leveren we aanwijzingen dat het aanpakken van mestcellen in atherosclerose een effectieve therapeutische strategie zou kunnen zijn. Door hun sterk geactiveerde toestand te remmen of door de rekrutering van mestcellen in de plaque aan te pakken, kan de atherosclerose mogelijk worden verminderd. Aangezien onze data aantoonden dat IgE een belangrijke bijdrage zou kunnen leveren aan de activatie van mestcellen in de plaque, zal het interessant zijn om patiënten te behandelen met IgE-blokkerende antilichamen, zoals Omalizumab[53], om te zien hoe dit de progressie van atherosclerose beïnvloedt. Hoewel we de belangrijkste rekruteringsroutes die betrokken zijn bij de migratie van mestcellen naar de atherosclerotische plaque nog niet hebben kunnen definiëren, zijn we ervan overtuigd dat het cruciaal is om dit in de toekomst verder te onderzoeken.

Naast het vinden en valideren van mogelijke geneesmiddelaangrijpingspunten, kunnen single-cell technologieën ook worden toegepast om de diagnostiek te verbeteren. Op dit moment is vroegtijdige opsporing van atherosclerotische hart- en vaatziekten een belangrijke pijler in het onderzoeksveld. Daarom is het essentieel om nieuwe *biomarkers* voor deze ziekte te definiëren. Een biomarker is een meetbare en specifieke indicator die een voorspelling geeft van de ernst van de ziekte. Als klinische parameters in verband kunnen worden gebracht met bepaalde pathologische celtypes, zou dit de voorspelling voor het risico op klinische complicaties kunnen verbeteren. Door te onderzoeken of de in de plaque gedetecteerde celtypes ook voorkomen in het bloed of als we voorlopers van pathogene celtypes kunnen vinden, kunnen deze mogelijk worden gebruikt als biomarker. Op basis van het werk in dit proefschrift zou het interessant kunnen zijn om verder te bepalen of de $CCR4^{+}CCR10^{+}$ voorloper $CD4^{+}$ T-cellen geassocieerd kunnen worden met toekomstige cardiovasculaire complicaties. Daarnaast zou het meten van mestcelvoorlopers in de circulatie mogelijk ook een hulpmiddel kunnen zijn om plaque stabiliteit te voorspellen. Ten slotte ligt er een groot potentieel in het gebruik van single-cell technologieën voor stratificatie van patiënten en om het effect van geneesmiddelen te voorspellen door de aan- of afwezigheid van therapeutisch relevante markers. Bij kanker wordt dit al toegepast om patiënten te definiëren die een grotere kans hadden op een goede respons op chemo- of immuuntherapie, bijvoorbeeld bij HER2 positieve of negatieve borstkanker. Bij atherosclerose is er reeds single-cell multi-omics toegepast om verschillen te analyseren tussen immuuncellen van patiënten met en zonder klinische symptomen[22], maar verder onderzoek is nodig om specifieke genen te identificeren die de respons op geneesmiddelen kunnen voorspellen. Verder is het essentieel om de data die gegenereerd is met single-cell sequencing te vergelijken tussen zowel plaques uit de carotis en de kransslagader. Een recente studie heeft deze vergelijking gemaakt voor macrofagen en gerapporteerd dat, afgezien van enige variatie tussen patiënten in de verhoudingen van de cellen, op beide locaties dezelfde macrofaagsubtypes gevonden werden.[22,54,55] Het verder uitbreiden van deze analyse voor andere celtypes zal een waardevolle bijdrage kunnen leveren aan de zoektocht naar gemeenschappelijke biomarkers en therapeutische aangrijpingspunten voor alle patiënten met slagaderverkalking.

Het werk in dit proefschrift laat zien dat single-cell multi-omics een zeer waardevol hulpmiddel is om de pathofysiologie van atherosclerose te onderzoeken en om nieuwe aangrijpingspunten voor interventie te identificeren. Het zal intrigerend zijn om te zien hoe de oneindige mogelijkheden van single-cell technologieën zullen bijdragen aan een verbeterde behandeling voor atherosclerose.

Referenties

1. World Health Organization. Noncommunicable diseases. https://www.who.int/news-room/fact-sheets/detail/noncommunicable-diseases (2022).
2. Timmis, A. *et al.* European Society of Cardiology: cardiovascular disease statistics 2021. *Eur Heart J* **43**, 716–799 (2022).
3. World Health Organization. Cardiovascular diseases (CVDs). https://www.who.int/news-room/fact-sheets/detail/cardiovascular-diseases-(cvds) (2021).
4. Grundy, S. M. *et al.* 2018 AHA/ACC/AACVPR/AAPA/ABC/ACPM/ADA/AGS/APhA/ASPC/NLA/PCNA Guideline on the Management of Blood Cholesterol: Executive Summary. *J Am Coll Cardiol* **73**, (2019).
5. Bäck, M., Yurdagul, A., Tabas, I., Öörni, K. & Kovanen, P. T. Inflammation and its resolution in atherosclerosis: mediators and therapeutic opportunities. *Nature Reviews Cardiology 2019 16:7* **16**, 389–406 (2019).
6. Bays, H. E. *et al.* Ten things to know about ten cardiovascular disease risk factors. *Am J Prev Cardiol* **5**, 100149 (2021).
7. Doran, A. C., Meller, N. & McNamara, C. A. Role of Smooth Muscle Cells in the Initiation and Early Progression of Atherosclerosis. *Arterioscler Thromb Vasc Biol* **28**, 812–819 (2008).
8. Rong, J. X., Shapiro, M., Trogan, E. & Fisher, E. A. Transdifferentiation of mouse aortic smooth muscle cells to a macrophage-like state after cholesterol loading. *Proceedings of the National Academy of Sciences* **100**, 13531–13536 (2003).
9. Li, H., Freeman, M. W. & Libby, P. Regulation of smooth muscle cell scavenger receptor expression in vivo by atherogenic diets and in vitro by cytokines. *J Clin Invest* **95**, 122–133 (1995).
10. Shankman, L. S. *et al.* KLF4-dependent phenotypic modulation of smooth muscle cells has a key role in atherosclerotic plaque pathogenesis. *Nat Med* **21**, 628–637 (2015).
11. Ridker, P. M. *et al.* Antiinflammatory Therapy with Canakinumab for Atherosclerotic Disease. *New England Journal of Medicine* **377**, 1119–1132 (2017).
12. Chung, E. S., Packer, M., Lo, K. H., Fasanmade, A. A. & Willerson, J. T. Randomized, Double-Blind, Placebo-Controlled, Pilot Trial of Infliximab, a Chimeric Monoclonal Antibody to Tumor Necrosis Factor-α, in Patients With Moderate-to-Severe Heart Failure. *Circulation* **107**, 3133–3140 (2003).
13. Nidorf, S. M. *et al.* Colchicine in Patients with Chronic Coronary Disease. *New England Journal of Medicine* **383**, 1838–1847 (2020).
14. Tardif, J.-C. *et al.* Efficacy and Safety of Low-Dose Colchicine after Myocardial Infarction. *New England Journal of Medicine* **381**, 2497–2505 (2019).
15. Opstal, T. S. J. *et al.* Long-Term Efficacy of Colchicine in Patients With Chronic Coronary Disease: Insights From LoDoCo2. *Circulation* **145**, 626–628 (2022).
16. Kashima, Y. *et al.* Single-cell sequencing techniques from individual to multiomics analyses. *Experimental & Molecular Medicine 2020 52:9* **52**, 1419–1427 (2020).
17. van Kuijk, K. *et al.* Human and murine fibroblast single-cell transcriptomics reveals fibroblast clusters are differentially affected by ageing and serum cholesterol. *Cardiovasc Res* **119**, 1509–1523 (2023).
18. Winkels, H. *et al.* Atlas of the Immune Cell Repertoire in Mouse Atherosclerosis Defined by Single-Cell RNA-Sequencing and Mass Cytometry. *Circ Res* **122**, 1675–1688 (2018).
19. Cochain, C. *et al.* Single-Cell RNA-Seq Reveals the Transcriptional Landscape and Heterogeneity of Aortic Macrophages in Murine Atherosclerosis. *Circ Res* **122**, 1661–1674 (2018).

20. Kim, K. *et al.* Transcriptome Analysis Reveals Nonfoamy Rather Than Foamy Plaque Macrophages Are Proinflammatory in Atherosclerotic Murine Models. *Circ Res* **123**, 1127–1142 (2018).
21. Willemsen, L. & de Winther, M. P. J. Macrophage subsets in atherosclerosis as defined by single-cell technologies. *J Pathol* **250**, 705–714 (2020).
22. Fernandez, D. M. *et al.* Single-cell immune landscape of human atherosclerotic plaques. *Natuere Medicine* **25**, 1576–1588 (2019).
23. Owens, G. K., Kumar, M. S. & Wamhoff, B. R. Molecular regulation of vascular smooth muscle cell differentiation in development and disease. *Physiol Rev* **84**, 767–801 (2004).
24. Gomez, D. & Owens, G. K. Smooth muscle cell phenotypic switching in atherosclerosis. *Cardiovasc Res* **95**, 156–164 (2012).
25. Chowdhury, R. R. *et al.* Human Coronary Plaque T Cells Are Clonal and Cross-React to Virus and Self. *Circ Res* **130**, 1510–1530 (2022).
26. Wigren, M. *et al.* Lack of Ability to Present Antigens on Major Histocompatibility Complex Class II Molecules Aggravates Atherosclerosis in ApoE -/- Mice. *Circulation* **139**, 2554–2566 (2019).
27. Slütter, B. & Kuiper, J. Immune Responses in Context: An Anti-Inflammatory Role for Major Histocompatibility Complex Class II Presentation in the Atherosclerotic Lesion? *Circulation* **139**, 2567–2569 (2019).
28. Bot, I. *et al.* Perivascular mast cells promote atherogenesis and induce plaque destabilization in apolipoprotein E-deficient mice. *Circulation* **115**, 2516–2525 (2007).
29. Bot, I. *et al.* Mast cell chymase inhibition reduces atherosclerotic plaque progression and improves plaque stability in ApoE-/- mice. *Cardiovasc Res* **89**, 244–252 (2011).
30. Bot, I., Shi, G. P. & Kovanen, P. T. Mast cells as effectors in atherosclerosis. *Arterioscler Thromb Vasc Biol* **35**, 265 (2015).
31. Shi, G. P., Bot, I. & Kovanen, P. T. Mast cells in human and experimental cardiometabolic diseases. *Nat Rev Cardiol* **12**, 643–658 (2015).
32. Willems, S. *et al.* Mast cells in human carotid atherosclerotic plaques are associated with intraplaque microvessel density and the occurrence of future cardiovascular events. *Eur Heart J* **34**, 3699–3706 (2013).
33. Sinkiewicz, W. *et al.* Immunoglobulin E as a marker of the atherothrombotic process in patients with acute myocardial infarction. *Cardiol J* **14**, 266–73 (2007).
34. Langer, R. D., Criqui, M. H., Feigelson, H. S., McCann, T. J. & Hamburger, R. N. IgE predicts future nonfatal myocardial infarction in men. *J Clin Epidemiol* **49**, 203–209 (1996).
35. Smit, V. *et al.* Single-cell profiling reveals age-associated immunity in atherosclerosis. *Cardiovasc Res* (2023) doi:10.1093/CVR/CVAD099.
36. Blasco, M. P. *et al.* Age-dependent involvement of gut mast cells and histamine in post-stroke inflammation. *J Neuroinflammation* **17**, (2020).
37. Pilkington, S. M., Barron, M. J., Watson, R. E. B., Griffiths, C. E. M. & Bulfone-Paus, S. Aged human skin accumulates mast cells with altered functionality that localize to macrophages and vasoactive intestinal peptide-positive nerve fibres. *Br J Dermatol* **180**, 849–858 (2019).
38. Gunin, A. G., Kornilova, N. K., Vasilieva, O. V. & Petrov, V. V. Age-related changes in proliferation, the numbers of mast cells, eosinophils, and cd45-positive cells in human dermis. *J Gerontol A Biol Sci Med Sci* **66**, 385–392 (2011).
39. Chatterjee, V. & Gashev, A. A. Aging-associated shifts in functional status of mast cells located by adult and aged mesenteric lymphatic vessels. *Am J Physiol Heart Circ Physiol* **303**, (2012).
40. Bulfone-Paus, S. & Bahri, R. Mast Cells as Regulators of T Cell Responses. *Front Immunol* **6**, (2015).

41. Heller, E. A. *et al.* Inhibition of atherogenesis in BLT1-deficient mice reveals a role for LTB4 and BLT1 in smooth muscle cell recruitment. *Circulation* **112**, 578–586 (2005).
42. Aiello, R. J. *et al.* Leukotriene B4 receptor antagonism reduces monocytic foam cells in mice. *Arterioscler Thromb Vasc Biol* **22**, 443–449 (2002).
43. Subbarao, K. *et al.* Role of leukotriene B4 receptors in the development of atherosclerosis: potential mechanisms. *Arterioscler Thromb Vasc Biol* **24**, 369–375 (2004).
44. Mehrabian, M. *et al.* Identification of 5-lipoxygenase as a major gene contributing to atherosclerosis susceptibility in mice. *Circ Res* **91**, 120–126 (2002).
45. Lasoudris, F. *et al.* IL4I1: an inhibitor of the $CD8^+$ antitumor T-cell response in vivo. *Eur J Immunol* **41**, 1629–1638 (2011).
46. MacKinnon, A. *et al.* 705 Anti-tumor activity of CB-668, a potent, selective and orally bioavailable small-molecule inhibitor of the immuno-suppressive enzyme Interleukin 4 (IL-4)-Induced Gene 1 (IL4I1). *J Immunother Cancer* **8**, A423.2-A424 (2020).
47. Mocan-Hognogi, D. L. *et al.* Immune Checkpoint Inhibitors and the Heart. *Front Cardiovasc Med* **8**, 726426 (2021).
48. Poels, K. *et al.* Antibody-Mediated Inhibition of CTLA4 Aggravates Atherosclerotic Plaque Inflammation and Progression in Hyperlipidemic Mice. *Cells* **9**, (2020).
49. Nilsson, J. & Hansson, G. K. Vaccination Strategies and Immune Modulation of Atherosclerosis. *Circ Res* **126**, 1281–1296 (2020).
50. Zhou, X., Caligiuri, G., Hamsten, A., Lefvert, A. K. & Hansson, G. K. LDL Immunization Induces T-Cell–Dependent Antibody Formation and Protection Against Atherosclerosis. *Arterioscler Thromb Vasc Biol* **21**, 108–114 (2001).
51. Palinski, W., Miller, E. & Witztum, J. L. Immunization of low density lipoprotein (LDL) receptor-deficient rabbits with homologous malondialdehyde-modified LDL reduces atherogenesis. *Proceedings of the National Academy of Sciences* **92**, 821–825 (1995).
52. Freigang, S., Hörkkö, S., Miller, E., Witztum, J. L. & Palinski, W. Immunization of LDL Receptor–Deficient Mice With Homologous Malondialdehyde-Modified and Native LDL Reduces Progression of Atherosclerosis by Mechanisms Other Than Induction of High Titers of Antibodies to Oxidative Neoepitopes. *Arterioscler Thromb Vasc Biol* **18**, 1972–1982 (1998).
53. Kawakami, T. & Blank, U. From IgE to Omalizumab. *J Immunol* **197**, 4187–4192 (2016).
54. Zernecke, A. *et al.* Integrated single-cell analysis-based classification of vascular mononuclear phagocytes in mouse and human atherosclerosis. *Cardiovasc Res* **119**, 1676–1689 (2023).
55. Wirka, R. C. *et al.* Atheroprotective roles of smooth muscle cell phenotypic modulation and the TCF21 disease gene as revealed by single-cell analysis. *Nat Med* **25**, 1280–1289 (2019).

Appendix

Curriculum vitae

Curriculum vitae

Marie Depuydt werd geboren op 14 januari 1994 in Leiderdorp. In 2012 behaalde ze haar gymnasium diploma aan het Stedelijk Gymnasium in Leiden. In datzelfde jaar startte ze met de bacheloropleiding Bio-Farmaceutische Wetenschappen aan de Universiteit Leiden. Na haar bachelorstage bij de divisie BioTherapeutics van het Leiden Academic Centre for Drug Research (LACDR) haalde Marie haar Bachelor of Science-graad in 2015.

Marie vervolgde haar opleiding met de master Bio-Pharmaceutical Sciences. Haar eerste wetenschappelijke stage werd wederom uitgevoerd bij de divisie BioTherapeutics van het LACDR. Deze stage werd afgesloten met een verslag getiteld "Understanding the role of Apoliprotein E in adrenal steroidogenesis". Dit heeft geleid tot twee wetenschappelijke publicaties in de wetenschappelijke tijdschriften *Molecular and Cellular Endocrinology* en *Biochimica et Biophysica Acta (BBA) – Molecular and Cell Biology of Lipids*. Marie heeft haar tweede wetenschappelijke stage uitgevoerd onder begeleiding van dr. Daniel Engelbertsen en prof. dr. Andrew Lichtman bij Harvard Medical School in Boston (VS). Deze stage is afgerond met een verslag getiteld "IL-23R deficiency does not affect atherosclerotic lesion development" en heeft geresulteerd in een wetenschappelijke publicatie in het tijdschrift *Journal of the American Heart Association*. In 2017 behaalde ze haar Master of Science-graad *cum laude*.

Van november 2017 tot april 2022 was Marie werkzaam als promovendus onder begeleiding van prof. dr. Johan Kuiper, dr. Bram Slütter en dr. Ilze Bot bij de divisie BioTherapeutics van het LACDR. Voor het presenteren van het onderzoek uit dit proefschrift ontving Marie in 2019, 2022 en 2023 de Young Investigator Fellowship voor het congres van de European Atherosclerosis Society. Verder ontving ze in 2019 een prijs voor haar poster bij de NVVI Annual meeting en in 2021 bij het LACDR Spring Symposium. Ze ontving een prijs voor haar presentatie bij het congres van de European Mast Cell and Basophil Research Network in 2021 en bij het congres van de Dutch Atherosclerosis Society in 2023. Tot slot eindigde ze in 2023 op de tweede plaats van de WCN Onderzoeksprijs voor haar paper in *Nature Cardiovascular Research*.

Sinds mei 2022 is Marie werkzaam als post-doctoraal onderzoeker bij de divisie BioTherapeutics van het LACDR om hier haar onderzoek voort te zetten.

Appendix

Scientific publications

Full papers

M. Mulholland, **M.A.C. Depuydt**, G. Jakobsson, I. Ljungcrantz, A. Grentzmann, F. To, E. Bengtsson, E. Jaensson Gyllenbäck, C. Grönberg, S. Rattik, D. Liberg, A. Schiopu, H. Björkbacka, J. Kuiper, I. Bot, B. Slütter, D. Engelbertsen. IL1RAP blockade limits development of atherosclerosis and reduces plaque inflammation. *Cardiovascular Research*. 2024; *accepted for publication*.

V. Smit , J. de Mol , F.H. Schaftenaar, **M.A.C. Depuydt**, R.J. Postel , D. Smeets, F.W.H. Verheijen, L. Bogers, J. van Duijn, R.A.F. Verwilligen, H.W. Grievink, M.N.A. Bernabé Kleijn, E. van Ingen, M.J.M. de Jong, L. Goncalves, A.H.M. Peeters, H.J. Smeets, A. Wezel, J.K. Polansky, M.P.J. de Winther, C.J. Binder, D. Tsiantoulas, I. Bot, J. Kuiper, A.C. Foks. Single-cell profiling reveals age-associated immunity in atherosclerosis. *Cardiovascular Research***.** 2023; 119, 2508–2521.

E. Diez Benavente, S. Karnewar, M. Buono, E. Mili, R.J.G. Hartman, D. Kapteijn , L. Slenders, M. Daniels, R. Aherrahrou, T. Reinberger, B.M. Mol, G.J. de Borst, D.P.V. de Kleijn, K.H.M. Prange, **M.A.C. Depuydt**, M.P.J. de Winther, J. Kuiper, J.L.M. Björkegren, J. Erdmann, M. Civelek, M. Mokry, G.K. Owens, G. Pasterkamp, H.M. den Ruijter. Female Gene Networks Are Expressed in Myofibroblast-Like Smooth Muscle Cells in Vulnerable Atherosclerotic Plaques. *Arteriosclerosis Thrombosis Vascular Biology*. 2023; 43: 1836-1850.

W. In het Panhuis, M. Schönke, M. Modder, H.E. Tom, R.A. Lalai, A.C.M. Pronk, T.C.M. Streefland, L.W.M. van Kerkhof, M.E.T. Dollé, **M.A.C. Depuydt**, I. Bot, W.G. Vos, L.A. Bosmans, B.W. van Os, E. Lutgens, P.C.N. Rensen, S. Kooijman. Time-restricted feeding attenuates hypercholesterolaemia and atherosclerosis development during circadian disturbance in APOE*3-Leiden.CETP mice. *eBioMedicine*. 2023; 93, 104680.

E. Hemme, D. Biskop, **M.A.C. Depuydt**, V. Smit, L. Delfos, M.N.A. Bernabé Kleijn, A.C. Foks, J. Kuiper, I. Bot. Bruton's Tyrosine Kinase inhibition by Acalabrutinib does not affect early or advanced atherosclerotic plaque size and morphology in Ldlr-/-mice. *Vascular Pharmacology*. 2023; 150: 107172.

M.A.C. Depuydt, F.H. Schaftenaar, K.H.M. Prange, A. Boltjes, E. Hemme, L. Delfos, J. de Mol, M.J.M. de Jong, M.N.A. Bernabé Kleijn, A.H.M. Peeters, L. Goncalves, A. Wezel, H.J. Smeets, G.J. de Borst, A.C. Foks, G. Pasterkamp, M.P.J. de Winther, J. Kuiper, I. Bot, B. Slütter. Single-cell T cell receptor sequencing of paired human atherosclerotic plaques and blood reveals autoimmune-like features of expanded effector T cells. *Nature Cardiovascular Research*. 2023; 2:112-125.

M. Mokry, A. Boltjes, L. Slenders, G. Bel-Bordes, K. Cui, E. Brouwer, J.M. Mekke, **M.A.C. Depuydt**, N. Timmerman, F. Waissi, M.C. Verwer, A.W. Turner, M. Daud Khan, C.J. Hodonsky, E. Diez Benavente, R.J.G. Hartman, N.A.M. van den Dungen, N. Lansu, E. Nagyova, K.H.M. Prange, J.C. Kovacic, J.L.M. Björkegren, E. Pavlos, E. Andreakos, H. Schunkert, G.K. Owens, C. Monaco, A.V. Finn, R. Virmani, N.J. Leeper, M.P.J. de Winther, J. Kuiper, G.J. de Borst, E.S.G. Stroes, M. Civelek, D.P.V. de Kleijn, H.M. den Ruijter, F.W. Asselbergs, S.W. van der Laan, C.L. Miller, G. Pasterkamp. Transcriptomic-based clustering of human atherosclerotic plaques identifies subgroups with different underlying biology and clinical presentation. *Nature Cardiovascular Research*. 2022; 1, 1140–1155.

M.A.C. Depuydt, F.D. Vlaswinkel, E. Hemme, L. Delfos, M.N.A. Bernabé Kleijn, P.J. van Santbrink, A.C. Foks, B. Slütter, J. Kuiper, I. Bot. Blockade of the BLT1-LTB4 axis does not affect mast cell migration towards advanced atherosclerotic lesions in LDLr$^{-/-}$ mice. *Scientific Reports*. 2022; 12:18362.

L. Slenders, L.P.L. Landsmeer, K. Cui, **M.A.C. Depuydt**, M. Verwer, J. Mekke, N. Timmerman, N.A.M. van den Dungen, J. Kuiper, M.P.J. de Winther, K.H.M. Prange, W.F. Ma, C.L. Miller, R. Aherrahrou, M. Civelek, G.J. de Borst, D.P.V. de Kleijn, F.W. Asselbergs, H.M. den Ruijter, A. Boltjes, G. Pasterkamp, S.W. van der Laan, M. Mokry. Intersecting single-cell transcriptomics and genome-wide association studies identifies crucial cell populations and candidate genes for atherosclerosis. *European Heart Journal Open*. 2021; 2:1-14.

M.A.C. Depuydt, K.H.M. Prange, L. Slenders, T. Örd, D. Elbersen, A. Boltjes, S.C.A. de Jager, F.W. Asselbergs, G.J. de Borst, E. Aavik, T. Lönnberg, E. Lutgens, C.K. Glass, H.M. den Ruijter, M.U. Kaikkonen, I. Bot, B. Slütter, S.W. van der Laan, S. Yla-Herttuala, M. Mokry, J. Kuiper, M.P.J. de Winther, G. Pasterkamp. Microanatomy of the Human Atherosclerotic Plaque by Single-Cell Transcriptomics. *Circulation Research*. 2020; 127:1437-1455.

R.J. van der Sluis, **M.A.C. Depuydt**, M. van Eck, M. Hoekstra. VLDL/LDL serves as the primary source of cholesterol in the adrenal glucocorticoid response to food deprivation. *Biochimica et Biophysica Acta (BBA) – Molecular and Cell Biology of Lipids*. 2020; 1865(7): 158682.

H. Douna, J. Amersfoort, F.H. Schaftenaar, M.J. Kröner, M.B. Kiss, B. Slütter, **M.A.C. Depuydt**, M.N.A. Bernabé Kleijn, A. Wezel, H. Smeets, H. Yagita, C.J. Binder, I. Bot, G.H.M. van Puijvelde, J. Kuiper, A.C. Foks. BTLA stimulation protects against atherosclerosis by regulating follicular B cells. *Cardiovascular Research*. 2020; 116(2): 295-305.

D. Engelbertsen, A. Autio, R.A.F. Verwilligen, **M.A.C. Depuydt**, G. Newton, S. Rattik, E. Levinsohn, G. Saggu, P. Jarolim, H. Wang, F. Velazquez, A.H. Lichtman, F.W. Luscinskas. Increased lymphocyte activation and atherosclerosis in CD47-deficient mice. *Scientific Reports*. 2019; 9(1):10608.

J. van Duijn, M. van Elsas, N. Benne, **M.A.C. Depuydt**, A. Wezel, H.J. Smeets, I. Bot, W. Jiskoot, J. Kuiper, B. Slütter. CD39 identifies a microenvironment-specific anti-inflammatory $CD8^+$ T-cell population in atherosclerotic lesions. *Atherosclerosis*. 2019; 285:71-78.

R.J. van der Sluis, **M.A.C. Depuydt**, R.A.F. Verwilligen, M. Hoekstra, M. van Eck. Elimination of adrenocortical apolipoprotein E production does not impact glucocorticoid output in wild-type mice. *Molecular and Cellular Endocrinology*. 2019; 490:21-27.

E. Kritikou, **M.A.C. Depuydt**, M.R. de Vries, K.E. Mulder, A.M. Govaert, M.D. Smit, J. van Duijn, A.C. Foks, A. Wezel, H.J. Smeets, B. Slütter, P.H.A. Quax, J. Kuiper, I. Bot. Flow Cytometry-Based Characterization of Mast Cells in Human Atherosclerosis. *Cells*. 2019; 8(4).

D. Engelbertsen, **M.A.C. Depuydt**, R.A.F. Verwilligen, S. Rattik, E. Levinsohn, A. Edsfeldt, F. Kuperwaser, P. Jarolim, A.H. Lichtman. IL-23R Deficiency Does Not Impact Atherosclerotic Plaque Development in Mice. *Journal of the American Heart Association*. 2018; 7(8).

Published abstracts

F.L. Vigario, I.S. Vesperinas, **M.A.C. Depuydt**, I. Bot, P. Van Veelen, J. Bouwstra, A. Kros, B. Slütter. Immunopeptidomic analysis of human atherosclerosis identifies novel ApoB100-derived antigenic drivers of atherosclerosis. *Atherosclerosis*. 2023; 379, S8-S9

V. Smit, J. de Mol, F.H. Schaftenaar, **M.A.C. Depuydt**, R.J. Postel, D. Smeets, F.W.H. Verheijen, L. Bogers, J. van Duijn, R.A.F. Verwilligen, W.H. Grievink, M.N.A. Bernabé Kleijn, L. Goncalves, A.H.M. Peeters, H.J. Smeets, A. Wezel, J. Polansky-Biskup, M.P.J. de Winther, C.J. Binder, D. Tsiantoulas, I. Bot, J. Kuiper, A.C. Foks. Single-cell profiling reveals age-associated immune cells in atherosclerosis. *Atherosclerosis*. 2023; 379, S37

L. Delfos, **M.A.C. Depuydt**, A.C. Foks, M.N.A. Bernabé Kleijn, J. Kuiper, M. Chemaly, A. Peace, V. McGilligan, I. Bot. NLRP3 inflammasome inhibition by the novel bispecific antibody inflamab inhibits atherosclerosis in apolipoprotein E-deficient mice. *Atherosclerosis*. 2023; 379, S2

E. Hemme, **M.A.C. Depuydt**, L. Delfos, J. Kuiper, I. Bot. Leukemia inhibitory factor receptor inhibition in atherosclerosis. *Atherosclerosis*. 2023; 379, S36

R. Snijckers, J. de Mol, V. Smit, R.J. Postel, E. Lievaart, M.N.A Bernabé Kleijn, **M.A.C. Depuydt**, I. Bot, J. Kuiper, A.C. Foks. IL-21R blockade reduces atherosclerosis development. *Atherosclerosis*. 2023;379, S26

M.A.C. Depuydt, V. Smit, F. Lozano Vigario, M.N.A. Bernabé Kleijn, M.R. de Vries, P.H.A. Quax, A. Wezel, H.J. Smeets, J. Kuiper, A.C. Foks, I. Bot, B. Slütter. Granzyme $B^{+}CD4^{+}$ T cells associate with an unstable plaque phenotype in advanced human atherosclerosis. *Cardiovascular Research*. 2022; 118(Supplement_1): cvac066.229.

E. Hemme, L. Delfos, **M.A.C. Depuydt**, M.N.A. Bernabé Kleijn, F.H. Schaftenaar, A.C. Foks, J. Kuiper, I. Bot. Bruton's tyrosine kinase inhibition to suppress mast cell activation in atherosclerosis. *Atherosclerosis*. 2022; 355, 17-18

R.J. Postel, V. Smit, J. de Mol, M.N.A. Bernabé Kleijn, M.J.M. de Jong, L. Delfos, E. Hemme, **M.A.C. Depuydt**, I. Bot, J. Kuiper, A.C. Foks. IL-21R blockade reduces atherosclerosis development in $LDLR^{-/-}$ mice. *Atherosclerosis*. 2022; 355: 23.

M.J.M. De Jong, **M.A.C. Depuydt**, F. Lozano Vigario, P.A. van Veelen, J. Kuiper, B. Slütter. Virus specific CD8⁺ T-cells accumulate, but do not recognize antigen, in the atherosclerotic lesion. Cardiovascular Research 2022; 118 (Supplement_1), cvac066. 228

S.W. van der Laan, L. Slenders , **M.A.C. Depuydt**, K.H.M. Prange, L. Granneman, D. Elbersen, A. Boltjes, S. de Jager, B. Slütter, I. Bot, M.P.J. de Winther, J. Kuiper, M. Mokry, F.W. Asselbergs, G. Pasterkamp. Mapping genes to cardiovascular susceptibility loci at a single-cell resolution. *Atherosclerosis*. 2019; 287: E21-E21.

M.A.C. Depuydt, K.H.M. Prange, L. Slenders, D. Elbersen, A. Boltjes, S.C.A. de Jager, B. Slütter, I. Bot, S.W. van der Laan, M. Mokry, G. Pasterkamp, M.P.J. de Winther, J Kuiper. Microanatomy of advanced human atherosclerotic plaques through single-cell transcriptomics. *Atherosclerosis* 2019;287: E5-E5.

M. Mokry, **M.A.C. Depuydt**, K.H.M. Prange, L. Slenders, D. Elbersen, L.E.C. Granneman, S.C.A. de Jager, B. Slütter, I. Bot, M.P.J. de Winther, J. Kuiper, F.W. Asselbergs, S.W. van der Laan, G. Pasterkamp. Single cell RNA-sequencing identifies numerous cell sub-types and suggests lineage plasticity in human atherosclerotic plaques. *Atherosclerosis*. 287: E96-E97.

J. van Duijn, M. van Elsas, N. Benne, **M.A.C. Depuydt**, A. Wezel, H.J. Smeets, I. Bot, W. Jiskoot, J. Kuiper, B. Slütter. Continuous TCR signaling in the atherosclerotic environment induces immunomodulatory CD8⁺ T-cells expressing CD39. *Atherosclerosis*. 2019;287: e17-e18.

B. Slütter, **M.A.C. Depuydt**, J. van Duijn, I. Bot, A. Wezel, H. Koppejan, R. Toes, J. Kuiper. Mass cytometry identifies CD8 T-cell diversity in human atherosclerotic lesions. *Atherosclerosis*. 2018;275: e8.

Appendix

PhD portfolio

PhD portfolio

Courses

2017	Laboratory Animal Science	Leiden University
2018	LACDR PhD Introductory Course on Drug Research	Leiden University
	Introduction to teaching and supervision	Leiden University
	Time management, self-management	Leiden University
	Data management course	Leiden University
	Atherosclerosis and Thrombosis course	Dutch Heart Foundation
	R for data science	Leiden University
	Advanced course on Atherosclerosis, Dyslipidemia and inflammation	European Atherosclerosis Society
2019	Follow-up workshop teaching and supervision	Leiden University
	10X Genomics course	EMBL
2022	Scientific conduct	Leiden University

Presentations at (inter)national conferences

Oral presentations

2019	87th European Atherosclerosis Society congress, Maastricht, The Netherlands
	Gordon Research Seminar in Atherosclerosis, Newry ME, United States of America
	3rd Translational Cardiovascular Research Meeting, Utrecht, The Netherlands
2020	LACDR Spring Symposium (online)
	11th Rembrandt Symposium (online)
2021	12th Rembrandt Symposium (online)
	5th DCVA Translational Cardiovascular Research meeting (online)
2022	90th European Atherosclerosis Society congress, Milan, Italy
	10th EMBRN International Mast Cell and Basophil Meeting, Utrecht, The Netherlands
	SCOG Workshop 'Single Cell Omics in Clinical Applications', Bonn, Germany

Presentations at (inter)national conferences

Oral presentations

	13th Rembrandt Symposium, Noordwijkerhout, The Netherlands
	NVVI Annual Meeting, Noordwijkerhout, The Netherlands
2023	91st European Atherosclerosis Society congress, Mannheim, Germany
	Dutch Atherosclerosis Society Symposium, Amersfoort, The Netherlands
	WCN Onderzoekscongres, Amsterdam, The Netherlands

Poster presentations

2018	LACDR PhD Introductory Course on Drug Research, Leiden, The Netherlands
	LACDR Spring Symposium, Leiden, The Netherlands
	9th Rembrandt Symposium, Noordwijkerhout, The Netherlands
2019	LACDR Spring Symposium, Leiden, The Netherlands
	Gordon Research Conference Atherosclerosis, Newry ME, United States of America
	10th Remrandt Symposium, Noordwijkerhout, The Netherlands
	NVVI Annual Meeting, Noordwijkerhout, The Netherlands
2020	VIB Single Cell Conference (online)
	NVVI Annual Meeting (online)
2021	LACDR Spring Symposium (online)
	6th European Congress of Immunology (online)
2022	Frontiers in CardioVascular Biomedicine (FCVB), Budapest, Hungary
	LACDR Spring Symposium, Leiden, The Netherlands
2023	Gordon Research Seminar in Atherosclerosis, Barcelona, Spain
	Gordon Research Conference Atherosclerosis, Barcelona, Spain